# A Comparative Analysis of the Performance and the Microbial Ecology of Biological Sulphate Reducing Reactor Systems

Tomas Hessler


Thesis presented for the Degree of

Doctor of Philosophy

In the Department of Chemical Engineering

University of Cape Town

February 2020

Supervisors: Dr Robert Huddy and Prof Susan T. L. Harrison

# Declaration

I, *Tomas Hessler*, hereby declare that the work on which this dissertation is based is my original work (except where acknowledgements indicate otherwise) and that neither the whole work nor any part of it has been, is being, or is to be submitted for another degree in this or any other university.

I empower the university to reproduce for the purpose of research either the whole or any portion of the contents in any manner whatsoever.

Signature: ……Signed by candidate

Date: 27th July 2020

# Acknowledgements

I would like to thank the following people who played a key role in bringing this work together:

Firstly, I would like to thank my supervisor, Dr Robert Huddy, for the fantastic insight into microbiology and the guidance and mentorship;

Prof Sue Harrison, my co-supervisor, for your encouragement, mentorship and great insights into bioprocess engineering;

Prof Jill Banfield, for the invaluable opportunity to visit your lab and for the training in genome-resolved metagenomics;

Dr Thanos Kotsiopoulos, for your assistance with the modelling of reactor performance data;

Joachim Mackie, for the building of reactors used in this study and consultation on technical aspects of the project;

Miranda Waldron, for the many hours of great work on the scanning electron microscope;

Tynan Marias and Sarah Fernandes, for all your help in the lab getting the reactors running and keeping them going;

Fadzai Kadzinga, for the assistance with many of the engineering aspects of this work and for your support during difficult stages of the project;

Kate Lane, Patrick West, and everyone in the Banfield lab, for the training in genome-resolved metagenomics and for being so welcoming;

Tich Samkange, Sue Jobson and all CeBER staff and students, for your time, generosity and your friendship.

And very special thanks to my family for all the support and encouragement and to Cynthia Fan for your whole-hearted and endless support and patience.

# Abstract

Acid rock drainage (ARD) is defined as acidic waste-water contaminated with sulphate and heavy metals which is generated through the oxidation of sulphidic ores in the presence of water and oxygen. Mining activities accelerate this process by bringing these ores to the surface where they are further crushed and, eventually end up in waste rock dumps and tailing impoundments where they continue to generate ARD into perpetuity.

Active mining operations are mandated to prevent the discharge of ARD into the environment. This ARD is commonly remediated by expensive yet highly effective active treatment strategies such as high-density sludge processes and reverse osmosis. South Africa has an extensive history of gold and coal mining which has left abandoned mine workings with associated waste rock dumps throughout northern and eastern parts of the country. As many of these mines have long been abandoned, the responsibility to mitigate the environmental impact of the generated ARD lies solely with government. Although these diffuse sites often generate smaller volumes of less aggressive ARD compared to that generated through mine water rebound, the sheer number and the continual ARD generation from these sites is a severe threat to South Africa's already poor water security.

Biological sulphate reduction (BSR) has long been considered an attractive option for the long-term remediation of these low-volume sources of ARD – but its implementation has shown mixed success. BSR is a process catalysed through the innate metabolism of sulphate-reducing bacteria (SRB) which coexist within complex microbial communities. SRB themselves are a highly diverse group of anaerobic microorganisms which use sulphate as a terminal electron acceptor. The sulphide and bicarbonate produced during BSR can be used to precipitate heavy metals and aid in the neutralisation of the ARD, respectively. The implementation of BSR is, therefore, a comprehensive remediation strategy for diffuse sources of ARD. The study of BSR, using various reactor configurations and operating conditions shows much promise. However, the microbial ecology of the complex communities within BSR systems, and their links to the performance of BSR processes, has received far less attention in published literature. This is not a result of underappreciation of the role microbial communities but rather a historical lack of tools, specifically high-throughput techniques, available to assess complex microbial consortia.

It is asserted that the success of a sustainable BSR process developed for the long-term remediation of ARD requires an in-depth understanding the microbial communities associated with this process. The identification of the microorganisms which are key to the process, those

which threaten the stability of the community and the optimal growth conditions of these microorganisms, can be used to inform how these bioreactors are designed and operated. This study investigated the performance and microbial ecology of several continuous BSR reactors using culture-independent metagenomic sequencing approaches. The performance and microbial ecology of these reactors were evaluated at a range of hydraulic residence times (HRT) over the course of approximately 1000 days of continuous operation, from five- through to one-day(s). The tested reactor configurations included a continuous stirred tank reactor (CSTR), an up-flow anaerobic packed bed reactor (UAPBR) and a linear flow channel reactor (LFCR) that were each operated in duplicate and supplemented with either lactate or acetate as an electron donor. The different reactor configurations and supplied electron donors, as well as the varied applied HRT, generated a range of microenvironments which were hypothesised to lead to the divergence of the initial microbial community of the inoculum and generate numerous distinct microbial communities throughout and across the reactor systems. 16S rRNA gene amplicon sequencing was used to assess the microbial community structure of the numerous populations across the reactor systems and monitor how these communities responded to the change in the applied HRT. Genome-resolved metagenomics was employed in parallel to recover the genomes of all predominant microorganisms identified through gene amplicon sequencing. This allowed the interrogation of the composition of the respective microbial communities as well as the genetic potential of each microorganism and encompassing the communities represented within specific reactor environments.

The CSTRs were selected as these systems are characterised as well-mixed, support solely suspended biomass and kinetic equilibriums are achieved rapidly. This allows the performance of these reactors to be predictable and provides a benchmark to which the LFCRs and UAPBRs could be compared. The lactate-supplemented CSTR performed largely as anticipated based on available literature, demonstrating a maintained sulphate conversion of approximately 55% over the course of the study. The reactor achieved a maximum observed volumetric sulphate reduction rate (VSRR) of 17 mg/ℓ.h at a one-day HRT. The system supported a low SRB diversity, constituted almost entirely by a *Desulfomicrobium* and two *Desulfovibrio* operational taxonomic units (OTUs). The acetate-supplemented CSTR was able to maintain sulphate reducing performance at HRT where complete washout of SRB had been predicted based on literature. This reactor exhibited a maximum VSRR of 10.8 mg/ℓ.h at a 1.5-day HRT and was dominated by the same *Desulfovibrio* and *Desulfomicrobium* observed in the lactate-supplemented CSTR, along with several other SRB genera at lower abundance.

The LFCRs demonstrated an approximately ten-fold greater biomass retention than the corresponding CSTRs. This was facilitated through the incorporation of carbon microfibres, which

facilitated microbial colonisation and biofilm formation within the reactors. Surprisingly, the lactate-supplemented LFCR, underperformed compared to the lactate-supplemented CSTR, achieving a maximum VSRR of 14.8 mg/ℓ.h at a one-day HRT. This reduced performance, in spite of the enhanced biomass retention, was concluded to result from the out-competition of lactate-oxidising SRB in the reactor by *Veillonella* and *Enterobacter* OTUs. The acetate-supplemented LFCR exhibited a period of underperformance before recovering and subsequently demonstrated a maximum VSRR of 17.1 mg/ℓ.h at a one-day HRT. Evaluations of the microbial communities of this system during the HRT study revealed a dramatic shift in the SRB communities from being dominated by *Desulfatitalea* and *Desulfovibrio* to being dominated predominantly by *Desulfomicrobium* and *Desulfobacter*.

The UAPBRs are governed by plug-flow which resulted in the generation of gradients of decreasing substrates and increasing products throughout the height of the reactors. This, as hypothesised, resulted in the stratification of the microbial communities throughout the height of these reactors. This allowed many associations to be made between specific microorganisms and their ideal growth environments. Both UAPBRs demonstrated competitive sulphate reducing performance. The lactate-supplemented UAPBR proved especially successful as this system was able to maintain >95% sulphate conversion at one-day HRT, corresponding with a VSRR of 40.1 mg/ℓ.h. The performance of this reactor was attributed to the significant quantity of retained biomass and the successful harbouring of lactate-oxidising SRB towards the inlet zone of the reactor as well as propionate- and acetate-oxidising SRB towards the effluent zones of the reactor. The acetate-supplemented UAPBR exhibited a maximum VSRR of 23.2 mg/ℓ.h at a one-day HRT and a maximum sulphate conversion of 79% at a 2.3-day HRT. The stratification of the microbial communities within the acetate-supplemented UAPBR was less pronounced than the lactate-supplemented UAPBR, as a result of the fewer available volatile fatty acid species. However, the stratification which was observed in this system could be used to postulate the growth kinetics associated with the identified SRB – a *Desulfobulbus* was associated with rapid acetate oxidation in the inlet zone while a *Desulfatitalea* and a *Desulfosarcina* could be implicated in sulphate scavenging in the effluent zone of this reactor. This proved particularly valuable for elucidating the roles of these same SRB in the well-mixed reactor systems.

Genome-resolved metagenomics was employed to recover the genomes of the microorganisms identified in these systems and determine the metabolic potential of these microorganisms. Hydrogen-evolving hydrogenase genes were found to be widespread in genomes not capable of sulphate reduction. In contrast, hydrogen-consuming hydrogenases as well as autotrophic gene pathways were common amongst SRB genomes. The ubiquity of hydrogenase genes in these environments indicated that inter-species hydrogen transfer was an important feature within these

microbial communities. The dual consumption of both acetate and hydrogen was concluded to have facilitated the maintained sulphate reducing performance of the acetate-supplemented reactor systems at short HRT where system failure had been predicted. Indices of replication (iRep) were used to estimate the instantaneous growth rates of the microorganisms from metagenomic shotgun sequencing datasets. This revealed that, at a four-day HRT, the microorganisms within the biofilms were comparably active to planktonic microorganisms. This, together with the dynamic changes in the composition of these biofilms during the HRT study, suggests these biofilms are even more active and competitive than previously thought.

The combined use of next-generation gene amplicon sequencing and genome-resolved metagenomics has given unprecedented insights into the microbial communities of BSR reactor systems. Using this approach, it was possible to uncover a seldom discussed form of hydrogen cycling within BSR systems and has shown that there is no 'one-size-fits-all' approach when inoculating BSR reactors. The SRB within these systems were often highly specialised to particular environments, specific electron donors and each showed differing growth kinetics. The success of long-term, semi-passive BSR reactor systems would benefit greatly from the tailoring of SRB inoculums informed by the chosen reactor configuration and operating conditions. The outcomes of the kinetic reactor experiments have led to several recommendations for the design and operation of these systems.

# Contents

# List of Figures

# List of Tables

# Abbreviations

| | |
|---|---|
| AMD | Acid mine drainage |
| ARD | Acid rock drainage |
| ATP | Adenosine triphosphate |
| BESA | Bromoethanesulphonate |
| BSR | Biological sulphate reduction |
| COD | Chemical oxygen demand |
| CSTR | Continuous stirred tank reactor |
| DNA | Deoxyribonucleic acid |
| DSR | Dissimilatory sulphite reductase |
| EPS | Extracellular polymeric substances |
| GRG | Generalised reduced gradient |
| HMM | Hidden Markov Model |
| HPLC | High Performance Liquid Chromatography |
| HRT | Hydraulic retention time |
| IQR | Interquartile range |
| iRep | Indices of replication |
| LFCR | Linear flow channel reactor |
| NADH | Nicotinamide adenine dinucleotide (reduced) |
| NGS | Next generation sequencing |
| ORF | Open reading frame |
| OTU | Operational taxonomic unit |
| PBR | Packed bed reactor |
| PBS | Phosphate-buffered saline |
| PCR | Polymerase chain reaction |
| PFR | Plug flow reactor |
| RNA | Ribonucleic acid |
| rpS3 | Ribosomal protein S3 |
| rRNA | Ribosomal ribonucleic acid |
| rTCA | Reverse Tricarboxylic acid cycle |
| SEM | Scanning electron microscopy |
| SRB | Sulphate-reducing bacteria |

| | |
|---|---|
| SSE | Sum of squared errors |
| TCA | Tricarboxylic acid cycle |
| UAPBR | Up-flow anaerobic packed bed reactor |
| VFA | Volatile fatty acid |
| VSLR | Volumetric sulphate loading rate |
| VSRR | Volumetric sulphate reduction rate |
| YE | Yeast extract |

# Nomenclature

| SYMBOL | | UNITS |
|---|---|---|
| $C_X$ | Biomass concentration | g/ℓ |
| D | Dilution rate | $h^{-1}$ |
| e- | Electron | |
| F | Flow rate | ℓ/h |
| k | rate constant | (variable) |
| $K_S$ | Saturation constant | g/ℓ |
| $r_A$ | Volumetric sulphate reduction | g/ℓ.h |
| $r_S$ | Reaction rate | g/ℓ.h |
| S | Substrate concentration | g/ℓ |
| $S_0$ | Feed substrate concentration | g/ℓ |
| T | Temperature | °C |
| μ | Specific microbial growth rate | $h^{-1}$ |
| $\mu_{max}$ | Maximum specific microbial growth rate | $h^{-1}$ |
| V | Working reactor volume | ℓ |
| $X_S$ | Substrate conversion | |
| $Y_{X/S}$ | Biomass yield coefficient | g/g |
| ΔG°' | Gibbs free energy of formation | kJ/mol |

# Publications arising from this work

- Hessler, T., Harrison, S.T. and Huddy, R.J. (2020, accepted). Linking performance and microbial ecology in a newly developed biological sulphate reducing reactor system. Hydrometallurgy.
- Hessler, T., Harrison, S.T. and Huddy, R.J. (2019). Biological sulphate reduction as sustainable treatment of acid mine drainage: the performance of an acetate supplemented Linear Flow Channel Reactor. International Biohydrometallurgy Symposium (IBS), Fukuoka City, Japan. (Conference proceeding and oral presentation)
- Hessler, T., Harrison, S.T. and Huddy, R.J. (2018). Stratification of microbial communities throughout a biological sulphate reducing up-flow anaerobic packed bed reactor, revealed through 16S metagenomics. Research in Microbiology, 169(10), pp.543-551.
- Hessler, T., Harrison, S. T. and Huddy, R.J. (2018). The preferential localisation of SRB in an acetate supplemented up-flow anaerobic packed bed reactor. International Mine Water Association (IMWA) conference, Pretoria, South Africa. (Conference proceeding and oral presentation)
- Hessler, T., Marais, T., Huddy, R. J., van Hille, R., and Harrison, S. T. (2017). Comparative Analysis of the Sulfate-Reducing Performance and Microbial Colonisation of Three Continuous Reactor Configurations with Varying Degrees of Biomass Retention. Solid State Phenomena, 262, 638–642. International Biohydrometallurgy Symposium (IBS), Freiberg, Germany. (Conference proceeding and poster presentation)

# Chapter 1 Introduction

## 1.1 Background

Acid rock drainage (ARD) is a serious environmental threat associated with current and historic mining activities in many countries. South Africa is a semi-arid country fast approaching a national water crisis due to prolonged droughts and increasing demand on freshwater resources that, in mining areas, is exacerbated by ARD contamination. ARD is formed through the weathering of sulphidic ores when exposed to oxygen and water. This produces low pH solutions with elevated concentrations of sulphate and heavy metal ions (Johnson and Hallberg, 2005). This process occurs spontaneously and can be further accelerated by the microbial oxidation of these sulphide compounds (Zagury and Neculita, 2007). ARD formation is significantly enhanced by mining operations which expose acid-generating ores to oxygen and water. Furthermore, the processing of these ores greatly enhances the liberation of the sulphide minerals and their surface area available for oxidation.

South Africa has an extensive history of mining and experienced large scale mine closures during the late 1900s (Mulunda, 2013) continuing currently. Several legislation acts were passed during the 1990s aimed at regulating the remediation of ARD (Matsumoto et al., 2016), however, the treatment of historic mine water pollution has been left exclusively to the state. As a result, ARD is regarded as the most severe threat to South Africa's long-term freshwater security. The sources of ARD in South Africa can be broadly categorised into two groups: (i) ARD emanating from groundwater rebound through abandoned mine workings and (ii) ARD originating from more diffuse sources, such as abandoned coal and gold tailing impoundments, waste rock dumps and unworked pits. The latter generates smaller seasonal volumes of less aggressive ARD. The Witwatersrand Gold Fields, the O'Kiep Copper District (McCarthy, 2011) as well as the Mpumalanga coalfields (Gunther, 2006) have shown severe ARD discharge generated from mine water rebound. These are currently treated by a high-density sludge process (Aube and Payant, 1997) and reverse osmosis (Hutton et al., 2009). While this process can treat large volumes of ARD, it is very costly (McCarthy, 2011). In contrast, the number of these sites and longevity of the generation of the diffuse ARD sources has created a problem not readily addressed by chemical treatments. Instead, sustainable alternatives are crucial for the remediation of this form of ARD.

Numerous studies have demonstrated the use of biological sulphate reduction (BSR) as an effective strategy for the remediation of low-volume ARD sources (Kolmert and Johnson, 2001; Lens et al.,

2002; Boshoff et al., 2004; Zagury and Neculita, 2007). These processes make use of mixed consortia of sulphate-reducing bacteria (SRB). This diverse group of anaerobic microorganisms use sulphate ($SO_4^{2-}$) as the terminal electron acceptor in the oxidation of organic compounds, resulting in the formation of hydrogen sulphide and bicarbonate (Muyzer and Stams, 2008). The produced hydrogen sulphide can be used to precipitate heavy metals and the bicarbonate aids in neutralisation of the solution, making BSR-based processes ideal for the treatment of low-volume ARD effluents. The success of a BSR process tasked with the remediation of ARD must overcome several challenges, including (i) the efficient use of a cost-effective carbon source and electron donor, (ii) overcoming the relatively low growth rates of SRB, to enable greater reaction rates, and (iii) the proper handling of the toxic sulphide which is generated during the process.

Overcoming each these challenges depends on the choice of reactor configuration and operating conditions (Harrison et al., 2014). BSR reactors must provide environments where the SRB, within mixed microbial communities, are able to effectively compete for the available electron donors. These systems also should facilitate SRB biomass retention to allow the decoupling of the hydraulic and the biomass retention times, thereby allowing greater reaction rates to be achieved. Finally, these systems should be configured to enable the removal of the generated sulphide (van Hille et al., 2011) as this represents a toxic by-product and one which can also spontaneously re-oxidise to sulphate if not properly managed. Solutions to address these challenges are seldom informed from the direct analyses of these BSR microbial communities. This has left many important questions surrounding the link between system performance and microbial ecology of BSR systems only partially answered. These relate to which SRB are key to reactor performance given the provision of particular electron donor(s); which microbial niches are essential for overall community stability; what are the ideal growth conditions of these SRB and key-stone microorganisms within a mixed microbial culture; which microorganisms are detrimental to system performance; and what reactor configurations and operating conditions can select against these microorganisms. Addressing these questions would undoubtedly inform the design and operation of BSR systems and thereby enhance system performance and robustness.

Another frequent difficulty when operating these systems, and likely a symptom of our limited understanding of the complex microbial communities within these bioreactors, has been the vulnerability of SRB to perturbations that lead to unpredictable reactor performance (Zagury and Neculita, 2007). The microbial diversity and the structure-function relationships within these consortia have typically been poorly, or little studied. This has not been due to an underestimation of the importance of investigating the microbial ecology, but due to the limitations in the available technologies. The advent of culture-independent techniques, including next-generation sequencing (NGS) technologies, has allowed unprecedented insights into the structure-function relationships

within mixed microbial communities (Breitbart et al., 2003). The use of gene amplicon sequencing, routinely targeting the 16S rRNA gene, allows the rapid assessment of the composition of microbial communities in high-resolution and simultaneously across multiple samples (Langille et al., 2013). This technique is now used more frequently to study BSR systems (Zheng et al., 2014; Zhou et al., 2015; Vasquez et al., 2018). Genome-resolved metagenomics has been used to characterise the microbial communities and their metabolic potential within environmental samples and, notably, several biotechnological processes, including thiocyanate biodegradation (Kantor et al., 2015; Kantor et al., 2017; Rahman et al., 2017), municipal wastewater treatment (Roume et al., 2015) and anaerobic digestion (Vanwonterghem et al., 2016). However, the use of genome-resolved metagenomics has not yet been applied to biological sulphate reducing systems.

This study investigates the performance of three BSR reactor configurations, each operated in duplicate and supplemented with acetate and lactate, separately. These electron donors, despite current limitations to their commercial use, represent the most promising electron donors for this purpose. Lactate is an expensive electron donor but supports some of the higest SRB growth rates compared with other organic electron donors. Lactate is typically supplied at concentrations in excess needed for complete sulphate removal via incomplete lactate oxidation. In this study, lactate was supplied at concentrations which theoretically allow a maximum of 64% of the supplied sulphate to be reduced via incomplete lactate oxidation. Further sulphate conversion requires the subsequent utilisation of by-products of lactate oxidation, namely acetate and propionate, by SRB. Supplementation of lactate at this concentration greatly reduces the amount of lactate required and the associated operating costs. Acetate is a low-cost electron donor but supports low SRB growth rates and is often poorly utilised. This study aimed to identify the operating conditions and the microbial consortia required for efficient acetate utilisation and competitive reaction rates. The criteria used for the selection of these reactor configurations and operating conditions were based on previous BSR reactor studies which have shown effective semi-passive operation. Secondly, the reactor systems were selected to generate a range of physiochemical conditions as a result of differences in reactor hydrodynamics, supplied electron donors and inclusion of solid support structures - all of which aimed to stimulate the development of a range distinct microbial communities. The performance of these six BSR reactors was monitored over the course of a hydraulic residence time (HRT) study. These reactors were simultaneously inoculated with the same inoculum and were initially operated at long HRT. The HRT was then iteratively reduced, acting as a further selective pressure on the microbial communities. Genome-resolved metagenomics was employed to characterise the composition and metabolic potential of the microbial consortia within each of these reactor systems, in combination with 16S rRNA gene amplicon sequencing which allowed for the composition of these microbial communities to be monitored as the hydraulic retention time was reduced. This approach allowed many microbial

communities associated with BSR reactor systems to be evaluated and for this information to be integrated with reactor performance. This enabled the contribution of individual microorganisms, and groups of microorganisms, towards system performance and robustness to be determined.

## 1.2 Thesis overview

Literature relating to this study are critically reviewed in Chapter 2. Topics addressed include the generation of ARD; different strategies to remediate ARD with a strong focus on biological sulphate reduction and its use in semi-passive ARD remediation; ecology and metabolism of SRB which catalyse BSR; and the use of metagenomics, next-generation sequencing (NGS) and bioinformatics for the evaluation of the composition and metabolic potential of mixed microbial communities. This chapter closes through motivating the scope of this study, followed by the setting out the hypotheses and aligned research activities. The methodologies used in this study are described in detail in Chapter 3 and the experimental plan is also further outlined.

Chapters 4,5 and 6 present the studies of microbial ecology and reactor performance of the continuous stirred-tank reactors (CSTR), linear flow channel reactors (LFCR) and the up-flow anaerobic packed bed reactors (UAPBR), respectively, using acetate and lactate separately as electron donor. The acetate- and lactate-supplemented reactors are presented in separate sections within each of these chapters. The performance and microbial ecology associated with each reactor is evaluated during an HRT study. The results of each reactor study and their discussion are presented in separate sections.

The comparison of the microbial ecology across the six reactors is presented as an integrated discussion in Chapter 7, having presented the ecology of individual reactors in detail in Chapters 4 to 6. The genome-resolved metagenomic analyses of the six reactor systems are presented in Chapter 8. The final conclusions and the recommendation for further study are discussed in Chapter 9.

# Chapter 2 Literature review

## 2.1 Acid rock drainage

Acidic and sulphate-rich wastewater streams are generated by a number of industries including coal power plants (Johnson, 2000), the tannery industry (Galiana-Aleixandre et al., 2011), chemical industries (Sarti and Zaiat, 2011) and, chiefly, mining (Johnson and Hallberg, 2005). Acid Rock Drainage (ARD) refers to the acidified water that results from the natural weathering of sulphide containing ores, including pyrite ($FeS_2$), chalcopyrite ($CuFeS_2$) and arsenopyrite (FeAsS), in the presence of oxygen and water to produce low pH waters with an increased concentration of dissolved sulphate and heavy metal ions (Equations 2.1 to 2.4; Johnson and Hallberg, 2005; Akcil and Koldas, 2006). These ores remain chemically stable underground in the absence of oxygen. However, during mining activities these ores are brought to the surface where they are crushed, greatly increasing the liberation and exposed surface area on which these reactions are able to occur (Hoffert, 1947).

### 2.1.1 ARD formation

The coal and gold deposits in South Africa are largely associated with pyrite and, therefore, the process of ARD generation from pyrite is discussed here. Briefly, pyrite reacts with oxygen and water generating ferrous iron, sulphate and acidity (Equation 2-1). Ferrous iron then reacts with oxygen to form ferric iron (Equation 2-2). At a pH above 2.3, ferric iron precipitates to form ferric hydroxide which results in the release of additional protons (Equation 2-3). The generated protons, in turn, further accelerate the oxidation of ferrous iron (Equation 2-2). As the pH decreases and the solubility of ferric iron rises, the amount of ferric iron able to chemically attack the pyrite surface increases (Equation 2-4), greatly accelerating the rate of ARD generation. In addition, the oxidation of pyrite and ferrous iron is accelerated through the activity of aerobic chemolithotrophic iron-oxidising bacteria and archaea (Equations 2-1and 2-2; Baker and Banfield, 2003; Zagury et al., 2006; Denef et al., 2010) which increase the rates of these reactions by several orders of magnitude (Johnson and Hallberg, 2005). When the pH is sufficiently low (>2) the formation of secondary minerals can be produced (Equation 2-5) along with sulphate, acidity and ferric iron.

$FeS_2 + 7/2\ O_2 + H_2O \rightarrow Fe^{2+} + 2\ SO_4^{2-} + 2\ H^+$ Equation 2-1

$Fe^{2+} + 14\ O_2 + H^+ \rightarrow Fe^{3+} + 12\ H_2O$ Equation 2-2

$Fe^{3+} + 3\ H_2O \rightarrow Fe(OH)_3 + 3\ H^+$ Equation 2-3

$FeS_2 + 14\ Fe^{3+} + 8\ H_2O \rightarrow 15\ Fe^{3+} + 2\ SO_4^{2-} + 16\ H^+$ Equation 2-4

$16\ FeS_2 + 60\ O_2 + 60\ H_2O \rightarrow Fe_8O_8(SO_4)(OH)_6 + 8\ Fe^{3+} + 38\ H_3O^+ + 31\ SO_4^2$ Equation 2-5

### 2.1.2 Environmental impacts of ARD

The extent of the environmental impact of ARD is dependent on the stage of ARD formation, the geomorphology of the ore deposit and several factors concerning the local climate (McCarthy, 2011). These ultimately influence the extent of the generation of acidity, sulphate and the release of heavy metals. Decreased pH and the release of even low concentrations of heavy metals into the environment can have severe consequences for terrestrial and aquatic ecosystems (Feris and Kotze, 2014) as well as human health (Tomlinson et al., 1980; Duruibe et al., 2007).

ARD treatments often focus predominantly on acid neutralisation and the removal of contaminating heavy metals, whilst paying less attention to elevated sulphate concentrations (Arnold et al., 2016). This is a result of the lower environmental threat of elevated sulphate concentrations and less stringent regulatory guidelines. Similarly, the acidity associated with diffuse ARD discharge is often neutralised through dilution in larger water bodies and several chemical reactions. However, the sulphate concentration in many South African dams has been steadily increasing over the past 25 years (McCarthy, 2011). This can have serious implications for the agricultural industries which use this water for irrigation and for livestock.

The World Health Organization (WHO) and US Environmental Protection Agency have stressed that drinking water should contain no more than 250 mg/ℓ sulphate (US EPA, 1999; Balintova et al., 2015) However, the legal guidelines for the industrial discharge of sulphate into the environment varies from country to country, with an upper permissible limit of 600 and 500 mg/ℓ in South Africa and the USA, respectively (Arnold et al., 2016). The sulphate concentration, even in neutral rock drainage (Figure 2-1) routinely exceeds these guidelines, indicating that the majority of ARD sources require treatment to reduce the sulphate concentration for safe and legal discharge into the environment. Within this thesis acid rock drainage, saline rock drainage and neutral rock drainage are all termed as acid rock drainage.

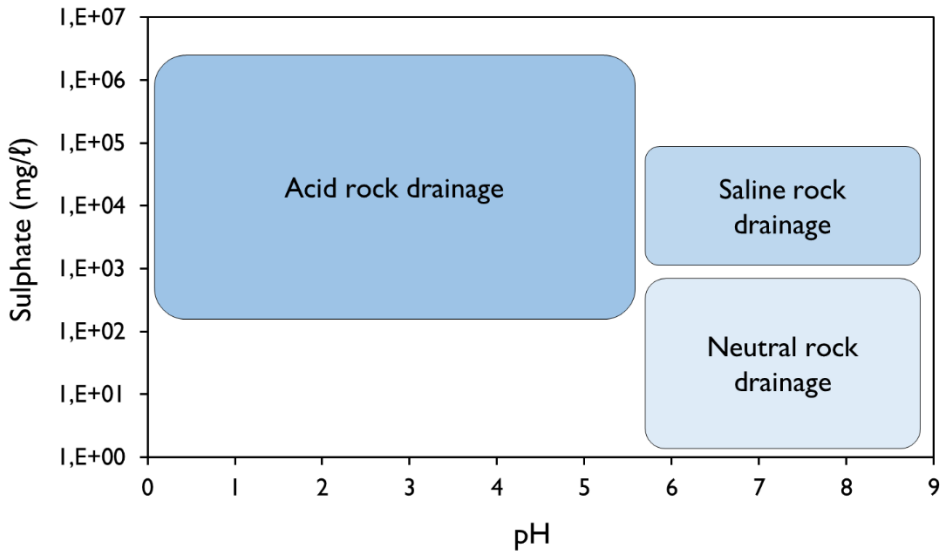


Figure 2-1 Schematic showing acid rock drainage, saline rock drainage, neutral rock drainage as a function of pH and sulphate concentration, adapted from Plumlee et al. (1999).

## 2.2 ARD remediation strategies

The prevention of ARD is regarded as favourable over remediation of ARD due to the longevity of its generation (Johnson and Hallberg, 2005). However, in many instances, this is not feasible, particularly when dealing with mining sites which have long been generating ARD. Broadly, strategies for the remediation of ARD should aim to neutralise the acidity and, remove the heavy metals and sulphate ions (Johnson and Hallberg, 2002). ARD treatment options can be categorised into chemical or biological remediation strategies and these can both be further sub-divided into either active or passive treatment processes (Johnson and Hallberg, 2005). The choice of treatment strategy is dependent on the volumes of ARD being produced, the concentration of sulphate and metals, and the pH of the produced ARD (Gazea et al., 1996). Smaller mines and more diffuse sources of ARD which generate less extreme forms of ARD are typically more amenable to passive process (Figure 2-2). This is largely due to the associated costs of remediation and the frequent lack of infrastructure. More aggressive forms of ARD which tend to result from mine water rebound, are more suitably treated using more expensive active treatment systems due to the volumes of ARD generated and the severity of the ARD.

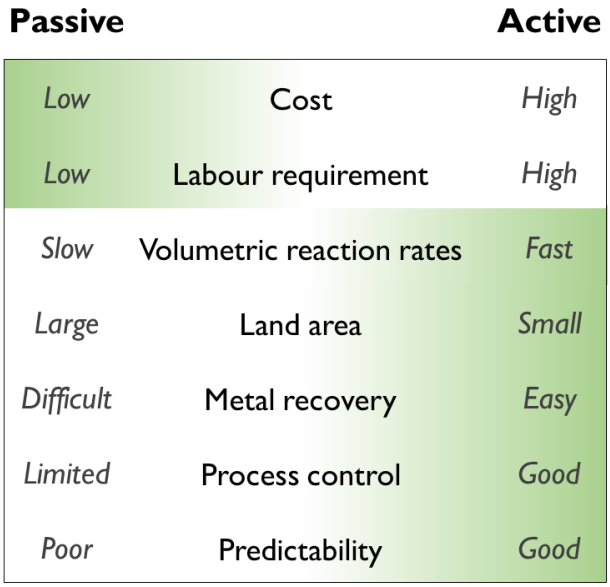


Figure 2-2 The trade-offs between passive and active treatments of ARD regarding the operational parameters and the effectiveness of the process, adapted from Kaksonen and Puhakka (2007).

### 2.2.1 Active treatment

The Karroo supergroup is a large geological formation containing one of the world's largest gold deposits. Historical and current large-scale mining in this small area has led to the continuous generation of large volumes of highly acidic, saline and heavy metal-rich ARD (McCarthy, 2011). The severity of the environmental impact of this ARD and the volumes produced mean that remediation via active treatments are essential. Active ARD treatment systems require the continuous input of materials, maintenance and labour. The implementation of active treatments generally requires the construction of a treatment facility comprising specialised equipment with large capital and operating expenditures (Gazea et al., 1996). The tight regulation of the operational conditions, the high kinetic rates and the short residence times associated with active treatment means that ARD streams of large volumes, low pH and high heavy metal and sulphate concentrations are best suited to this form of treatment.

The most commonly used active ARD treatment involves the addition of an alkaline chemical for neutralisation (Coulton et al., 2003). Lime is typically used for this purpose due to its lower cost compared to other alkaline reagents such as sodium hydroxide. However, lime is hydrophobic and requires considerable energy input to ensure sufficient mixing in solution (Skousen et al., 2000). The addition of alkaline chemicals results in metal precipitation and the formation of a high-density sludge that has traditionally been stored. This process can be performed in sequential steps whilst monitoring of the pH, allowing for the selective precipitation of various heavy metals as hydroxides (Aube and Payant, 1997) and the precipitation of sulphate as gypsum.

A second promising active treatment is the use of membrane technologies which have the advantage of generating potable water as a by-product (Liu et al., 2011). These processes, such as reverse osmosis and nanofiltration, are expensive and difficult to maintain due to fouling of the membranes (Simate and Ndlovu, 2014). However, with routine maintenance and pre-treatment steps to minimise fouling, these processes can be sustainably operated (Nasir et al., 2016; Hutton et al., 2009).

Many mining areas in South Africa have shown extensive discharge of aggressive ARD, including the Witwatersrand Gold Fields and the O'Kiep Copper District (McCarthy, 2011) as well as the Mpumalanga coalfields (Gunther, 2006). The ARD generated in these areas is not suitable to be treated by passive treatments due to the large volumes produced. Instead, the approach for the treatment of these sources of ARD is the use of high-density sludge (Aube and Payant, 1997) for neutralisation, heavy metal removal and substantial dewatering in order to reduce the cost of disposal and storage (Johnson and Hallberg, 2005). The eMalahleni Water Reclamation Plant (Figure 2-3; Hutton et al., 2009) as well as the Optimum coal mine (Cogho and van Niekerk, 2009) in Mpumalanga, South Africa, have demonstrated use of ultrafiltration and reverse osmosis for further treating the water stream following removal of this sludge as dewatered sludge cake. This generates potable water and a highly concentrated brine solution which is stored in evaporation ponds.

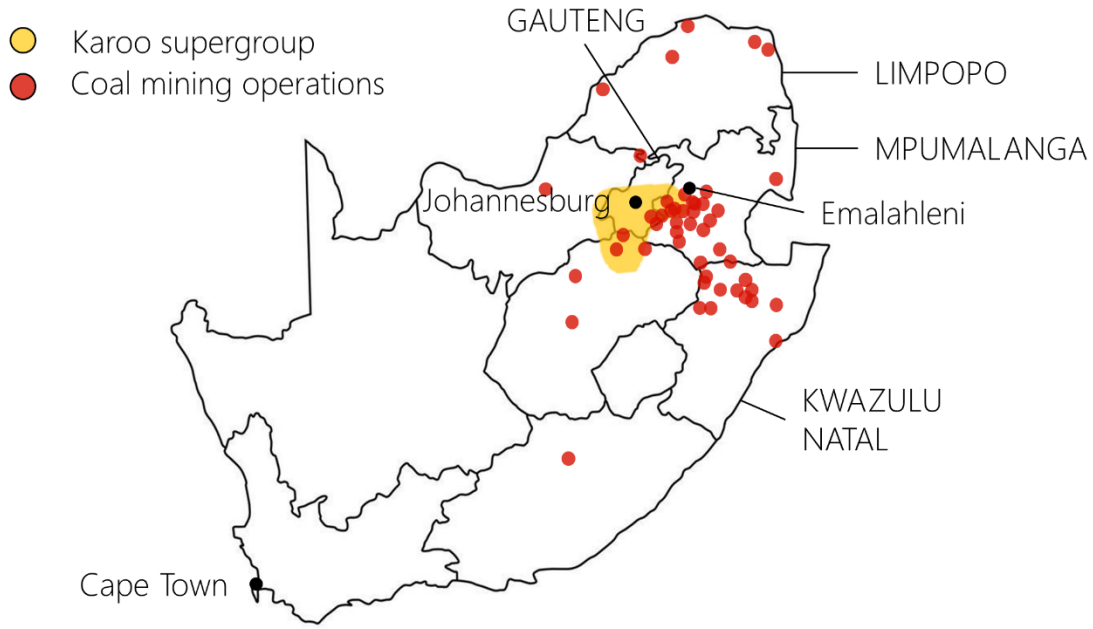


Figure 2-3 Annotated map of South Africa showing the gold-rich Karoo supergroup and current coal mining operations. Adapted from McCarthy (2011) and Council for Geosciences, South Africa.

The Alkaline barium chloride (ABC) process was developed by The Council for Scientific and Industrial Research (CSIR) as a cost-effective active treatment for the remediation of ARD (de Beer et al., 2010). The ABC process pilot-scale plant was able to neutralise and remove heavy metals as well as the sulphate associated with ARD originating from a gold mine in the Western Basin in Gauteng, South Arica (de Beer et al., 2010). The first stage of this process involves the precipitation of metals in a pre-treatment using CaS, $Ca(HS)_2$ or $Ca(OH)_2$. The majority of the sulphate is removed through gypsum crystallisation followed by precipitation using barium carbonate, generating gypsum as a value-added product. This two-step process reduced the sulphate concentration in the ARD from 4500 mg/ℓ to less than 100 mg/ℓ. This process was designed to use chemical reagents which were widely available in the region, at low costs. These reagents could then be regenerated from the final sludge processing stage of the process.

### 2.2.2 Passive treatment

Passive treatment options do not generally require any further labour nor additional materials after the process has been installed (Johnson and Hallberg, 2005). A common passive chemical treatment option for ARD remediation is the use of anoxic limestone drains (Kleinmann et al., 1998). These limestone drains raise the pH of the solution and maintain iron as ferrous iron ($Fe^{2+}$) to prevent the precipitation of ferric hydroxide which can create a passivation layer and cause

impermeabilisation of the limestone. In the case where the concentration of iron and other metals are too high, biological treatment using anaerobic wetlands becomes more viable (Hao, 2000). These are large ponds rich in organic matter, often supplied in the form of compost, which is oxidised by aerobic microorganisms resulting in the removal of oxygen from the water (Johnson and Hallberg, 2005). This creates anoxic conditions suitable for the proliferation of anaerobic microorganisms, including sulphate-reducing bacteria (SRB), methanogens and nitrate-reducing bacteria (Johnson and Hallberg, 2002). These ponds are often supplemented with a limestone bed below the compost layer to further aid in neutralisation of acidic ARD (Younger et al., 2003). However, these wetlands need to be established in a large area. Estimation of the size of the wetland needed can be difficult (Johnson and Hallberg, 2002) and if the area requirement is not met, the reduced residence time in the prevents adequate treatment.

### 2.2.3 Semi-passive biological treatment

A comparative summary of the main characteristics of passive and active treatment is shown in Figure 2-2 (Kaksonen and Puhakka, 2007). These comparisons demonstrate the trade-off between process control and the costs of the process. The stark contrasts between active and passive remediation strategies have stimulated interest in the development of semi-passive processes with lower associated costs, compared to active treatments, but which allow a greater degree of control and higher reaction rates over passive systems (Harrison et al., 2014). Semi-passive systems require the continual addition of materials but with minimal power or labour requirements (Trumm, 2010). Semi-passive ARD treatment processes are typically performed in bioreactors, employing biological sulphate reduction (BSR) (Nielsen et al., 2018).

The successful development of a semi-passive process would be hugely beneficial within a South African context and in other countries with a legacy on mining of sulphidic deposits over a large land area. The ARD generated by the numerous tailings impoundments, waste rock dumps and unworked pits associated with coal mining across South Africa (Figure 2-3) are most suitably addressed by passive to semi-passive treatment processes due to the rural nature and low infrastructure available at many of these sites, and the number and distribution of these sites.

### 2.2.4 Biological Sulphate Reduction

Active and passive biological treatment of ARD effluents typically employ biological sulphate reduction (BSR). This process is catalysed by SRB, a diverse group of anaerobic microorganisms capable of using sulphate as their terminal electron acceptor. The term sulphate-reducing bacteria (SRB) is used interchangeably with sulphate reducing microorganisms or prokaryotes due to the capacity for dissimilatory sulphate reduction occurring in several species of archaea (Itoh et al., 1999). In addition to the reduction of sulphate, this process generates alkalinity and metals can be

precipitated with the generated sulphide, thereby effectively reversing the process of ARD generation. The feasibility of the application of BSR for semi-passive treatment of ARD is dependent on the availability and cost of electron donors and their efficient use (Section 2.3, Gopal, 2005; Harrison et al., 2014). Further, the reaction rates of the process need to be maximised to ensure feasibility in terms of reactor sizing and cost (Gopal, 2005; Harrison et al., 2014). A major weakness of this process has been the susceptibility of SRB to perturbations leading to unpredictable reactor performance (Zagury and Neculita, 2007) i.e. lack of resilience. These perturbations include changes in ambient temperatures (Lefticariu et al., 2015), changes in the applied HRT (Baskaran and Nemati, 2006) and the gradual change in the composition of the complex organic electron donor (Das et al., 2012; Mirjafari and Baldwin, 2016; Sato et al., 2018). The reactor configurations used for semi-passive BSR treatment of ARD are discussed in Section 2.5.

## 2.3 Sulphate-reducing bacteria

### 2.3.1 The ecology of SRB

SRB are found in a wide variety of anaerobic environments including deep-sea hydrothermal vents (Thauer et al., 2007), rice fields (Loubinoux et al., 2002), ARD effluents (Barton, 1995), anoxic river sediments (Sul et al., 2009) and the gastrointestinal tracts of ruminant animals (Rabus, et al. 2006). As of 2008, all identified SRB were classified within only five bacterial and two archaeal phyla, with the majority of SRB genera classified to the classes, Deltaproteobacteria and Clostridia (Muyzer and Stams, 2008). However, the discovery of new taxa of SRB had relied largely upon targeted *dsrAB* gene surveys using molecular techniques. The subsequent characterisation of SRB historically relied on cultivation which hugely limited the number of SRB which could be studied. Since then, genome-resolved metagenomics (Section 2.8.3) has facilitated the recent identification of numerous microorganisms capable of dissimilatory sulphate reduction within an environment and thoroughly assessed their metabolic potential (Bendall et al., 2016; Probst et al., 2017; Timmers et al., 2018). A genomic survey for genes involved in the sulphur cycle, performed by Anantharaman et al. (2018), brought the total number of bacterial and archaeal phyla in which SRB belonged to 18 and four, respectively (Figure 2-4). This has serious implications for the reliance on 16S rRNA gene sequencing alone for the identification of SRB and assessment of SRB diversity within complex microbial communities.

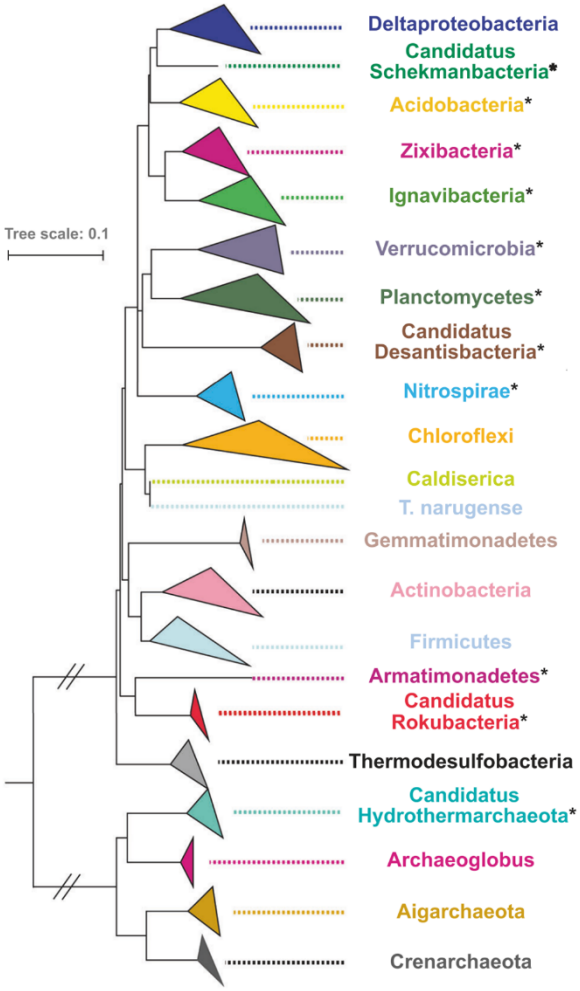


Figure 2-4 Phylogenetic consensus neighbour-joining and maximum-likelihood tree of 16S rRNA gene sequences of microorganisms with the genetic capacity to perform dissimilatory sulphate reduction, presented by Anantharaman et al. (2018). Sequences are collapsed at the phylum level and are so labelled. Asterisks indicate phyla which were found to contain sulphate reducers by Anantharaman et al. (2018).

### 2.3.2 Molecular mechanism of sulphate reduction

Dissimilatory sulphate reduction occurs in four main steps (Figure 2-5) following the transport of sulphate across the membrane by a sulphate transporter embedded in the cell membrane. The reduction of sulphate to sulphite is performed in two steps due to the sulphate-sulphite redox couple being too negative for NADH or ferredoxin oxidation ($E^{\circ\prime}$ = -516 mV; Muyzer and Stams, 2008). Sulphate is first activated to adenosine 5-phosphosulfate (APS) by sulphate adenylyltransferase (Sat; Shen and Buick, 2004). The redox potential of APS-sulphite is just $E^{\circ\prime}$ = -60 mV and therefore the oxidation of NAD and ferredoxin becomes favourable ($E^{\circ\prime}$ of -314 mV and -398 mV, respectively). APS is subsequently oxidised by APS reductase (AprAB) to sulphite, with the two electrons being donated from the membrane-bound QmoABC complex (Oliveira et al., 2011). The produced sulphite becomes covalently bound to the active site of the dissimilatory

sulphite reductase complex (DsrAB). It was understood that the further reduction of sulphite to sulphide was energetically favourable but the mechanism for this was unknown until recently.

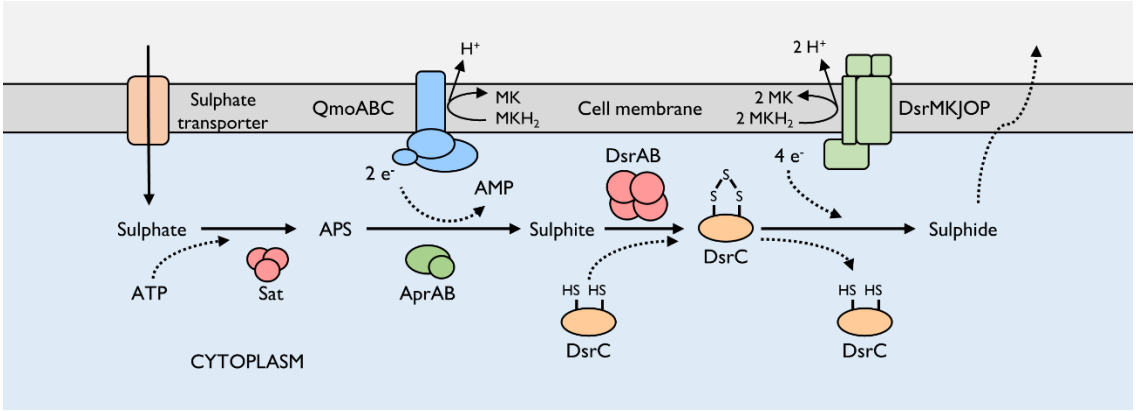


Figure 2-5 The dissimilatory sulphate reducing pathway adapted from Santos et al. (2015) and Ruckert (2016).

Oliveira et al. (2011) resolved the first crystal structure of DsrAB with and without being complexed to a DsrC subunit. Analysis of the active site of this complex led the authors to conclude that DsrC was not merely a structural subunit of the Dsr complex but was also a co-substrate of DsrAB which is directly involved in the reduction of sulphite to sulphide. This was confirmed experimentally by Santos et al. (2015) who demonstrated that a trisulphide forms between two cysteine residues on DsrC, catalysed by DsrAB. The final reduction of this trisulphide bound to DsrC is likely catalysed by DsrMKJOP with electrons originating from the menaquinol pool (Grein et al., 2010; Oliveira et al., 2011; Santos et al., 2015). The generated hydrogen sulphide is then able to freely diffuse across the cell membrane and into the environment.

## 2.4 Electron donors and carbon sources for BSR

SRB commonly use low molecular weight volatile fatty acids (VFAs) as electrons donors, including formate, acetate, lactate, propionate, ethanol, butyrate and citrate (Liamleam and Annachhatre, 2007; Stams et al., 2009). In anaerobic environments, these VFAs arise through the hydrolysis of complex organic macromolecules to monomers and their fermentation by different groups of microorganisms (Muyzer and Stams, 2008). SRB are conventionally grouped into two groups, namely incomplete and complete oxidisers, based on their ability to use these electron donors. Incomplete oxidisers degrade organic molecules to form acetate, whilst complete oxidisers oxidise organic molecules, including acetate, completely to carbon dioxide (Muyzer and Stams, 2008).

Common reactions catalysed by SRB and competing microorganisms are shown in Table 2-1.

Table 2-1 Common sulphate-reducing, lactate fermenting and methanogenic reactions. Adapted from Thauer et al. (1977).

| Reaction equation | ΔG°' (kJ/reaction) | |
|---|---|---|
| $4\ H_2 + SO_4^{2-} + H^+ \rightarrow HS^- + 4\ H_2O$ | - 51.9 | Equation 2-6 |
| $Acetate^- + SO_4^{2-} \rightarrow 2\ HCO_3^- + HS^-$ | - 47.6 | Equation 2-7 |
| $Ethanol + 0.5\ SO_4^{2-} \rightarrow Acetate + 0.5\ HS^- + 0.5\ H^+ + H_20$ | -15.9 | Equation 2-8 |
| $Propionate^- + 0.75\ SO_4^{2-} \rightarrow Acetate^- + HCO_3^- + 0.75\ HS^- + 0.25\ H^+$ | - 37.7 | Equation 2-9 |
| $Lactate^- + 0.5\ SO_4^{2-} \rightarrow Acetate^- + HCO_3^- + 0.5\ HS^-$ | - 80.2 | Equation 2-10 |
| $2\ Lactate^- + 3\ SO_4^{2-} \rightarrow 6\ HCO_3^- + 3\ HS^- + H^+$ | - 225.3 | Equation 2-11 |
| $3\ Lactate^- \rightarrow Acetate- + 2\ Propionate^- + HCO_3^- + H^+$ | - 70.0 | Equation 2-12 |
| $Acetate^- + H_2O \rightarrow CH_4 + HCO_3^-$ | - 31.0 | Equation 2-13 |

### 2.4.1 Lactate

Lactate is one of the most widely used substrates for the cultivation of SRB by researchers (Rabus et al., 2015). Within lactate-oxidising microorganisms, lactate is transported over the membrane by a permease and first converted to pyruvate through the action of one of several lactate dehydrogenases. Pyruvate is then converted to acetate via one of several pathways. Several *Desulfovibrio* species perform this using pyruvate dehydrogenase (EC:1.2.4.1) which participates in the conversion of pyruvate to acetyl-CoA. Phosphate acetyltransferase (EC:2.3.1.8) then converts the acetyl-CoA to acetyl-phosphate and finally, acetate kinase (EC:2.7.2.1) dephosphorylates the acetyl-phosphate to produce acetate (Pereira et al., 2007; Wall et al., 2008).

In contrast, lactate can be fermented to propionate and acetate via the methylmalonyl and acrylyl pathways by fermentative microorganisms and some SRB (Grandgirard et al., 2002). The acrylyl pathway involves the conversion of lactate to lactoyl-CoA by propionate CoA-transferase (EC:2.8.3.1) and is converted to acryloyl-CoA, propanoyl-CoA and finally to propionate (Selmer et al., 2002). The methylmalonyl pathway involves many enzymes of the TCA cycle acting in reverse, eventually producing succinyl-CoA, from pyruvate, which is then acted upon by a suite of enzymes, including methylmalonyl-CoA mutase (EC:5.4.99.2), to produce propionyl-CoA and finally propionate (Grandgirard et al., 2002). This pathway has been well studied in *Veillonella* species (Hilpert and Dimroth, 1991).

Biological sulphate reduction coupled to the predominant incomplete oxidation of lactate to acetate can be described by Equation 2-10. Many bacteria are able to compete for lactate as a

carbon source (Laanbroek et al., 1982) through anaerobic lactate fermentation (Equation 2-12) to form acetate and propionate. Oyekola et al. (2012) investigated the competition between fermentative bacteria and SRB in a mixed culture with lactate as the primary electron donor. The maximum specific growth rates of the lactate fermenters and oxidisers (SRB) were determined to be 0.3 and 0.2 $h^{-1}$ respectively (Figure 2-6). The saturation constant ($K_s$) for lactate was determined to be 3.3 g/ℓ for fermentative microorganisms and 0.6 g/ℓ for SRB. The notably smaller $K_s$ of SRB indicates that these microorganisms will outcompete fermentative microorganisms at lower lactate concentrations.

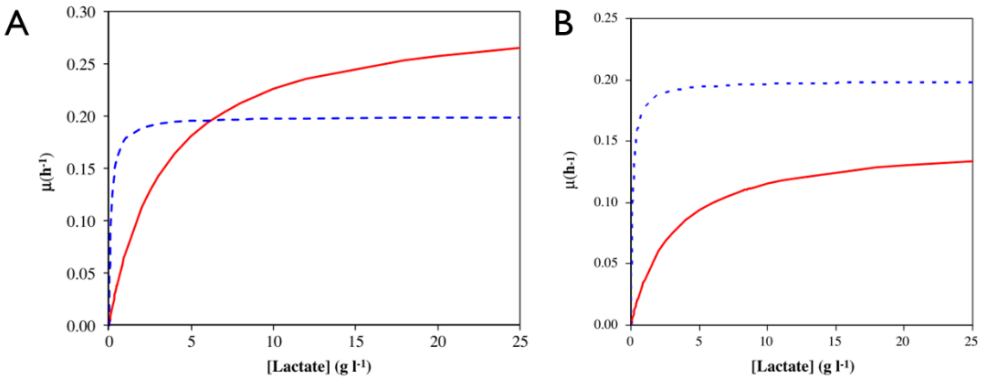


Figure 2-6 Modelled growth rates of lactate-oxidising SRB (dotted, blue line) and lactate-fermenting microorganisms (red, solid line) at varied lactate concentrations in the (A) absence and (B) presence of >0.5 g/ℓ sulphide as performed by Oyekola et al. (2012). This data highlights the susceptibility of fermentative microorganisms, contrasted to SRB, to sulphide inhibition.

Sulphide generation due to BSR results in the inhibition of growth of many microorganisms (Weedon et al., 1940). Oyekola et al. (2012) investigated how the kinetic constants for both lactate fermenters and oxidisers would change in the presence of a high concentration of sulphide (>0.5 $g.\ell^{-1}$). It was found that the kinetic constants for SRB growth remained unchanged, while the apparent affinity for fermentative growth on lactate remained unchanged and the maximum specific growth rate was halved at sulphide concentrations greater than 0.5 g/ℓ (Figure 2-6). This suggests that once an SRB community has become sufficiently dominant in an environment, the sulphide produced will further suppress fermentative microorganisms. The simultaneous growth of SRB and fermenters at a range of lactate feed concentrations was also investigated by Oyekola et al. (2009) in a CSTR. It was found that initial feed sulphate concentrations of 2.5, 5.0 and 10.0 g/ℓ (at a fixed molar ratio to lactate) resulted in a mixture of lactate oxidation and lactate fermentation. However, only incomplete oxidation of lactate was seen at an initial feed sulphate concentration of 1 g/ℓ. This was attributed to the lower $K_s$ of SRB than fermentative microorganisms for lactate leading to a higher effective specific growth rate. This study also found the greatest diversity of SRB to occur at longer HRT and low substrate concentrations. Similar observations of the performance of lactate-supplemented CSTR were made by White and Gadd (1996) who noted

the highest observed volumetric sulphate reduction rates occurred when lactate concentrations were supplied below 40 mM (3.6 g/ℓ lactate).

Lactate is a common electron donor used to supplement BSR reactor systems due to the favourable lactate oxidation kinetics by SRB. Although a wide spectrum of SRB are able to metabolise lactate, the primary disadvantage of this electron donor for supplementation of BSR reactor systems is its relatively high cost (Hao et al., 2014) and the competition for this electron donor by fermentative microorganisms (Oyekola et al., 2009). The potential cultivation of SRB within these BSR reactors capable of oxidising lactate or acetate completely to $CO_2$ can therefore substantially reduce the amount of required lactate, reducing the associated operating costs and need for subsequent treatment to decrease its organic content.

### 2.4.2 Propionate

Propionate utilisation has been exhibited by a small number of SRB, typically using enzymes of the methylmalonyl pathway in reverse. SRB known to consume propionate as an electron donor include *Desulfobulbus propionicus* (Pagani et al., 2011), *Desulfobacterium autotrophicum* (Brysch et al., 1987) and *Desulfococcus multivorans* (Stieb and Schink, 1989). Although the kinetics of SRB growth on propionate are favourable for use in BSR reactors, the reduced diversity of SRB able to metabolise propionate often sees it overlooked as an electron donor in favour of lactate (Hao et al., 2014).

### 2.4.3 Acetate

A number of SRB are capable of sulphate reduction linked solely to acetate oxidation via a variety of pathways. In all instances, acetate must first be activated to form acetyl-CoA through the action of acetyl-CoA synthetase (EC:6.2.1.1) or the sequential action of acetate kinase (EC:2.7.2.1) and phosphate acetyltransferase (EC:2.3.1.8), the latter requiring the consumption of one molecule of ATP (Bergmeyer et al., 1963; Möller et al., 1987).

Brandis-Heep et al. (1983) demonstrated that *Desufobacter postgatei* was able to metabolise acetate using the TCA cycle. Acetate was first activated to acetyl-Coa by acetyl-CoA synthetase with coenzyme-A originating from the cleavage of succinyl-CoA to form succinate. Acetyl-CoA was then able to enter the TCA cycle through the action of citrate synthase (EC: 2.3.3.1) which catalyses the reaction between acetyl-CoA, oxaloacetate and water to form citrate and coenzyme-A.

Elferink et al. (1999) fist isolated and characterised *Desulfobacca acetoxidans* which was found to be capable of acetate oxidation via the carbon monoxide dehydrogenase pathway, also known as the acetyl-CoA pathway. This pathway was first discovered by Schauder et al. (1986) in a number

of SRB including *Desulfobacterium*, *Desulfosarcina*, *Desulfococcus*, *Desulfovibrio baarsii*, *Desulfobacterium*, and *Desulfotomaculum*. This pathway uses many enzymes common to the Wood-Ljunghdalh pathway but catalysing these reactions in reverse and not involving the TCA cycle. Using this pathway, acetyl-CoA is converted to carbon monoxide by 5-methyltetrahydrofolate corrinoid/iron-sulphur protein methyltransferase (EC:2.1.1.258) and finally to carbon dioxide by carbon-monoxide dehydrogenase (EC:1.2.7.4).

One of the earliest published studies that demonstrated simultaneous acetate consumption and carbon dioxide fixation was performed by Sorokin (1966). This study showed that when a *Desulfovibrio desulphuricans* strain was grown on acetate, hydrogen and $^{14}$carbon labelled $CO_2$, 30-50% of the cell-carbon was derived from the $^{14}$carbon labelled $CO_2$. This phenomenon was further investigated by Badziong et al. (1979) using *Desulfovibrio vulgaris* cultured on acetate, hydrogen and $CO_2$. These authors found that alanine, aspartate, glutamate and ribose phosphate were synthesised from both acetate and $CO_2$, and concluded this was facilitated through a modified TCA cycle. The now well-known modified-TCA cycle involves the conversion of acetate and $CO_2$ to pyruvate by pyruvate ferredoxin oxidoreductase (EC:1.2.7.1). The pyruvate then enters the TCA cycle through either the action of pyruvate carboxylase (EC:6.4.1.1) or the sequential action of pyruvate dikinase (EC:2.7.9.2) and phosphoenolpyruvate carboxylase (EC:4.1.1.31) to produce oxaloacetate.

SRB oxidise acetate using sulphate as the terminal electron acceptor as described by Equation 2-7. Acetate is the primary substrate for methanogenic microorganisms (Equation 2-13) and results in competition between SRB and methanogens for acetate. The growth of methanogens can, however, be completely inhibited by 2-bromoethane sulfonate (BESA; Gunsalus et al., 1978). A kinetic analysis of the growth of a mixed SRB culture supplemented with acetate as an electron donor was performed by Moosa et al. (2002) and Moosa et al. (2005). The $K_s$ of the sulphate reducing, acetate oxidising culture increased linearly from 0.027 to 0.125 g/ℓ sulphate with the increasing initial sulphate concentrations from 1.0 to 10.0 g/ℓ. However, the maximum specific growth rate ($\mu_{max}$) increased only marginally with increasing initial sulphate concentration with an average of 0.061 $h^{-1}$. The increasing $K_s$ with unaffected $\mu_{max}$ suggested competitive substrate inhibition, according to Michaelis-Menten kinetics, as was previously reported (Chen and Hashimoto, 1980).

The growth kinetics of pure cultures of *Desulfobacter postagei, Desulfuromonas acetoxidans* and *Desulfonema magnum* were studied by Flaherty (1998). Each of these SRB were determined to have a $\mu_{max}$ between 0.018 and 0.063 $h^{-1}$ in accordance with the studies conducted by Moosa et al. (2002). These SRB pure cultures were also shown to have a $K_s$ for sulphate between 0.02 and 0.045 g/ℓ. Ingvorsen et al. (1984) performed a similar kinetic experiment using a pure culture of *D.*

*postgatei* DSM2034 cultured on sulphate and acetate, and determined the $K_s$ for acetate and sulphate to be 0.00413 and 0.0192 g/ℓ, respectively. In addition, acetate consumption was observed at concentrations below 1 μM (0.059 mg/ℓ), whilst sulphate consumption halted between 0.48 and 1.92 mg/ℓ. Although the theoretical maximum doubling time of acetate oxidising SRB, presented in this literature, is long (16-56 hours), the high affinity of SRB for acetate and for sulphate allows these microorganisms to sustain growth at low substrate concentrations.

The low growth rates of acetate oxidising microorganisms and the preferential utilisation of other organic acids, such as lactate and propionate (Brand et al., 2014; Huang et al., 2012; Liamleam and Annachhatre, 2007), can make acetate difficult to remove from wastewater and BSR reactor systems. However, the high affinity of select SRB for acetate can lead to efficient conversion of this substrate with the accumulation of sufficient biomass (Harada et al., 1994). The wide availability and low cost of this substrate, as well as its potential to be sourced from waste streams such as anaerobic digestion, make acetate an attractive electron donor for the supplementation of semi-passive BSR systems.

### 2.4.4 Autotrophy

SRB are known to fix $CO_2$ via several pathways including previously mentioned modified TCA cycle. The Wood-Ljungdahl pathway is employed by a number of SRB using hydrogen as an electron donor (Ragsdale, 2008), such as *Desulfosporosinus orientis* and *Desulfobacterium autotrophicum* (Schauder et al., 1989). In contrast to a number of carbon fixation pathways, the Wood-Ljunghdahl pathway relies on the reduction of $CO_2$ to formate or carbon monoxide instead of carboxylation onto an already existing organic molecule. This carbon fixation mechanism is more kinetically favourable than carboxylation and may, therefore, offer increased growth rates and biomass yields (Cotton et al., 2018). Key enzymes in this pathway include carbon-monoxide dehydrogenase (EC: 1.2.7.4), formate dehydrogenase (EC: 1.17.1.10) and CO-methylating acetyl-CoA synthase (EC: 2.3.1.169). This pathway was first found in SRB by Jansen et al. (1984) who identified this pathway in *Desulfovibrio baarsii* grown solely on $CO_2$ and hydrogen.

The reverse or reductive TCA (rTCA) cycle is another carbon fixation pathway employed by SRB, such as *Desulfobacter hydrogenophilus* (Schauder et al., 1987). This cycle uses many enzymes of the TCA but operating in reverse. Key enzymes of the rTCA cycle are 2-oxoglutarateferrodoxin reductase (EC:1.2.7.3) which catalyses the formation of 2-oxoglutarate from succinyl-CoA and $CO_2$; and pyruvate ferredoxin oxidoreductase (EC:1.2.7.1) which catalyses the carboxylation of acetyl-CoA to form pyruvate.

### 2.4.5 Hydrogen

As previously outlined, many SRB are capable of participating in hydrogen metabolism, either through hydrogen consumption as an electron donor (Equation 2-6) or through the generation of hydrogen during fermentation (Pagani et al., 2011). Hydrogenases are categorised based on the metal co-factors in their active sites (Peters et al., 2015). NiFe hydrogenase can be both associated with hydrogen consumption and generation. Membrane-bound Group 1 NiFe hydrogenases are implicated in hydrogen uptake (Greening et al., 2016) and are commonly found in *Desulfovibrio* (Fauque et al., 1988) and *Desulfomicrobium* (Garcin et al., 1999). Two commonly found hydrogen evolving hydrogenases found in SRB are FeFe hydrogenases (Nicolet et al., 1999) and membrane-bound Group 4 NiFe hydrogenases (Morais-Silva et al., 2013; Greening et al., 2016). The ability of SRB to use hydrogen as an electron donor allows the proliferation of these microorganisms in organic carbon limited environments and show higher affinities for hydrogen than other common hydrogen consuming microorganisms including methanogens (Lovley et al., 1982; Cord-Ruwisch et al., 1988).

The use of hydrogen as an electron donor for BSR, with either acetate or $CO_2$ as the carbon source, has been successfully applied in a number of BSR reactor systems (Hao et al., 2014). The major advantage of this electron donor is the more favourable change in free energy of SRB catalysed $H_2$ oxidation compared to that of methanogens (Table 2-1, Thauer et al., 1977), the main competitor of SRB for hydrogen. This allows operating conditions to be manipulated to minimise the competition for- and wastage of this electron donor (Davidova and Stams, 1996). A second advantage of this electron donor is the minimal COD discharged in the effluent of these reactors: the residual COD can be a major issue when using organic electron donors with incomplete oxidation and particularly when using complex carbon sources (Widdel, 1988). The drawback of using hydrogen, however, is the safety requirements and the difficulty in the handling of compressed hydrogen (Esposito et al., 2006). This, therefore, sees hydrogen used primarily in active BSR processes such as the Paques Thiopaq® process (Janssen and Buisman, 1998).

### 2.4.6 Complex carbon sources

Several BSR processes have shown effective reactor performance with supplementation of complex carbon sources such as manure (Das et al., 2012), sewerage (Rose, 2013; Section 2.8.3), woodchips (Neale et al., 2018) and compost (Vasquez et al., 2016). The macromolecules of these complex carbon sources are broken down, eventually to carbon dioxide, in much the same way as for anaerobic digestion. Several separate groups of microorganisms are involved in the different stages of anaerobic digestion from the hydrolysis of the macromolecules, to the fermentation of the produced monomers, the acetogenic reactions arising from the oxidation of the produced volatile fatty acids and eventual oxidation of the produced acetate (Vanwonterghem et al., 2016).

SRB are able to partake in each of these stages (Pareek et al., 2001; Muyzer and Stams, 2008) but are predominantly associated with volatile fatty acid oxidation as described above (Kaksonen et al., 2004; Liamleam and Annachhatre, 2007; Hao et al., 2014).

## 2.5 Microbial biofilms

Microorganisms can exist in two broad physical modes: as unicellular free-floating cells (termed here as planktonic cells) or as multicellular sessile biofilms, with the latter being more commonly observed in nature (Kolter, 2010). The development of biofilms within continuous bioprocesses can be important as this allows the decoupling of the hydraulic retention time and the biomass retention time within continuous reactors. The development of microbial biofilms can be encouraged through the provision of plentiful surface area for attachment (O'Toole and Wong, 2016). In addition, microorganisms within biofilms have also been shown to perform heavy metal sorption (Konhauser et al., 1993). Microorganisms in biofilms, following adhesion to a solid surface, produce extracellular polymeric substances (EPS) constituted predominantly by high molecular weight polysaccharides, proteins, nucleic acids, and lipids (Flemming and Wingender, 2010) which provide structural integrity to the biofilm. Living within a biofilm offers several advantages including defence from antimicrobial agents within the solution (Lee et al., 2014), protection from eukaryotic grazers (Matz and Kjelleberg, 2005) and cooperation with other microorganisms within the biofilm (Burmølle et al., 2014). In reality, the microorganisms within biofilms establish complex ecological webs (Faust and Raes, 2012) where competition and antagonism are also rife (Rendueles and Ghigo, 2015). As a result, the microbial communities within biofilms are considered highly competitive and versatile (Haagensen et al., 2015; Nadell and Drescher, 2016).

## 2.6 Reactor configurations used for BSR

In this section, the reactor configurations which have been applied for the study of BSR are discussed. The section focusses largely on reactor configurations which are suitable for long-term semi-passive treatment of low-flow ARD due to their low associated energy requirements and operating and maintenance costs.

### 2.6.1 Overview of BSR reactor configurations

#### Overcoming low SRB growth rates

BSR reactor configurations, intended for implementation for the remediation of ARD, use various strategies to increase biomass retention within the reactors leading to the decoupling of the biomass and hydraulic retention times (HRT). Increased biomass retention allows greater sulphate

reduction rates to be achieved at shorter HRT, allowing large volumes of ARD to be treated in shorter time periods or in smaller reactors. This has been accomplished by: (i) increasing the internal surface area of the reactor for biofilm formation which has been used in the baffled reactor (Barber and Stuckey, 2000), the linear flow channel reactor (LFCR; Marais et al., 2020) and packed bed reactors (PBR, Janssen and Buisman, 1998); (ii) sludge granulation of SRB in up-flow anaerobic sludge bed reactors (UASB, Lettinga et al.,1980; Celis et al., 2013) and (iii) the use of semi-permeable membranes (Chuichulcherm et al., 2001) to prevent cell washout. These reactor configurations are shown below (Figure 2-7).

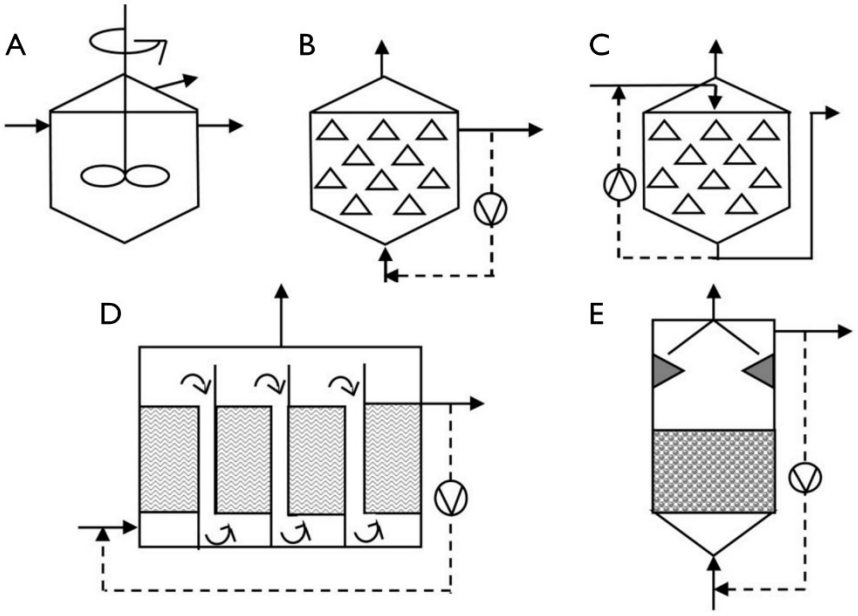


Figure 2-7 Continous bioreactor configurations used for the study of BSR for passive to semi-passive treatment of ARD effluents including (A) the continuous stirred-tank reactor, (B) the up-flow anaerobic packed bed reactor (UAPBR), (C) the down-flow anaerobic packed bed reactor (DFPBR), (D) the baffled reactor and (E) the up-flow anaerobic sludge blanket reactor (UASB). Diagrams adapted from Kaksonen and Puhakka (2007).

The exhibited performance, chosen operating conditions and the SRB identified in a number of BSR studies employing these and similar reactor systems are summarised in Table 2-2, below. Thorough discussion of these studies and other studies can be found within the Discussion sections of Chapters 4 to 6.

Table 2-2 Summary of the performance and the identified SRB of lab- and pilot-scale BSR reactors using various electron donors and applied HRT.

| Reactor | Electron donor | Sulphate (mg/ℓ) | HRT (h) | max VSRR (mg/ℓ.h) | Predominant SRB | Reference |
|---|---|---|---|---|---|---|
| PBR | woodchips, hay, manure etc. | 3000 | 168 | 17.0 | n.d. | Neale et al. (2018) |
| PBR | rice bran, rice husk | 310 | 25 | 2.4 | *Desulfomonile tiedjei* | Hamai et al. (2018) |
| Baffled reactor | molasses | 500 | 24 | 20.2 | n.d. | Vossoughi et al. (2003) |
| PBR | manure, mushroom compost etc. | 2500 | 24 | 41.7 | *Desulfovibrio; Desulfomicrobium; Desulfobulbus; Desulfobacter* | Vasquez et al. (2016) Vasquez et al. (2018) |
| passive | manure | 2500 | 24 | 23.1 | n.d. | Novhe et al. (2016) |
| PBR | spent mushroom compost | 3000 | 408 | 1.5 | n.d. | Dvorak et al. (1992) |
| passive | spent mushroom compost | 2600 | 321 | 7.1 | n.d. | Das et al. (2012) |
| PBR | rice bran | 325 | 8 | 28.1 | *Dechloromonas aromatica; Desulfovibrio mexicanus; Desulfatirhabdium butyrativorans* | Aoyagi et al. (2017) |
| Baffled reactor | lactate | 1000 | 48 | 18.4 | n.d. | Bayrakdar et al. (2009) |
| Baffled reactor | lactate | 2000 | 48 | 37.5 | n.d. | Bayrakdar et al. (2009) |
| LFCR | lactate | 1000 | 48 | 10.8 | *Desulfovibrio; Desulfomicrobium; Desulfocurvus* | Marais (under review) |
| LFCR | acetate | 1000 | 48 | 11.0 | *Desulfobacter; Desulfovibrio; Desulfomicrobium; Desulfocurvus* | Marais (under review) |
| DPBR | acetate | 900 | 60 | 13.0 | n.d. | Lin and Lee (2001) |
| DPBR | methanol | 900 | 60 | 72.0 | n.d. | Tsukamoto and Miller (1999) |
| Anaerobic filter reactor | acetate | 2500 | 20 | 17.1 | n.d. | El Bayoumy et al. (1999) |
| UASB | acetate | 3242 | 9.75 | 69.4 | *Desulfobacterium* sp. | Omil et al. (1997) |
| FBR | lactate | 2300 | 16 | 92.5 | *Desulfovibrio; Desulfobulbus; Desulfomaculum; Desufitobacteriumn* | Kaksonen (2004) |
| FBR | ethanol | 2300 | 16 | 96.7 | *Desulfovibrio; Desulfobulbus; Desulfomaculum; Desufitobacteriumn* | Kaksonen (2004) |
| UAPBR | lactate | 900 | 6.5 | 15.0 | *Desulfovibrio desulfuricans* | Chen et al. (1993) |

Table 2-2 continued

| Reactor | Electron donor | Sulphate (mg/ℓ) | HRT (h) | max VSRR (mg/ℓ.h) | Predominant SRB | Reference |
|---|---|---|---|---|---|---|
| UAPBR | lactate | 1500 | 22 | 31.0 | n.d. | Elliott et al. (1998) |
| UAPBR | lactate | 1000 | 4.6 | 200.0 | n.d. | Baskaran et al. (2005) |
| CSTR | lactate | 1217 | 48 | 17.1 | n.d. | White and Gadd (1996) |
| CSTR | lactate | 1000 | 14.6 | 38.2 | *Desulfobulbus propionicus*, *Desulfobacter postgatei*, *Desulfovibrio gigas*, *Desulfosarcina variabilis* | Oyekola (2008) |
| CSTR | acetate | 1000 | 90 | 6.9 | n.d. | Moosa (2000) |
| CSTR | acetate | 2500 | 60 | 33 | *Desulfonema; Desulfobulbus* | Moosa (2000); Icgen et al. (2007) |

n.d. – not determined

**The effective handling and the uses of the sulphide produced during BSR**

The sulphide which is produced during BSR can be used to precipitate metals in the incoming ARD stream. BSR and metal precipitation can be performed using a single reactor unit which reduces the initial capital costs but faces difficulties in recovering the metal-sulphides and can result in heavy metal toxicity to SRB (Hao, 2000). Two-stage processes recycle sulphide generated in the BSR reactor to a primary reactor where metals in the ARD are precipitated before the solution enters the BSR reactor (Haas, 1993). When sulphide is not removed through precipitation with heavy metals the sulphide must be removed via an alternate method before being discharged. Sulphur oxidising bacteria (SOB) have been used in both active (Janssen and Buisman, 1998). and semi-passive BSR processes (Marais et al., 2020) to oxidise the produced sulphide, generating elemental sulphur as a value-added product and an effluent stream which can be safely discharged into the environment.

### 2.6.2 Continuous stirred tank reactors

CSTRs have been used to study BSR as, at steady state, constant reactor conditions can be generated at which the rate constant and performance associated with these conditions can be easily and reliably determined (Levenspiel, 1990; Moosa et al., 2002; Oyekola et al., 2009). However, these systems are typically not used in practice for the implementation of BSR due to the low biomass concentrations supported, the constraint of hydraulic residence time by the growth rate of the microorganism required and the potential for washout of active biomass (Speece, 1983; Lens et al., 2003). The continuous stirred tank reactor (CSTR) represents an ideal well-mixed reactor with its contents distributed uniformly through its bulk liquid with mixing provided by an internal impeller. As the inlet stream enters the reactor, it instantaneously becomes evenly distributed throughout the reactor (Levenspiel, 1999). The reactor provides minimal surface area for microbial attachment and therefore supports a primarily planktonic microbial culture, making the microbial culture easy to quantify and monitor. The rate of reaction ($r_s$) is derived from a substrate mass balance (Equation 2-14). The rate equation (Equation 2-15) finds the consumption of substrate ($S$) within a CSTR to be dependent on the inlet substrate concentration ($S_0$), the volume of the reactor ($V$) and the volumetric flow rate ($F$), assuming no accumulation taking place (Levenspiel, 1999):

$$V\frac{dS}{dt} = F\,.S_0 - F.S - r_s.V$$

Equation 2-1

At steady state where $V\frac{dS}{dt} = 0$

$$-r_s = \frac{F}{V}.(S_0 - S)$$

Equation 2-25

A cell mass balance across a CSTR finds the concentration of biomass within a CSTR (Equation 2- 16), at steady state, to be a function of the biomass yield coefficient ($Y_{X/S}$), the concentration of the limiting substrate in the feed ($S_0$), the applied dilution rate ($D$), the saturation constant of that microorganism(s) for said substrate ($K_S$) and the maximum growth rate of the microorganism(s) ($\mu_{max}$; Pirt, 1965). This assumes no cell maintenance, cell death or product formation.

$$C_X = Y\,{}^{X}/_{S} \cdot \left( S_0 - \frac{D \cdot K_S}{\mu\, max - D} \right)$$

Equation 2-36

### 2.6.3 Packed bed reactors

The ideal packed bed reactor (PBR) behaves as a steady-state plug flow reactor (PFR) whereby the flow of fluid through the reactor travels parallel to the axis of the reactor with no mixing along the flow path (Levenspiel, 1999). These reactors can be operated as down-flow (Zaluski et al., 1999) or up-flow anaerobic PBRs (UAPBR; Maree and Strydom, 1985). Various solid support structures have been used as packing materials within these reactors, including glass beads (Baskaran and Nemati, 2006), sand (Elliott et al., 1998) and polyurethane beads (Dev et al., 2016), to support biomass retention.

The rate of the reaction in this and other PFRs is dependent on the concentration of the available substrate ($S$) at each point in the reactor. The differential mass balance with regards to reactor volume ($V$) is given in Equation 2-17. The flow rate ($F$) and inlet substrate concentration ($S_0$) remain constant; however, the reaction rate ($r_s$) and conversion of the substrate ($X_s$) vary along the length of the reactor (Levenspiel, 1999).

$$F\,.\,dXs = (-r_s).dV$$

Equation 2-47

The rate of the reaction will, therefore, decrease along the length of the reactor as the substrate(s) are consumed and product(s) accumulate, assuming a reaction order above zero for sulphate reduction. The integration of Equation 2-17 results in an expression which describes the reaction rate over the entire reactor (Equation 2-18).

$$\int_0^V \frac{dV}{F} = \int_0^{Xs} \frac{dXs}{-r_s}$$

Equation 2-58

### 2.6.4 Upflow Anaerobic Sludge Blanket Reactor

Upflow anaerobic sludge blanket (UASB) reactor hydrodynamics are governed by plug flow moving through settled SRB granular sludge. No solid support structures are incorporated into UASBs and therefore these reactors rely entirely on granulation of the microbial biomass. While this has been successfully performed in several BSR studies (Dries et al., 1998; Omil et al., 1998; Li et al., 2014) it is well recognised that SRB granules are difficult to develop and maintain (Steed et al., 2000; Bertolino et al., 2012).

### 2.6.5 Baffled reactor

The baffled reactor was developed by Bachmann et al. (1985) and is an adaptation of the UASB reactor whereby wastewater is sequentially forced over and under a series of baffles throughout the reactor in the vertical orientation or around baffled in the horizontal design. This reactor configuration boasts a number of advantages over conventional reactor configurations including observed system robustness (Barber and Stuckey, 2000) in response to changes in HRT and sulphate loading rates owing to the zoning of the reactor, long sludge retention times (Speece, 1996) and minimal start-up and operating costs (Vossoughi et al., 2003).

### 2.6.6 Linear flow channel reactor

The linear flow channel reactor (LFCR) was first developed by Molwantwa and Rose (2013) to address the need for ARD remediation strategy which could be operated long-term with minimal operating costs. van Hille et al. (2011) further developed this reactor to perform sulphate reduction and sulphide oxidation simultaneously within a single reactor unit. Sulphide oxidation at the air-liquid interface of this reactor produces the ideal conditions for the formation of a floating sulphur biofilm which allowed anaerobic conditions to be maintained in the reactor for sulphate reduction. The elemental sulphur can be harvested and used for a variety of applications, including soil amelioration (Marais et al., 2020). Complete mixing within this reactor at the small scale, well within a single hydraulic residence time, is achieved passively thereby transporting sulphide generated by SRB in the bulk liquid to the surface where it is partially oxidised by sulphide oxidising bacteria (SOB) (Marais et al., 2017; Marais et al., 2020). Harrison et al. (2014) and van Hille et al. (2016) further improved the reactor configuration by incorporating carbon microfibres anchored to a stainless steel frame which spans the length of the reactor. This increased the internal surface

area for biofilm formation, allowing for the decoupling of the hydraulic and biomass retention times.

## 2.7 Implemented BSR technologies

In this section, some of the most pertinent applications of BSR for the bioremediation of ARD at both full-scale and pilot-scale are discussed.

### 2.7.1 Reducing and alkalinity producing systems

Reducing and alkalinity producing systems (RAPS; Watzlaf et al., 2000), also known as vertical flow wetlands, are a widely implemented passive BSR technology. Within these systems acidic mine water is collected in ponds with a limestone base, on top of which lies an organic layer. In this organic layer oxygen is consumed, preventing the precipitation of iron in the limestone, and sulphate is reduced by SRB. The sulphate reduction results in partial neutralisation before the solution passes through the limestone where it is fully neutralised. This solution is then drained into an aerobic wetland where metal oxidation and precipitation takes place.

### 2.7.2 Paques Thiopaq process

The Paques Sulfateq™ treatment process (Figure 2-8) is predominantly used for the active treatment of industrial effluents containing high concentrations of sulphate and heavy metals, including ARD (Janssen and Buisman, 1998). The first stage of this process makes use of an anaerobic sulphate-reducing gas lift reactor with a mixed culture of SRB immobilised on a porous matrix. When treating high sulphate loads, hydrogen and carbon dioxide are provided as the electron donor and carbon source, respectively (Boonstra et al., 1999). At lower sulphate loading, the use of ethanol or butanol becomes more economically viable and serve as both the electron donor and carbon source. Metal sulphide precipitates are passed to a settling tank and the solids-free effluent of this reactor is fed into an aerobic gas lift reactor where the sulphide is biologically oxidised, partially, to elemental sulphur which is recovered as a value-added product.

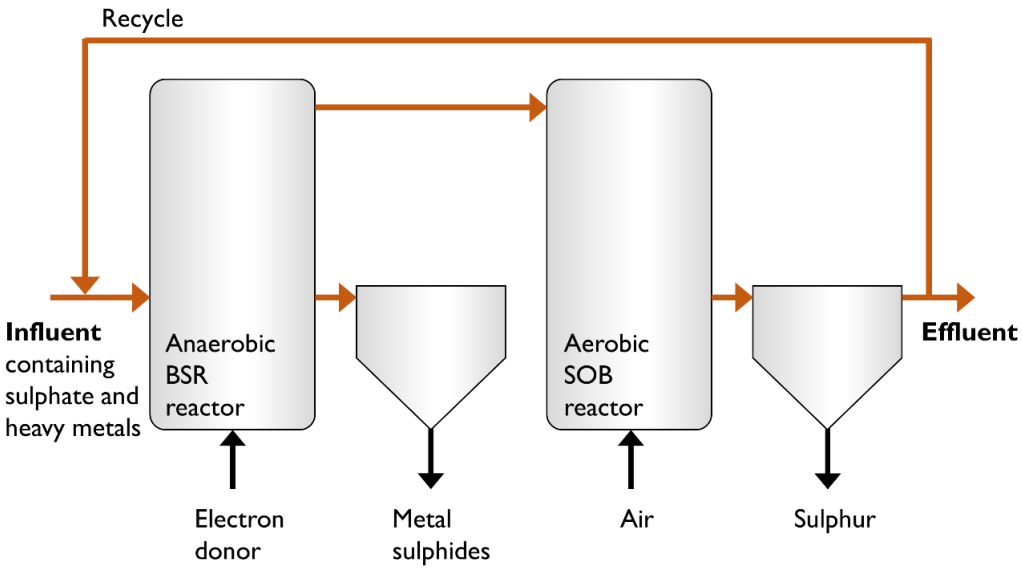


Figure 2-8 The Paques Sulfateq™ process used for the bioremediation of sulphate- and heavy metal-containing wastewater. This process uses two gas lift reactors, the first performs BSR with SRB immobilised on an inert packing and using hydrogen or other organic compounds as electron donors. The second gas lift reactor is used to partially oxidise the produced sulphide to form elemental sulphur which is recovered as a value-added product (adapted from http://en.paques.nl/products/other/sulfateq).

### 2.7.3 The Biosulphide process

The Biosulphide process is a profitable commercial operation which is not aimed at removing sulphate from ARD, but was instead developed for the recovery of metals from mine drainage as (Ashe et al., 2008). Within this process sulphide is generated through the activity of sulphur-reducing bacteria in an anaerobic reactor supplemented with sulphur and, typically, acetic acid as the electron donor. The generated sulphide is passed through the metal solution in a seprate reactor and the metal sulphide precipitates are subsequently recovered by clarification and filtration.

### 2.7.4 Mintek-Anglo American BSR process

The Mintek-Anglo American BSR pilot plant (Neale et al., 2018) was installed to treat ARD in a tailings dam on a coal mine in Mpumalanga, South Africa. This process makes use of three down-flow packed bed reactors (DFPBRs) in series using woodchips, hay, manure and other complex carbon sources as packing and electron donor. This reactor system was able to reduce sulphate concentrations from approximately 3 g/ℓ to less than 500 mg/ℓ during continuous operation at long hydraulic residence times (7 days). Prior to this, several factors led to unstable and poor performance including reduced ambient temperatures, lack of control of the influent pH and the need to optimise the replenishment of the complex carbon sources. Similar challenges are frequently reported in the literature (Section 2.2.4).

### 2.7.5 The BioSURE process

The BioSURE process, developed at Rhodes University in South Africa in the 1990s and piloted at the Grootvlei mine (East Rand, South Africa) to treat 10 Mℓ/day around 2005 (Holtzhausen, 2005), utilises primary sewage sludge (PSS) as the electron donor for sulphate reduction to remediate ARD (Rose, 2013). The process, making use of a novel Up-flow Recycling Sludge Bed Reactor, is able to reduce the sulphate concentration to below 100 mg/ℓ at an HRT as short as 12 hours. The process has also shown to be highly effective at removing the metals in the ARD through precipitation with the produced sulphide in a second reactor unit. The main vulnerability of this process identified by Rose (2013) was the potential for the production of toxic sulphide in the effluent at levels which could become hazardous.

## 2.8 Metagenomics

### 2.8.1 Introduction

Many bioremediation strategies employ mixed microbial communities whose activity and microbial composition have not been fully understood during initial operation. These processes were typically developed and refined based on iterative modifications and observation, while the microbial communities were viewed as a 'black-box'. These mixed microbial cultures typically prove to be more effective than pure cultures, likely due to the expanded metabolic capabilities across multiple microorganisms and the synergism between these microorganisms (Hays et al., 2015). Ideally, ensuring the robustness of mixed microbial processes requires an understanding of both the effect of environmental pressures and perturbations on the inhabiting microbial communities within these systems (Shade et al., 2012) and on their performance.

Initial microbial ecology studies relied on traditional culture-based methods but were limited by the fact that the huge majority of microorganisms in a given habitat cannot be cultured *in vitro* (Amann et al., 1995). The first metagenomic based studies involved PCR amplification from metagenomic DNA and cloning followed by functional screening (Schrenk et al., 1998). Metagenomics has since been defined as the direct genetic analysis of the total metagenomic DNA representing all microorganisms in a given environmental sample (Thomas et al., 2012). This approach allowed an initial shift from culture-based methods to molecular techniques generally targeting the 16S ribosomal RNA (rRNA) gene as a phylogenetic marker gene using clone libraries, terminal restriction fragment length polymorphism (T-RFLP), denaturing gradient gel electrophoresis (DGGE), and quantitative real-time PCR (Nocker et al., 2007; Kim et al., 2013)

The phylogenetic diversity of SRB meant that 16S rRNA sequencing was not always a suitable approach for the evaluation of SRB diversity in environmental samples and, therefore, the techniques mentioned above were often applied to genes, including *dsrAB*, specifically involved in sulphate reduction (Wagner et al., 1998; Klein et al., 2001; Zverlov et al., 2005) and *apr* (Meyer and Kuever, 2007). Although not classically defined under 'metagenomics', the use of fluorescence *in situ* hybridisation (FISH; Amann et al., 1990) has played a valuable role in the detection and quantification of SRB in environmental (Stubner, 2004; Foti et al., 2007) and BSR reactor systems (Icgen and Harrison, 2006).

The advent of next-generation DNA sequencing (NGS) enabled the development of high-throughput gene amplicon sequencing (Section 2.7.2) for the comprehensive evaluation of complex microbial communities (Caporaso et al., 2010; Caporaso et al., 2012). Further advances in DNA sequencing and bioinformatic analyses facilitated the direct random shotgun sequencing of environmental DNA and reconstruction of the individual genomes from these high-resolution metagenomic datasets (Tyson et al., 2004; Kim et al., 2012; Sharon et al., 2013; Kantor et al., 2015). This allowed for the phylogenetic composition to be analysed without PCR bias and/or influence of variation in copy number of the phylogenetic marker genes (Louca et al., 2018) introduced during gene amplicon sequencing. Furthermore, the metagenomic approach allows an unprecedented understanding of the metabolisms and roles of individual microorganisms in highly complex microbial communities (Hug and Co, 2018).

In discussing the key NGS techniques in more detail below, their role within a suite of tests for the detailed study of mixed microbial systems and their performance are highlighted.

### 2.8.2 Gene amplicon sequencing

Gene amplicon sequencing involves the next-generation sequencing of a PCR amplified gene of interest and is most commonly used to sequence a fragment the 16S rRNA gene in mixed microbial samples (Caporaso et al., 2012). This allows for the phylogeny and abundance of all microorganisms in complex microbial communities to be resolved. The generated short-read sequences of the sequenced marker genes are processed, clustered into OTUs, the taxonomy of OTUs assigned and further analysed using one of several available bioinformatic tools including Mothur (Schloss et al., 2009), QIIME (Caporaso et al., 2010), and DADA (Callahan et al., 2016) as shown in Figure 2-9. The major drawback of 16S rRNA gene amplicon sequencing, and all quantitative analyses based on the 16S rRNA gene, apart from extraction and PCR bias, is that this gene occurs in varying copy numbers within and between microbial phyla (Acinas et al., 2004; Baldrian, 2013; Louca et al., 2018). This can lead to a distortion in the determined relative abundance of microorganisms with 16S rRNA gene copy numbers below or above the average copy number in a community.

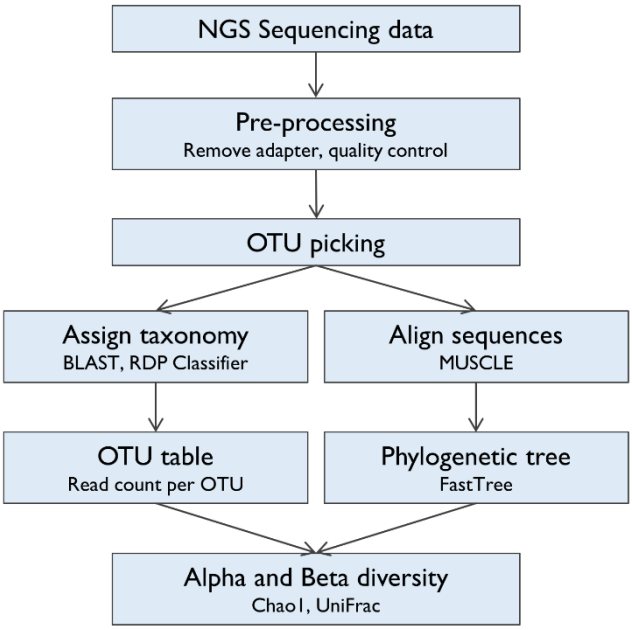


Figure 2-9 Overview of the steps performed during the processing of gene amplicon Next-generation sequencing data, from pre-processing to analysis. Adapted from Caporaso et al. (2010).

### 2.8.3 Genome-resolved metagenomics

Amplicon sequencing has been employed successfully to thoroughly characterise the microbial communities in a number of areas in microbiology (Turnbaugh et al., 2007; Shin et al., 2016). However, the 16S rRNA gene and other phylogenetic marker genes offer limited information about the roles of microorganisms within a community, particularly when considering that even closely related microorganisms can have distinctive metabolic traits (Kantor, 2016). An alternative strategy into understanding the roles of microorganisms in complex microbial communities is to employ genome-resolved metagenomics.

This approach comprises of four mains steps (Figure 2-10): (i) shotgun sequencing of metagenomic DNA; (ii) assembly of the generated reads into larger contiguous fragments, 'contigs',; (iii) the open reading frames and genes on these contigs are predicted and annotated; and (iv) the annotated contigs are 'binned' into collections of contigs representing original individual organisms. Total metagenomic DNA can be shotgun sequenced using several NGS platform to produce millions of short paired-end sequencing reads, representing all DNA within a sample. These are assembled into contigs and complete genome sequences (Luo et al., 2012). The most applicable NGS platform include nanopore sequencing (Branton et al., 2010), Pacific Biosciences' Single Molecule Real-Time Sequencing (SMRT; Flusberg et al., 2010) and Roche 454 (Luo et al., 2012), but the most widely applied NGS platform for microbial metagenomics is the short-read sequencing-by-synthesis (SBS) offered by Illumina due to its low-cost and high accuracy.

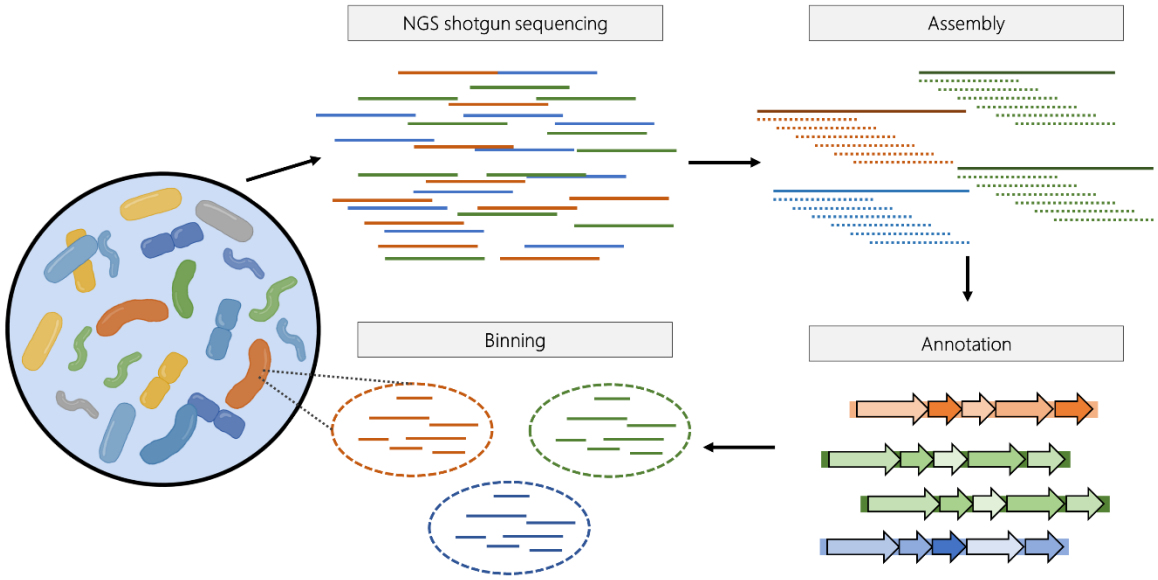


Figure 2-10 Overview of the processing steps involved in the generation of annotated genome bins from metagenomic shotgun DNA sequencing datasets. Refer to Section 2.8.3 for additional detail.

### Assembly

The reads generated during NGS are assembled into longer contiguous fragments, termed 'contigs' (Thomas et al., 2012). Current assembly programmes break reads into k-mers and construct these contigs using de Bruijn graphs (Compeau et al., 2011). This approach greatly reduces assembly time compared to previously used assemblers (Scholz et al., 2012). Some of the current, best-performing metagenomic assemblers include Megahit (Li et al., 2015), IDBA (Peng et al., 2012) and MetaSpades (Nurk et al., 2017; Vollmers et al., 2017).

### Binning

Contigs are grouped into 'bins' which represent an individual genome or that of multiple closely related microorganisms (Thomas et al., 2012). Some of the best available binning tools include CONCOCT (Alneberg et al., 2014), Metabat (Kang et al., 2015) and Maxbin (Wu et al., 2016). All of these tools separate contigs into bins based on differential coverage and genome attributes such as GC-content and k-mer frequency (Sharon et al., 2013). The determined quality of the generated bins is largely based on the presence of ubiquitous and single-copy genes which are critical for the growth of most microorganisms (excluding the candidate phyla radiation and DPANN (Hug et al., 2016). This is evaluated by CheckM (Parks et al., 2015) which determines the number of missing and duplicate BSCGs and assigns each genome bin a score for completeness and contamination.

**Annotation and metabolic analysis**

The metabolic potential of each genome is assessed by first determining the open reading frames (ORFs) using Prodigal (Hyatt et al., 2010), on each contig and annotating these using USEARCH (Edgar, 2010) and HMMER against KEGG (Kanehisa and Goto, 2000), UniRef100 and Uniprot (Consortium, 2009) databases.

### 2.8.4 Applications of metagenomics in bioremediation

Investigations into the microbial communities whose metabolic activity facilitate many water treatments processes have been ongoing for some time. The goals of these studies have remained similar over the years but the techniques which are used have advanced considerably.

The microbial communities of several BSR reactors fed with various electron donors were evaluated by Dar et al. (2007) using the PCR amplification of 16S rRNA and *dsrAB* genes, and subsequent DGGE and clone libraries. This study was able to conclude that the SRB which became dominant in these reactors, originating from the same inoculum, were selected for by the supplied electron donors, with *Desulfobulbus*, *Desulfovibrio* and *Desulfobacca* species appearing in ethanol-fed reactors and *Desulfosarcina* and *Desulfoarculus* species occurring in reactors fed a mixture of organic compounds. The same approach was employed by these authors (Dar et al., 2008) to monitor the competition between SRB, fermentative microorganisms and methanogens in lactate-supplemented bioreactors. Burns et al. (2012) used a similar method to characterise the microbial communities before, during and after entering a passive BSR reactor treating coal ARD. A single SRB could be identified, a *Desulfobacca* species, and led the authors to suggest that the bioreactor be modified in order to stimulate the growth of additional SRB.

The use of NGS became more well-spread and facilitated the shift from molecular techniques to high-throughput DNA sequencing for the rapid and high-resolution evaluation of multiple microbial communities simultaneously. Illumina amplicon sequencing was employed by Shu et al. (2015) to gain insight into the effect of various VFAs on the microbial communities and functional potential within Anammox bioreactors using 16S rRNA, anammox (*hzsB*) and nitrate reductase (*napA*, *narG*, *nirK*, *nirS*, *nosZ) genes*.

A similar approach has recently been applied in several BSR reactor studies. Marais (under review) used 16S rRNA gene amplicon sequencing to assess the microbial communities of several LFCR operated under a range of operating conditions. This study found the microbial communities, and the SRB which were present, to be strongly influenced by the supplied electron donor, the feed sulphate concentration and the differences in the conditions experienced by cells in biofilms and free-floating cells in the bulk liquid. Vasquez et al. (2018) studied a passive bioreactor and sampled from throughout the height of this reactor. Although some evidence of stratification was present,

the major influencers on microbial community structure appeared to be the operated HRT and the length of time which was allowed for the communities to become stable. The predominant SRB identified in the is study were *Desulfovibrio*, *Desulfomicrobium*, *Desulfobulbus* and *Desulfobacter*.

Vanwonterghem et al. (2014) used 16S rRNA gene amplicon sequencing to definitively show that deterministic processes shape the microbial community structures within three identical anaerobic digester (AD) reactors seeded with the same inoculum. These authors then resolved the microbial community of an AD reactor using genome-resolved metagenomics and were are able to assign each of the more than one hundred recovered genomes with a putative role within the system (Vanwonterghem et al., 2016).

The seasonal effect on the microbial communities associated with a wastewater treatment plant was investigated by Roume et al. (2015) using genome-resolved metagenomics, metatranscriptomics and metaproteomics. The composition of the microbial community associated with this process varied greatly between seasons. However, genes involved in nitrification, denitrification and ammonium oxidation were highly expressed throughout, despite these genes being found in low copy number and present in relatively few microorganisms. These genes were concluded to be 'key-stone' genes for the functioning of this system, regardless of the specific make-up of the microbial community.

Kantor et al. (2015) performed a genome-resolved metagenomic analysis of a bioreactor performing thiocyanate degradation. These authors discovered a novel thiocyanate degrading gene operon in a dominant *Thiobacillus* species present in this bioreactor. Although this system was supplemented with molasses, a thorough investigation into the metabolism of this predominant thiocyanate degrader found this *Thiobacillus* could grow autotrophically and derive energy from sulphide oxidation using the *sox* gene cluster, following thiocyanate degradation.

These studies illustrate the capacity of metagenomics, using various molecular, DNA sequencing, and bioinformatic techniques to resolve complex microbial communities, understand key microorganisms from a process perspective leading to a better understanding of the fundamental mechanisms within these processes. This can, in turn, inform how these systems should be designed and operated for improved performance and system robustness.

## 2.9 Research rationale and motivation

The review of the literature discussed above revealed that many areas relating to BSR are well studied and well understood. These include the phylogenetics of SRB which was recently expanded by Anantharaman et al. (2018); the molecular mechanism of sulphate reduction which was largely

understood through biochemical experimentation and recently fully characterised (Oliveira et al., 2011; Santos et al., 2015); the metabolism of select SRB which are well documented through study in pure culture (Sorokin, 1966; Thauer et al., 1977; Schauder et al., 1986); the characterisation of SRB growth kinetics and substrate utilisation (White and Gadd, 1996; Moosa et al., 2002; Moosa et al., 2005; Oyekola et al., 2012); and establishment of several BSR processes for the remediation of various waste streams (Janssen and Buisman, 1998; Neale et al., 2018; Rose, 2013). However, the challenges faced by BSR systems, including the slow growth rates of SRB and the need for a cost-effective electron donor which can be efficiently competed for by SRB means that successful BSR systems rely on trade-offs between reactor performance and the reactor configurations, the choice and quantity of electron donor, and the applied volumetric sulphate loading rates. Therefore, the development of a sustainable semi-passive BSR process requires extensive optimisation of the operating conditions and the design of these systems. Inseparable from each of these considerations is the underlying microbial communities which catalyse this process. Furthermore, a current drawback of BSR processes is the instability of the SRB community in response to system perturbations (Zagury and Neculita, 2007), resulting in unpredictable long-term reactor performance.

Considering the longevity of ARD generation there exists a need to thoroughly investigate the BSR microbial communities of a range of differing BSR systems, operated under a range of operating conditions, to understand which microorganisms facilitate reactor functioning and community stability. The SRB communities of well-functioning BSR reactors have been investigated using a suite of molecular techniques (Dar et al., 2007; Dar et al., 2008; Burns et al., 2012) and some process operating conditions which lead to changes within the SRB community have been identified (Oyekola 2008; Marais 2020). However, due to the limited number of investigations, the link between the microbial ecology and the performance of BSR systems is still difficult to determine.

The advent of NGS, gene amplicon metagenomics and genome-resolved metagenomics has allowed unprecedented access to the microbial community dynamics, structure and metabolic potential within several mixed microbial bioprocesses including anammox bioreactors (Shu et al., 2015), wastewater treatment (Roume et al., 2015), anaerobic digestion (Vanwonterghem et al., 2014) and thiocyanate degradation (Kantor et al., 2015). The application of metagenomics in the field of BSR shows strong promise for deepening the understanding of these microbial communities. This can inform the further design and operation of these systems for improved system robustness and performance. This is essential for the development of sustainable, passive to semi-passive BSR processes which are aimed to continually remediate ARD effluents for many years to come.

## 2.10 Research scope

The goal of this study was to overlay the reactor performance of six BSR reactor systems with the microbial ecology and metabolic potential present within these systems as the hydraulic residence time of the reactors is iteratively reduced. This approach facilitates the building of an understanding of both the microbial community structure and the impact of the microbial ecology on BSR reactor performance. By understanding the microbial ecology, including the communities of SRB, competing microorganisms and syntrophic microorganisms, within the microbial communities, as a function of electron donor, residence time, location in the reactor and the associated performance of this portion of the reactor, the desirable reactor configurations and operating conditions can be better defined to favour the growth of identified key-stone microorganisms, leading to greater system performance and robustness.

The initial hypotheses surrounding reactor performance and general microbial community structure are outlined below.

### 2.10.1 Research hypotheses

**Hypothesis 1**

The SRB community within multiple BSR systems have been concluded to be influenced by the supplemented electron donor. BSR plug flow reactors exhibit an inverse gradient of products and reactants which generates a range of microbial selective pressures. Well-mixed BSR reactors have a different uniform selective pressure throughout. This will result in the development of dissimilar microbial communities throughout a "PFR" and uniform microbial communities throughout a "well-mixed" reactor when inoculated with an identical diverse microbial culture.

**Hypothesis 2**

Lactate-oxidising SRB typically have higher respective growth rates than that of acetate-oxidising SRB. Incomplete lactate oxidation by SRB and fermentative microorganisms leads to the generation of acetate. Within a lactate-supplemented well-mixed continuous reactor which supports solely planktonic cells, some acetate oxidation will occur at long HRT. However, acetate oxidation will be abolished as the HRT is reduced and acetate-oxidising SRB are washed out of the reactor The incorporation of solid support structures for the promotion of biofilm formation within well-mixed systems will enable these slower-growing acetate-oxidising SRB to become immobilised in these reactors and catalyse the oxidation of the produced acetate at HRT where acetate oxidation is abolished in solely-planktonic cell supporting system.

**Hypothesis 3**

The reduction of the hydraulic residence time and the corresponding increase of the volumetric sulphate loading rate allows higher volumetric sulphate reduction rates to be achieved in BSR reactor systems. However, the reduction of the hydraulic residence time of BSR reactor systems will result in a gradual loss of planktonic species whose doubling time is longer than the operated residence time, leading to their washout. Comparison of changes in the microbial communities and changes in the associated performance in the acetate and lactate supplemented CSTR systems will lead to the identification of SRB species with greater growth rates and identification of SRB which are responsible for the greatest sulphate conversions. These organisms will remain in the biofilm communities of the LFCR and confer these reactors with enhanced sulphate reducing performance at short residence times.

### 2.10.2 Research activities

The following research activities were devised to address the research scope of this study and test the hypotheses presented above.

**Activity 1**

Maintain several SRB stock reactors on various electron donors and ensure high sulphate reducing performance prior to the inoculation of the six continuous BSR reactors with a composite culture made from these stock reactors. Operate the continuous reactors at a long hydraulic residence time and collect performance data until steady-state is achieved. At steady-state collect thorough performance data as well as biological samples for gene amplicon and genome-resolved metagenomics.

**Activity 2**

Operate the reactors under increasingly demanding conditions by iteratively reducing the hydraulic residence time across the reactors step-wise after steady-state at each residence time is achieved. Collect performance data and biological samples to generate a time series of the changing microbial ecology across all six of the reactor systems.

**Activity 3**

Employ 16S rRNA gene amplicon sequencing to characterise the planktonic and biofilm communities within each zone of each BSR reactor and further monitor these communities at several reduced hydraulic residence times.

**Activity 4**

Characterise the microbial communities of the BSR reactors at steady-state at a four-day HRT using shotgun Illumina sequencing. Process the generated sequencing reads through bioinformatic pipelines established by Prof. Banfield's research group at the University of California Berkeley to yield and annotate the genomes of the microorganisms associated with these reactor systems.

**Activity 5**

Integrate the performance data collected from the six continuous reactors with the gene amplicon and genome-resolved metagenomics from activities 3 and 4 and ascribe specific species and communities with functional characteristics. These will be assessed for the refinement of parameters needed for the design and operation of sulphate reducing bioreactor system.

# Chapter 3 Materials and Methodology

## 3.1 Microbial culture

The SRB culture used to inoculate the bioreactors within this study was obtained from the Department of Microbiology, Biochemistry and Biotechnology, Rhodes University in 2001. The SRB stock culture was maintained in several batch reactors using Postgate B medium (0.42 g/ℓ $KH_2PO_4$, 1 g/ℓ $NH_4Cl$, 1 g/ℓ $MgSO_4.7H_2O$, 0.9 g/ℓ $Na_2SO_4$, 0.4 g/ℓ yeast extract, 0.3 g/ℓ sodium citrate, neutral pH) supplemented with several electron donors, including acetate; lactate; ethanol; a composite of lactate, ethanol and acetate; and anaerobic digestate from an anaerobic digestor fed spirulina biomass. The BSR batch reactors were further enriched by the addition of samples of anoxic river sediment and an industrial oxidation pond. These batch reactors were maintained at a sulphate concentration of 1 g/ℓ and a COD:$SO_4$ ratio of 0.7 to favour the growth of SRB.

## 3.2 Reactor medium

The bioreactors of this study were maintained on 1.0 g/ℓ (10.41 mM) sulphate Postgate B medium containing the following: 0.42 g/ℓ (2.41 mM) $KH_2PO_4$, 1 g/ℓ (18.69 mM) $NH_4Cl$, 1 g/ℓ (4.06 mM) $MgSO_4.7H_2O$, 0.3 g/ℓ (1.16 mM) sodium citrate, 0.9 g/ℓ (6.33 mM) $Na_2SO_4$, 0.4 g/ℓ yeast extract and either 0.92 g/ℓ (11.2 mM) sodium acetate or 1.5 g/ℓ (13.32 mM) sodium lactate as the supplemented electron donor. The concentrations of lactate and of acetate used in the media were independantly selected for optimal sulphate reducing performance and efficient electron donor utilisation, based on kinetic studies described in Chapter 2.

Citrate was incorporated into the medium to prevent precipitation of media components during autoclaving. The medium was not deaerated following autoclaving meaning that low concentrations of oxygen (approximately 8 mg/L/0.25 mM) were present in the media entering the reactors. This concentration of oxygen was deemed to be negligible when considering the oxidation of organic electron donors.

## 3.3 Reactor units

Three reactor configurations were used in this study, namely continuous stirred-tank reactors (CSTRs), linear flow channel reactors (LFCRs) and up-flow anaerobic packed bed reactors (UAPBRs). The CSTRs and LFCRs are well-mixed reactors whilst the UAPBRs are governed by plug flow. The CSTRs support primarily a free-floating planktonic microbial culture whilst solid support structures were incorporated into the LFCR and UAPBR in order to facilitate additional

biofilm communities in these systems. These reactor configurations are discussed in further detail below.

### 3.3.1 Continuous stirred-tank reactor

Studies were carried out in two identical glass stirred-tank reactors with a working volume of 1 ℓ (Figure 3-1). The reactors had a height of 200 mm, a diameter of 104 mm and a liquid height of 118 mm. These reactors were similar to those used by Moosa et al. (2002) and Oyekola et al. (2009) to conduct kinetic analyses of BSR. Mixing was achieved using a Heidolph overhead stirrer which powered a four-blade Rushton impeller (D/T = 0.303) and was operated at 300 rpm. Vortex formation was prevented using four vertical baffles. The lids of the reactors were modified to prevent air ingress into the reactors. Briefly, the shaft of the impellor passed through a column in the lid and was held in place by three rubber O-rings. The reactors were operated continuously by means of a variable speed peristaltic pump (Masterflex) which continuously fed reactor medium into the reactors via the inlet port. Sampling was performed using a single sampling port which extended to near the base of the reactor. Effluent was discharged by gravity from the reactor via an overflow port. Heated water was passed through external glass jackets, by a circulating water bath, to maintain a constant temperature of 30°C in the reactor.

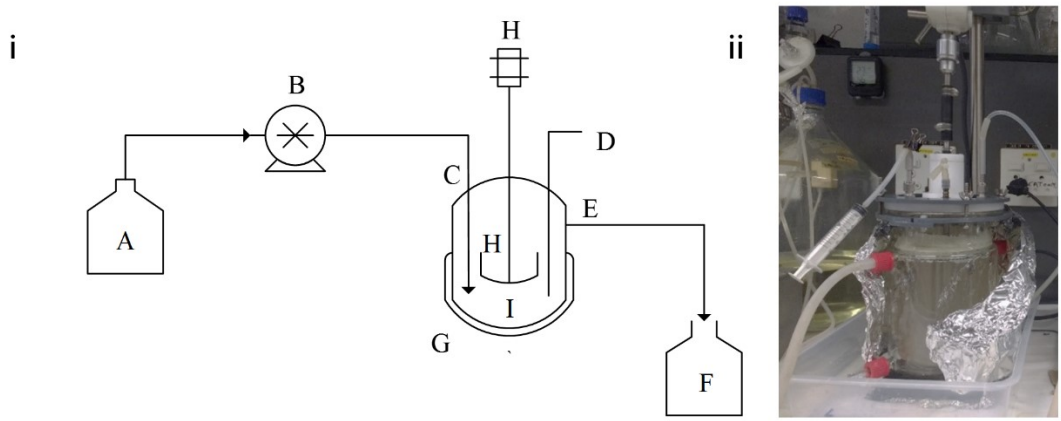


Figure 3-1 Schematic diagram (i) and photograph (ii) of a 1ℓ Continuous stirred-tank reactor operated in this study. A: feed reservoir; B: pump; C: feed inlet; D: sampling port; E: effluent port; F: effluent collection; G: glass heating jacket; H: Rushton impellers; I: CSTR

### 3.3.2 Linear flow channel reactor

The 2.4 ℓ Linear flow channel reactors (LFCRs) used in this study (Figure 3-2, Figure 3-3,) were constructed from 12 mm thick Perspex. The reactor had external dimensions of length: 275 mm, width: 123 mm and height of 112 mm. The reactor had an internal length of 247 mm, width of 100 mm and height, from base to inlet and effluent ports, of 100 mm. The reactor had a working volume of 2.4 ℓ and a headspace of 1.25 ℓ. A silicone gasket was placed between the top of the reactor and the Perspex lid which were securely bolted to the reactors to prevent the ingress of oxygen and loss of volatile sulphide from the reactor. Heated water was pumped through internal stainless-steel heating coils using a circulating water bath to maintain the temperature within the reactor at 30°C. Carbon microfibres were incorporated into the LFCR to increase the internal surface area for the formation of biofilms within the reactor. These carbon microfibres were anchored to- and extended above and below three stainless-steel metal frames which spanned the length of the reactor from the inlet to the effluent port as shown in Figure 3-2 and Figure 3-3 The LFCR is demarcated into two zones of equal volume, the inlet and effluent zone, as shown in (Figure 3-2). The inlet-zone encompassed the full height and width of the reactor but extends from the inlet port to the middle of the length of the reactor. The effluent zone extended from the middle of the length of the reactor to the effluent port. Sampling was performed on these two reactor-zones independently.

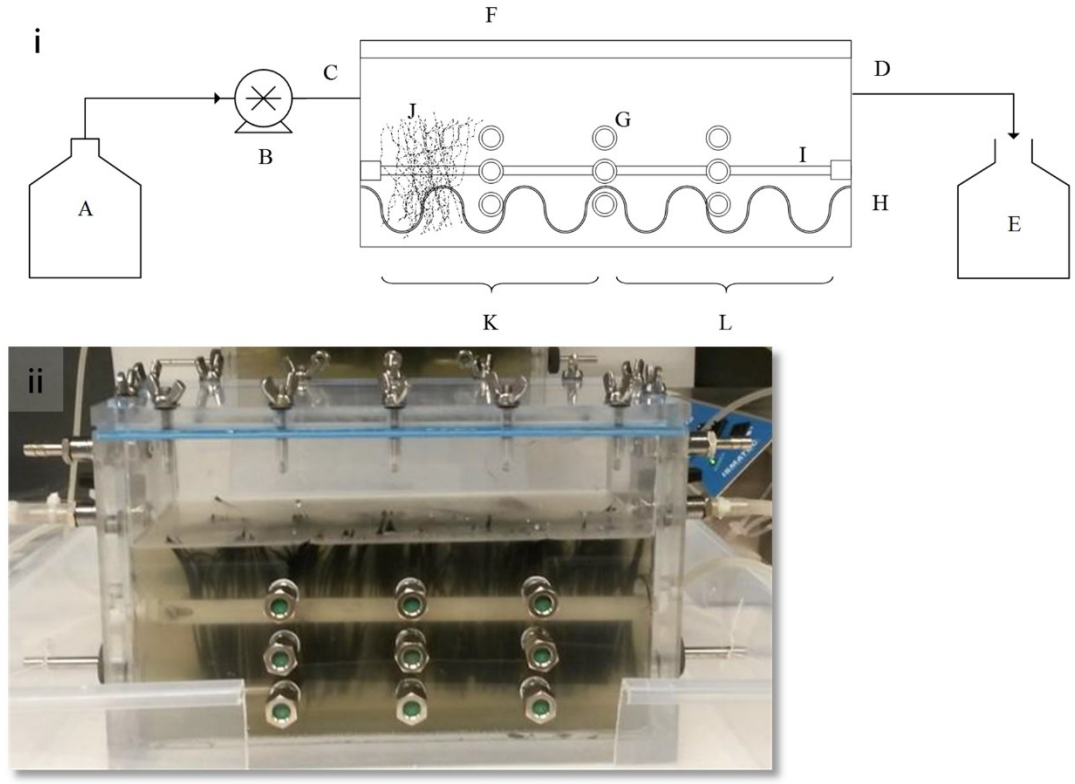


Figure 3-2 Schematic diagram (i) and photograph (ii) of a Linear flow channel reactor (LFCR) operated in this study. The reactor had a working volume of 2.4 ℓ and a headspace of 1.25 ℓ. A: feed reservoir; B: pump; C: feed inlet; D: effluent port; E: effluent collection; G: sampling port; H: internal heating coil; I: carbon fibre support scaffold; J: carbon microfibres which extend across the reactor, anchored to the carbon fibre support scaffold, K: inlet zone; L: effluent zone

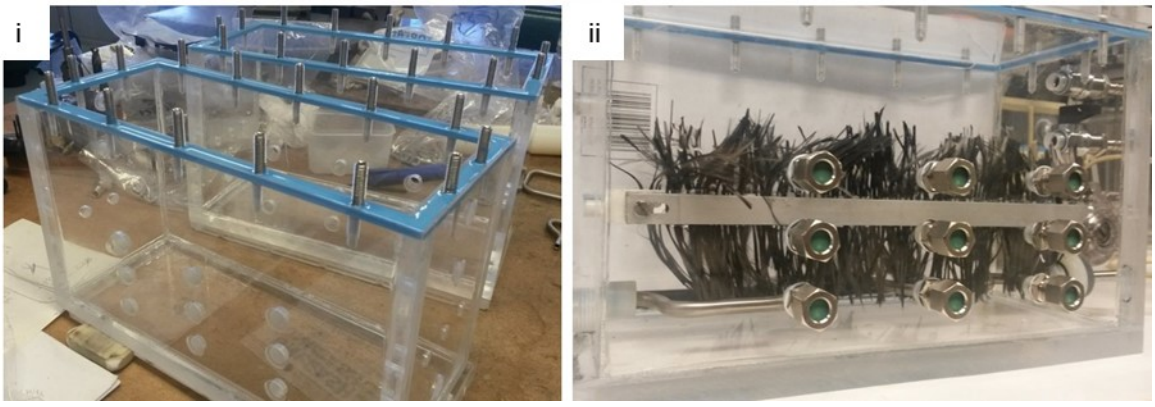


Figure 3-3 Photographs of the Perspex LFCR (A) during assembly and (B) after carbon microfibres had been fitted within the reactor, prior to inoculation.

The LFCR has been demonstrated to achieve complete mixing within one hydraulic residence time by Marais et al. (2020) and this study (Appendix A.2).

### 3.3.3 Up-flow anaerobic packed bed reactor

Two glass Up-flow anaerobic packed bed reactor (UAPBRs) were operated in this study as shown in Figure 3-4. These reactors were held vertical and bolted to a metal frame. Reactor medium (Section 3.2) was continuously pumped into the reactors using a variable speed peristaltic pump via the inlet port positioned of the base of the reactors. Effluent from these reactors was discharged by gravity via effluent ports positioned near the top of the reactor. Water was pumped through external heating jackets, using a circulating water bath, to maintain a temperature of 30°C within the reactors. Sampling pipes were fitted to the base and top of the reactor which extend to the boundary between the inlet and middle zones, middle and effluent zones and just below the effluent port. These reactors were packed with open-cell polyurethane foam cubes (20 mm x 20 mm x 20 mm) to act as a biomass support matrix for the formation of microbial biofilms within the reactors. This foam occupied approximately 40 $cm^3$ (4%) of the internal 1ℓ working volume.

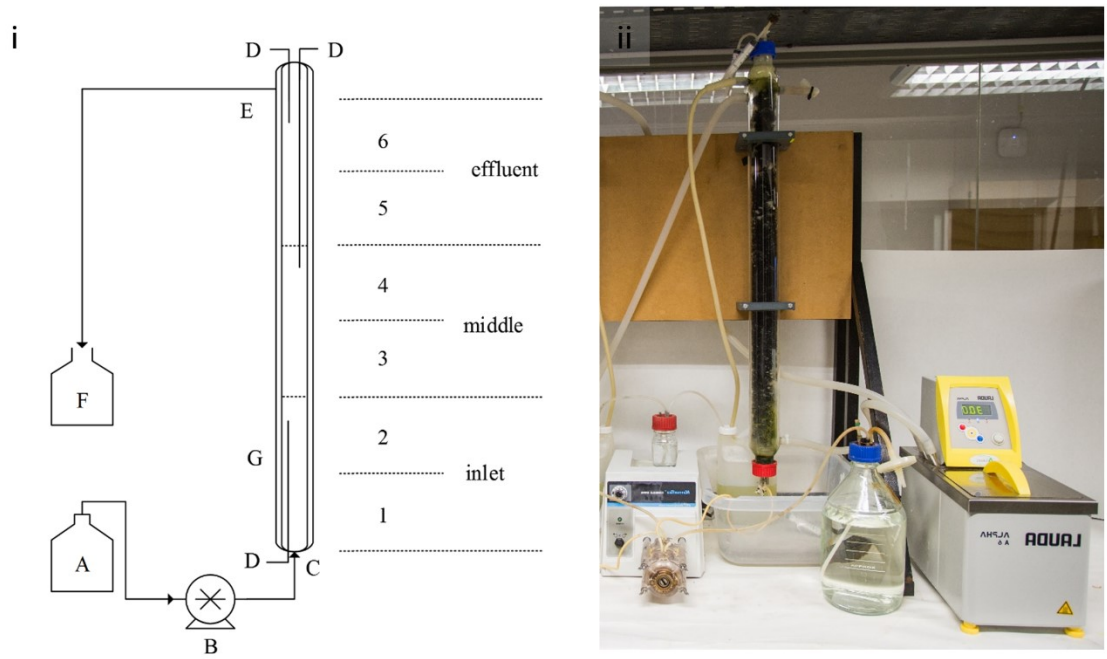


Figure 3-4 Schematic diagram (i) and photograph (ii) of a UAPBRs operated in this study. The reactors had a working volume of 1ℓ, an internal diameter of 40 mm and a height of 80 mm. The reactor was demarcated into three 0.33 ℓ sequential zones. These were demarcated as the inlet, middle and effluent zones, and these were further divided to six sequential 0.167 ℓ sub-zones that were numbered one, at the inlet, to six at the effluent. A: feed reservoir; B: peristaltic pump; C: feed inlet; D: sampling ports; E: effluent port; F: effluent reservoir; G: external heating jacket; J: inlet zone; K: middle zone; L: effluent zone.

## 3.4 Reactor operation

### 3.4.1 Reactor inoculation and start-up

The three duplicate reactor systems (Section 3.3) were filled to half of the reactor working volume with sterile Postgate B media supplemented with an appropriate electron donor (each duplicate reactor receiving either acetate or lactate, Section 3.2). SRB Inoculum, described in Section 3.1, was added to each reactor to fill them to the respective working volumes. The lids of the reactors were tightly sealed, and the headspace of each reactor was sparged with nitrogen gas for two minutes to ensure anaerobic conditions.

The six reactors were operated as batch systems for a period of seven days, with 10% (v/v) of the liquid volume being replaced with fresh, sterile reactor medium supplemented with the appropriate electron donor (Section 3.2) every 48 hours. The reactors were sampled regularly and assayed for sulphate, sulphide and VFA concentrations, pH and redox as described in Section 3.5.

### 3.4.2 Continuous reactor operation

The reactors were changed to continuous operation after being operated as batch reactors for seven days. Sterilised reactor medium, supplemented with either acetate or lactate as the electron donor, was continuously supplied to the respective reactor via a peristaltic pump. The CSTRs (Section 3.3.1) were initially operated at a five-day HRT (0.008 $h^{-1}$) and the LFCR (Section 3.3.2) and UAPBR (Section 3.3.3) at a four-day HRT (0.010 $h^{-1}$). The sulphate reducing performance of the CSTRs was expected to be abolished at longer HRT compared to the LFCR and UAPBRs based on the susceptibility of these systems to cell washout at short HRT. Therefore, the CSTRs were operated initially at five-day HRT prior to the reduction in the HRT to four-days to increase the number of steady-state performance points. The methanogenic inhibitor BESA (sodium 2-bromoethanesulfonate; Sigma Aldrich) was added to the six continuous reactors after 30 days of continuous operation to a final concentration of 10 mM within the LFCRs and CSTRs and 20 mM to the UAPBRs. This was done to reduce the competition for acetate between SRB and any potential methanogens present in the inoculum.

Each reactor zone of each reactor was sampled at least once per hydraulic residence time during monitoring and three times per HRT during defined steady-state periods. Sampling was performed by drawing 7 mℓ of bulk liquid via the respective sampling ports using a 10 mℓ syringe. Standard assays involved sulphate, sulphide and VFA analysis (Section 3.5) using 2 mℓ of solution drawn from

the reactors, whilst 5 mℓ of solution was used for pH and redox potential measurements (Section 3.5).

As the CSTRs are well-mixed, only a single representative sample was taken from each of these reactors. The LFCR, although relatively well-mixed, were sampled from the inlet and effluent zone via sampling ports positioned at the far-left and far-right of the reactor, in the middle row (Figure 3-2). In addition, approximately 10 mℓ of solution was collected from the effluent of this reactor. This solution was assayed as described above but no sulphide measurements were taken as the solution was exposed to the atmosphere for extended periods of time making sulphide analysis variable and not representative of the sulphide leaving the reactor. Solution leaving the UAPBRs' inlet, middle and effluent zones were sampled via sampling ports connected to sampling pipes which extend to the relevant zone as shown in Figure 3-4.

Upon reaching steady-state conditions within each zone of a reactor, the performance of each reactor zone was monitored closely and steady-state sampling was performed (Section 3.4.3) before the hydraulic residence applied to the system was reduced. This was performed iteratively as described in Table 3-1. When results from this study are reported, the HRT at which data was collected will be stated and the corresponding dilution rate, applied over the entire reactor, will be shown in parentheses.

Table 3-1 The hydraulic residence times (HRT) and corresponding applied dilution rates at which the steady-state performance of the acetate- and lactate-supplemented CSTR, LFCR and UAPBR were evaluated during the course of this study. The performance of the CSTRs was evaluated at two additional HRT, compared to the LFCR and UAPBR, due to these reactors rapidly reaching steady state following a change in the HRT.

| HRT (days) | dilution rate ($h^{-1}$) | CSTR | LFCR | UAPBR |
|---|---|---|---|---|
| 5 | 0.0083 | • | | |
| 4 | 0.0104 | • | • | • |
| 3 | 0.0139 | • | • | • |
| 2.6 | 0.0157 | • | • | • |
| 2.3 | 0.0179 | • | • | • |
| 2 | 0.0208 | • | • | • |
| 1.75 | 0.0238 | • | | |
| 1.5 | 0.0278 | • | • | • |
| 1.3 | 0.0321 | • | • | • |
| 1 | 0.0417 | • | • | • |

### 3.4.3 Steady-state sampling

Steady-state conditions were defined as consistent residual sulphate concentrations in each reactor zone, for a minimum of three HRT, with less than 10% variation in the observed sulphate concentration. In addition, the gradient of a fitted linear trendline across the steady-state residual sulphate concentrations, against time in days, fell within -2.0 to 2.0 mg $SO_4$/ℓ.day.

In addition to standard sampling analyses for sulphate, sulphide, VFA, pH and redox potential which were performed at least three times per hydraulic residence time during steady-state, the concentration of bicarbonate in the effluent of each reactor was also determined during defined steady-state periods (Section 3.5.5).

The biomass retention was estimated for the planktonic communities of each reactor zone at each defined steady-state using a modified detachment and direct cell counting protocol as described in Section 3.6.1 (Table 3-2). Total metagenomic DNA from the planktonic communities was extracted from duplicate samples (Section 3.8.2).

Biofilm-attached and biofilm-associated cells were quantified at the four-day (0.010 $h^{-1}$) and ultimate one-day HRT (0.042 $h^{-1}$) as described in Section 3.6.2 (Table 3-2). These biofilm communities were not quantified at HRT between a four-day and one-day HRT due to the potential impact, of exposing these systems to oxygen, on reactor performance. Total metagenomic DNA was extracted and purified from representative biofilm-attached and -associated communities in parallel to biomass quantification. In addition, solid support structures were removed and visualised using scanning electron microscopy (SEM; Section 3.6.3). Representative biofilm communities were quantified and total metagenomic DNA extracted from the inlet and effluent zones of the LFCRs. Whereas, biofilm communities were quantified and total metagenomic DNA extracted and purified from zones 1 and 6 of the UAPBRs (Figure 3-4) at a four-day HRT, and from zones 1 through 6 at a one-day HRT. The biofilm communities of only two zones were sampled at a four-day HRT due to the substantial perturbation caused to the UAPBRs' microbial communities due to unpacking of the polyurethane foam from all reactor zones.

Table 3-2 The (P) planktonic and (B) biofilm-associated and -attached communities, from the CSTR, LFCR and UAPBR reactor zones, which were sampled at steady-state for biomass qunatification during the HRT study.

| Reactor | Zone | | 5 | 4 | 3 | 2.6 | 2.3 | 2 | 1.75 | 1.5 | 1.3 | 1 | HRT (days) |
|---|---|---|---|---|---|---|---|---|---|---|---|---|---|
| | | | 0.008 | 0.010 | 0.014 | 0.016 | 0.018 | 0.021 | 0.024 | 0.003 | 0.032 | 0.042 | dilution rate ($h^{-1}$) |
| CSTR | n/a | | P | P | P | P | P | P | P | P | P | P | |
| LFCR | inlet | | | P/B | P | P | P | P | | P | P | P/B | |
| | effluent | | | P/B | P | P | P | P | | P | P | P/B | |
| UAPBR | inlet | 1 | | B | | | | | | | | B | |
| | | 2 | | P | P | P | P | P | | P | P | P/B | |
| | middle | 3 | | | | | | | | | | B | |
| | | 4 | | P | P | P | P | P | | P | P | P/B | |
| | effluent | 5 | | | | | | | | | | B | |
| | | 6 | | P/B | P | P | P | P | | P | P | P/B | |

## 3.5 Analytical methods

### 3.5.1 Sulphate

The standard turbidimetric method (Greenberg and Eaton, 1999) was used to determine residual sulphate concentrations. This assay is based on the reaction of sulphate ions with barium to form barium sulphate. The insoluble barium sulphate forms small particles of relatively uniform size. This results in an increase in the turbidity of the solution which is quantified using a spectrophotometer at a wavelength of 420 nm. Briefly, zinc chloride solution was added immediately to 2 mℓ of sample to a final concentration of 0.167% (w/v) and vortexed for five seconds. This precipitated any sulphide in solution as zinc sulphide and prevents the oxidation of any sulphide to sulphate during the assay. The solution was clarified by centrifugation at 10 000 g in a benchtop microfuge for 10 minutes. The sample was then passed through a 0.22 μm syringe filter to remove any remaining cells and/or particulate matter. The sample was then suitably diluted with deionised water to a total volume of 5 mℓ. Subsequently, 250 μℓ of conditioning reagent was added to the diluted sample and vigorously mixed using a benchtop vortex for 10 seconds. A 'micro-scoop' of barium chloride salt (Sigma Aldrich, analytical grade, 30 mesh minimum size) was added and the solution and vigorously mixed using a benchtop vortex for approximately one minute. The turbidity of the solution was determined by the absorbance of the solution at 420 nm. The concentration of sulphate was determined relative to a sulphate standard curve made using analytical grade $Na_2SO_4$ at varying concentrations (Appendix A.1.2).

### 3.5.2 Sulphide

The aqueous sulphide generated in the reactors was quantified using the colourimetric DMPD method (Cline, 1969). This assay is based on the reaction, catalysed by $Fe^{3+}$ ions, of aqueous sulphide with N,N-dimethyl-p-phenylenediamine to form methylene blue which can be quantified

spectrophotometrically. A suitable volume of sample (typically 20-50 uℓ) was added to 200 µℓ of 1% (w/v) zinc acetate to stabilise the aqueous sulphide and prevent the protonation of aqueous sulphide ($HS^-$) to gaseous sulphide ($H_2S$). Thereafter the volume was made up to 5 mℓ using deionised water. Thereafter, N,N-dimethyl-p-phenylenediamine and ferric chloride were added sequentially, to final concentrations of 0.033 and 0.133% (w/v), respectively. The sample was mixed vigorously using a bench-top vortex for 10 seconds and allowed to react for a further five minutes. Thereafter the absorbance of the samples was measured at a wavelength of 670 nm using a benchtop V-1200 VWR spectrophotometer and the concentration of sulphide determined against a sulphide standard curve (Appendix A.1.3).

### 3.5.3 pH and redox potentials

Routine pH measurements were performed using a Cyberscan 2500 micro pH meter fitted with an XS Sensor 2-Pore T DHS pH probe. The pH probe was calibrated using Accsen Instrumental standard buffering solutions (pH 4.0 and 7.0) immediately prior to use. The redox potential of reactor samples was measured using the Metrohm 827 pH lab meter fitted with a Pt-ring (Ag/AgCl reference) 3 M KCl electrode (Metrohm model 6.0451.100). Redox potentials are reported relative to standard hydrogen electrode (Eh values).

### 3.5.4 Volatile fatty acids

The concentrations of several volatile fatty acids (VFAs) were determined by high-performance liquid chromatography (HPLC) on a Waters Breeze 2 system. This system was equipped with a Bio-Rad Organic Acids ROA column and UV (210 nm wavelength) detector and operated at a flow rate of 0.6 mℓ/min using a mobile phase of 10 mM $H_2SO_4$. The concentrations of acetate, lactate, propionate, butyrate, citrate and valerate were determined against a standard curve of these VFAs at concentrations between 100 and 600 mg/ℓ. Standard solutions of each VFA were made using analytical grade reagents (Sigma).

### 3.5.5 Alkalinity

The concentration of bicarbonate alkalinity in the effluent of the reactors was assayed using the APHA standard titration method (APHA method 2320, 1975). Briefly, 20 mℓ of reactor effluent was collected and 0.1 N $H_2SO_4$ continuously added whilst monitoring the pH using a Cyberscan 2500 micro pH meter. The initial pH of the solution and five further pH measurements were collected during titration until the pH reached the endpoint pH of 3 ± 0.2. The volume of $H_2SO_4$

utilized during the titration was recorded. The Gran function (Fx, Equation 3-1) was calculated for each pH measurement using the following equation (APHA method 2320, 1975):

$$F_x = -10^{-pH_x}(V_s + V_x) \qquad \text{Equation 3-1}$$

Where $V_s$ is the volume of sample, $V_x$ is the volume of acid added and $pH_x$ is the measured pH of the solution. Linear regression is used to determine the value of $V_x$ where $F_x$ is equal to zero. This is termed the equivalence point, $V_e$. The alkalinity is then calculated using the following equation (APHA method 2320, 1975; Equation 3-2):

$$A_T = \frac{V_e C_a}{V_s} \qquad \text{Equation 3-2}$$

Where $A_T$ is the concentration of alkalinity, $V_e$ is the calculated equivalence point, $C_a$ is the concentration of acid and $V_s$ is the volume of the sample.

Expected bicarbonate concentrations were calculated based on the degree of observed electron donor utlisation and the stoichiometric equations presented in Table 2-1. This considered the pKa1 of carbonic of 6.37 and the pH within the given reactor zone.

## 3.6 Cell biomass isolation and quantification

The isolation and quantification of the distinct microbial communities associated with discrete phases each reactor system was necessary for the complete characterisation of a given reactor system. The methods described below detail the isolation of the planktonic, biofilm-associated and biofilm-attached communities from each appropriate reactor configuration. The planktonic cells were defined as free-floating microbial cells found solely within the bulk liquid of each reactor. The biofilm-associated cells were defined as those cells associated with the surface of biofilms but not directly attached and, therefore, could be removed (as described below) through gentle agitation. Biofilm-attached cells were those cells colonising the surface of the solid support structures and/or embedded in EPS anchored to these supports. Recovery of whole cells from biofilm attached communities required vigorous agitation and use of non-ionic detergent to detach biofilms from the solid support structures and to liberate cells from the EPS. The separate isolation of these communities was necessary not only for accurate quantification of the microorganisms colonising these, respective, phases but it also enables the independent microbial speciation of each of these communities (Sections 3.8 - 3.10). This was facilitated through the use of a modified cell detachment and recovery protocol. This protocol was adapted from Chiume et al. (2012) and

Govender et al. (2013) who each successfully used this approach to recover microbial cells from the surface of low-grade chalcopyrite ore. This approach has also been successfully applied by Makaula (2019). This protocol was adapted and validated for the detachment of cells from colonised carbon microfibres and polyurethane foam (Appendix A.3).

The quantified cell concentrations determined for the biofilm-attached and biofilm-associated communities of the LFCRs and UAPBRs are presented as cell concentrations given per reactor working volume. This was calculated by estimating the total amount and volume of solid support structures present in a reactor and reactor zone.

### 3.6.1 Direct microscope cell counting

Direct microscope cell counting was used to determine the concentration of microbial cells in a given solution. This included planktonic cells within a solution drawn directly from a bioreactor or solution generated during the cell detachment protocol.

Cell concentrations were quantified by direct microscope counting using a Thoma counting chamber and an Olympus BX40 phase contrast microscope using 1000x magnification. Briefly, 1.1 µℓ of an appropriately diluted sample was pipetted into the centre of the Thoma counting chamber and covered with a coverslip. The sample was viewed using oil immersion phase contrast microscopy on an Olympus BX40. Cells within 16 blocks of the Thoma counting chamber, representing one quadrant, were counted in duplicate. The concentration of cells in the original sample were calculated using Equation 3-3, below:

$$C_N = \frac{C \times \left(\frac{N_T}{N_L}\right)}{D \times A} \times \frac{1}{d} \times 10^3 \qquad \textbf{Equation 3-3}$$

where:

| | |
|---|---|
| $C_N$ | = Cell concentration (cells/mℓ) |
| C | = Number of cells counted in the large squares |
| $N_T$ | = Total number of large squares (= 16) |
| $N_L$ | = Number of large squares where cells were counted |
| D | = Depth of the chamber (0.02 µm) |
| A | = Area |
| d | = Dilution |

### 3.6.2 Recovery of whole microbial cells from solid support structures

Carbon microfibres were incorporated into the LFCRs and open-pore polyurethane foam pieces were incorporated into the UAPBRs to increase the surface area for microbial attachment and biofilm formation within these reactors. Microbial colonisation of these supports was confirmed using SEM. The modified cell detachment protocol was, therefore, validated for use to recover the biofilm-associated and -attached cells from these support structures (Appendix A.3). The following protocol was performed using colonised polyurethane foam pieces (2 $cm^3$) from the UAPBRs or carbon microfibres (approximately 2.5 cm in length) removed from the stainless-steel support structures of the LFCRs. This protocol was performed in duplicate in each instance.

Three units of support structures were removed from the respective reactor configuration. These were placed into 50 mℓ Sterilin tubes containing 30 mℓ of Postgate B media (Section 3.4) without a supplemented electron donor. The tubes containing the solid support structures were swirled by hands for five seconds. This gentle agitation was performed to remove the biofilm-associated cells from the surface of the biofilms and introduce these cells into the medium. These cells were recovered through centrifugation at 10 000 g for 10 minutes. For quantification of the biofilm-associated cells, the resulting cell pellets were resuspended in 2 mℓ of 1x PBS buffer and counted using a Thoma counting chamber (Section 3.6.1). For speciation of the biofilm-associated cells, the resulting cell pellets were resuspended in lysis buffer and DNA extraction and purification performed as described in Section 3.8.2. Purified DNA was stored at -60 °C until DNA sequencing was performed.

The biofilm-attached cells were immediately recovered from the solid support structures following the removal of the biofilm-associated cells. The solid support structures were aseptically transferred to new 50 mℓ Sterilin tubes containing 30 mℓ of Postgate B media with no supplemented electron donor but containing 0.4% (w/v) Tween® 20 detergent. The sterilin tubes were vigorously agitated for two minutes at 3200 rpm using a benchtop vortex - this represents the first Tween® 20 wash step. The solid support structures were then aseptically transferred to a new Sterilin tube containing 30 mℓ Postgate B media, without an electron donor but containing 0.4% (w/v) Tween® 20 detergent and vigorously agitated as described above. This was repeated for a total of seven Tween® 20 wash steps. Seven wash steps had been previously demonstrated to recover the majority of biofilm-attached cells from the surface of colonised carbon microfibres (Appendix A.3). The supernatant of the seven Tween® 20 wash steps was recovered, pooled and the cells recovered by centrifugation at 10 000 g for 10 minutes. The harvested biofilm-attached cells were resuspended in 2 mℓ of 1x PBS buffer and quantified by direct microscope cell counting (Section 3.6.1).

### 3.6.3 Scanning electron microscopy

The surface of colonised solid support structures from the LFCR and UPABR and uncolonized control support structures were visualised using scanning electron microscopy (SEM). Solid support structures were cut into smaller pieces using sterile stainless-steel scissors and placed in 2.5% (v/v) glutaraldehyde (Sigma) for 8 to 12 hrs at 4°C. The support structures were then rinsed in 1x PBS and subsequently with deionised water. The support structures were then dehydrated through an alcohol series of 30, 50, 70, 90, 95, 99, 100% (v/v) ethanol for ten minutes each at 4°C. The support structures were then glued to an aluminium stub using carbon tape and critical point dried using hexamethyldisilane (HMDS; Sigma). The mounted solid support structures were then sputter-coated with carbon and viewed using an FEI NOVA NANO SEM 230 at various magnifications.

## 3.7 Physiochemical and kinetic data handling

### 3.7.1 General kinetic equations

**Sulphate conversion**

The sulphate conversion achieved by a reactor or reactor zone was calculated by the general equation below:

$$Sulphate\ conversion = \frac{S_0 - S}{S_0} \times 100 \qquad \text{Equation 3-4}$$

Where $S_0$ represents the incoming sulphate concentration and $S$ represents the residual sulphate concentration leaving the respective reactor or reactor zone.

**Expected sulphide**

The expected sulphide concentration was calculated based on the observed residual sulphate concentration with respect to the initial feed sulphate concentration as shown below

$$Expected\ sulphide = \frac{S_0 - S}{3} \qquad \text{Equation 3-5}$$

Where $S_0$ and $S$ represent the feed sulphate (1 g/ℓ or 10.4 mM) and residual sulphate concentration, respectively.

**Volumetric sulphate loading rate**

The volumetric sulphate loading rate (VSLR) applied to each reactor and reactor zone was calculated based on the applied dilution rate and feed sulphate concentration as shown below:

$$VSLR = S_0 \times D \qquad \text{Equation 3-6}$$

where $S_0$ represents the concentration of sulphate in the incoming stream (1 g/ℓ or 10.4 mM for CSTR, LFCR and UAPBR inlet zones, variable for UAPBR middle and effluent zone) and $D$ represents the dilution rate (time$^{-1}$).

**Volumetric sulphate reduction rate**

The volumetric sulphate reduction rate (VSRR) was calculated, as shown below, where $S_0$ represents the concentration of sulphate in the incoming stream and $S$ represents the residual sulphate concentration leaving a reactor or reactor zone.

$$r_s = (S_0 - S)\,D \qquad \text{Equation 3-7}$$

### 3.7.2 Predicting cell biomass concentrations in a continuous stirred-tank reactor

The predicted biomass concentrations of mixed and pure SRB cultures, under various operating conditions, were estimated from kinetic constantans reported in the literature using Equation 3-8. This equation derives from a cell mass balance in a well-mixed continuous system (Pirt, 1965), assuming no cell maintenance:

$$C_X = Y_{X/S} \cdot \left(C_0 - \left(\frac{D \cdot K_S}{\mu\, max - D}\right)\right) \qquad \text{Equation 3-1}$$

The biomass concentration ($Cx$) is calculated using the biomass yield coefficient ($Y_{X/S}$), the dilution rate ($D$) applied to the system, the limiting substrate concentration ($C_0$) in the inlet stream, the saturation constant ($K_S$) for that substrate and the theoretical maximum growth rate ($\mu_{max}$) of the microorganism(s). The biomass concentration cannot be calculated when the biomass yield coefficient is not available. However, the proportionality between two or more biomass concentrations under varying substrate concentrations and dilution rates can be calculated by making the $Y_{X/S}$ term equal to one.

### 3.7.3 Modelling of UAPBR kinetic data

The sulphate reducing performance of the UAPBRs were modelled as ideal plug flow reactors

$$\frac{dX}{dV} = \frac{-rA}{F.C_0}$$

according to

Equation 3-9, where $X$ is the sulphate conversion, $V$ is the volume of the reactor, or tested reactor region, $-r_A$ is the reaction rate, $F$ is the flow rate (volume per time) and $C_0$ is the concentration of substrate entering the reactor or reactor zone.

$$\frac{dX}{dV} = \frac{-rA}{F.C_0} \qquad \text{Equation 3-9}$$

A generalised rate equation (Equation 3-10) was substituted into Equation 3-9 yielding an overall expression describing the rate of an n$^{th}$ order irreversible reaction with rate constant *k* and starting substrate concentration $C_A$, in an ideal plug flow reactor (Equation 3-11).

$$r_A = -k.{C_A}^n \qquad \text{Equation 3-10}$$

$$\frac{dX}{dV} = \frac{-k.{C_A}^n}{F.C_0} \qquad \text{Equation 3-11}$$

Equation 3-9, was rearranged to yield Equation 3-12:

$$dX = -\frac{1}{C_0} dC_A \qquad \text{Equation 3-12}$$

This was resubstituted into Equation 3-11 to give Equation 3-13:

$$\frac{-\frac{1}{C_0}\, dC_A}{dV} = \frac{-k.{C_A}^n}{F.C_0} \qquad \text{Equation 3-13}$$

This was rearranged to give Equation 3-14:

$$\frac{dC_A}{{C_A}^n} = \frac{k}{F} d\mathrm{V} \qquad \text{Equation 3-14}$$

Performing integration and solving for $C_A$ results in Equation 3-15:

$$C_A = \left(C_0^{(-n+1)} + (n-1) \cdot k \cdot \frac{V}{F}\right)^{\frac{1}{(-n+1)}} \qquad \text{Equation 3-15}$$

This equation was substituted into Equation 3-16, an equation describing the volumetric reaction rate over a volume of reactor:

$$r_A = -\frac{F}{V}(C_A - C_0)$$

Equation 3-16

This yielded a general equation for a PFR following a spontaneous, irreversible chemical reaction (Equation 3-17) with constants *k* representing the rate constant, and *n* the order of the reaction. The solving for these constants using experimental data is discussed below.

$$r_A = \frac{V}{F}\left(\left(C_0^{(-n+1)} + (n-1)\cdot k \cdot \frac{V}{F}\right)^{\frac{1}{(-n+1)}} - C_0\right)$$

Equation 3-17

$$\text{where n} \neq 1$$

In Equation 3-17, the order of the reaction, *n*, cannot be equal to one as this would cause the exponent of the term from Equation 3-15 to become undefined. As this equation would not be suitable for a first-order reaction, a new expression was formulated assuming first-order kinetics. The *n* term in Equation 3-10 was made to be equal to one (Equation 3-189, shown below)

$$\frac{dX}{dV} = \frac{k.C_A}{F.C_0}$$

Equation 3-19

Performing integration and solving for $C_A$ results in Equation 3-20:

$$C_A = \frac{C_0}{e^{\frac{V.k}{F}}}$$

Equation 3-20

Equation 3-20 was substituted into Equation 3-16 to give Equation 3-21:

$$r_A = -\frac{F}{V}\left(\frac{C_0}{e^{\frac{V.k}{F}}} - C_0\right)$$

Equation 3-21

Equation 3-21 describes a spontaneous, first-order, irreversible chemical reaction in a plug flow reactor where the constant *k* is the rate constant with units of time$^{-1}$.

As previously stated, the UAPBRs were sampled at three heights: at the boundary between the inlet and middle zone, between the middle and effluent zone, and immediately below the effluent of the reactor. The initial sulphate concentration, $C_0$, at the inlet is equal to the media sulphate concentration of 1000 mg/ℓ. However, the sulphate concentration entering the middle and effluent

zones varied according to the concentration of sulphate consumed in the inlet, and the inlet and middle zones respectively. Experimental data collected from the UAPBRs at each tested flow rate and each reactor zone (Figure 3-5 and Table 3-3) was recorded according to the volume (*V*) of the zone, the applied flow rate (*F*), the sulphate concentration entering the zone ($C_0$), the sulphate concentration leaving the zone ($C_A$) and the reaction rate across the zone calculated from Equation 3-16.

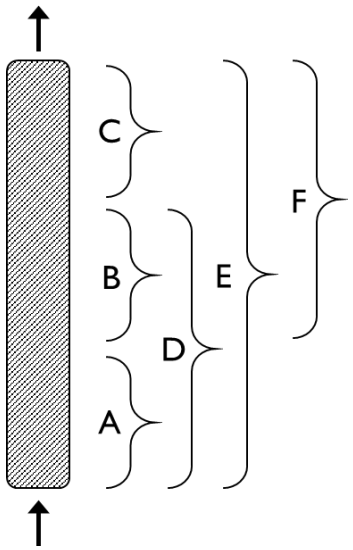


Figure 3-5 Schematic of the UAPBR reactor zones and composite zones from which kinetic data was inputted into the reactor kinetic Equation 3-17 and Equation 3-21.

Table 3-3 The UAPBR reactor zones (A-C) and composite zones (D-F) from which collected kinetic data were inputted into the reactor kinetic Equation 3-17 and Equation 3-21. The volume and the starting sulphate concentrations are shown. Refer to Figure 3-5 for the position of reactor zones and composite zones A to F.

| Label on Figure 3-5 | Zone | Volume (ℓ) | $C_0$ (mg $SO_4^{2-}$ /ℓ) |
|---|---|---|---|
| A | inlet | 0.333 | 1000 |
| B | middle | 0.333 | variable |
| C | effluent | 0.333 | variable |
| D | inlet:middle | 0.666 | 1000 |
| E | inlet:effluent | 1 | 1000 |
| F | middle:effluent | 0.666 | variable |

Each flow rate, volume, and initial substrate concentration combination tested was substituted into Equation 3-17 and Equation 3-21. Non-linear regression using the iterative, generalised reduced gradient (GRG) method was employed to solve for constants *k* and *n* (Warren, 1976). This was done using the SOLVER function of Microsoft Excel (Microsoft Office 365 ProPlus). This feature varies *k* and *n* to yield a modelled rate for each $C_0$, *F* and *V* tested which produces the lowest standard squared error (SSE) against the observed rate. The standard squared error is calculated according to:

$$SSE = \sum(y - y_{fit})^2$$

Equation 3-22

where *y* is the observed rate and $y_{fit}$ is the modelled rate.

The goodness of fit of the models, with predicted *k* and *n* values, was done by calculating the coefficient of determination $R^2$ (Kvalseth, 1983) according to:

$$R^2 = 1 - \frac{\sum(y - y_{fit})^2}{\sum(y - y_{mean})^2}$$

Equation 3-23

where *y* is the observed reaction rate, $y_{fit}$ is the modelled reaction rate using the *k* and *n* values calculated, and $y_{mean}$ is the mean of all observed reaction rates ($r_A$).

Confidence intervals were calculated by two-tailed inverse of the Student's t-distribution using a probability of 95% and degrees of freedom equal to the number of reaction rates used to solve for *k* and *n*. The produced critical t-value was multiplied by the standard error (SE; Equation 3-24), to yield a 95% confidence interval.

$$SE = \sqrt{\frac{SSE}{degrees\ of freedom}}$$

Equation 3-24

## 3.8 Approach to time-course sequencing and provision of metadata

### 3.8.1 Rationale of the sequencing approach

Gene amplicon sequencing of the 16S rRNA gene from metagenomic DNA samples was used to monitor changes in the composition of the microbial communities and identify microorganisms pertinent to system performance. Genome-resolved metagenomics was used in parallel to resolve the metabolic potential of these identified microorganisms.

Gene amplicon sequencing was initially used to characterise the microbial communities of the planktonic, biofilm-associated and attached communities of the six BSR reactors at longer HRT (Table 3-4). A selection of these samples was then sequenced by Illumina shotgun metagenomic sequencing. The choice of samples for shotgun metagenomic sequencing was based on the minimum number of samples which would allow for recovery of genomes from the majority of the microorganisms identified by the initial 16S rRNA gene amplicon sequencing. Further 16S rRNA gene amplicon sequencing was subsequently used to monitor the changes in these microbial communities during the course of the HRT study, as shown in Table 3-4.

Table 3-4 Metagenomic sequencing strategy used to assess the microbial communities of this study. Metagenomic DNA samples were assessed by 16S rRNA amplicon sequencing during the first (■) and second (●) round of sequencing of acetate and lactate reactor samples, and the reactor inoculum. Metagenomic samples which were assessed by genome-resolved metagenomics are starred (*). Recovered DNA samples that have not been sequenced are also shown ( ○)

| Reactor | Zone | Phase | HRT (days) | | | | | | | | | |
|---|---|---|---|---|---|---|---|---|---|---|---|---|
| | | | 5 | 4 | 3 | 2,66 | 2,33 | 2 | 1.75 | 1.5 | 1.3 | 1 |
| CSTR | n/a | planktonic | ● | ■* | ● | ○ | ○ | ● | ○ | ○ | ○ | ● |
| LFCR | inlet | planktonic | | ■* | ● | ○ | ○ | ● | ○ | ○ | ○ | ● |
| | | associated | | ■ | | | | | | | | |
| | | attached | | ■* | | | | | | | | |
| | effluent | planktonic | | ■ | ● | ○ | ○ | ● | ○ | ○ | ○ | ● |
| | | associated | | ■ | | | | | | | | ● |
| | | attached | | ■ | | | | | | | | ● |
| UAPBR | inlet (1) | associated | | ■ | | | | | | | | ● |
| | | attached | | ■* | | | | | | | | ● |
| | inlet (2) | planktonic | | ■* | ● | ○ | ○ | ● | ○ | ○ | ○ | ● |
| | | associated | | | | | | | | | | ● |
| | | attached | | | | | | | | | | ● |
| | middle (3) | associated | | | | | | | | | | ● |
| | | attached | | | | | | | | | | ● |
| | middle (4) | planktonic | | ■* | ● | ○ | ○ | ● | ○ | ○ | ○ | ● |
| | | associated | | | | | | | | | | ● |
| | | attached | | | | | | | | | | ● |
| | effluent (5) | associated | | | | | | | | | | ● |
| | | attached | | | | | | | | | | ● |
| | effluent (6) | planktonic | | ■* | ● | ○ | ○ | ● | ○ | ○ | ○ | ● |
| | | associated | | ■ | | | | | | | | ● |
| | | attached | | ■* | | | | | | | | ● |

### 3.8.2 Total DNA extraction

Total genomic DNA was extracted and purified from planktonic, biofilm-associated and -attached microbial communities from the BSR reactors of this study using a NucleoSpin® soil genomic DNA extraction kit (Machery-Nagel, Germany) as per manufacturer's instructions. Additional details and deviations from this protocol are outlined below.

Planktonic cells were recovered from the respective reactors by removing 15 mℓ of bulk liquid from each reactor zone via a sampling port. The cells were harvested by centrifugation at 10 000 g for 10 minutes in a benchtop microfuge. The biofilm-associated cells (i.e. no firm attachment) were isolated as described in Section 3.6.2. Briefly, solid support structures were removed from the respective bioreactor and gently agitated in 30 mℓ of sterile reactor medium containing no supplemented electron donor, for ten seconds. The biofilm-associated cells were recovered through centrifugation of this solution at 10 000 *g* for 10 minutes. Pelleted cells from the associated and planktonic samples were resuspended in lysis buffer before being transferred to DNA extraction tubes. Following the removal of biofilm-associated cells, sterile stainless-steel scissors were used to dissect the solid support structures into smaller pieces which could be placed directly into a DNA extraction tube. The biofilm-attached cells were then extracted directly from the solid support structures. Prior to the final step of the DNA extraction and purification protocol (DNA elution), elution buffer was heated to 60°C and incubated on the DNA-bound membrane column for 5 minutes before elution.

## 3.9 16S rRNA gene amplicon sequencing

Purified metagenomic DNA was sent to Macrogen Korea for sample preparation, Illumina MiSeq® sequencing, sample pre-processing, OTU clustering and taxonomic assignment. Dual-index barcoded 16S rRNA gene V3-V4 sequence libraries were generated by limited cycle polymerase chain reaction (PCR) using the 16S rRNA gene amplicon PCR forward (FwOvAd_341F; 5′-TCGTCGGCAGCGTCAGATGTGTATAAGAGACAGCCTACGGGNGGCWGCAG-3’) and reverse primers (ReOvAd_785R; 5′-GTCTCGTGGGCTCGGAGATGTGTATAAGAGACAGGACTACHVGGGTATCTAATCC-3’) to yield a ~460 bp product. This PCR was performed using the conditions: denaturation at 95°C for 3 min; 25 cycles of denaturation at 95°C for 30 s, 55°C annealing for 30 s, 72°C elongation for 30 s; and a final extension at 72°C for 4 min. Amplicon libraries were sequenced on an Illumina MiSeq® sequencer generating 300 bp paired-end reads.

Paired-end reads were merged using Fast Length Adjustment of Short reads (FLASH 1.2.11; http://ccb. jhu.edu/software/FLASH/; Magoč and Salzberg, 2011). CD-HIT-OUT (http://weizhongli-lab.org/cd-hit-otu/; Li et al., 2012) was used for raw read trimming and filtering, and OTU picking which was performed at a distance cut-off of 0.03. OTU taxonomy assignment was performed using the RDP 16S rRNA classifier algorithm (https:// rdp.cme.msu.edu/index.jsp; Edgar et al., 2010) by QIIME, UCLUST (Langille et al., 2013).

OTUs presented in the results and discussion sections are described by their highest taxonomic classification, up to the genus level, followed by an ‘OTU number’- a unique whole number given

to each defined OTU. The distribution of the abundance of OTUs across multiple samples was resolved using hierarchical clustering using the Pearson correlation and single linkages using Clustvis (Metsalu and Vilo, 2015; https://biit.cs.ut.ee/clustvis/).

It is imperative that 16S rRNA gene amplicon sequencing data are interpreted with an understanding that the differing copy number of the 16S rRNA gene between different species can lead to substantial distortion in the relative abundance of microorganisms within a sample (Baldrian, 2013). Less emphasis should be placed on the interpretation of the composition of a single sample in isolation. Instead, the composition of multiple samples should be compared concurrently, with larger emphasis being placed on the ratio between shared microorganisms since the copy number of the 16S rRNA gene stays fixed within a single microorganism. The cell concentration of individual OTUs was estimated by multiplying the relative abundance of an OTU by the total cell concentration determined for that sample. The estimated cell concentrations were faced by the same limitations as relative abundance but allowed better-informed comparisons between samples to made.

The enrichment of OTUs under specific physicochemical conditions was tested using the Walds t-test provided in Microsoft Excel (Microsoft Office 365 ProPlus). This variation of a two-tailed t-test assumes unequal variance. The distribution of abundances of an OTU across a microbial community exposed to a physiochemical condition was compared against the distribution of said OTU across microbial communities where the physiochemical condition was not observed. The physiochemical conditions tested included exposure to lactate and the retention within a biofilm (Chapter 7 ). Many of the samples which were compared are not truly independent of one another (for example biofilm and planktonic communities within the same reactor zone). Therefore, the statistical significance which is reported requires further experimentation to be confirmed.

## 3.10 Genome-resolved metagenomics

### 3.10.1 Metagenomic DNA sequencing

A selection of 17 metagenomic DNA samples (Table 3-4) isolated from the BSR reactor communities at steady-state at a four-day HRT, and the reactors' inoculum, were shotgun sequenced using an Illumina® HiSeq4000®. These were sampled and sequenced in duplicate to determine the reproducibility of the sampling. The sequencing generated 2.5 Gbp of sequencing data for each of the 34 sequenced samples. Sequencing generated 150 bp paired reads with an insert size of 400 to 800 bp. The Illumina® CASAVA pipeline (version 1.8) was used to process raw sequencing data.

### 3.10.2 Read processing, assembly and annotation

Prior to read processing, duplicate sequencing read files (2.5 Gbp) were concatenated into single files (5 Gbp) and are referred to hereafter as concatenated samples. The individual 2.5 Gbp sequencing files and the newly generated 5 Gbp concatenated sequenced samples were processed from read processing to genome binning and annotation in parallel.

Sickle (https://github.com/najoshi/sickle) was used to remove Illumina adapters and perform read trimming of raw sequencing reads, using default parameters. The trimmed reads of the 17 concatenated samples and 34 duplicate samples underwent assembly using MEGAHIT version 1.1.3 (Li et al., 2015) with the following default parameters: --k-min 21, --k-max 99, --k-step 10, --min—count 2. Larger scaffolds were then constructed from the assembled contigs using Scaffold and default parameters. Bowtie2 (Langmead and Salzberg, 2012) was used to determine the coverage of each scaffold by mapping trimmed reads to the assemblies. Open reading frames (ORFs) were predicted using Prodigal's metagenome procedure (Hyatt et al., 2010) for all assemblies. The predicted ORFs were then annotated using USEARCH (Edgar, 2010) against KEGG (Kanehisa and Goto, 2000), UniRef100 and Uniprot (Consortium, 2009) databases. The tentative phylogeny of each scaffold was assigned using Uniref100 gene hits across each gene on a scaffold.

### 3.10.3 Binning of metagenomes

The scaffolds constructed from each assembly were binned independently using a number of binning strategies in parallel. MaxBin (Yu-Wei et al., 2016), Metabat (Kang et al., 2015) and Concoct (Alneberg et al., 2014) were used to perform assemblies on each duplicate and concatenated sample assembly. Concoct was then employed to generate genome bins using differential coverage abundance patterns across all 17 concatenated and 34 duplicate samples. Genome bins were manually generated using ggKbase (ggkbase.berkeley.edu) on the basis of GC content, coverage and consensus taxonomy. The completeness of the manually binned genomes was informed by the recovery of 43 bacterial-single-copy genes (BSCGs; Bork, 2007). The number and phylogeny of the Rps3 genes in each assembly were used to confirm that the genomes of all abundant microorganisms within an assembly had been binned during manual binning.

The completeness and degree of contamination within each bin was determined using CheckM (Parks et al., 2015). Das Tool (Sieber et al., 2018) was used to select for a set of non-redundant genome bins generated from all five binning approaches for each of the 51 assemblies. A set of non-redundant genome bins from all 51 assemblies was then selected by dRep (Olm et al., 2017) using an average nucleotide identity (ANI) of 99%.

### 3.10.4 Metabolic analyses

The final set of non-redundant genome bins originating from all 51 assemblies were uploaded to ggKbase for metabolic analysis. Metabolic pathways were identified from gene annotations searched by name using ggKbase. The list of genes required for the ascribing of a microbial genome with a metabolic pathway is described in Appendix A.5.1.

In addition to KEGG, UniRef100 and Uniprot annotated ORFs, genes were predicted using HMMSEARCH to match ORF against Hidden Markov Models (HMM) built with protein sequence alignments from TIGRfam protein database. The construction of these HMMs are described by Anantharaman et al. (2016). This allowed the identification of the genes associated with major pathways, as well as several NiFe and FeFe hydrogenases, with a high degree of confidence.

### 3.10.5 Phylogenetic analyses

The phylogeny of genome bins was putatively assigned based on the classification of the rpS3 gene by UniRef100 annotation. These classifications were validated through analysis of sixteen recovered ribosomal genes. The 16 ribosomal protein sequences (RPL 2, 3, 4, 5, 6, 14, 15, 16, 18, 22, and 24, and RPS 3, 8, 10, 17, and 19) were aligned using MUSCLE v3.8.31 (Edgar, 2004) and then concatenated to form one alignment which was trimmed using Geneious. A custom set of 16 ribosomal proteins, as used in Hug et al. (2016), was included in a second alignment with the ribosomal proteins recovered in this study. Phylogenetic reconstruction of these two alignments were performed using FastTree and default parameters (Price et al., 2009) and viewed on iTol (Letunic et al., 2006). These can be viewed at https://itol.embl.de/ by viewing the shared project of hsstom001.

### 3.10.6 Genome indices of replication

Indices of replication (iRep; Brown et al., 2016), a measure of instantaneous genome replication rates, were determined for genomes recovered in this study. This method assigns an index of replication to a genome, based on the difference in coverage between the predicted origin of replication and terminus. Reads from each sample were mapped to each recovered genome within a sample and iRep.py (Brown et al., 2016) was used to predict the origin and terminus and assign an index of replication based on the difference in coverage between these two positions in the genome.

# Chapter 4 Continuous stirred tank reactors

## 4.1 Introduction

Continuous stirred-tank reactor (CSTR) systems were selected for this study to act as a reference to which the well-mixed LFCRs (Chapter 5 ) and plug-flow governed UAPBRs (Chapter 6 ) could be compared, both in terms of performance and their microbial ecology at a range of tested HRTs.

These reactors were chosen as they select for a suspended microbial community due to their low surface area to volume ratio, limiting biofilm formation. The microbial cultures which these reactors support are therefore vulnerable to cell washout at dilution rates which are equal to and greater than the maximum specific growth rate of the individual microorganism. These reactors are also well-suited to the collection of robust kinetic data under defined conditions.

## 4.2 Lactate CSTR Results

This section describes the performance of the lactate CSTR across the tested dilution rates applied to the system with a constant sulphate (1.0 g/ℓ or 10.41 mM) and lactate (1.2 g/ℓ or 13.3 mM) feed concentration. The cell concentrations supported by the CSTR are shown, followed by the 16S rRNA gene amplicon sequencing results, which describe the microbial community structure of the system at a phylum- and class-taxonomic levels, followed by the abundances and classification of the dominant OTUs in the system.

### 4.2.1 Reactor performance

The lactate CSTR achieved a sulphate conversion of 64% at a five-day HRT (0.008 $h^{-1}$; Figure 4-1 A). This decreased gradually to 52% at a 2.6-day HRT (0.016 $h^{-1}$) and remained stable with increasing dilution rate until an HRT of 1.75 days (0.024 $h^{-1}$). A linear increase in the residual sulphate concentration with increasing dilution rate was then observed between a 1.75- and 1.0-day HRT (0.024-0.042 $h^{-1}$) with a final sulphate conversion of 40%. The expected sulphide and measured sulphide concentrations differed by a maximum of 12% between a four- and one-day HRT (0.010-0.042 $h^{-1}$).

No residual lactate was detected within the reactor, above 10 mg/ℓ (0.11 mM) between a five- and 1.75-day HRT (0.008-0.024 $h^{-1}$; Figure 4-1 B). The residual lactate concentration then increased gradually with further reduction in HRT from 15 mg/ℓ (0.17 mM) at a 1.5 day-HRT (0.028 $h^{-1}$), to 26 mg/ℓ (0.29 mM) at a 1.3-day HRT (0.032 $h^{-1}$) and to 47 mg/ℓ (0.52 mM) at a one-day HRT (0.042 $h^{-1}$). The utilisation of 1,153 mg/ℓ (12.80 mM) at a one-day HRT represents a lactate conversion

and utilisation rate of 96% and 48 mg/ℓ.h, respectively. Propionate was detected in the reactor at each HRT, indicating the presence of lactate fermenting microorganisms (Equation 2-12), with an average propionate concentration of 132 mg/ℓ (1.81 mM) between a five- and 1.5-day HRT (0.008 - 0.028 $h^{-1}$) The propionate concentration then increased to 154 mg/ℓ (2.11 mM) at a 1.3-day HRT (0.032 $h^{-1}$) and 225 mg/ℓ (3.08 mM) at a one-day HRT (0.042 $h^{-1}$) indicating a greater degree of lactate fermentation had taken place at these reduced HRT. This corresponds with the reduced sulphate conversions seen at a 1.3- and 1.0-day HRTs. The highest observed residual acetate concentration of 801 mg/ℓ (13.34 mM) was seen at a four-day HRT (0.010 $h^{-1}$), after which it decreased to a minimum of 679 mg/ℓ (11.31 mM) at a 1.5-day HRT (0.028 $h^{-1}$). The acetate concentration then increased to 718 mg/ℓ (11.96 mM)at a one-day HRT (0.042 $h^{-1}$). No citrate, which was incorporated at 222 mg/ℓ (1.16 mM) in the reactor medium, was detected in the reactor at any of the tested dilution rates.

The redox potential remained highly negative throughout the HRT study with a gradual increase from -172 mV at a five-day HRT to -119 mV at a one-day HRT (Figure 4-1 C), indicating that anaerobic conditions were maintained for the duration of the study. The pH within the reactor was highest at a five-day HRT at 7.5 before decreasing to 7.1 at a four-day HRT (0.010 $h^{-1}$) where it remained stable until a one-day HRT (0.042 $h^{-1}$) where the pH dropped to 6.9.

The observed bicarbonate concentration remained stable between and including the four- and 2.3-day HRT (0.010-0.018 $h^{-1}$) at approximately 24 mM (Figure 4-1 D). At lower HRTs, the bicarbonate decreased to an average of 20 mM. This decrease in production of bicarbonate from a 1.75-day HRT (0.024 $h^{-1}$) corresponds with the reduced electron donor utilisation and reduced sulphate conversion seen at these shorter HRTs.

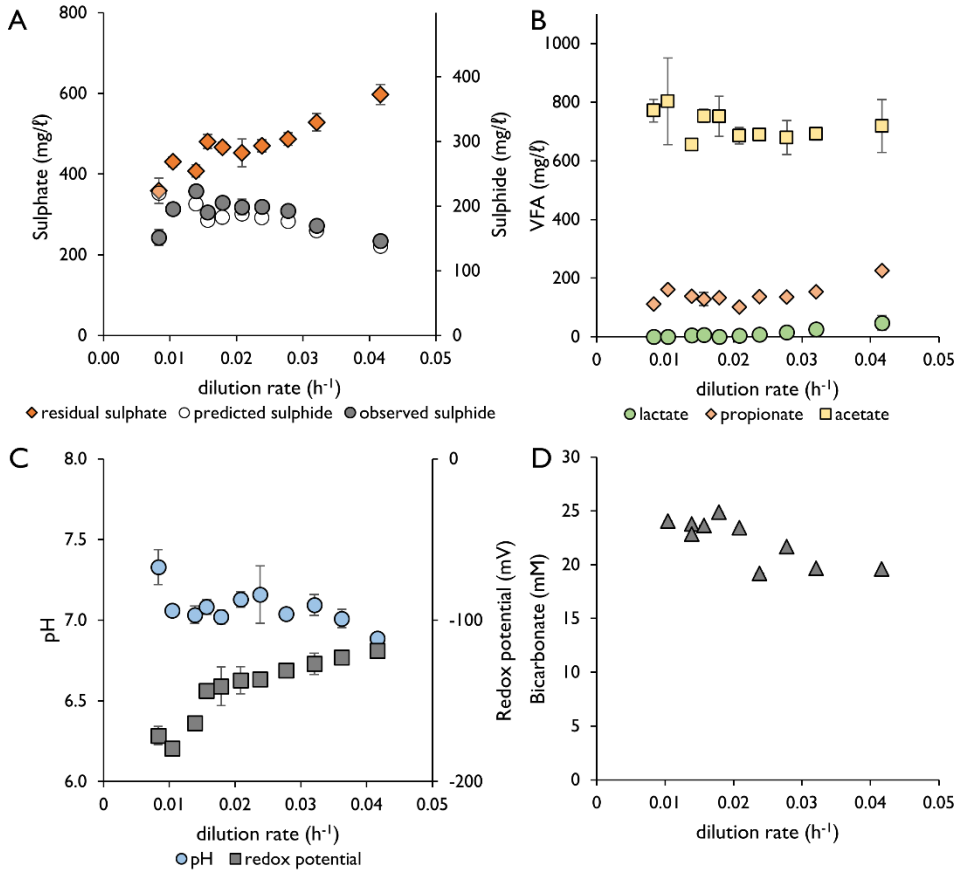


Figure 4-1 Steady-state kinetic data of the lactate-supplemented CSTR at a range of tested dilution rates, including (A) the residual sulphate, the produced sulphide and the predicted sulphide concentration based on the observed sulphate reduced; (B) the observed volatile fatty acid profile; (C) pH and redox potential (reported relative to a standard hydrogen electrode); and (D) the produced bicarbonate concentration calculated from the difference between the observed and feed bicarbonate concentrations. Error bars represent one standard deviation from the mean.

The lactate CSTR supported 1.1 x $10^9$ cells/mℓ at a five-day HRT (Figure 4-2). The cell concentration exhibited minor fluctuations between HRT but showed a stable cell concentration between and including the four- and 1.5-day HRT (0.010 – 0.028 $h^{-1}$). The cell concentration then decreased at shorter HRTs, exhibiting a cell concentration of 3.2 x $10^8$ cells/mℓ at a one-day HRT (0.042 $h^{-1}$), representing a reduction in cell concentration of 70% between a one- and five-day HRT.

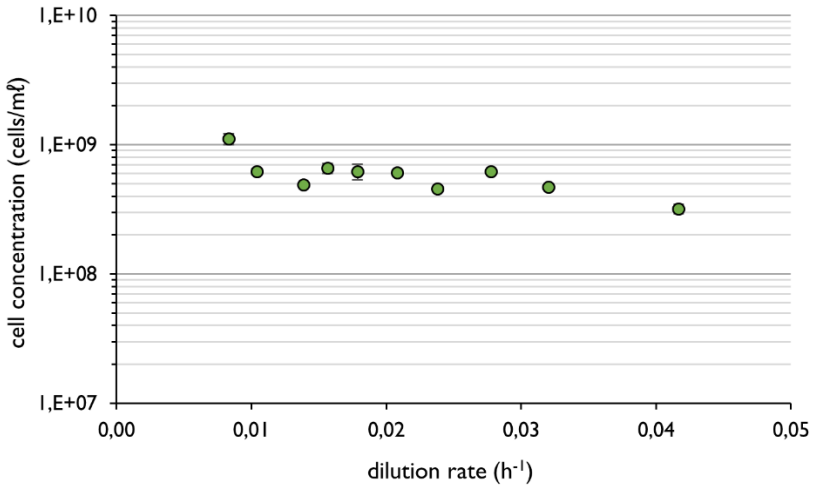


Figure 4-2 The microbial cell concentration supported by the lactate-supplemented CSTR as a function of applied dilution rate. Error bars represent one standard deviation from the mean of duplicate samples each counted in duplicate.

### 4.2.2 Microbial ecology

The microbial community of the lactate CSTR, at all HRTs studied, was largely made up of the phyla Proteobacteria, Bacteroidetes, Firmicutes, Spirochaetes and Synergistetes (Figure 4-3). A considerable reduction in Negativicutes, a class of Firmicutes, was seen between a five- and four-day HRT (0.008 - 0.010 $h^{-1}$) before recovering at a three-day HRT (0.014 $h^{-1}$) and making up 49% of the community. The representation of Negativicutes was almost entirely constituted by a *Veillonella* OTU (Figure 4-4), a common lactate fermenting microorganism (Rogosa, 1963). A genome bin was classified as *Veillonella* and showed similar abundance patterns across the reactor samples at a four-day HRT and therefore was concluded to represent the genome of this *Veillonella* OTU. Its ability to ferment lactate was confirmed through analysis of its recovered genome (Chapter 8 , Metagenomics).

The relative abundance of Deltaproteobacteria, the class to which all identified SRB in this CSTR belong and of which all members are SRB, was variable, between 18 and 35% between the 5- and 3- day HRT. It decreased gradually from 39% at a 2.6-day HRT (0.016 $h^{-1}$) to 14% at a one-day HRT (0.042 $h^{-1}$). The temporary decrease in Deltaproteobacteria from 33% relative abundance at a four-day HRT (0.010 $h^{-1}$) to 16% relative abundance at a three-day HRT (0.014 $h^{-1}$) corresponded with the increase in the relative abundance of Firmicutes in the reactor.

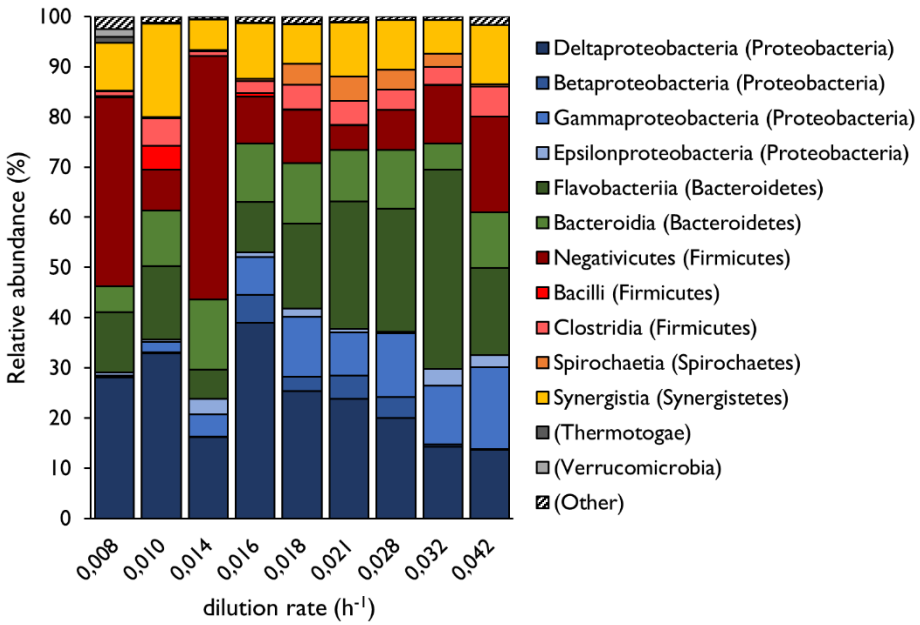


Figure 4-3 The microbial community structure, at the phylum and class taxonomic level, of the lactate-supplemented CSTR as a function of applied dilution rate.

The most abundant OTUs present in the lactate CSTR remain in the top six ranked OTUs, in terms of relative abundance, for the duration of the HRT study, with the abundance of these OTUs fluctuating with increasing dilution rate (Figure 4-4). The cell concentration of these OTUs were estimated by multiplying the relative abundance of an OTU by the total cell concentration determined at the time of sampling, as discussed in Section 3.9. The majority of the OTUs present in the lactate-supplemented CSTR at long HRTs were still present at a one-day HRT (0.042 $h^{-1}$) but each at a reduced cell concentration (Figure 4-5). *Desulfomicrobium* (1) was the most abundant of the SRB OTUs for the duration of the study. *Desulfovibrio* (6) was abundant at a five- and four-day HRT (0.008-0.010 $h^{-1}$) but was largely undetected at shorter HRT, whilst a second *Desulfovibrio* OTU (39) appeared in the system at low abundances for the duration of the HRT study, increasing slightly at short HRT. *Pustulibacterium* (3), a Bacteroidetes showed marked dominance over other OTUs from a 2.3-day HRT (0.018 $h^{-1}$). The class of Gammaproteobacteria made up almost entirely by *Enterobacter* (16), showed increased and sustained dominance in the community, too, from a 2.6-day HRT (0.016 $h^{-1}$).

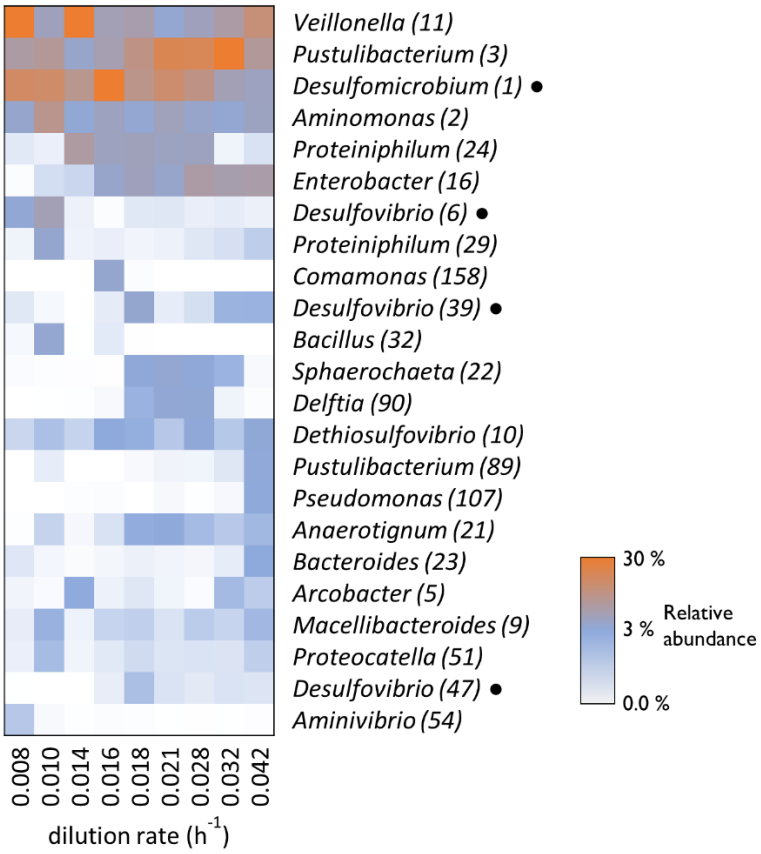


Figure 4-4 The microbial community of the lactate CSTR shown as relative abundance (%) of the 23 most abundant OTUs at the tested dilution rates. SRB are indicated (●). The unique number given to each detected OTU is shown in parentheses.

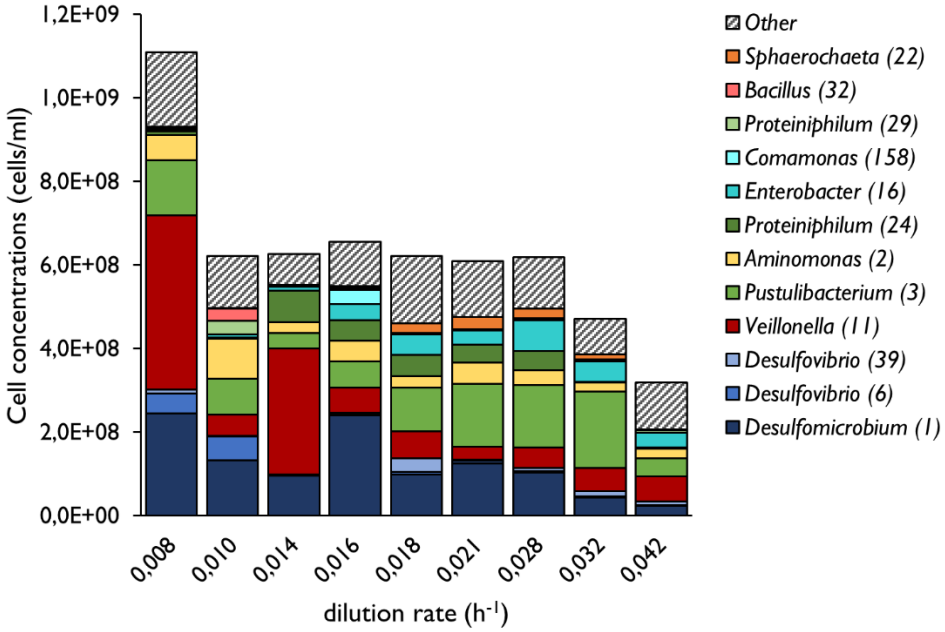


Figure 4-5 The microbial community structure of the ten most abundant OTUs present in the lactate-supplemented CSTR, as a function of HRT, represented as estimated cell concentrations of predominant OTUs. OTU cell concentrations were calculated by multiplying the relative abundance (%) of each OTU by the determined total cell concentration of that sample (Figure 4-4). OTUs confirmed to contain genes for sulphate reduction through genomes-resolved metagenomics (Chapter 8 are *Desulfovibrio* (6 and 39) and *Desulfomicrobium* (1).

## 4.3 Lactate CSTR Discussion

The performance data collected from the lactate CSTR is discussed in the context of studies presented in the literature. The competition between lactate oxidising SRB and fermentative microorganisms are discussed based on a physiochemical basis, followed by the analysis of the microbial communities through combining the cell concentration and the 16S rRNA gene amplicon sequencing dataset.

### 4.3.1 Achieved VSRR in the context of literature

The volumetric sulphate reduction rate (VSRR) exhibited in the lactate supplemented CSTR is plotted as a function of volumetric sulphate loading rate (VSLR) in Figure 4-6 and compared to the results from BSR continuous stirred tank reactor studies presented by White and Gadd (1996), Dar et al. (2008) and Oyekola et al. (2010). In the lactate CSTR described in this thesis, a sulphate conversion of 55% was maintained between a five- and 1.75-day HRT, corresponding to a dilution rate of 0.008 - 0.024 $h^{-1}$ and a VSLR of 8 to 24 mg/ℓ.h and a VSRR of 5.3 to 12.6 mg/ℓ.h. On further reduction of the HRT, a gradual reduction in sulphate conversion between a 1,5- and one-day

HRT (0.028 - 0.042 $h^{-1}$) was observed, with a 40% conversion at a one-day HRT. The highest VSRR of 17 mg/ℓ.h was seen at a one-day HRT, corresponding to a VSLR of 42 mg/ℓ.h.

Oyekola et al. (2010) evaluated a mixed SRB culture using the same reactors and similar operating conditions, namely 35°C operating temperature, Postgate B medium supplemented with 1 g/ℓ (10.41 mM) $SO_4^{2-}$ and 2.25 g/ℓ (25 mM) lactate. Oyekola et al. (2010) demonstrated an 80% sulphate conversion with the higher lactate concentration before the VSRR began to plateau with increasing VSLR between a 24- and 12-hour HRT (0.041 - 0.082 $h^{-1}$), exhibiting a sulphate conversion and maximum VSRR of 50% and 41.4 mg/ℓ.h, respectively. The difference in sulphate conversion between these two studies is accounted for by the nearly two-fold difference in supplied lactate concentrations. The VSRR exhibited by the lactate CSTR of this study begins to plateau earlier, between a 1,5- and 1,3-day HRT (0.028 - 0.032 $h^{-1}$). This is attributed to the lower growth rates supported on the reduced lactate concentration compared to Oyekola et al. (2012).

Dar et al. (2008) observed near complete sulphate reduction at a two-day HRT on feeding 1.8 g/ℓ (20 mM) lactate and 0.9 g/ℓ (9.4 mM) sulphate (Figure 4-6). This was achieved through the inoculation of the system with sludge from a wastewater treatment plant treating lactate containing wastewater. The biomass concentration would therefore not represent steady-state conditions as it would continuously decrease as a result of cell washout. This does, however, indicate that complete sulphate conversion, of 0.9 g/ℓ sulphate and a lactate concentration similar to that used by Oyekola et al (2010), can be achieved with sufficient, SRB-enriched, biomass accumulation. White and Gadd (1996) modelled data from a continuous stirred tank reactor which was operated with feed lactate concentrations ranging between 3.6 and 78 mM (0.32 – 7.02 g/ℓ ) at varied applied dilution rates between 0.01 $h^{-1}$ to 0.08 $h^{-1}$. These modelled results are similar to those of this study in terms of achieved VSRR at the tested VSLRs, exhibiting VSRRs of 7.3 and 17.1 mg/ℓ.h at VSLRs of 8.4 and 26 mg/ℓ.h, respectively (Figure 4-6). Their results also indicate a greater degree of lactate fermentation (not shown) over SRB-linked oxidation at higher lactate concentrations, in accordance with Oyekola et al. (2012).

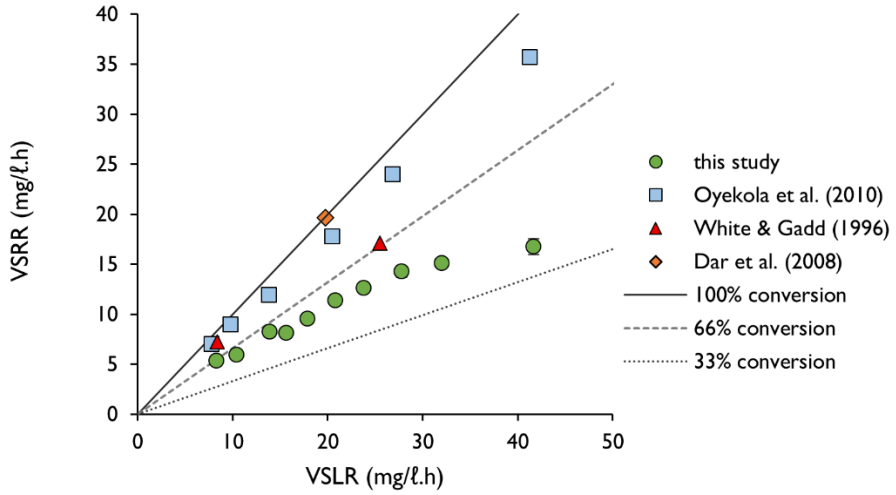


Figure 4-6 The volumetric sulphate reduction rate (VSRR) achieved by the lactate-supplemented CSTR of this study (1.2 g/L lactate, 1 g/L sulphate, 30 °C) compared to the sulphate reducing, lactate-supplemented systems of Oyekola et al. (2010; 2.4 g/L lactate, 1.0 g/L sulphate, 35 °C), Dar et al. (2008; sludge inoculum; 0.9 g/L sulphate, 1.8 g/L lactate) and, White and Gadd (1996; modelled kinetic data, 20°C, 1.2 g/L sulphate, 0.9 g/L lactate) at varied volumetric sulphate loading rates, varied through the reduction in the hydraulic retention time applied to the systems.

### 4.3.2 Sulphate reduction is linked to the oxidation of lactate and small quantities of additional electron donors

Between the five and 1.5-day HRT (0.008 - 0.028 $h^{-1}$) approximately 80% of the 13.6 mM lactate supplied in the reactor feed is estimated to have been used via incomplete or complete oxidation by SRB (Equation 2-10 and Equation 2-11), with the remaining 20% metabolised via fermentation (Equation 2-12, Figure 4-7). The proportion of lactate used by SRB decreased to 72% at a 1.3-day HRT (0.032 $h^{-1}$) and 62% at a one-day HRT. This coincided with a reduction in the sulphate conversion and an increased proportion of lactate fermentation over this period (Figure 4-7).

The sulphate conversion exhibited at a five-, four- and three-day HRT (0.008-0.014 $h^{-1}$) was greater than that expected from the oxidation of the available lactate via incomplete lactate oxidation by SRB (Equation 2-10). The amount of lactate available for sulphate reduction was calculated based on the assumption that all propionate produced originated from lactate fermentation (Equation 2- 12), and that no propionate was subsequently oxidised. The validity of these assumptions are addressed below.

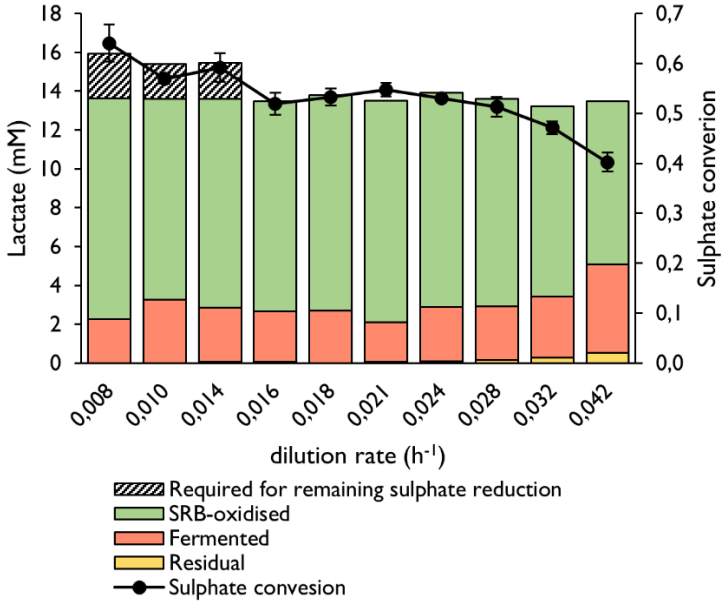


Figure 4-7 The concentration of lactate undergoing lactate fermentation (Equation 2-12) calculated from the observed propionate concentration; undergoing incomplete lactate oxidation by SRB (Equation 2-10) calculated from the observed sulphate reduction but allowing to exceed the feed lactate concentration of 13.6 mM, residual lactate remaining in the reactor and the theoretical concentration of lactate required to allow for degree of sulphate conversion observed at each tested dilution rate.

With these assumptions, all lactate can be accounted for, within 5% (of 13.6 mM feed lactate) between a 2,66- and a one-day HRT (0.016-0.042 $h^{-1}$) based on the produced propionate and residual sulphate concentrations. However, at longer HRT (0.008 - 0.014 $h^{-1}$), the quantity of lactate estimated to have been oxidised by SRB, using incomplete oxidation, does not account for the observed degree of sulphate reduced at these steady-states. Between the 5- and 3-day HRTs (0.008 - 0.014 $h^{-1}$), the sulphate conversion averaged 60%, whereas the average conversion between 2.66- and 1.75-days was 53%. This additional sulphate reduction which was not linked to lactate oxidation indicates some complete lactate oxidation, the oxidation of the produced acetate (lined area, Figure 4-7). The difference between the sulphate linked to lactate oxidation and total sulphate reduced would correspond with approximately 1 mM of oxidised acetate. Agreement between the observed and predicted acetate concentrations in this reactor systems are addressed throughout the following sections.

### 4.3.3 Genomic potential for citrate oxidation by SRB

Citrate was included in the reactor medium at 1.16 mM and was not detectable at any tested HRT in this reactor. A number of SRB within this reactor had the genetic potential to oxidise acetate (Chapter 8 , Metagenomics) and therefore there is a strong possibility that the additional sulphate reduction observed, or a proportion of, is linked to acetate oxidation. Only one of the SRB had the operon required for citrate uptake and fermentation. This *Desulfovibrio* (OTU 6; Figure 4-4; Section 4.2.2) was matched to the genome bin BSR_Ace_C_na_Desulfovibrio_desulfuricans_58_43 (Chapter 8 , Metagenomics), based on ascribed taxonomy and relative abundance across 16 samples. This genome contained the genes for citrate lyase which catalyses the conversion of citrate to oxaloacetate; a trans-membrane citrate transporter and a GntR family transcriptional regulator which is likely the transcriptional regulator (*citO*) of this operon (Blancato et al., 2008). The presence of this operon provides evidence that this *Desulfovibrio* is capable of citrate oxidation as an electron donor for sulphate reduction. However, this *Desulfovibrio* experienced a considerable reduction in relative abundance between a four- and three-day HRT (0.010 - 0.014 $h^{-1}$). The maintained 'complete lactate oxidation' at a three-day HRT indicates that it is unlikely that the sulphate reduction observed at these longer HRT was linked to citrate oxidation.

### 4.3.4 Exploiting differing stoichiometry of SRB-linked lactate oxidation and lactate fermentation

The competition between lactate oxidising SRB and lactate fermentative microorganisms was effectively evaluated by Oyekola et al. (2009) by taking advantage of the differing stoichiometry of the products and reactants of lactate oxidation by these two groups of microorganisms (Equation 2-10 and Equation 2-12). Instead of using these ratios to quantify the competition between these groups, the following section will assume that the degree of lactate fermentation estimated from the amount of propionate produced is correct along with associated assumptions (Section 4.3.2). The observed molar ratios of products and reactants are used to validate these assumptions.

**Lactate oxidised: sulphate reduced**

Incomplete lactate oxidation by SRB (Equation 2-10) consumes two moles of lactate per mole of sulphate reduced. The total quantity of lactate oxidised per mole of sulphate reduced across HRT is shown in Figure 4-8 (red circles). At a five-day HRT (0.008 $h^{-1}$) this ratio is equal to two and would suggest all lactate supplied in the reactor feed was oxidised incompletely by SRB. However, residual propionate at this HRT indicates 2.27 mM of lactate was oxidised via fermentation. As described in Section 4.3.2, increased sulphate conversion seen between a five- and three- day HRT, compared to subsequent HRT, is presumed to be linked to acetate utilisation. The ratio of lactate

oxidised to sulphate reduced increased to 2.41 between a 2.66- and a 1.5-day HRT (0.016 and 0.028 $h^{-1}$).

The concentration of lactate available for sulphate reduction (lactate provided in the medium minus lactate fermented), divided by the amount of sulphate reduced is plotted in Figure 4-8 (green circle). Between the 2.66- and 1.0- day HRTs, this ratio is approximately 2.0 in accordance with Equation 2-10. However, this ratio is approximately 1.7 between a five- and three-day HRT (0.008-0.014 $h^{-1}$). This indicates either a mixture of complete and incomplete lactate oxidation by SRB or incomplete lactate oxidation and the oxidation of a different electron donor linked to sulphate reduction at these longer HRT. The increasing ratio of observed lactate oxidised per sulphate reduced reflects the increased proportion of lactate used by fermentative microorganisms.

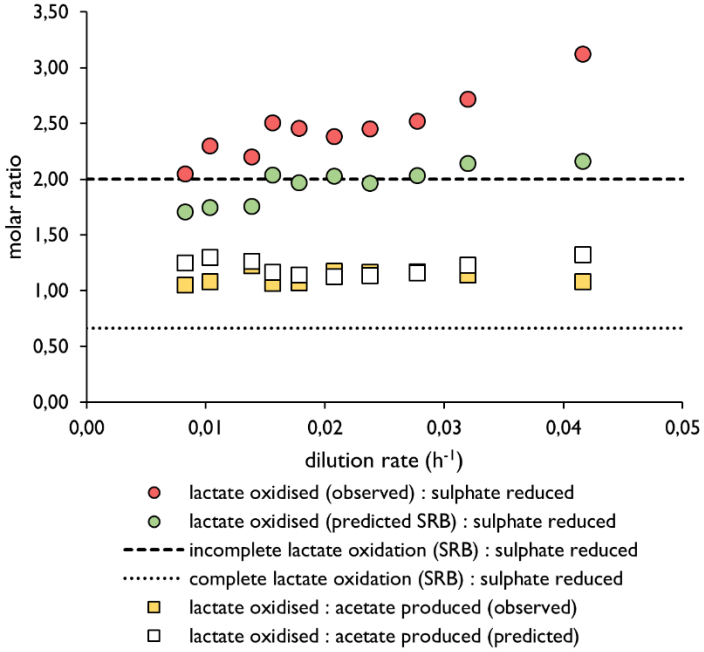


Figure 4-8 The predicted and observed steady-state molar ratios of products and reactants arising from lactate oxidation by SRB (Equation 2-10) and lactate fermentation (Equation 2-12). The lactate predicted to have been oxidised by SRB was calculated by subtracting the lactate oxidised by fermentation (Figure 4-7) from the feed lactate concentration (13.6 mM) and confirming through the observed sulphate reduced according to Equation 2-12. The observed lactate oxidised was calculated by subtracting the residual lactate in the reactor from the inlet lactate feed concentration. The predicted acetate produced was calculated according to the degree of lactate oxidation by SRB and fermenters (Equation 2-10 and Equation 2-12) shown in Figure 4-7. The theoretical ratio of 'lactate oxidised to sulphate reduced' arising from complete and incomplete lactate oxidation by SRB are plotted.

**Lactate oxidised / acetate produced**

The fermentation of lactate and the incomplete oxidation of lactate by SRB generates differing amounts of acetate per mole of lactate. The acetate concentration, given the estimated degree of

fermentation and incomplete oxidation, was predicted and compared to the observed acetate concentration to validate the assumptions made in Section 4.3.2.

One mole of acetate is produced from the oxidation of one mole of lactate through incomplete lactate oxidation by SRB (Equation 2-10), whereas a single mole of acetate is produced from the fermentation of three moles of lactate (Equation 2-12). The ratio of acetate produced: lactate oxidised is shown in Figure 4-8. A predicted acetate concentration, based on the degree of lactate fermentation and SRB-linked lactate oxidation, is plotted alongside. The observed ratio lies between 1.02 – 1.19 for the duration of the HRT study and corresponds well with predicted values. An observed ratio greater than that predicted would have indicated further acetate consumption. The observed and predicted acetate concentration, based on the lactate reactions shown in Figure 4-7 are shown below in Figure 4-9. It is demonstrated in Section 4.4.2 that the oxidation of yeast extract contributes to some acetate generation. The agreement between the predicted and observed acetate concentrations, for the majority of this study, indicates that minimal yeast extract oxidation was occurring in the lactate-supplemented CSTR during this study.

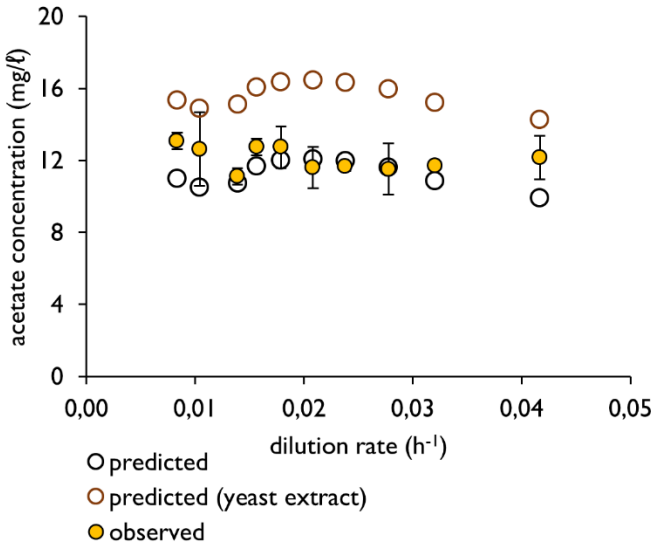


Figure 4-9 The observed and predicted acetate concentration in the lactate-supplemented CSTR at a range of applied dilution rates which correspond to HRT between four- and one-day HRTs. Acetate predictions were calculated according to the generation of acetate from lactate oxidation reactions including fermentation and complete and incomplete lactate oxidation by SRB, as shown and estimated in Figure 4-7. A second acetate concentration was predicted, 'predicted (yeast extract)', which also considered the generation of 4.54 mM of acetate from the oxidation of yeast extract as demonstrated in the Acetate CSTR and described in Section 4.4.2. Error bars represent one standard deviation from the mean.

### Lactate oxidised / bicarbonate produced

Lactate fermentation generates a mole of bicarbonate and carbon dioxide per three moles of lactate consumed. Therefore, a 'lactate utilised' to 'bicarbonate produced' ratio of three would

indicate all lactate was oxidised via fermentation (Equation 2-12), whilst a ratio of one indicates all lactate oxidisation via incomplete oxidation by SRB (Equation 2-10). This assumes no other reactions, such as citrate and yeast extract oxidation, contribute to the formation of bicarbonate. These observed and expected ratios, given the quantified lactate fermentation and oxidation, are plotted in Figure 4-10. The observed ratio was approximately a third that of the expected, which lies at approximately 1.5, indicating that the concentration of bicarbonate in the reactor was far higher than expected and reactions other than those described by Equation 2-10 and Equation 2-12 are taking place to produce this bicarbonate. This has already been demonstrated by the sulphate reduction being coupled to complete lactate oxidation or citrate oxidation (Figure 4-7 and Figure 4-8) and that yeast extract (Section 4.4.2) and citrate oxidation had been confirmed. Complete oxidation of citrate would yield 6.9 mM bicarbonate. The expected ratio, incorporating complete oxidation of citrate better accounts for the reduced ratio of observed lactate oxidation to bicarbonate produced.

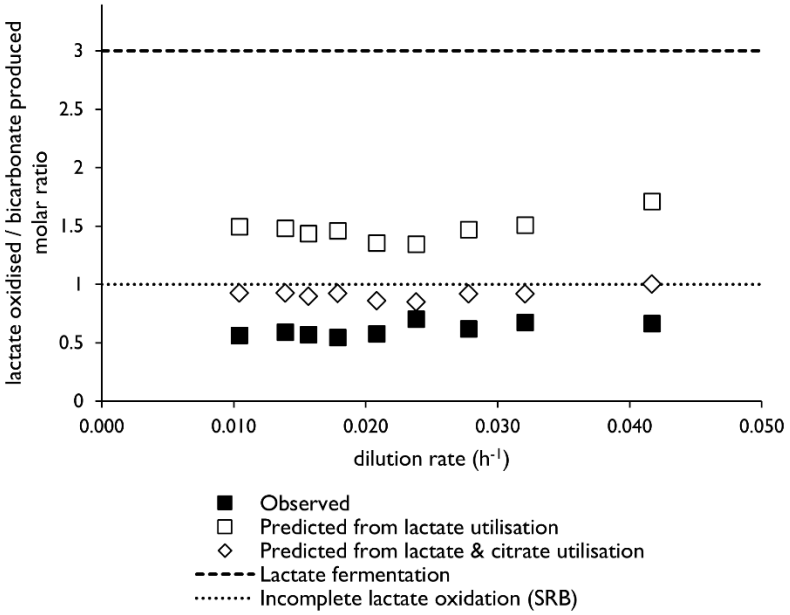


Figure 4-10 The observed and predicted steady-state molar ratios of "lactate oxidised" to "bicarbonate produced". The predicted amount of bicarbonate produced was predicted according to the degree of lactate undergoing lactate fermentation (Equation 2-12) and incomplete oxidation (Equation 2-10; Figure 4-7) and, in a second predicted, assuming complete citrate oxidation. Theoretical lactate oxidised: bicarbonate produced are plotted according to incomplete lactate oxidation (Equation 2-10; dotted line) and complete lactate fermentation (Equation 2-12; dashed line) assuming no other reactions contribute to the production of bicarbonate in this system.

### 4.3.5 Sulphate reduction and the proportion SRB in the CSTR communty

The calculated cell concentrations of SRB was at a maximum at a five-day HRT and represented 40% of the microbial community (Figure 4-11). The cell concentrations of SRB remained stable between a four- and 1.5-day HRT (0.010 - 0.028 $h^{-1}$). The SRB cell concentration then decreases between a 1.5- and 1.3-day HRT (0.028 - 0.032 $h^{-1}$), and again between a 1.3- and one-day HRT (0.032 - 0.042 $h^{-1}$). The ratio of *Desulfomicrobium* (1) to remaining SRB was 5:1 at a two-day HRT (0.021 $h^{-1}$) and decreased to 1.7:1 at one day HRT, with a difference in sulphate conversion of just 0.14. This indicates that the 'remaining SRB' consume more sulphate per unit biomass than the dominant *Desulfomicrobium* (1) OTU. Therefore, the contribution to overall sulphate reduction of these lower abundance SRB OTUs is likely not reflected in their abundance within the community.

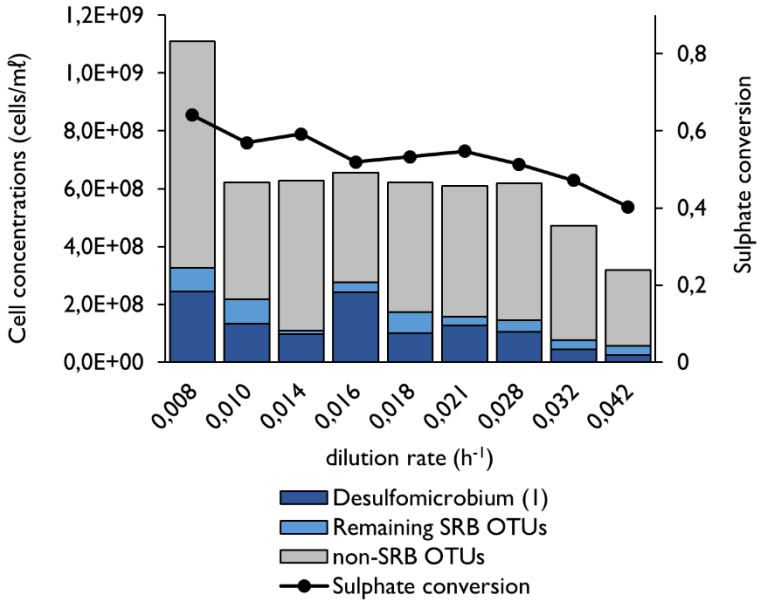


Figure 4-11 The estimated cell concentrations of the SRB OTU *Desulfomicrobium* (1), the remaining SRB OTUs and OTUs shown to not possess the capacity for sulphate reduction (Chapter 8, Metagenomics) at all tested dilution rates. The estimated cell concentrations were calculated by multiplying the relative abundance of an OTU by the determined total cell concentration within a sample. The sulphate conversion observed at steady-state at these dilution rates are plotted alongside.

The decrease in the cell concentrations of Deltaproteobacteria, the class to which all SRB identified within this system were classified, between a four- and three-day HRT (0.010 - 0.014 $h^{-1}$) coincides with a substantial increase in the cell concentration of the *Veillonella* (11) OTU (Figure 4-4). During this period the total cell concentration supported within the CSTR remained constant and the sulphate conversion improved.

The phylum Firmicutes, to which *Veillonella* (11) is classified, contain some of the highest recorded 16S rRNA gene copy numbers (Baldrian 2013). Baldrian (2013) reviewed 395 Firmicute genomes

and found an average of 5.8 16S rRNA gene copies per genome, whereas the average Deltaproteobacteria copy number, from 43 reviewed genomes, was 2.7. This may account for the apparent decrease in Deltaproteobacteria at a three-day HRT (0.014 $h^{-1}$) during a relatively stable period. This decrease may instead be an overestimation of the proportion of the community made up by *Veillonella*. This would account for an outlier of Deltaproteobacteria cell concentration in an otherwise relatively stable period of performance and community structure. Should this be accurate, the cell concentrations of other OTUs, including Deltaproteobacteria at a five-day HRT (0.008 $h^{-1}$), would also be underestimated due to the apparent dominance of *Veillonella* (11) at this HRT.

The calculated cell concentrations of the OTUs in this system were adjusted using the 16S rRNA gene copy number by phyla according to Baldrian (2013; Figure 4-12 B). Comparison between the calculated cell concentrations of OTUs assuming uniform and varied 16S rRNA gene copy number demonstrated that the microbial community structure of the lactate CSTR is largely unaffected by fluctuations in most phyla, excluding Firmicutes. Where Firmicutes were abundant, the cell concentrations of OTUs belonging to other phyla may be underestimated.

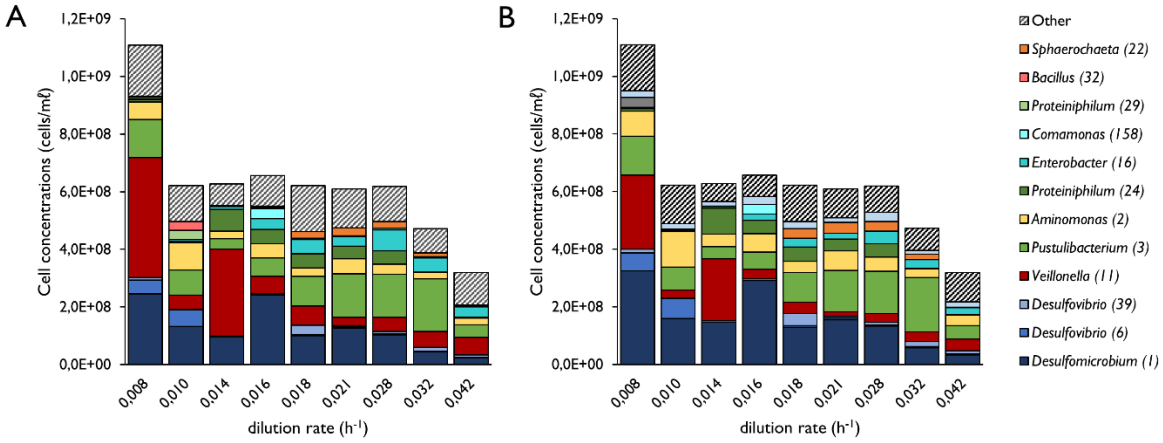


Figure 4-12 The estimated cell concentrations of the most dominant OTUs in the lactate CSTR at each tested dilution rate, assuming 16S rRNA gene copy numbers are (A) uniform across all identified microorganisms or (B) varied by phyla as described by Baldrian (2013). Largest variations between the two assumed copy numbers distributions occurred when Firmicutes (*Veillonella* (11), red) were abundant.

### 4.3.6 Low but stable SRB diversity maintained with increasing dilution rate

The most abundant OTUs in the lactate-supplemented CSTR were largely maintained at each HRT, with the majority of these OTUs persisting at the final one-day HRT (0.042 $h^{-1}$; Figure 4-13). Two exceptions to this are *Spirochaeta* (22) and *Proteiniphillum* (24) which were present from a five-day HRT (0.008 $h^{-1}$) but not detectable at a one-day (0.042 $h^{-1}$) and a 1.3-day HRT (0.032 $h^{-1}$), respectively. The presence of the majority of the predominant OTUs at each tested dilution

rate indicates that the resulting microbial community structure is largely a result of competition between all these microorganisms and that each of these microorganisms have a maximal growth rate greater than all tested dilution rates.

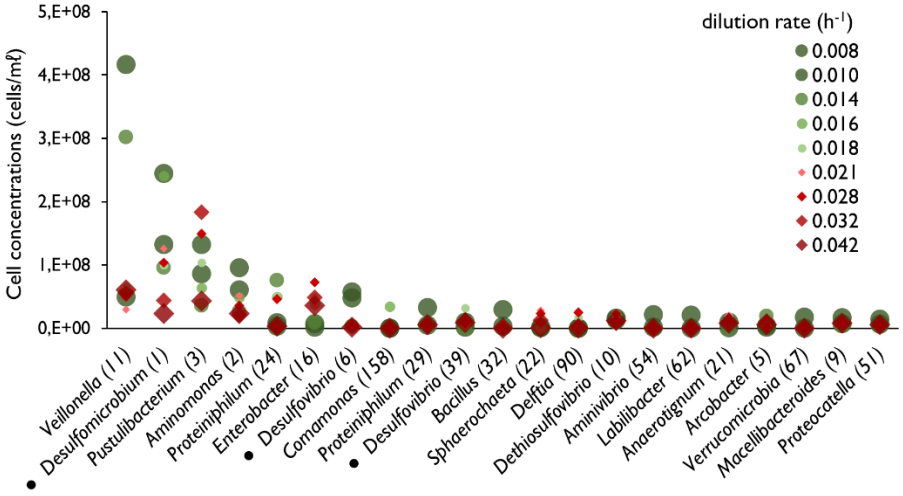


Figure 4-13 Rank abundance curves showing the estimated cell concentration of the 21 most abundant OTUs in the lactate-supplemented CSTR over the course of the HRT study. The dilution rate of each rank abundance curve is shown in the legend. OTU identified as SRB are indicated (●).

## 4.4 Acetate CSTR Results

The following sections describe the performance of the acetate CSTR across the tested dilution rates applied to the system with a constant sulphate (1.0 g/ℓ or 10.41 mM) and acetate (0.72 g/ℓ / 12.2 mM) concentration. The cell concentrations supported by the CSTR are shown, followed by the 16S rRNA amplicon sequencing results which describe the microbial community structure of the system at phylum- and class- taxonomic levels followed by the abundances and classification of the dominant OTUs in the reactor system.

### 4.4.1 Reactor performance

The acetate CSTR maintained a sulphate conversion (Figure 4-14 A) of 37% at a five-day HRT (0.008 $h^{-1}$). This conversion gradually improved with increasing dilution rate until a 51% sulphate conversion was achieved at a 2.3-day HRT (0.018 $h^{-1}$). The sulphate conversion then gradually decreased from a 2.3-day HRT until a 1.3-day HRT was reached (0.032 $h^{-1}$) where the conversion had decreased to 25%. With further reduction in HRT, to one-day (0.042 $h^{-1}$), the conversion

remained consistent at 23%. The expected sulphide concentration, from the determined sulphate reduced, had an average of 5% difference with the measured sulphide concentration.

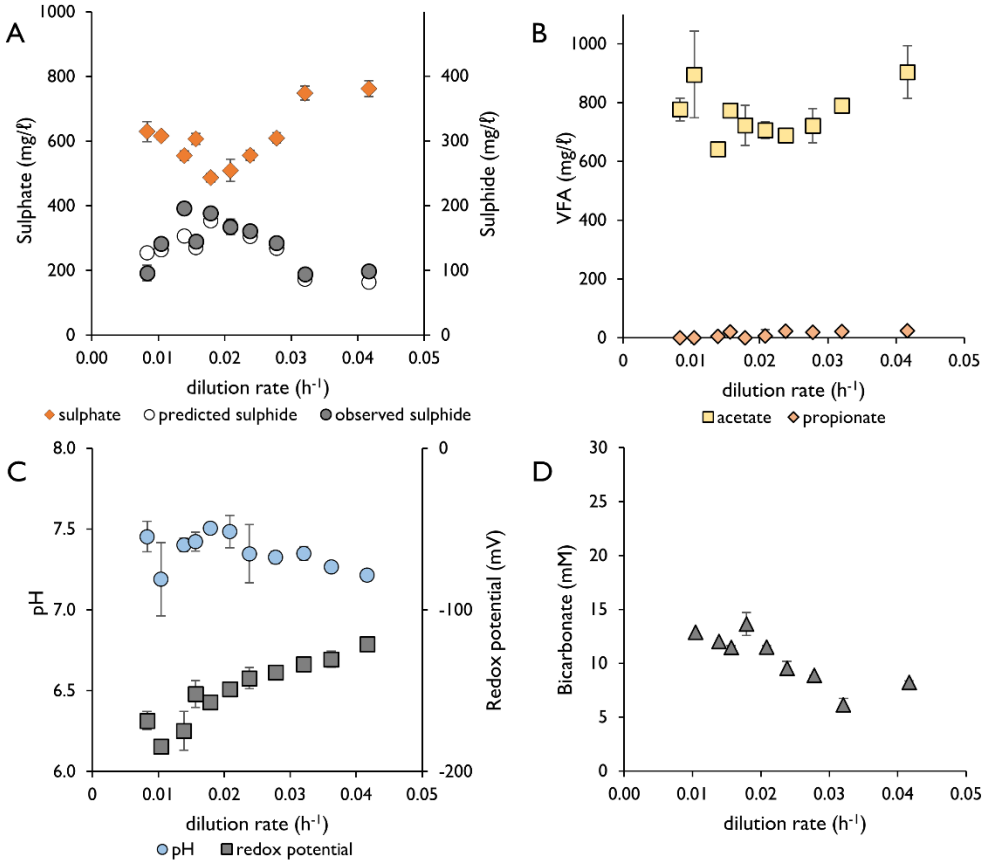


Figure 4-14 Steady-state kinetic data of the acetate-supplemented CSTR at a range of tested dilution rates, including (A) the residual sulphate, the produced sulphide and the predicted sulphide concentration based on the observed sulphate reduced; (B) the observed volatile fatty acid profile; (C) pH and redox potential (reported relative to a standard hydrogen electrode); and (D) the produced bicarbonate concentration calculated from the difference between the observed and feed bicarbonate concentrations.

The VFA profile (Figure 4-14 B) showed similar trends to that seen in the concentration of sulphate. The observed acetate concentration at a five-day HRT (0.008 $h^{-1}$) was 723 mg/ℓ (12.04 mM). An overall gradual decrease in the acetate concentration between a five- and 1.75-day HRT (0.008-0.024 $h^{-1}$) was observed. The acetate concentration then increased linearly with increasing dilution rate until a maximum observed concentration of 904 mg/ℓ (15.05 mM) was seen at a one-day HRT (0.042 $h^{-1}$). Citrate, incorporated in the reactor feed, was not detected in the reactor at any HRT. Low concentrations of propionate were detected, with an average

concentration of 12 mg/ℓ (0.16 mM) and a maximum of 23 mg/ℓ (0.31 mM) observed at a one-day HRT (0.042 $h^{-1}$).

The redox potential (Figure 4-14 C) within the reactor was highly negative, below -120 mV for the duration of the study indicating a highly anaerobic environment was maintained. Neutral conditions also persisted with a pH of 7.7 at a five-day HRT (0.008 $h^{-1}$) and decreased gradually with increasing dilution rate to 7.2 at a one-day HRT (0.042 $h^{-1}$).

The concentration of bicarbonate (Figure 4-14 D) decreased linearly with increasing dilution rate from 13 mM at a five-day HRT (0.008 $h^{-1}$) to 6 mM at a 1.3-day HRT (0.032 $h^{-1}$), before increasing to 8 mM at a one-day HRT (0.042 $h^{-1}$).

The acetate CSTR supported approximately 2.4 x $10^8$ cells/mℓ at a five-day HRT (0.008 $h^{-1}$; Figure 4-15). The supported cell concentration showed an undulating increase with increasing dilution rate, reaching a maximum of 4.6 x $10^8$ cells/mℓ at a 1.3-day HRT (0.032 $h^{-1}$).

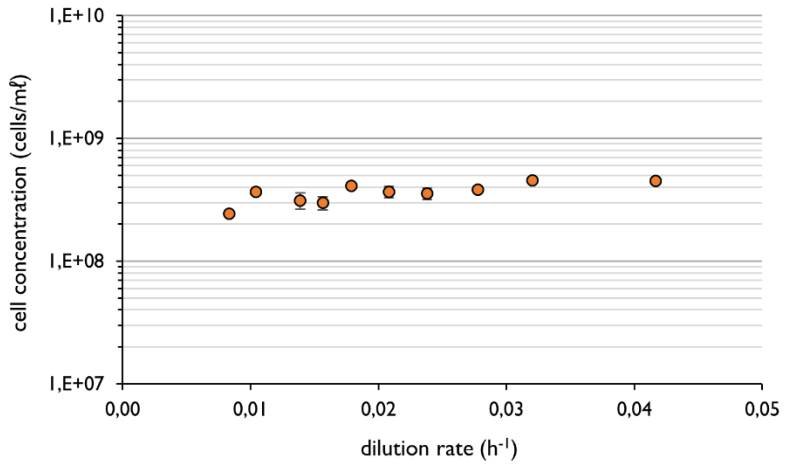


Figure 4-15 The microbial cell concentration supported by the acetate-supplemented CSTR at each tested dilution rate determined through direct cell counting. Error bars represent one standard deviation from the mean of duplicate samples each counted in duplicate.

### 4.4.2 Contribution of yeast extract to acetate generation

The acetate CSTR was operated at a five-day HRT for an extended period, prior to the start of the HRT study. It was observed, over a period defined as steady-state, that the residual acetate concentration was approximately 1200 mg/ℓ (21 mM; Figure 4-16). This was far greater than expected given acetate was included in the reactor medium at 720 mg/ℓ (15.6 mM), and the reactor was achieving a sulphate conversion of 46%, therefore, acetate was also being consumed. Subsequently, the yeast extract concentration in the medium was reduced from 1.0 to 0.4 g/ℓ. This

resulted in the residual acetate concentration in the reactor decreasing from 1200 to 770 mg/ℓ (13.2 mM). The generation of acetate per gram of yeast extract was estimated based on the observation that removing 0.6 g/ℓ yeast extract in the reactor medium resulted in the reduction in acetate concentration by 520 mg/ℓ (8.66 mM). Several assumptions were made with these calculations: all sulphate reduction was solely linked to acetate oxidation; 0.4 g/ℓ yeast extract was not growth-limiting; and all yeast extract was oxidised to acetate in this reactor at this five-day HRT (0.008 $h^{-1}$). The sulphate conversion decreased from 46 to 37% and the difference in degree of assumed sulphate linked acetate oxidation was considered. This allowed the approximate concentration of acetate generated from the 0.4 g/ℓ yeast extract which was incorporated in the feed to be estimated to be 268 mg/ℓ (4.54 mM) or 0.67 g acetate per 1 g of yeast extract.

Yeast extract was included in the reactor medium as a source of vitamins, trace metals and amino acids. Although not incorporated to act as an electron donor, yeast extract has been shown to be an effective electron donor for sulphate reduction (Sáez- Navarrete et al., 2009). However, the gradual increase in the residual sulphate of only 90 mg/ℓ (0.94 mM), when the yeast extract concentration was reduced by 60% indicates that this is not the primary electron donor for sulphate reduction. Instead, it is more likely that SRB benefit indirectly, consuming the products of yeast extract oxidation performed by other microorganisms.

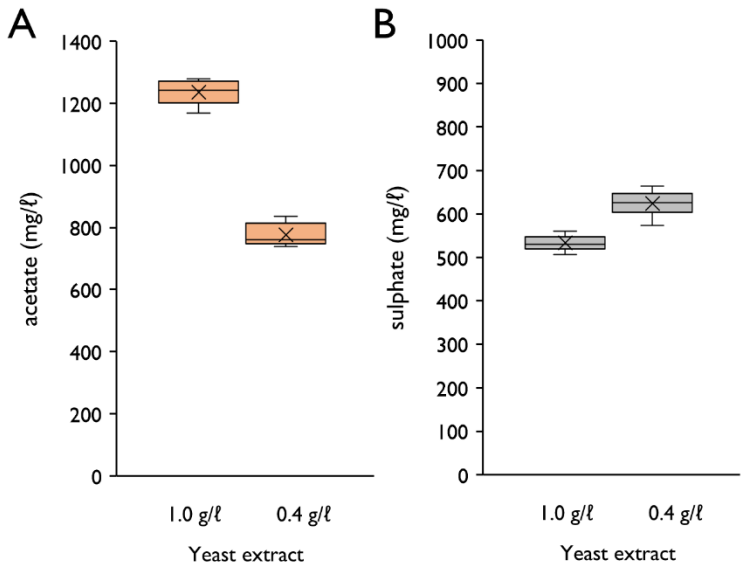


Figure 4-16 The steady-state residual (A) acetate and (B) sulphate concentration in the acetate-supplemented CSTR, at a five-day HRT, following the reduction in the yeast extract concentration, supplemented in the feed, from 1.0 to 0.4 g/ℓ. The data are displayed as boxplots showing the interquartile ranges of each reading during the defined steady-state period. The mean acetate and sulphate concentrations are shown as a cross.

### 4.4.3 Microbial ecology

The acetate CSTR microbial community (Figure 4-17), for the duration of the HRT study, was largely made up of the phyla Proteobacteria, Bacteroidetes, Synergistetes and Spirochaetes. Verrumicrobia were in high abundance at four- and three-day HRT (0.010 and 0.014 $h^{-1}$), before decreasing in abundance with increasing dilution rate. Spirochaetes showed considerable change in abundance throughout the study, appearing at 4% relative abundance at a five-day HRT, before increasing to 48% at a 1.5-day HRT (0.028 $h^{-1}$) and maintaining this dominance at a one-day HRT (0.042 $h^{-1}$). Bacteroidetes showed the inverse trend, decreasing in abundance with shortening HRT. All OTUs classified as Deltaproteobacteria were identified as SRB. In addition to the SRB classified as Deltaproteobacteria, a *Desulfitobacterium* (222), belonging to the phylum Firmicutes, was also found at low relative abundances in this reactor throughout the HRT study. The proportion of the community which was represented by SRB changed intermittently with increasing dilution rate, making up a maximum of 14% and a minimum of 3% over the HRT study.

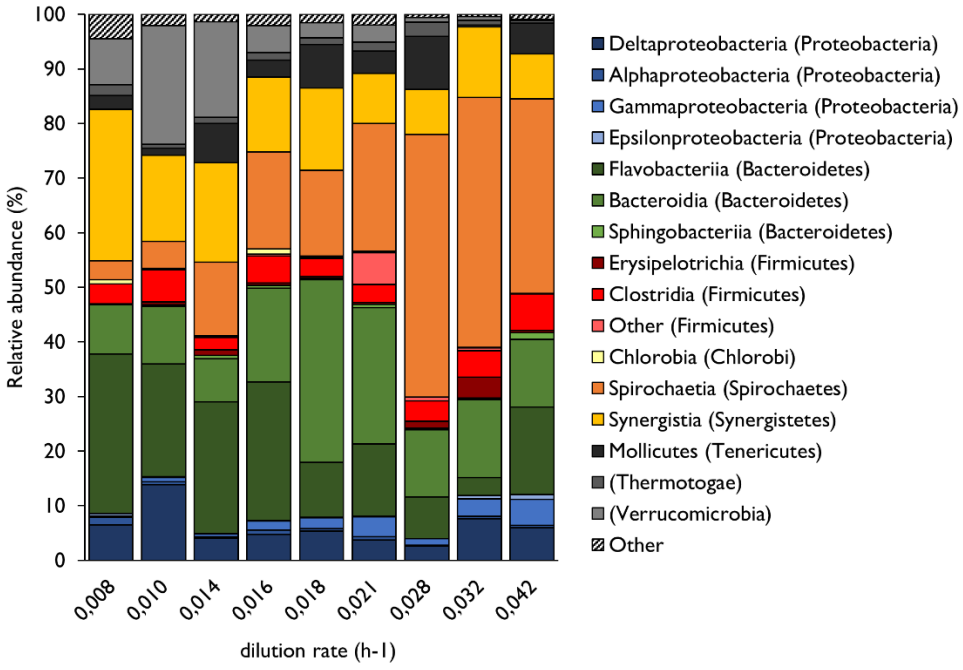


Figure 4-17 The relative abundance of the classes and phyla identified in the acetate supplemented CSTR microbial community at a range of tested dilution rates, determined by 16S rRNA gene amplicon sequencing. Phyla are shown in parentheses.

The community structure of the acetate CSTR at the OTU level (Figure 4-18) showed that members which were dominant at longer HRT were outcompeted by lower abundant OTUs at shorter HRT. Most notably, a Spirochaetes, *Sphaerochaeta* (22), was present at low cell

concentrations at a five-day HRT (0.008 $h^{-1}$) but became the most dominant organism in the reactor from a 1.5-day HRT (0.028 $h^{-1}$). Inversely Verrumicrobia (67), was the most dominant organism in the reactor at a four-day HRT (0.010 $h^{-1}$) but decreased in cell concentration at subsequent shorter HRT. Two SRB were detected in this reactor above 1% relative abundance, namely *Desulfomicrobium* (1) and *Desulfovibrio* (6). The *Desulfovibrio* was the dominant SRB in the reactor at a five-day HRT (0.008 $h^{-1}$) but was observed to be washed out of the reactor between a four- and three-day HRT (0.010 and 0.014 $h^{-1}$, respectively). Inversely the *Desulfomicrobium* increased from low abundance at a five- and four-day HRT to become the dominant SRB in the system from a three-day HRT (0.014 $h^{-1}$).

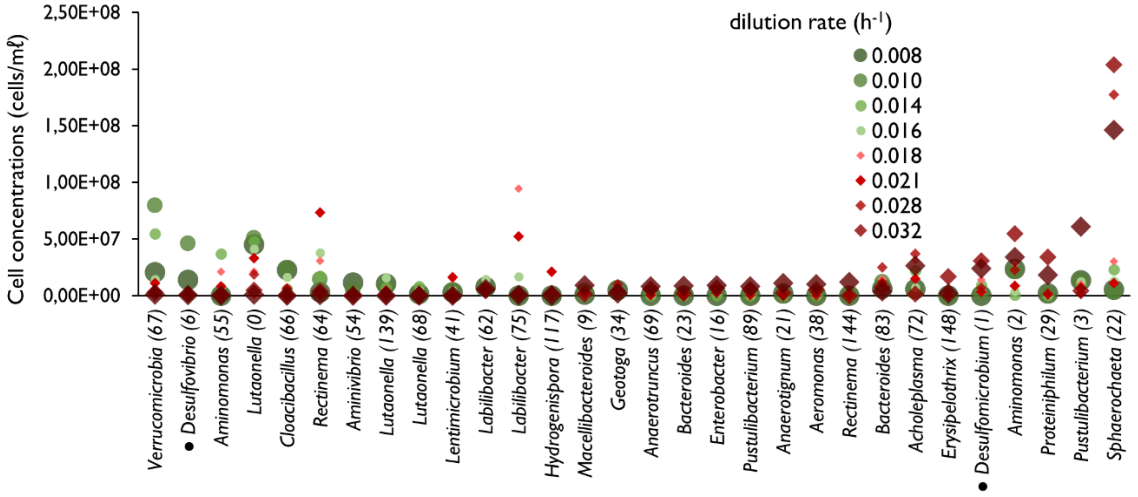


Figure 4-18 Rank abundance curves of the estimated cell concentrations of the dominant OTUs present in the acetate supplemented CSTR, determined by 16S rRNA gene amplicon sequencing at a range of dilution rates. Tested dilution rates are shown in the legend. OTU reference numbers are shown in parentheses. Sulphate-reducing bacteria are indicated (•).

In addition to the two dominant SRB, namely *Desulfovibrio* (6) and *Desulfomicrobium* (1), several lower abundant SRB were also detected in the reactor (Figure 4-19). Collectively these microorganisms showed the greatest abundance between a three- and two-day HRT (0.014 – 0.021 $h^{-1}$) and show a marked reduction at a 1.5- through to a one-day HRT (0.028 – 0.042 $h^{-1}$). The most prominent of these low abundance SRB, which exhibited washout between the described HRT, are *Desulfovibrio* (108), *Desulfitobacterium* (222), *Desulfobacter* (18) and *Desulfobulbus* (58).

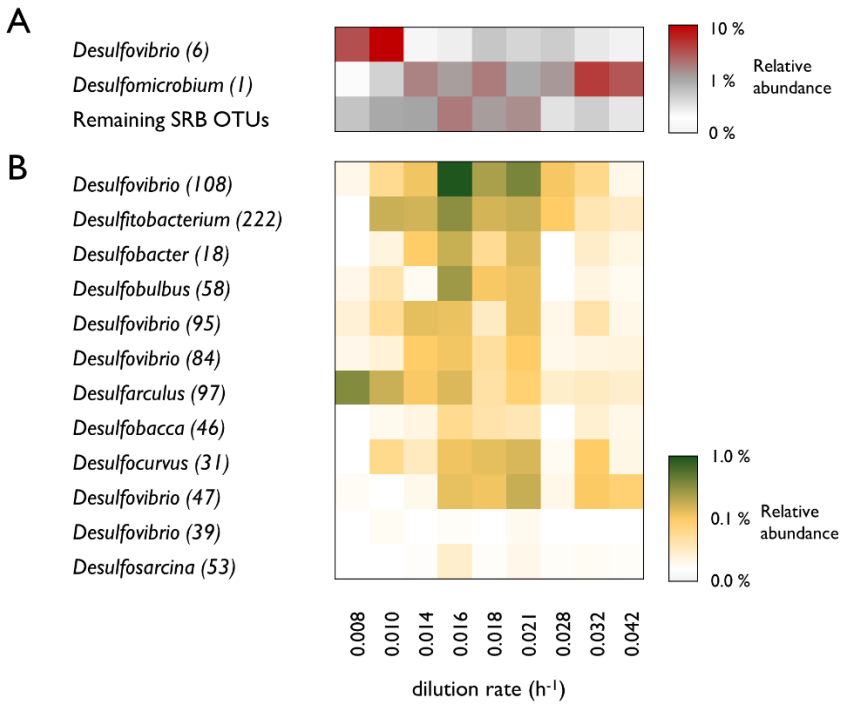


Figure 4-19 The relative abundance of the OTUs identified as SRB in the acetate-supplemented CSTR which appear in this system (A) at greater than 1% compared to the summed remaining SRB OTUs, and (B) SRB OTUs which appear at less than 1%, as a function of dilution rate.

## 4.5 Acetate CSTR Discussion

The following sections discuss the performance exhibited by the acetate CSTR compared with similar studies presented in the literature. The exhibited sulphate reduction is overlaid with the VFA profile. The resulting microbial communities cell concentrations and the 16S rRNA gene sequencing results are subsequently discussed.

### 4.5.1 Achieved VSRR and literature context

The VSRR performance of the acetate CSTR (Figure 4-20 A) can be described as three sequential phases. Between a five- and 2.6-day HRT (0.008 - 0.016 $h^{-1}$), the VSRR increases linearly with increasing VSLR, with an average sulphate conversion of 40%. The sulphate conversion then abruptly increases to 51% at a 2.3-day HRT (0.018 $h^{-1}$), corresponding to a VSRR of 9.1 mg/ℓ.h, increasing from 6.2 mg/ℓ.h at a 2.6-day HRT (0.016 $h^{-1}$). The exhibited VSRR plateaus from a 2.3-day HRT to a 1.5-day HRT, with the VSRR increasing with smaller increments between each subsequent HRT. A substantial reduction in the VSRR was then observed between a 1.5- and 1.3-day HRT (0.028 - 0.032 $h^{-1}$) decreasing from 10.8 to 8.1 mg/ℓ.h. The VSRR of 8.1 mg/ℓ.h corresponded to a sulphate conversion of 25%. This conversion remained relatively stable at a

one-day HRT (0.042 $h^{-1}$). The reduction in the VSRR from a 1.5- to 1.3-day HRT (0.028 - 0.032 $h^{-1}$) corresponded with the washout of a number of low-abundance SRB described in Section 4.4.3.

Moosa et al. (2002) presented the results from a similarly operated acetate supplemented CSTR, differing in operating temperature (35°C) and media composition but with 1 g/ℓ sulphate and 2.5 g/ℓ sodium acetate. This reactor exhibited considerably different performance (Figure 4-20 A). A constant VSRR was achieved between a five- and 3.7-day HRT (0.008 - 0.011 $h^{-1}$), corresponding to a decrease in sulphate conversion from 88 to 66%. The VSRR decreased with each further reduction of the HRT with eventual abolishment of sulphate reduction between a 2.5- and two-day HRT (0.017 - 0.021 $h^{-1}$).

The growth of a number of acetate-oxidising SRB described by O'Flaherty et al. (1998), and a mixed microbial sulphate reducing culture described by Vavilin et al. *(*1994), were modelled using the reported kinetic constants ($K_S$ for sulphate; $\mu_{max}$), as steady-state cultures operated under conditions used in this study (dilution rates of 0.008 - 0.042 $h^{-1}$; 1 g/ℓ sulphate; excess acetate) as described in Section 3.7.2 (Figure 4-20 B). The Deltaproteobacteria *Desulfuromonas acetoxidans* was one example, described by Flaherty (1998), of an acetate-oxidising SRB which would be capable of maintaining growth, and therefore sulphate reducing performance at HRT shorter than one-day (0.042 $h^{-1}$) under the operating conditions employed in this study. Whereas *Desulfobacter postgatei* and *Desulfonema magnum* would have experienced washout at an HRT of 1.1 days (0.037 $h^{-1}$) and 2.4 days (0.017 $h^{-1}$) respectively. The SRB within the mixed microbial community described by Vavilin et al. (1994) would theoretically have experienced washout at a 1.6-day HRT (0.026 $h^{-1}$). These examples demonstrate that it is feasible that some SRB may be able to sustain growth rates up to 0.042 $h^{-1}$ using acetate as a sole electron donor but this is not common.

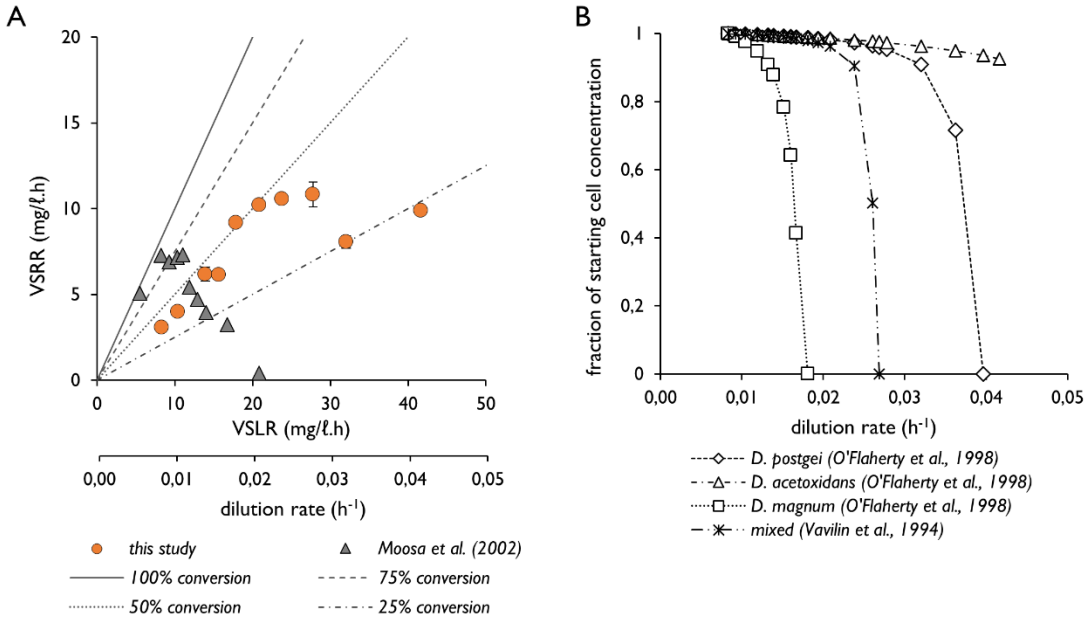


Figure 4-20 Steady-state VSRR achieved by the acetate-supplemented CSTR of this study, at a range of tested dilution rates, (A) plotted against the applied VSLR and alongside the VSRR achieved by the similarly operated CSTR reported by Moosa et al. (2002) (1 g/ℓ sulphate, 2.5 g/ℓ acetate and 35°C) with theoretical sulphate conversions plotted, and (B) the modelled fraction (Section 3.7.2) of a starting cell concentration of a range of acetate-oxidising SRB (Flaherty et al., 1998) and the mixed SRB community described by Vavilin et al. (1994) over the same dilution rates and experimental conditions used in this study.

The contrasting performance of the CSTR operated in this study and that of Moosa et al. (2002) (Figure 4-20 A) may simply be the result of differing SRB ecology between the two systems. However, the major difference in operation of the CSTRs between these two studies is the supplementation of yeast extract in this study. Yeast extract was concluded to not be a direct substrate for sulphate reduction in Section 4.4.2, due to the stability in sulphate reducing performance immediately following the reduction in the yeast extract concentration from 1.0 to 0.4 g/ℓ. The constituents of yeast extract may not be directly linked to sulphate reduction, instead, the breakdown of these constituents is hypothesised to provide an indirect, supplementary, electron donor for sulphate reduction in the form of hydrogen. Substantial evidence for this theory is provided through genome-resolved metagenomics of this CSTR community. This is expanded in Section 4.5.4 of this chapter and Section 8.11 of Chapter 8, Metagenomics.

### 4.5.2 Sulphate reduction is linked to acetate oxidation

The residual acetate concentration in the acetate-supplemented CSTR is plotted below, alongside three different predicted acetate concentrations (Figure 4-21). These predictions are made assuming all sulphate reduced was linked to acetate oxidation as described by Equation 2-7. The

feed acetate concentration was 12.2 mM and therefore the reduction of approximately 4 mM of sulphate, at a five-day HRT (0.008 $h^{-1}$), is predicted to correspond to a residual acetate concertation of 8.2 mM. However, as discussed in Section 4.4.2, the inclusion and oxidation of yeast extract in the reactor medium led to the generation of approximately 4.6 mM of acetate. This is included in the second predicted acetate concentration and is largely in agreement with the observed residual acetate concentration. The similar trend across the tested dilution rates between the predicted and observed residual acetate concentrations provides evidence that supports the assumption that the observed sulphate reduction is linked to acetate oxidation, and the oxidation of yeast extract to acetate is performed by a second group of microorganisms. A third acetate concentration was predicted which, in addition to the feed and yeast extract derived acetate, accounted for the theoretical amount of acetate which could have arisen from the complete oxidation of the 1.16 mM of citrate in the reactor medium. This represents a theoretical maximum and any observed acetate concentration above this prediction would disprove the assumption that all sulphate reduced is linked to acetate oxidation. This predicted residual acetate concentration is greater than the observed at every tested dilution rate. This indicates that citrate was oxidised completely at most HRT.

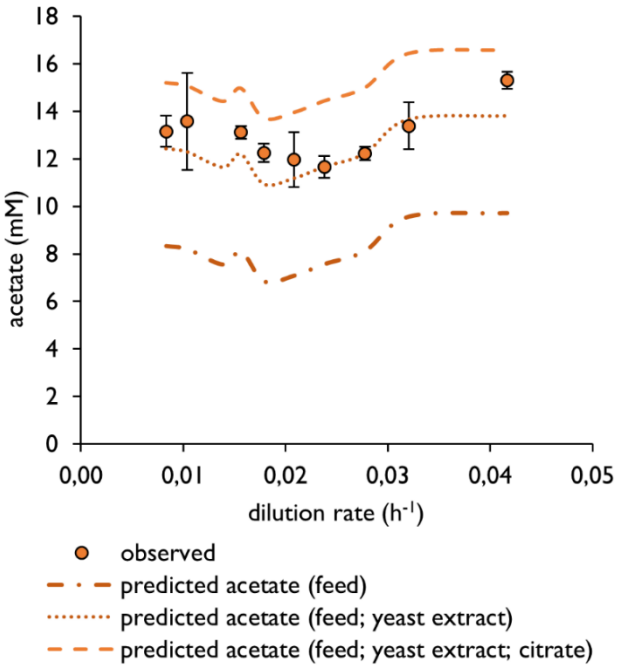


Figure 4-21 The observed and predicted acetate concentration within the acetate-supplemented CSTR at a range of tested dilution rates. The predicted acetate concentrations are determined by subtracting the theoretical amount of acetate oxidised by SRB according to Equation 2-7, from the sum of the amount of acetate supplied in the feed, arising from yeast extract oxidation (Section 4.4.2) and from the theoretical maximum concentration of acetate arising from the oxidation of citrate. Error bars represent one standard deviation from the mean ($n$>4).

### 4.5.3 Enhanced sulphate reduction linked to low-abundance acetate-oxidising SRB

The two most dominant SRB OTUs, namely *Desulfovibrio* (6) and *Desulfomicrobium* (1), show the greatest cell concentrations at a four- and 1.3-day HRT (0.010 and 0.032 $h^{-1}$), respectively (Figure 4-22 A). The cell concentration of *Desulfovibrio* (6) decreased by nearly 100-fold between a four- and three-day HRT (0.010 - 0.014 $h^{-1}$), after which *Desulfomicrobium* (1) became the dominant SRB OTU in the system. However, the combined cell concentrations of the lower abundance SRB OTUs increased from a five-day HRT (0.008 $h^{-1}$) and collectively become greater than that of *Desulfomicrobium* (1) at a 2.6-day HRT (0.016 $h^{-1}$). The concentration of residual acetate in the CSTR decreased between a four- and two-day HRT (0.008 - 0.021 $h^{-1}$), from 13.6 to 12.0 mM, respectively (Figure 4-22 A). The increased apparent acetate oxidation and the improved sulphate conversion seen between a four- and 1.5-day HRT (0.010 - 0.028 $h^{-1}$; Figure 4-22 B) corresponds with increased cell concentration of these low-abundance SRB. The cell concentration of *Desulfomicrobium* (1) and the sum of the lower abundance SRB OTUs inversely oscillate between a three- and 1.5-day HRT (0.010 - 0.028 $h^{-1}$) - a strong indication of competition between these two groups for one or more substrates. From a 1.75-day HRT (0.024 $h^{-1}$), the acetate concentration increased linearly to a maximum observed concentration of 15.31 mM at a one-day HRT (0.042 $h^{-1}$) and corresponds with the reduced sulphate conversion over these HRT and the reduction in cell concentration of low-abundance SRB OTUs.

The greater cell concentrations of *Desulfovibrio* (6) at a four-day HRT (0.010 $h^{-1}$) and *Desulfomicrobium* (1) at a 1.3- to 1.0-day HRT (0.032 - 0.042 $h^{-1}$), with the lowest observed sulphate conversions (Figure 4-22 B), indicate that these high-abundance SRB have a higher biomass yield per unit of sulphate. Inversely, the low abundance SRB OTUs which collectively become abundant at and between a 2.6- and 2.0-day HRT (0.016 - 0.021 $h^{-1}$) collectively have a far lower biomass yield per unit sulphate compared to *Desulfovibrio* (6) and *Desulfomicrobium* (1).

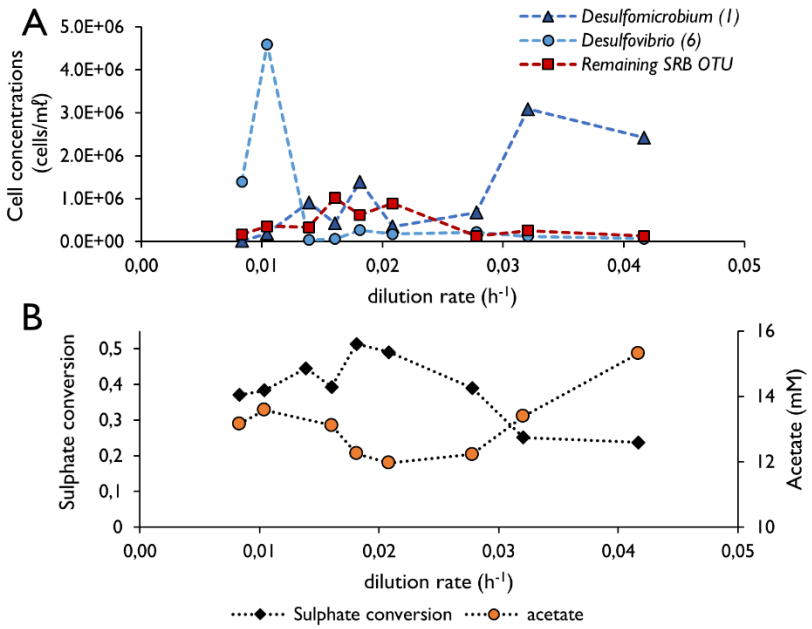


Figure 4-22 The (A) competition between the two dominant SRB OTUs, *Desulfovibrio* (6) and *Desulfomicrobium* (1), and the sum of the remaining SRB OTUs shown as estimated cell concentrations; and (B) the achieved sulphate conversion and residual acetate concentrations at varied applied dilution rates.

### 4.5.4 Mixotrophic sulphate reduction

Several results from this chapter and from genome-resolved metagenomics (Chapter 8) suggest that acetate may not have been the sole electron donor for the observed sulphate reduction. These include the maintained sulphate reducing performance at dilution rates greater than the expected maximal SRB growth rate, the distribution of hydrogen-consuming and -evolving hydrogenase genes amongst the CSTR microbial community (Section 8.5.5), the carbon fixation pathways found within SRB genomes (Section 8.5.4) and the low bicarbonate concentrations in the reactors Figure 4-23.

The bicarbonate produced in the reactor is plotted in Figure 4-23-A against the predicted bicarbonate concentration. The predicted 'produced bicarbonate' concentration assumes all bicarbonate produced arises from the observed sulphate reduction, which is assumed to be entirely linked to acetate oxidation. This predicted bicarbonate concentration assumes no additional bicarbonate generation by microorganisms other than SRB. As SRB constituted only 3 - 14% of the entire microbial community, this assumption provides a still unrealistic minimum concentration of produced bicarbonate in the reactor. This assumption also does not consider the bicarbonate generated through yeast extract and citrate oxidation. The observed bicarbonate concentration and the bicarbonate concentration predicted based on acetate-linked sulphate

reduction show little difference between a two- and 1.3-day HRT (0.021 - 0.032 $h^{-1}$). Therefore, bicarbonate produced by non-SRB, 86 - 97% of the remaining microbial community, is unaccounted for. This phenomenon is not observed in the lactate CSTR (Figure 4-23 B) which had a nearly two-fold greater observed bicarbonate concentration than predicted from the degree of total lactate oxidation throughout the HRT study. This phenomenon suggests that a larger proportion of feed carbon was incorporated into cell biomass in the acetate system. The meachnaism for this is not yet understood but it is proposed that the unaccounted-for bicarbonate in the acetate CSTR may have fixed by autotrophic bacteria, potentially including autotrophic SRB. More evidence to substantiate this theory is described in Section 8.5.4 (Chapter 8, Metagenomics) but is discussed briefly below.

Two metabolic pathways involved in carbon fixation were identified in the CSTR metagenome including the reverse-TCA and Wood–Ljungdahl pathways. These were found in several SRB genomes. Evaluations of the genomes present in the CSTRs at a four-day HRT revealed that a number of non-sulphate reducing microorganisms, present in both acetate and lactate supplemented systems, were capable of amino acid oxidation and citrate uptake and oxidation. These microorganisms also contained hydrogen-evolving hydrogenases further indicating their role in substrate fermentation. Hydrogen consuming hydrogenases were commonly found within the same genomes as those with autotrophic pathways - many of which were SRB. It was concluded that these facultative autotrophic microorganisms consumed hydrogen and potentially fixed produced bicarbonate.

As discussed in this chapter acetate oxidation was prominent. This led to the development of the BSR mixotrophic metabolic model. In this model, sulphate reduction is coupled to both acetate oxidation and to hydrogen consumption. This form of metabolism in SRB is not novel and has been discussed in pure and co-culture (Abram and Nedwell, 1978; Badziong et al., 1979; Eselsberg 1987). However, this is rarely discussed in the context of mixed SRB enrichment cultures nor passive wastewater remediation.

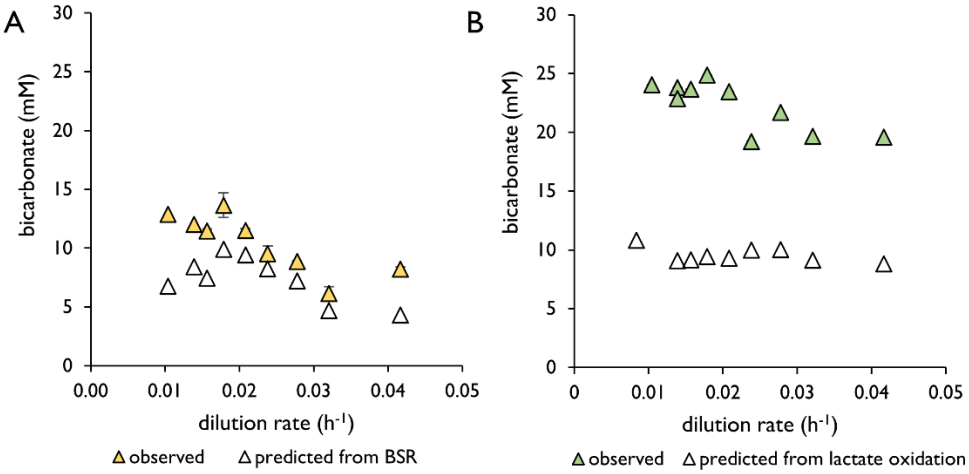


Figure 4-23 Steady-state bicarbonate concentrations observed in the (A) acetate- and (B) lactate-supplemented CSTRs across a range of dilution rates, plotted against the predicted bicarbonate concentration in each CSTR. Error bars represent one standard deviation from the mean (*n*=2). In the acetate system, the predicted bicarbonate concentration is calculated assuming only acetate-linked sulphate reduction (Equation 2-7), whilst in the lactate system, the prediction is based on the sulphate reduction linked to incomplete lactate oxidation (Equation 2-10) lactate fermentation (Equation 2-12) and acetate oxidation by SRB (Equation 2-7) as shown in Figure 4-7.

## 4.6 Conclusions

Both the acetate- and lactate-supplemented CSTRs showed comparable performance throughout the HRT study compared to other studies presented in the literature. The lactate CSTR maintained an average of 55% sulphate conversion between a five- and 1.5-day HRT and demonstrating a maximum VSRR of 16.8 mg/ℓ.h at a one-day HRT (0.042 $h^{-1}$). The acetate CSTR maintained sulphate reduction for the duration of the tested dilution rates, exhibiting an average sulphate conversion of 45% between a four- and 1.75-day HRT (0.010 - 0.024 $h^{-1}$), with a maximum exhibited VSRR of 10.8 mg/ℓ.h at a 1.5-day HRT (0.028 $h^{-1}$). The sulphate conversion then decreased to 25% at a 1.5- and 1.3-day HRT (0.028 and 0.032 $h^{-1}$). These results indicate competitive and robust SRB cultures.

A CSTR provides a uniform selective pressure throughout the reactor and selects for a solely-planktonic microbial community. This combined with the simple carbon sources used in this study makes the level of the diversity in the SRB identified, although at low cell concentrations, surprising. *Desulfomicrobium* (1) and *Desulfovibrio* (6) were identified at high abundance in both the acetate- and lactate-supplemented systems and each demonstrates similar trends in cell concentrations with increasing dilution rates between the two systems. From both the systems it can be concluded that these OTU have a high biomass yield coefficient, per unit of sulphate,

compared to collective low-abundance SRB OTUs. The performance of both systems is, therefore, attributed to both the high abundant OTU and collectively, the low-abundant SRB OTUs.

The community structure of the acetate system was impacted greatly by the increase in dilution rate, exhibiting a nearly total change in the community structure between a five- and one-day HRT. However, the approximately six most abundant OTUs in the lactate system remain in the reactor for the duration of the study, but at reduced cell concentrations at short HRT.

Within the lactate-supplemented CSTR, the competition between lactate-oxidising SRB and fermentative microorganisms was effectively monitored through both physiochemical data and 16S rRNA gene sequencing data. The bulk of the sulphate reduction seen in this reactor could be attributed to incomplete lactate oxidation. The remainder of the sulphate reduction was presumed to be linked to acetate oxidation. Within the acetate-supplemented system, the sulphate reduced was attributed to primarily acetate oxidation. However, the low bicarbonate concentrations, the metagenomic evidence of hydrogen metabolism and autotrophy within this community, and the sustained sulphate reducing performance at high dilution rates indicates that mixotrophic sulphate reduction is likely occurring. This is thought to include acetate oxidation, the oxidation of hydrogen produced by fermentative microorganisms and possibly the fixation of bicarbonate produced through the degradation of organic compounds within the reactor. This hypothesised metabolic theory is discussed further in Section 8.11 of Chapter 8.

# Chapter 5 Linear flow channel reactors

## 5.1 Introduction

### 5.1.1 Background

The linear flow channel reactor (LFCR) was first developed by Molwantwa and Rose (2013) to perform long-term biological sulphate reduction for the remediation of ARD. This reactor system was further developed by van Hille et al. (2011), as a hybrid LFCR, to perform simultaneous sulphate reduction and sulphide oxidation. The oxidation of the sulphide, producing chemically stable elemental sulphur, takes place at the liquid-air interface producing a floating sulphur biofilm. This prevents oxygen ingress into the bulk volume and allows the reactor to become anaerobic. This was incorporated into the process to limit the amount of toxic sulphide which was discharged from the reactor and allow the recovery of sulphur, a product with monetary value. Complete mixing within this reactor, well within a single hydraulic residence time, is achieved passively thereby transporting sulphide generated by SRB in the bulk liquid to the surface where it is oxidised (Marais et al., 2017; this study - Appendix A-2). Harrison et al. (2014) and Van Hille et al. (2016) further improved the reactor configuration by incorporating carbon microfibres anchored to a stainless steel frame which spans the length of the reactor. This increased the internal surface area for microbial colonisation and biofilm formation, allowing for the decoupling of the hydraulic and biomass retention times. The performance of this hybrid sulphate-reducing and sulphide-oxidising system has been demonstrated using both acetate and lactate as electron donors (Marais et al., 2017; Marais et al., 2020). The purpose of the overall study is to investigate the microbial communities associated with BSR and therefore the LFCRs were sealed from the atmosphere - preventing the activity of sulphur-oxidising bacteria and associated communities. The LFCRs also provide a unique environment to study the development of the respective microbial communities – the planktonic and biofilm communities within a well-mixed bioreactor at varied HRT. The physiochemical conditions generated by the LFCR contrasts the well-mixed CSTRs which do not support any biofilm communities and contrasts the UAPBRs which support both planktonic and biofilm communities but are governed by plug-flow hydrodynamics and therefore the reactions and reaction rates within these reactors vary spatially.

### 5.1.2 Experimental approach

The LFCRs were simultaneously inoculated, along with the two CSTRs and two UAPBRs, from the same composite culture originating from a number of stock reactors (Section 3.4.1). The LFCRs were initially operated at a four-day HRT. The reactors, although demonstrated to be relatively well-mixed, were demarcated into two zones of equal volume which were sampled independently for physicochemical data and metagenomic DNA to verify that the conditions within these two zones were the same. Due to the little difference between the solution chemistry and microbial ecology between these two zones, results obtained from the effluent zone are shown unless stated.

Once a period defined as steady-state had been observed the HRT was iteratively reduced as described in Section 3.4. Steady-state physiochemical data was collected as described in Section 3.5. At each steady-state, the concentration of planktonic cells was determined through direct cell counting. The attached and associated biofilm communities were quantified using the developed detachment and quantification protocol (Section 3.6) and the community dynamics assessed through 16S rRNA metagenomic sequencing at the initial and final four- and one-day HRT, respectively. This was performed only twice to minimise the impact of oxygen and desiccation stresses on the microbial communities associated with these reactors. The microbial communities assessed through genome-resolved metagenomics (reported in Chapter 8 ) and 16S rRNA gene amplicon sequencing are described in Section 5.2.2 and 5.4.2.

## 5.2 Lactate LFCR Results

The following sections describe the performance (Section 5.2.1) of the lactate-supplemented LFCR across the range of dilution rates applied to the system with a constant sulphate (1.0 g/ℓ or 10.41 mM) and lactate (1.2 g/ℓ or 13.3 mM) concentration in the feed. The cell concentrations supported by the LFCR in the planktonic and biofilm phases are reported (Section 5.2.1). The results of the 16S rRNA gene amplicon sequencing (Section 5.2.2) are presented which describe the microbial community structure of these communities at a phylum- and class- taxonomic levels (Section 5.2.2), followed by the abundances and classification of the dominant OTUs in the system (Section 5.2.2).

### 5.2.1 Reactor performance

The lactate-supplemented LFCR achieved a maximum sulphate conversion of 76% at a four-day operated HRT (0.010 $h^{-1}$; Figure 5-1A). This corresponded to a VSRR of 7.9 mg/ℓ.h (Figure 5-2) at a VSLR of 10.4 mg/ℓ .h. Reduction in the applied HRT from four- (0.010 $h^{-1}$) to three-days (0.014 $h^{-1}$), resulted in both the sulphate conversion and VSRR decreasing to 50% and 6.9 mg/ℓ.h,

respectively. The exhibited VSRR remained at approximately 7 mg/ℓ.h between and including a three- and 2.3-day HRT (0.014 and 0.018 $h^{-1}$). The sulphate conversion decreased to 38% over this period. The reactor then maintained, on average, a 40% sulphate conversion from a two- to a 1.3-day HRT (0.021 $h^{-1}$ – 0.032 $h^{-1}$), before decreasing further to 35% at a one-day HRT (0.042 $h^{-1}$). The maintained sulphate conversion between a two- and one-day HRT corresponded with an increasing VSRR with further increasing VSLR. A maximum VSRR of 14.8 mg/ℓ.h was observed at a one-day HRT (0.042 $h^{-1}$). The observed sulphide concentration in the reactor differed from the predicted sulphide concentration, predicted based on the observed degree of sulphate reduction, by less than 7%, on average over the course of the HRT study. The highest sulphide concentration, of 231 mg/ℓ (6.77 mM) , was observed at a four-day HRT (0.010 $h^{-1}$). The sulphide concentration decreased to 171 mg/ℓ (5.02 mM) at a three-day HRT (0.014 $h^{-1}$) and continued to gradually decrease to 125 mg/ℓ (3.67 mM) at a one-day HRT (0.042 $h^{-1}$).

The propionate concentration present in the reactor (Figure 5-1B) increased from 32 mg/ℓ (0.42 mM) at a four-day HRT, to a maximum observed of 266 mg/ℓ (3.64 mM) at a three-day HRT. This concentration then decreased gradually with every further reduction in the HRT before reaching 196 mg/ℓ (2.68 mM) at a one-day HRT (0.042 $h^{-1}$). No citrate was detected in the reactor or reactor effluent at any applied HRT, being included in the reactor medium at 1.16 mM.

The acetate concentration in the reactor decreased from 813 mg/ℓ (13.54 mM) at a three-day HRT (0.014 $h^{-1}$) to 567 mg/ℓ (9.44 mM) at a 2.3-day HRT where it remained stable for the remainder of the HRT study. Inversely, the residual lactate in the reactor remained below 25 mg/ℓ (0.28 mM) between a four- and 2.3-day HRT (0.010 – 0.018 $h^{-1}$) but increased to 74 mg/ℓ (0.82 mM) at a two-day HRT (0.021 $h^{-1}$) and to a maximum of 167 mg/ℓ (1.85 mM) at a one-day HRT (0.042 $h^{-1}$).

The pH within the reactor remained stable for the duration of the HRT study at 7.1 (Figure 5-1D). The redox potential within the reactor and the effluent leaving the reactor increased gradually from approximately -180 mV at a four-day HRT (0.010 $h^{-1}$) to -125 mV at a one-day HRT (0.042 $h^{-1}$). The bicarbonate produced within the reactor (Figure 5-1C) decreased gradually from 27 mM at a four-day HRT (0.010 $h^{-1}$) to 23.5 mM at a one-day HRT (0.042 $h^{-1}$).

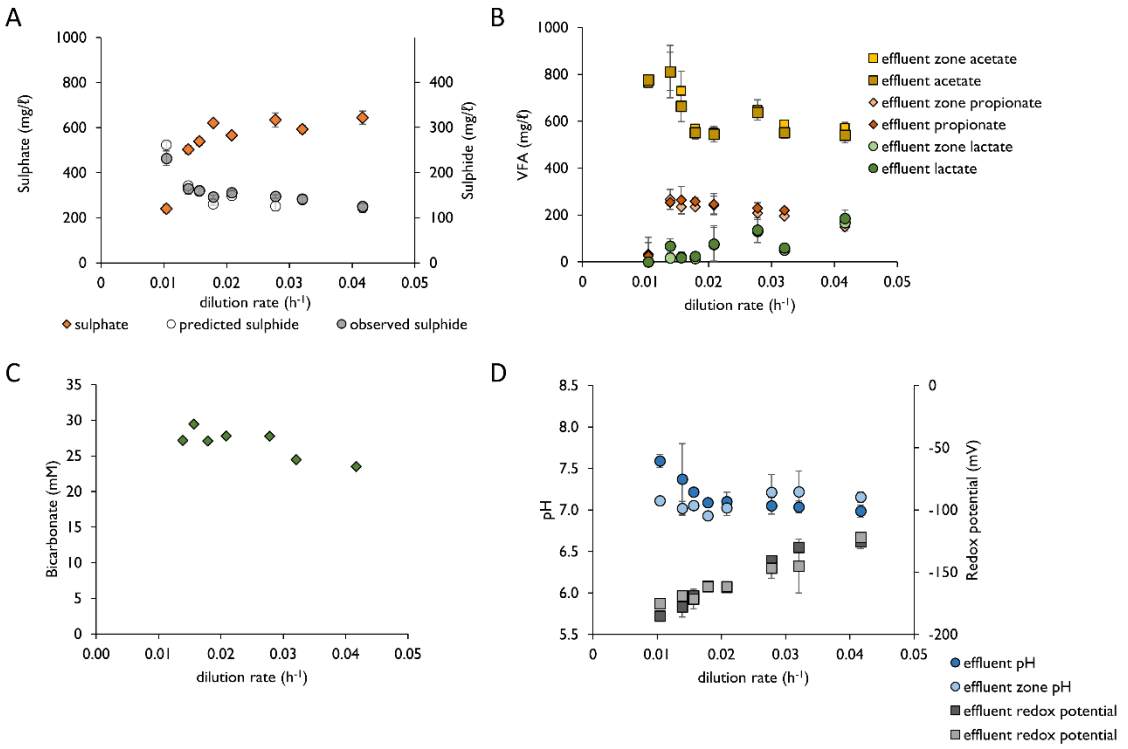


Figure 5-1 Steady-state kinetic data of the lactate-supplemented LFCR at a range of tested dilution rates, including (A) the residual sulphate, the produced sulphide and the predicted sulphide concentration, based on the observed sulphate reduced; (B) the observed volatile fatty acid profile; (C) the produced bicarbonate concentration present in the reactor effluent calculated from the difference between the observed and feed bicarbonate concentrations and (D) the pH and redox potential (reported relative to a standard hydrogen electrode). The VFA profile, redox potential and pH are reported for solution chemistry drawn from the effluent-zone of the reactor and the reactor effluent. Error bars represent one standard deviation from the mean.

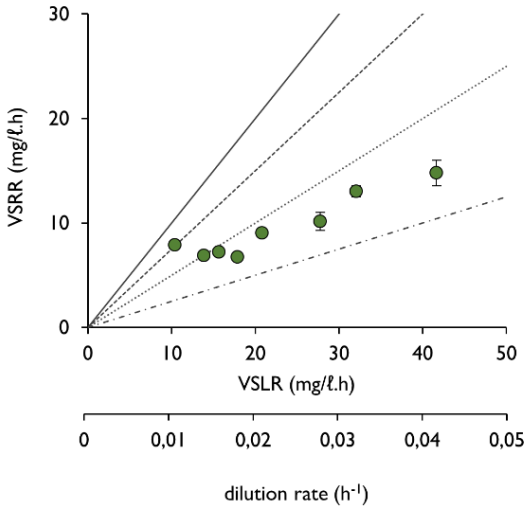


Figure 5-2 The VSRRs achieved by the lactate-supplemented LFCR at varied volumetric sulphate loading rates, varied through the reduction in the hydraulic retention time applied to the systems. Sulphate conversion can be visually determined through comparisons with plotted lines: 100% conversion – solid line, 75% conversion – dashed line; 50% conversion – dotted line, 25% - composite dashed and dotted line.

**Biomass retention**

The planktonic cell concentration supported within the inlet and effluent zones of the lactate-supplemented LFCR differed by less than 10% at each tested HRT. The planktonic cell concentration in the reactor was maintained at approximately 3 x $10^8$ cells/mℓ between a four- and 2.6-day HRT (0.010 - 0.016 $h^{-1}$; Figure 5-3). The cell concentration then decreased to an average of 1.9 x $10^8$ cells/ml at further reduced HRT which was approximately maintained for the remainder of the HRT study. The concentration of planktonic cells within the lactate-supplemented CSTR was, on average over the course of the HRT study, 1.7-fold greater than the planktonic cell concentration maintained within the LFCR.

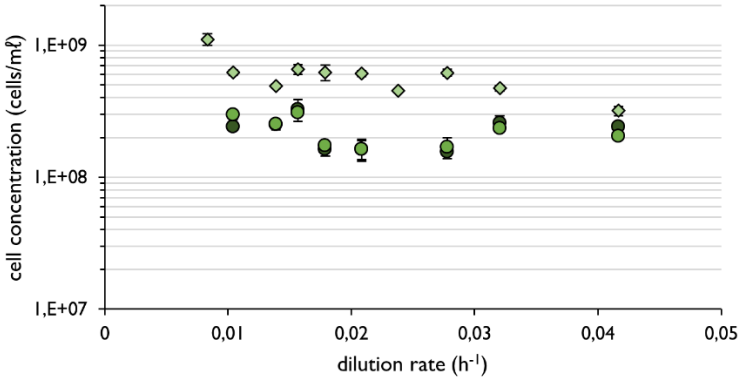


Figure 5-3 The planktonic cell concentration supported in the (●) inlet and (●) effluent zone of the lactate-supplemented LFCR at a range of tested dilution rates corresponding to HRTs ranging from four- to one-day(s). The concentration of planktonic cells supported by the similarly operated (♦) lactate-supplemented CSTR is shown for comparison. Cell concentrations were determined through direct cell counting on solution drawn directly from the respective reactor zone. Cell counts were performed in duplicate and error bars represent one standard deviation from the mean.

The biomass retained within the biofilm-associated and biofilm-attached communities of the lactate supplemented LFCR was evaluated at the initial four- and the final one-day HRT (0.010 and 0.042 $h^{-1}$; Figure 5-204). This found the concentration of cells within the associated communities to be slightly lower than that of the planktonic communities. At a four-day HRT, the associated communities of the inlet and effluent zones were 1.1 x $10^9$ and 1.8 x $10^8$ cells/mℓ, respectively. This decreased to 1.77 x $10^8$ and 1.24 x $10^8$ cells/mℓ, respectively, at a one-day HRT. The attached cell concentration, however, was approximately 10-fold greater than that of the planktonic cell concentration within each zone at both HRT.

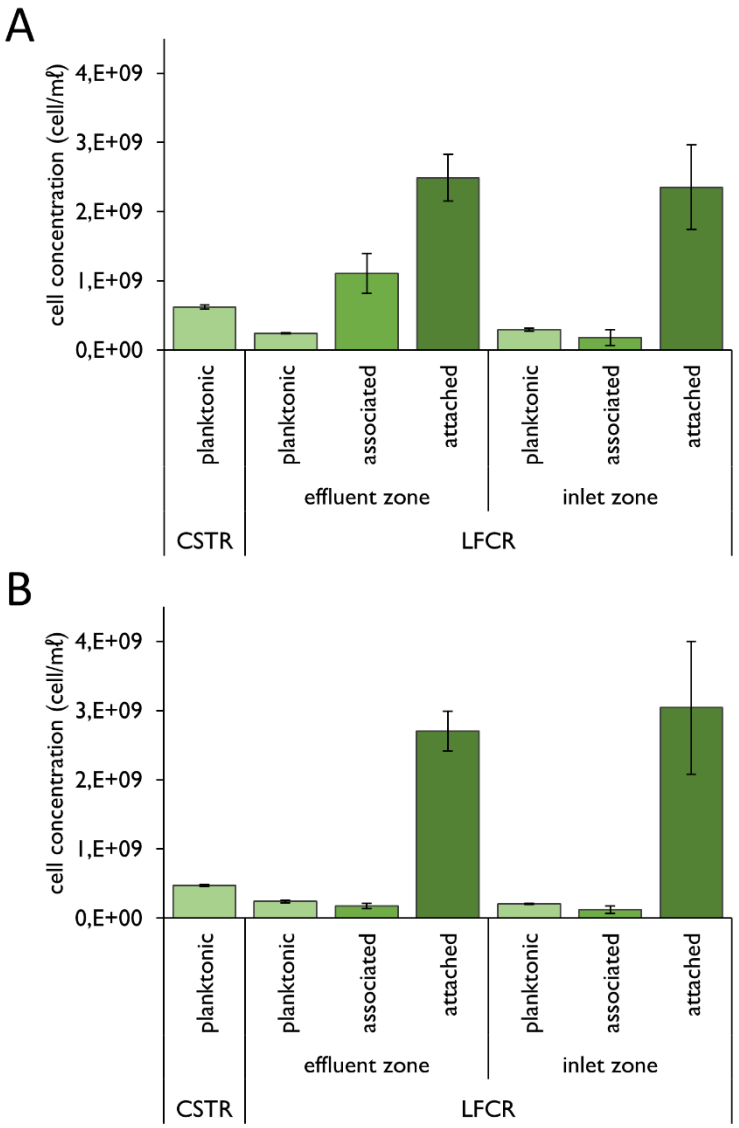


Figure 5-4 The concentration of planktonic, biofilm-associated and -attached communities of the lactate-supplemented LFCR and, as a comparison, the planktonic cell concentration of the lactate-supplemented CSTR at a (A) four- and (B) one-day HRT. The microbial communities of both the effluent and inlet zones of the LFCR were assessed independently. Biofilm communities were sampled in duplicate and cell counts were then performed in duplicate. Error bars represent one standard deviation from the mean.

Scanning electron microscopy was used to visually inspect the biofilm which had formed on the surface of the carbon microfibres of the lactate-supplemented LFCR at a four- and one-day HRT.

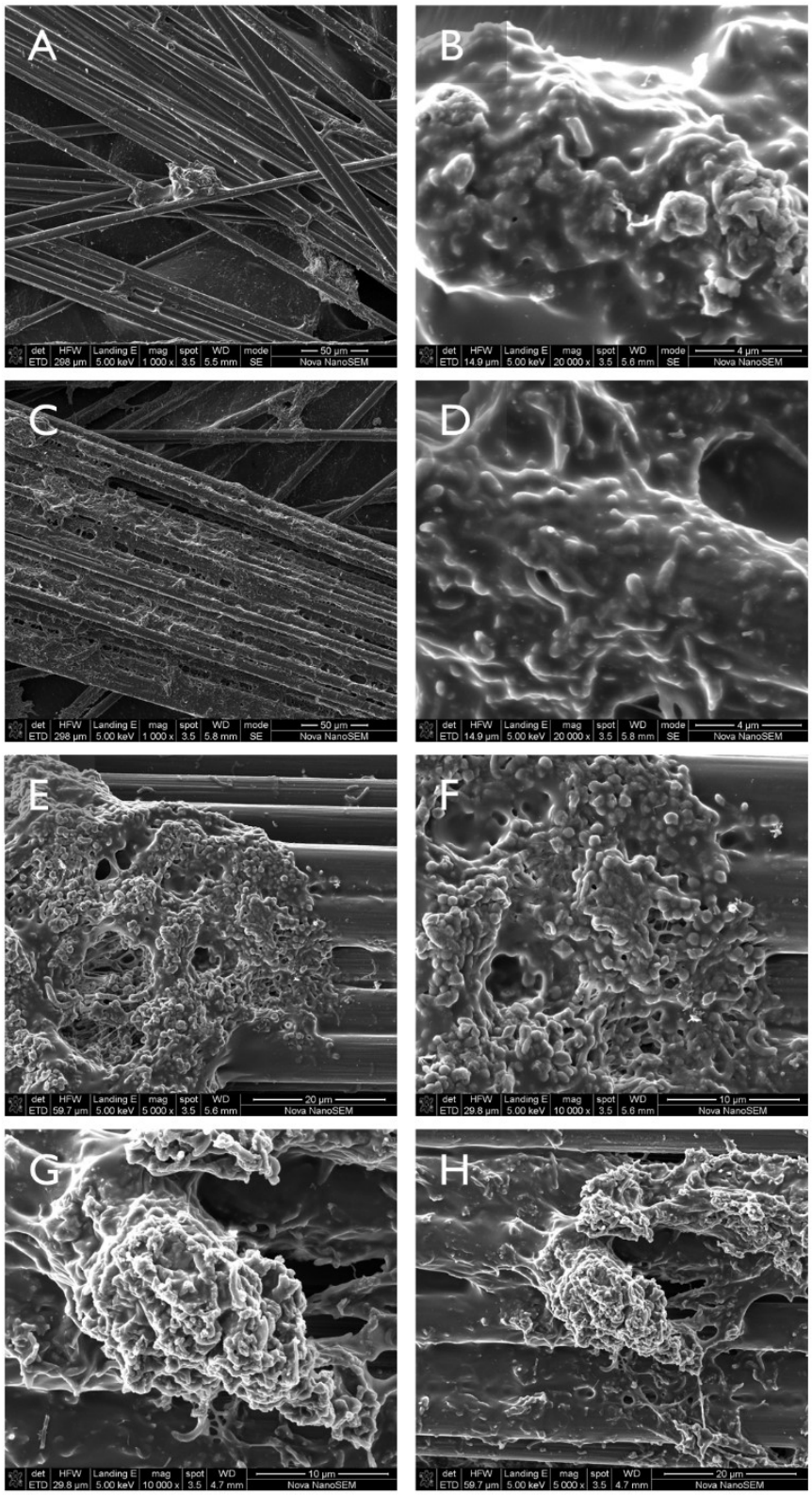


Figure 5-5 Scanning electron micrographs of the carbon microfibres recovered from the lactate-supplemented LFCR. Carbon microfibres were recovered at a four-day HRT from the (A, B) inlet zone and (C, D) effluent zone, and at a one-day HRT, fibres were again recovered from the (E, F) inlet and (G, H) and effluent zones. Scale bars are shown in each micrograph.

Mature biofilms were observed on the carbon fibres from both the inlet and effluent zones of the LFCR at a four- and one-day HRT (Figure 5-5). Pores and channels through the depth of the biofilm were most prevalent in micrographs of fibres isolated from the effluent zone at a one-day HRT. A range of cell morphologies were present within these biofilms, including lemon-shaped, vibrio, rods and cocci.

### 5.2.2 Microbial ecology

The attached and associated communities of the lactate-supplemented LFCR, at a four- and one-day HRT, were dominated by Proteobacteria and Synergistetes (Figure 5-6). Microorganisms from these two phyla accounted for 54 to 77% relative abundance of these biofilm communities. Firmicutes, which were widely implicated in lactate oxidation in the other lactate-supplemented reactors of this study, were present between at only 5 and 13% of these biofilm communities. Firmicutes were present at similar abundances in the planktonic microbial community at a four-day HRT too, but the proportion of this phyla, at a three-, 1.5- and one-day HRT increased to between 24 and 51%. Bacteroidetes were higher in abundance in the planktonic communities (23 - 34%) compared to the biofilm communities (6-13%) at each tested HRT.

All SRB which could be putatively identified in this reactor system were classified as Deltaproteobacteria and constituted all of the Deltaproteobacteria identified. Deltaproteobacteria constituted approximately 24% of the planktonic communities at a four-day HRT but decreased to approximately 7% at a three-day HRT. The proportion of Deltaproteobacteria increased at the further reduced HRT of 1.5-days, to approximately 18% relative abundance, but decreased again to 8% at a one-day HRT. The reduction in the HRT had little effect on the abundance of Deltaproteobacteria in the associated and attached biofilm communities where this class of microorganisms were present at, on average, 29 and 31% relative abundance, respectively.

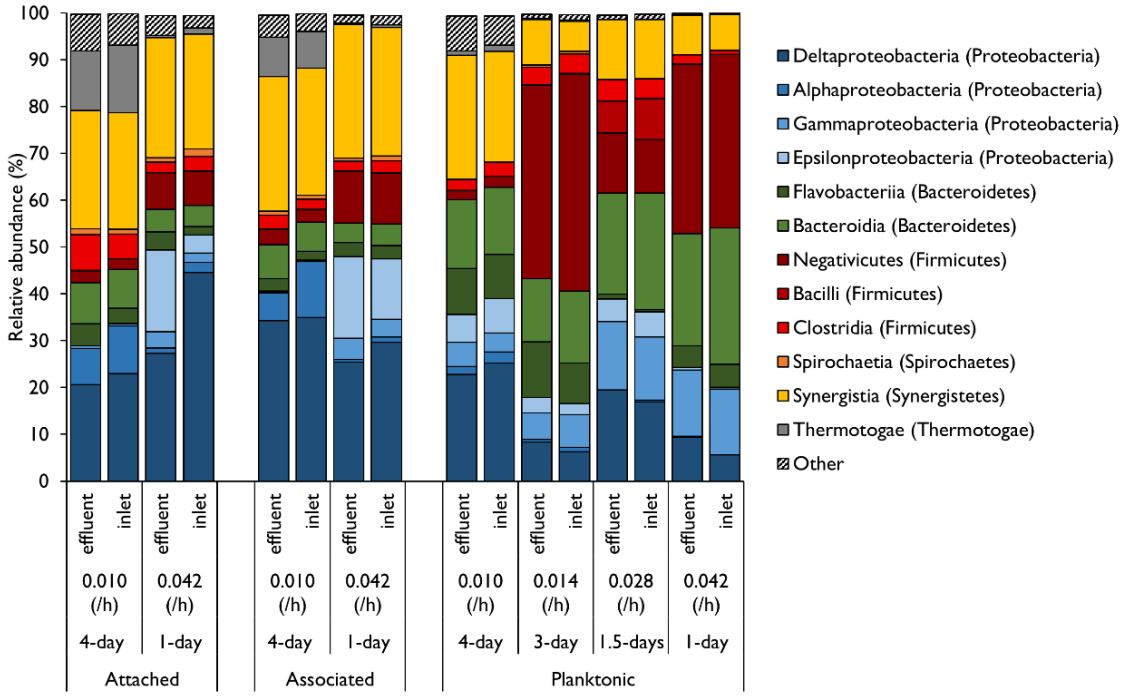


Figure 5-6 Relative abundance of the predominant microbial classes within the planktonic, attached and associated communities of the inlet and effluent zones of the lactate-supplemented LFCR at dilution rates corresponding to four- (0.010 $h^{-1}$), three- (0.014 $h^{-1}$), 1.5- (0.028 $h^{-1}$) and one-day (0.042 $h^{-1}$) HRTs. The phyla to which each class belongs are shown in parentheses.

Many of the predominant OTUs in the lactate-supplemented LFCR were shared in the biofilm and planktonic microbial communities (Figure 5-7). The SRB which were present at a four-day HRT in these communities also did not differ greatly from those present at the final one-day HRT. One or both *Desulfomicrobium* (1) and *Desulfovibrio* (6) were present in each microbial community. *Desulfomicrobium*, however, exhibited washout between a 1.5- and one-day HRT.

Several *Desulfovibrio* OTUs were present in the planktonic and biofilm communities of this reactor. *Desulfovibrio* (108) was present in the attached communities at each HRT, *Desulfovibrio* (39) and *Desulfovibrio* (47) became abundant in the biofilm communities at a one-day HRT with *Desulfovibrio* (39) becoming dominant within the planktonic communities from a 1.5-day HRT. A *Desulfarculus* OTU (97) was present within the biofilm communities at a four-day HRT but showed greatly reduced abundance at a one-day HRT. This SRB OTU was present within the biofilm communities of the inlet zones of both the acetate- and lactate-supplemented UAPBRs (Chapter 6 ).

*Veillonella* (11) was the most abundant Firmicute in the reactor system, accounting for most of this phylum present in both the planktonic and biofilm communities. The abundance of Synergistales was predominantly made up of two OTUs, *Aminomonas* (2) and *Dethiosulfovibrio* (10). Both OTUs were present in the biofilm and planktonic communities too, but *Dethiosulfovibrio* (10) decreased in abundance within the planktonic community with each reduction in the HRT.

Notable changes occurred in the composition of OTUs classified within Proteobacteria during the HRT study. *Aliidongia* (52), present in the biofilm communities at a four-day HRT, appeared to be replaced by *Arcobacter* (5) in the biofilm communities at a one-day HRT. *Arcobacter* (5) was present in the planktonic community at a four-day HRT but itself appears to have washed out with reducing HRT. *Enterobacter* (16) then became the predominant non-Deltaproteobacteria Proteobacteria in the planktonic communities at reduced HRT.

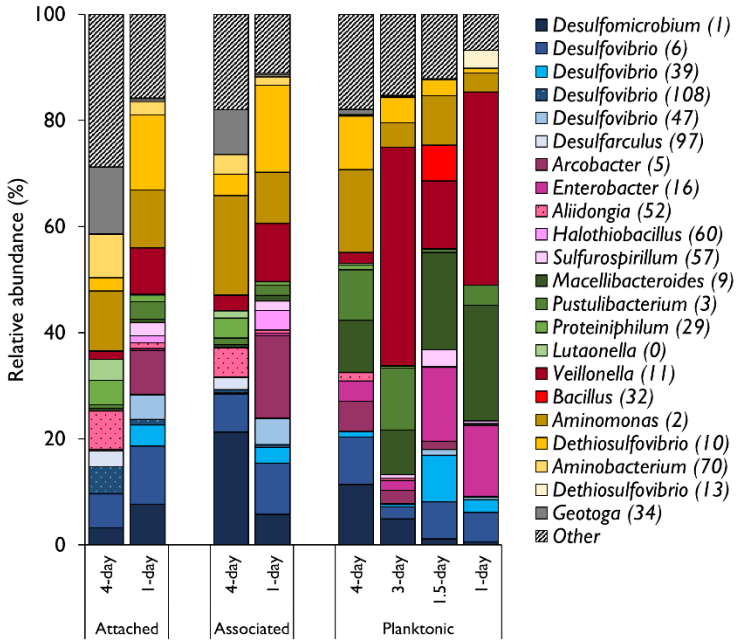


Figure 5-7 The relative abundance of the most abundant OTUs in the biofilm-associated, attached and planktonic communities of the effluent zone of the lactate-supplemented LFCRs at dilution rates corresponding to a four- (0.010 $h^{-1}$), three- (0.014 $h^{-1}$), 1.5- (0.028 $h^{-1}$) and one-day (0.042 $h^{-1}$) HRT. OTUs are broadly coloured by taxonomy: Deltaproteobacteria – blue, other Proteobacteria – purple, Bacteroidetes – green, Firmicutes – red, Synergistetes – yellow, other phyla – grey.

## 5.3 Lactate LFCR discussion

The following sections aim to determine the extent of lactate and acetate oxidation by SRB and lactate fermentation by competing fermentative microorganisms in lactate-supplemented LFCR. This is attempted through an assessment of the collected physiochemical data including the reduced sulphate, removed lactate and produced VFAs and bicarbonate in the reactor. The microbial ecology, in terms of cell concentration and taxonomy, are subsequently overlaid with the performance data to estimate the influence of particular microorganisms with the observed reactor performance.

### 5.3.1 Evaluation of the competition for lactate using physiochemical data

The competition for lactate between SRB and lactate fermentative microorganisms was initially evaluated based on the observed degree of sulphate reduction and the production of propionate in the reactor (Figure 5-8). At a four-day HRT, when the sulphate conversion averaged 76%, it was estimated that 13.0 mM of the 13.6 mM feed lactate was linked to sulphate reduction, with 0.6 mM lactate being fermented and giving rise to the observed propionate. This 13.0 mM lactate, accounts for 6.5 mM of the observed 7.9 mM sulphate reduced through incomplete lactate oxidation. Incomplete lactate oxidation, therefore, does not account for all the sulphate which was reduced which suggests a portion of lactate was oxidised completely to bicarbonate (Equation 2-11). The sulphate conversion decreased substantially, to 50%, at a three-day HRT which corresponded with the estimated amount of lactate being fermented increasing from 0.6 mM at a four-day HRT to 5.4 mM at a three-day HRT. The remaining 8.2 mM lactate was still not sufficient for the observed sulphate reduced and again indicated that a portion of this lactate was oxidised completely to bicarbonate. The amount of lactate estimated to be used by SRB decreased gradually with each iterative increase in the applied dilution rate, from 5.4 mM at a three-day HRT (0.014 $h^{-1}$) to 3.0 mM at a one-day HRT. Evidence of complete oxidation of lactate by SRB was last observed at a two-day HRT (0.021 $h^{-1}$). The residual lactate concentration in the reactor began to increase gradually from almost negligible at a 2.3-day HRT (0.018 $h^{-1}$) to 1.9 mM at a one-day HRT (0.042 $h^{-1}$).

The molar ratios employed by Oyekola et al. (2009) to monitor the competition between SRB and lactate fermentative microorganisms were used to further evaluate the competition between the SRB and fermentative microorganisms for lactate in this study (Figure 5-9). A molar ratio of 'lactate oxidised to sulphate reduced' of 2:1 indicates lactate was incompletely oxidised by SRB to acetate (Equation 2-10). A ratio of 1:0.667 indicates that all lactate underwent complete oxidation by SRB (Equation 2-11) and a ratio above 2 indicates that at least a degree of lactate oxidation is occurring which is not linked to sulphate reduction.

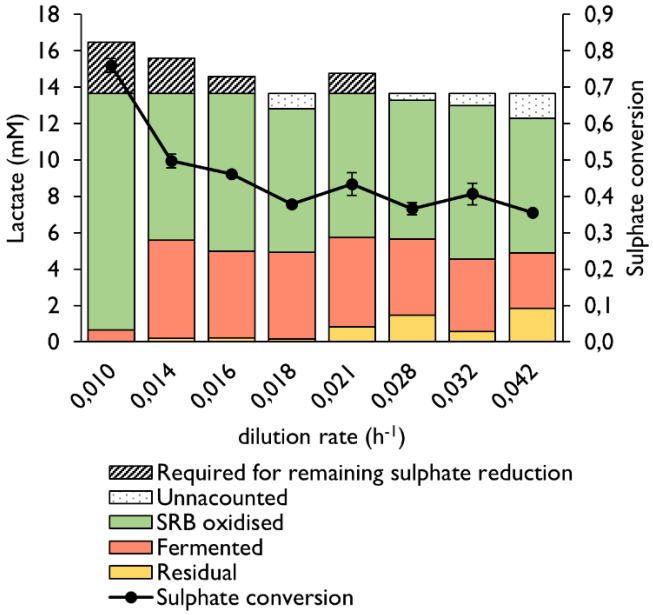


Figure 5-8 The predicted fate of the 13.6 mM lactate supplied in the reactor medium of the LFCR at a range of tested dilution rates corresponding to HRT between a four- and one-day. These include the concentration of lactate undergoing lactate fermentation (Equation 2-12) calculated from the observed propionate concentration; undergoing incomplete lactate oxidation by SRB (Equation 2-10) calculated from the observed sulphate reduced but not allowing to exceed the feed lactate concentration of 13.6 mM; residual lactate remaining in the reactor, lactate unaccounted for from sulphate reduction and lactate fermentation; and the theoretical concentration of lactate required to allow for degree of sulphate conversion observed at each tested dilution rate.

The ratio of observed 'lactate oxidised to sulphate reduced' (Figure 5-9) increased from 1.7 at a four-day HRT (0.010 $h^{-1}$) to 2.6 at a three-day HRT (0.014 $h^{-1}$). This further attests to the predicted degree of lactate oxidation by fermentative microorganisms at a three-day HRT (0.014 $h^{-1}$) as shown in Figure 5-8. Lactate oxidation by SRB in this lactate-supplemented LFCR was far more prevalent than observed in the lactate-supplemented CSTR at a four-day HRT. An observed ratio of lactate oxidised to sulphate reduced of 2.6:1 was also observed in the CSTR at a three-day HRT (0.014 $h^{-1}$) but this ratio is approximately maintained in the CSTR at further reduced HRT, until the final one-day HRT where this observed ratio was 3:1. The LFCR reached a maximum 'lactate oxidised to sulphate reduced' ratio of 3.4 at a 2.3-day HRT (0.018 $h^{-1}$) indicating a large proportion of the supplied lactate was utilised by lactate fermenting microorganisms. This degree of lactate fermentation was the highest observed in any of the lactate-supplemented reactor systems operated in this study.

The amount of lactate estimated to have been oxidised by SRB, as shown in Figure 5-8, was used to calculate the ratio of lactate oxidised by SRB to sulphate reduced (Figure 5-9). This was calculated by assuming all lactate which oxidised but was not linked to lactate fermentation through

the accounting of produced propionate, was linked to sulphate reduction. Therefore, a ratio of 'lactate oxidised by SRB (predicted): sulphate reduced' above two would indicate lactate that was oxidised but is not accounted for by sulphate reduction or fermentation using the assumptions made above. This unaccounted-for lactate likely underwent lactate fermentation and the propionate which was produced subsequently oxidised.

The observed 'lactate oxidised by SRB (predicted): sulphate reduced' lying between 1.5:1 and 2:1 at HRT between four- and two-days, omitting the 2.3-day HRT (0.018 $h^{-1}$) indicates that some of the lactate oxidised by SRB at these HRT was completely oxidised to bicarbonate. At the applied HRT of 1.5- to one-day(s) this ratio lies above two indicating that sulphate reduction was linked to incomplete lactate oxidation and the degree of lactate fermentation was potentially underestimated.

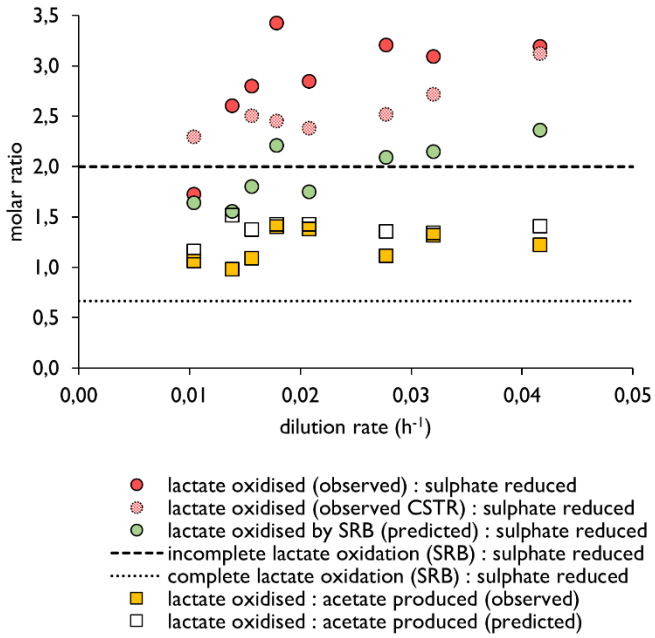


Figure 5-9 The predicted and observed steady-state molar ratios of products and reactants arising from lactate oxidation by SRB (Equation 2-10) and lactate fermentation (Equation 2-12) within the effluent zone of the lactate LFCR at a range of tested dilution rates. The lactate predicted to have been oxidised by SRB was calculated by subtracting the lactate oxidised by fermentation (Figure 5-8) and the residual lactate observed in the reactor from the feed lactate concentration (13.6 mM). The predicted acetate concentration was calculated according to the degree of lactate oxidation by SRB and fermentative microorganisms (Equation 2-10 and Equation 2-12) shown in Figure 5-8 as well as assuming all sulphate reduced which was not accounted by the available lactate oxidised, was linked to acetate oxidation. The observed and predicted ratio lactate oxidised to acetate produced are shown.

The concentration of acetate in the reactor was predicted based on the oxidation of lactate via incomplete and complete oxidation by SRB and through the determined lactate fermentation, as described in Figure 5-8. In this prediction, sulphate reduced which was not linked to lactate oxidation is assumed to have been linked, instead, to the oxidation of acetate. The ratio of lactate oxidised to observed acetate produced is plotted in Figure 5-9, along with the ratio of lactate oxidised to predicated acetate concentration. Where this predicted ratio is greater than observed, this indicates that there is more acetate in the reactor than predicted. This degree of additional acetate in the reactor was observed at a three- (0.014 $h^{-1}$), 2.6- (0.016 $h^{-1}$) and 1.5-day (0.028 $h^{-1}$) HRT. This indicates that additional acetate is generated in this reactor through the oxidation of substrates other than lactate. The observed and predicted acetate concentrations, based on the lactate oxidation and sulphate reduction reactions discussed above at each tested HRT, are shown in Figure 5-10. The observed acetate concentration showed the greatest difference from this predicted acetate concentration at a three- (0.014 $h^{-1}$), 2.6- (0.016 $h^{-1}$) and 1.5-day (0.028 $h^{-1}$) HRT. At each other HRT, the difference between the observed and predicted acetate concentrations differed by, on average, just 0.6 mM acetate. The additional observed acetate in this reactor was expected to have originated from the oxidation of yeast extract as described in Section 4.4.2. The predicted acetate concentration in the LFCR at a three-, 2.6- and 1.5-day HRT are lower than the second predicted acetate concentration in Figure 5-10 which also considers 4.37 mM of acetate generation from yeast extract oxidation. The agreement with the first prediction and the observed acetate concentration, at most HRT, suggests that yeast extract oxidation was less prevalent in this reactor compared to the acetate-supplemented CSTR, and acetate-supplemented LFCR (Section 5.5.1). This suggests that this microbial culture preferentially oxidises lactate over the lower concentrations of yeast extract constituents as an electron donor and carbon source. The high acetate concentrations in the effluent of this reactor represents an unutilised electron donor occurring even in the presence of high concentrations of sulphate. This likely speaks to the absence of both sulphate- and non-sulphate reducing microorganisms able to effectively metabolise acetate in this reactor.

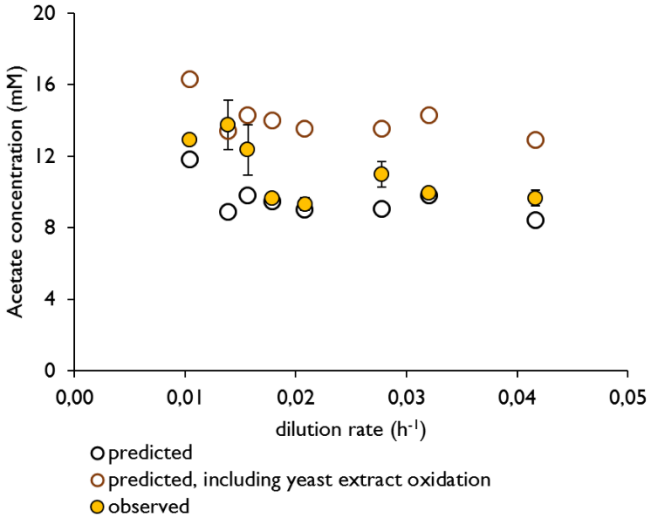


Figure 5-10 The observed and predicted acetate concentrations in the lactate-supplemented LFCR at each tested HRT. The acetate concentrations were predicted based on the determined lactate oxidation by fermentation reactions as shown in Figure 5-8. A second acetate prediction was made including 4.37 mM of acetate being generated from yeast extract oxidation, as observed in the acetate-supplemented CSTR and discussed in Section 4.4.2.

Although the observed acetate concentrations are largely as predicted in the reactor, the concentration of bicarbonate was far greater than anticipated based on the determined lactate and acetate oxidation reactions (Figure 5-11). The observed bicarbonate concentration was, on average across the HRT study, 8.8 mM greater than that predicted.

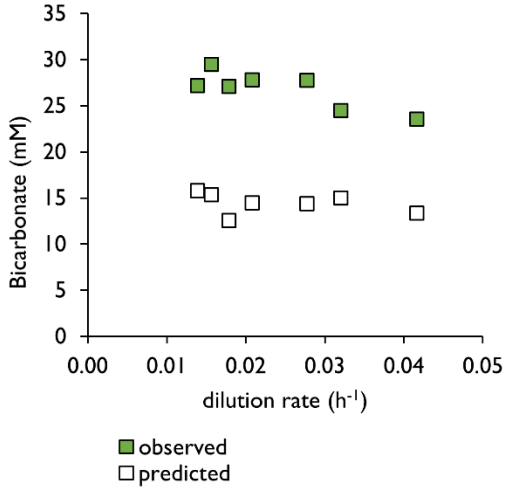


Figure 5-11 The (green) observed and (white) predicted bicarbonate concentrations present in the lactate-supplemented LFCR at a range of applied dilution rates, corresponding to HRT between four- and one-day (0.010 – 0.042 $h^{-1}$). The predicted concentrations of bicarbonate in the reactor were calculated based on the degree of determined lactate fermentation, incomplete lactate oxidation and complete lactate oxidation as shown in Figure 5-8.

The ratio of 'lactate oxidised to bicarbonate produced' at each HRT, is plotted in Figure 5-12. The bicarbonate concentration was approximately two-fold higher than predicted at each tested HRT and lies below 1:1 for the duration of the HRT study. A ratio of one would typically indicate that complete lactate oxidation by SRB was the prevailing reaction taking place in the reactor. The generation of bicarbonate from the oxidation of substrates other than lactate, however, is leading to this misinterpretation. This ratio is, therefore, not a good performance indicator of lactate oxidation under these conditions. As little yeast extract was thought to have been oxidised in this reactor, the majority of this additional bicarbonate is thought to originate from the oxidation of citrate which was not detected in the reactor at any tested HRT.

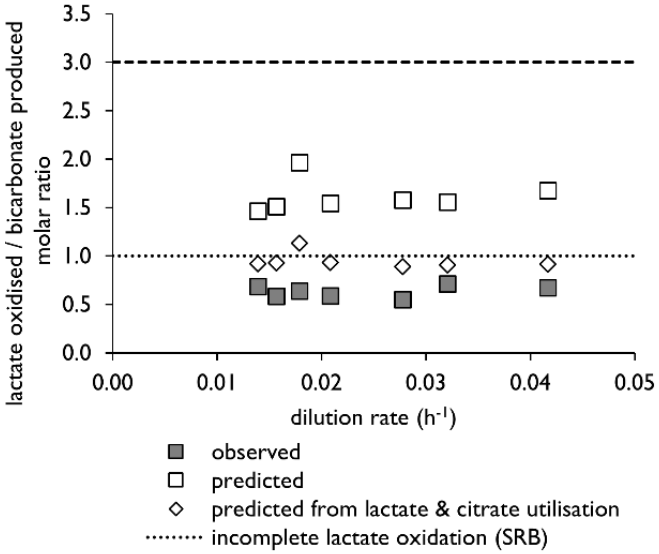


Figure 5-12 The observed and predicted 'lactate oxidised to produced bicarbonate' ratio within the lactate-supplemented LFCR at a range of applied dilution rates, corresponding to HRT between and including a four- and one-day HRT (0.010 – 0.042 $h^{-1}$). The predicted ratios were calculated based on the degree of lactate oxidation by SRB (Equation 2-10 and Equation 2-11), lactate fermentation (Equation 2-12). The ratios of 'lactate oxidised to bicarbonate produced' based on the theoretical consumption of all lactate by SRB (1:1) and by fermentative microorganisms (3:1) are shown.

### 5.3.2 Comparison of the performance of the lactate-supplemented LFCR and CSTR

The VSRR achieved by the lactate-supplemented LFCR, with increasing VSLR and dilution rates, is plotted alongside that achieved by the similarly operated CSTR in Figure 5-13. The lactate LFCR achieved a VSRR of 7.9 mg/ℓ.h at a four-day HRT (0.010 $h^{-1}$) compared to the CSTR which achieved 5.8 mg/ℓ.h at this HRT. However, at every subsequent tested HRT, the lactate CSTR exhibited higher VSRRs than the LFCR, even at a one-day HRT (0.042 $h^{-1}$) where the planktonic cell

concentrations in this CSTR were greatly reduced (Section 4.2.1). This is particularly surprising given the greater degree of biomass retention achieved within the LFCR.

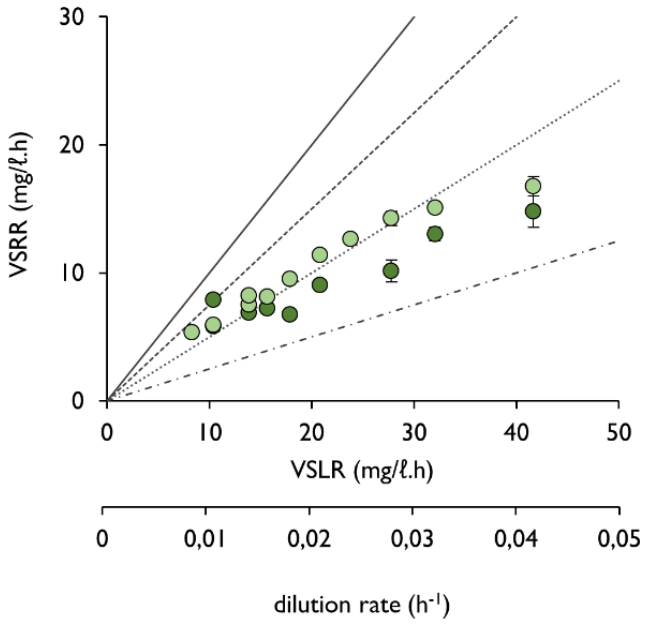


Figure 5-13 The VSRRs achieved by the lactate-supplemented (●) LFCR and similarly operated (●) CSTR of this study at varied volumetric sulphate loading rates, varied through the reduction in the hydraulic retention time applied to the systems. Sulphate conversion can be visually determined through comparisons with plotted lines: 100% conversion – solid line, 75% conversion – dashed line; 50% conversion – dotted line, 25% - composite dashed and dotted line. Error bars represent one standard deviation from the mean.

The cell concentration of SRB within the lactate-supplemented LFCR was estimated by multiplying the cumulative relative abundance of the OTUs putatively identified as SRB by the total determined cell concentration of each microbial community (Figure 5-14). Far higher cell concentrations of SRB were calculated to be present in the attached communities, $5.5 \times 10^8 – 1.3 \times 10^9$ cells/mℓ, compared to the planktonic communities of the LFCR ($1.1 \times 10^7 – 7.6 \times 10^7$ cells/mℓ) and CSTR ($4.3 \times 10^7 – 3.1 \times 10^8$ cells/mℓ). The reduced performance of the LFCR may, therefore, be explained by the presence of specific microorganisms within this reactor which were outcompeting the SRB in this reactor for the available lactate.

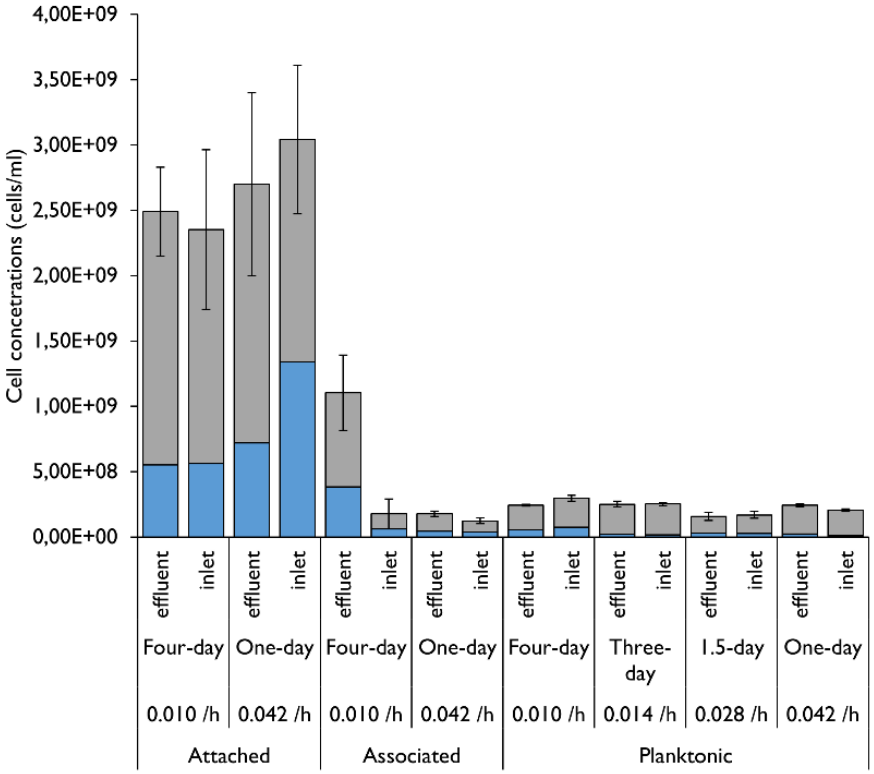


Figure 5-14 The proportion of identified SRB (blue) and non-SRB (grey) of the attached, associated and planktonic communities of the inlet and effluent zones of the lactate-supplemented LFCR, at a range of tested HRT including four-, three-, 1.5- and one-day HRT. The total magnitude of these communities was determined by direct cell counting, following, were applicable to, the use of the modified detachment protocol. The proportion of SRB within a community was determined through the putative identification of SRB OTUs following 16S rRNA amplicon sequencing. Genome-resolve metagenomics, where possible, was used to supplement and validify the identification of these SRB. Error bars represent one standard deviation from the mean.

### 5.3.3 Integration of reactor performance and microbial ecology

The sulphate conversion exhibited by the lactate-supplemented LFCR roughly correlated with the determined SRB cell concentration in the planktonic phase, which was made up largely by *Desulfomicrobium* (1), *Desulfovibrio* (6) and *Desulfovibrio* (39) (Figure 5-15). These are likely performing incomplete and complete lactate oxidation. The sulphate conversion was also roughly anticorrelated with the determined cell concentration of *Veillonella* (11). As previously mentioned, the genus *Veillonella* has been demonstrated in the literature to be an effective lactate oxidiser (Rogosa, 1963; Ng and Hamilton, 1971; Seeliger et al., 2002; Scheiman et al., 2019). This microorganism was also shown to possess the genes required to oxidise lactate through genome-resolved metagenomics (Section 8.5). Further, a survey of the microbial communities across all six of the bioreactors operated in this study (Chapter 7 ), revealed that this *Veillonella* (11) OTU was significantly enriched in zones where lactate oxidation occurred and within planktonic microbial

communities. When this *Veillonella* OTU did appear in biofilm communities across the six bioreactors, it averaged just 4.6% relative abundance. However, this *Veillonella* OTU was found at high abundances in the attached and associated communities of this LFCR. At a one-day HRT, *Veillonella* (11) was found at approximately 10% relative abundance in each of these biofilm communities (Figure 5-16).

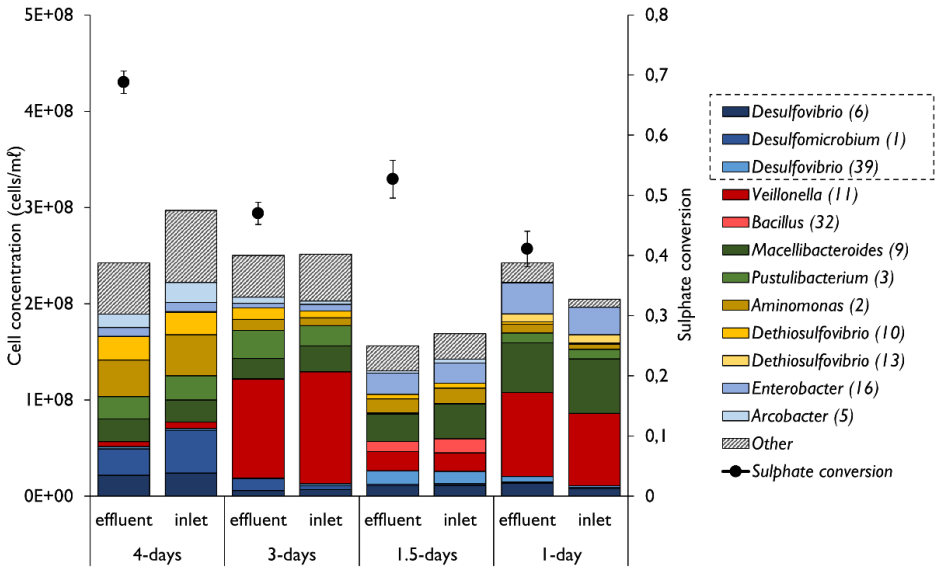


Figure 5-15 The calculated cell concentrations of the predominant OTUs in the effluent zone planktonic communities of the lactate-supplemented LFCR at a range of tested dilution rates. Cell concentrations were estimated through multiplying the relative abundance of an OTU by the total cell concentration determined at each respective steady-state through direct cell counting. The sulphate conversion achieved at each HRT is shown in the secondary y-axis. OTUs are coloured by taxonomy: Deltaproteobacteria – blue, other Proteobacteria – purple, Bacteroidetes – green, Firmicutes – red, Synergistetes – yellow, other phyla – grey. OTUs putatively identified are SRB are circled by a dotted line in the legend.

This was one of the many microorganisms which became more abundant at reduced HRT in the biofilm communities (Figure 5-16). Two *Desulfovibrio* OTUs, namely 39 and 47, also appeared in the biofilm communities at a one-day HRT. The growth of these OTUs in the biofilm likely accounts for their sudden appearance in the planktonic communities at reduced HRT, having likely being seeded from this biofilm.

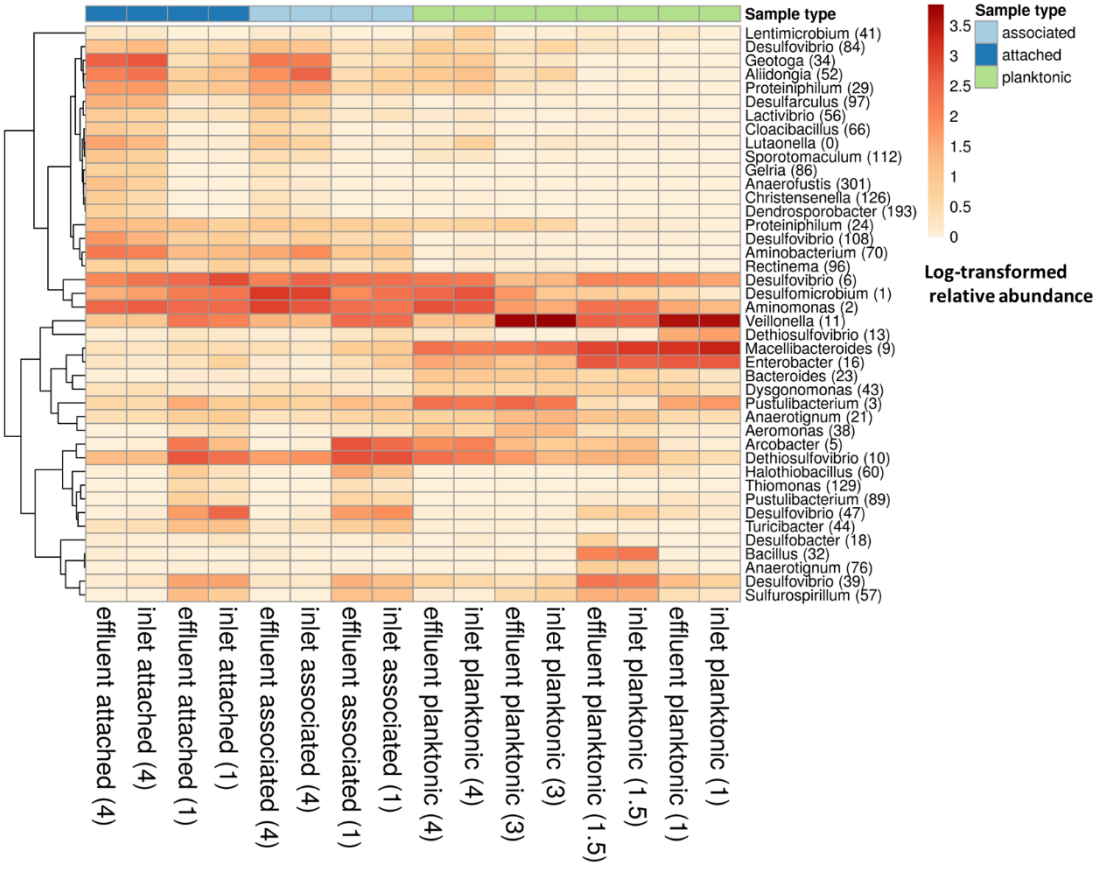


Figure 5-16 Hierarchical clustering of the relative abundance of the predominant OTUs in the planktonic, associated and attached microbial communities of the lactate-supplemented LFCR at a range of tested HRT including four-, three-, 1.5- and one-day HRTs (shown in parentheses in the column names). Relative abundances were ln(x +1) transformed and hierarchical clustering was performed using correlation distance and average linkage. No row centring was performed. The reactor zone from which each sample was isolated, the microbial phase and the HRT at which the sample was recovered is shown above the heatmap and the legend shown on the right of the heatmap.

It is interesting to note the sustained presence of *Desulfovibrio* (6), *Aminomonas* (2) and *Dethiosulfovibrio* OTUs in the biofilm and planktonic communities between a four- and one-day HRT – making these core members of these communities (Figure 5-16). The genera of *Dethiosulfovibrio* and *Aminomonas* is commonly implicated in amino acid and citrate oxidation in literature (Baena et al., 1999; Surkov et al., 2001; Jumas-Bilak et al., 2009) and many of the recovered genomes of Synergistales in these reactors were found with complete or near-complete gene pathways for the urea cycle, citrate oxidation and lactate oxidation (Section 8.5). These microorganisms are thought likely to perform amino acid and citrate oxidation within this reactor. The basis of this conclusion, based on genetic potential and distribution throughout reactor communities, is further discussed in Chapters 7 and 8.

The correlation between the sulphate conversion exhibited by the lactate-supplemented LFCR and the estimated SRB cell concentrations suggest that the sulphate which is reduced at HRT

where SRB cell concentrations are greatly reduced, namely 470 mg/ℓ (4.90 mM) sulphate at a three-day HRT and 411 mg/ℓ (4.28 mM) sulphate at a one-day HRT, is largely reduced by SRB present within the biofilm communities. The sulphate reducing performance of the current reactor configuration, therefore, is expected to outcompete that of the CSTR at further increased dilution rates only where total planktonic SRB cell washout would take place.

It is expected that the performance of this reactor could be improved by maximising the surface area for biofilm formation thereby limiting the growth of microorganisms within the planktonic phase which are competing with the SRB for lactate. The prevalence of the *Veillonella* OTU in the planktonic and attached communities is thought to account for the degree of lactate fermentation observed in this reactor. The performance of this reactor in the context of other studies described in the literature is described in Section 5.6.

## 5.4 Acetate-supplemented LFCR Results

The following sections describe the performance of the acetate-supplemented LFCR across the tested dilution rates applied to the system with a constant sulphate (1.0 g/ℓ or 10.41mM ) and acetate (0.72 g/ℓ or 11.2 mM) concentration. The cell concentrations supported by the LFCR in the planktonic and biofilm phases are reported. The results of the 16S rRNA gene amplicon sequencing results are presented which describe the microbial community structure of these communities at a phylum- and class- taxonomic levels, followed by the abundances and classification of the dominant OTUs in the system.

### 5.4.1 Reactor performance

The acetate-supplemented LFCR, at a four-day HRT (0.010 $h^{-1}$) achieved a sulphate conversion of 69% (Figure 5-17A), corresponding to a VSRR of 7.2 mg/ℓ.h at a VSLR of 10.4 mg/ℓ.h (Figure 5-18). The sulphate conversion then decreased to 47% at a three-day HRT (0.014 $h^{-1}$) and gradually decreased further to 39% at a 2.3-day HRT (0.018 $h^{-1}$). The VSRR exhibited between a four- and 2.3-day HRT (0.010 - 0.018 $h^{-1}$) remained fairly stable, at approximately 6.9 mg/ℓ.h. The dramatic decrease in sulphate conversion between a four- and three-day HRT (0.010 - 0.014 $h^{-1}$) coincided in the acetate concentration in the reactor increasing from 643 mg/ℓ (10.71 mM) to nearly 800 mg/ℓ (13.32 mM; Figure 5-17B). No citrate was observed in the reactor at any applied HRT. The acetate concentration decreased to 670 mg/ℓ (11.16 mM) at a 2.3-day HRT (0.018 $h^{-1}$) where it remained stable for the remainder of the study. The residual sulphate in the reactor, however, decreased from 608 mg/ℓ (6.33 mM) at a 2.3-day HRT to 422 mg/ℓ (4.40 mM) at a two-day HRT (0.021 $h^{-1}$). This sudden improvement in sulphate conversion corresponds with an increase in the VSRR from 7.0 mg/ℓ.h at a 2.3-day HRT (0.018 $h^{-1}$) to 12.0 mg/ℓ.h at a 2-day HRT (0.021 $h^{-1}$). The sulphate conversion decreases gradually with subsequent reduction in the applied HRT, achieving

a sulphate conversion of 41% at a one-day HRT (0.042 $h^{-1}$). The VSRR continues to increase over this period, from 12.0 mg/ℓ.h at a two-day HRT to 17.1 mg/ℓ.h at the one-day HRT (0.042 $h^{-1}$).

The measured sulphide concentration within the reactor (Figure 5-17A) was largely consistent with the predicted sulphide concentration based on the stoichiometric reduction of sulphate in the reactor. The sulphide concentration reached 212 mg/ℓ (6.22 mM) at a four-day HRT before decreasing to 135 mg/ℓ (3.96 mM) at a 2.3-day HRT (0.018 $h^{-1}$). The maximum observed sulphide concentration, of 216 mg/ℓ, (6.33 mM) was reached at a two-day HRT. The sulphide concentration then decreased linearly with increasing dilution rate, reaching 137 mg/ℓ (4.02 mM) at a one-day HRT (0.042 $h^{-1}$). The pH within the reactor remained steady, on average 7.4, for the duration of the HRT study (Figure 5-17D). The redox potential within the reactor was fairly stable but decreased gradually from -175 to -137 mV over the course of the HRT study.

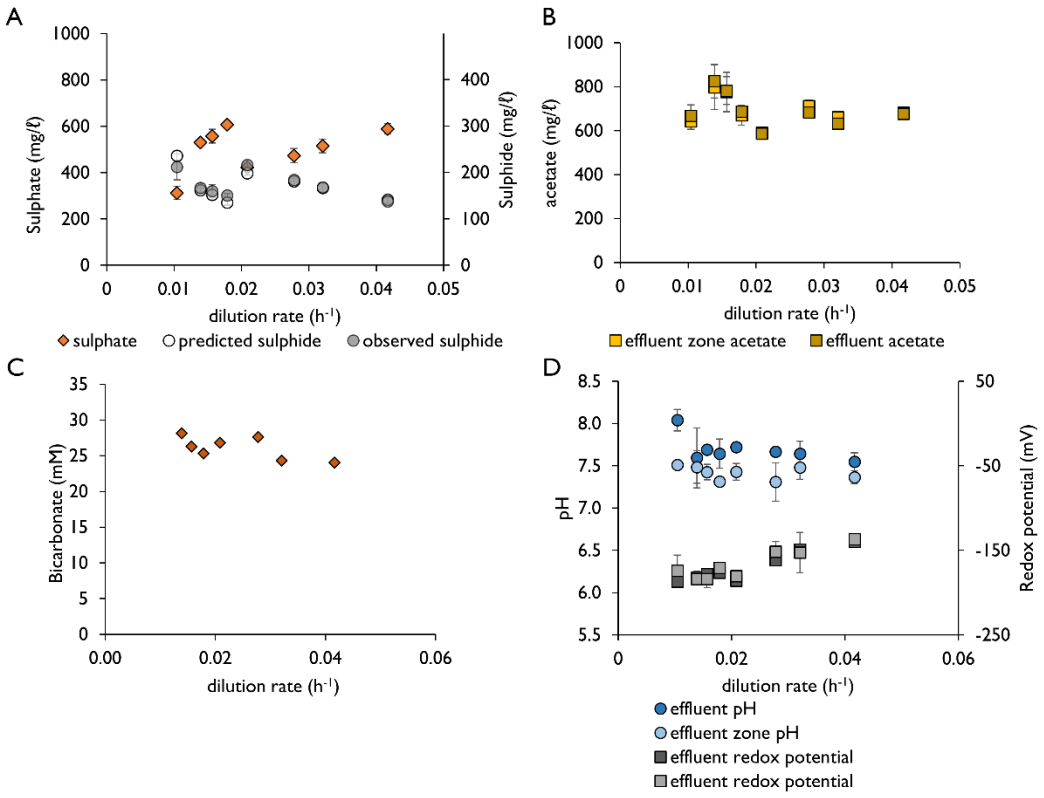


Figure 5-17 Steady-state kinetic data collected from the acetate-supplemented LFCR, at a range of tested dilution rates, including (A) the residual sulphate, the produced sulphide and the predicted sulphide concentration, based on the observed sulphate reduced,; (B) the observed residual acetate concentration; (C) the produced bicarbonate concentration present in the reactor effluent calculated from the difference between the observed and feed bicarbonate concentrations and (D) the pH and redox potential (reported relative to a standard hydrogen electrode). The observed residual acetate concentration, redox potential and pH are reported for solution chemistry drawn from the effluent-zone of the reactor and the reactor effluent. Error bars represent one standard deviation from the mean.

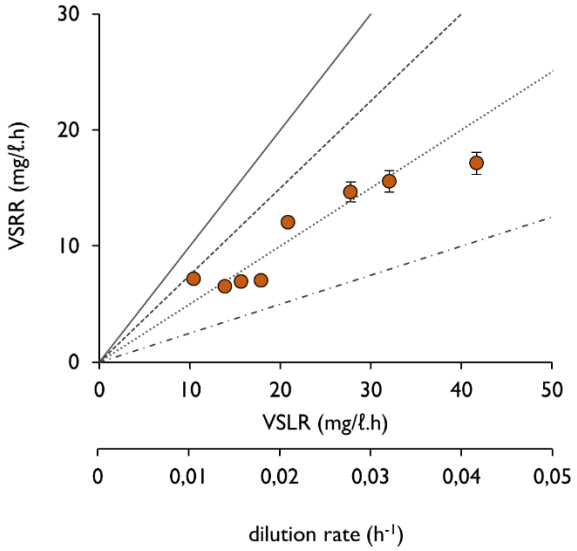


Figure 5-18 The VSRRs achieved by the acetate-supplemented LFCR at varied volumetric sulphate loading rates, varied through the increase in the applied dilution rate, corresponding to HRT between four- and one-days. Sulphate conversion can be visually determined through comparisons with plotted lines: 100% conversion – solid line, 75% conversion – dashed line; 50% conversion – dotted line, 25% - composite dashed and dotted line. Error bars represent one standard deviation from the mean.

**Biomass retention**

The planktonic cell concentration supported within the inlet and effluent zones of the acetate-supplemented LFCR differed by, on average, 15% of the concentration of cells supported within the effluent zone. The cell concentration supported within the reactor at a four-day HRT (0.010 $h^{-1}$) varied between 2.4 - 2.55 x $10^8$ cells/mℓ (Figure 5-19). The concentration of supported cells decreased at a three-day HRT (0.014 $h^{-1}$) to 1.7 - 2.0 x $10^8$ cells/mℓ. The planktonic cell concentration then increased to a maximum of 2.3-3.0 x $10^8$ cells/mℓ at a two-day HRT before gradually decreasing to 1.5 - 1.6 x $10^8$ cells/mℓ at a one day HRT (0.042 $h^{-1}$). The cell concentration supported by similarly operated CSTR was, on average across each tested HRT, 120% greater in magnitude than supported within the effluent zone of the LFCR.

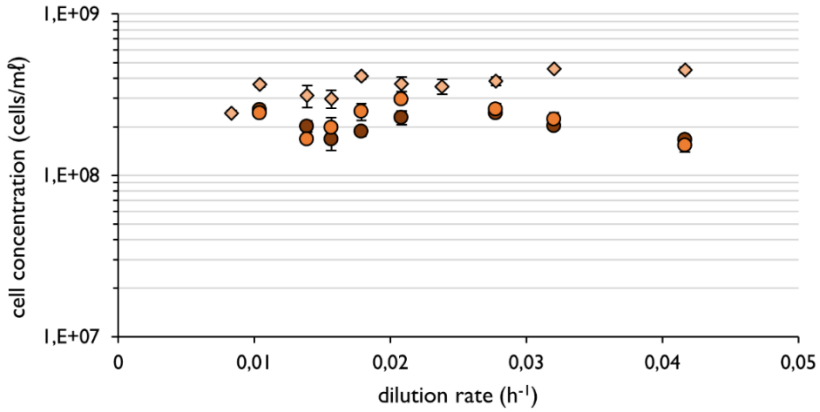


Figure 5-19 The planktonic cell concentration supported in the (●) inlet- and (●) effluent-zones of the lactate-supplemented LFCR at a range of tested dilution rates corresponding to HRTs ranging from four- to one-day. The concentration of planktonic cells supported by the similarly operated (♦) lactate-supplemented CSTR are shown for comparison. Cell concentrations were determined through direct cell counting on solution drawn directly from the respective reactor zone. Cell counts were performed in duplicate and error bars represent one standard deviation from the mean.

The biomass retained within the biofilm-associated and biofilm attached communities of the acetate supplemented LFCR was evaluated at the initial four- and one-day HRTs (0.010 and 0.042 $h^{-1}$; Figure 5-20). This found the concentration of cells within the associated communities to be similar to the concentration of cells found within the planktonic communities. At a four-day HRT, the concentration of cells within the associated communities of the inlet and effluent zones were 4.7 x $10^8$ cells/mℓ and 3.8 x $10^8$ cells/mℓ, respectively. This decreased to 1.3 x $10^8$ and 1.5 x $10^8$ cells/mℓ, respectively, at a one-day HRT. The attached cell concentration, however, was more than 10-fold that of the planktonic cell concentration within each zone and at both HRT. The attached cell concentration decreased from 2.58 x $10^9$ - 2.88 x $10^9$ cells/mℓ at a four-day HRT to 1.74 x $10^9$ - 2.01 x $10^9$ cells/mℓ at a one-day HRT.

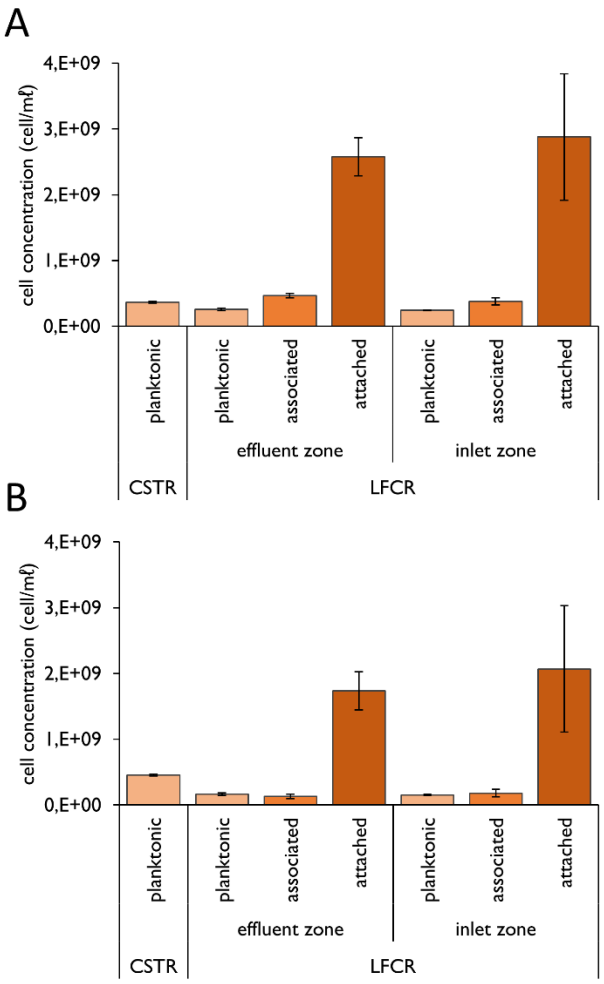


Figure 5-20 The concentration of planktonic, biofilm-associated and attached communities of the acetate-supplemented LFCR and the planktonic cell concentration in the acetate-supplemented CSTR at a (A) four- and (B) one-day HRT. The microbial communities of both the effluent and inlet zones of the LFCR were assessed independently. Biofilm communities were sampled in duplicate and cell counts were then performed in duplicate. Error bars represent one standard deviation from the mean.

SEM was used to visually inspect the surface of the carbon microfibres which were removed from the acetate-supplemented LFCR at a four- and one-day HRT (Figure 5-21). At both the four- and one-day HRT, cells embedded within a thick layer of EPS were visible spread over the surface of the fibres. These cells were mostly rod and vibrio in morphology. Large crystalline precipitates were also attached to these fibres (Figure 5-21C) at both tested HRT. Similar crystalline precipitates were described by Marais (under review) when operating a LFCR under similar conditions. Marais (under review) used Energy Dispersive Spectroscopy to show these precipitates largely comprised magnesium and phosphorus.

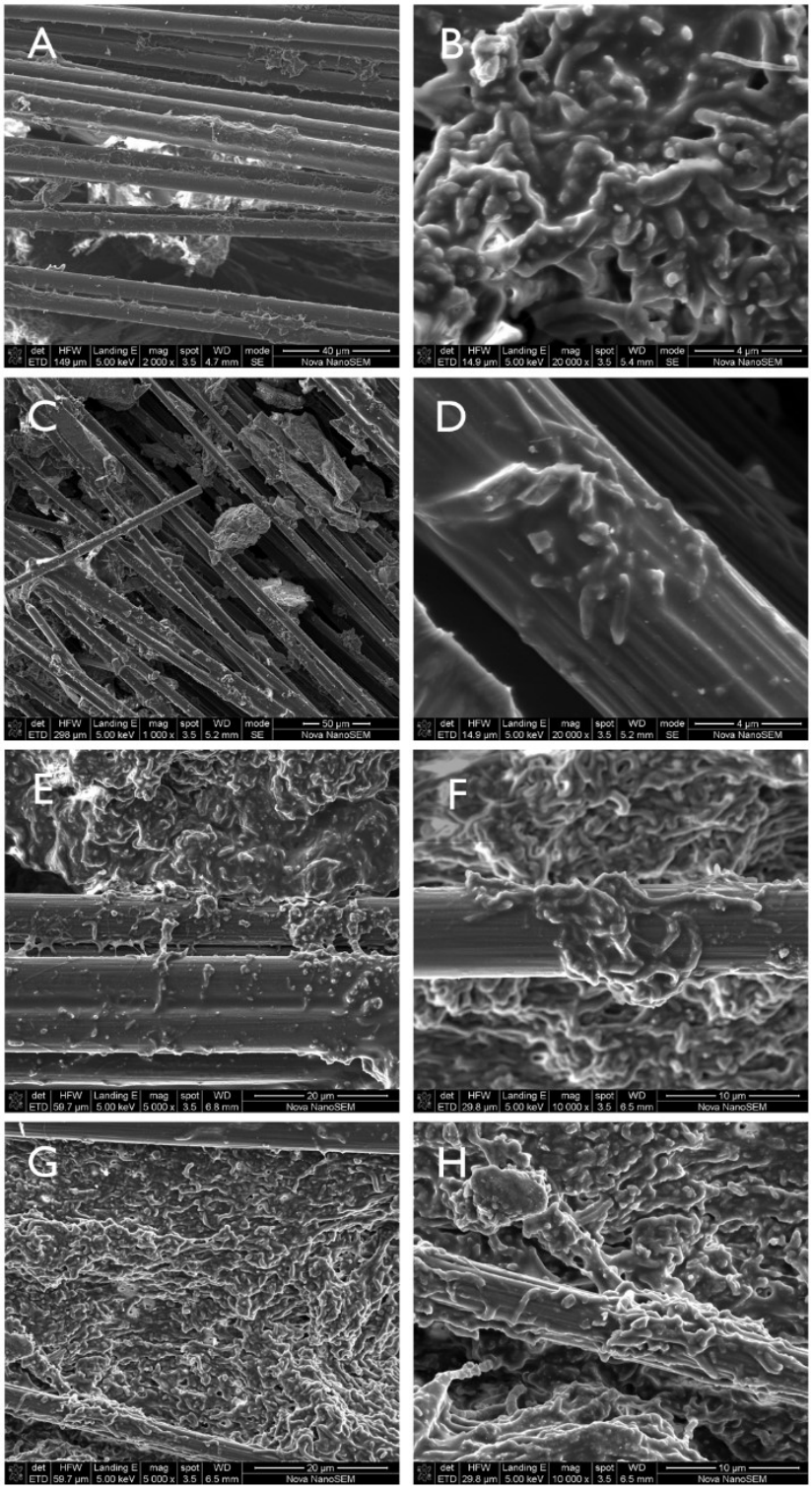


Figure 5-21 Scanning electron micrographs of the carbon microfibres recovered from the acetate-supplemented LFCR. Carbon microfibres were recovered at a four-day HRT from the (A, B) inlet zone and (C, D) effluent zone, and at a one-day HRT, fibres were again recovered from the (E, F) inlet and (G, H) effluent zones. Scale bars are shown in each micrograph.

### 5.4.2 Microbial ecology

The acetate-supplemented LFCR, at the phylum and class level, was dominated by two classes of Bacteroidetes: Flavobacteria and Bacteroidia (Figure 5-22). These two classes constituted more than 50% of each of the planktonic, associated and attached communities at a four-day HRT (0.010 $h^{-1}$). Deltaproteobacteria, entirely comprised putatively identified SRB, made up 10 to 20% relative abundance of the attached and associated communities at a four- and one-day HRTs. The relative abundance of this class fluctuated, however, within the planktonic communities. Briefly, the relative abundance in the four-day planktonic communities ranged between 13 - 14% but decreased to 4-5% at a three-day HRT. The abundance then increased to 14 - 21% at a 1.5-day HRT before decreasing to 7 - 9% at a one-day HRT.

The class composition of the planktonic communities saw large changes between the four- and one-day HRTs. The abundance of Flavobacteria decreased from 30 - 34% at a four- and three-day HRT to 8 - 12% relative abundance at a 1.5-day HRT. This class was present at less than 1% relative abundance at a one-day HRT. The relative abundance of the other predominant class of Bacteroidetes, Bacteroidia, appears to be almost unaffected by the reduced HRT. The Firmicutes class of Bacilli increases from almost undetectable in the planktonic communities at the longer HRT to 3% and 20 - 34% relative abundance of the planktonic communities at a 1.5- and one-day HRTs, respectively.

Bacilli also constituted a large proportion of the attached and associated communities at a one-day HRT, after being almost undetected at a four-day HRT. The class of Synergistia and Clostridia show little change a result of applied dilution rate. Synergistia made up roughly 10% of the attached communities, 15% of the associated communities and 20% of the planktonic communities.

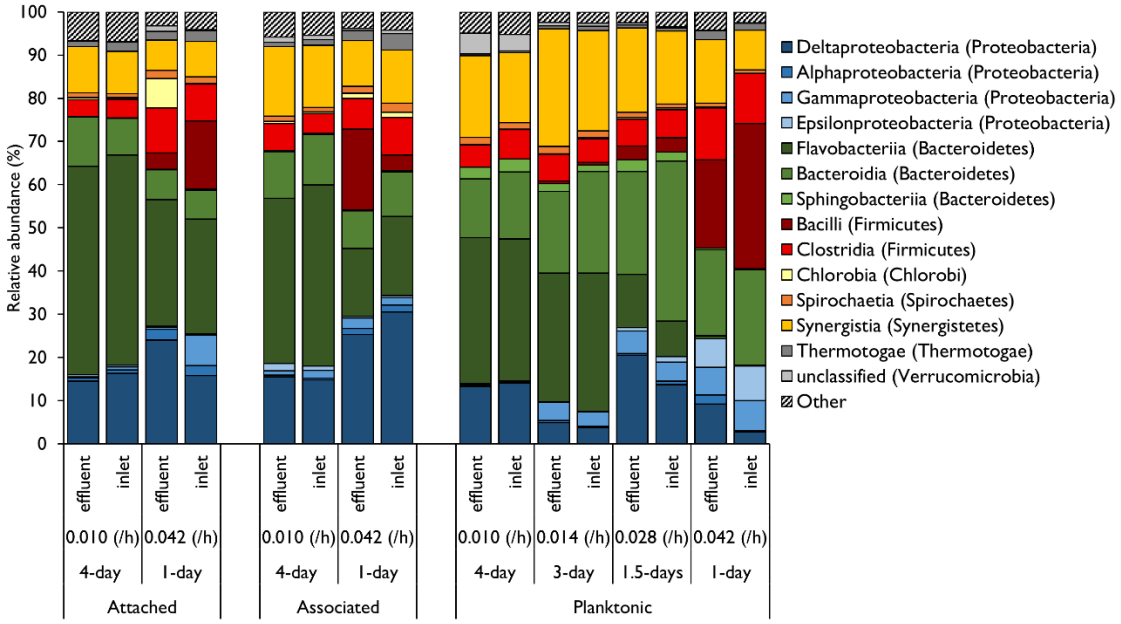


Figure 5-22 Relative abundance of the predominant microbial classes within the planktonic, attached and associated communities of the inlet and effluent zones of the acetate-supplemented LFCR at dilution rates corresponding to four- (0.010 $h^{-1}$), three- (0.014 $h^{-1}$), 1.5- (0.028 $h^{-1}$) and one-day (0.042 $h^{-1}$) HRTs. The phyla to which each class belongs are shown in parentheses.

Although not evident at the class taxonomic level, the OTUs which constituted the planktonic and biofilm communities were highly dissimilar (Figure 5-23). The Flavobacteria classified *Lutaonella* (0) was the largest constituting OTU within the biofilm-associated and attached communities at a four- and one-day HRT. A different Flavobacteria classified microorganism, *Pustulibacterium* (3), was the most abundant OTU within the planktonic communities at a four- and three-day HRT. This OTU then exhibits a considerable reduction in abundance at a 1.5-day HRT and is detected at less than 0.1% relative abundance at a one-day HRT.

Not only were the biofilm communities and planktonic communities dissimilar, but the OTU composition of each of these communities changed substantially between a four- and one-day HRT. Three putatively identified SRB were identified within the biofilm communities at a four-day HRT. These were *Desulfatitalea* (177), *Sporotomaculum* (112) and a small proportion of *Desulfobacter* (18). *Sporotomaculum* (112) was identified as an SRB through matching with a recovered Clostridial classified genome bin in Chapter 8 (Section 8.5), Desulfotomaculum_gibsoniae_47_21, which contains the genes required for dissimilatory sulphate reduction. The three SRB OTUs present in the biofilms at a four-day HRT had almost entirely been replaced by *Desulfobacter* (18) and *Desulfomicrobium* (1) at a one-day HRT. The planktonic communities, too, show large changes in the constituting SRB with the changing in the applied

HRT. At a four-day HRT, these SRB communities largely comprised *Desulfovibrio* (6) as well as *Sporotomaculum* (112) and a small proportion of *Desulfomicrobium* (1). At a 1.5- and one-day HRTs, these SRB communities are almost entirely made up of *Desulfobacter* (18) and *Desulfomicrobium* (1).

A further observation is the inverse abundances of the Synergistales OTUs *Aminomonas* (2) to *Dethiosulfovibrio* (13) in the planktonic communities between a four- and one-day HRT. The *Aminomonas* OTU was dominant at longer HRT, while the *Dethiosulfovibrio* OUT subsequently became dominant at shorter HRT.

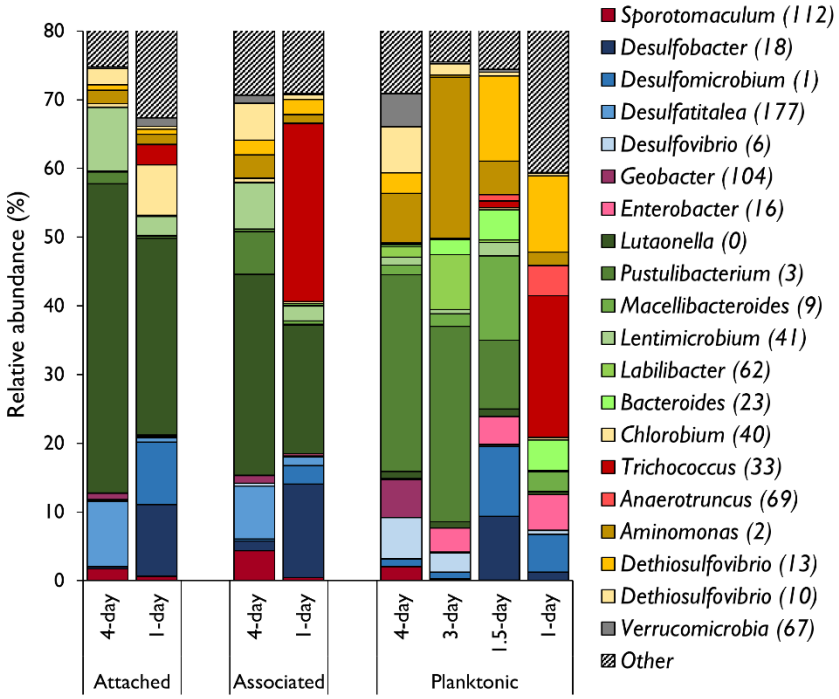


Figure 5-23 The relative abundance of the most abundant OTUs in the associated, attached and planktonic communities of the effluent zone of the lactate-supplemented LFCRs at dilution rates corresponding to a four-, three-, two- and one-day HRT. OTUs are coloured by taxonomy: Deltaproteobacteria – blue, other Proteobacteria – purple, Bacteroidetes – green, Firmicutes – red, Synergistetes – yellow, other phyla – grey.

## 5.5 Acetate-supplemented LFCR Discussion

The following sections aim to determine the extent of acetate oxidation by SRB and competing microorganisms in the acetate-supplemented LFCR. This is attempted through an assessment of the collected physiochemical data including the reduced sulphate, removed acetate, and the produced bicarbonate in the reactor. Subsequently the microbial ecology, in terms of cell

concentration and taxonomy, is overlaid with this performance data to estimate the influence of specific microorganisms with the observed reactor performance.

### 5.5.1 Prevailing metabolisms in the acetate-supplemented LFCR

The concentration of acetate predicted to be present in the LFCR at each HRT was predicted using a set of assumptions. Firstly, all sulphate reduced was linked to acetate oxidation (Equation 2-7). According to this equation, the reduction of one mol of sulphate is coupled to the oxidation of 1 mol of acetate. The second assumption is that all acetate which was oxidised in the reactor was oxidised by SRB. The first plotted prediction, shown in Figure 5-24, assumes that the only acetate available for sulphate reduction was the 11 mM acetate supplied in the reactor medium. The second prediction assumes that, in addition to this acetate, a further 4.37 mM acetate is generated from the oxidation of yeast extract, as demonstrated in Section 4.4.2. The observed acetate concentration at each HRT differs from this predicted acetate concentration, by on average, 8.6% of the predicted value. A third predicted acetate concentration is also plotted in this figure which accounts for the potential of acetate generation through citrate oxidation. This final prediction represents a theoretical maximum acetate concentration which could be observed in the reactor if assumption one and two are true. If a residual acetate concentration should have been found above this prediction, this would have indicated that the assumption that sulphate reduction was linked to acetate oxidation would be proved to be false.

The relatively small difference between the observed and predicted acetate concentration, predicted assuming the generation of acetate from yeast extract oxidation, provides strong evidence that sulphate reduction is linked, predominantly, to acetate oxidation.

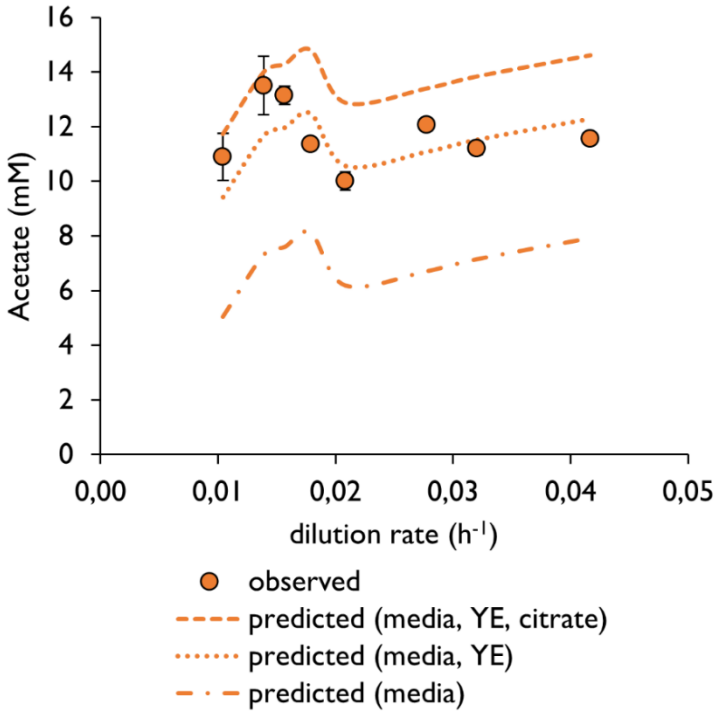


Figure 5-24 The observed and predicted residual acetate concentration in the acetate-supplemented LFCR at a range of dilution rates which correspond to HRT between four- and one-day HRT (0.010 - 0.042 $h^{-1}$). Predicted acetate concentrations were based on the degree of sulphate reduction being solely linked to oxidation of acetate present in the media, according to Equation 2-7, and including the concentration of acetate generated from yeast extract oxidation Section 4.4.2 and including the concentration of acetate potentially generated from the oxidation of 1.16 mM citrate.

The concentration of bicarbonate produced in the reactor varied between 24 and 28 mM for the duration of the HRT study. The predicted 'produced bicarbonate' is plotted alongside this observed concentration in Figure 5-25. This prediction is based solely on the bicarbonate produced through acetate-linked sulphate reduction, according to Equation 2-7. The observed bicarbonate concentration was greater than this 'SRB produced' bicarbonate concentration by, on average across the HRT study, just 11%. Within the lactate-supplemented LFCR, the observed bicarbonate concentration was greater than predicted by, on average, 49%. The bicarbonate concentration within the lactate system was calculated based on the oxidation of lactate by SRB and by fermentative microorganisms, and the oxidation of acetate by SRB whereas the bicarbonate concentration in the acetate-supplemented LFCR was calculated solely on the metabolism of SRB.

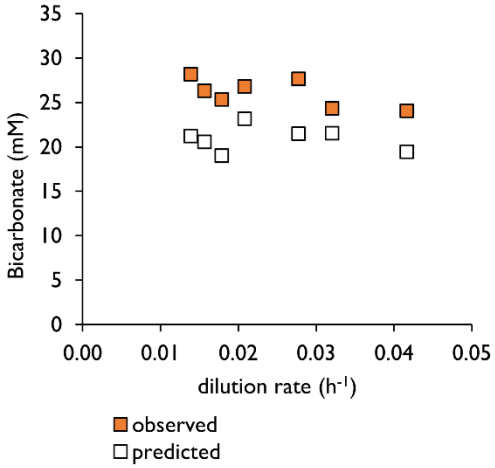


Figure 5-25 The observed and predicted produced bicarbonate concentrations in the acetate-supplemented LFCR at a range of tested dilution rates corresponding to HRT between and including four- and one-day (0.010 – 0.042 $h^{-1}$). Predicted produced bicarbonate concentrations were based on the observed sulphate reduction, assuming all sulphate reduction was linked to oxidation of acetate in the reactor medium according to Equation 2-7.

The difference of 25% between the observed and predicted produced bicarbonate concentrations in the acetate system is surprisingly small as this 25% is all that would indicate the presence of microorganisms other than SRB. This is also low considering the 86% difference between the observed and predicted produced bicarbonate concentrations in the lactate system, which was concluded to have been generated through citrate and yeast extract oxidation, both of which are occurring in the acetate system. The estimated relative abundance of non-SRB ranges from 79-91% in the planktonic communities and 68-82% in the biofilm communities of the acetate LFCR. Furthermore, considering that 4.37 mM of acetate was concluded to be generated from yeast extract oxidation, as shown in Figure 5-24, this should be accompanied by the production of additional bicarbonate. Since the acetate LFCR was identical in configuration to the lactate LFCR, showed similar pH to the lactate LFCR (where additional bicarbonate accumulated) and all sulphide generated from sulphate reduction could be accounted for, it is concluded that negligible bicarbonate was lost as gaseous carbon dioxide. The reason for the deficit of bicarbonate is still unclear, however, genome resolved metagenomics (Section 8.5.4) indicates autotrophic growth in this community is possible.

Genome-resolved metagenomics revealed that hydrogen evolving and consuming hydrogenases were widespread among the BSR reactor microbial communities (Chapter 8). It was concluded from the almost uniformity in the distribution of these genes amongst the microorganisms of these systems that hydrogen cycling was occurring in these systems. Examination of the genomes of the identified SRB revealed that all SRB contained genes encoding hydrogen consuming, group 1 NiFe

hydrogenases and would, therefore, be able to oxidise any hydrogen produced within these systems. Therefore, a portion of the sulphate reduction was linked to the oxidation of hydrogen produced through the fermentation of yeast extract and/or citrate by non-SRBs. Autotrophic pathways, present in an estimated 47% of the biofilm community at a four-day HRT, were found together within hydrogen consuming hydrogenases genes amongst several Bacteroidetes and Proteobacteria. It is therefore possible that autotrophic fixation of bicarbonate in the reactor was performed by SRB and additional microorganisms.

### 5.5.2 Comparison of the performance of the acetate-supplemented LFCR and CSTR

The acetate-supplemented LFCR and CSTR showed similar trends in the exhibited VSRR at increased VSLRs and dilution rates (Figure 5-26). The acetate CSTR maintained a sulphate conversion of 39% between a five- and 2.6-day HRT (0.008 – 0.018 $h^{-1}$). The sulphate conversion then increased to 51% at a 2.3-day HRT. This improved sulphate conversion was attributed to the increased, cumulative abundance of low-abundance SRB in this reactor. The LFCR also showed an improved sulphate conversion at similar applied dilution rates. The sulphate conversion increased from 39% at a 2.3-day HRT (0.018 $h^{-1}$) to 58% at a two-day HRT (0.021 $h^{-1}$). As discussed below, this is thought to be a consequence of the changing microbial community composition. In both reactors, *Desulfovibrio* (6) is the predominant SRB at a four-day HRT (0.010 $h^{-1}$). However, this OTU subsequently experiences near-complete washout at a three-day HRT(0.014 $h^{-1}$). The loss of this microorganism may have been the likely trigger for the subsequent changes in the composition of these SRB communities. This is discussed in more detail in Sections 5.5.4 below.

The acetate-supplemented CSTR exhibited a substantial decrease in sulphate conversion between a 1.5- (0.028 $h^{-1}$) and 1.3-day HRT (0.032 $h^{-1}$) corresponding to the VSRR decreasing from 10.8 to 8.1 mg/ℓ.h (Figure 5-26). The LFCR, although exhibiting a decreased sulphate conversion from 53 to 48% over this period, does not show a decrease in VSRR. Maintaining the VSRR is attributed to the SRB retained within the biofilm communities associated with the carbon microfibres of this reactor.

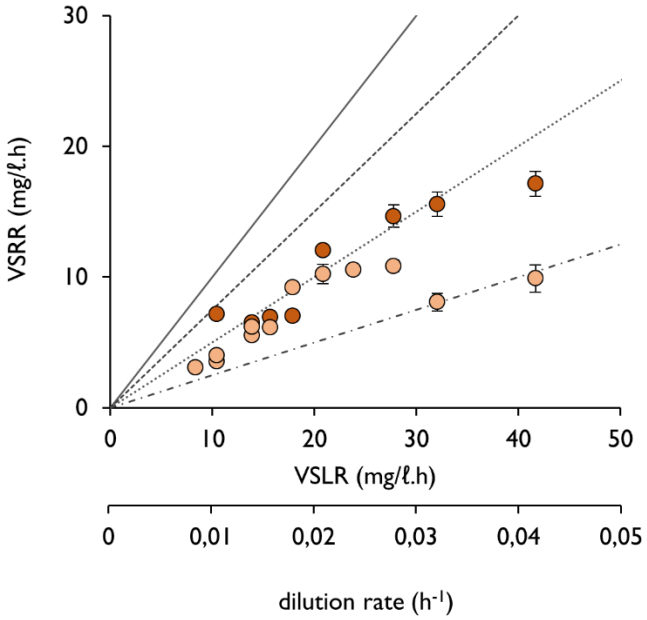


Figure 5-26 The VSRRs achieved by the acetate-supplemented (●) LFCR and similarly operated (●) CSTR at VSLR, varied through the reduction in the HRT applied to the systems. Sulphate conversion can be determined through comparisons with plotted lines: 100% conversion – solid line, 75% conversion – dashed line; 50% conversion – dotted line, 25% - composite dashed and dotted line.

### 5.5.3 Estimated SRB-biomass retention

The cell concentration of SRB in the microbial communities of the acetate-supplemented LFCR were estimated by multiplying the summed relative abundance of the putatively identified SRB OTUs, at each HRT, by the total cell concentration of that community (Figure 5-27). The decreasing SRB cell concentrations present in planktonic microbial communities during the HRT study reflects the sulphate conversion profile, as illustrated in Figure 5-27 below. At a four-day HRT the combined cell concentration of *Sporotomaculum* (112), *Desulfovibrio* (6) and *Desulfomicrobium* (1) was 2.5-2.6 x $10^7$ cells/mℓ. This decreased to 8.2 x $10^6$ cells/mℓ at a three-day HRT corresponding with the decrease in sulphate conversion from 69 to 47%. The increased conversion from 47% at a three-day HRT to 53% at a 1.5-day HRT coincided with the increase in concentration of cumulative planktonic SRB to 4.2 x $10^8$ cells/mℓ. The SRB, at this HRT, are almost entirely made up by *Desulfomicrobium* (1) and *Desulfobacter* (18). These two SRB OTUs are still present within the reactor at a one-day HRT, but cumulatively at a 4.2-fold lower cell concentration.

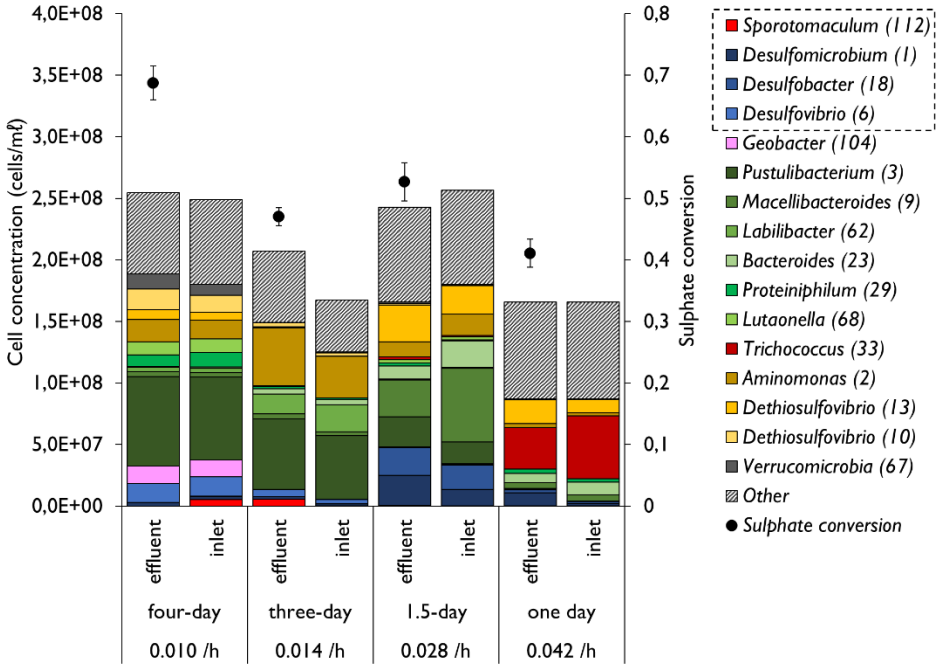


Figure 5-27 The estimated cell concentrations of the predominant OTUs in the planktonic communities of the lactate-supplemented LFCR at a range of tested dilution rates. Cell concentrations were estimated through multiplying the relative abundance of an OTU by the total cell concentration determined at each respective steady-state through direct cell counting. The sulphate conversion achieved at each HRT is shown in the secondary y-axis. OTUs are coloured by taxonomy: Deltaproteobacteria – blue, other Proteobacteria – purple, Bacteroidetes – green, Firmicutes – red, Synergistetes – yellow, other phyla – grey. OTUs putatively identified as SRB have been circled by a dotted line in the legend.

The decrease in planktonic SRB by more than 4-fold between a 1.5- and one-day HRT and the resulting sulphate conversion decreasing by just 7% suggests that the SRB held within the biofilm are the major contributors to the sulphate reducing performance of this reactor, certainly at a one-day HRT. The estimated concentration of total SRB cells within the planktonic, associated and attached communities of the acetate-supplemented LFCR and are shown in Figure 5-28. The large majority of SRB held within this reactor, $2.9 \times 10^8 – 4.2 \times 10^8$ cells/mℓ, are held within the attached biofilm communities. In contrast, the estimated SRB cell concentration in the planktonic phase ranged from $4.5 \times 10^6$ to $4.9 \times 10^7$ cells/mℓ.

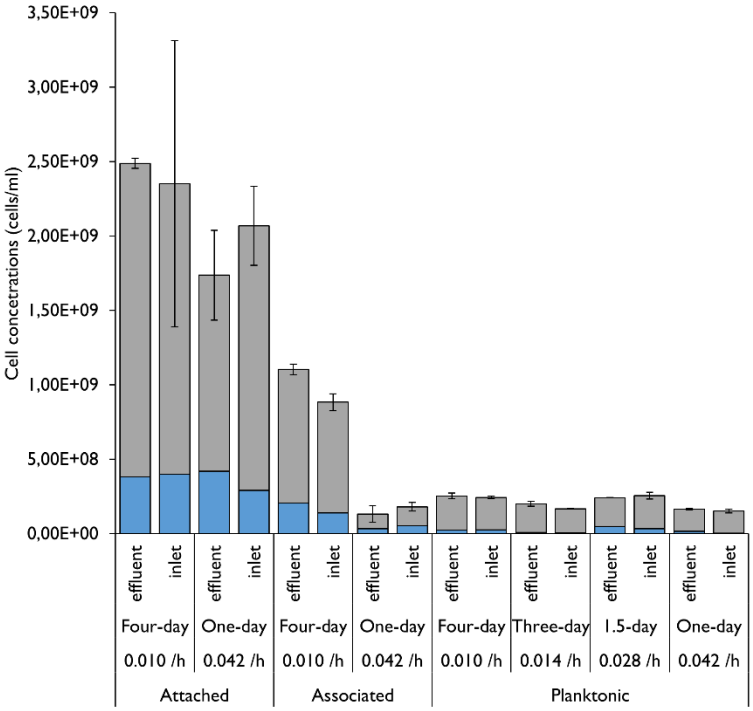


Figure 5-28 The estimated cell concentrations of identified SRB (blue) and non-SRB (grey) of the attached, associated and planktonic communities of the lactate-supplemented LFCR, at a range of tested HRT including four-, three-, 1.5- and one-day HRT. The total magnitude of these communities was determined by direct cell counting, following, where applicable to, the use of the modified detachment protocol. The proportion of SRB within a community was determined through the identification of SRB OTUs following 16S rRNA amplicon sequencing. Genome-resolve metagenomics, where possible, was used to supplement and validify the identification of these SRB. Error bars represent one standard deviation are from the mean, as described in Figure 5-20.

### 5.5.4 Changes in OTU composition linked to reactor performance

Both the planktonic and biofilm communities showed extensive changes in the OTU composition of these communities as a result of decreasing the HRT. Hierarchical clustering was used to resolve the predominant OTUs of these communities based on their abundance across the inlet and effluent zone attached, associated and planktonic communities at a range of tested HRT into four all-encompassing clusters (Figure 5-29). One of these clusters grouped OTUs present predominantly in the biofilm communities at a four-day HRT. This included the SRB OTUs *Desulfobulbus* (58), *Desulfatitalea* (177) and *Desulfarculus* (97). *Desulfatitalea* (177), the most abundant of these SRB OTUs, was also identified in the effluent zone attached community of the acetate-supplemented UAPBR at a four-day HRT and previously concluded in Hessler et al. (2018) to play a role in sulphate scavenging in the effluent of this reactor.

*Desulfovibrio* (6) and *Sporomaculum* (112) were present in the planktonic communities at a four-day HRT but show almost complete washout at a three-day HRT. These SRB OTUs are not replaced by any other SRB in the planktonic communities until a two-day HRT when

*Desulfobacter* (18) and *Desulfomicrobium* (1) become the predominant planktonic SRBs. These were also the predominating SRB within the biofilm communities at a one-day HRT. *Desulfobacter* (18) was identified within the biofilm community of the inlet zone of the acetate-supplemented UAPBR at a four-day HRT. This localisation of this OTU within the UAPBR suggests that it favours higher concentrations of sulphate and may play a role in the higher VSRR achieved in the inlet zone of this UAPBR.

The sulphate conversion of the acetate-supplemented LFCR decreased from 69%, at a four-day HRT, to 47% at a one-day HRT and coincided with the washout of the *Desulfovibrio* (6) and *Sporotomaculum* (112). The poor performance of the acetate-supplemented LFCR at three-day to a 2.3-day HRTs is, therefore, attributed to the washout of these planktonic SRB. The resulting increased sulphate concentration in the reactor is thought to have prompted the changes in the SRB biofilm communities between a four- and one-day HRT. These changes in the biofilm communities were likely gradual, as is evident in the maintained VSRR of 6.9 mg/ℓ.h between a four- and 2.3-day HRT. The OTUs *Desulfobacter* (18) and *Desulfomicrobium* (1) found in the planktonic communities at a 1.5-day HRT are thought to have been seeded from the biofilm communities in which they were found at a one-day HRT. The role of the SRB within the biofilm, therefore, changes from that of scavenging sulphate not removed by the abundant planktonic *Desulfovibrio* (6) and *Sporotomaculum* (112) at a four-day HRT to becoming the predominant SRB within the reactor at a one-day HRT.

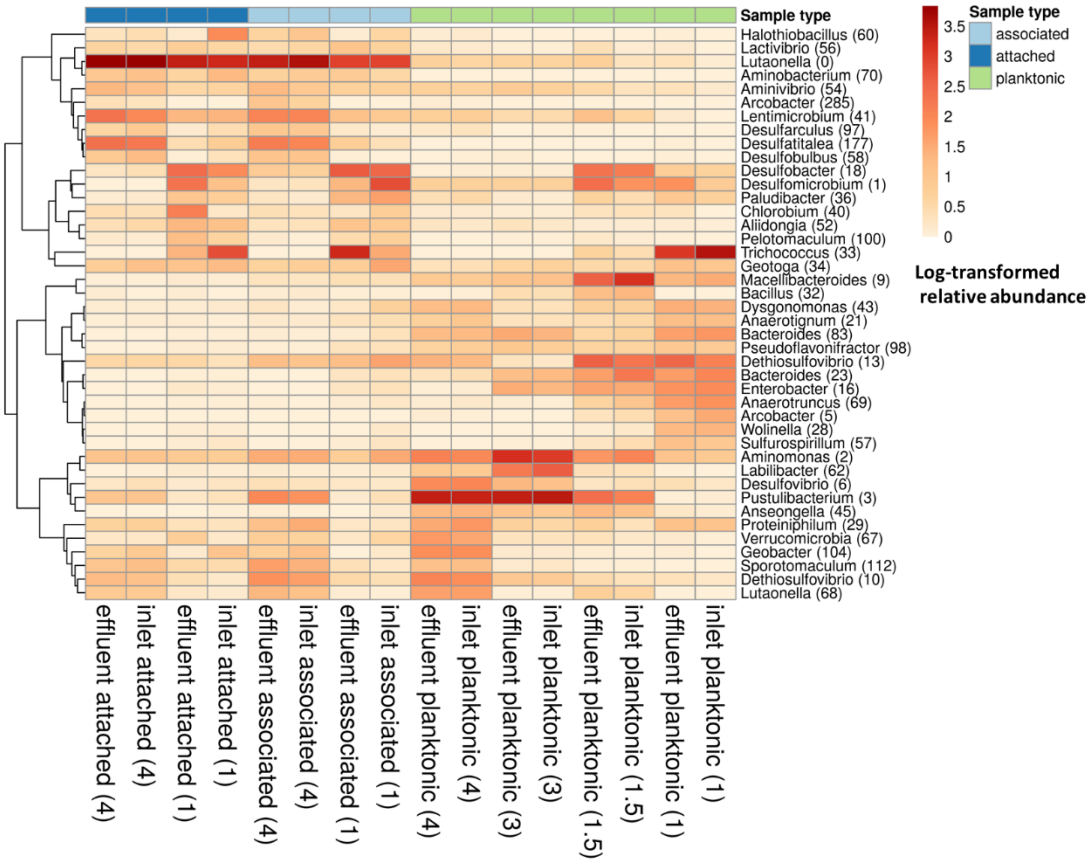


Figure 5-29 Hierarchical clustering of the relative abundance of the predominant OTUs in the planktonic, associated and attached microbial communities of the acetate-supplemented LFCR at a range of tested HRT including four-, three-, 1.5- and one-day HRTs (shown in parentheses in the column names). Hierarchical clustering of the coloumns (samples) was not performed. Relative abundances were ln(x +1) transformed and hierarchical clustering was performed using correlation distance and average linkage (Section 3.9). No row centring was performed. The reactor zone from which each sample was isolated, the microbial phase and the HRT at which the sample was recovered is shown above the heatmap and the legend shown on the right of the heatmap.

The observed changes in the microbial composition of the biofilm and planktonic communities, omitting *Lutaonella* (0), means that the active sulphate reducing microorganisms at the start of the study were distinct from those performing sulphate reduction at a one-day HRT. The non-sulphate reducing microorganisms present in these communities, too, are distinct between the longest and shortest HRT. The change in the composition of the planktonic communities as a result of the increased dilution rates applied to the LFCRs was anticipated. However, the observed changes in the biofilm communities, of both LFCRs, was not. Few changes were expected to take place within the biofilms due to their resistance to cell washout at reduced HRTs. The observed changes indicate that the biofilms are far more dynamic than previously thought. It appears that these communities do not change as a direct result of the increased dilution rate but rather due to changes in the physiochemical environment as a consequence of changes within the planktonic

microbial communities. This is an important observation when considering the inoculum which should be used in these systems, as these may be optimised depending on the specified operating conditions. This was highlighted by Pruden et al. (2007) who saw differing performance in identical reactors which were inoculated with SRB inoculums from different sources.

Substantial changes in the microbial communities of bioreactors, as a result of differing operating conditions, has been noted in various fields, including BSR (Zheng et al., 2014), wastewater treatment (Ding et al., 2019) and anaerobic digestion (Xu et al., 2018). The effect of various pH conditions on the resulting sulphate reducing microbial communities of bio-electrochemical systems was tested by Zheng et al. (2014). The communities which inhabited the studied bioreactor systems at pH of 4.5 and 6.5 were somewhat similar but shared no community members with an identical reactor operated at a pH of 8.5. The microbial communities of anaerobic digesters operated at differing hydraulic retention times, of 20- and 15-days, and organic loading rates were evaluated by Xu et al. (2018). These authors concluded that these varied conditions were strong deterministic factors based on changes seen these microbial communities. Ding et al. (2019) found that the HRT applied to wastewater-treating membrane bioreactors was a major selection factor for the resulting microbial communities of these systems. This was a remarkable finding considering cell-washout was prevented in these systems through the use of membranes.

Apart from ensuring that BSR reactor inoculums contain a diverse group of SRB, it should be possible to design or supplement the inoculum with SRB known to perform well at the desired operating conditions, thus further ensuring robust performance. The re-inoculation of the acetate-supplemented LFCR at a three-day HRT, with *Desulfobacter* (18) and *Desulfomicrobium* (1), may have allowed a more rapid recovery in reactor performance which was only seen at a two-day HRT. Whereas re-inoculation with a *Desulfovibrio* (6) rich culture may not have led to a significant improvement in reactor performance.

## 5.6 The performance of the acetate- and lactate-supplemented LFCRs in the context of reported literature

The performance of the acetate- and lactate-supplemented LFCRs was compared to that of other continuous semi-passive reactor systems described in the literature in Figure 5-30. The VSRR achieved by each of these reactors is shown against the applied VSLR. The number of variables which were controlled between these studies is minimal, often using genuine ARD from different mines, with differing complex substrates, differing pH and temperatures, making the comparison

of these studies difficult. However, the differences in the performance of each of these systems are discussed on the basis of the conclusions made within each of these studies.

Spent mushroom compost (SMC) is a commonly used reactor matrix and complex carbon source for passive BSR systems. Das et al. (2012) demonstrated that a VSRR and sulphate conversion of 8.1 mg/ℓ.h and 88%, respectively, could be achieved using synthetic ARD with a pH of 2.8, sulphate concentration of 2.6 g/ℓ and SMC as the substrate for sulphate reduction. These authors noted, however, that the SMC, needed to be replenished after 13 weeks. Similar conditions were used by Dvorak et al. (1992) and, even at the relatively long applied HRT of over seven days, were unable to observe considerable sulphate reduction. However, the sulphide which was generated in this reactor was enough to precipitate the majority of the metals entering the system.

The passive to semi-passive reactor systems described in literature which achieve the highest VSRR, achieved through short operated HRT, are commonly supplemented with manure as a substrate for sulphate reduction (Vossoughi et al., 2003; Novhe et al., 2016; Vasquez et al., 2016; Neale et al., 2018). It is interesting to note that the acetate-supplemented LFCR demonstrates lower but comparable VSRR to that of Vasquez et al. (2016) at VSLR between 26-28 mg/ℓ.h. This demonstrates that the use of acetate and low concentrations of fermentable material, including yeast extract and citrate, can be employed to achieve similar VSRR and sulphate conversions achieved using potentially more expensive complex electron donors.

Bayrakdar et al. (2009) demonstrated a VSRR and corresponding sulphate conversions of 37.5 mg/ℓ.h and 90%, respectively, at VSLR of 42 mg/ℓ.h. This result was achieved using a baffled reactor supplemented with a lactate to sulphate ratio similar to that used in this study. The VSRR achieved by this reactor, using 1 g/ℓ sulphate and an HRT of two-days was nearly double that achieved by the lactate-supplemented LFCR described in this study. This indicates that the performance of the LFCR can be improved through minimising the proportion of lactate which is oxidised by fermentative microorganisms.

The performance of the anaerobic acetate- and lactate-supplemented LFCRs, within this study, were compared to that of the hybrid LFCRs operated by Marais et al. (2020). These reactors were operated with the same reactor feed, temperature, volume, sulphate concentrations and similar HRT. The comparison, therefore, sought to identify whether the operation of these reactors as a hybrid, sulphate reducing and sulphide oxidising, system would hinder sulphate reducing performance through the routine collapsing and harvesting of the floating sulphur biofilm. This was performed by Marais et al. (2020) and was shown to lead to brief periods of oxygen ingress. At a two-day HRT, the acetate- and lactate-supplemented hybrid LFCRs both achieved a VSRR of approximately 11 mg/ℓ.h corresponding to sulphate conversions of approximately 52%. This was similar to the 12 mg/ℓ.h VSRR achieved by the acetate-supplemented LFCR of this study, at a two-

day HRT, and greater than the 9.0 mg/ℓ.h VSRR achieved by the lactate-supplemented LFCR within this study. This indicates that the sulphate reducing performance of these LFCRs is not substantially hindered by the operation of these systems as hybrid reactor systems.

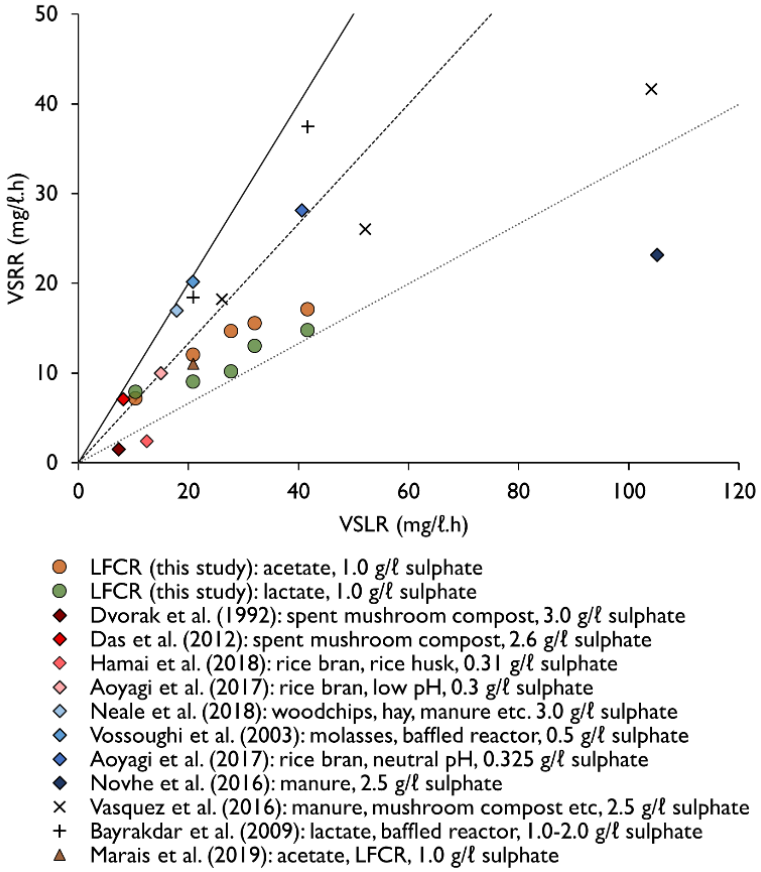


Figure 5-30 The volumetric sulphate reduction rate (VSRR) achieved by the acetate- and lactate-supplemented LFCRs of this study and selected continuous reactor studies from literature, at varied volumetric sulphate loading rates (VSLR) as shown in the legend. Details of the selected study are included in the figure legend including the sulphate concentration and supplied electron donor. Numerous operating conditions and environmental factors vary between these studies and are too numerous to describe here. Sulphate conversion can be visually be determined through comparisons with lines plotted: 100% conversion – solid line, 66% conversion – dashed line, 33% conversion – dotted line.

The BioSURE process utilised primary sewage sludge as an electron donor for sulphate reduction within a reactor system remediating ARD (Rose, 2013). This process was able to reduce sulphate concentrations to below 100 mg/ℓ (1.04 mM) at HRT as short as 12 hours. The process has also shown to be highly effective at removing the metals in the ARD through precipitation with the sulphide produced through sulphate reduction. The main vulnerability of this process identified by Rose (2013) was the potential for the production of toxic sulphide in the effluent at levels which become hazardous. Few studies, including those described above, address the management and

release of sulphide into the environment. An alternative approach to prevent the release of sulphide into the environment is to directly remove sulphate in the ARD through precipitation and not through sulphate reduction to sulphide. This formed the major rationale for the ABC process developed by the CSIR (de Beer et al., 2010). Although highly effective at addressing the acidity, heavy metals and sulphate associated with aggressive ARD the application of this process is dependent on the availability of these reagents and has large CAPEX and OPEX requirements.

The LFCR supplemented with acetate shows considerable sulphate-reducing performance compared with other studies in the literature. This competitive performance achieved using this inexpensive electron donor warrants further investigation. The LFCR supplemented with lactate, however, does show reduced performance against other semi-passive systems using lactate, and even the acetate-supplemented LFCR. The current configuration and operation of this reactor would require modification and improved performance before further scale-up using this electron donor.

## 5.7 Conclusions

The lactate-supplemented LFCR underperformed against the lactate-supplemented CSTR and the acetate-supplemented LFCR. This outcome was surprising considering this reactor had an approximately ten-fold higher biomass retention than the CSTR and the kinetics of SRB growth on lactate far exceeds the respective growth using acetate. This reactor was able to achieve a maximum VSRR of 14.8 mg/ℓ.h of at a one-day HRT, corresponding to a sulphate conversion of just 35%. This provided a valuable opportunity to study the changes in the microbial communities of this reactor as the performance of this reactor declined from well-functioning at a four-day HRT.

The SRB within the planktonic community of this reactor were highly susceptible to the reduction in HRT, with considerable reductions in the abundance of *Desulfovibrio* (6) and *Desulfomicrobium* (1) occurring between a four- and three-day HRT. Inversely, a dramatic increase in the abundance of *Veillonella* (11) occurred during the same period. The high concentration of sulphide likely prevented the growth of this *Veillonella* at a four-day HRT but, with the decrease of the planktonic SRB and the corresponding sulphide concentration, was able to become dominant from a three-day HRT onwards. This fermentative microorganism, particularly within the planktonic phase, is thought to be one of the major competitors with SRB for lactate, while the reliance on the planktonic SRB for sulphate reduction ultimately led to the poor performance of the reactor.

In addition to the poor lactate conversion by SRB in this reactor, little acetate oxidation by SRB or non-sulphate reducing microorganisms was observed within this system during the study. This not only represents an unutilised electron donor for sulphate reduction but also an unwanted by-

product which was expected to have been removed by microorganisms through immobilisation of biomass on the incorporated solid support structures. No SRB specifically implicated in acetate oxidation within other reactors were identified in this system. Inoculation or re-inoculation of this reactor with an acetate-utilising, sulphidogenic microbial culture would have likely aided in both sulphate reduction and COD removal in this reactor system.

In contrast, the acetate-supplemented LFCR performed well compared to the BSR reactors operated in this study and semi-passive reactor systems described in literature. The performance of this solely anaerobically-operated LFCR was similar to that of the dual sulphate reducing and sulphide oxidising LFCR operated by Marais et al. (2020). This indicates that the exposure of these hybrid BSR reactors to brief periods of oxygen ingress, whilst the floating sulphur biofilm is still forming, does not substantially hinder the sulphate reducing performance.

The acetate-supplemented LFCR exhibited a maximum observed VSRR of 17.1 mg/ℓ.h at a one-day HRT. The relatively small difference between the observed and predicted acetate concentration in this reactor provides strong evidence that the sulphate reduction is predominantly linked to acetate oxidation. However, the widespread distribution of genes encoding hydrogen-generating and hydrogen-consuming hydrogenases, together with genes for autotrophic pathways in a number of SRB and other Proteobacteria and Bacteroidetes (Chapter 8) is thought to indicate hydrogen cycling and potential autotrophy in this reactor. This was particularly evident in the agreement between the observed bicarbonate and that predicted to be produced as a result of acetate oxidation linked sulphate reduction – not accounting for the metabolisms of citrate and yeast extract consuming microorganisms. This, therefore, indicated a deficit of bicarbonate. This deficit in bicarbonate is not fully understood, however, autotrophic growth provides a possible explanation.

The planktonic and biofilm communities of this reactor showed remarkable changes in their composition as a result of the reduction in the applied HRT. *Desulfovibrio* (6) and *Sporotomaculum* (112) were the predominant SRB in the planktonic community at a four-day HRT but exhibited near-complete washout at a three-day HRT. *Desulfobacter* (18) and *Desulfomicrobium* (1) then became dominant in this community at a 1.5-day HRT, corresponding with improved reactor performance. It is concluded that these SRB were likely inoculated into the planktonic phase from the biofilm once they had become dominant in these biofilm communities. *Desulfobacter* (18) and *Desulfomicrobium* (1) replaced other SRB in these biofilm communities, the predominant of which was *Desulfatitalea* (177). This SRB had been identified in the effluent zone of the acetate-supplemented UAPBR and had consequentially been concluded to be a sulphate scavenger. It is therefore suggested that the role of SRB in the biofilm of this reactor changed from scavenging sulphate which was not consumed by dominant SRB present at a four-day HRT to becoming the

prevailing sulphate reducers in the reactor. The dramatic changes in the SRB composition in this reactor and the differing roles these likely SRB fulfil has important implications for the development and designing of BSR reactor inocula.

# Chapter 6 Up-flow anaerobic packed bed reactors

## 6.1 Introduction

The up-flow anaerobic packed bed reactor configurations (Section 3.3.3) were selected for this study as they offer a low-cost and highly implementable reactor configuration for the treatment of ARD. These reactor configurations offer high biomass retentions and are attractive for semi-passive treatment when operated as down-flow PBRs (Kaksonen and Puhakka, 2007). The 1 ℓ UAPBRs of this study were packed with polyurethane foam cubes of approximately 8 $cm^3$. The foam displaced 2.5% (40 mℓ) of the total volume of the reactor. Although displacing a relatively small proportion of the reactor volume, this carrier proved to be highly effective at retaining high biomass concentrations within the reactors. The incorporation of polyurethane foam was hypothesised to facilitate microbial colonisation through biofilm formation and thereby lead to the decoupling of the hydraulic and biomass retention times. It was also hypothesised that the microbial communities throughout the height of these reactors would show indications of stratification due to the continuum of changing reactor conditions along the length of these plug-flow reactors.

### 6.1.1 Experimental approach

The acetate- and lactate-supplemented UAPBRs were initially operated at a four-day HRT (0.010 $h^{-1}$) and upon stable operation, the HRT study was begun with the iterative reduction of the HRT, until a final tested HRT of one-day (0.042 $h^{-1}$). Solution chemistry data were collected from solution drawn via sampling ports positioned at the boundary between the 0.33 ℓ inlet- and middle zones, between the middle and effluent zones and just below the effluent port of the effluent zone. Solution chemistry data were analysed as described in Section 3.5 of Chapter 3 .

The planktonic communities were quantified by direct cell counting at steady-state at each tested HRT (Section 3.6.1). These communities were further assessed through 16S rRNA gene metagenomics at four-, three-, two- and one-day HRTs. The biofilm communities of these reactors were assessed twice during the study to minimise oxygen and desiccation stress to the microbial communities of these reactors. When assessing the biofilm communities in the reactors, each of the 0,33 ℓ zones of the UAPBRs was further demarcated into two zones of approximately 0.167 ℓ. These zones were numbered one to six (Figure 3-5), with one at the inlet port (bottom of the reactor) and six at the effluent port (top of the reactor). Biofilm communities were quantified using the modified detachment protocol, followed by direct cell counting, at a four- and one-day

HRT (Section 3.6.2). Biofilm associated microbial communities within these reactors were assessed through 16S rRNA metagenomic sequencing at four- and one-day HRTs.

## 6.2 Lactate UAPBR Results

### 6.2.1 Reactor performance

The lactate-supplemented UAPBR was able to convert over 90% of the 1000 mg/ℓ (10.41 mM) sulphate at each tested HRT, achieving greater than 95% conversion at five of the eight tested HRTs, including a one-day HRT (Figure 6-1A). The inlet zone of the lactate UAPBR consumed approximately 600 mg/ℓ (6.25 mM) sulphate at a four-day HRT (0.010 $h^{-1}$). The amount of sulphate consumed in this zone gradually decreased with increasing dilution rate to a minimum of 435 mg/ℓ (4.53 mM) at a one-day HRT (0.042 $h^{-1}$). The reduction in the HRT from four days to three-days and 2.6 days represented a notable perturbation to the performance of the inlet zone. The two residual sulphate concentrations leaving the inlet zone, at these two HRT, are taken to be outliers due to the subsequent increase in sulphate conversion (Figure 6-1A) and VSRR (Figure 6-4) exhibited by this zone improved at even further reduced HRT.

The sulphate leaving the inlet zone at each HRT was largely consumed in the middle-zone. The variation in sulphate consumption in this zone did not vary much with increasing dilution rates. The average sulphate consumed within the middle zone was 320 mg/ℓ (3.33 mM) sulphate with a standard deviation of 32 mg/ℓ (0.33 mM) when omitting the data points collected at 3- and 2.6-day HRTs (0.014-0.016 $h^{-1}$). The effluent zone saw little sulphate until a two-day HRT (0.021 $h^{-1}$), after which the sulphate consumption in this zone increased with increasing dilution rate. This zone consumed 130 mg/ℓ (1.35 mM) sulphate at a 1.5-day HRT, 166 mg/ℓ (1.73 mM)at a 1.3-day HRT and 212 mg/ℓ (2.21 mM) sulphate at a 1.0-day HRT.

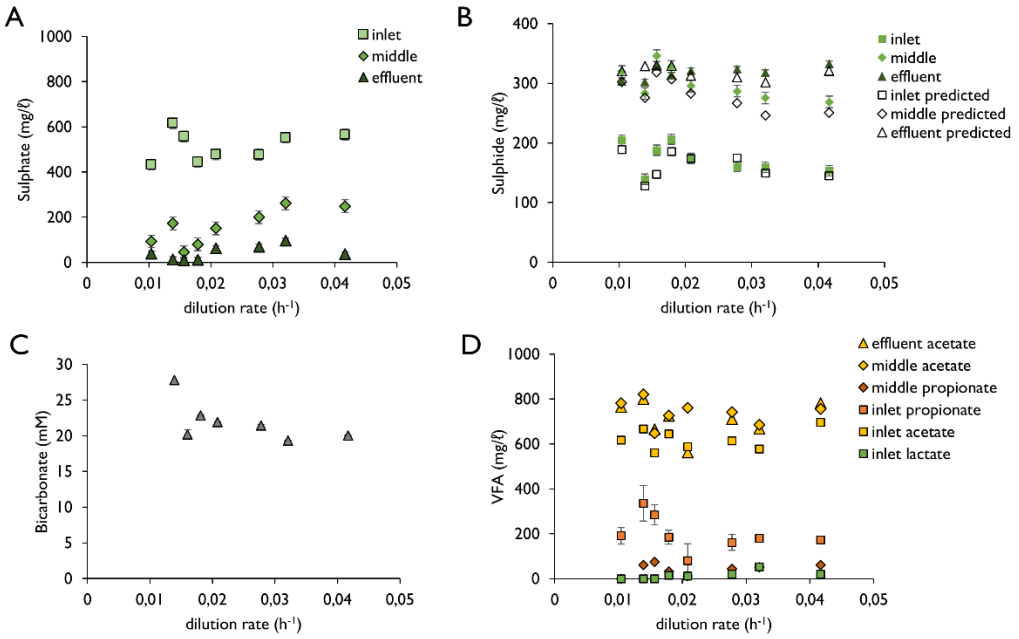


Figure 6-1 Steady-state kinetic data of the lactate-supplemented UAPBR across a range of dilution rates, including the residual sulphate (A), sulphide produced and the predicted sulphide concentration based on the observed sulphate reduced (B); the produced bicarbonate concentration calculated from the difference between the observed and feed bicarbonate concentrations (C); and the observed VFA profile describing the concentrations of acetate propionate and lactate leaving the sequential inlet, middle and effluent zones (D).

The predicted sulphide concentration, based on the observed sulphate reduced, (Figure 6-1B) largely agreed with the observed sulphide concentrations in each of the three zones. The lactate UAPBR showed the highest observed sulphide concentrations of any reactor investigated in this study. The sulphide concentration reached 150 - 200 mg/ℓ (4.4 - 5.9 mM)at the boundary between the inlet and middle-zones and in excess of 300 mg/ℓ (5.87 mM)in the reactor effluent at all tested HRT, corresponding with the high sulphate conversions achieved.

The produced bicarbonate concentrations remained stable (Figure 6-1C) between a 2.6- and 1.0-day HRT (0.016 - 0.042 $h^{-1}$) at approximately 20 mM. At a three-day HRT (0.014 $h^{-1}$), the bicarbonate concentration was elevated at 27 mM. Almost all lactate provided was consumed within the inlet zone at each tested HRT. Citrate, provided in the reactor feed at 1.1 mM, was consumed in the inlet zone at each tested HRT. Propionate was observed leaving the inlet zone at an average of 165 mg/ℓ (2.26 mM), omitting the three- and 2.6-day HRT where the detected propionate concentrations were elevated, to 336 (4.60 mM) and 285 mg/ℓ (3.90 mM), respectively. This elevated propionate concentration at a three- and 2.6-day HRT corresponds with the reduced sulphate reducing performance of the inlet zone at these HRT and increased metabolism of lactate by fermentation. The majority of the propionate produced in the inlet zone, at each tested HRT, was subsequently consumed within the middle-zone. High concentrations of acetate were

observed leaving each zone but are within predicted estimates based on the degree of lactate oxidation and sulphate reduction observed.

The pH remained between 7.0 and 7.5 in each zone for the duration of the HRT study, with the pH increasing gradually with progression through the reactor zones (Figure 6-2A). The redox potential remained highly negative, with little variation between reactor zones, throughout the study. However, the redox potential did increase between a three-day HRT (0.014 $h^{-1}$), where a redox potential of -195 mV was observed, and a two-day HRT (0.021 $h^{-1}$) where a redox potential of approximately -145 mV was observed and maintained for the remainder of the study.

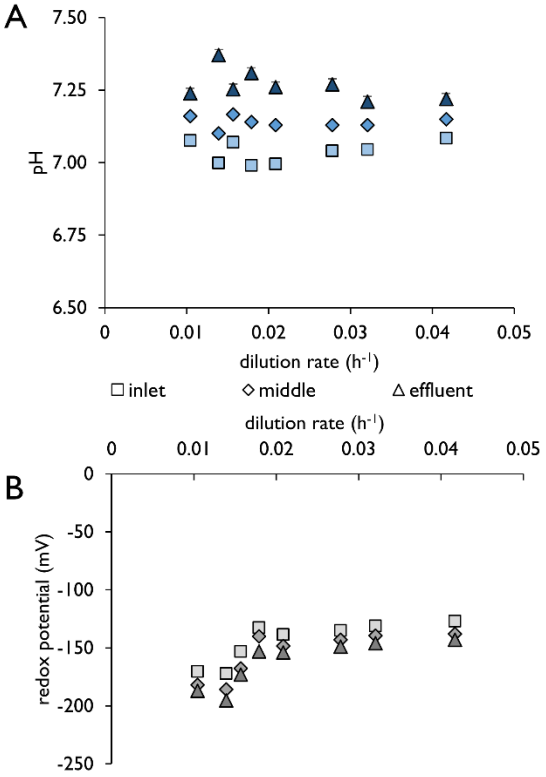


Figure 6-2 Steady-state kinetic data of the lactate-supplemented UAPBR at a range of tested dilution rates, including (A) the pH and (B) redox potential (reported relative to a standard hydrogen electrode) of the solution leaving each of the sequential inlet, middle and effluent zones.

The VSRR exhibited by the lactate supplemented UAPBR (Figure 6-3) increased linearly with increasing VSLR, maintaining a sulphate conversion of over 90% for the duration of the study and demonstrating a maximum VSRR of 40.1 mg/ℓ.h at a one-day HRT (0.042 $h^{-1}$). The UAPBR offered a nearly 50% increase in sulphate conversion, at each tested HRT, over the similarly operated lactate-supplemented CSTR (Section 4.2.1). The sulphate conversion exhibited by this CSTR showed the largest decrease between a 1.3- and 1.0-day HRT and corresponded with the decrease in cell concentration in this reactor. In contrast, a decreased sulphate conversion between a 1.3- and 1.0-day HRT was not observed for the lactate-supplemented UAPBR.

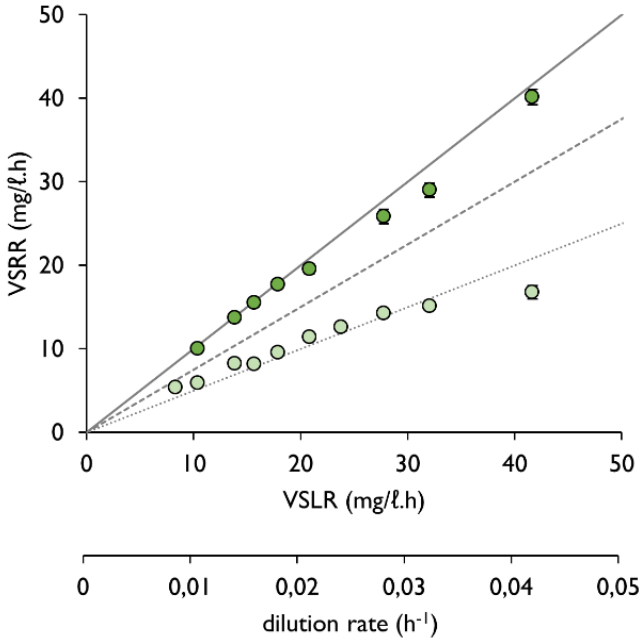


Figure 6-3 Volumetric sulphate reduction rates (VSRR) achieved by the (●) lactate-supplemented UAPBR at volumetric sulphate loading rates (VSLR) increased through the increasing of the dilution rate, corresponding to hydraulic retention times ranging from four- to one-day, whilst keeping the feed sulphate concentration constant at 1 g/ℓ. The VSRR achieved by the (●) similarly operated lactate-supplemented CSTR is shown for comparison. VSRRs were calculated based on the residual concentrations measured leaving the effluent of the reactors. Error bars representing one standard deviation from the mean are plotted. Sulphate conversion can be visually determined through comparisons with plotted lines: 100% conversion – solid line, 75% conversion – dashed line; 50% conversion – dotted line.

In the 0.33 ℓ inlet zone, a maximum VSRR of 54 mg/ℓ.h was achieved at a one-day HRT (0.042 $h^{-1}$). The VSRR of the inlet zone appeared to increase linearly ($R^2$ = 0.94; see Section 6.2.2) with increasing dilution rate, with the sulphate conversion ranging between 40 and 60%. The middle- and effluent-zones, receiving lower concentrations of sulphate, did not demonstrate VSRR of this magnitude. However, they were able to sustain higher conversions of the incoming sulphate in

each respective zone (53 to 92%) This ultimately led to near-complete sulphate conversion of the 1 g/ℓ sulphate over the length of the entire reactor.

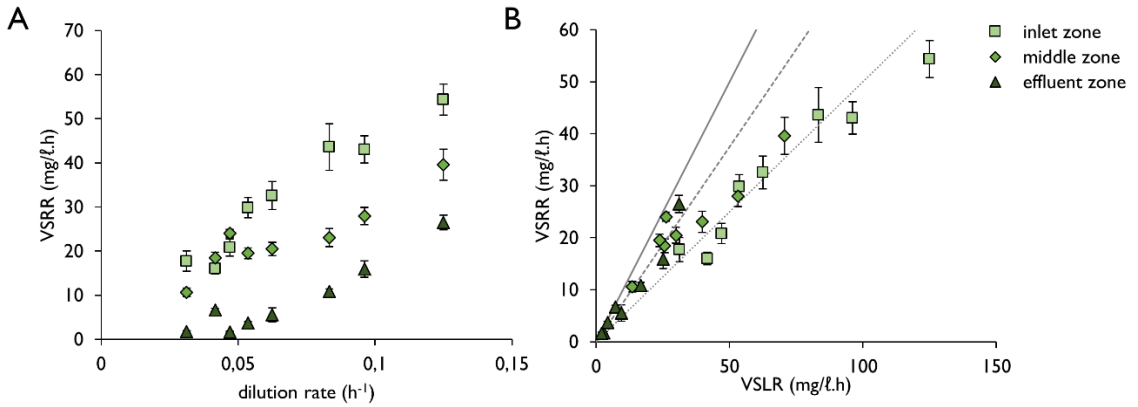


Figure 6-4 The volumetric sulphate reduction rate (VSRR) achieved by each of the lactate UAPBR's 0.33ℓ inlet, middle and effluent zones versus (A) the applied dilution rate to that zone and (B) the volumetric sulphate loading rate (VSLR) calculated based on the concentration of sulphate entering the zone and the applied flow rate. Sulphate conversions achieved by each zone can be visually determined against the plotted lines: 100% conversion – solid line; 75% conversion -dashed line; 50% conversion – dotted line.

**Biomass retention**

The planktonic cell concentrations of the middle and effluent zones remained relatively stable, at approximately 2 x $10^8$ cells/mℓ, for the duration of the HRT study (Figure 6-5). The planktonic cell concentration in the effluent zone was, on average, lower than that of the middle-zone by 5 x $10^7$ cells/mℓ. The inlet zone supported a similar concentration of planktonic cells to the middle- and effluent zones between and including a four-day and 2.3-day HRT (0.010 - 0.018 $h^{-1}$). The planktonic cell concentration in the inlet zone more than doubled between a 2.3- and two-day HRT (0.018 - 0.021 $h^{-1}$) reaching a maximum cell concentration of 1.5 x $10^9$ cells/mℓ at a 1.5-day HRT (0.028 $h^{-1}$). This increase in cell concentration corresponded with the change in the consistency of the solution drawn from this zone changing from a clear to an opaque-grey coloured and viscous solution. This may be from the gradual settling of planktonic cells and detached biofilm over the duration of the study, which had at this time been operated continuously for more than 985 days. The solution drawn directly from the inlet port was of similar colour and consistency.

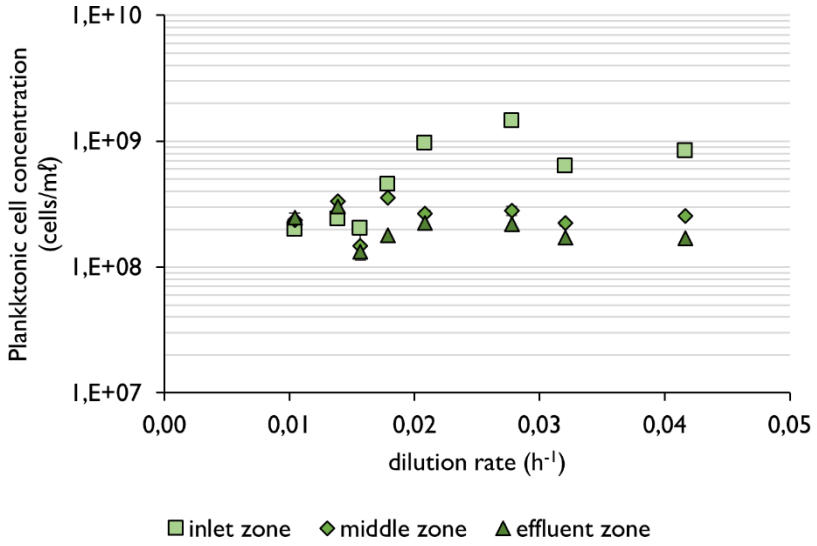


Figure 6-5 Planktonic cell concentrations in the lactate UAPBR inlet, middle and effluent zones at each tested dilution rate, determined through direct cell counting. All displayed data points carry error bars which represent one standard deviation from the mean.

The concentration of cells attached to- and associated with the polyurethane foam showed a clear decreasing trend through the zones of the UAPBR (Figure 6-6), at both the initial four- and one-day HRTs. The cell concentration in zone 1 of the inlet zone's attached community were 5.4 x $10^{10}$ and 2.2 x $10^{10}$ cells/ml at a four-day and one-day HRT, respectively. The biofilm communities of zones 2 to 5 were not quantified at a four-day HRT, however, polyurethane foam was recovered and biofilm-associated microbial communities assessed from each of the six zones of the UAPBR at a one-day HRT. At a one-day HRT (Figure 6-6B), the biofilm attached cell concentrations decrease gradually between 2.2 x $10^{10}$ cells/mℓ in zone 1, to 1.5 x $10^{10}$ cells/mℓ in zone 3. The biofilm attached cell concentration then decreased abruptly in zone 4 to 2.6 x $10^{9}$ cells/mℓ and further to 5 x $10^{8}$ cells/mℓ in zone 6. The concentration of attached cells in zone 6 at a one-day HRT, of 5 x $10^{8}$ cells/mℓ was ten-fold greater than the 5 x $10^{7}$ cells/mℓ cell concentration observed at a four-day HRT. The associated cell concentration, at a one-day HRT, decreased linearly from 8.8 x $10^{9}$ cells/mℓ in zone 1 to 1.5 x $10^{9}$ cells/mℓ in zone 5 ($R^2$ = 0.97) and to 1.2 x $10^{9}$ cells/mℓ in zone 6. The ratio of associated to attached cell concentration, therefore, decreases between the inlet to effluent zones, from 2.5:1 in zone 1 to almost 1:1 in zone 4. A similar observation was made at a four-day HRT, the associated cell concentration, in each zone at a one-day HRT, was approximately 10-fold greater than that of the planktonic cells within the same reactor zone.

SEM was used to visually inspect the surface of the polyurethane foam isolated from each of the six reactor zones at a one-day HRT (Figure 6-7). Thick microbial mats and amorphic clumps of

cells were visible colonising the surface of the polyurethane foam removed from each of the six (0.167 ℓ) zones of the UAPBRs.

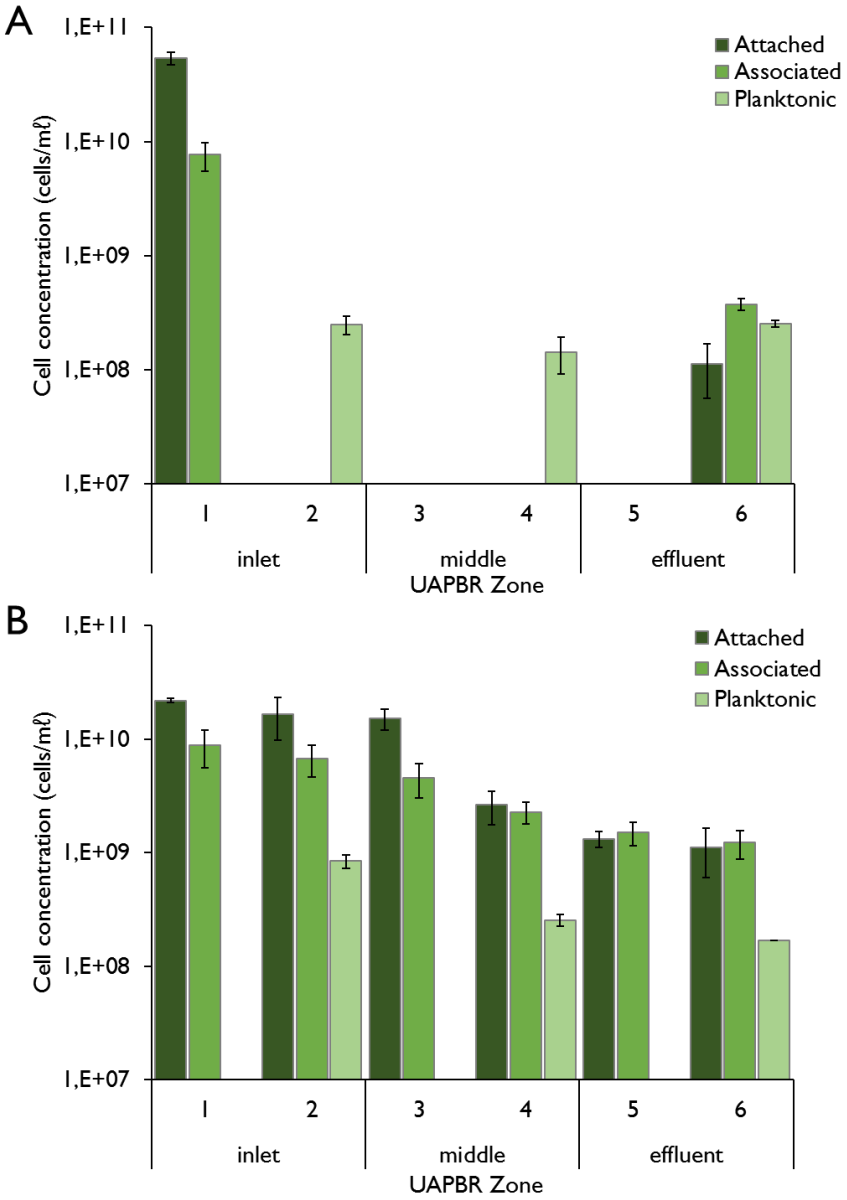


Figure 6-6 Cell concentration of the total cells present in the biofilm attached, biofilm-associated and planktonic microbial communities throughout the six sequential 0.167 ℓ zones of the lactate supplemented UAPBR at a four-day HRT (0.010 $h^{-1}$; A) and one-day HRT (0.042 $h^{-1}$; B). Error bars represent one standard deviation from the mean of two replicates each counted in duplicate.

The morphology of the cells, which made up these biofilms, were primarily rod and vibrio shapes with some cocci. Thick EPS was most evident on the polyurethane foam isolated from zones 1 and 2. Anchoring fibres and pores within the biofilm were evident on the surface of the foam isolated from each reactor zone. Lemon-shaped morphologies were observed in zones four, five and six and are likely *Desulfobulbus* (Widdel and Pfennig, 1982) which were detected in these attached communities using gene amplicon sequencing (Figure 6-14)

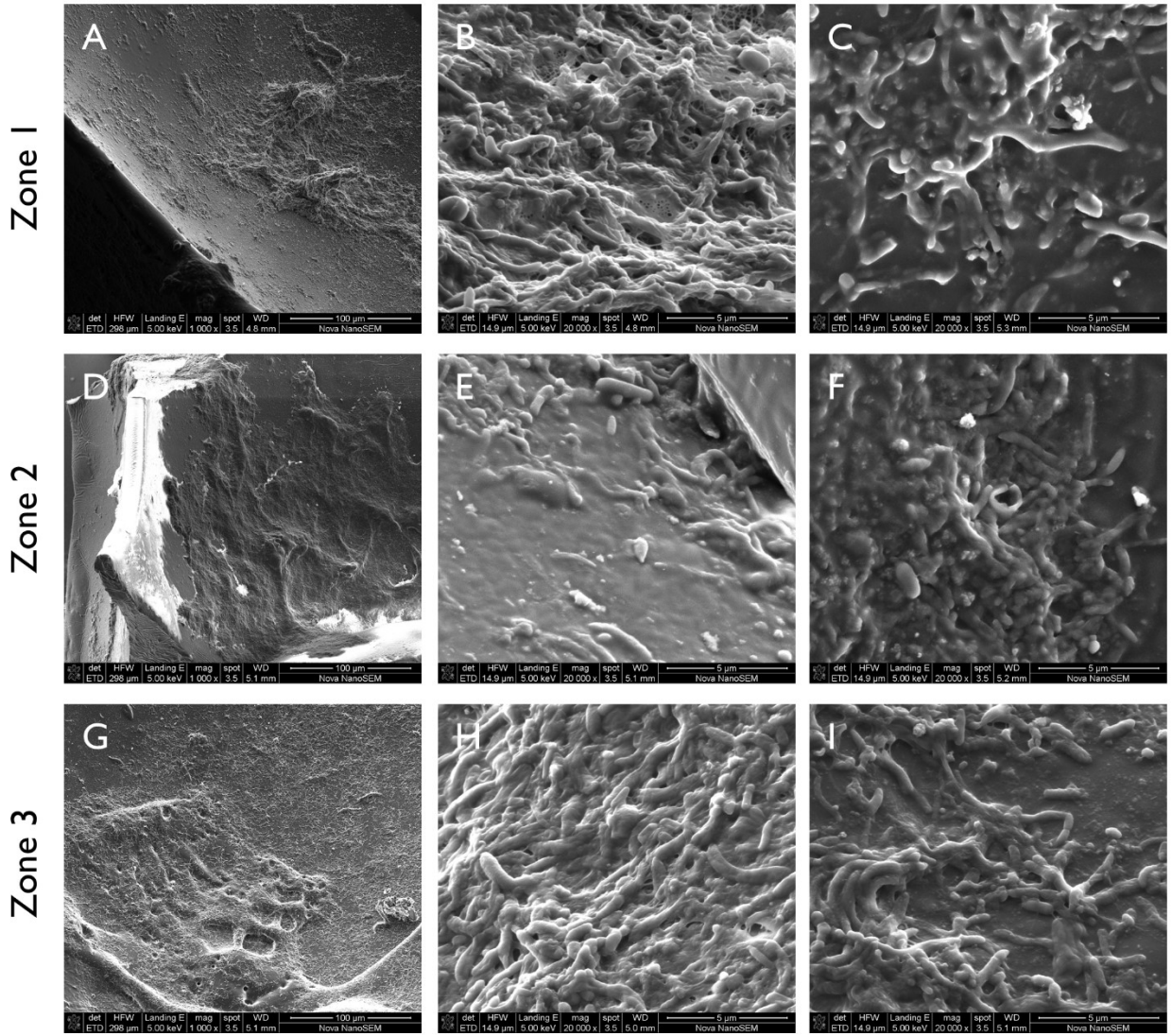


Figure 6-1 Scanning electron micrographs of the surface of the polyurethane foam packing within the lactate-supplemented UAPBR, isolated during the defined one-day HRT steady-state period. Polyurethane foam was isolated from zone 1(A-C), zone 2 (D-F), zone 3 (G-I), zone 4 (J-L), zone 5 (M-O) and zone 6 (P-R). Scale bars are shown in each micrograph.

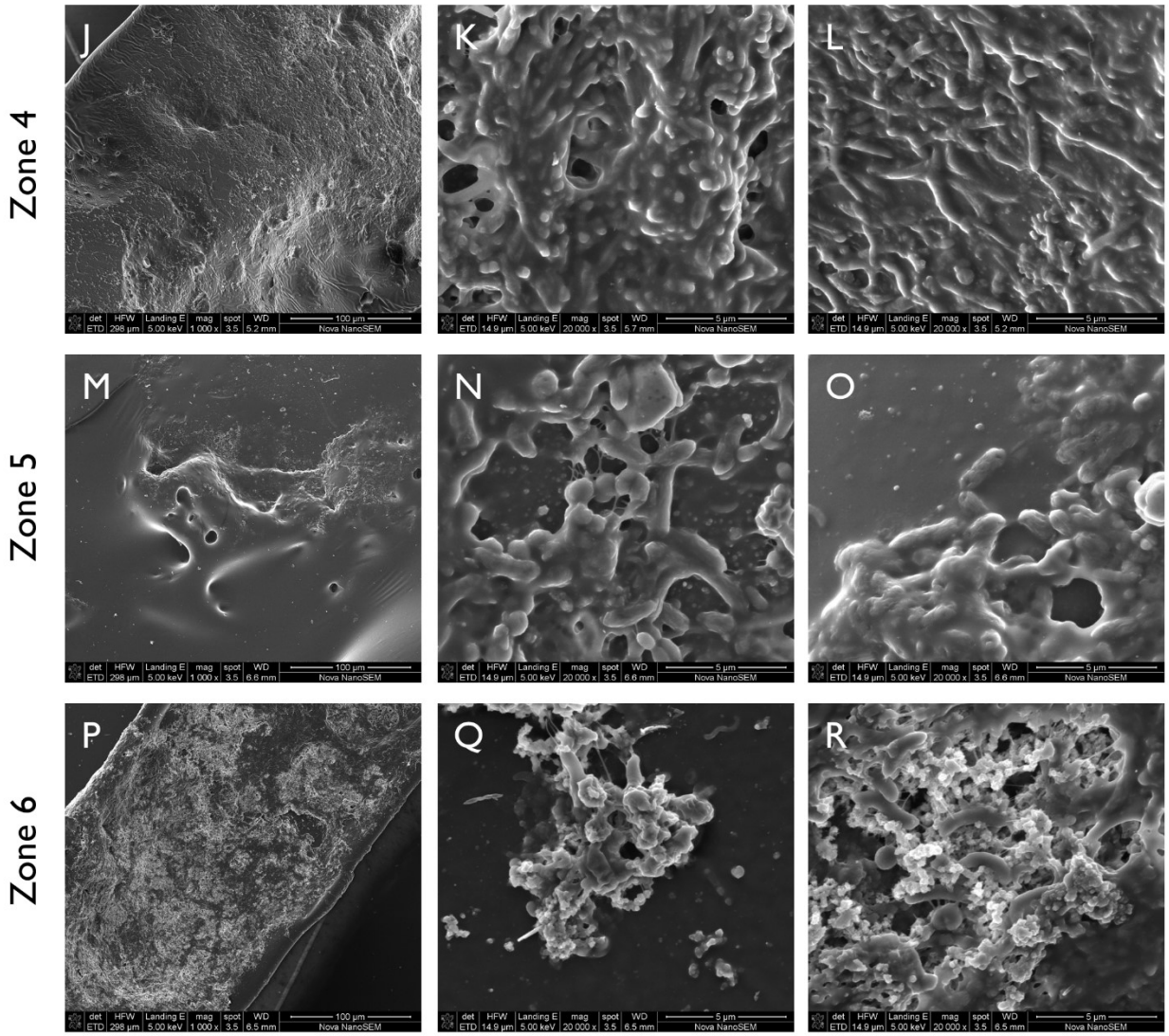


Figure 6-7 Continued

### 6.2.2 Sulphate reduction performance model

The sulphate reducing performance of the lactate UAPBR was modelled as a spontaneous, irreversible, $n^{th}$ order reaction, with rate constant *k*, according to Equation 3-17. This expression does not allow the order of reaction, *n*, to be equal to one as this causes the expression to become undefined. Solving for *n* with the boundary condition that $n \neq 1$ causes *n* to approach one from values above and below one (Figure 6-8).


Figure 6-8 Sum of squared error (SSE, Equation 3 22) of the observed data against that modelled using with various *k* and *n* values using Equation 3-17. The size of the circles is indicative of the magnitude of the SSE which is shown within the circle. Using this model, the SSE was minimised as *n* approached 1.0 with a rate constant, *k*, of 0.0695 $h^{-1}$.

This indicated that the sulphate reduction reaction in this reactor could be described by a first-order reaction and therefore was better described by Equation 3-21 (shown below) where $r_A$ is the volumetric sulphate reduction reaction rate, *F* is the flow rate applied to the reactor, *V* is the volume of the reactor or reactor zone(s), $C_0$ is the initial sulphate concentration entering the zone/reactor and *k* is the rate constant with the units $time^{-1}$.

$$r_A = -\frac{F}{V}\left(\frac{C_0}{e^{\frac{V.k}{F}}} - C_0\right)$$

Equation 3-21

Applying the non-linear regression generalised reduced gradient (GRG) method to the observed data produced a rate constant, *k,* of 0.06955 $h^{-1}$ (Figure 6-9 and Figure 6-10). The standard error associated with this model was 4.18, the 95% confidence interval equal to 8.41 and the model fits the data with an $R^2$ of 0.89 (Section 3.7.3). The first-order nature of the modelled reactor kinetic data indicates that the rate of sulphate reduction is directly proportional to the concentration of the sulphate substrate. According to this model, the rate of sulphate reduction approaches

71 mg/ℓ.h, with a starting sulphate concentration of 1000 mg/ℓ, as F/V approaches infinity. The rate of sulphate reduction, at this starting sulphate concentration of 1000 mg/ℓ, would reach 56 mg/ℓ.h at an F/V of 0.15.

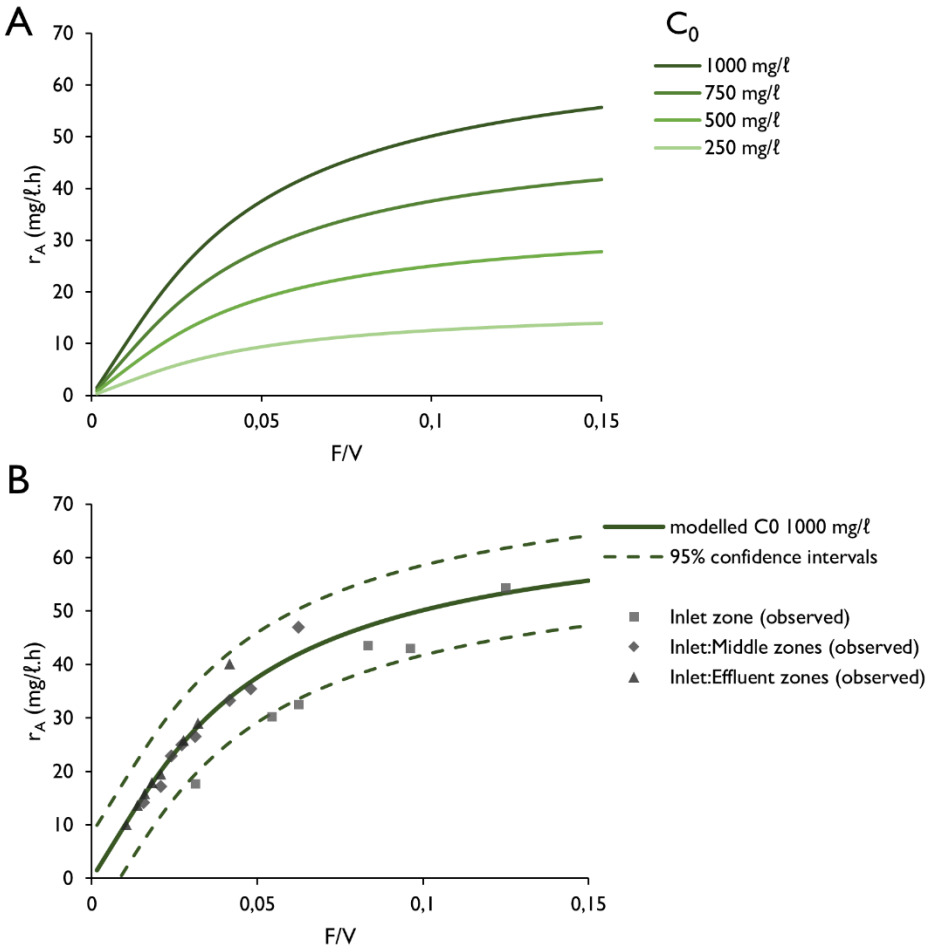


Figure 6-9 Modelled sulphate reduction reaction rate data at various flow rate to volume ratios (F/V) with (A) various starting sulphate starting concentrations ($C_0$) as shown in the legend. Observed sulphate reduction reaction rates (B) from the inlet, composite inlet and middle zone and entire reactor are plotted against the modelled reaction rate with $C_0$ of 1000 mg/ℓ sulphate and 95% confidence intervals.

The predicted and observed sulphate reduction rates, together with their residuals, of all zones and composite zones, are shown in Figure 6-10. The residuals of the observed and predicted rates for most zones and composite zones were relatively low. The difference between the residual and the predicted reaction rates differed by, on average, 12% of the predicted reaction rate. The residuals of the observed and predicted rates of the inlet zone alone, however, were some of the highest determined, with the predicted reaction rates generally being overestimated. The modelled

sulphate reduction of the 0.33 ℓ middle and effluent zones and the 0.66 ℓ middle-effluent zones agreed well with the sulphate reduction rates observed in these zones (Figure 6-10). The sulphate concentration entering these zones and composite zones was less than 1000 mg/ℓ and is the reason these observed and predicted sulphate reduction rates do not lie on the curve generated in Figure 6-9. The sulphate reduction rates observed in the middle- and effluent-zones at a one-day HRT, however, were considerably greater than those predicted.

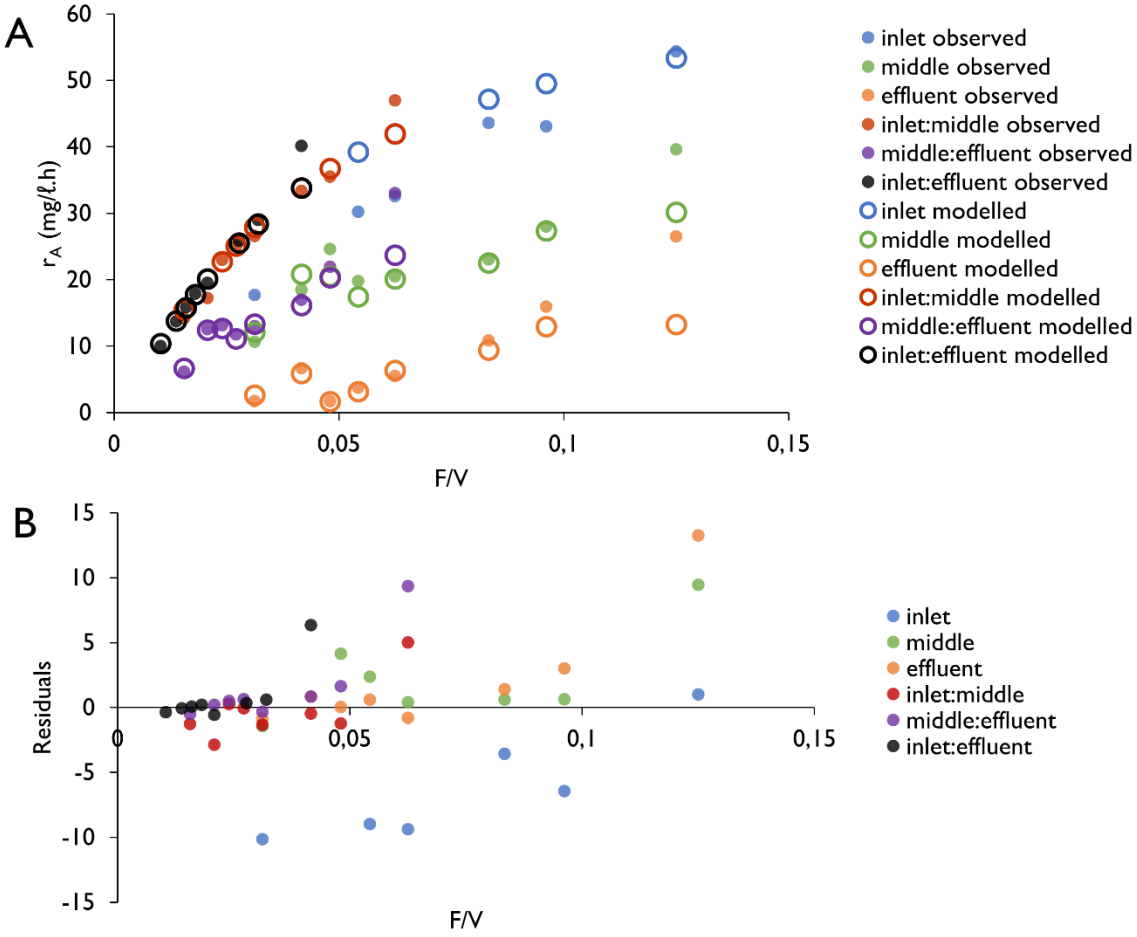


Figure 6-10 The (A) observed (closed circles) and predicted (open circles) sulphate reducing reaction rates of the individual and composite reactor zones of the lactate UAPBR at various tested flow rate to volume ratios (F/V). Predicted rates were based on Equation 3-21 which describes a spontaneous, first-order irreversible reaction in a plug flow reactor with a rate constant, *k*, of 0.069 $h^{-1}$. The residuals (B) of the observed rates minus the modelled rates are shown.

### 6.2.3 Microbial ecology of the planktonic communities

The microbial community structure of the UAPBR planktonic communities, at the phylum and class level, remained consistent across the HRT study. The communities, at each HRT, were made up of the Bacteroidetes, Proteobacteria, Firmicutes and Synergistetes to between 80 and 90% of the entire community (Figure 6-11). Proteobacteria classified to classes other than Deltaproteobacteria increased from <5% relative abundance at a four-day HRT (0.010 $h^{-1}$) to 7 - 30% at reduced HRT.

Comparing the communities at this level saw little variation between the inlet, middle and effluent zones – except, the relative abundance of Firmicutes. Firmicutes saw, on average, an 8-fold reduction in abundance between the inlet and middle zone planktonic communities. This reduction was only observed between the middle and effluent zones at a two-day HRT (0.021 $h^{-1}$), where the greatest degree of lactate fermentation had taken place (inferred from the propionate concentration, Figure 6-1) and the sulphate conversion in the inlet zone was the lowest observed (Section 6.2.1).

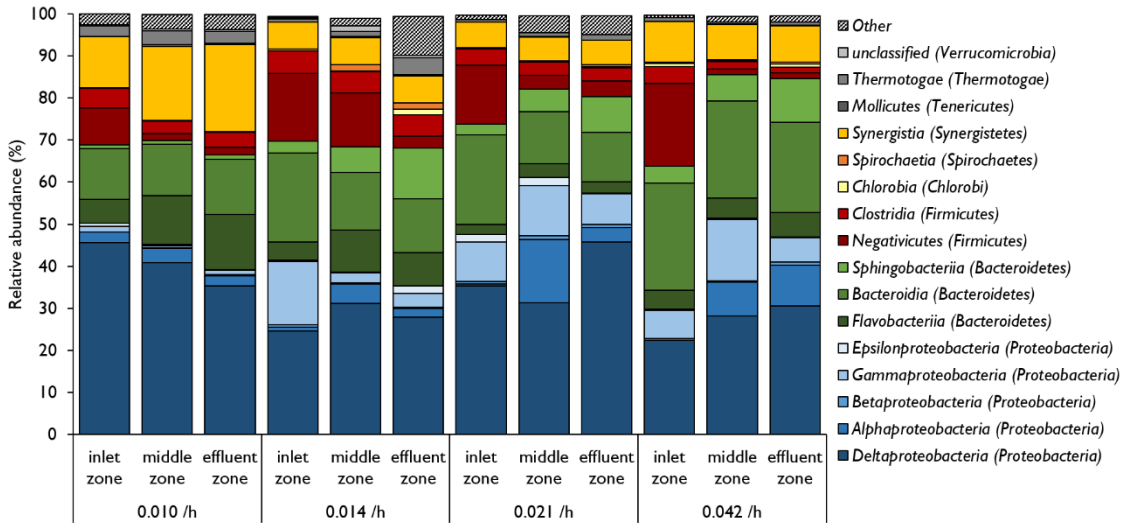


Figure 6-11 Relative abundance of the predominant microbial classes within the planktonic communities of the inlet, middle and effluent zones of the lactate UAPBR at dilution rates corresponding to four- (0.010 $h^{-1}$), three- (0.014 $h^{-1}$), two- (0.021 $h^{-1}$) and one-day (0.042 $h^{-1}$) HRTs, respectively. The phyla to which each class belongs are shown in parentheses.

The relative abundance of the 17 most abundant OTUs seen in the lactate UAPBR planktonic communities is shown in Figure 6-12. These 17 OTUs constitute between 69 and 88% of these communities at each of the four tested HRTs. The predominant SRB were two *Desulfovibrio* OTUS (OTU 6 and OTU 84, respectively) and a *Desulfomicrobium* OTU (OTU 1). *Desulfovibrio* (6) and *Desulfomicrobium* (1) were also the predominant SRB identified in the lactate CSTR (4.2.2). The

ratio between these SRB varies greatly between HRT and reactor zone. However, these fluctuations do not show a discernible pattern within this data. The *Veillonella* OTU (11) makes up a considerable proportion of the planktonic community of the inlet zone, but reduces considerably in the middle and effluent zones, corresponding with the class and phylum level data discussed above.

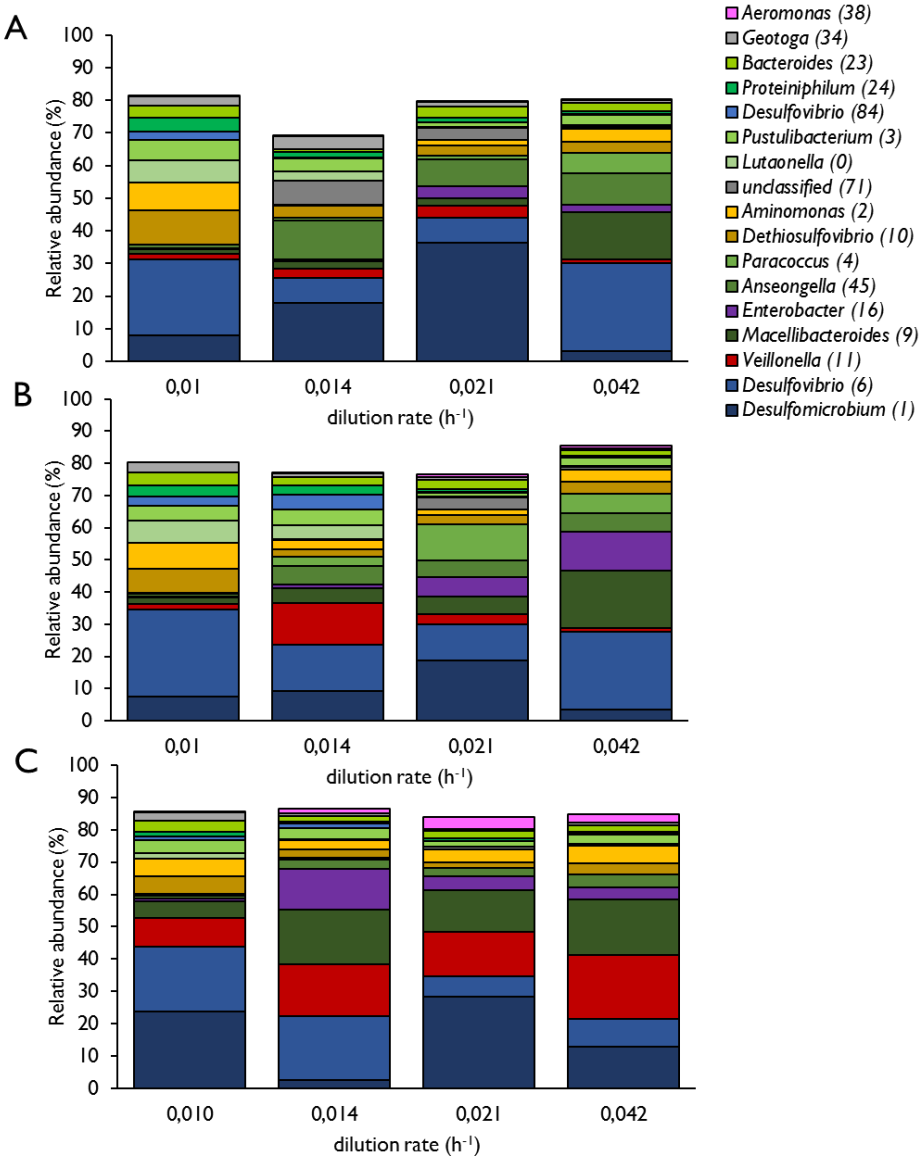


Figure 6-12 The relative abundance of the most abundant OTUs in the planktonic communities of the lactate UAPBRs (A) effluent, (B) middle and (C) inlet zones at dilution rates corresponding to a four-, three-, two- and one-day HRT. OTUs are coloured by taxonomy: Deltaproteobacteria – blue, other Proteobacteria – purple, Bacteroidetes – green, Firmicutes – red, Synergistetes – yellow, and other phyla – grey.

### 6.2.4 The microbial ecology of the biofilm communities

The biofilm communities of the lactate-supplemented UAPBR were dominated by Deltaproteobacteria up to 48% - the highest proportions seen in any of the six reactors operated in this study (Figure 6-13). This class was mostly constituted by SRB and, in some instances, an OTU classified as *Geobacter* - a microorganism implicated in metal, but not dissimilatory sulphate reduction (Methé et al., 2003; Barlett et al., 2012; Handley et al., 2013). The lack of genes for dissimilatory sulphate reduction, including *dsrAB*, *aprAB* and *sat*, in this microorganism was confirmed through the genome-resolved metagenomics employed in this study (Chapter 8 ). The classes of Bacteroidetes: Flavobacteria and Bacteroidia, together with Proteobacteria made up 55 - 85% of the total biofilm communities. Changes in the abundance of these classes were not observed across the six sequential 0.167 ℓ zones of this reactor. Firmicutes and Spirochaetes, however, were typically higher in abundance in the first three zones of the reactor. Inversely, the class of Thermotogae were enriched in the final three zones of this reactor, at both four- and one-day HRTs.

The proportion of Firmicutes present in the biofilm communities decreased from more than 20% at a four-day HRT to approximately 10% at a one-day HRT, with a corresponding increase in the Bacteroidetes class of Flavobacteria at a one-day HRT.

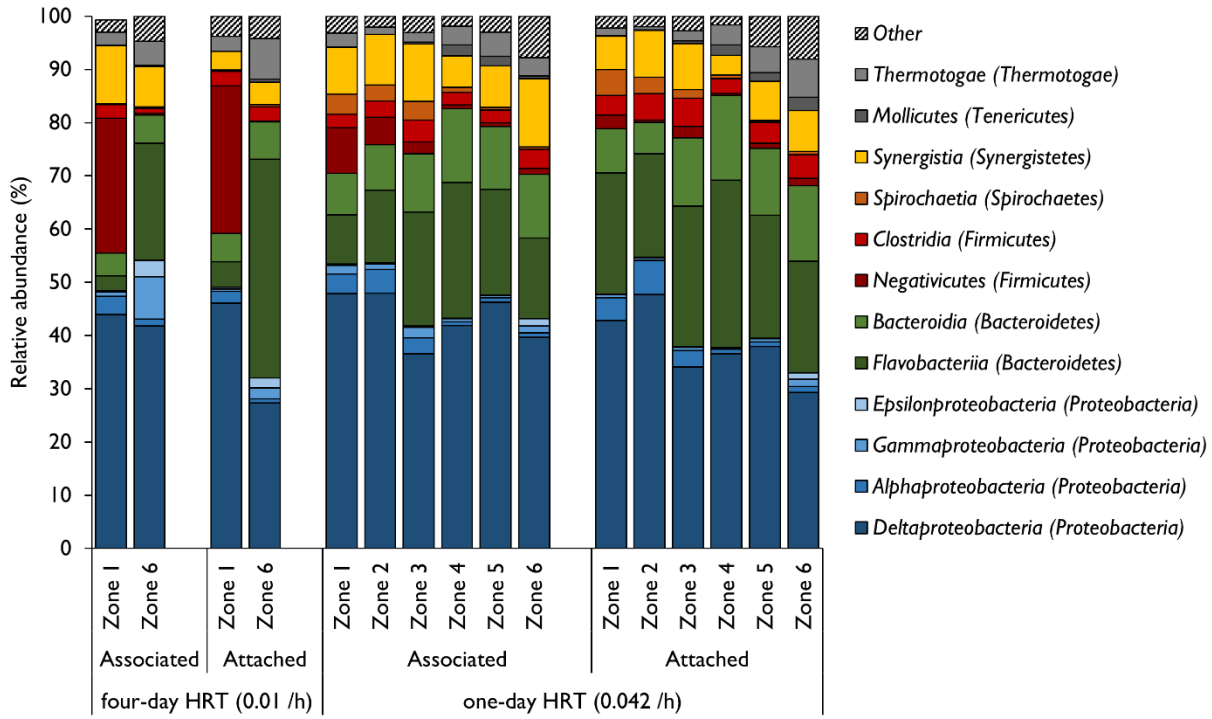


Figure 6-13 Relative abundance of the predominant microbial classes within the attached- and associated-biofilm communities of the six sequential zones of the lactate UAPBR at a four- and one-day operated HRTs. The phyla to which each class belongs are shown in parentheses.

Although not evident at the class taxonomic level, there was clear evidence of stratification of individual OTUs throughout the biofilm communities of the lactate-supplemented UAPBR. *Desulfovibrio* (6) and *Desulfomicrobium* (1) were the dominant SRB present in the attached and associated communities of zone one, at a four-day HRT, and zones one to three at a one-day HRT (Figure 6-14). At a four-day HRT *Desulfovibrio* (6) is greater than three-fold more abundant than *Desulfomicrobium* (1), however, this ratio inverts with *Desulfomicrobium* becoming the dominant SRB OTU in the biofilm at a one-day HRT. The SRB OTU *Desulfobulbus* (27), an OTU matching one of the few SRB genomes containing genes necessary for propionate oxidation (Section 8.5.2 and Figure 8-5), was dominant in zones 4 and 5 (>20% relative abundance). *Desulfobacter* (18) and *Desulfosarcina* (53) were present in zones 3 to 6, while *Desulfatiglans* (91) was dominant in zones 5 and 6.

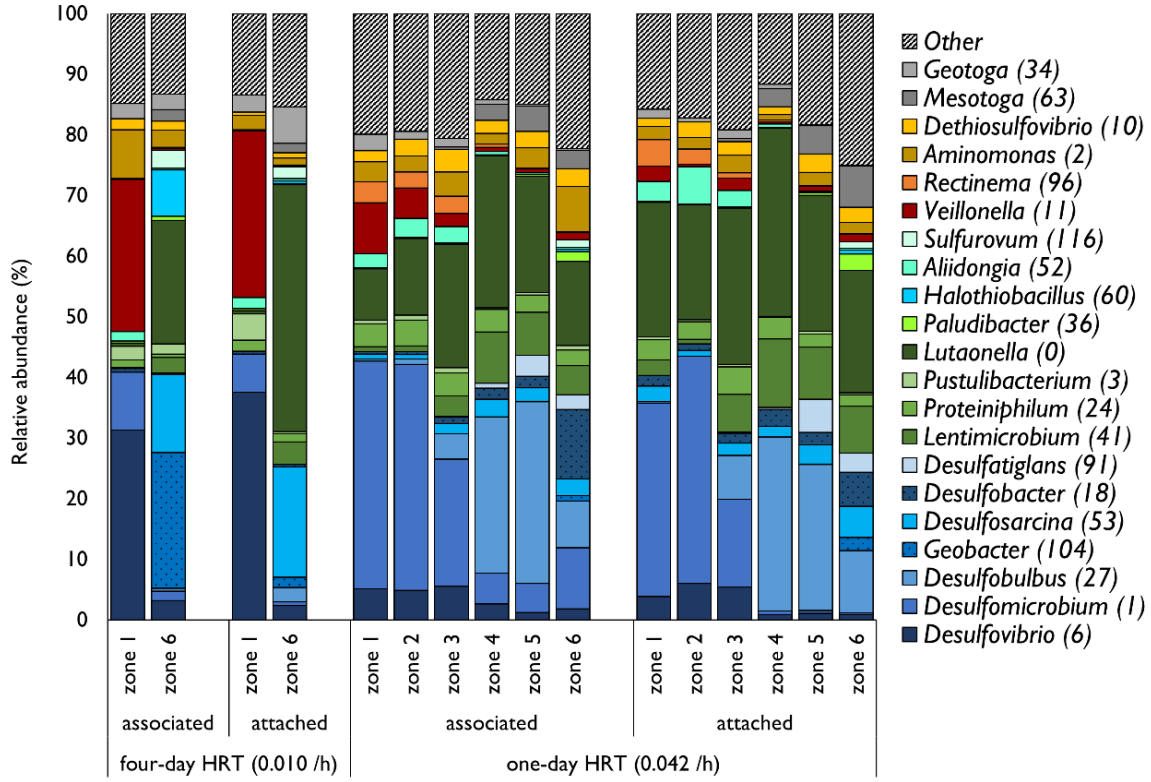


Figure 6-14 Relative abundance of the predominant OTUs within the attached- and associated-biofilm communities of the six sequential zones of the lactate UAPBR at four- and one-day HRTs. The OTUs are colour shaded based on their higher taxonomic classifications. Briefly, Deltaproteobacteria are shown in blue, Bacteroidetes in green, Firmicutes in red, Spirochaetes in orange, Synergistales in yellow and other phyla in grey.

## 6.3 Lactate UAPBR Discussion

### 6.3.1 The lactate UAPBR sulphate reduction rate model

The sulphate concentrations leaving each of the three reactor zones, at each tested flow rate, was predicted using the model described in Section 6.2.2 (Figure 6-15). The residual sulphate concentrations were predicted using a $C_0$ of 1000 mg/ℓ in the inlet zone, the concentration of sulphate leaving the inlet zone for the middle zone, and the concentration of sulphate leaving the middle for the effluent zone.

The observed and predicted sulphate concentrations, leaving the middle and effluent zones, differed by less than 100 mg/ℓ at each tested flow rate, with a mean difference of 35 mg/ℓ. However, this model was not able to accurately predict the sulphate reducing performance of the inlet zones at lower dilution rates. The deviation of the observed from the modelled reaction rates in the inlet zone could indicate limitations in the inlet zone that were not present in the rest of the reactor. This could include limited mass transfer through the thicker biofilm of the inlet zone or

through reaching a maximum biomass concentration in this zone. It is also possible that the mode or mechanism of the sulphate reduction reaction in the inlet zone differs from that in the middle and effluent zones and would, therefore, require a different equation to describe it.

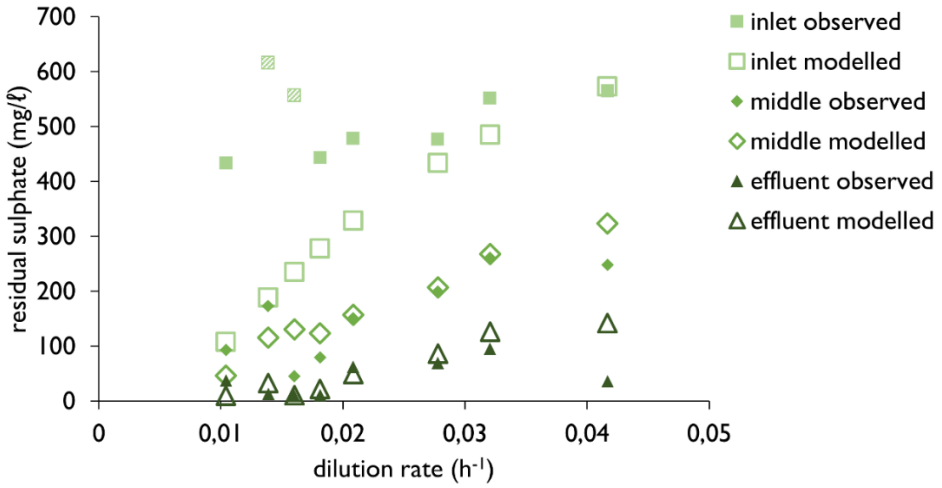


Figure 6-15 The observed and predicted residual sulphate concentrations leaving the inlet, middle and effluent zones of the lactate UAPBR at varying applied dilution rates. The predicted sulphate concentrations were predicted using the model described in Section 6.2.2. This model describes a first-order, spontaneous, irreversible chemical reaction in a plug-flow reactor with a rate constant, *k*, of 0.06955 $h^{-1}$. Predictions were made using the observed concentration of sulphate leaving the inlet zone as the initial sulphate concentration entering the middle zone, and the observed concentration leaving the middle zone as the initial concentration entering the effluent zone. Outliers in the data are lined. The sulphate concentration entering the inlet zone was maintained at 1000 mg/ℓ across the dilution rates tested.

Overlaying the VFA profile over the sulphate reduction rate profile across zones and tested HRT provides the simplest explanation. The sulphate reducing performance of the inlet zone at a 0.014 and 0.016 $h^{-1}$ dilution rate were excluded from the refining of the term for the rate constant as these were concluded to be outliers. These were deemed to be outliers as the sulphate conversion at these timepoints decreased from a dilution rate of 0.010 $h^{-1}$, but then improved substantially at even greater dilution rates. The propionate concentration leaving the inlet zone at these two dilution rates were the highest seen for this reactor (336 and 285 mg/ℓ, respectively) compared with an average of 162 mg/ℓ (2.22 mM) for all other tested dilution rates (Figure 6-1D). It is thought that the competition of SRB (using lactate oxidation) with other microorganisms (performing lactate fermentation) for lactate in the inlet zone is one of the factors which limits the rate of sulphate reduction. The degree of lactate fermentation in the lactate UAPBR was greater than observed in both the lactate-supplemented CSTR and LFCR (Figure 6-16).

The assumed constant rate constant, *k*, across the reactor and flow rates may not hold true for the inlet zone of the reactor. Lactate oxidation is restricted to the inlet zone. The competition for lactate in this zone between SRB and fermentative microorganisms may give rise to the greatest variability in performance due to fluctuating dominance between these two groups. This is evident in the reaction rates observed over the inlet zone at a three- and 2.6-day HRT (0.014 and 0.016 $h^{-1}$, respectively) which were assumed to be outliers and not included in the refining of the rate constant.

### 6.3.2 Electron donor utilisation within the inlet zone

The consumption of lactate by SRB and fermentative microorganisms was almost entirely restricted to the inlet zone. The highest concentration of lactate observed entering the middle zone was 53 mg/ℓ, having decreased from the lactate concentration of 1200 mg/ℓ (13.32 mM) in the feed, at a 1.3-day HRT (0.032 $h^{-1}$). The degree of lactate fermentation was calculated based on the molar concentration of propionate leaving the inlet zone (Figure 6-16). This calculation is performed assuming that no propionate had been consumed before leaving the inlet zone and that all propionate was produced through lactate fermentation. These assumptions are supported by the SRB OTU *Desulfobulbus* (27) being specifically enriched in zones of propionate oxidation. This OTU showed minimal abundance in zone 1 and 2 of the biofilm communities at a one-day HRT but was prevalent in zones 3 to 6 (Figure 6-14).

The degree of lactate fermentation showed little variation across the HRT study when data collected at dilution rates of 0.14 and 0.16 $h^{-1}$ was omitted (Figure 6-16). The average quantity of the 1200 mg/ℓ (13.32 mM) lactate feed undergoing fermentation was estimated to be approximately 25% (300 mg/ℓ) with a standard deviation of 5%. At dilution rates of 0.14 and 0.16 $h^{-1}$, the amount of lactate undergoing fermentation was estimated to be approximately 49% (591 mg/ℓ) and 42% (506 mg/ℓ), respectively. The elevated lactate fermentation at these two time-points corresponds with the lower than average sulphate conversions (38 and 44%, respectively) observed in the inlet zone. The degree of lactate fermentation in the lactate UAPBR was greater than that seen in the lactate CSTR (average of 22% feed lactate; Section 4.3.2) at almost all tested HRT. This may be either a consequence of the lower sulphide concentrations in the UAPBR near the inlet, leading to less inhibition of fermentative microorganisms, or the result of immobilisation of fermentative microorganisms on the polyurethane foam within this zone. It is assumed that the amount lactate that was oxidised, but not associated with fermentation, was instead linked to sulphate reduction by the SRB population within the reactor community. The amount of lactate oxidation which was not linked to sulphate reduction nor assumed to be fermented is shown as "unaccounted" in Figure 6-16 (occurring at dilution rates of 0.021 and 0.042 $h^{-1}$).

The amount of lactate metabolism linked to sulphate reduction averaged 75% (900 mg/ℓ or 9.99 mM ) of the feed lactate (1200 mg/ℓ or 13.3 mM) across the HRT study, again omitting the 3- and 2.6-day HRT data (0.014 and 0.016 $h^{-1}$, respectively). At longer HRT, this quantity of lactate does not entirely account for the degree of sulphate conversion observed and suggests some acetate and/or propionate had also been consumed by SRB. The amount of sulphate reduced which was not accounted for by lactate oxidation averaged, between and including the tested dilution rates of 0.010 $h^{-1}$ and 0.018 $h^{-1}$, 0.86 mols of sulphate (82 mg/ℓ) and corresponds to 1.7 mol of lactate which would be required for its reduction, or 0.86 mol of either acetate or propionate. The proportion of sulphate reduced which could be linked to lactate oxidation, at these dilution rates, is estimated at approximately 83%.

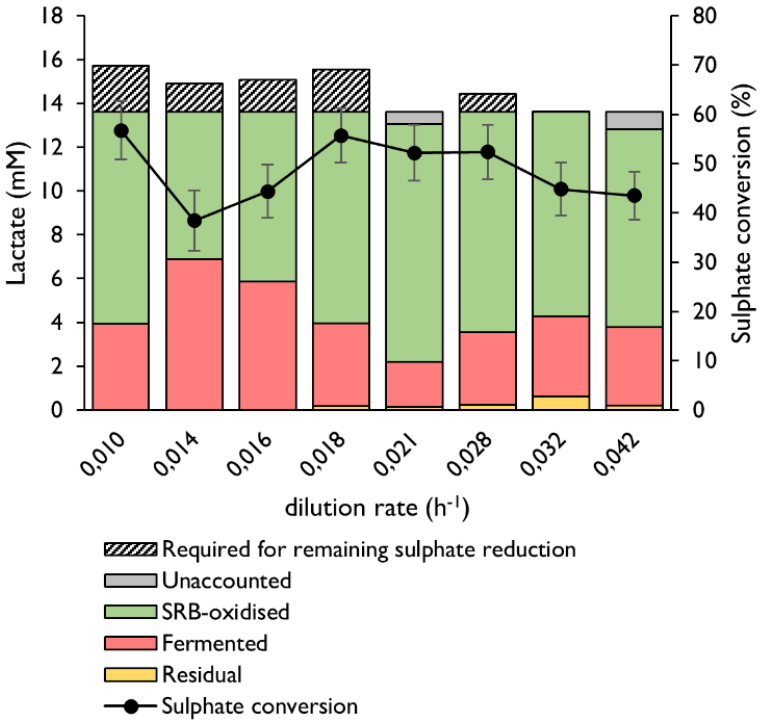


Figure 6-16 The concentration of lactate undergoing lactate fermentation (Equation 2-12) calculated from the observed propionate concentration; undergoing incomplete lactate oxidation by SRB (Equation 2-10) calculated from the observed sulphate reduced but not allowing to exceed the feed lactate concentration of 13.6 mM; residual lactate remaining in the reactor, lactate unaccounted for from sulphate reduction and propionate produced; and the theoretical concentration of lactate required to allow for degree of sulphate conversion observed at each tested dilution rate.

### Lactate oxidised/ sulphate reduced

The ratio of lactate oxidised to sulphate reduced increased with the increasing of the dilution rate (Figure 6-17). This was not a result of increased lactate fermentation but a decrease in the amount of acetate and/or propionate linked to sulphate reduction in this zone. The estimated "lactate oxidised by SRB" to "sulphate reduced" molar ratio was below 2.0 between a four- and 2.3-day HRT (0.010 to 0.018 $h^{-1}$) – indicating a degree of complete lactate oxidation. This observed ratio increased to approximately 2 at a two-day HRT (0.021 $h^{-1}$) where it remained for the duration of the HRT study. This ratio indicated the incomplete oxidation of lactate by SRB, with little further oxidation of additional electron donors.

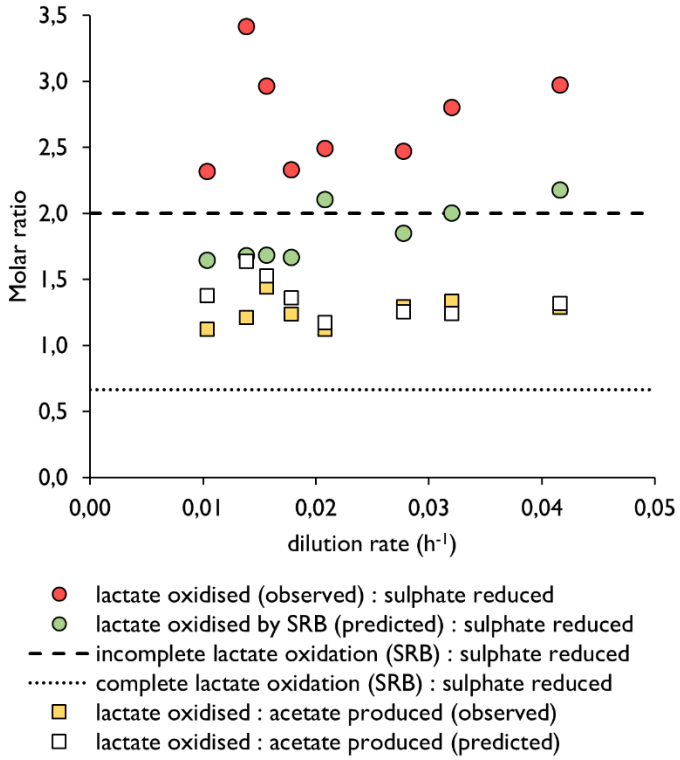


Figure 6-17 The predicted and observed steady-state molar ratios of products and reactants arising from lactate oxidation by SRB (Equation 2-10 and Equation 2-12) and lactate fermentation (Equation 2-12) within the inlet zone of the lactate UAPBR at a range of tested dilution rates. The lactate predicted to have been oxidised by SRB was calculated by subtracting the lactate oxidised by fermentation (Figure 6-16) from total lactate oxidised within the reactor and confirming through the observed sulphate reduced according to Equation 2-10. The observed lactate oxidised was calculated by subtracting the residual lactate in the reactor from the inlet lactate feed concentration. The predicted acetate produced was performed according to the degree of lactate and acetate oxidation by SRB and fermenters (Equation 2-7, Equation 2-10 and Equation 2-12) shown in Figure 6-16.

### Lactate oxidised / acetate produced

The predicted concentration of acetate leaving the inlet zone was calculated based on the degree of lactate oxidation by SRB and fermentative microorganisms and the subsequent oxidation of acetate of SRB based on the amount that was sulphate reduced which was not accounted for based on the observed lactate oxidation (Figure 6-15). The observed and predicted ratio of lactate oxidised to acetate produced were largely in agreement (Figure 6-17), providing evidence that the assumptions above hold true. The difference in the observed and predicted acetate concentration leaving the inlet zone differed by just 5% between a 2.6- and one-day HRT (0.016 – 0.0042 $h^{-1}$; Figure 6-18). However, the observed acetate concentrations leaving the inlet zone at a four- and three-day HRT (0.010 and 0.014 $h^{-1}$) were both greater than the predicted acetate concentration. The likely explanation for this additional acetate is the generation of acetate from yeast extract oxidation (Section 4.4.2). The maximum acetate generation from yeast extract oxidation is included in a 'predicted acetate' concentration shown in Figure 6-18 and the observed acetate concentrations lay between the two predictions. It is interesting to note that the generation of acetate from yeast extract oxidation does not seem to occur in the inlet zone at HRTs less than a three-day HRT (0.014 $h^{-1}$).

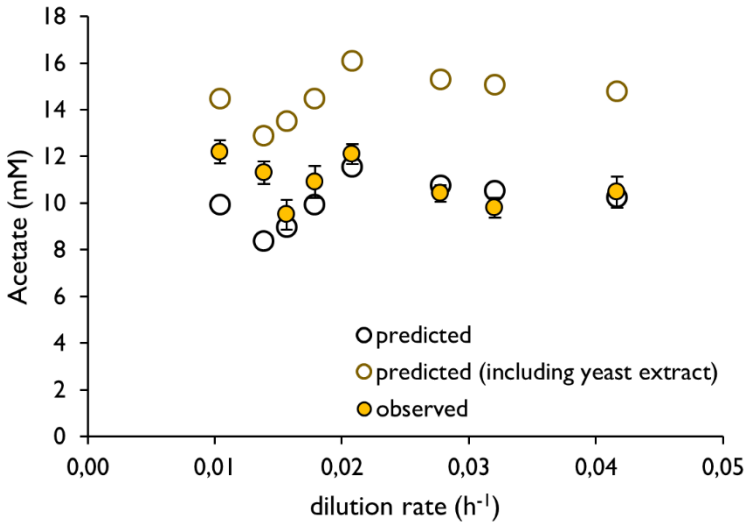


Figure 6-18 The observed and predicted acetate concentration leaving the inlet zone of the lactate-supplemented UAPBR at a range of tested dilution rates corresponding to HRT between four- and one-day(s). Predicted acetate concentrations were calculated using the degree of lactate oxidation by SRB (Equation 2-10), lactate fermentation (Equation 2-12) and complete oxidation of acetate by SRB (Equation 2-7) as shown in Figure 6-16. The theoretical acetate concluded to have been generated from yeast extract (Section 4.4.2)

was added to the initial prediction to generate a maximum predicted acetate concentration.

### 6.3.3 Electron donor utilisation within the middle and effluent zones.

Most of the propionate produced in the inlet zone was subsequently oxidised in the middle zone. This corresponded with an increase in the acetate concentration between entering and leaving the middle zone (Figure 6-1). This preferential oxidation of propionate over acetate led to the assumption that sulphate reduction would be linked to propionate if present, followed by acetate oxidation. It was also assumed that all propionate oxidised was linked to sulphate reduction. The remaining sulphate which was reduced and was not linked to lactate nor propionate oxidation, in the middle and effluent zones, was linked to acetate oxidation. These assumptions were used to estimate the quantity of lactate, propionate and acetate being consumed by SRB in the middle and effluent zones (Figure 6-19). It was predicted that the majority (79%) of the sulphate reduced in the middle zone was linked to propionate oxidation. The amount of sulphate reduced in the middle zone linked to acetate oxidation increases from approximately 0 mg/ℓ at a four- and three-day HRT (0.0.10 and 0.014 $h^{-1}$) to 67 mg/ℓ (0.70 mM), on average at reduced HRT.

Increased sulphate reduction and predicted electron donor oxidation by SRB occurred in the middle zone at a three- and 2.6-day HRT (0.014 and 0.016 $h^{-1}$). The elevated performance of this reactor zone ultimately led to the maintained sulphate conversion exhibited by the entire reactor, of over 95%. The sulphate consumed in the effluent zone varied between 0.5 and 2.1 mM and, based on physiochemical data and the assumptions made above, it was estimated that approximately half of this sulphate reduction was linked to acetate oxidation and the other half to propionate oxidation.

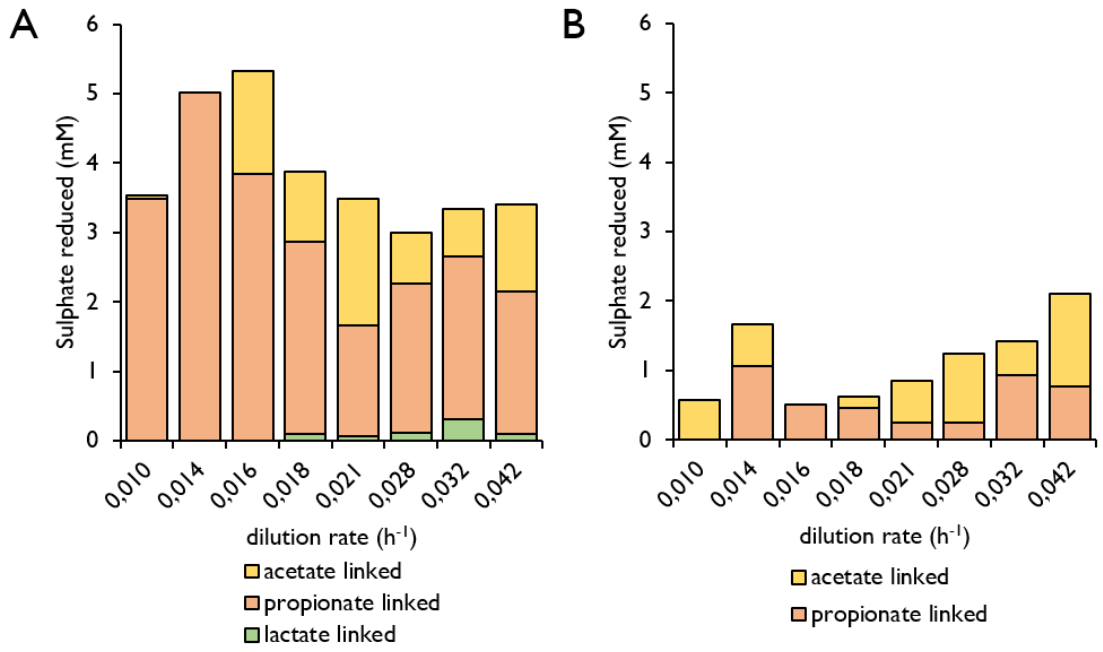


Figure 6-19 The electron donors putatively linked to the sulphate reduction observed in the (A) middle and (B) effluent zones at a range of tested dilution rates. This assumes all propionate oxidation was linked to sulphate reduction. Additional sulphate reduction which is not accounted for by propionate oxidation is assumed to be linked to acetate oxidation. The predicted acetate concentrations based on these assumptions are shown in Figure 6-20.

The predicted acetate concentration leaving the middle zone was calculated assuming the sulphate reduction coupled to the oxidation of propionate (Equation 2-9) and acetate (Equation 2-7) as shown in Figure 6-19A. The predicted and observed acetate concentrations agree only between a four- and 2.6-day HRT (0.010 to 0.016 $h^{-1}$). At lower HRTs, the observed acetate concentration averages 1.4 mM greater than predicted. The predicted and observed acetate concentration leaving the effluent zone are largely in agreement. It, therefore, appears that additional acetate is generated through yeast extract oxidation within the inlet zone at a four and three-day HRT (Figure 6-19) but as a result of the increased dilution rate this becomes restricted to the middle zone at further reduced HRT. The bicarbonate concentrations (Figure 6-20B) were greater than predicted from the observed oxidation of lactate, propionate and acetate. The additional bicarbonate is expected to have been generated through citrate and yeast extract oxidation which have been concluded to have taken place in this reactor.

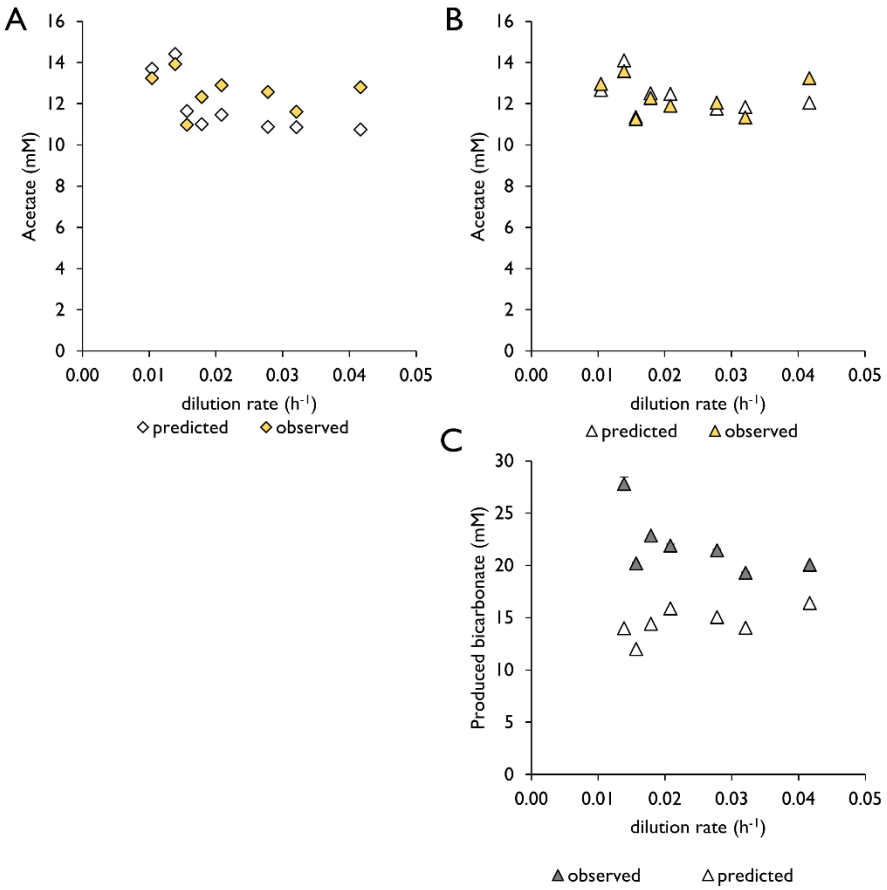


Figure 6-20 The observed and predicted (A) acetate concentrations leaving the (A) middle zone and (B) effluent zone, and the (B) observed and predicted bicarbonate concentrations in the effluent zone of the lactate UAPBR at a range of tested dilution rates. The concentration of acetate predicted leaving each zone was based on all observed propionate oxidation being linked to the observed sulphate reduction, and all further sulphate reduction being linked to acetate oxidation according to Equation 2-13. The produced bicarbonate concentrations were predicted based on the degree of lactate fermentation (Equation 2-12) and the oxidation by SRB (Equation 2-10), followed by acetate oxidation by SRB (Equation 2-7).

### 6.3.4 Reactor performance in the context of reported literature

The performance of the lactate-supplemented UAPBR, in terms of the entire 1 ℓ reactor and the 0.33 ℓ inlet zone, were compared against that of similarly operated reactors reported in the literature and shown in Figure 6-21. These studies used similar sulphate concentrations, reactor configurations with similar biomass retention capacity, and VSLRs to those used in this study. Baskaran et al. (2005) and Baskaran and Nemati (2006) operated UAPBRs, packed with sand and glass beads, respectively, which performed similarly to the 1 ℓ UAPBR of this study. These reactors both achieved sulphate conversions of over 90% at VSLRs between 25 and 50 mg/ℓ.h.

A UAPBR operated by Elliott et al. (1998), using sand as a carrier, exhibited similar performance to that of the 0.33 ℓ inlet zone of the UAPBR of this study. This UAPBR was operated, under acidic conditions, with an HRT of 22 hours and a feed sulphate concentration of 1.5 g/ℓ. The reactor was able to achieve a sulphate conversion and VSRR of approximately 46% sulphate and 31 mg/ℓ.h, respectively. This is similar to that of the inlet zone of the lactate-supplemented UAPBR at a two-day HRT.

Sand was also used as a biomass support matrix in a study by Chen et al. (1994) in a lactate-supplemented UAPBR. This reactor underperformed in comparison to other studies. This reactor was operated at a 6.5 hour HRT and a sulphate concentration of 0.9 g/ℓ, and achieved a VSRR of 15 mg/ℓ.h at a VSLR of 138 mg/ℓ.h. However, it was lactate limited and the performance would have likely improved with an increased feed lactate concentration.

Kaksonen et al. (2004) presented the performance of two fluidised bed reactors (FBRs) one supplemented with lactate and the other ethanol, using a sulphate concentrations of 2.3 g/ℓ and operated at an HRT of 16 hours. The lactate-supplemented FBR converted 65% of the 2.3 g/ℓ sulphate, corresponding to a VSRR of 92.5 mg/ℓ.h. The ethanol-supplemented reactor was able to achieve a sulphate conversion and VSRR of 81% sulphate and 97 mg/ℓ.h, respectively. Although the maximum VSRR that could be achieved by the lactate-supplemented UAPBR of this study was estimated at 71 mg/ℓ.h, using 1 g/ℓ sulphate, the reactor is expected to exhibit higher VSRR if the initial sulphate concentration was increased. Extrapolation of the kinetic model describing the performance data of the lactate-UAPBR within this study suggested that similar rates to that of Kaksonen et al. (2004) could be achieved in this reactor at flow rate: volume ratios of 0.059 when using a sulphate concentration of 2.3 g/ℓ. This corresponds to an HRT of 17 hours using the 1ℓ UAPBR.

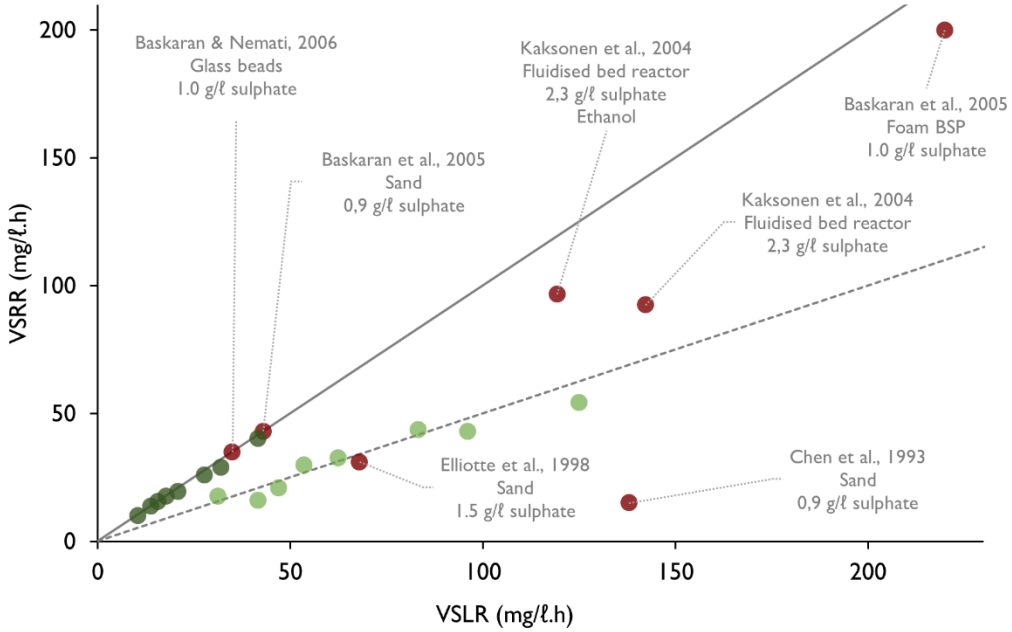


Figure 6-21 The volumetric sulphate reduction rate (VSRR) achieved by the lactate-supplemented (●) 1ℓ UAPBR of this study, (●) the 0.33 ℓ inlet zone of the UAPBR of this study and (●) selected continuous reactor studies from literature, at varied volumetric sulphate loading rates (VSLR). Sulphate conversion can be visually be determined through comparisons with lines plotted: 100% conversion – solid line, 50% conversion – dashed line. Details of the selected study are included in the figure including the sulphate concentration, carrier material, electron donor if not lactate and reactor configuration if not a UAPBR. These reactor studies were selected as these had similar starting sulphate concentrations and hydraulic retention times to those used in this study.

Baskaran et al. (2005) operated a UAPBR with foam carrier matrix and was able to maintain sulphate conversions above 90% at a VSLR of 220 mg/ℓ.h. This was achieved using a lactate and sulphate concentration of 5.5 and 1.0 g/ℓ, respectively. The achieved VSRR, therefore, comes at the cost of providing excess lactate – 4.6-fold higher than the lactate concentration used in this study.

### 6.3.5 Changes in the planktonic microbial communities between reactor zones

The change in abundance of the 17 most predominant OTUs, between the inlet and effluent zones of the lactate-supplemented system, across all tested HRT, was evaluated and is described in Figure 6-22. This data were used to implicate these OTUs in lactate oxidation in the inlet zone and propionate and/or acetate oxidation in the effluent zone. The large changes in abundance of these OTUs, whilst cell concentrations between these zones remain fairly constant, indicates that cells present in the middle and effluent zones are present not simply because they were carried upwards

to these zones by the hydrodynamics of this system. Instead, these OTUs would need to be metabolically active to maintain abundance in these zones.

*Veillonella* (11) and *Aeromonas* (38) showed an average decrease of more than 75% (2 log2 fold) between the inlet and effluent zones– indicating these OTUs were primarily active in the inlet zone and showing little further growth throughout the remainder of the reactor. These OTUs are, therefore, likely performing lactate fermentation. The *Veillonella* OTU was also found to be highly enriched in lactate samples after surveying the communities of all six BSR reactors of this study (Chapter 7 ), this genus is frequently implicated in lactate fermentation in literature (Rogosa, 1963; Ng and Hamilton, 1971; Seeliger et al., 2002; Scheiman et al., 2019) and is found nearly exclusively within zones of lactate oxidation in the lactate-supplemented UAPBR. Therefore, it is concluded that this is one of the SRB's major competitors for lactate in this reactor.

Inversely, three OTUs, namely unclassified (71), *Paracoccus* (4) and *Lutaonella* (0), each increased by more than four-fold from the inlet to the effluent zone. It is therefore hypothesised that these OTUs are involved in the consumption of acetate and/or propionate. *Paracoccus* (4) and *Lutaonella* (0) were also identified in the acetate-supplemented UAPBR planktonic communities (Figure 6-34), providing further evidence that these microorganisms consume acetate. Further evidence for these associations are described in Chapter 7 .

The two SRB OTUs identified in these planktonic communities, namely *Desulfovibrio* (6) and *Desulfomicrobium* (1), showed little change in abundance across the inlet and effluent zones. This suggests these microorganisms remained active throughout the length of the reactor, and that these SRB likely utilise lactate in the inlet zone as well as oxidising acetate and/or propionate throughout the rest of the column.

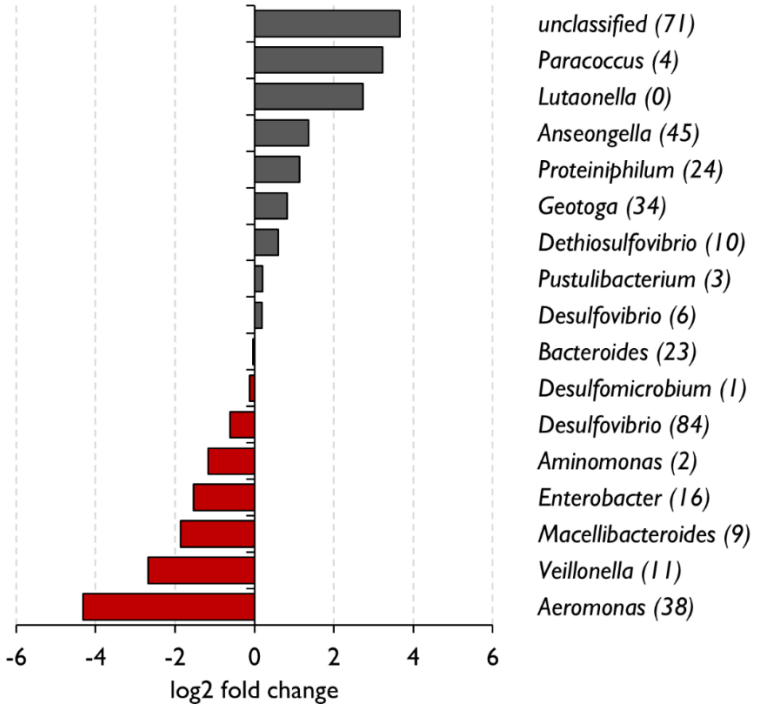


Figure 6-22 Log2 fold change of the predominant OTUs, in the lactate UAPBR planktonic communities, between the inlet and the effluent zones, averaged between the four-, three-, 1.5- and one-day HRTs. OTUs which show a reduced abundance between the inlet and effluent zones are shown in red, while those increasing in abundance are shown in grey.

### 6.3.6 Comparison of planktonic and biofilm communities

The composition of each planktonic and biofilm community from the lactate-supplemented UAPBR were compared (Figure 6-23). Using this approach, all the planktonic samples as well as the biofilm sample isolated from zone one at a four-day HRT clustered separately from all remaining biofilm communities. The three most abundant SRB in any of UAPBR's communities were *Desulfomicrobium* (1) which was a dominant microorganism in almost every sample excluding the biofilm communities of zones four, five and six, *Desulfovibrio* (6) which was primarily dominant in the planktonic communities, and *Desulfobulbus* (27) which was dominant in the biofilm communities of zones three to six at a one-day HRT.

One of the most striking differences between the biofilm communities present in zone one between a four-day and one-day HRT is the differing abundances of *Lutaonella* (0) and *Veillonella* (11). *Veillonella* (11) is highly abundant in the biofilm communities, and other UAPBR planktonic communities, at a four-day HRT, but is almost undetected at a one-day HRT in the biofilm communities. Whereas, the *Lutaonella* (0), present at very low abundance in the biofilm communities of zone one and six at a four-day HRT, becomes one of the most dominant microorganisms present in the biofilms throughout the lactate-supplemented UAPBR at a one-day. A survey of all the microbial communities of the six BSR reactors assessed by 16S rRNA gene

amplicon sequencing (Chapter 7 ) found *Lutaonella* (0) to be highly enriched in biofilm communities and, inversely, found *Veillonella* (11) to be enriched in planktonic samples. This shift in dominance between *Veillonella* (11) and *Lutaonella* (0) may be evidence of biofilm maturation and not a direct consequence of the changing dilution rate.

Attributing identified SRB within the biofilm communities with specific electron donor oxidation was done by overlaying the estimated VFA oxidation in each zone (Sections 6.3.1 and 6.3.3) to the SRB present within the biofilms at a one-day HRT (Section 6.2.4). This aligned *Desulfovibrio* (6) and *Desulfomicrobium* (1) in the biofilm communities of zone 1 and 2 with lactate oxidation within these zones, *Desulfobulbus* (27) dominant in zones 3 and 4 with propionate oxidation, *Desulfatiglans* (91) present in the effluent zone with acetate oxidation and sulphate scavenging and, *Desulfobacter* (18) and *Desulfacarina* (53) present in zones 3 to 6 to acetate and propionate oxidation.

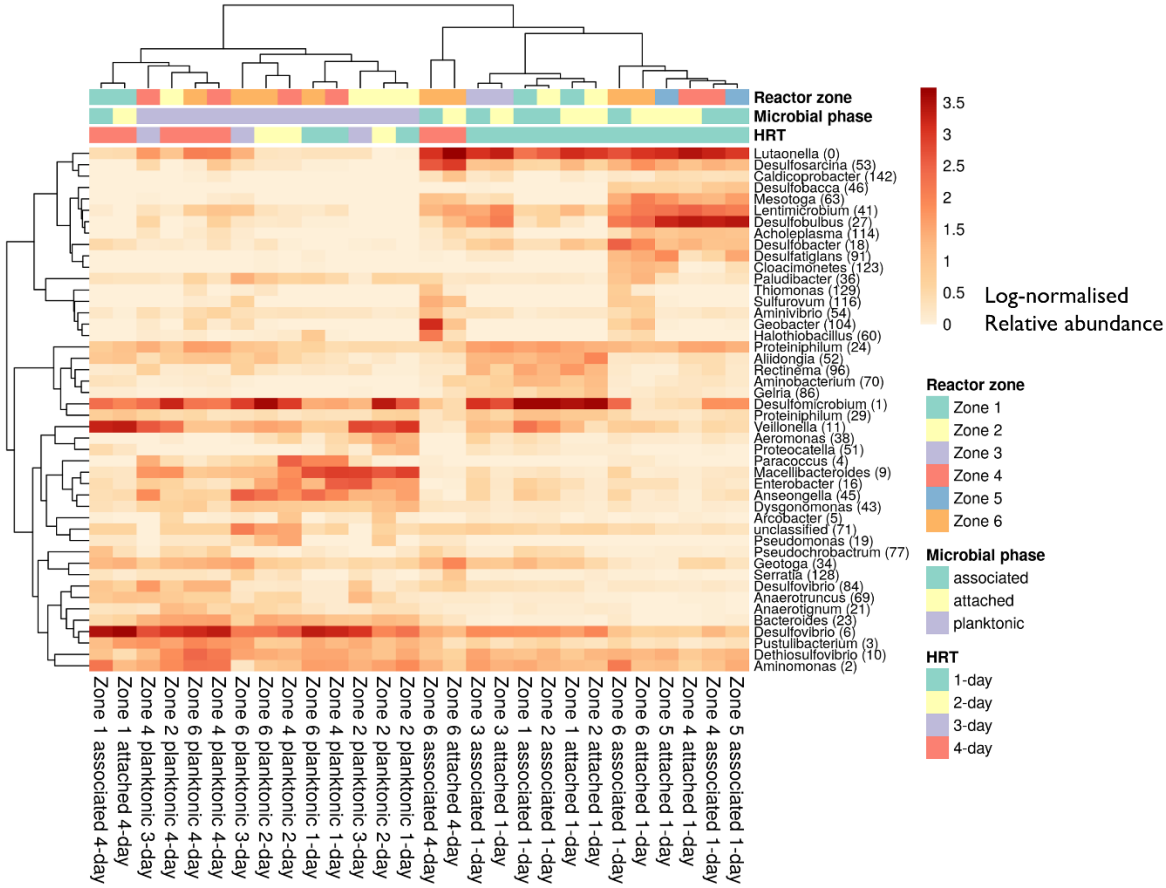


Figure 6-23 Hierarchical clustering of the relative abundances of the dominant OTUs in planktonic, associated and attached communities isolated from the six 0.167 ℓ zones of the lactate-supplemented UAPBR reactor zones, at hydraulic retention times of one-, two-, three- and four-days. Relative abundances were ln(x +1) transformed and hierarchical clustering was performed using correlation distance and average linkage (Section 3.9). No row centring was performed. The reactor zone from which each sample was isolated, the microbial phase and the HRT at which the sample was recovered is shown above the heatmap and the legend shown on the right of the heatmap.

## 6.4 Acetate UAPBR Results

### 6.4.1 Reactor performance

The acetate UAPBR had achieved near 95% sulphate conversion of the 1 g/ℓ feed sulphate (Figure 6-24A) at the boundary between the middle and effluent zones at a four-day HRT (0.010 $h^{-1}$). The reduction in the HRT to three-days (0.014 $h^{-1}$) had a detrimental effect on the performance of the inlet zone. The sulphate conversion achieved by the inlet zone decreased from 78 to 42% between the four- and three-day HRT (0.010 and 0.014 $h^{-1}$), respectively. These correspond with volumetric sulphate reduction rates of 24 and 18 mg/ℓ.h, respectively (Figure 6-27). Further reduction in the HRT resulted in improvement to both the VSRR and sulphate conversion achieved in this zone. The sulphate reducing performance at the three-day HRT is therefore assumed to be an outlier. Nevertheless, this data were included in further microbial analyses in order to associate this poor performance to the VFA profile and microbial ecology present within the reactor at the time.

The inlet zone of the acetate-supplemented UAPBR exhibited VSRRs comparable to that of the inlet zone of the lactate-supplemented UAPBR at each tested dilution rate. The middle and effluent zones of the acetate UAPBR, however, showed far lower VSRRs compared with those of the lactate UAPBR. The middle and effluent zones of the acetate UAPBR were only able to convert approximately 25% of the sulphate entering each of these zones (Figure 6-27). This compared to the lactate-supplemented UAPBR which saw the middle and effluent zones convert over 50% of the available sulphate (Figure 6-1).

The sulphide concentrations observed in each of the three zones were largely in agreement with those predicted from the degree of sulphate reduction (Figure 6-24B), although in some instances the observed was marginally higher than that predicted. The highest sulphide concentration observed leaving the inlet zone was 261 mg/ℓ.h at a four-day HRT (0.010 $h^{-1}$). The concentration increased to 340 mg/ℓ.h in the effluent of the reactor at this HRT. At a one-day HRT the concentration of sulphide leaving the inlet zone was 122 mg/ℓ.h and increased to 186 mg/ℓ.h in the reactor effluent. The bicarbonate concentration (Figure 6-24 C) present in the effluent decreased with increasing dilution rate, from 21 mM at a three-day HRT (0.014 $h^{-1}$) to 7 mM at a 1.3-day HRT (0.032 $h^{-1}$) and 10 mM at a one-day HRT (0.042 $h^{-1}$).

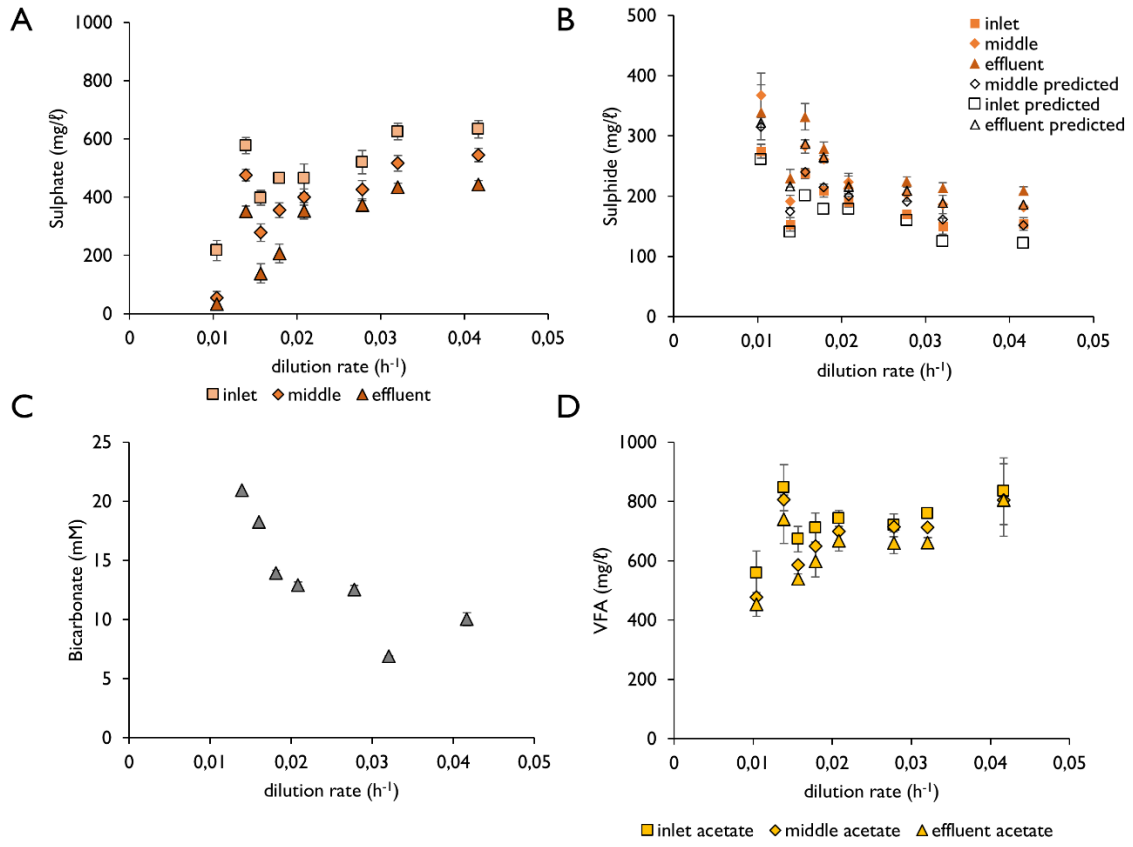


Figure 6-24 Steady-state kinetic data of the acetate-supplemented UAPBR at a range of tested dilution rates, including (A) the residual sulphate, (B) the produced sulphide and the predicted sulphide concentration based on the observed sulphate reduced; (C) the produced bicarbonate concentration present in the reactor effluent calculated from the difference between the observed and feed bicarbonate concentrations and (D) the observed volatile fatty acid profile.

The concentration of acetate in each zone, with increasing dilution rate, (Figure 6-24D) reflected that of the sulphate profile – gradually increasing with each reduction in the HRT. The acetate concentration in each of the three zones was elevated at three-day HRT (0.014 $h^{-1}$) compared with those seen at a four- and 2.6-day HRT (0.10 and 0.016 $h^{-1}$, respectively). This corresponds with the poor sulphate reducing performance observed at this HRT. The concentration of acetate decreases between each of the subsequent zones, observed at each tested HRT. The acetate concentration was at a minimum in the reactor effluent of 452 mg/ℓ (7.53 mM) at a four-day HRT (0.010 $h^{-1}$) and reached a maximum of 834 mg/ℓ (13.89 mM) in the inlet zone at a one-day HRT (0.042 $h^{-1}$).

The observed pH (Figure 6-25A), between the three zones and across the HRT study resided within a narrow band between 7.35 and 7.55. However, the pH was lowest at a three-day and one-day HRT, where the sulphate reducing performance was lowest. The redox potential (Figure 6-25B), showed a greater degree of variation, increasing from -195 mV in the effluent zone at a

one-day HRT (0.010 $h^{-1}$) to -161 mV at 2.3-day HRT (0.018 $h^{-1}$) where it remained at further reduced HRT.

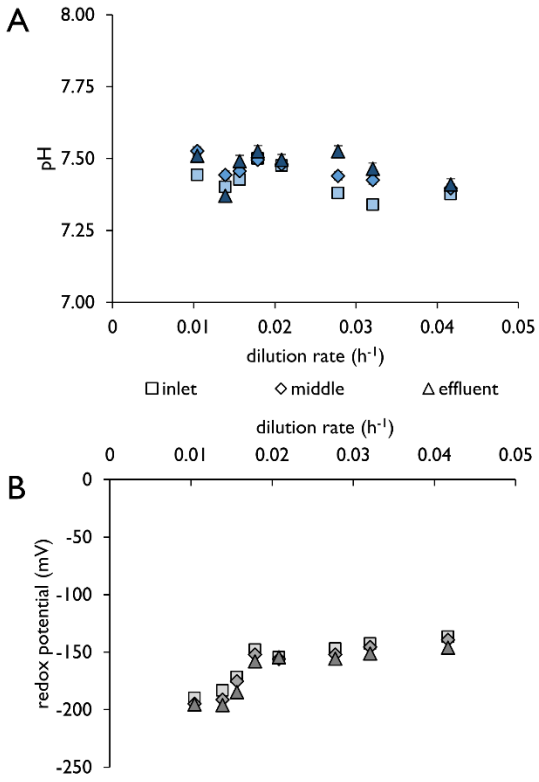


Figure 6-25 Steady-state kinetic data of the lactate-supplemented UAPBR at a range of tested dilution rates, including (A) pH and (B) redox potential (reported relative to a standard hydrogen electrode) in the inlet-, middle- and effluent zones of the acetate-supplemented UAPBR at each tested dilution rate. Error bars represent one standard deviation from the mean.

The acetate-supplemented UAPBR was able to maintain an increasing VSRR with increasing VSLR for all tested dilution rates (Figure 6-26), increasing from 10 mg/ℓ.h at a four-day HRT (0.010 $h^{-1}$) to a maximum VSRR of 23 mg/ℓ.h at a one-day HRT (0.042 $h^{-1}$). The conversion achieved by the reactor, however, decreased with the reduction of the HRT. The UAPBR maintained a sulphate conversion approximately two-fold greater than that exhibited by the similarly operated acetate CSTR at each tested HRT.

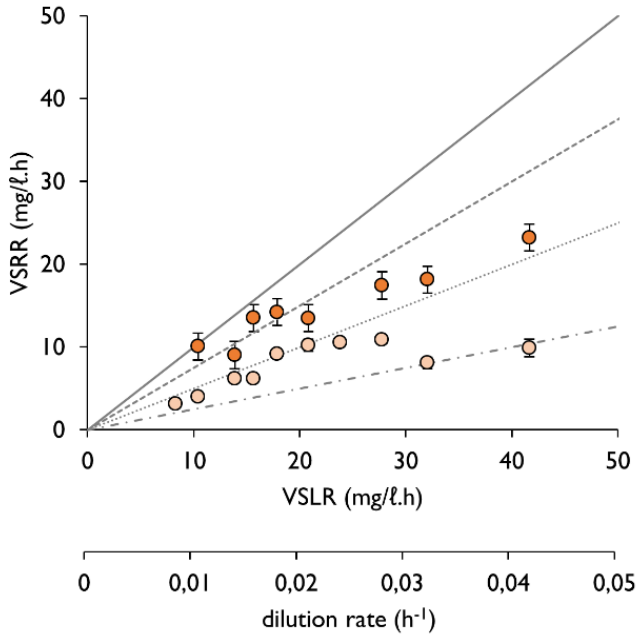


Figure 6-26 Volumetric sulphate reduction rates (VSRR) achieved by (●) the acetate-supplemented UAPBR at increasing volumetric sulphate loading rates (VSLR), increased through the increasing of the applied dilution rate, corresponding to hydraulic retention times ranging from four-days to one day, whilst keeping the feed sulphate concentration constant at 1 g/ℓ. The achieved VSRR of (●) the similarly operated acetate-supplemented CSTR is shown for comparison. VSRR were calculated based on the residual concentrations measured leaving the effluent of the reactor. Sulphate conversion can be visually be determined through comparisons with lines plotted: 100% conversion – solid line, 75% conversion – dashed line; 50% conversion – dotted line, 25% conversion – composite dotted-dashed line.

The majority of the sulphate reduced in the acetate UAPBR was reduced within the inlet zone at each tested HRT. The VSRR achieved by the 0.33 ℓ inlet zone (Figure 6-27) increased from 23 mg/ℓ.h at a four-day HRT (0.010 $h^{-1}$; 78% sulphate conversion) to 46 mg/ℓ.h at a one-day HRT (0.042 $h^{-1}$; 36% sulphate conversion). The middle and effluent zones achieved a maximum VSRR of 11 and 13 mg/ℓ.h, respectively, at a one-day HRT (0.042 $h^{-1}$).

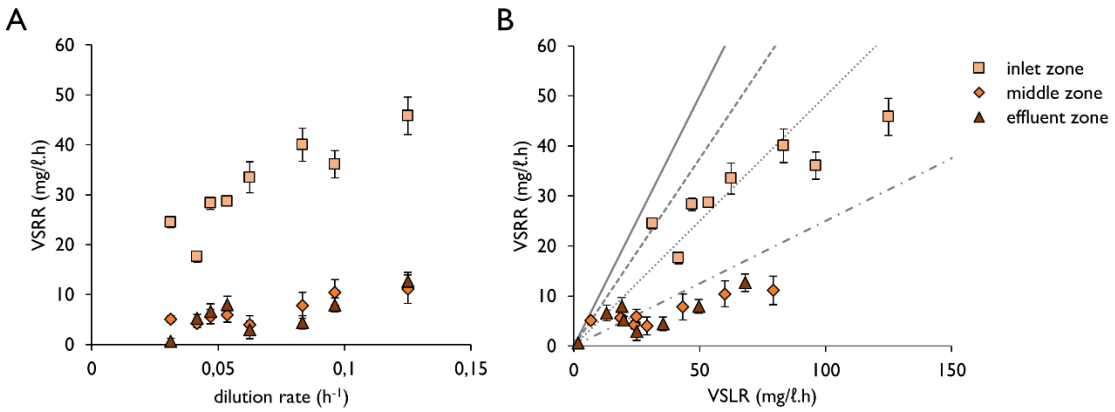


Figure 6-27 Volumetric sulphate reduction rate (VSRR) achieved by the three zones of the acetate UAPBR at (A) each tested dilution rate and (B) at the volumetric sulphate loading rate (VSLR) applied to each zone. Sulphate conversion can be visually be determined through comparisons with lines plotted: 100% conversion – solid line, 75% conversion – dashed line; 50% conversion – dotted line; 25% conversion – composite dotted-dashed line.

**Biomass retention**

The planktonic cell concentrations, from all zones and all tested HRT, remained stable for the duration of the study (Figure 6-28). The concentration of planktonic cells in the inlet were typically lowest, at approximately 1.5 x $10^8$ cells/mℓ and increased to 2 x $10^8$ cells/mℓ in the middle and effluent zones. These cell concentrations were significantly lower than the cell concentrations supported by the acetate CSTR (average of 3.6 x $10^8$ cells/mℓ) over the HRT study (*p*-value <0.05 calculated from two-tailed Students t-test).

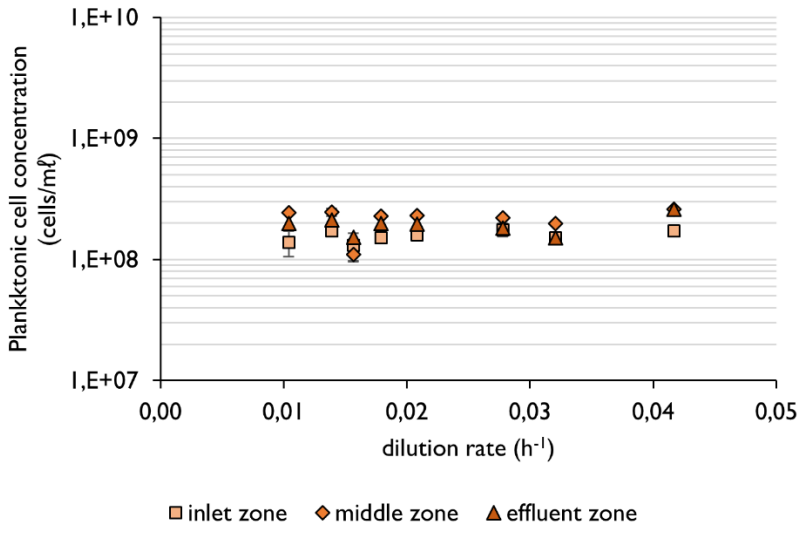


Figure 6-28 Planktonic cell concentrations in the acetate UAPBR inlet, middle and effluent zones at each tested dilution rate. Error bars represent one standard deviation from the mean.

The highest cell concentration of any microbial community observed in the acetate-supplemented UAPBR was seen in the biofilm attached community of zone one at a four-day HRT (0.010 $h^{-1}$; Figure 6-29). This community reached a cell concentration of 5.4 x $10^{10}$ cells/mℓ, which is more than 200-fold greater than that of the planktonic community present in the inlet zone at a four-day HRT. The biofilm-associated community of this zone was also highly concentrated at 7.7 x $10^{9}$ cells/mℓ.

The cell concentration of the attached and associated communities of zone one decreased to 9.0 x $10^{9}$ and 3.5 x $10^{9}$ cells/mℓ, respectively, at a one-day HRT. Furthermore, at this HRT, the biofilm attached cell concentration decreased approximately three-fold by zone two and reached a cell concentration of 7.2 x $10^{8}$ cells/mℓ in zone three, where it stayed relatively constant throughout the rest of the reactor.

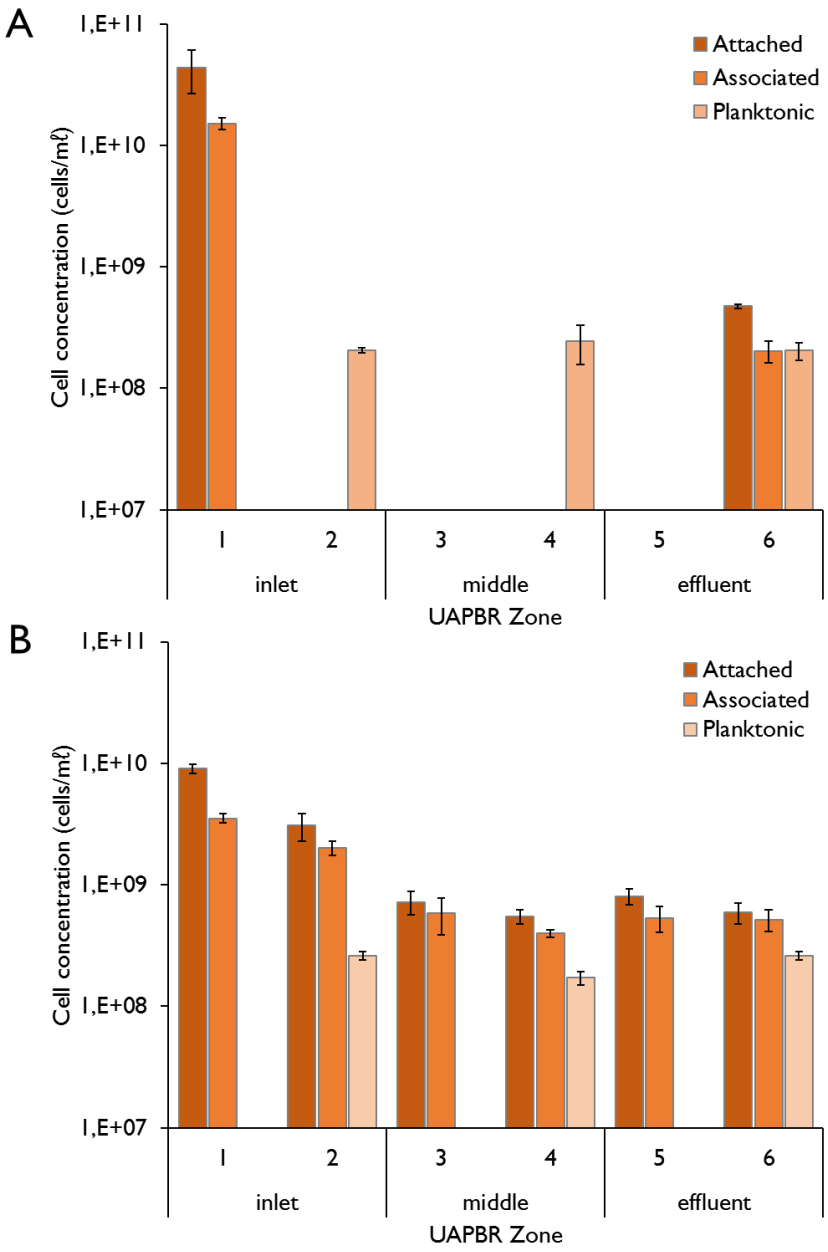


Figure 6-29 The cell concentrations of the biofilm-attached, -associated and planktonic communities found in the six sequential zones of the acetate-supplemented UAPBR, observed at a (A) four-day HRT (0.010 $h^{-1}$) and (B) one-day HRT (0.042 $h^{-1}$).

SEM was used to visually inspect the surface of the polyurethane foam isolated from each of the six reactor zones at a one-day HRT (Figure 6-30). Thick microbial mats were visible on the polyurethane foam removed from zones 1 and 2 of the acetate UAPBR. The cells which made up these biofilms were mostly vibrio and large cocci in morphology. The apparent density of cells present on the surface of the polyurethane decreased between zones two and three. Foam recovered from zones three to six showed cells scattered evenly over the surface. A variety of morphologies were present in these biofilms including rod, vibrio, spirochaete and lemon-shaped cells.

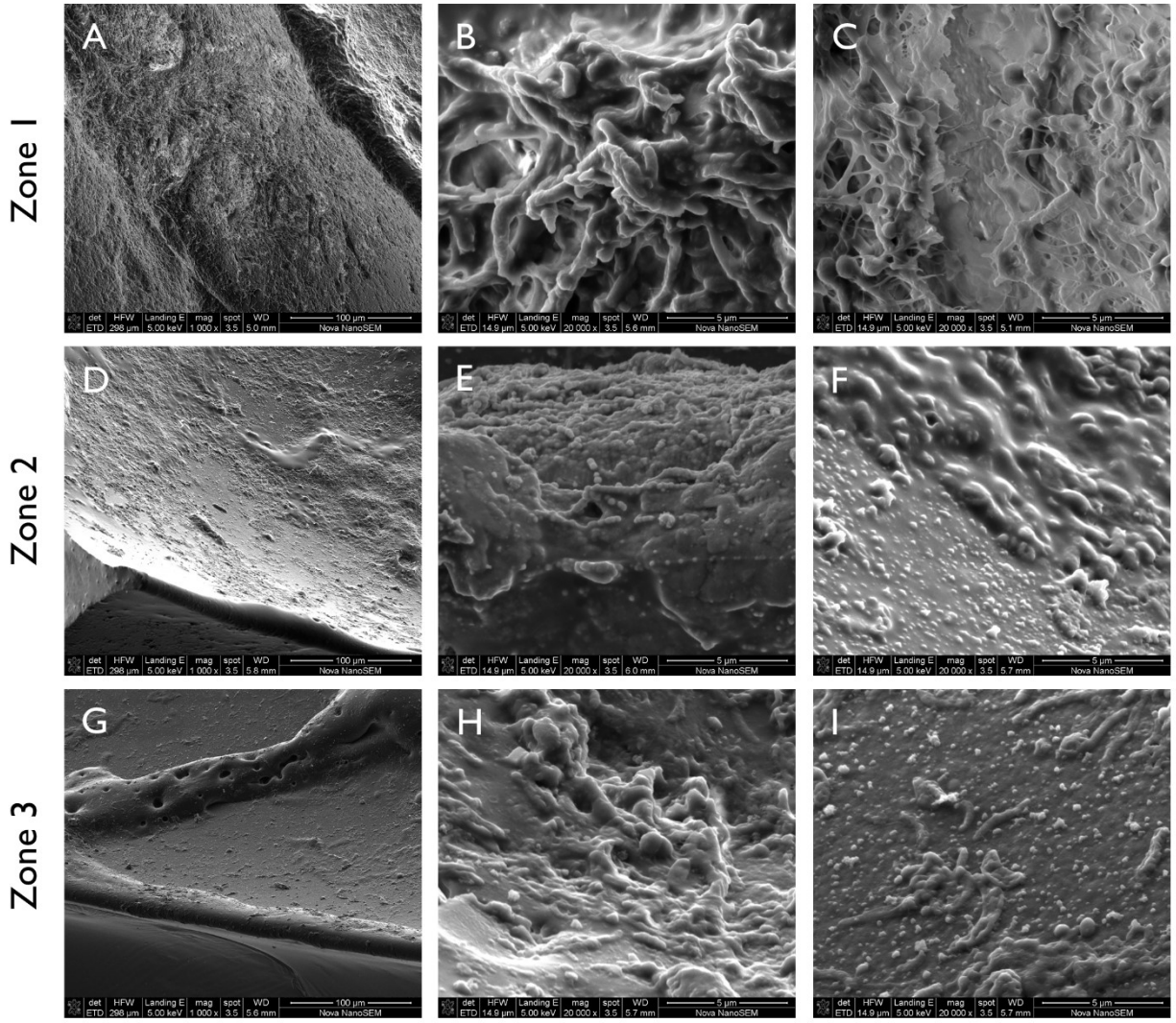


Figure 6-2 Scanning electron micrographs of the surface of the polyurethane foam packing within the Acetate supplemented UAPBR, isolated during the defined one-day HRT steady-state period. Polyurethane foam was isolated from zone 1(A-C), zone 2 (D-F), zone 3 (G-I), zone 4 (J-L), zone 5 (M-O) and zone 6 (P-R). Scale bars are shown in each micrograph.

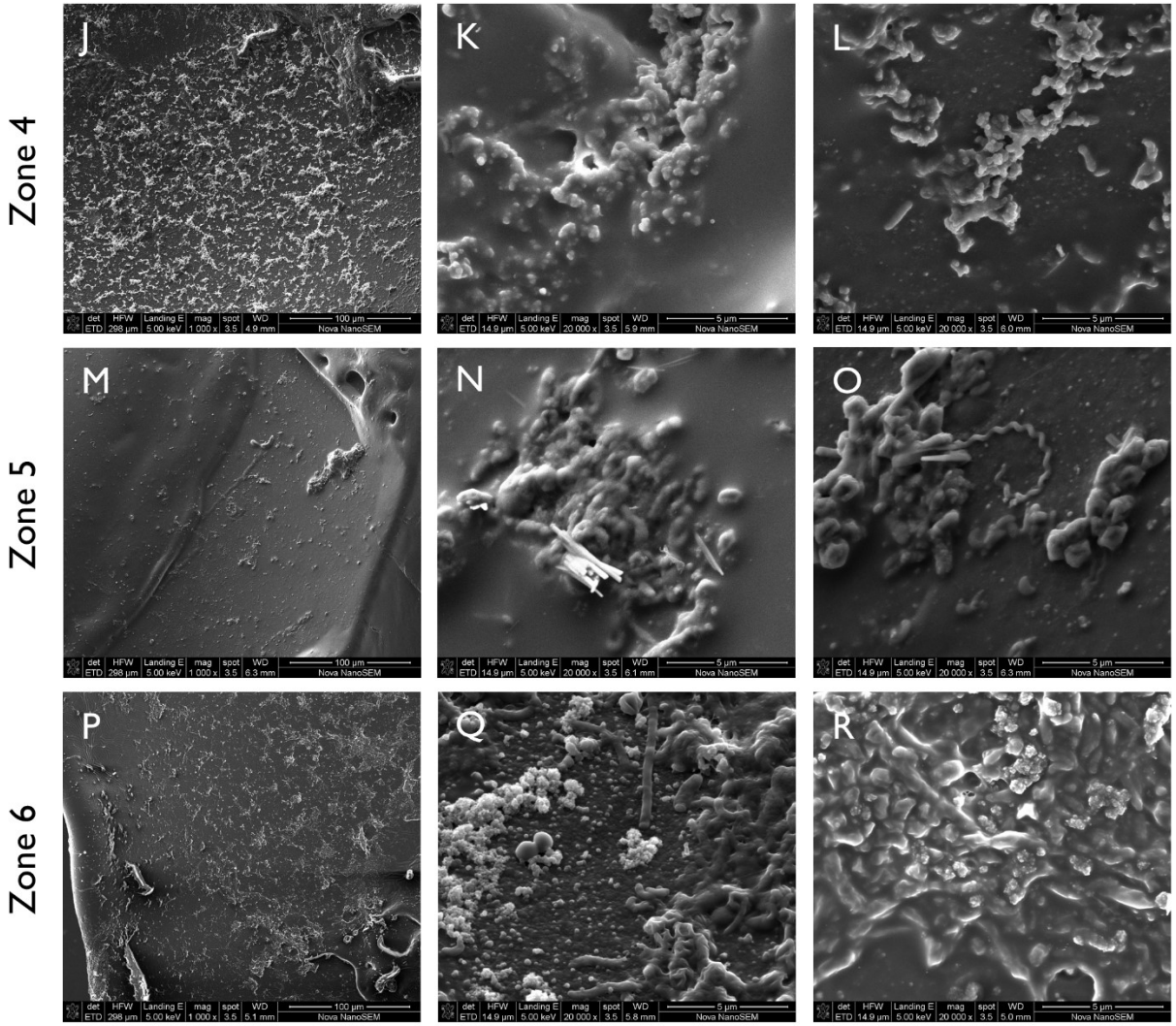


Figure 6-30 Continued

### 6.4.2 Sulphate reduction performance model

$$r_A = \frac{V}{F}\left(\left(C_0^{(-n+1)} + (n-1)\cdot k\cdot\frac{V}{F}\right)^{\frac{1}{(-n+1)}} - C_0\right)$$

The acetate UAPBR was modelled using

Equation 3-17 (Section 3.7.3) shown below as an n$^{th}$ order spontaneous, irreversible reaction in an ideal plug flow reactor (PFR).

$$r_A = \frac{V}{F}\left(\left(C_0^{(-n+1)} + (n-1)\cdot k\cdot\frac{V}{F}\right)^{\frac{1}{(-n+1)}} - C_0\right)$$

Equation 3-17

The non-linear regression generalised reduced gradient (GRG) method was used with collected reactor kinetic data, from the multiple zones and composite zones, to find the value for the order of the reaction, *n,* and for the rate constant, *k,* which resulted in the lowest sum of squared errors. The acetate UAPBR kinetic data were best described with this equation with a reaction order, *n*, of 2.9 and a rate constant, k, of 1.5 x $10^{-7}$ $mg^{-1,9}\ell^{1,9}h^{-1}$. Sulphate reduction data collected at a three-day HRT (0.014 $h^{-1}$) were concluded to be outliers and not included in this optimisation. The standard error associated with this model was 2.5, the 95% confidence interval of 5.08 mg/ℓ.h and the model fitted the data with an $R^2$ of 0.95 (Figure 6-31).

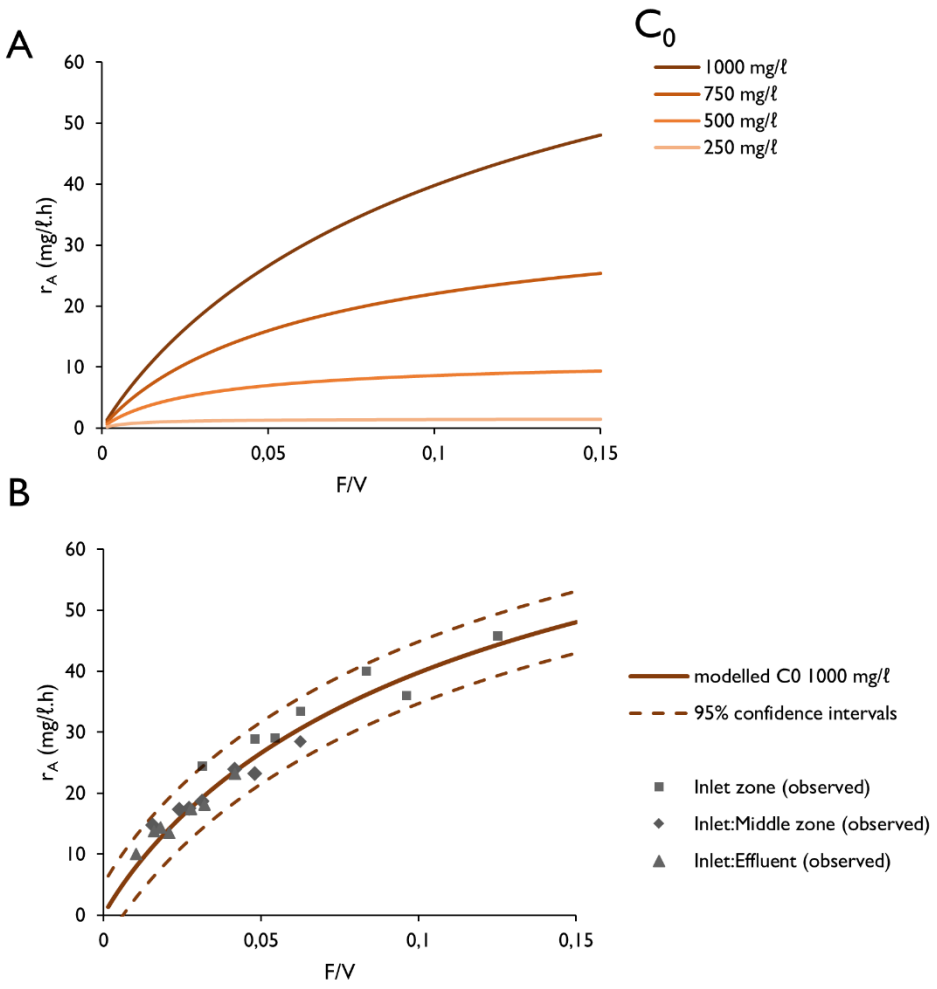


Figure 6-31 Modelled reaction rate data at various flow rate to volume ratios (F/V) with (A) various starting sulphate starting concentrations ($C_0$) as shown in the legend. Observed reaction rates (B) from the inlet zone (0.33 ℓ), composite inlet and middle zone (0.66 ℓ) and entire reactor (1.0 ℓ) are plotted against the modelled reaction rate with the modelled reaction rates with a $C_0$ of 1000 mg/ℓ sulphate. 95% confidence intervals are shown.

The modelled data predict VSRRs achieved by this reactor, at a flow rate to volume ratios of 0.15, with incoming sulphate concentrations of 1000, 750, 500 and 250 mg/ℓ to be equal to 48.2, 25.4, 9.3 and 1.4 mg/ℓ.h, respectively.

The difference between the observed and corresponding predicted sulphate reduction rates, from each zone and composite reactor zone, from each HRT, were found to be similar. These differed by, on average 14% of the predicted VSRR (Figure 6-32). The residuals between the observed and predicted sulphate reduction rates (Figure 6-31), assessed collectively from all samples, appear to largely be normally distributed when not considering which zone(s) or composite zones the data originated. However, residuals tended to decrease from positive to negative with increasing flow rate to volume ratios for individual and composite reactor zones. This indicates predictions made at low F/V ratios are overestimated and are underestimated at higher F/V ratios.

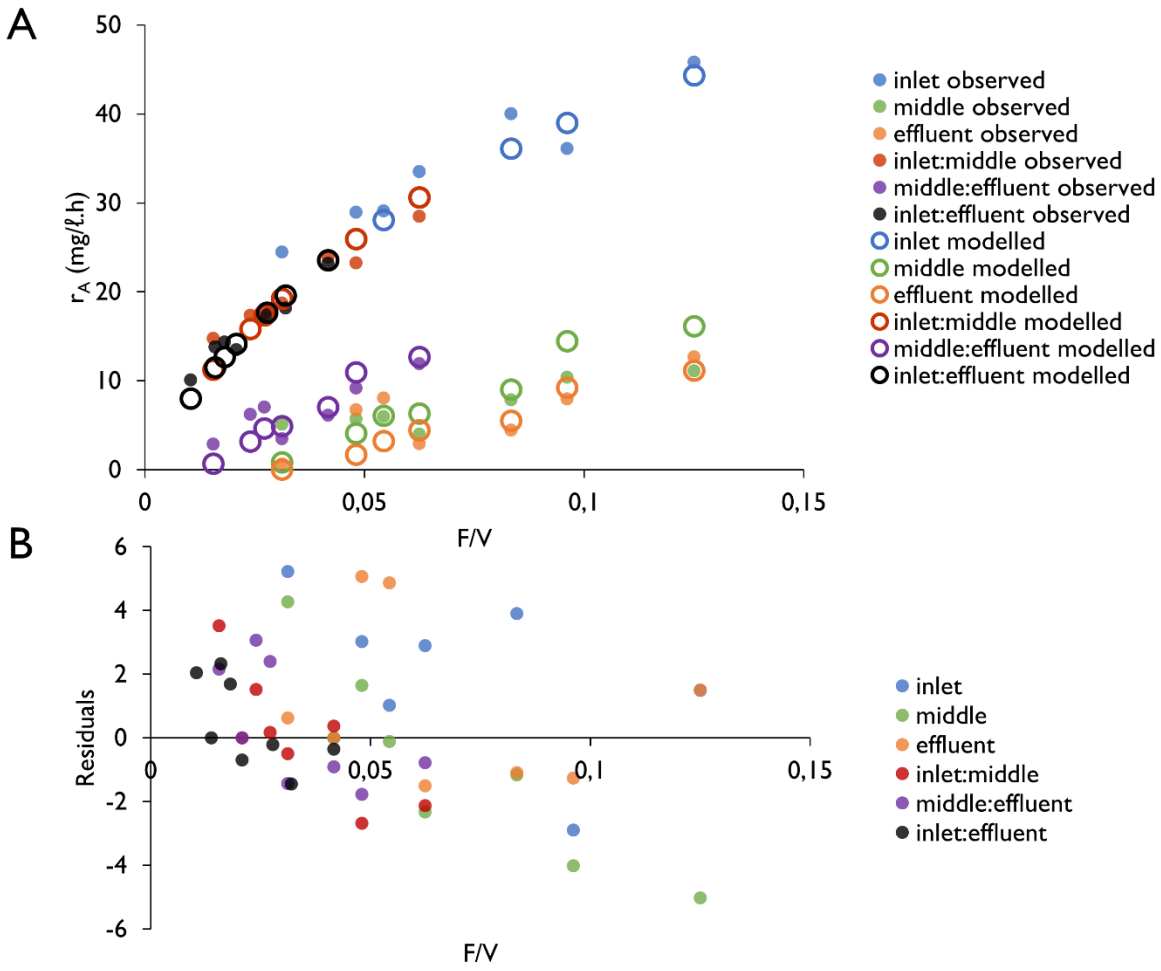


Figure 6-32 The (A) observed (closed circles) and predicted (open circles) sulphate reducing reaction rates over the individual and composite reactor zones of the acetate UAPBR at various tested flow rate to volume ratios (F/V). Predicted rates were based on eq () which describes a spontaneous, first-order irreversible reaction in a plug flow reactor with a rate constant, k, of 0.069 $h^{-1}$. The residuals (B) of the observed rates minus the modelled rates are shown.

### 6.4.3 Microbial ecology of the planktonic communities

The planktonic communities of the acetate UAPBR were dominated by Bacteroidetes at all tested dilution rates (Figure 6-33). The proportion of SRB, made up by Deltaproteobacteria, was also greatly diminished compared to that seen in the lactate UAPBR. Bacteroidetes were particularly dominant and, inversely, Deltaproteobacteria particularly reduced at a three-day HRT (0.014 $h^{-1}$) – the HRT where the sulphate conversions were some of the lowest observed. Some Firmicutes were also present but little to no Negativicutes, of which the lactate fermenting microorganism *Veillonella* is a member. Verrumicrobia were present in all three zones at four-day HRT (0.010 $h^{-1}$) but absent at further reduced HRT. Verrumicrobia were also observed in the acetate CSTR (Chapter 4) and experienced a considerable reduction in abundance at HRT shorter than four-

days. Apart from these changes, little other variation can be seen between the multiple zones and multiple dilution rates at the phylum and class taxonomic level.

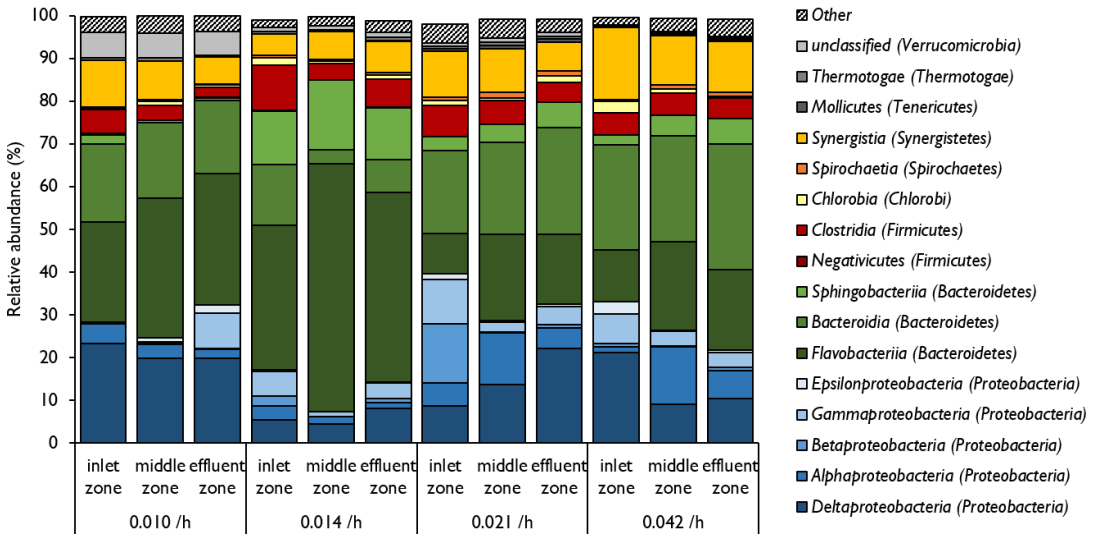


Figure 6-33 Relative abundance of the predominant microbial classes within the planktonic communities of the inlet, middle and effluent zones of the acetate UAPBR at dilution rates corresponding to four-, three-, two- and one-day HRTs. The phyla to which each class belongs are shown in parentheses.

The dominant SRB OTUs were *Desulfovibrio* (6) and *Desulfomicrobium* (1) in the planktonic communities of this reactor (Figure 6-34), as seen in the acetate CSTR. Like the CSTR, *Desulfovibrio* (6) was abundant at a four-day HRT (0.010 $h^{-1}$) but showed a substantial reduction in abundance at reduced HRT, where *Desulfomicrobium* (1) became more dominant. The abundance of these OTUs was considerably reduced at the three-day HRT (0.014 $h^{-1}$) where sulphate conversion, VSRRs and acetate conversion were some of the lowest observed. At this three-day HRT (0.014 $h^{-1}$), the Bacteroidetes OTU *Pustulibacterium* (3) was particularly dominant, present above 50% relative abundance in the middle zone planktonic community. A number of additional Proteobacteria classified to classes other than Deltaproteobacteria where seen throughout the planktonic communities (Shown in pink-purple in Figure 6-34), including the OTUs *Halothiobacillus* (60) at a four-day HRT, and both *Aquamicrobium* (26) and *Paracoccus* (4) at a two- and one-day HRT (0.021 and 0.042 $h^{-1}$).

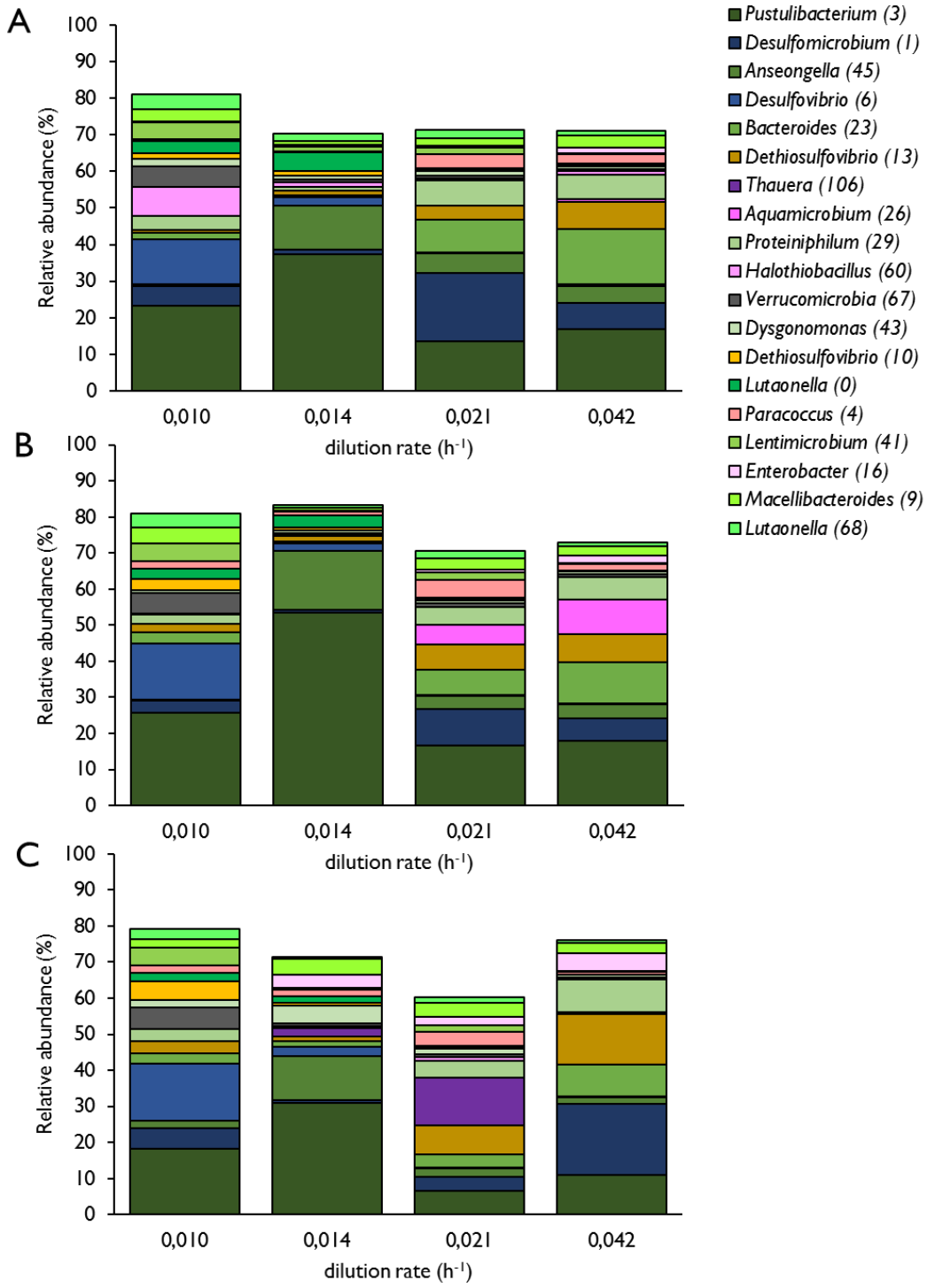


Figure 6-34 The relative abundance of the most abundant OTUs in the planktonic communities of the acetate-supplemented UAPBRs (A) effluent, (B) middle and (C) inlet zones at dilution rates corresponding to a four-, three-, two- and one-day HRT. OTUs are colour shaded by taxonomy: Deltaproteobacteria – blue, other Proteobacteria – purple, Bacteroidetes – green, Firmicutes – red, Synergistetes – yellow, other phyla – grey.

### 6.4.4 Microbial ecology of the biofilm communities

Stratification of the microbial communities from zone to zone of the acetate-supplemented UAPBR was not evident at the phylum and class taxonomic level. The attached and associated biofilm communities of the acetate-supplemented UAPBR were made up of relatively few microbial phyla (Figure 6-35). Proteobacteria and Bacteroidetes typically constituted more than 70% of these communities, with Clostridia, Chlorobia, Synergistia, Thermotogae and Mollicutes constituting a further 20%. All but one of the OTUs classified as Deltaproteobacteria were thought to be likely SRB (Figure 6-36). This *Geobacter* OTU was predominant in the attached community of zone 6 at a four-day HRT.

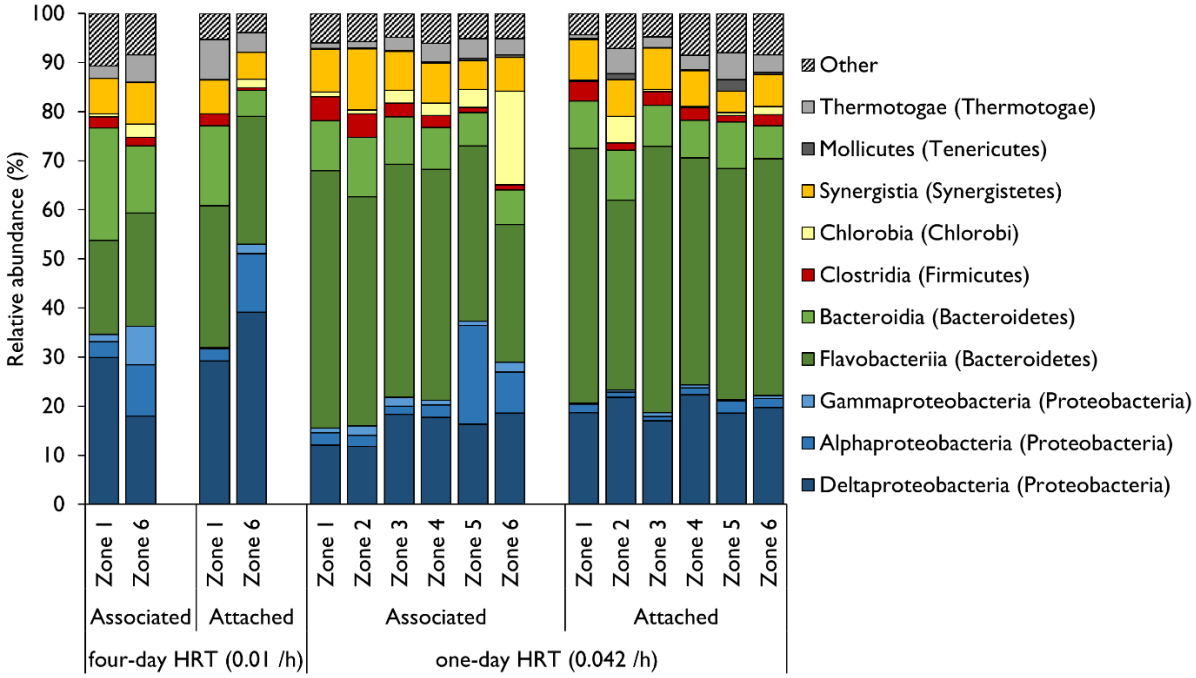


Figure 6-35 Relative abundance of the predominant microbial classes within the attached- and associated-biofilm communities of the six sequential zones of the acetate UAPBR at four- and one-day operated HRTs. The phyla to which each class belongs are shown in parentheses.

Six predominant SRB OTUs could be putatively identified within the biofilm communities of the acetate UAPBR (Figure 6-36). *Desulfovibrio* (6), which was dominant in the planktonic communities at a four-day HRT, was also present in the associated communities at a four-day HRT. This OTU was not detected, however, at a one-day HRT. *Desulfobulbus* (58), observed in the lactate UAPBR biofilm communities, was one of the most dominant SRB OTUs in these communities. This OTU was dominant in attached and associated communities, at both a four- and one-day HRT,

throughout the zones of the UAPBR. *Desulfosarcina* (53) and *Desulfobacca* (46) was present in the biofilm communities at a one-day HRT and became dominant OTUs from zone two and three to six respectively. The Bacteroidetes classified OTU, *Lutaonella* (0), made up a large proportion of the biofilm communities at a one-day HRT, between 34 and 52% relative abundance. This OTU was present in the biofilm communities at a four-day HRT but to a far less of an extent. A *Chlorobium* OTU, *Chlorobium* (40), and a handful of non-Deltaproteobacteria OTUs, *Aquamicrobium* (26), Rhizobium (30) and *Halothiobacillus* (60) became abundant in the associated communities of zones five and six, at a one-day HRT.

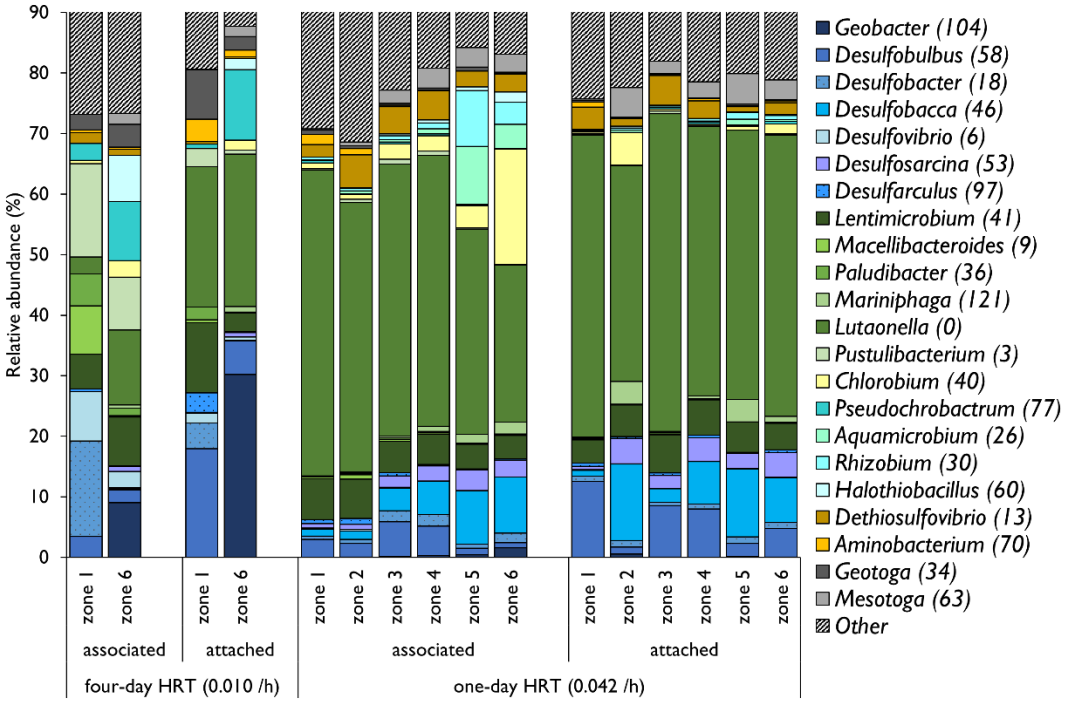


Figure 6-36 Relative abundance of the predominant OTUs within the attached- and associated-biofilm communities of the six sequential zones of the acetate-supplemented UAPBR at four- and one-day operated HRTs. The genus to which each OTU was classified is shown in the legend with OTU number shown in parentheses. The OTUs are colour shaded based on higher their higher taxonomic classifications: Deltaproteobacteria are shown in blue, Other Proteobacteria in turquoise, Bacteroidetes in green, Synergistales in yellow and other phyla in grey.

## 6.5 Acetate UAPBR Discussion

### 6.5.1 The sulphate reduction rate model

The acetate UAPBR sulphate reducing model described in Section 6.4.2 was used to predict the concentration of sulphate leaving each of the three zones of the acetate UAPBR at each tested HRT (Figure 6-37). The concentration of sulphate observed leaving the inlet and middle zones

were considered when predicting the concentration of sulphate that would leave the middle and effluent zone respectively. This model was able to predict 19 of the 24 data points to within 100 mg/ℓ (1.04 mM)sulphate and the maximum observed difference between observed and predicted was just 167 mg/ℓ (1.74 mM) sulphate. The greater deviations occurred at a four- and three-day HRT. These few points would be better described by differing reaction orders, *n*, and rate constants, *k*, than characterised for the entire reactor performance dataset. This may result from changes in the composition or cell concentration of these communities between the four- and three-day reactor communities, with more stable communities forming at a 2.6- to a one-day HRT.

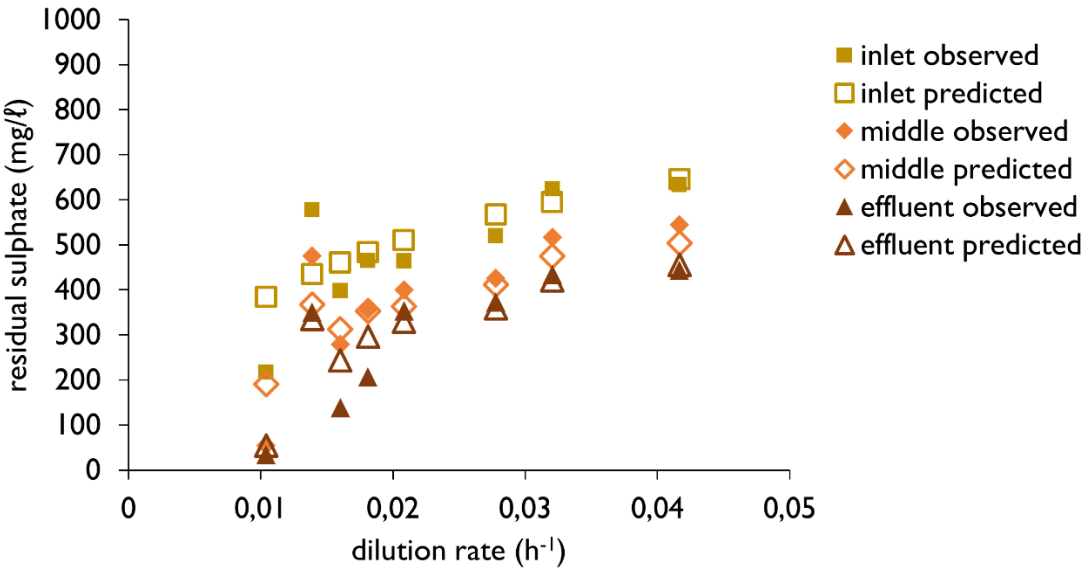


Figure 6-37 The observed and predicted residual sulphate concentrations leaving the inlet, middle and effluent zones of the acetate UAPBR at varying applied dilution rates. The predicted sulphate concentrations were predicted using the model described in Section 6.2.2. This model describes a spontaneous, irreversible chemical reaction in a plug-flow reactor with an order, n, of 2.9 and rate constant, k, of 1.5 x $10^{-7}$ $h^{-1}$. Predictions were made using the observed concentration of sulphate leaving the inlet zone as the initial sulphate concentration entering the middle zone, and the observed concentration leaving the middle zone as the initial concentration entering the effluent zone.

The maximum growth rate of acetate oxidising SRB are typically far lower than lactate-oxidising SRB (Section 2.4) – yet the inlet zone of the acetate UAPBR performed similarly to that of the lactate UAPBR. This is presumed to be a result of the decoupling of the biomass retention and hydraulic retention times, therefore allowing for high VSRR to be achieved.

The nearly third-order nature of this model indicates that the rate of sulphate reduction decreases exponentially with decreasing sulphate concentrations. This was illustrated in Figure 6-31A and that seen in the observed VSRR of the inlet, middle and effluent zones at multiple HRT (Figure

6-27). This observation is not consistent with kinetic studies in literature (Ingvorsen et al., 1984; Flaherty,1998; Moosa et al., 2002). Acetate-oxidising SRB have been shown to have a high affinity for both acetate and sulphate, with determined *Ks* values in the order of $10^{-2}$ g/ℓ for sulphate and for acetate. Moosa et al. (2002) characterised an acetate-oxidising SRB culture and found the maximum growth rate, the biomass yield per unit sulphate and per unit acetate, to vary little with initial sulphate concentration. However, the saturation constant, *Ks*, showed an increasing linear relationship with increasing initial sulphate concentrations. Therefore, according to Monod growth kinetics, the growth rate of an acetate consuming SRB culture should be close to *μmax* for sulphate concentrations much greater than *Ks*. This, therefore, implies a reaction order between zero and one, even at low sulphate concentration (approximately 10 mg/ℓ).

The characterised third-order of the acetate UPABR kinetic model is therefore unusual. A possible explanation to this observation may be that a compound in the reactor, which is in excess in the inlet zone, may become growth-limiting in successive zones in the reactor. This may include trace metals and/or nitrogen compounds included in the medium as yeast extract. The very high biomass retention in the system, particularly in zone one and two, followed by a rapid decrease in attached and associated cell concentrations from zone three to six would have supported this, however, a similar degree of biomass retention within the inlet zone was observed in lactate-supplemented UAPBR. The kinetic model describing the lactate UAPBR was characterised as a first-order reaction and the model was able to accurately predict the VSRR in zones receiving little sulphate. Many SRB are common to both the acetate- and lactate-supplemented UAPBRs (*Desulfobulbus* (27), *Desulfomicrobium* (1) and *Desulfovibrio* (6)) and therefore the nutrient requirements of these SRB are thought to be similar in both reactors. However, the nutrient requirements of the non-sulphate reducers in these reactors may differ substantially. The effect of a growth-limiting compound such as a trace metal or nitrogen species is, therefore, unlikely.

An alternative to this explanation is the mixotrophic SRB metabolic model first introduced in Chapter 4. The fermentation of yeast extract is postulated to lead to the generation of hydrogen. This is based largely on the widespread distribution of genes encoding the enzymes of the urea cycle co-occurring with hydrogen evolving hydrogenases within the majority of non-sulphate reducing microorganisms in the BSR reactor samples (Chapter 8). The acetate UAPBR kinetic model may be better described by using a rate equation which considers the concentration of sulphate and the concentration of hydrogen. This may account for higher reaction order. Evidence to support the occurrence of the metabolism described in the mixotrophic metabolic model is described in Chapter 8.

### 6.5.2 Reactor performance in the context of reported literature

The performance of the acetate-supplemented 1ℓ UAPBR and the 0.33 ℓ inlet zone of the UAPBR was compared with other studies reported in the literature (Figure 6-38). Dries et al. (1998) operated a sulphate reducing UASBR using acetic acid as the electron donor. This study was able to demonstrate remarkably high VSRRs (>150 mg/ℓ.h) at very short HRT. This reactor was inoculated with a highly concentrated sludge and operated continuously for a short period of time. So, although the degree of biomass retention observed in this study may have not been sustained long-term, this does indicate possible rates in well-performing acetate-supplemented BSR reactor configurations.

The UAPBR of this study performed similarly to the down-flow packed bed reactors (DPBRs) operated by Lin and Lee (2001). These authors operated a DPBR packed with plastic ballast rings and supplemented with acetate at a 60-hour HRT. This reactor achieved a VSRR of 13 mg/ℓ.h and a sulphate conversion of 87% of the 0.9 g/ℓ sulphate. Tsukamoto and Miller (1999) used a similar reactor configuration and sulphate concentration but packed with sand and supplemented instead with methanol, which allowed this reactor to achieve a sulphate conversion of 53% at a 6.6-hour HRT. This corresponded to a VSRR of 72 mg/ℓ.h.

The kinetic model developed to explain the data collected from the acetate-supplemented UAPBR of this study predicts that a flow rate to volume ratio of 0.617 would be required , with a starting concentration of 1 g/ℓ sulphate, to achieve a VSRR of 72 mg/ℓ.h in this reactor. This corresponds to an HRT of 1.6 hours and a sulphate conversion of just 12%. Similar VSRR and sulphate conversion were reported by (Omil et al., 1997). These authors operated a UASB with sulphate concentrations between 1 – 4 g/ℓ sulphate and applied short HRT of under 12 hours. This UASB was able to achieve VSRR of over 60 mg/ℓ.h but a sulphate conversion of approximately 20%. This UASB was also operated for a short period of time (approximately 200 days) and, therefore, the long-term performance of this reactor is not certain.

The UAPBR of this study out-performed the acetate-supplemented anaerobic filter reactor (AFR) operated by El Bayoumy et al. (1999b). These authors operated this reactor configuration using a starting sulphate concentration of 2.5 g/ℓ and an HRT of 20 hours. However, the relatively poor sulphate reducing performance of this reactor was likely a consequence of the elevated metal concentrations present in the medium.

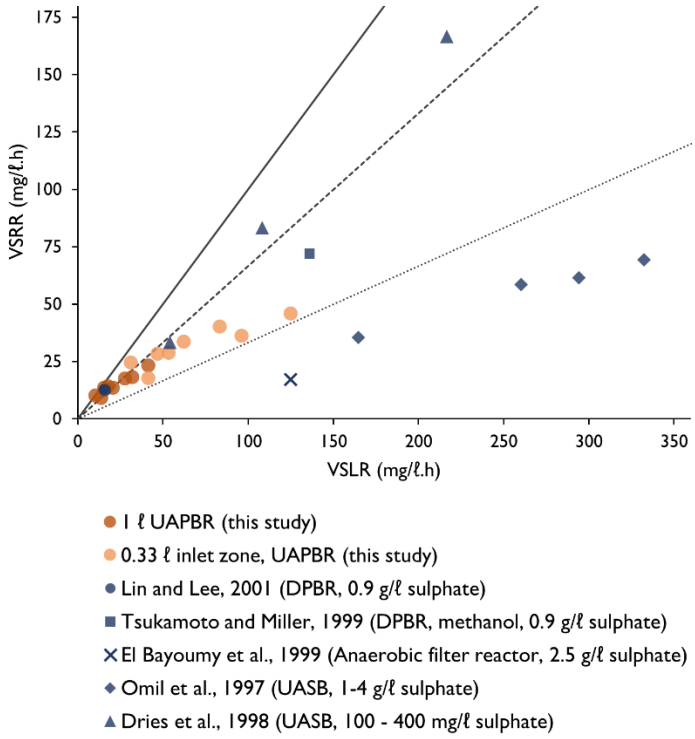


Figure 6-38 The volumetric sulphate reduction rate (VSRR) achieved by the lactate-supplemented 1ℓ UAPBR of this study, 0.33 ℓ inlet zone of the UAPBR of this study and selected continuous reactor studies from literature, at varied volumetric sulphate loading rates (VSLR) as shown in the legend. Sulphate conversion can be visually be determined through comparisons with lines plotted: 100% conversion – solid line, 66% conversion – dashed line, 33% conversion – dotted line. Details of the selected case studies are included in the figure including the sulphate concentration, carrier material, electron donor if not acetate and reactor configuration. These reactor studies were selected as these had similar starting sulphate concentrations and hydraulic retention times to those used in this study.

### 6.5.3 Sulphate reduction linked predominantly to acetate oxidation

The observed degree of sulphate reduction was used to predict the acetate concentration (Figure 6-39) leaving the inlet zone of the UAPBR, according to Equation 2-7. The predicted acetate concentration was consistently lower than that observed by, on average, 5.5 mM acetate. The concentration of acetate concluded to be generated from the oxidation of yeast extract, namely 4.5 mM, was then included in the predicted acetate concentration. This predicted acetate and the observed acetate concentration leaving the inlet zone differed by less than 10% that of the observed acetate concentrations.

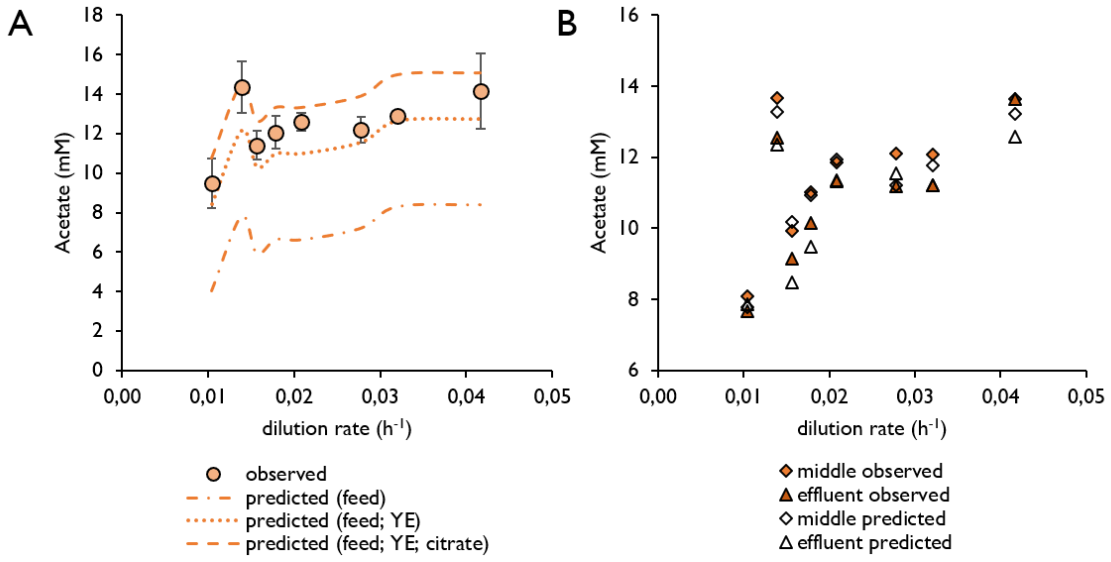


Figure 6-39 The observed and predicted acetate concentrations in the (A) inlet and (B) middle and effluent zones of the acetate-supplemented UAPBR at multiple dilution rates. Predicted acetate concentrations in the inlet zone are based on the reduction of sulphate linked to acetate oxidation as described by Equation 2-7. No oxidation of acetate by non-SRB was assumed to be taking place. The starting acetate concentration of 12 mM ('feed') and considering the generation of 4.45 mM acetate from yeast extract oxidation ('feed, YE') and from the oxidation of 1.16 mM citrate ('feed, YE, citrate').

The predicted acetate concentrations leaving the middle and effluent zones (Figure 6-39) were based on the observed sulphate reduction which was presumed to be linked to acetate oxidation (Equation 2-7). These calculations were performed using the observed acetate and sulphate concentrations entering and the sulphate concentrations leaving each zone. The predicted and observed values differed by an average and a maximum of 2.2 and 7.7% of the predicted acetate concentration. This degree of accuracy indicates little to no acetate generation from yeast extract oxidation occurred in these zones. The agreement between the predicted and observed acetate concentrations indicates that sulphate reduction in this reactor is largely associated with acetate oxidation. However, this agreement also suggests that all observed acetate oxidation was linked to sulphate reduction. The source of carbon that supports the presence of non-SRB, which make up the majority of each assessed microbial community, is therefore not accounted for. It is possible that non-SRB are performing yeast extract and citrate oxidation within the inlet zone, but there is no evidence of these reactions throughout the rest of the reactor. Genome-resolved metagenomics revealed that few non-SRB possessed genes for autotrophy and hydrogen consumption. It can, therefore, be concluded that the non-SRBs within the acetate-UAPBRs are likely heterotrophs.

It is therefore concluded that these non-SRB too are using acetate as an electron donor, as this was the only form of organic carbon available in the middle and effluent zones. Therefore Equation 2-7 can account for only a portion of the acetate consumed, and therefore only a portion of the

sulphate reduced. It is proposed that hydrogen generated from yeast extract oxidation provides the additional electrons required for the observed sulphate reduction. Further metagenomic evidence to support this model is described below.

The observed concentration of produced bicarbonate leaving the effluent of the acetate UAPBR is also in agreement with the predicted bicarbonate concentration based on all sulphate reduction being linked to acetate oxidation according to Equation 2-7 (Figure 6-40). This, however, does not account for bicarbonate produced from the oxidation of yeast extract nor citrate and does not account for any bicarbonate which would be generated by non-SRB. The non-SRB make up more than 50% relative abundance of every acetate UAPBR community. iRep values determined for genomes present in the BSR reactor systems at a four-day HRT (Chapter 8 ) demonstrated that the planktonic and biofilm communities, even in the effluent of the reactor were actively dividing. The changing proportions of the planktonic microbial communities throughout the zones of the UAPBR at multiple HRT (Figure 6-411, discussed below) indicate that these planktonic communities are active, even in the effluent zone of the reactor. Given that these non-SRB are active and predominantly heterotrophs, and must be generating bicarbonate, the assumption that all sulphate reduction is linked to acetate oxidation via Equation 2-7 must be false. The deficit of bicarbonate in this reactor provides additional evidence for the BSR mixotrophic metabolic model. The deficit of bicarbonate, therefore, indicates that bicarbonate being produced in the reactor, by non-SRB, may be subsequently fixed via autotrophy into biomass.

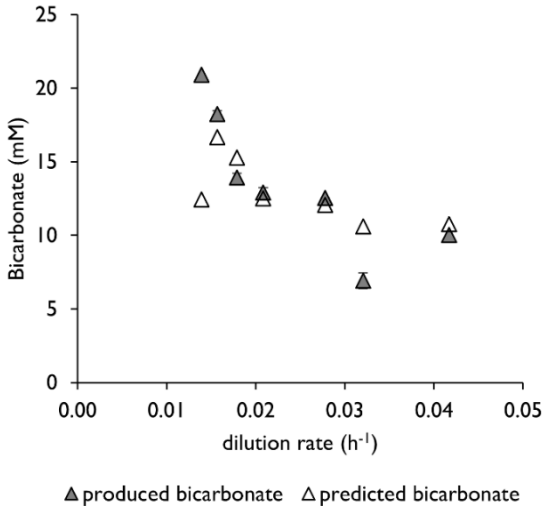


Figure 6-40 The observed and predicted produced bicarbonate concentrations leaving the effluent of the acetates-supplemented UAPBR at range of tested dilution rates. Predicted bicarbonate concentrations were estimated using the observed degree of sulphate reduction according to Equation 2-7 of sulphate reduction linked to acetate oxidation. Bicarbonate produced from the oxidation of yeast extract, citrate or oxidation of acetate by non-SRB is not considered.

### 6.5.4 Comparisons of the planktonic and biofilm microbial communities

The reduced abundance of Firmicutes between the inlet and effluent zones of the UAPBR (Figure 6-33) indicates that plug flow does not carry the planktonic community, regardless of its activity, throughout the column. Instead, the decreased abundance of Firmicutes indicates that the community which persists within the middle and effluent zones is active. This is reaffirmed by activity from iRep values determined for these planktonic communities from whole genome sequencing and analysis (Section 8.4).

The predominant SRB within the planktonic communities of the acetate supplemented UAPBR, *Desulfovibrio* (6) and *Desulfomicrobium* (1) showed little change in abundance between the inlet and effluent zones (Figure 6-41), indicating sustained activity. On the whole, most of the abundant OTUs in the planktonic communities do not vary greatly between these two zones – contrasting to the changes seen in the lactate UAPBR planktonic communities (Figure 6-22). However, a Firmicute OTU, *Halothiobacillus* (60) saw a more than eight-fold increase (3 log2 fold change) between the inlet and effluent zone. Zhou et al. (2015) identified a *Halothiobacillus* within a formate-supplemented haloalkaliphilic sulphate reducing bioreactor. This genus is implicated in sulphide oxidation and autotrophy (Beller et al., 2006; Shi et al., 2011). In contrast, the Proteobacteria, *Thauera* (106), a selenite reducing microorganism (Schröder et al., 1997), decreased in abundance 32-fold (5 log2 fold) between these two zones, suggesting primarily citrate and/or yeast extract fermentation.

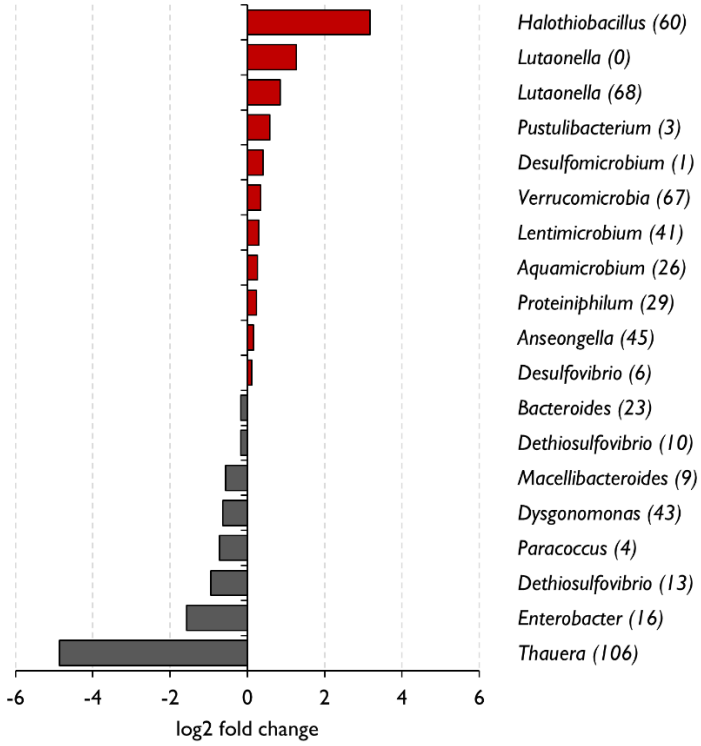


Figure 6-41 Log2 fold change of the predominant OTUs, in the lactate UAPBR planktonic communities, between the inlet and the effluent zones. OTUs which show a reduced abundance are shown in red, while those increasing in abundance are shown in grey.

Hierarchical clustering resolved the microbial communities based on the abundance of the predominating OTUs across each assessed acetate UAPBR community into two all-encompassing clusters (Figure 6-42). All attached and associated biofilm communities from a one-day HRT, together with the four-day attached and associated community of zone 6 and the four-day HRT attached community of zone 1, into a single cluster. All of these samples were dominated by *Lutaonella* (0), *Desulfobulbus* (58), *Lentimirobium* (41) and *Dethiosulfovibrio* (13). Other SRB OTUs which were common to these communities included *Desulfarculus* (97), *Desulfobacter* (18), *Desulfobacca* (46), *Desulfosarcina* (53) and *Desulfovibrio* (95). The planktonic communities, together with the associated community of zone 1 at a four-day HRT, formed a separate cluster. The planktonic samples clustered into further smaller clusters on the basis of tested HRT, indicating gradual changes in the composition of these communities as the HRT was reduced. *Desulfovibrio* (6) was one of the OTUs to be washed out of this reactor at reduced HRT. Other SRB belonging to this group of OTUs was a *Desulfobacter* OTU (18) and *Desulfomicrobium* (1) which becomes dominant at a two-day HRT. It is the absence of predominant SRB in the planktonic community of the acetate UAPBR which is thought to account for the decreased sulphate conversions at reduced HRT.

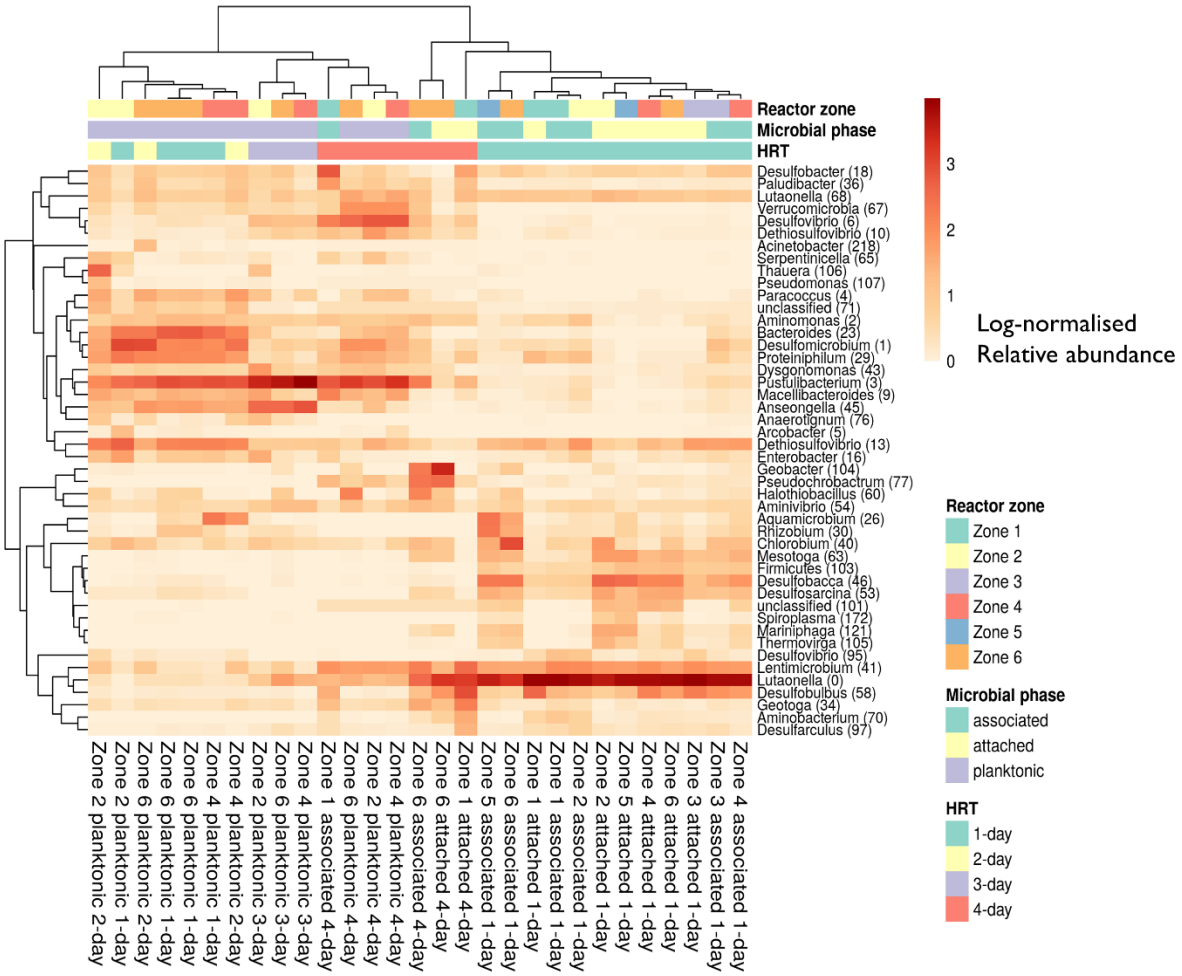


Figure 6-42 Hierarchical clustering of the relative abundances of the dominant OTUs in planktonic, associated and attached communities isolated from the six 0.167 ℓ zones of the acetate-supplemented UAPBR reactor zones, at hydraulic retention times of one-, two-, three- and four-days. Relative abundances were ln(x +1) transformed and hierarchical clustering was performed using correlation distance and average linkage (Section 3.9). No row centring was performed. The reactor zone from which each sample was isolated, the microbial phase and the HRT at which the sample was recovered is shown above the heatmap and the legend shown on the right of the heatmap.

## 6.6 Conclusion

The acetate- and lactate-supplemented UAPBRs described in this chapter showed literature competitive sulphate reducing performance at a range of HRTs.

### Acetate UAPBR

The acetate UAPBR demonstrated a maximum VSRR of 23 mg/ℓ.h at a one-day HRT. This corresponded to a sulphate conversion of 56%. The inlet zone of this reactor exhibited a maximum VSRR of 46 mg/ℓ.h at a one-day HRT, corresponding a sulphate conversion of 37%. The sulphate reduction rate data collected from the three zones of the acetate-supplemented UAPBR were

used to model the rate of sulphate reduction across the reactor at a range of HRT. This found that the rate of sulphate reduction in this reactor could be modelled as an irreversible 2.9$^{th}$ order reaction, with rate constant, k, of 1.5 x $10^{-7}$ $mg^{-1,9}\ell^{1,9}h^{-1}$ within an ideal plug flow reactor.

The dramatic decrease in the rate of sulphate reduction at decreasing concentrations of sulphate, as evident in the reaction order of 2.9, is thought to be the result of the consumption of a rate-limiting substance, predominantly, in the inlet zone of the reactor.

Evidence that sulphate reduction was linked to electron donors other than acetate was seen in the agreement in the observed and predicted acetate and bicarbonate concentrations in the middle and effluent zones. These predictions were based on the observed degree of sulphate reduction being solely linked to acetate oxidation. The considerable retention of non-SRB in these microbial communities indicates that the substrate consumption by these non-SRBs is not negligible. Instead, these microorganisms likely perform acetate oxidation in the middle and effluent zones. It is therefore concluded that the SRB in these reactors are likely consuming acetate and hydrogen generated by the fermentation of yeast extract constituents in the inlet zone. The rate of reaction, dependent on the concentration of both sulphate and hydrogen would potentially account for the increased reaction order.

The performance of the acetate-supplemented UAPBR is largely attributed to the degree of biomass retention within this system. The biofilm attached and associated communities of the inlet zone's zone 1 was 9.0 x $10^9$ cells/mℓ and 3.5 x $10^9$ cells/mℓ respectively, at a one-day HRT, whereas the planktonic cell concentration in the inlet zone at this HRT was just 2.6 x $10^8$ cells/mℓ. The biofilm attached cell concentration decreased approximately three-fold by zone two and reached a cell concentration of 7.2 x $10^8$ cells/mℓ in zone three, where it stayed relatively constant throughout the rest of the reactor.

These attached and associated communities, at a one-day HRT, were dominated by the Bacteroidetes OTU, *Lutaonella* (0). Notable SRB identified in these biofilm communities include *Desulfobulbus* (58) present in zones 1 to 4, and *Desulfobacca* (46), *Desulfosarcina* (53) present in these communities in zones 2 to 6. The planktonic communities of this reactor were dominated by the Bacteroidetes OTU *Pustulibacterium* (3) at each tested HRT. *Desulfomicrobium* (1) and *Desulfovibrio* (6) were the dominant SRB in these communities but decrease in abundance between a four- and three-day HRT. This corresponded to poor reactor performance at the three-day HRT and is concluded to result from the reduction of these OTUs due to washout. Unlike *Desulfomicrium* (1), the abundance of *Desulfovibrio* (6) does not recover at subsequent HRT - a phenomenon observed in many reactors discussed in this thesis.

**Lactate UAPBR**

The lactate UAPBR demonstrated a maximum VSRR of 40 mg/ℓ.h at a one-day HRT. This corresponded to a sulphate conversion of 96%. The inlet zone of this reactor exhibited a maximum VSRR of 54 mg/ℓ.h at a one-day HRT, corresponding a sulphate conversion of 54%. The sulphate reduction rate data collected from the three zones of the acetate-supplemented UAPBR was used to model the rate of sulphate reduction across the reactor at a range of HRT. This found that the rate of sulphate reduction in this reactor could be modelled as an irreversible first-order reaction, with rate constant, *k*, of 0.06955 $h^{-1}$ within an ideal plug flow reactor.

Sulphate reduction linked to lactate oxidation was largely restricted to the inlet zone of this reactor, with an estimated 75% of the 1.2 g/ℓ feed lactate linked to sulphate reduction. This was higher than observed in the lactate CSTR and is postulated to result from the lower sulphide concentrations present at the inlet of this reactor, compared to the bulk liquid of the CSTR, or the immobilisation of lactate fermenters within the biofilm communities of the inlet zone leading to higher biomass concentrations.

The sulphate reduced within the middle and effluent zone was concluded to be linked predominantly to propionate oxidation in the middle zone, and an equal combination of acetate and propionate oxidation in the effluent zone.

As concluded for the acetate-supplemented UAPBR, the performance of the lactate-supplemented UAPBR is largely attributed to the levels of biomass retention provided through the incorporation of polyurethane foam packing. The concentration of planktonic cells in this reactor was approximately $2 \times 10^8$ cells/mℓ. The attached cell concentrations of zone 1, at a one-day HRT, was $2.2 \times 10^{10}$ mℓ.

The SRB present in the biofilm communities changed considerably between the inlet and effluent of the reactor. *Desulfovibrio* (6) and *Desulfomicrobium* (1) were highly abundant in the inlet zone, *Desulfobulbus* (27) was the predominant SRB in the middle zone, *Desulfatiglans* (91) was dominant in the effluent zone and *Desulfobacter* (18) and *Desulfacarina* (53) were present in both the middle and effluent zones. It is possible therefore to link these SRB to the oxidation of particular electron donors due to the localisation of lactate in the inlet zone, propionate oxidation primarily occurring in the middle zone and a combination of acetate and propionate oxidation in the effluent zone. The predominant non-SRB present in the biofilm communities from the inlet to the effluent of the reactor was the Bacteroidetes OTU *Lutaonella* (0).

This Bacteroidetes OTU was implicated in acetate and/or propionate oxidation in the planktonic communities of this reactor, due to its increase in abundance in the planktonic community between the inlet and the effluent of the reactor. Inversely, a *Veillonella* (11) and an *Aeromonas* (38)

OTU showed a decreased abundance between these zones and are therefore concluded to be the major competitors with SRB for lactate in these planktonic communities. The abundance of the planktonic SRB, *Desulfomicrobium* (1) and *Desulfovibrio* (6) did not vary considerably between these two zones and therefore were likely consuming lactate in the inlet zone and acetate and/or propionate in the middle and effluent zones.

# Chapter 7 Integration of the microbial ecology and reactor performance

## 7.1 Introduction

While the microbial ecology within each of the six BSR reactor of this study are described independently in Chapters four to seven, this chapter aims to compare microbial ecology across these reactor systems. The BSR reactors are compared based on the observed diversity and the distribution of individual microorganisms across the six reactor systems. The distribution of SRB across all reactor samples and reactor environments is subsequently compared and related to the exhibited performance of the six BSR reactors towards the end of the chapter.

## 7.2 Results and Discussion

### 7.2.1 Alpha diversity and OTU richness

The samples analysed in this investigation include all planktonic, biofilm-associated and biofilm-attached assessed using 16S rRNA gene amplicon sequencings from each of the six reactor systems, across the HRT study. The mean and median read count per sample was approximately 29 000 and 30 600 respectively with a minimum goods coverage of 0.996 indicating adequate sampling depth had been reached to detect the vast majority of OTUs in these samples. The diversity of the microbial communities isolated from each of the six BSR reactors, over the course of the HRT study, were evaluated using Shannon indices (Hutcheson, 1970) and are summarised in Figure 7-1. Shannon indices are an ecological measure of diversity and are calculated considering both the number of OTUs detected and the evenness of the distribution in abundance between these organisms.

The mean and median Shannon indices for the microbial communities within each of the six BSR reactor were similar, between 3.5 and 4.5 (Figure 7-1A). These represent reasonably simple microbial communities compared to, for example, highly diverse soil microbial communities which are often described by Shannon indices greater than 10.0 (Lei et al., 2019). The mean and median OTU count within the acetate-supplemented CSTR was the lowest observed in the acetate reactors with the UAPBR displaying the highest (Figure 7-1B). The lactate-supplemented UAPBR showed a similar distribution of supported OTUs in its microbial communities compared to that of the acetate reactors. However, the mean and median OTU count for the lactate-supplemented

CSTR and LFCR were considerably lower than the other four BSR reactors, at approximately 170 OTUs. Lactate was the predominant electron donor within these two reactors, with little subsequent acetate oxidation. This suggests that lactate supports fewer OTUs than acetate, possibly due to the greater-supported growth rates and increased competition for this substrate.

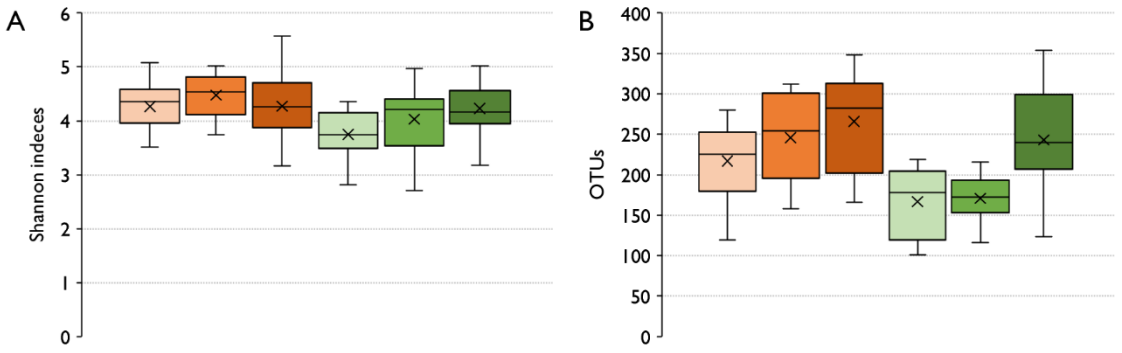


Figure 7-1 Box and whisker plots of the (A) Alpha diversity, represented as Shannon indices, and (B) OTU richness of the microbial communities isolated from the acetate-supplemented (■) CSTR, (■) LFCR and (■) UAPBR and the lactate-supplemented (■) CSTR, (■) LFCR and (■) UAPBR. The top and bottom of each box represent the 75th and 25th quartiles respectively. The mean within each reactor is shown as a cross.

The acetate CSTR, over the course of HRT study, supported a total of 528 unique OTUs, whilst the acetate supplemented LFCR and UAPBR supported 901 and 1129 OTUs, respectively. A similar observation was made for the number of OTUs supported within the lactate-supplemented reactor configurations, with the CSTR supporting 535 OTUs whilst the LFCR and UAPBR supported 638 and 1207 OTUs, respectively. The increased number of OTUs supported by LFCRs over the CSTRs is explained by the increased physiochemical environments provided through both the planktonic and biofilm environments. The increased number of OTUs supported by the UAPBRs over the LFCRs is similarly explained by the increased physiochemical environments generated in the UABPRs a result of plug-flow in these systems.

### 7.2.2 Variation within individual communities

The variation in the microbial composition within individual communities was assessed by performing gene amplicon sequencing on duplicate metagenomic DNA samples isolated from the acetate- and lactate-supplemented CSTR (Figure 7-2), LFCR (Figure 7-3) and UAPBR (Figure 7-4) reactor communities, simultaneously.

Variation in the abundance of individual OTUs was low, particularly within planktonic samples. Little variation between planktonic communities in the CSTRs and LFCRs (Figure 7-2 and Figure

7-3) were expected because of the degree of mixing within these systems. The similarity in planktonic samples simply indicates that the two samples were representative of the individual planktonic communities. The variation that was observed occurred in the biofilm-associated and attached microbial communities of the acetate and lactate supplemented LFCRs (Figure 7-3). However, within these samples, the variation occurred within only a handful of OTUs. This indicates that the communities within these reactors are largely stable and formed through deterministic factors, but antagonistic effects or simply competition between a few dominant microorganisms led to observed differences in the microbial community. The consistency in the composition of these biofilm communities and the differences in only a handful of OTUs may indicate social interactions are leading to spatial developments within these biofilms (Nadell et al., 2016). Considering this variation involves the SRB *Desulfomicrobium* (1), this warrants further investigation using tools such as fluorescent *in situ* hybridisation.

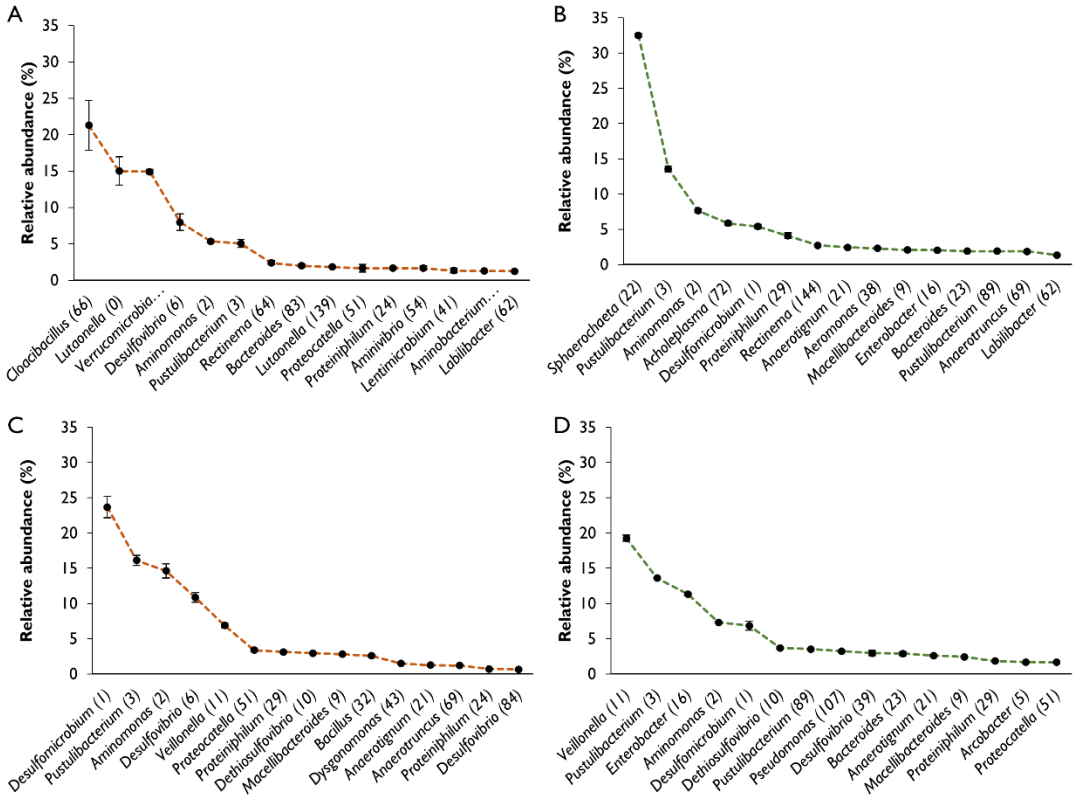


Figure 7-2 Rank abundance curves of the planktonic microbial communities isolated from the (A, C) acetate- and (B, D) lactate-supplemented CSTRs at a (A, B) four- and (C, D) one-day HRT, in duplicate. Error bars represent one standard deviation from the mean.

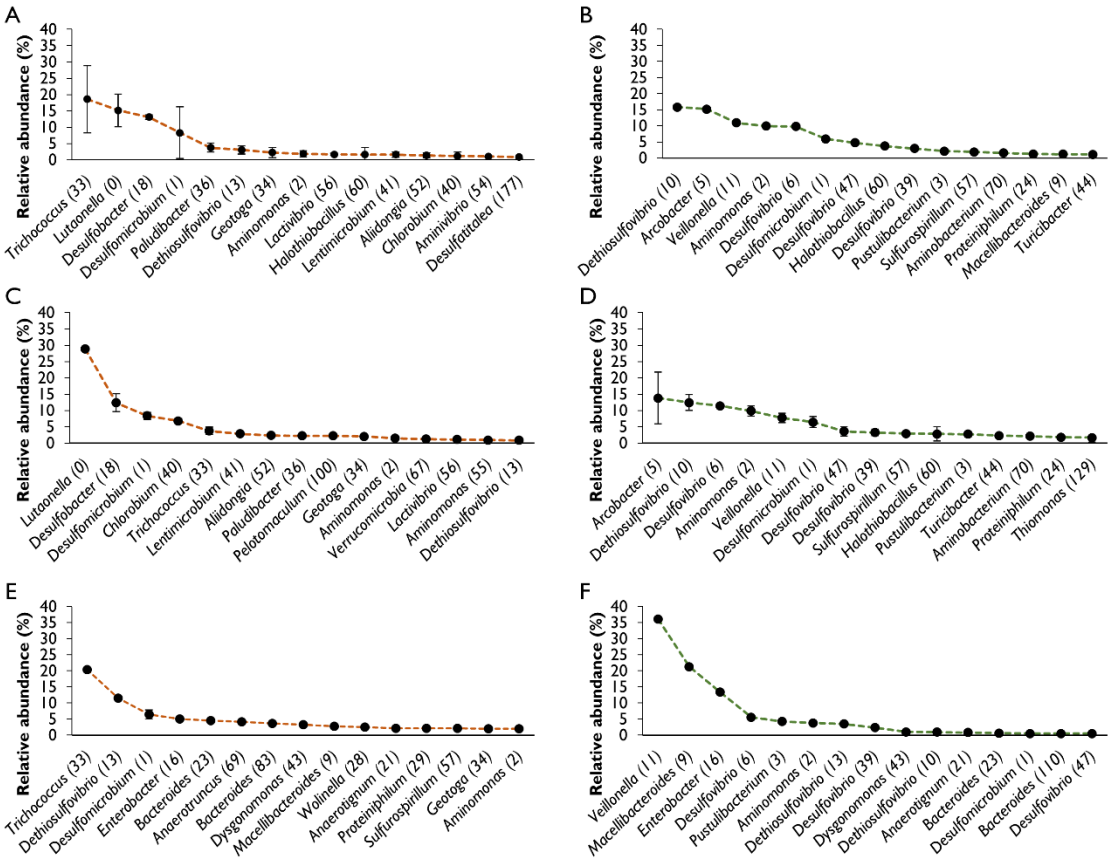


Figure 7-3 Rank abundance curves of the (A, B) biofilm-associated, (C, D) biofilm attached and (E, F) planktonic microbial communities isolated from the (A, C, E) acetate- and (B, D, F) lactate-supplemented LFCRs at a one-day HRT, in duplicate. Error bars represent one standard deviation from the mean.

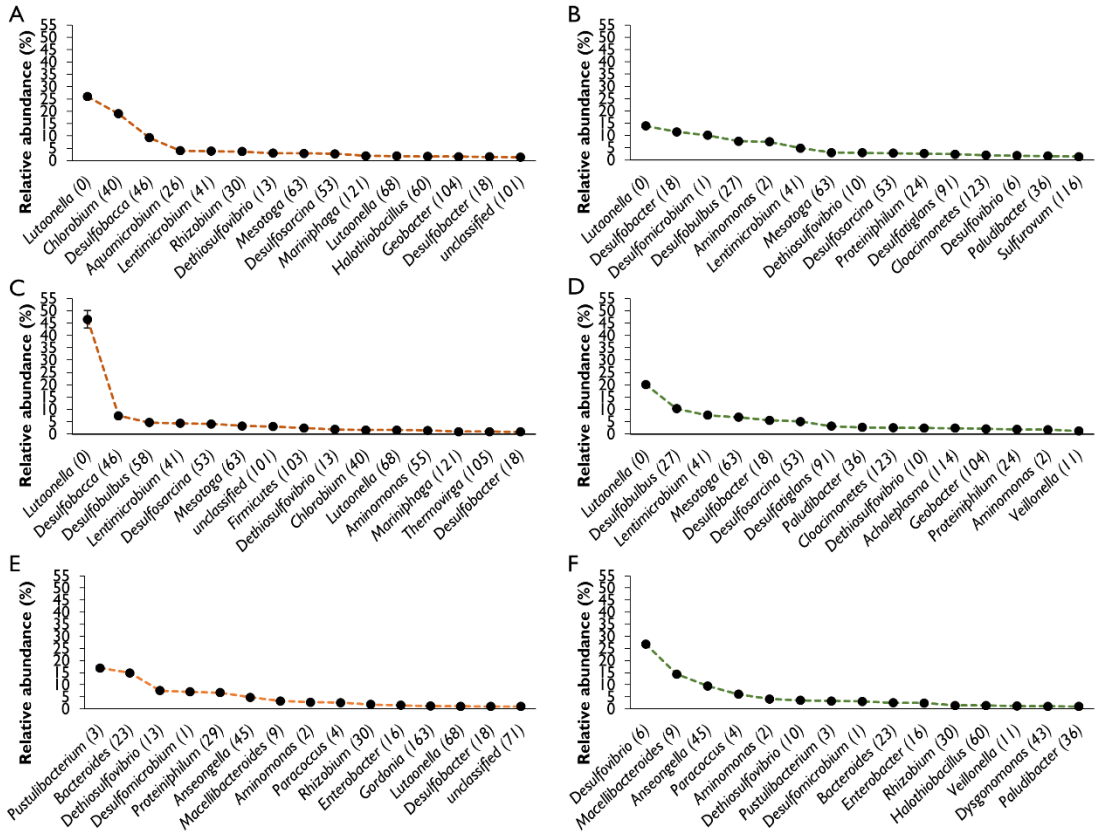


Figure 7-4 Rank abundance curves of the (A, B) biofilm-associated, (C, D) biofilm attached and (E, F) planktonic microbial communities isolated from the effluent zones of the (A, C, E) acetate- and (B, D, F) lactate-supplemented UAPBR at a one-day HRT, in duplicate. Error bars represent one standard deviation from the mean.

### 7.2.3 Distribution of frequently occurring OTUs between prevailing reactor environments

Many observations were made in Chapters four to six relating to the apparent preferential conditions for the growth of particular microorganisms. These included the apparent affinity of *Veillonella* (11) for lactate and the enrichment of *Lutaonella* (0) in biofilm communities. To provide stronger evidence for these conclusions, the abundances of OTUs when present under a specific environmental condition were compared against when these OTUs were present but the environmental condition was not prevailing. A relative abundance cut-off of 0.01% was used to determine whether an OTU was present in a sample.

The first condition tested was the enrichment of OTUs in microbial communities were lactate oxidation was prevalent, versus communities where only acetate and/or propionate oxidation was taking place. The SRB OTU *Desulfomicrobium* (1) was found to be significantly enriched in reactor environments were lactate oxidation was occurring (Figure 7-5). This SRB OTU was found at a

median abundance of about15% in lactate oxidising samples, compared to a median abundance of less than 5% in communities where only acetate and or propionate oxidation was occurring. However, there were instances when this OTU achieved above 15% relative abundance in acetate/propionate oxidising reactor zones indicating this OTU's propensity for multiple electron donors. The other frequently occurring SRB OTU, *Desulfovibrio* (6), was found to be similarly abundant in both reactor zones where lactate and where acetate/propionate oxidation was taking place. The distribution of other identified SRB OTUs are further described in Section 7.2.4.

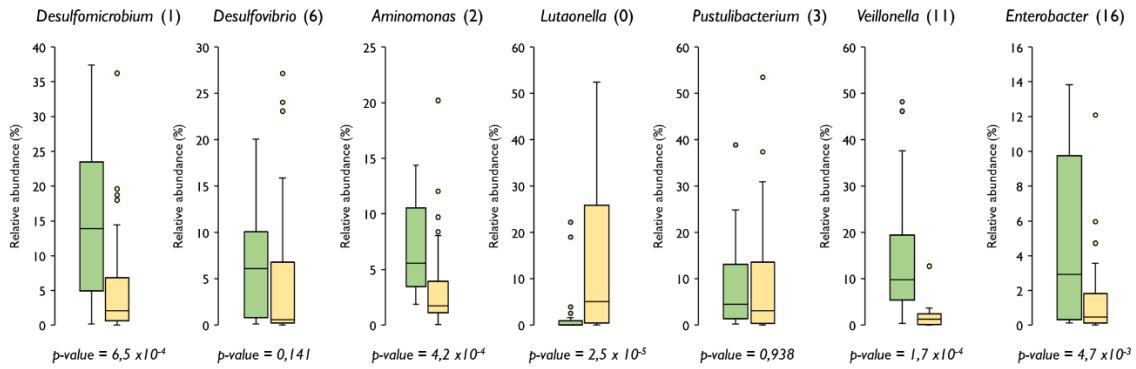


Figure 7-5 The relative abundance of frequently occurring OTUs across the six reactor systems present in microbial communities where lactate oxidation (Green) occurs, and in zones where propionate and/or acetate oxidation occurs in the absence of lactate oxidation (Yellow). A cut-off of 0.1% relative abundance was used to determine whether an OTU was 'present' in a sample. The data are presented as box plots representing the four interquartile ranges. The minimum and maximum of each box plot were calculated by multiplying the interquartile range by 1.5. Two-tailed Student t-tests, assuming unequal variance (Welch's test), were used to determine statistical significance. Refer to Table 7-1 for the number of times an OTU was present under a specific environmental condition.

Several other frequently occurring non-SRB OTUs were shown to be enriched in reactor zones where lactate oxidation was occurring (Figure 7-5). These included the Synergistales classified *Aminomonas* (2), the Proteobacteria *Enterobacter* (16) and the highly abundant and frequently occurring *Veillonella* (11) OTU. This provides strong evidence that these OTUs are competing with SRB for lactate. These OTUs were also present, at far lower abundances, in zones where no lactate oxidation was taking place. The presence of these microorganisms in these environments indicates that these microorganisms can effectively compete with other microorganisms for substrates other than lactate but are adept at competing for lactate.

Two Bacteroidetes OTUs, namely *Pustulibacterium* (3) and *Lutaonella* (0) were also investigated for their propensity for differing reactor environments. *Pustulibacterium* (3) was equally prevalent in both lactate and non-lactate oxidising environments. This may indicate the ability of this Bacteroidetes to effectively compete for multiple substrates or that it is sourced substrates common to both environments, such as amino acids in the yeast extract or citrate and/or. In contrast, *Lutaonella* (0) was highly enriched in zones where no lactate oxidation was determined

to have occurred but acetate and/or propionate were found. It was present within these zones with a high frequency (Table 7-1) – indicating that this OTU likely performs acetate oxidation.

This *Lutaonella* (0) OTU was also highly enriched in biofilm environments compared to planktonic environments (Figure 7-6). This *Lutaonella*, when appearing in a biofilm community, had a median abundance of 25% and a maximum observed abundance of 55%. This OTU, under acetate-limiting conditions, may compete with SRB for acetate. However, the acetate concentration present in the effluent of each of these reactors was high - largely owing to acetate generation from yeast extract oxidation. This Bacteroidetes OTU may be desirable for the removal of acetate from the effluent of the reactor – a frequent problem little addressed in BSR reactor literature (Widdel, 1988; Harada et al., 1994). *Paracoccus* (4) was another OTU which showed enrichment in communities were acetate oxidation was prominent. *Paracoccus* (4) was identified in a total of 40 communities, 37 of these communities were identified in zones without lactate oxidation and 33 of these were planktonic communities. *Paracoccus* (4), like *Lutaonella* (0), may be an OTU beneficial for the removal of COD from the reactor without substantially hindering reactor performance.

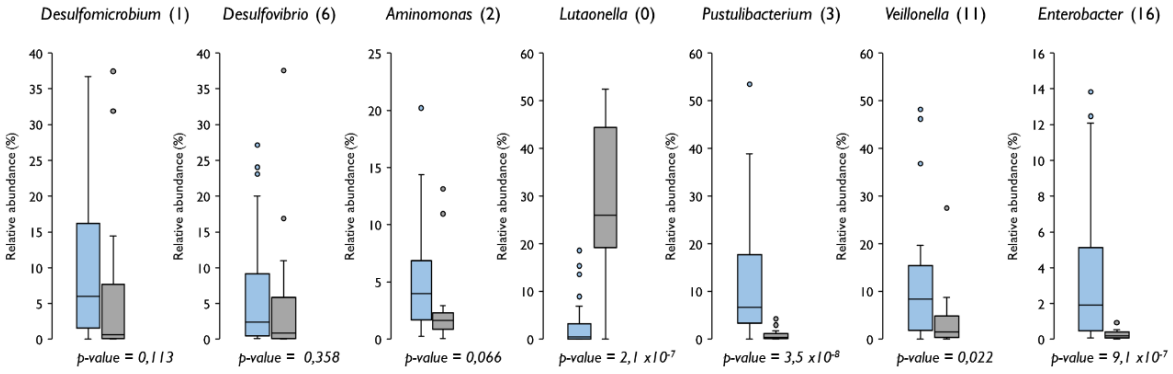


Figure 7-6 The relative abundance of frequently occurring OTUs across the six reactor systems present in planktonic microbial communities (Blue) and in biofilm attached communities (Grey). A cut-off of 0.1% relative abundance was used to determine whether an OTU was 'present' in a sample. The data are presented as box plots representing the four interquartile ranges. The minimum and maximum of each box plot were calculated by multiplying the interquartile range by 1.5. Outliers are shown as points. Two-tailed Student t-tests, assuming unequal variance (Welch's test), were used to determine statistical significance. Refer to Table 7-1 for the number of times an OTU was present under a specific environmental condition.

Abundant and frequently occurring OTUs which were enriched in planktonic environments, over biofilm communities, included *Pustulibacterium* (3), *Enterobacter* (16) and *Veillonella* (11). As previously stated, *Veillonella* (11) and *Enterobacter* (16) are likely the predominant competitors with SRB for lactate. The propensity of these OTUs for the planktonic phase indicates that oxidation of lactate by SRB could be further favoured by decreasing the proportion of total planktonic cells of the total microbial biomass within a BSR reactor.

The SRB OTUs *Desulfomicrobium* (1) and *Desulfovibrio* (6) were not enriched in planktonic nor biofilm communities. These OTUs did, however, have a higher median abundance in planktonic communities, indicating these SRB OTUs were more likely to become dominant in planktonic environments. These SRB are therefore dynamic, being able to thrive in both planktonic and biofilm environments and sustain competitive growth rates on various electron donors. *Aminomonas* (2), too, did not show enrichment in either planktonic nor biofilm communities but similarly showing a greater median abundance in planktonic communities (Figure 7-6 and Table 7-1).

Table 7-1 The frequency of the occurrence of OTUs present within the microbial communities of the six BSR reactor configurations at various HRT, including the SRB *Desulfomicrobium* (1) and *Desulfovibrio* (6). A relative abundance cut-off of 0.1 % was used to determine whether an OTU was present within a sample. The total number of times an OTU was present is shown in the furthest left column of the table. The number of times an OTU was present under differing reactor conditions are shown. These include zones where the determined predominant electron donors are lactate (Lactate), or either acetate and/or propionate Acetate or Propionate), planktonic environments and Biofilm environments. The number of samples analysed, falling within each category are shown in parentheses in each column heading.

| | Total observations (74) | Acetate or Propionate (50) | Lactate (24) | Biofilm (24) | Planktonic (50) |
|---|---|---|---|---|---|
| *Lutaonella (0)* | 73 | 50 | 23 | 24 | 49 |
| *Desulfomicrobium (1)* | 73 | 49 | 24 | 23 | 50 |
| *Aminomonas (2)* | 74 | 50 | 24 | 24 | 50 |
| *Pustulibacterium (3)* | 74 | 50 | 24 | 24 | 50 |
| *Paracoccus (4)* | 40 | 36 | 4 | 7 | 33 |
| *Arcobacter (5)* | 64 | 40 | 24 | 17 | 47 |
| *Desulfovibrio (6)* | 74 | 50 | 24 | 24 | 50 |
| *Macellibacteroides (9)* | 73 | 49 | 24 | 23 | 50 |
| *Dethiosulfovibrio (10)* | 74 | 50 | 24 | 24 | 50 |
| *Veillonella (11)* | 41 | 17 | 24 | 13 | 28 |
| *Enterobacter (16)* | 72 | 48 | 24 | 23 | 49 |

### 7.2.4 Distribution of SRB across reactor environments and implications for reactor performance

Most of the identified SRB could not be included in the statistical analyses of Section 7.2.3 because many of the identified SRB occurred in few samples. This section examines the precise location of each of the identified SRB. The distribution of these SRB is related to the exhibited performance of each of the tested BSR reactors.

All of the SRB which were identified in the acetate planktonic environments were also present in biofilms where acetate/propionate oxidation was prominent (Figure 7-7). This was true also of SRB in lactate planktonic samples and biofilm samples. The total SRB diversity was therefore held

within the biofilms in these reactors. A number of SRB were isolated to biofilms where acetate and/or propionate were the only available electron donors.

Two *Desulfovibrio* OTUs, namely OTUs 39 and 47, were only identified in communities where lactate was present (Figure 7-7), whereas the remaining SRB identified in zones of lactate oxidation were also observed in zones where acetate or propionate oxidation was prominent. This suggests the latter group of SRB can metabolise both lactate and acetate as electron donors.

Six SRB were only identified where acetate and/or propionate oxidation were the predominant electron donors, and lactate oxidation was not taking place. This is remarkable because both acetate and sulphate were available in the zones where lactate oxidation was taking place. These SRB become dominant in the middle and effluent zones of the UAPBRs indicating their absence in the zones of lactate oxidation are not due to out-competition for sulphate or constituents of yeast extract. The 'out-competition' of these acetate-oxidising SRB appears to depend on the proximity to lactate oxidising microorganisms. Therefore, the growth of these six SRB appears to be inhibited, possibly through the production of antimicrobial compounds (Hibbing et al., 2010), or simply out-competed for space by lactate-oxidising microorganisms.

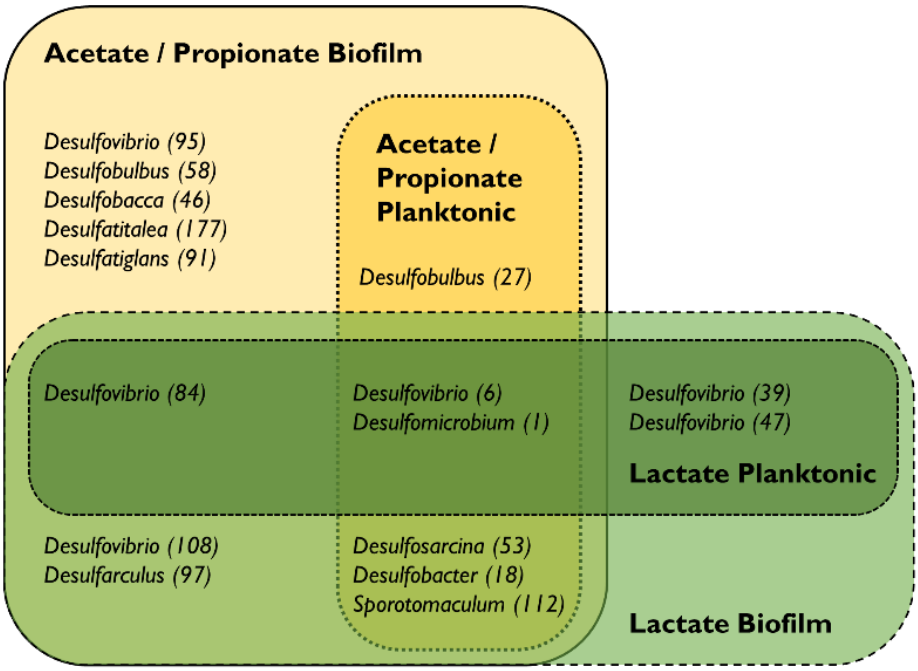


Figure 7-7 The presence of the putatively identified SRB OTUs, at ≥1% relative abundance, in the biofilm and planktonic communities within reactor zones where lactate or acetate and propionate are the determined predominant electron donors. The predominant electron donor in the effluent zone of the lactate-supplemented UAPBR, for example, is classified as Acetate/Propionate.

Only two SRB were present in acetate and lactate planktonic and biofilm communities, namely *Desulfovibrio* (6) and *Desulfomicrobium* (1). These frequently occurring SRB appeared in each of the six BSR reactors, within most reactor zones and microbial phases (Figure 7-8). *Desulfobacter* (18) was also highly prevalent, present in both UAPBRs, the acetate-supplemented LFCR and lactate-supplemented CSTR (Figure 7-8). This SRB OTU was found in biofilm communities where lactate was the predominant electron donor and where acetate and/or propionate were the predominant electron donors (Figure 7-7).

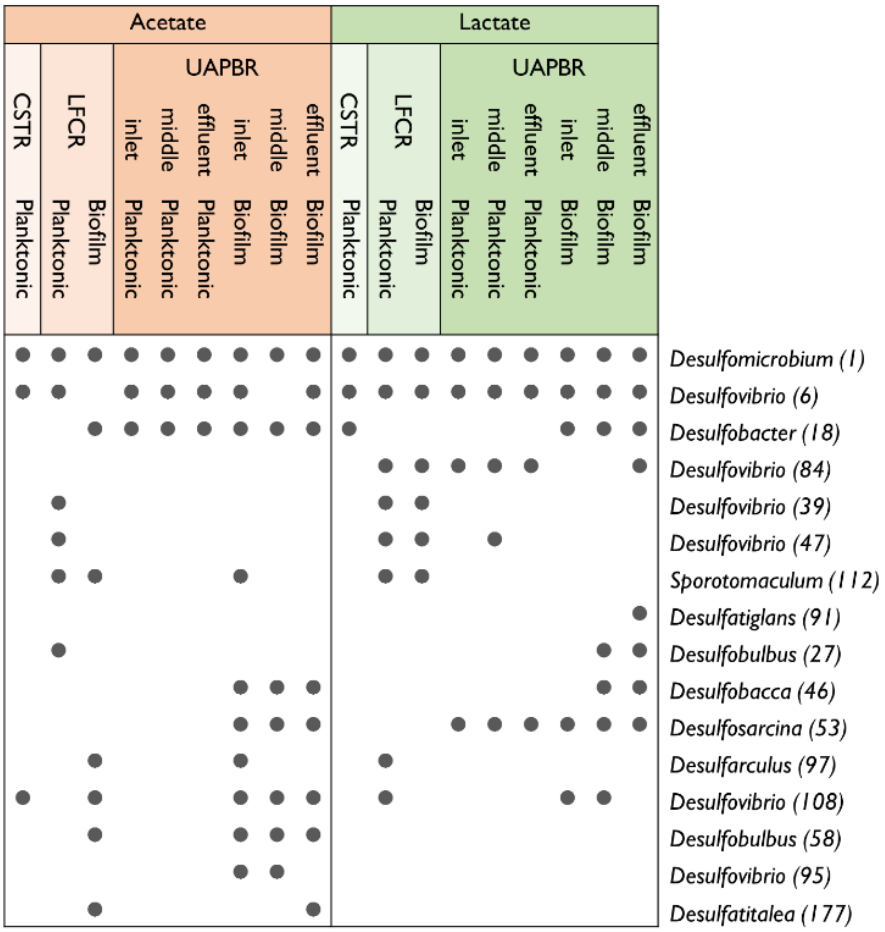


Figure 7-8 The presence of the putatively identified SRB OTUs, at ≥1% relative abundance, in the biofilm and planktonic communities of the acetate- and lactate-supplemented CSTR, LFCR and UAPBRs during the course of the HRT study.

The CSTR held less SRB diversity (above 1% relative abundance) than the respective LFCR and UAPBRs. This is likely a result of the single environmental condition created in the CSTRs as discussed in Section 7.2.1. This single environment likely results in a trade-off, selecting for faster-growing SRB with a lower affinity for sulphate and against SRB which are slower growing but have a higher affinity for acetate and sulphate which would confer the system with improved sulphate conversions.

The acetate-supplemented UAPBR and LFCR both performed well compared with other acetate supplemented reactors described in the literature, as discussed in Chapters five and six. The UAPBR achieved sulphate conversions approximately 21% higher than the LFCR at each tested HRT (Figure 7-9 A). Both of these systems supported relatively diverse SRB consortiums which were both more diverse than those supported by the CSTR. A number of SRB that were identified in both the LFCR and UAPBR including *Desulfarculus* (97) *Desulfovibrio* (108) *Desulfobulbus* (58) and *Desulfatitalea* (177). The SRB OTUs *Desulfobulbus* (58) and *Desulfatitalea* (177) were only found in

zones where no lactate oxidation occurred, while *Desulfatitalea* (177) occurred in the effluent zone of the UAPBR, indicating that this SRB is likely adept at scavenging sulphate.

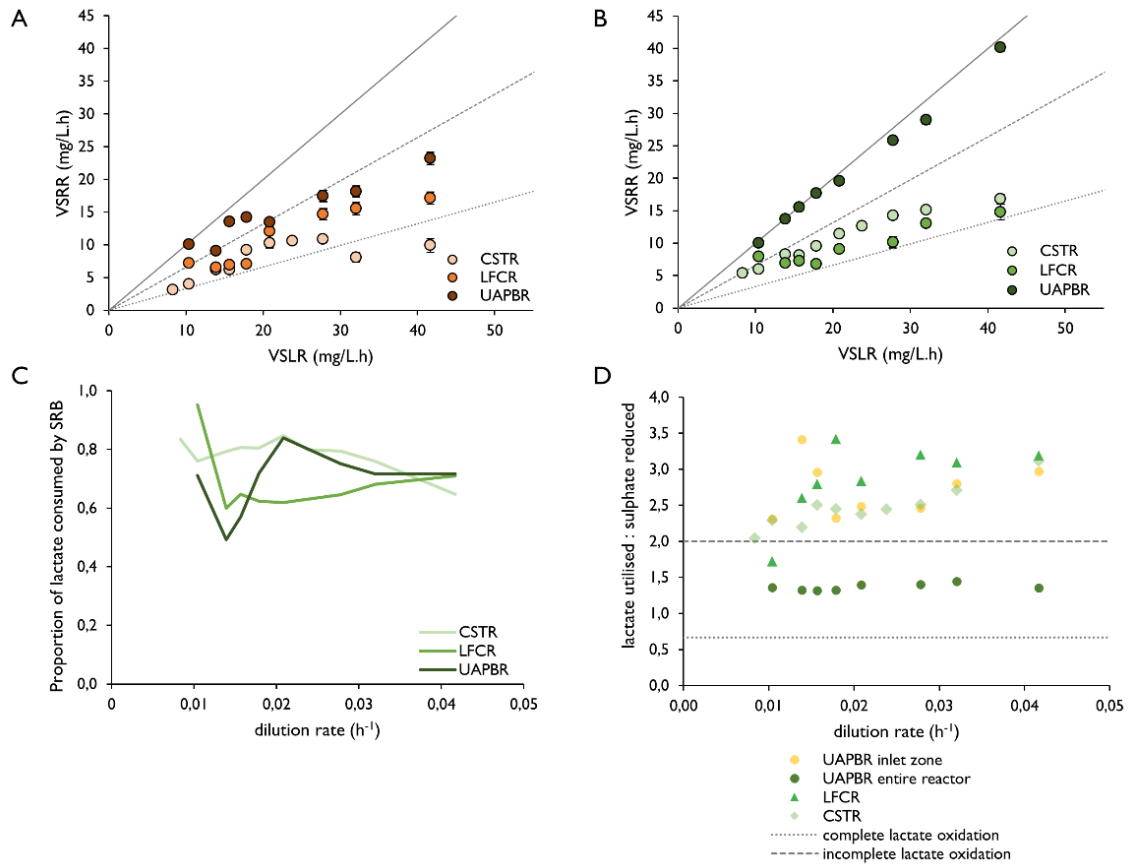


Figure 7-9 The integrated performance of the (A) acetate-supplemented and (B) lactate-supplemented CSTRs, LFCRs and UAPBRs in terms of the volumetric sulphate reduction rates (VSRRs) achieved at increasing volumetric sulphate loading rates (VSLRs), increased through the reduction in the applied HRT. The error bars represent one standard deviation from the mean. The theoretical sulphate conversions of 100% (solid line), 66% (dashed line) and 33% (dotted line) are plotted alongside. The competition for lactate between SRB and fermentative microorganisms in the lactate-supplemented BSR reactors was assessed through (C) estimating the proportion of feed lactate which was consumed by SRB and (D) comparing the molar ratio of lactate utilised to sulphate reduced in the three lactate-supplemented BSR reactors.

As discussed in Chapter 5, the lactate-supplemented LFCR underperformed compared to the lactate-supplemented CSTR. The LFCR held a great deal more SRB diversity than the CSTR but this diversity alone was not sufficient to ensure adequate system performance. The lactate-supplemented CSTR, LFCR and UAPBR displayed similar proportions of lactate estimated to have been consumed by SRB (Figure 7-9 C). The degree of lactate oxidation by SRB, on average over the course of the HRT study, was only marginally lower in the LFCR than the other two reactor configurations. This is counterintuitive when considering the far greater VSRR achieved by the

UAPBR compared with the other reactor configurations (Figure 7-9 B). The lactate-supplemented UAPBR was able to maintain near complete sulphate removal during the HRT study, reaching a maximum VSRR of 40.1 mg/ℓ.h at a one-day HRT. This performance is partially attributed to the out-competition of lactate fermenting microorganisms by SRB in the inlet zone but is similarly attributed to the subsequent acetate and propionate oxidation in the middle and effluent zones by a largely distinct SRB consortium (Figure 7-8).

The role of acetate and propionate oxidising SRB in the lactate-supplemented UAPBR is particularly evident when comparing the ratio of 'lactate utilised to sulphate reduced' by each lactate-supplemented reactor (Figure 7-9 D). This ratio observed above 2.0 in the CSTR and LFCR indicates incomplete lactate oxidation and lactate fermentation. A ratio of above 2.0 is also observed leaving the inlet zone of the lactate-supplemented UAPBR but this decreased to approximately 1.4 when considering the entire length of the reactor. This indicates a large degree of complete lactate oxidation – oxidation of the produced acetate and propionate. The UAPBR was, therefore, the only reactor able to effectively use lactate and acetate. The SRB isolated to the middle and effluent zones of this reactor included *Desulfovibrio* (84), *Desulfatiglans* (91), *Desulfobulbus* (27) and *Desulfobacca* (46). These SRB were not identified in either of the lactate-supplemented CSTR nor LFCR, but some were identified in the acetate-supplemented UAPBR and LFCR. The performance of the lactate-supplemented LFCR would likely be improved by enabling this system to harbour more of these acetate oxidising SRB. As demonstrated in Figure 7-7, these SRB appear to be isolated to zones where no lactate oxidation is occurring simultaneously, indicating that the cultivation of these SRB in this system requires zoning.

## 7.3 Conclusions

The diversity of microbial communities within BSR reactors supplemented with lactate were found to be lower than within reactors supplemented with acetate. Similarly, the CSTRs held less total diversity than the LFCRs and the LFCRs appeared less diverse than the UAPBRs. It is not certain whether increased microbial diversity is advantageous for reactor performance and remains an observation.

The sequencing of duplicate microbial metagenomic samples indicated that the microbial populations are largely stable and differences are likely the result of deterministic factors. Most gene amplicon sequencing performed in this study was performed using individual samples and this provides evidence these individual samples are representative of their microbial communities. Some variation in the relative abundance of few OTUs is seen between duplicate biofilm samples and warrants further study into the spatial distribution of microorganisms within biofilms of BSR systems.

There is clear evidence that many OTUs within the BSR reactors show strong preferences for differing physiochemical environments. These include the enrichment of *Veillonella* (11) and *Enterobacter* (16) in zones where lactate is available. These two OTUs were also shown to be enriched in the planktonic phases. These are concluded to be the major competitors of SRB for lactate and therefore the minimising of the planktonic phase within lactate supplemented BSR reactors should be investigated. Inversely, other OTUs show enrichment in acetate environments and biofilm communities. These non-dissimilatory sulphate-reducing microorganisms may improve reactor performance by contributing to the removal of COD in the form of acetate.

Assessing the distribution of SRB across reactors allowed several valuable observations to be made. Firstly, SRB diversity was held within biofilm communities, with every SRB identified in a planktonic community also being identified within a biofilm, but not vice-versa. Secondly, many SRB only became dominant in microbial communities where lactate is not available. These acetate and propionate oxidising SRB appear to be inhibited or out-competed by lactate-oxidising microorganisms. It is these SRB which are expected to confer BSR reactors with high sulphate conversions because of the sustained dominance of these acetate-oxidising SRB in reactors zones with little available substrate. Thirdly, the SRB communities showed changes throughout the height of the UAPBRs and show substantial differences with the SRB held in the LFCRs. This provides strong evidence in support of hypothesis 1 (Section 2.10.1). This hypothesis stated that the communities throughout plug-flow reactors would change throughout the height of the reactors and these communities would be different from those within well-mixed reactors. This was based on the varying conditions generated as a result of the differing hydrodynamics.

The success of the lactate-supplemented UAPBR was attributed largely to the ability of this reactor to harbour both lactate- and acetate-oxidising SRB. This allowed nearly complete removal of the feed 1 *g/ℓ* sulphate. The effective use of lactate as an electron donor for semi-passive BSR treatment requires that the generated acetate and propionate be used for sulphate reduction. This allows less lactate to be required, offering lower operating costs, and prevents the discharge of high COD from these reactors.

It is important to note that few to no SRB implicated in acetate-oxidation in the UAPBRs were present in either of the lactate-supplemented LFCR nor CSTR. The success of the LFCR supplemented with lactate, therefore, requires the system to be modified so as to allow acetate-oxidising SRB to become dominant. This did not occur and therefore provides strong evidence against hypothesis 2. This hypothesis anticipated slower-growing acetate oxidising bacteria to become dominant on the carbon microfibres and confer the reactor with acetate oxidation linked to sulphate reduction. It is suggested that zoning this reactor, to spatially separate lactate and acetate oxidation, is required to stimulate the growth of these acetate-oxidising SRB.

# Chapter 8 Genome-resolved metagenomics of BSR reactor systems

## 8.1 Background

Metagenomic DNA samples isolated from the six continuous reactor systems, at a four-day steady-state and the original inoculum used to inoculate the reactors, were sequenced by whole-genome shotgun sequencing as described in Section 3.10. The reactor samples selected for whole-genome sequencing are described in more detail in Table 8-1below.

Table 8-1 Metagenomic samples selected for whole-genome shotgun sequencing. These samples are described by the reactor configuration these samples originate (for both acetate and lactate systems) and whether they originate from a free-floating planktonic microbial sample or were extracted directly off solid support structures (attached). Each sample was sequenced in duplicate.

| Reactor | Reactor Zone | Phase |
|---|---|---|
| Inoculum | n/a | Planktonic |
| CSTR | n/a | Planktonic |
| LFCR | Inlet zone | Planktonic |
| | | Attached |
| UAPBR | Inlet zone | Planktonic |
| | | Attached |
| | Middle zone | Planktonic |
| | Effluent zone | Planktonic |
| | | Attached |

These reactor samples were selected in order to recover as many microbial genomes associated with the BSR process as possible. The generated sequencing data were quality controlled as described in Section 3.10.2 before undergoing assembly, annotation and binning as described in Section 3.10.2 and Section 3.10.3.

## 8.2 Genome statistics

A total of 163 microbial genomes, 162 bacterial and a single archaeal genome, were recovered from the 34 duplicate sequenced samples after genome dereplication. Less than 1% of the contigs within each metagenome were classified as eukaryotic and were present at low coverage. As a result no eukaryotic genomes could be recovered. Viral genomes were recovered but are not

reported in this thesis. All recovered microbial genomes were deemed high-quality due to an average and minimum completeness of 95 and 75%, respectively, based on the recovery of bacterial and archaeal single-copy genes (Figure 8-1). This excludes a Microgametes genome which recorded a completeness of 64% and a genome size of just 0.9 Mbp. This organism is classified as a member of the candidate phyla radiation (CPR) which typically have greatly reduced genomes sizes, which initially led to the speculation that these microorganisms must live symbiotically with a host microorganism (Hug et al., 2016). Although lacking many common bacterial single-copy genes, it is expected that this genome is relatively complete. A summary of the statistics associated with the most prevalent of the recovered genomes is shown in Table 8-2. The degree of contamination between genome bins was low, with 90% of the genome bins having an estimated contamination of less than 4%. This level of contamination and completeness is attributed to the relatively simple reactor microbial communities – with few microorganisms dominating any given sample. It was found that half of the genomes which appeared in a sample above 1% relative abundance would do so in more than one sample. This enabled improved binning of these genomes through a "time-series binning" approach (Section 3.10.3) and dereplication of the highest quality of the repeated genomes. Although the occurrence of genomes in multiple samples led to improved genome bins, individual genomes would co-occur in relatively few samples. The varied ecology between these similarly operated reactors indicates that the different reactor environments suggest substantial heterogeneous selective pressure on the original inoculum community. Although, there is room to discuss whether many of these resulting microorganisms are present due to deterministic or stochastic factors (Stegen et al., 2012; Dini-Andreote et al., 2015), the enrichment of particular genes and gene pathways independent of the microorganism in which they are found, is almost certainly a result of deterministic factors (see Section 8.6). Instances of this are discussed throughout this chapter. The differing growth kinetics between microorganisms with similar metabolism would also likely explain many of these differences between microorganisms with similar metabolic attributes. Relatively few 16S rRNA genes were binned with the recovered genomes (Table 8-2). This is not uncommon, as the highly conserved regions and multi-copy of this nature of this gene make it exceedingly difficult to accurately bin (Yuan et al., 2015). Future efforts to further curate these genomes should allow the recovery of more 16S rRNA gene sequences from the remaining un-binned contigs.

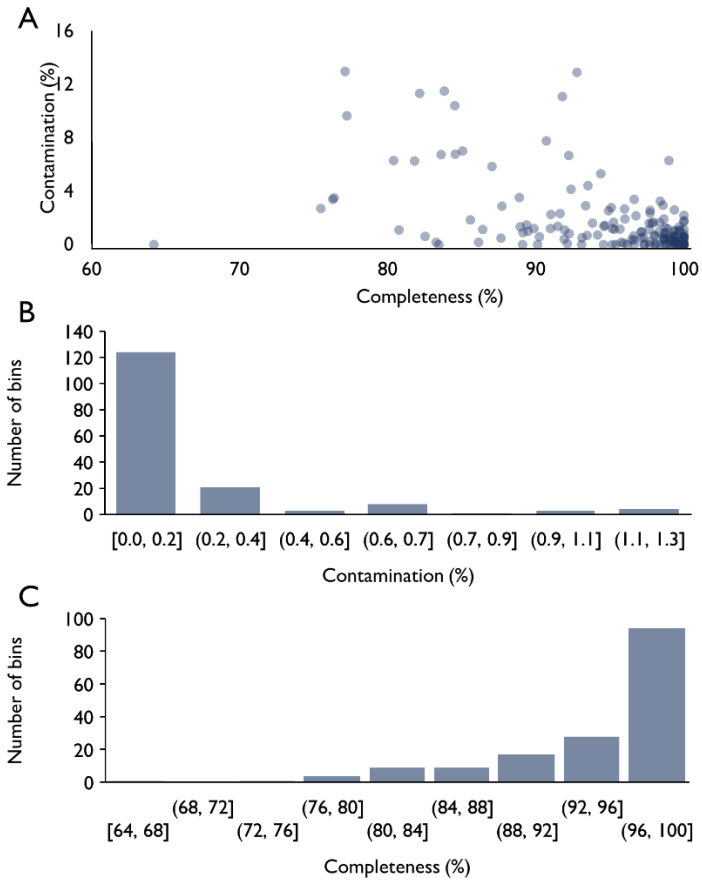


Figure 8-1 Genome bin quality shown as (A) genome contamination as a function of genome completeness for each of the 163 recovered genomes bins from the BSR reactor and inoculum communities. The number of genome bins lying in a particular range of (B) contamination and (C) completeness is shown, with the majority of these bins showing 0-2% contamination and >96% completeness.

Table 8-2 Genome statistics of the 68 most abundant of the 163 recovered microbial genome bins. These genome bins are described by their GC percentage, the average coverage from the dereplicated genome bin, the number of contigs in the genome bin, the number of features/genes, the bacterial and archaeal single-copy genes and the number of multi-copies (MC) of each, the estimated genome completeness and contamination, the size of the genome, the median contig length in each bin (N50), the presence of 16S rRNA gene(s), and the number of times a genome appeared in one of the 17 samples above one and above five percent relative abundance (RA). Genome statistics of all 163 recovered genomes can be found in Section A.5.

| genome bin | GC (%) | coverage | contigs | features | BSCG [/51] (MC) | ASCG [/38] (MC) | completeness (%) | contamination (%) | genome size (Mbp) | N50 (bp) | 16S rRNA | frequency (>1 % RA) | frequency (>5 % RA) |
|---|---|---|---|---|---|---|---|---|---|---|---|---|---|
| BSR_Ace_LFCR_na_at_2_Desulfobacterales_57_55 | 57 | 55 | 72 | 5265 | 50 (1) | n/a | 98 | 3 | 5.8 | 1.7E+05 | ☑ | 5 | 3 |
| BSR_Ace_UAPBR_inlet_at_2_Synergistales_64_17 | 64 | 17 | 156 | 2483 | 51 (0) | n/a | 100 | 0 | 2.6 | 3.7E+04 | ☑ | 14 | 11 |
| BSR_Lac_UAPBR_inlet_at_Bacteroidia_47_18 | 47 | 18 | 31 | 1604 | 51 (0) | n/a | 95 | 1 | 1.8 | 1.5E+05 | | 2 | 2 |
| BSR_Ace_C_na_Sphaerochaeta_globosa_51_113 | 51 | 113 | 335 | 3337 | 32 (1) | n/a | 90 | 1 | 3.4 | 2.3E+04 | | 13 | 7 |
| BSR_Ace_LFCR_na_p_Geobacter_lovleyi_46_94 | 46 | 94 | 69 | 3300 | 51 (0) | n/a | 99 | 0 | 3.4 | 1.2E+05 | | 9 | 2 |
| BSR_Ace_C_na_2_Bacteroidetes_44_67_(50) | 44 | 67 | 90 | 2215 | 51 (0) | n/a | 95 | 2 | 2.5 | 5.8E+04 | | 12 | 3 |
| BSR_Lac_LFCR_na_p_Bacteroidia_39_30 | 39 | 30 | 37 | 2195 | 51 (0) | n/a | 97 | 0 | 2.5 | 4.1E+05 | ☑ | 6 | 3 |
| BSR_Ace_UAPBR_effluent_at_Desulfarculus_baarsii_66_20 | 66 | 20 | 66 | 3341 | 51 (0) | n/a | 99 | 0 | 3.6 | 1.4E+05 | ☑ | 3 | 2 |
| BSR_Ace_UAPBR_middle_p_1_Bacteroidia_44_46 | 44 | 46 | 86 | 3205 | 51 (0) | n/a | 100 | 1 | 3.7 | 9.9E+04 | | 5 | 1 |
| BSR_Ace_UAPBR_inlet_at_2_BJP_IG2103_Bacteroidetes_41_9_47_32 | 47 | 32 | 161 | 3533 | 51 (0) | n/a | 98 | 2 | 4.4 | 6.4E+04 | ☑ | 13 | 4 |
| BSR_Ace_C_na_Sphaerochaeta_globosa_53_73 | 53 | 73 | 389 | 3657 | 50 (0) | n/a | 98 | 2 | 3.6 | 2.2E+04 | | 9 | 4 |
| BSR_Ace_C_na_Desulfovibrio_desulfuricans_58_43 | 58 | 43 | 43 | 2859 | 51 (0) | n/a | 100 | 0 | 3.5 | 1.7E+05 | | 9 | 6 |
| BSR_Ace_LFCR_na_p_Sphaerochaeta_globosa_51_20 | 51 | 20 | 55 | 2929 | 50 (1) | n/a | 98 | 0 | 3.1 | 1.0E+05 | | 11 | 6 |
| BSR_Ace_UAPBR_inlet_at_2_Desulfobulbus_propionicus_52_45 | 52 | 45 | 36 | 2519 | 51 (0) | n/a | 100 | 0 | 2.8 | 1.6E+05 | | 1 | 1 |
| BSR_Ace_UAPBR_inlet_p_GWF2_Bacteroidetes_43_11_curated_39_33 | 39 | 33 | 98 | 3143 | 51 (0) | n/a | 98 | 2 | 4.1 | 6.3E+04 | | 3 | 1 |
| BSR_Ace_UAPBR_inlet_at_1_Desulfovibrio_64_36 | 64 | 36 | 37 | 3090 | 51 (0) | n/a | 100 | 0 | 3.4 | 1.5E+05 | ☑ | 4 | 1 |
| BSR_Ace_UAPBR_effluent_at_Synergistales_59_15 | 59 | 15 | 161 | 3972 | 51 (1) | n/a | 100 | 0 | 4.2 | 5.5E+04 | | 4 | 2 |
| BSR_Ace_C_na_Klebsiella_oxytoca_56_23 | 56 | 23 | 93 | 5737 | 51 (0) | n/a | 100 | 0 | 6.0 | 1.3E+05 | | 3 | 1 |
| BSR_Ace_C_na_2_Bacteroidia_49_19 | 49 | 19 | 46 | 2988 | 51 (0) | n/a | 97 | 2 | 3.8 | 1.7E+05 | | 1 | 1 |
| BSR_Ace_UAPBR_effluent_at_2_Deltaproteobacteria_63_50 | 63 | 50 | 95 | 4046 | 50 (1) | n/a | 99 | 3 | 4.4 | 7.8E+04 | ☑ | 9 | 4 |
| BSR_Ace_UAPBR_effluent_p_Bacteroidetes_40_41 | 40 | 41 | 28 | 2366 | 51 (0) | n/a | 97 | 1 | 2.8 | 2.2E+05 | | 7 | 3 |
| BSR_Ace_C_na_2_Bacteroidales_35_10 | 35 | 10 | 183 | 2567 | 51 (0) | n/a | 99 | 1 | 3.0 | 2.8E+04 | | 1 | 1 |
| BSR_Ace_LFCR_na_p_Dysgonomonas_39_22 | 39 | 22 | 27 | 3408 | 51 (0) | n/a | 99 | 0 | 4.1 | 3.2E+05 | | 7 | 1 |
| BSR_Ace_UAPBR_inlet_p_1_Dethiosulfovibrio_peptidovorans_54_25 | 54 | 25 | 50 | 2592 | 50 (0) | n/a | 100 | 0 | 2.7 | 1.3E+05 | | 2 | 0 |
| BSR_Ace_C_na_2_Microgenomates_37_51 | 37 | 51 | 24 | 965 | 47 (0) | n/a | 64 | 0 | 0.9 | 2.4E+05 | ☑ | 6 | 0 |
| BSR_Ace_LFCR_na_p_RIFOXYB2_FULL_Tenericutes_36_25_curated_36_10 | 36 | 10 | 120 | 1606 | 51 (0) | n/a | 99 | 1 | 1.6 | 2.0E+04 | | 2 | 0 |
| BSR_Lac_C_na_Bacteroidia_44_10 | 44 | 10 | 253 | 3064 | 42 (4) | n/a | 93 | 1 | 3.4 | 3.0E+04 | ☑ | 6 | 0 |
| BSR_Ace_LFCR_na_p_1_Bacteroidales_43_13 | 43 | 13 | 49 | 2671 | 51 (0) | n/a | 100 | 1 | 3.2 | 1.1E+05 | ☑ | 3 | 0 |
| BSR_Lac_C_na_Desulfovibrio_70_18 | 70 | 18 | 74 | 3273 | 51 (0) | n/a | 100 | 0 | 3.6 | 2.0E+05 | ☑ | 2 | 0 |
| BSR_Ace_C_na_Synergistales_61_23 | 61 | 23 | 36 | 3215 | 50 (0) | n/a | 100 | 2 | 3.4 | 2.2E+05 | | 5 | 0 |
| BSR_Ace_LFCR_na_p_Desulfotomaculum_gibsoniae_47_21 | 47 | 21 | 33 | 3029 | 50 (0) | n/a | 97 | 1 | 3.1 | 1.5E+05 | | 5 | 0 |
| BSR_Ace_LFCR_na_p_1_Clostridiales_58_10 | 58 | 10 | 86 | 3043 | 51 (2) | n/a | 98 | 0 | 3.1 | 6.5E+04 | | 3 | 0 |
| BSR_Lac_UAPBR_effluent_at_1_GWC2_Bacteroidetes_46_850_curated_52_9 | 52 | 9 | 120 | 1776 | 51 (1) | n/a | 97 | 1 | 2.0 | 2.4E+04 | | 1 | 0 |
| BSR_Ace_C_na_Bacteroidia_43_15 | 43 | 15 | 97 | 3695 | 51 (3) | n/a | 99 | 1 | 4.5 | 1.1E+05 | | 2 | 0 |
| BSR_Ace_UAPBR_effluent_at_Phycisphaerae_63_30 | 63 | 30 | 66 | 4332 | 48 (0) | n/a | 100 | 1 | 5.3 | 1.3E+05 | ☑ | 4 | 0 |
| BSR_Ace_UAPBR_middle_p_Bacteria_50_28 | 50 | 28 | 52 | 2215 | 49 (0) | n/a | 95 | 1 | 2.8 | 1.1E+05 | ☑ | 4 | 0 |
| BSR_Ace_C_na_Bacteroidales_43_22 | 43 | 22 | 35 | 2824 | 51 (0) | n/a | 100 | 1 | 3.4 | 1.6E+05 | | 1 | 0 |
| BSR_Lac_UAPBR_effluent_p_2_Desulfomicrobium_baculatum_60_28 | 60 | 28 | 38 | 3782 | 51 (0) | n/a | 99 | 0 | 4.1 | 3.6E+05 | | 2 | 0 |
| BSR_Ace_UAPBR_effluent_p_Clostridiales_54_14 | 54 | 14 | 35 | 3038 | 49 (3) | n/a | 99 | 0 | 3.2 | 1.7E+05 | ☑ | 2 | 0 |
| BSR_Ace_LFCR_na_p_Sphaerochaeta_globosa_45_14 | 45 | 14 | 64 | 2994 | 50 (0) | n/a | 98 | 1 | 3.3 | 8.6E+04 | | 2 | 0 |
| BSR_Ace_UAPBR_inlet_p_Bacteroidales_40_21 | 40 | 21 | 67 | 3329 | 51 (0) | n/a | 100 | 1 | 4.0 | 9.9E+04 | ☑ | 4 | 0 |
| BSR_Lac_C_na_Clostridiales_55_36 | 55 | 36 | 53 | 3098 | 51 (3) | n/a | 99 | 0 | 3.6 | 1.5E+05 | | 1 | 0 |
| BSR_Ace_C_na_Clostridiales_57_14 | 57 | 14 | 63 | 3532 | 51 (2) | n/a | 98 | 1 | 3.7 | 1.7E+05 | | 1 | 0 |
| BSR_Lac_C_na_Aeromonas_veronii_59_14 | 59 | 14 | 35 | 4213 | 51 (0) | n/a | 100 | 0 | 4.5 | 2.5E+05 | | 1 | 0 |
| BSR_Lac_LFCR_na_p_Clostridiales_36_11 | 36 | 11 | 85 | 2442 | 51 (2) | n/a | 97 | 0 | 2.5 | 5.0E+04 | | 2 | 0 |
| BSR_Lac_LFCR_na_at_1_Alphaproteobacteria_54_165 | 54 | 165 | 43 | 2098 | 50 (0) | n/a | 90 | 0 | 2.1 | 1.6E+05 | ☑ | 1 | 0 |
| BSR_Lac_UAPBR_middle_p_Sphaerochaeta_55_11 | 55 | 11 | 78 | 1948 | 48 (0) | n/a | 98 | 0 | 2.1 | 4.6E+04 | | 3 | 0 |
| BSR_Ace_C_na_Bacteroidetes_33_15 | 33 | 15 | 56 | 2079 | 51 (0) | n/a | 97 | 1 | 2.4 | 1.3E+05 | | 5 | 0 |
| BSR_Ace_UAPBR_effluent_at_Bacteria_64_7 | 64 | 7 | 669 | 4147 | 43 (2) | n/a | 89 | 4 | 4.9 | 9.2E+03 | ☑ | 3 | 0 |
| BSR_Ace_UAPBR_middle_p_Parabacteroides_42_25 | 42 | 25 | 71 | 3556 | 51 (0) | n/a | 99 | 0 | 4.2 | 1.1E+05 | ☑ | 4 | 0 |
| BSR_Ace_C_na_Bacteroidia_47_14 | 47 | 14 | 182 | 2191 | 50 (4) | n/a | 92 | 4 | 2.4 | 2.2E+04 | | 1 | 0 |
| BSR_Ace_C_na_Burkholderiales_68_7 | 68 | 7 | 588 | 4356 | 51 (1) | n/a | 88 | 0 | 4.3 | 8.9E+03 | ☑ | 1 | 0 |
| BSR_Lac_UAPBR_middle_p_1_Thermotogae_38_9 | 38 | 9 | 229 | 2310 | 49 (2) | n/a | 93 | 1 | 2.3 | 1.3E+04 | | 1 | 0 |
| BSR_Ace_LFCR_na_p_Parabacteroides_42_11 | 42 | 11 | 412 | 3591 | 51 (2) | n/a | 98 | 3 | 4.0 | 2.0E+04 | ☑ | 5 | 0 |
| BSR_Ace_LFCR_na_p_Oscillibacter_valericigenes_56_9 | 56 | 9 | 161 | 2816 | 51 (2) | n/a | 99 | 0 | 2.8 | 2.8E+04 | | 1 | 0 |
| BSR_Ace_UAPBR_effluent_at_Gammaproteobacteria_63_27 | 63 | 27 | 157 | 2921 | 51 (0) | n/a | 100 | 0 | 3.1 | 4.5E+04 | | 7 | 0 |
| BSR_Ace_UAPBR_effluent_p_Chlorobium_limicola_53_20 | 53 | 20 | 55 | 2443 | 51 (0) | n/a | 98 | 0 | 2.6 | 1.1E+05 | | 1 | 0 |
| BSR_Ace_UAPBR_effluent_p_2_Thiomonas_65_14 | 65 | 14 | 129 | 2942 | 51 (0) | n/a | 99 | 1 | 3.0 | 4.1E+04 | ☑ | 1 | 0 |
| BSR_Ace_LFCR_na_at_Clostridiales_56_12 | 56 | 12 | 21 | 1929 | 51 (2) | n/a | 95 | 0 | 1.9 | 1.8E+05 | | 1 | 0 |
| BSR_Lac_LFCR_na_at_2_Bacteroidia_44_21 | 44 | 21 | 90 | 3694 | 51 (2) | n/a | 100 | 2 | 4.6 | 7.9E+04 | | 4 | 0 |
| BSR_Lac_C_na_Spirochatetes_56_14 | 56 | 14 | 26 | 2811 | 48 (0) | n/a | 99 | 0 | 3.0 | 1.6E+05 | ☑ | 1 | 0 |
| BSR_Ace_UAPBR_inlet_at_Bacteria_57_9 | 57 | 9 | 165 | 2368 | 49 (1) | n/a | 96 | 0 | 2.5 | 2.1E+04 | | 2 | 0 |
| BSR_Ace_LFCR_na_p_Clostridiales_45_11 | 45 | 11 | 50 | 1754 | 51 (0) | n/a | 95 | 0 | 1.8 | 6.5E+04 | ☑ | 1 | 0 |
| BSR_Lac_UAPBR_effluent_p_2_Desulfovibrio_65_51 | 65 | 51 | 74 | 3562 | 51 (0) | n/a | 100 | 0 | 3.9 | 1.3E+05 | | 2 | 0 |
| BSR_Lac_UAPBR_effluent_at_Firmicutes_36_25 | 36 | 25 | 4 | 1139 | 50 (0) | n/a | 99 | 0 | 1.2 | 6.0E+05 | ☑ | 1 | 0 |
| BSR_Lac_LFCR_na_at_Clostridiales_48_8 | 48 | 8 | 228 | 2376 | 51 (1) | n/a | 91 | 1 | 2.3 | 1.4E+04 | | 6 | 0 |
| BSR_Ace_UAPBR_inlet_at_Firmicutes_56_7 | 56 | 7 | 466 | 3096 | 44 (3) | n/a | 81 | 1 | 3.1 | 7.7E+03 | ☑ | 1 | 0 |
| BSR_Ace_UAPBR_effluent_at_Armatimonadetes_related_68_12 | 68 | 12 | 542 | 5961 | 49 (1) | n/a | 94 | 4 | 8.6 | 2.3E+04 | ☑ | 1 | 0 |

## 8.3 Phylogeny

The genome bins were initially classified using the rpS3 gene sequences and confirmed using a phylogenetic tree built (Figure 8-2) using concatenated alignments of 16 ribosomal protein sequences, as described in Section 3.10.5. Nearly three-quarters of the genomes recovered were classified to either Proteobacteria, Bacteroidetes or Firmicutes. Of the 22 genomes capable of dissimilatory sulphate reduction (Section 8.5.1 - Sulphur metabolism) 21 were classified as Deltaproteobacteria and one as a Clostridia (class of Firmicutes). Other phyla to which a number of genomes were classified, and showed high abundances in a number of samples, include Verrumicrobia, Thermotogae, Synergistetes and Spirochaetes. A number of phyla were only constituted by a single recovered genome. None of these microorganisms were dominant, above 2.5 % relative abundance, in any of the samples and included a Euryachaeota, the only recovered archaea genome, a Microgenomates, an Actinobacteria, a Chlorobi, an Atribacteria and a Cloacimonetes (Figure 8-2).

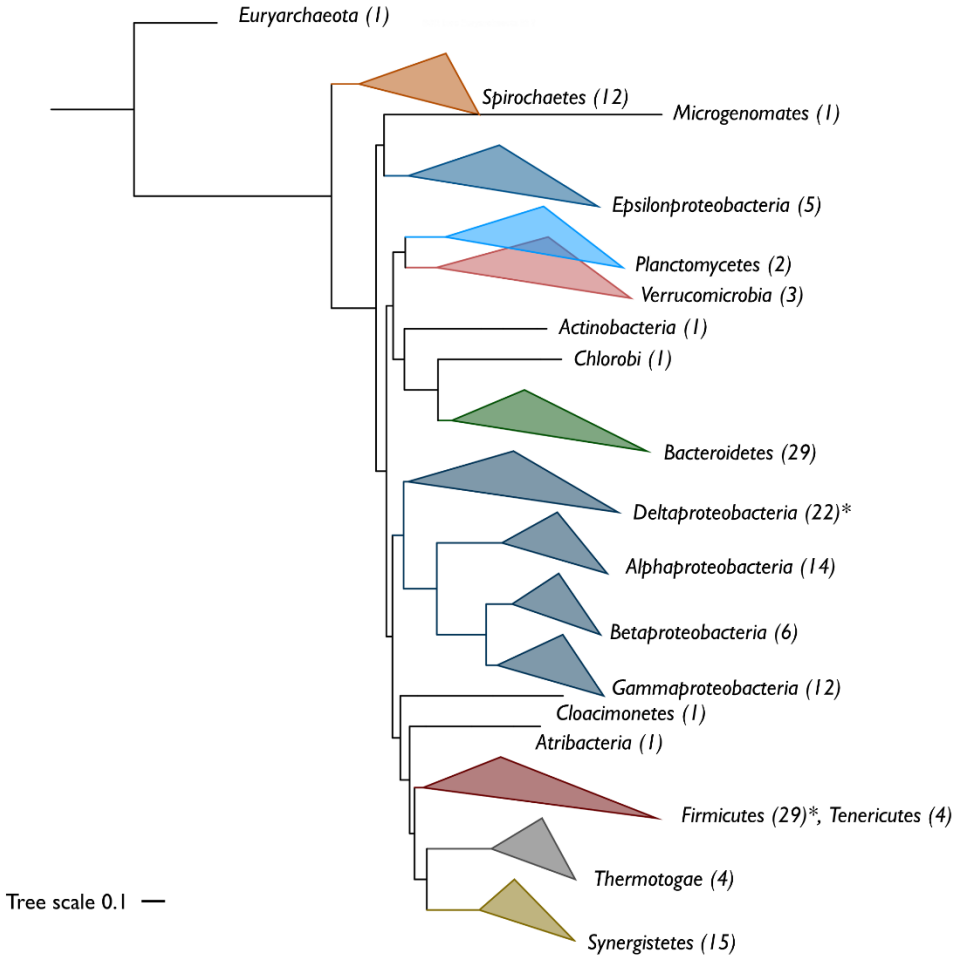


Figure 8-2 The phylogeny and phylum-level classification of the recovered genomes from the BSR reactor and inoculum microbial communities. This phylogenetic tree was constructed by the neighbour-joining method, using FastTree v2.1, of concatenated ribosomal protein

sequence alignments as described in Section 3.10.5. Branch orders were improved by applying maximum-likelihood rearrangements using the Jukes-Kantor model. The branches of the tree have been collapsed at the phylum level and the number of microorganisms classified to each phylum is shown in parentheses. Note that the phylum Tenericutes branches from within the Firmicutes phylum and therefore these two phyla are collapsed together. Phyla which contain confirmed SRB are denoted by an asterisk. A detailed phylogenetic tree with bootstrap values and reference sequences can be viewed at https://itol.embl.de/ (shared project of hsstom001).

## 8.4 Community stability and instantaneous growth rates

iRep values (Brown et al., 2016) were calculated for all recovered bins which met the required criteria of ≥5x coverage, ≥98% of the genome remaining after iRep coverage filtering and $r^2$ values of greater than 0.9 for fitted iRep regressions (Section 3.10.6). The distribution of iRep values of genome bins with ≥1% relative abundance are shown for each reactor sample (Figure 8-3).

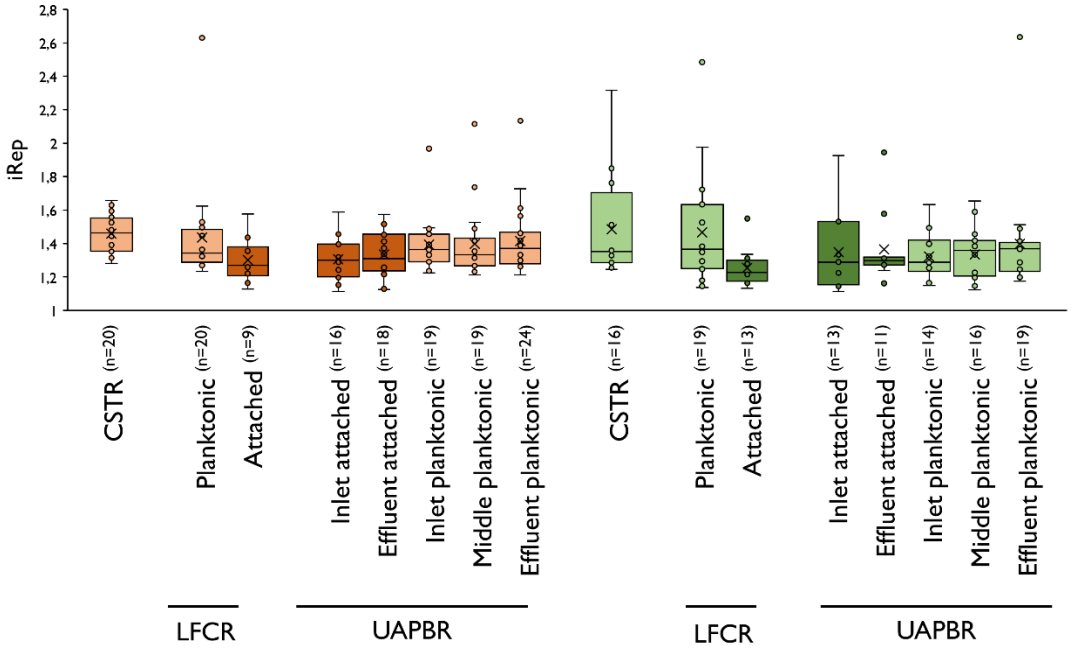


Figure 8-3 Community stability represented as iRep values calculated for dominant organisms (present at ≥1% relative abundance) in the acetate (orange) and lactate (green) planktonic (light) and attached (dark) microbial communities of the CSTRs, LFCRs and UAPBRs at a four-day HRT. Mean iRep values of each sample are indicated by a cross.

The operated HRT of four-days (0.01 $h^{-1}$) was one of the longest tested and limits the observed microbial doubling time, at steady-state, to an average of 0.01 $h^{-1}$ in the planktonic phases of the reactors. All 16 reactor community samples exhibited mean and median iRep values between 1.2 and 1.5, respectively (Figure 8-3). The majority of these samples showed little variance from the respective means indicating stability in the composition of these microbial communities. However, the lactate CSTR, the lactate LFCR planktonic and the inlet attached community of the lactate

UAPBR showed a high degree of variance in the observed iRep scores. This suggests a degree of fluctuation in the composition of the microbial communities at the time of sampling. One can expect microorganisms with low iRep values to decrease in rank abundance with time, while the inverse is true for microorganisms with higher iRep values (Brown et al., 2016).

The mean and median iRep values in the inlet planktonic phases of both UAPBRs is similar to that observed in the respective CSTR communities (Figure 8-3). The distribution of iRep values across the two UAPBR's planktonic microbial communities did not vary throughout the length of the reactors. It was observed that the sulphate reduction, lactate oxidation and citrate oxidation rates were far higher in the inlet zones than the middle- and effluent zones. The largely constant planktonic cell concentration and the little variation in iRep values within and between the three planktonic communities of the UAPBRs suggests that these communities are not responsible for the magnitude of the observed reactions in the inlet zones. Instead, this data suggests that the degree of substrate utilisation of the biofilm communities is substantial enough to severely restrict the growth of the planktonic communities. This resulted in similar planktonic cell concentrations in the inlet and effluent zones despite the considerable difference in substrate concentrations. This conclusion is supported by far the greater cell concentrations within the bioilm communities compared to the planktonic communitiies in the inlet zones. Furhther, mean iRep value of the attached communities of the inlet and effluent zones of both UAPBRs was greater than 1.3. This indicates that these biofilms represent metabolically active communities. There were no outliers below the calculated minimum iRep score, indicating that all organisms in the biofilms above 1% relative abundance were active and reproducing. Some of the highest volumetric sulphate reduction rates observed in this study were observed within the inlet zones of the UAPBRs (Section 6.2.1 and Section 6.4.1). It was concluded in chapter five, from the high biomass retention on the polyurethane foam, that the biofilm-associated communities contributed more substantially to the VSRR than the planktonic phase and this is further supported by the observed iRep values. This contributes to the body of evidence that highlights the significance of biofilm communities in these BSR reactor systems (Kuo and Shu, 2004; Harrison et al., 2014; van Hille et al., 2015; Zhang et al., 2016; Hessler et al., 2017). This was further substantiated by the reduced planktonic concentration of the LFCRs and UAPBRs in comparison to that of the purely planktonic CSTRs (Sections 5.2.1 and 5.4.1).

## 8.5 Metabolism overview

This section describes the inferred metabolic potential of the microorganisms and microbial communities within the BSR systems, based on their genetic features. It is important to note that the presence of a pathway in a genome does not alone provide evidence that this pathway is actively expressed. Numerous metabolic features are only transcribed under conditions which may not have been prevailing at the time of sampling (Neidhardt et al., 1990). Contrary to this, the absence of a particular metabolic pathway within an organism's genome provides strong evidence against that microorganism partaking in that form of cellular metabolism. The combination of metagenomics together with metatranscriptomics, metaproteomics and/or metabolomics as well as, in this instance, detailed physiochemical data and reaction kinetics, can be used to elucidate the role of particular organisms, or groups of microorganisms, within a mixed microbial community (Desai et al., 2010; Simon and Daniel, 2011; Starke et al., 2016). The following section provides a detailed overview of the metabolic capacity of the recovered metagenomes and the most abundant microorganisms present in the bioreactor samples.

### 8.5.1 Sulphur metabolism

Genes required for dissimilatory sulphate reduction were found in 22 genomes and these microorganisms could, therefore, be characterised as SRB. Approximately 21 of these genomes classified as Deltaproteobacteria and one to the phylum Firmicutes, namely - *Desulfotomaculum gibsoniae* (Figure 8-5). These genomes contained at least two of three *dsrABD* dissimilatory sulphite reductase subunits as well as either *aprA* (adenylylsulphate reductase, EC:1.8.99.2) or *sat* (sulphate adenylyltransferase, EC: 2.7.7.4). The majority of these identified contained a full pathway for dissimilatory sulphate reduction. Two low abundance genomes, classified as *Desulfovibrio*, lacked a *dsr* subunit as well as either *sat* or *aprA*. It is speculated that these genes exist on contigs belonging within this genome bin but were not binned as a result of the low coverage. The cumulative abundance of the detected SRB was highly variable throughout the 16 reactor samples (Figure 8-4). SRB were most dominant in the lactate UAPBR reactor communities (50-60% of these reactor communities), but only comprised approximately 7% of the total acetate CSTR microbial community. The specific sulphate reduction rate, per SRB cell, is far higher in the acetate CSTR than any other reactor.

Assimilatory sulphate reduction was also investigated. Assimilatory sulphate reduction gene pathways were found in only three non-SRB genomes. The supplementation of yeast extract is likely to have removed the selective pressure for microorganisms to perform assimilatory sulphate reduction for the synthesis of sulphur-containing amino acids. The minimal representation of assimilatory sulphate reduction in the genomes is, therefore, unsurprising.

Although little sulphur was unaccounted for, based on the degree of sulphate reduction and sulphide generation, the ability to perform sulphide oxidation using the *sox* gene cluster was investigated. Nine genomes contained at least one subunit of each *soxAX*, *soxYZ* and *soxCD* as well as contained *soxB*. All of these genomes were classified as Proteobacteria. The presence of *sox* genes in these genomes may not be notable for the functioning of the reactor systems of this study but has implications for the subsequent processes required to remove the sulphide these systems generate (Marais, 2019). The presence of these microorganisms should allow spontaneous biological sulphide oxidation to occur, upon the exposure of this community to oxygen. Therefore, the microbial community present within these anaerobic BSR reactor systems contains the required microorganisms necessary for the inoculation of theoretical biological sulphide oxidation system.

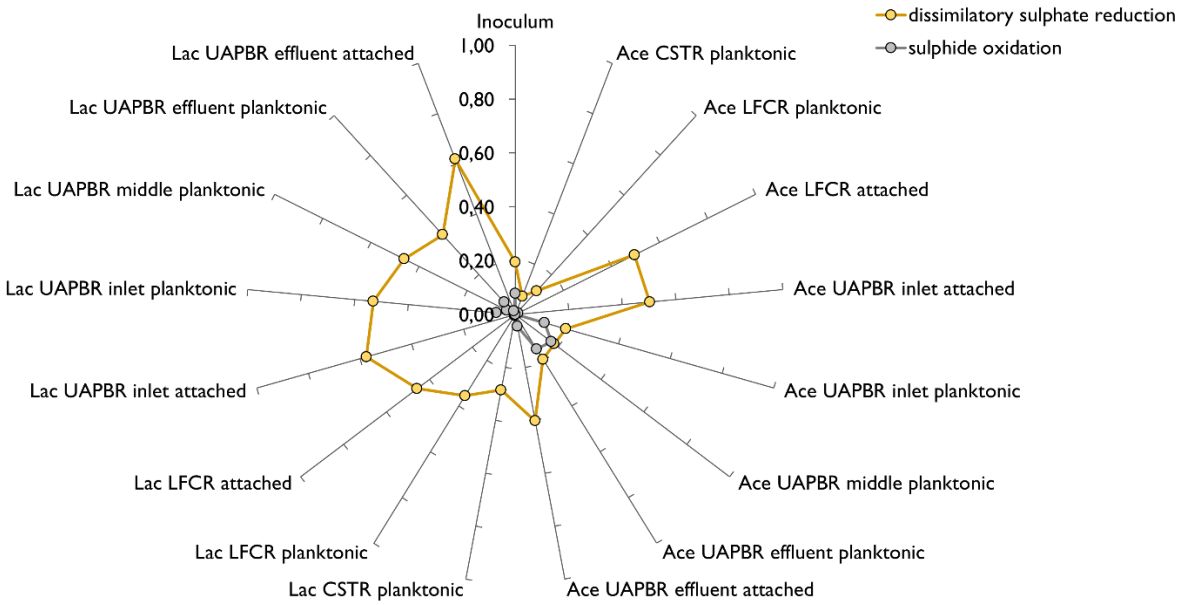


Figure 8-4 The cumulative proportions of the BSR reactor and inoculum microbial communities with the genetic capacity to perform dissimilatory sulphate reduction and sulphide oxidation. The proportion of each microorganism within a microbial community, possessing genes for these processes, were summed and displayed as a spider plot. Reactor samples are described by the reactor's supplemented electron donor [acetate (Ace) or lactate (Lac)], the reactor configuration and reactor zone, and the microbial phase [planktonic or biofilm (attached) community].

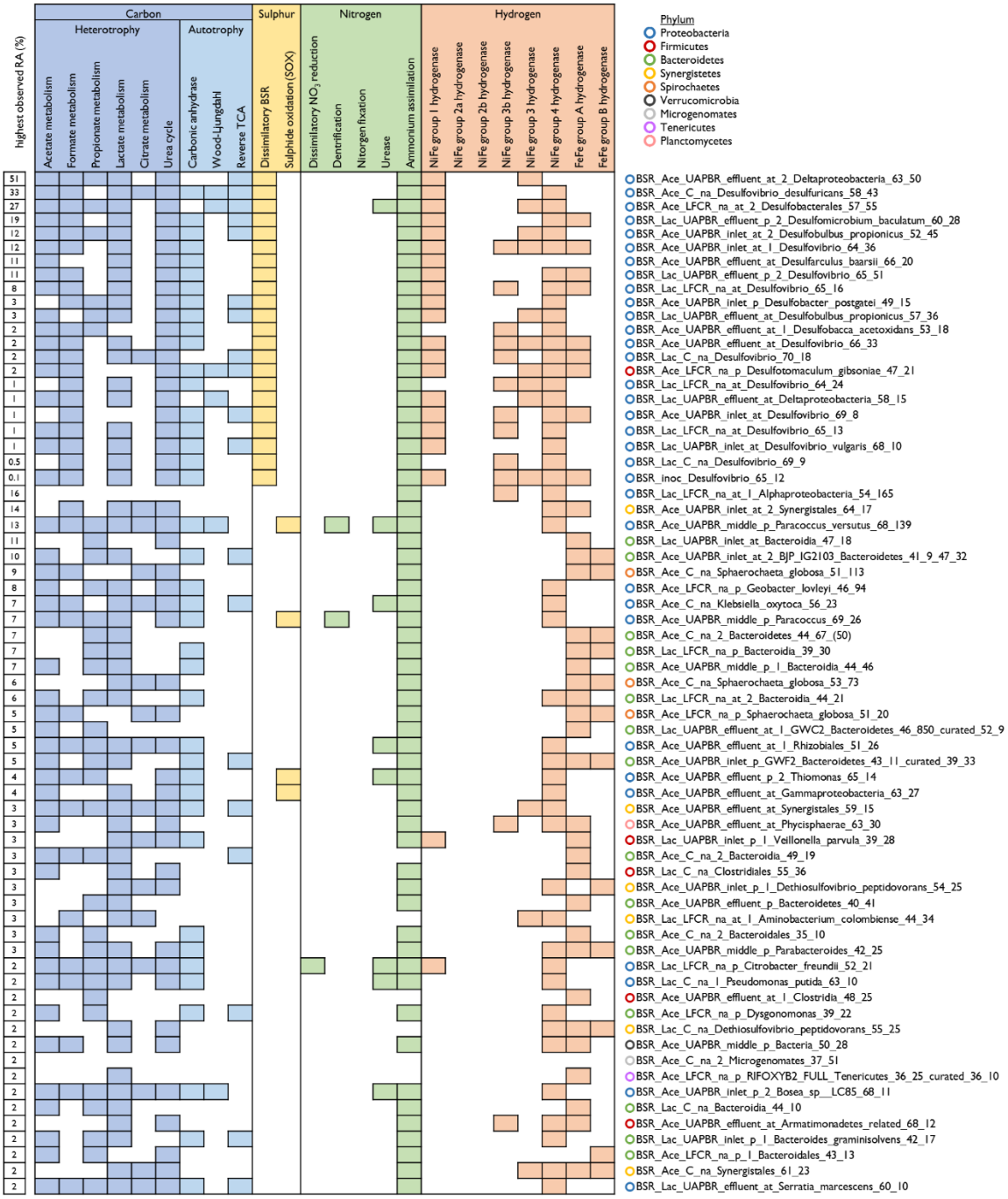


Figure 8-5 Metabolic features of the most abundant of the 163 recovered microbial genome bins. Genes and genes pathways used to attribute genomes with particular metabolic functions are described in detail in Appendix A.5.1. Genomes containing genes for dissimilatory reduction are ordered first followed by non-SRB ordered from highest to lowest observed relative abundance (RA) in any one reactor sample.

### 8.5.2 Volatile fatty acid metabolism

Some of the major conclusions arising from the 16S rRNA amplicon sequencing, described in Chapters 4-7, were the association of specific microorganisms with the oxidation of particular electron donors. The recovery and annotation of the genomes in these systems has allowed for

the validation of these associations between particular microorganisms and these metabolic reactions. The presence of genes demonstrating the capacity to metabolise the provided electron donors were investigated.

Many enzymes in the following pathways are bidirectional and many of the overall reactions can be catalysed by the sequential action of various sets of enzymes. Attributing a particular metabolic feature to a particular microorganism is dependent on the presence of various enzymes, some of which are crucial for these forms of metabolism (Appendix A.5.1, Section 2.4). However, in many instances, it is difficult to discern whether a microorganism is able to consume and/or produce particular VFAs based on genome annotation alone. The extent of oxidation of these VFAs in the reactor systems confirms these oxidation reactions are readily occurring, but the assumption of the direction of these pathways in a microorganism may still risk being a false positive.

**Lactate oxidation**

The capacity for a microorganism to metabolise lactate was inferred from the presence of one or more gene(s) encoding a lactate dehydrogenase (EC: 1.1.1.27; EC: 1.1.2.4; EC: 1.1.2.5; EC: 1.1.5.12; EC: 1.1.1.28; EC: 1.1.2.4) and one of several enzyme pathways for lactate oxidation including the incomplete oxidation of lactate to propionate via the Methylmalonyl and Acrylyl pathways, and the incomplete oxidation of lactate to acetate via a variety of enzyme catalysed reactions.

One or more lactate dehydrogenase genes were found in 124 genomes. All of these genomes had the genetic capacity to oxidise lactate incompletely to acetate and 75 genomes were found to be capable of lactate degradation via the Methylmalonyl pathway, but none via the Acrylyl pathway. The few genome bins which were unable to metabolise lactate included 8 Firmicute, 7 Bacteroidetes and 5 Spirochaetes genomes (Table 8-3). Genes relating to lactate metabolism were found in all but three SRB genomes. These three genomes were classified as *Desulfotomaculum gibsoniae*, *Desulfobacca acetoxidans* and a low abundance *Desulfovibrio* genome (Figure 8-5). The absence of genes relating to lactate metabolism in the recovered *Desulfobacca acetoxidans* genome is in accordance with other reports (Göker et al., 2011).

The proportion of the communities capable of lactate oxidation, in reactor zones where lactate oxidation was observed, varied from 70 to 85% (Figure 8-6). The remaining proportion of these communities must, therefore, sustain growth on alternate sources of organic carbon, or through autotrophy. Similar proportions of microorganisms capable of lactate oxidation were observed in several acetate reactor communities. The proportion of the planktonic microbial communities of the lactate UAPBR capable of lactate oxidation decreased from 85% in the inlet-zone to 75 and 73% in the middle-and effluent-zones, respectively. The inverse trend was observed for the proportion of the communities able to oxidise propionate (Figure 8-6) increasing from 22% in the

inlet zone to 36% in the middle-zone and then decreasing to 32% in the effluent-zone. This change in genetic potential corresponds with the localisation of the observed lactate and propionate consumption in this reactor.

**Acetate metabolism**

The ability to metabolise acetate was inferred from a genome by the presence of genes encoding for enzymes required for the first step of acetate oxidation, the conversion of acetate to acetyl-CoA (Section A.5, Methodology). The conversion of acetate to acetyl-CoA can be catalysed by either acetyl-CoA synthetase (EC:6.2.1.1) or by sequential action of acetate kinase (EC:2.7.2.1) and phosphate acetyltransferase (EC:2.3.1.8). Subsequently, the mechanism of acetate oxidation was investigated and included the reverse Wood Ljungdahl pathway, the TCA cycle (reference pathway ko00020) and the modified TCA (Londry and Des Marais, 2003). Genes required for acetate oxidation were fairly common amongst the recovered genomes, present in 93 of the 163 recovered genomes. Of these genomes, 7 could perform acetate oxidation via the reverse Wood Ljungdahl pathway (reference pathway ko00720) and 79 via a modified TCA cycle using pyruvate ferredoxin oxidoreductase (EC: 1.2.7.1). These pathways were particularly abundant in Proteobacteria, Bacteroidetes and Spirochaetes genomes (Table 8-3). Genes for acetate oxidation were less prevalent than those for lactate oxidation, appearing in a minimum proportion of 46% of the acetate CSTR community and observed at a maximum of 76% of the lactate UAPBR effluent attached community (Figure 8-6).

**Formate metabolism**

During some forms of anaerobic respiration, pyruvate is acted on by formate C-acetyltransferase (EC: 2.3.1.54) to form acetyl-CoA and formate. This generated formate can in turn act as a valuable substrate for many anaerobic microorganisms and represents an important intermediate in syntrophic anaerobic environments (Jormakka et al., 2003).

Genes encoding formate dehydrogenase were found in 86 of the 163 recovered genomes. Formate dehydrogenases have been shown to catalyse the oxidation of formate linked to the reduction of $NAD^+$ but have also been shown to act in reverse in carbon fixation pathways (Yu et al., 2017). These genes were represented in an average of 51% of the microorganisms within each reactor system. In most instances, the representation of these genes in a reactor community was somewhat correlated with the representation of autotrophic pathways (Section 8.5.4) in these communities, perhaps indicating a more anabolic role of these genes. However, the representation of formate dehydrogenase (EC: 1.2.1.2 / EC: 1.2.2.1) genes was greater than that of autotrophic pathways in the acetate CSTR, lactate LFCR and lactate CSTR communities, respectively. This may indicate that a proportion of these microorganisms were involved catabolic oxidation of formate

to $CO_2$. Formate could arise in these organisms from the action of formate c-acetyltransferase (EC: 2.3.1.54) acting on pyruvate, generated from lactate, citrate, or amino acid oxidation, to form acetyl-CoA and formate (KEGG reaction R00212). In this instance, microorganisms will use organic carbon as an electron acceptor resulting in the generation of formate. Both formate and hydrogen can be formed during anaerobic metabolisms as electron sink products (Grobicki and Stuckey, 1989), but the production of formate, over of hydrogen production, appears to only be favoured at above neutral pH (Zoetemeyer et al., 1982; Voolapalli and Stuckey, 2001). Considering that the pH in the BSR reactors of this study rarely reached beyond 7.5, the far greater prevalence of hydrogen evolving hydrogenases (See Section 8.5.5) compared to formate metabolising genes is in line with other studies.

Formate dehydrogenases can, however, also be involved in methane oxidation. However, the gene encoding methane monooxygenase (EC: 1.14.13.25), catalysing the first reaction of methane oxidation, was only present in two low-abundance genomes, Thiomonas_65_14 and Brevundimonas_diminuta_67_12, indicating this reaction is unlikely to be occurring in these systems.

Genes involved in methanogenesis were detected in the single archaeal genome found exclusively in the inoculum and was not present in any of the reactor communities. The absence of methanogens in these reactors is explained by the treatment of the inoculum with the methanogenic inhibitor BESA. This was intended to allow acetate oxidising SRB to dominate the reactors and ensure successful SRB colonisation, minimising the start-up period. It is notable that this dominance was maintained absolutely for the duration of the study.

**Propionate oxidation**

It was demonstrated in Chapters 3 to 5 that a portion of lactate underwent fermentation to form propionate and acetate. Evidence of propionate oxidation was most prevalent in the lactate UAPBR where propionate generated in the inlet zone was not detected leaving the middle zone of the reactor. The capacity to oxidise propionate was therefore investigated and was inferred by the presence of one or more of three genes which encode enzymes which act on propanoyl-CoA and convert this to (S)-2-Methylmalonyl-CoA (Methylmalonyl carboxyltransferase (EC:2.1.3.1) or propanoyl-CoA carboxylase (EC:6.4.1.3)) or 2-methylcitrate synthase (EC:2.3.3.5). At least one of these three genes were present in 75 genome bins, most of which contained the gene for methylcitrate synthase (EC:2.3.3.5). All genomes classified as Bacteroidetes, approximately half of Proteobacteria and a third of Firmicutes genomes were found to be capable of propionate oxidation (Table 8-3). A *Desulfobulbus* detected in the attached and associated community of zones three through to six of the lactate UAPBR, by 16S rRNA gene amplicon sequencing, was implicated in propionate oxidation as described in Section 6.2.4, based on relative abundance across 17

samples. Three other SRB contained genes indicating the propensity of these microorganisms to oxidise propionate: Desulfobacterales_57_55, Desulfobulbus_propionicus_52_45 and Desulfobacca_acetoxidans_53_18.

Vanwonterghem et al. (2016) performed a genome-resolved metagenomic analysis of an anaerobic digestor and used a similar method to identify potential propionate oxidising microorganisms. These authors identified three Syntrophobacterales microorganisms which were likely capable of propionate oxidation. These three microorganisms were credited with maintaining low propionate concentrations in this reactor. The very high propionate concentrations seen in the lactate-supplemented BSR (>150 mg/ℓ) reactors of this study explain the pervasiveness of these genes through the BSR reactor communities.

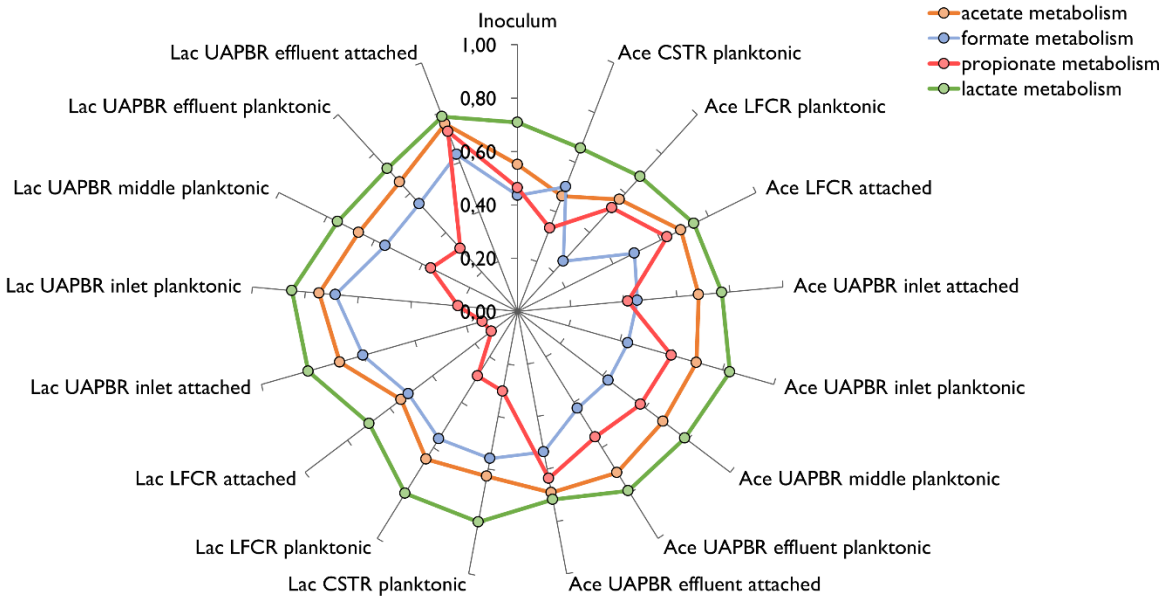


Figure 8-6 The cumulative proportions of the BSR reactor and inoculum microbial communities with the genetic capacity to perform several forms of volatile fatty acid oxidation. The proportion of each microorganism within a microbial community, capable of performing the described volatile fatty acid oxidation, were summed and displayed as a spider plot. Reactor samples are described by the reactor's supplemented electron donor [acetate (Ace) or lactate (Lac)], the reactor configuration and reactor zone, and the microbial phase [planktonic or biofilm (attached) community].

Table 8-3 Overview of the metabolic capacity of the 163 recovered genomes from the 17 sequenced bioreactor and inoculum samples. Metabolic features include the capacity to oxidise several volatile fatty acids, oxidise amino acids via the urea cycle, hydrogen metabolism, carbon fixation, dissimilatory sulphate reduction and sulphide oxidation. Genes investigated within each pathway are described in detail in Appendix A.5.1. The total number of recovered genomes classified to each phylum are shown in parentheses. The total number of genomes ascribed with a metabolic feature is displayed in the bottom row.

| | lactate metabolism | acetate metabolism | formate metabolism | propionate metabolism | citrate metabolism | urea cycle | hydrogen metabolism | autotrophy | dissimilatory sulphate reduction | sulphide oxidation (sox) |
|---|---|---|---|---|---|---|---|---|---|---|
| Proteobacteria (59) | 49 | 50 | 47 | 31 | 15 | 55 | 57 | 19 | 21 | 9 |
| Firmicutes (29) | 21 | 5 | 11 | 8 | 6 | 18 | 27 | 1 | 1 | 0 |
| Bacteroidetes (28) | 21 | 20 | 4 | 28 | 2 | 9 | 28 | 7 | 0 | 0 |
| Synergistetes (15) | 14 | 3 | 9 | 1 | 10 | 10 | 15 | 2 | 0 | 0 |
| Spirochaetes (12) | 7 | 7 | 6 | 0 | 5 | 9 | 12 | 0 | 0 | 0 |
| Thermotogae (4) | 2 | 0 | 3 | 3 | 1 | 0 | 4 | 0 | 0 | 0 |
| Tenericutes (4) | 3 | 0 | 1 | 0 | 2 | 0 | 3 | 0 | 0 | 0 |
| Planctomycetes (2) | 2 | 2 | 0 | 0 | 0 | 2 | 2 | 0 | 0 | 0 |
| Atribacteria (1) | 1 | 0 | 1 | 0 | 0 | 0 | 1 | 0 | 0 | 0 |
| Verrucomicrobia (3) | 3 | 3 | 1 | 1 | 1 | 3 | 3 | 0 | 0 | 0 |
| Microgenomates (1) | 0 | 0 | 0 | 0 | 0 | 0 | 0 | 0 | 0 | 0 |
| Chlorobi (1) | 0 | 1 | 0 | 0 | 0 | 1 | 1 | 1 | 0 | 0 |
| Cloacimonetes (1) | 0 | 0 | 1 | 1 | 0 | 0 | 0 | 0 | 0 | 0 |
| Actinobacteria (1) | 1 | 1 | 1 | 1 | 0 | 1 | 0 | 0 | 0 | 0 |
| Euryarchaeota (1) | 0 | 1 | 1 | 1 | 0 | 0 | 1 | 1 | 0 | 0 |
| Total (163) | 124 | 93 | 86 | 75 | 42 | 108 | 154 | 31 | 22 | 9 |

### 8.5.3 Alternate organic carbon sources

#### Citrate

Citrate was included in the reactor medium at 1.16 mM to prevent precipitation of media components during autoclaving. Citrate oxidation was observed in each reactor (Section 4.2.1, Section 4.4.1, Section 5.2.1, Section 5.4.1, Section 6.2.1 Section 6.4.1) and therefore the presence of genes required for citrate oxidation was investigated. The genes encoding citrate lyase (EC: 2.3.3.8), responsible for the conversion of citrate to oxaloacetate, and a citrate transporter were found in 42 genomes (Table 8-3). These were commonly found in a number of phyla including Synergistetes, Spirochaetes, Proteobacteria and Firmicute genomes, and were observed in only two low-abundance Bacteroide and five Spirochaete genomes (Table 8-3).

The abundance of the microorganisms with genes for citrate oxidation was commonly lowest in the attached microbial communities (Figure 8-7), appearing in an average of 14% of the microorganisms within these communities – omitting the lactate UAPBR inlet attached community where these genes were found in 47% of the community. Inversely, the average proportion of the planktonic microbial communities which contain citrate oxidation genes was 32%. This suggests that the microorganisms responsible for citrate oxidation are commonly enriched in the planktonic phases. The representation of these genes decreases across the length of both acetate and lactate

UAPBRs' planktonic communities – as they are observed to be highest in the inlet-zone decreasing in subsequent reactor zones. This corresponds with observed citrate oxidation observed in these reactors which occurred exclusively in the inlet zones.

### Amino acid oxidation

Yeast extract included in the reactor medium is a complex source of many micro and macro nutriets and is largely constituted of amino acids and small peptides (Izzo and Ho, 1991). Fermentative bacterial growth has been studied using yeast extract and has been found to be supported through amino acid utilisation (Benthin and Villadsen, 1996). The incomplete oxidation of yeast extract to acetate was demonstrated in each of the reactors and is discussed in Section 4.4.2, of Chapter 4. The ability to utilise amino acids as a carbon source was inferred from the presence of genes for the urea cycle (reference pathway ko00220). These genes encode argininosuccinate lyase (EC: 4.3.2.1), argininosuccinate synthase (EC: 6.3.4.5), carbamoyl-phosphate synthase (EC: 6.3.5.5), ornithine carbamoyltransferase (EC: 2.1.3.3) and ureohydrolase arginase (EC: 3.5.3.1). These genes were found in 108 genomes, which included 55 of the 56 recovered Proteobacteria genomes and high proportions of Synergistetes and Spirochaetes genomes. The representation of these genes in the reactor and inoculum microbial communities was, in most samples, the second most prevalent form of organic carbon metabolism following acetate oxidation – present in, on average, 65% of each microbial community (Figure 8-7).

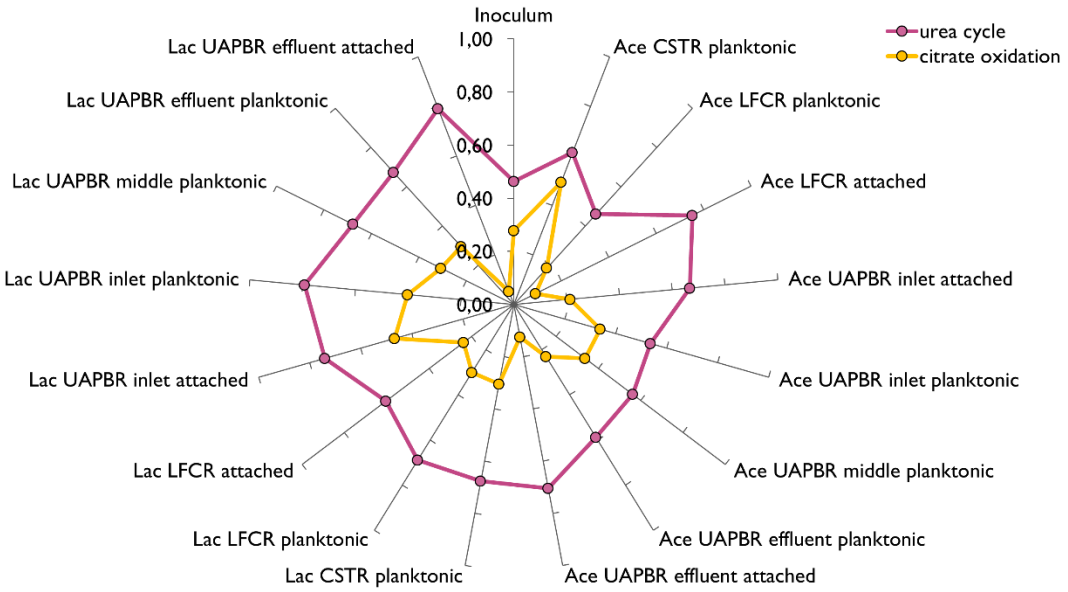


Figure 8-7 The cumulative proportions of the BSR reactor and inoculum microbial communities with the genetic capacity to use citrate and amino acids as a carbon source and electron donor. The ability of a microorganism to utilise citrate was inferred by the presence of genes encoding a citrate transporter and citrate lyase. The ability to utilise amino acids was inferred from the presence of genes for enzymes involved in the urea cycle (Appendix A.5.1). The proportion of each microorganism within a microbial community, capable of performing citrate or amino acid oxidation, were summed and displayed as a spider plot.

Reactor samples are described by the reactor's supplemented electron donor [acetate (Ace) or lactate (Lac)], the reactor configuration and reactor zone, and the microbial phase [planktonic or biofilm (attached) community].

### 8.5.4 Autotrophy

It was evident that bicarbonate concentrations in the acetate-supplemented reactors were far lower than predicted (Section 4.5.4, Section 5.5.1 and Section 6.5.3). The potential for bicarbonate to be fixed into biomass through carbon fixation pathways was investigated. The pH of the reactors, lying largely between 7.0 and 8.0, would result in 82-97% of the produced bicarbonate remaining as bicarbonate. The remaining bicarbonate would be protonated to form carbon dioxide and water. Carbon fixation could, therefore, proceed through direct fixation of lower concentrations of dissolved carbon dioxide, or through the conversion of bicarbonate to carbon dioxide catalysed by carbonic anhydrase within the cell. Genes encoding bicarbonate anhydrases were widespread amongst genomes with autotrophic pathways (Figure 8-5).

Evidence of autotrophic genes was found in 31 genomes, 24 of which also contained the gene for carbonic anhydrase. Eleven of the 31 genomes were also capable of dissimilatory sulphate reduction. Three carbon fixation pathways were investigated. Nine genomes contained genes for the Wood Ljungdahl pathway (reference pathway ko00720, M00377) of which seven were found in Proteobacteria genomes (Figure 8-5). No genomes contained a complete CBB pathway (reference pathway ko0070, M00165). Carbon fixation via reverse TCA cycle (reference pathway ko00720, M00173) was found in 25 genomes, most of which were Bacteroidetes or Proteobacteria.

No genome containing the genes for autotrophy did not also contain genes for either acetate or lactate oxidation (Figure 8-5). Therefore, these organisms are likely facultative autotrophs. The presence of these autotrophic gene pathways in a sample, therefore, does not implicitly indicate autotrophy is occurring. Autotrophic genes were represented in each BSR reactor community, commonly co-occurring with NiFe group 1 and/or group 3 hydrogenases (see below; Figure 8-10).

### 8.5.5 Hydrogen metabolism

Hydrogenase genes were ubiquitous throughout the genomes from the BSR reactor systems, represented in 156 of the 163 recovered genomes. Particularly remarkable is the pervasiveness of these genes amongst phyla not ubiquitously implicated in hydrogen metabolism. Genes for FeFe hydrogenases were found in 93% of Firmicute, 89% of Bacteroidetes and all Spirochete genomes recovered from the BSR reactor systems (Table 8-4). Peters et al. *(*2015) surveyed nearly 3000 published bacterial and archaeal genomes for hydrogenase genes and found FeFe hydrogenase

genes in 9 of 94 surveyed Bacteroidetes genomes, 160 of 622 Firmicutes and 20 of 65 Spirochaete genomes. The enrichment of these microorganisms in the BSR reactor systems from phyla not ubiquitously implicated in hydrogen metabolism, as well as the presence of multiple forms of hydrogenase genes throughout the entire microbial community, is indicative of hydrogen evolution and consumption being an important form of metabolism in these reactors.

Similar conclusions were made by Probst et al. (2017) who performed a genome-resolved metagenomic analysis of a microbial community within a subsurface aquifer. These authors identified a number of mixotrophic bacteria with autotrophic gene pathways as well as several hydrogenase genes. It was concluded that these mixotrophic bacteria were likely consuming hydrogen generated by fermentative microorganisms and fixing $CO_2$ which was abundant in the environment.

Table 8-4 Distribution of hydrogenase genes among the microbial phyla recovered from the BSR reactor microbial communities. The predicted function of these hydrogenases are as described in Peters *et al. (*2015). The number of genomes containing a class of hydrogenase gene is shown. The total number of genomes recovered per phylum is shown in parentheses. All gene predictions were made using HMMs described by Anantharaman et al. (2016).

| | group 1 [NiFe] (uptake) | group 2a [NiFe] (uptake) | group 2b [NiFe] (regulatory) | group 3b [NiFe] (bidirectional) | group 3c/3d [NiFe] (bidirectional) | group 4 [NiFe] (evolving) | group A [FeFe] (evolving) | group B1 [FeFe] (evolving) |
|---|---|---|---|---|---|---|---|---|
| Proteobacteria (59) | 26 | 2 | 1 | 14 | 10 | 55 | 8 | 0 |
| Firmicutes (29) | 5 | 0 | 0 | 1 | 1 | 5 | 24 | 14 |
| Bacteroidetes (28) | 0 | 0 | 0 | 0 | 1 | 9 | 23 | 12 |
| Synergistetes (15) | 0 | 0 | 0 | 0 | 6 | 12 | 8 | 8 |
| Spirochaetes (12) | 0 | 0 | 0 | 0 | 0 | 0 | 12 | 8 |
| Thermotogae (4) | 0 | 0 | 0 | 0 | 0 | 3 | 4 | 1 |
| Tenericutes (4) | 0 | 0 | 0 | 0 | 0 | 1 | 3 | 0 |
| Planctomycetes (2) | 0 | 0 | 0 | 1 | 1 | 1 | 2 | 0 |
| Atribacteria (2) | 0 | 0 | 0 | 0 | 0 | 2 | 2 | 0 |
| Verrucomicrobia (2) | 0 | 0 | 0 | 0 | 0 | 2 | 1 | 0 |
| Microgenomates (1) | 0 | 0 | 0 | 0 | 0 | 0 | 0 | 0 |
| Chlorobi (1) | 1 | 0 | 0 | 1 | 0 | 1 | 0 | 0 |
| Lentishphaerae (1) | 0 | 0 | 0 | 0 | 0 | 1 | 1 | 1 |
| Cloacimonetes (1) | 0 | 0 | 0 | 0 | 0 | 0 | 0 | 0 |
| Actinobacteria (1) | 0 | 0 | 0 | 0 | 0 | 0 | 0 | 0 |
| Euryarchaeota (1) | 0 | 0 | 0 | 0 | 1 | 1 | 0 | 0 |
| Total (163) | 32 | 2 | 1 | 17 | 20 | 93 | 88 | 44 |

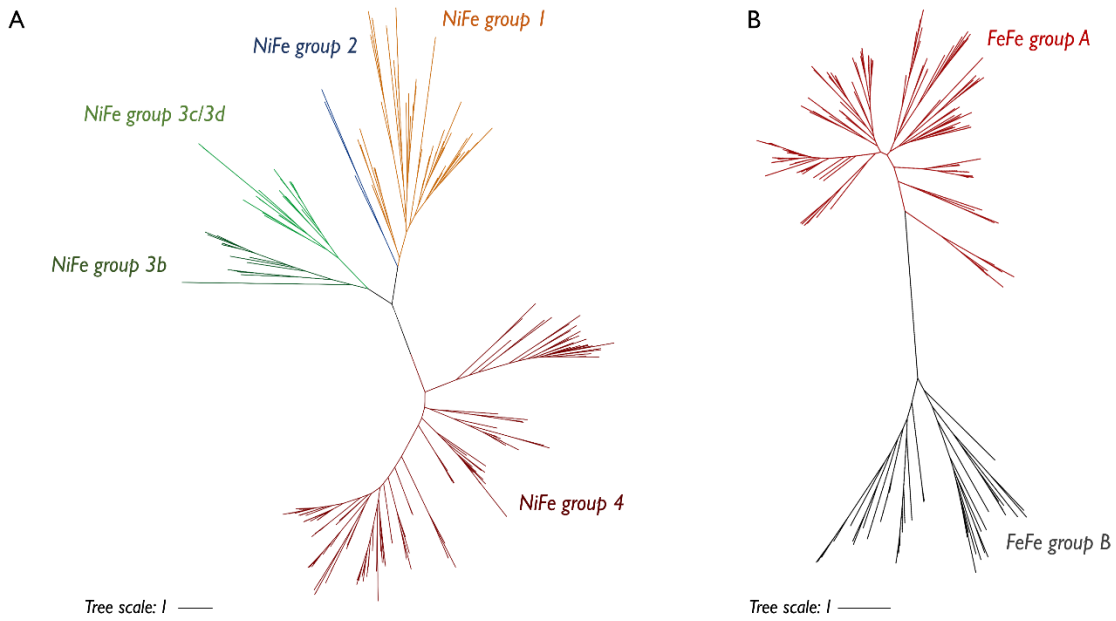


Figure 8-8 The phylogeny of the (A) NiFe and (B) FeFe hydrogenase genes identified from 156 of the total 163 genomes recovered from the BSR reactor and inoculum communities. Hydrogenase gene sequences identified by HMMs were muscle aligned and neighbour-joined in this unrooted tree. The branches of the tree are coloured based on the classifications of the HMM from which they were identified.

The most common hydrogenase genes identified were NiFe group 4 and FeFe group A hydrogenases (Table 8-4, Figure 8-8 and Figure 8-9), commonly predicted to catalyse the evolution of hydrogen (Vignais and Colbeau, 2004; Greening et al., 2016). The proportion of these two hydrogenases represented in a microbial community were often anticorrelated (Figure 8-9) and largely reflects the competition of Proteobacteria and Synergistetes (NiFe hydrogenases) with Bacteroidetes, Firmicutes and Spirochaetes (FeFe hydrogenases; Table 8-4). The prevalence of group 4 NiFe and FeFe hydrogenases were typically higher in the three lactate systems, reflecting the additional degree of fermentation taking place in these reactors.

The presence of the hydrogen evolving hydrogenases is believed to have been selected for by the absence of alternate electron acceptors for anaerobic growth in these reactors. No nitrate was included in the reactor medium, although sulphate reduction was highly prevalent little to no elemental sulphur was generated, and the original inoculum was incubated with the methanogenic inhibitor BESA preventing oxidised carbon being used as an electron acceptor. This leaves few alternatives for anaerobic microorganisms other than to remove electrons from the cells in the form of organic carbon or hydrogen. The generation of this energy-rich molecule would, in turn, lead to the selection of microorganisms which can oxidise this hydrogen using alternative forms

of hydrogenase genes. The electrons extracted from hydrogen could then be captured as sulphide when using sulphate as the terminal electron acceptor, and/or be incorporated into microbial biomass in combination with autotrophy.

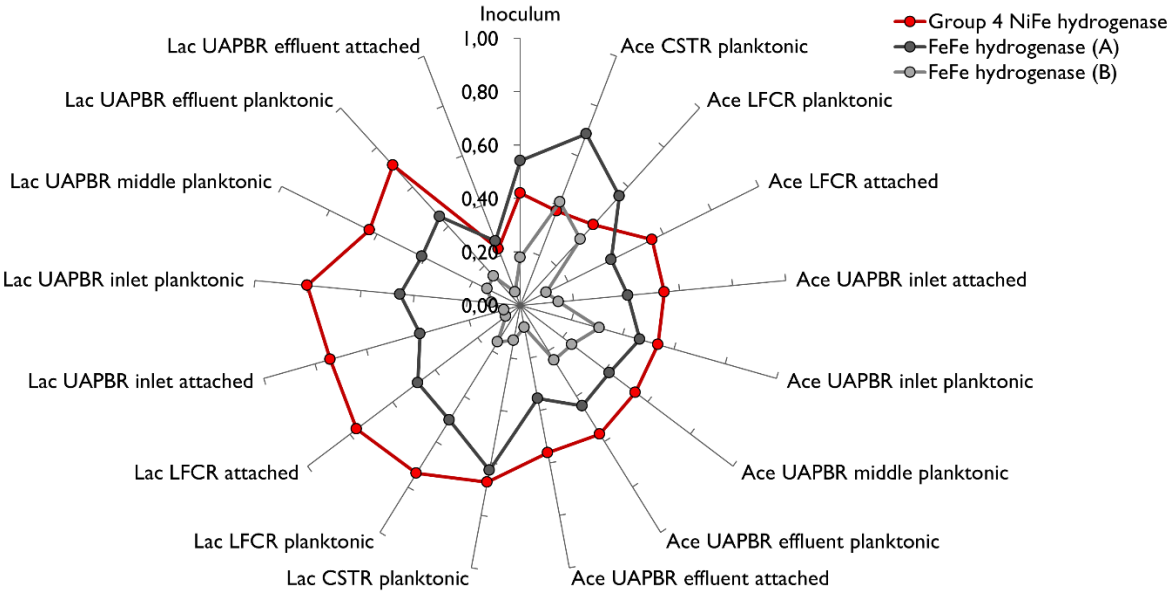


Figure 8-9 The cumulative proportions of the BSR reactor and inoculum microbial communities containing genes for group 4 NiFe hydrogenases, group A FeFe hydrogenases and group B FeFe hydrogenases. The proportion of each microorganism within a microbial community containing these genes were summed and displayed as a spider plot. Reactor samples are described by the reactor's supplemented electron donor [acetate (Ace) or lactate (Lac)], the reactor configuration and reactor zone, and the microbial phase [planktonic or biofilm (attached) community].

It is therefore unsurprising that several group 1 and 3 NiFe hydrogenases genes were also detected across multiple phyla in the BSR reactor systems, most frequently in Proteobacteria as well as some Firmicutes and Synergistetes. NiFe group 1 hydrogenases are commonly membrane-bound and function by oxidising hydrogen and transferring the acquired electron to the quinone pool via a cytochrome (Peters et al., 2015). The presence of a group 1 hydrogenase is a strong indicator of the ability to consume hydrogen. This hydrogenase is commonly found in *Desulfovibrio* species (Fauque et al., 1988) and has been shown to be essential for the activity of *Desulfovibrio gigas* grown on sulphate and hydrogen (Morais-Silva et al., 2013). All identified SRB contained gene(s) for group 1 hydrogenase and, therefore, the abundance of these genes co-occurred with dissimilatory sulphate reduction genes across most samples (Figure 8-5, Figure 8-10).

NiFe group 3 hydrogenase genes were found to be abundant in almost all attached microbial communities, with little representation in any of the planktonic communities (Figure 8-10). These hydrogenases are bidirectional and are able to catalyse both $H_2$ consumption or generation (Houchins, 1981; Ma et al., 1993; Berney et al., 2014).

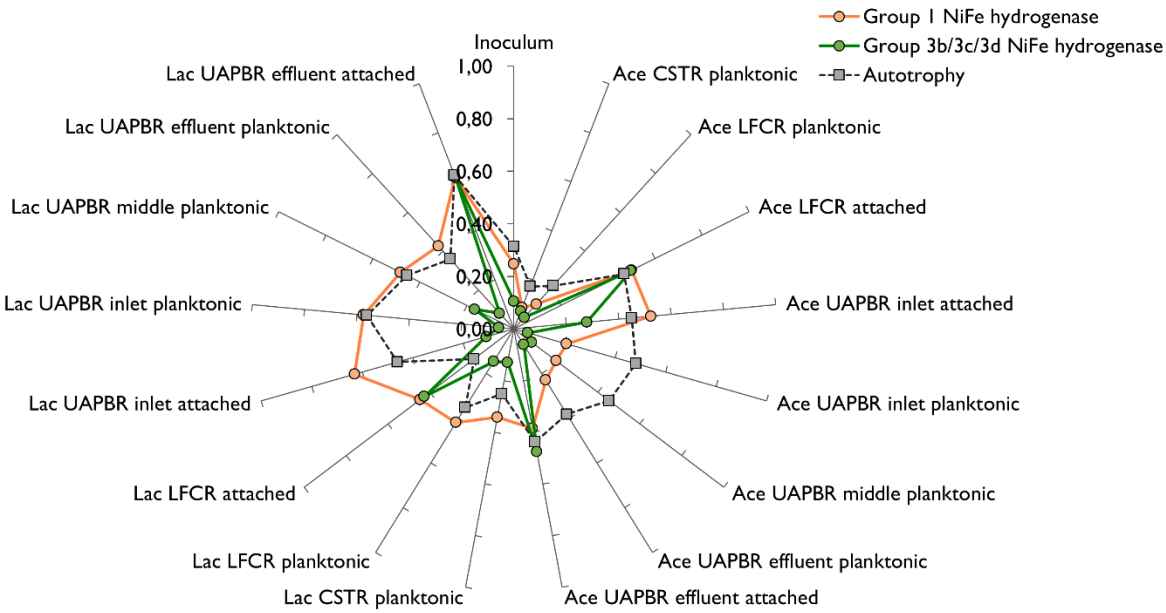


Figure 8-10 The cumulative proportions of the BSR reactor and inoculum microbial communities containing genes for group 1 NiFe hydrogenases, group 3 NiFe hydrogenases and either the reverse TCA or Wood Ljungdahl pathway for autotrophic growth. The proportion of each microorganism within a microbial community containing these genes were summed and displayed as a spider plot. Reactor samples are described by the reactor's supplemented electron donor [acetate (Ace) or lactate (Lac)], the reactor configuration and reactor zone, and the microbial phase [planktonic or biofilm (attached) community]. The proportion of the communities containing group 2 NiFe hydrogenases are not displayed as these genes were not present at greater than 5% in any microbial community.

## 8.6 Co-occurrence of metabolic features across reactor samples

The BSR reactor microbial samples were compared based on the abundance of metabolic features discussed in Section 8.5 using hierarchical clustering (Figure 8-11). This revealed that biofilm communities in zones exposed to acetate in the absence of lactate ("acetate attached", includes the lactate UAPBR effluent attached community) had a similar distribution in observed metabolic features. This was similarly true of all acetate planktonic samples, while both lactate planktonic and lactate attached samples clustered together. Although there are large variations in the individual microorganisms which dominate each of the sixteen reactor communities, it is apparent that the metabolic potential which results is deterministically driven.

The acetate planktonic communities showed some of the highest prevalence of citrate oxidation genes (Figure 8-7). Unlike within the lactate supplemented systems, citrate would be the most reduced carbon species in the acetate supplemented systems. The prevalence of these genes in the acetate systems is, therefore, to be expected. It is interesting to note that the prevalence of these genes was greatly reduced in the acetate attached samples. Citrate oxidation genes co-occurred with FeFe group A and B hydrogenase genes, suggesting fermentative citrate oxidation, leading to the evolution of hydrogen. This provides some evidence against dissimilatory sulphate

reduction linked to citrate oxidation by *Desulfovibrio_desulfuricans_58_43*, due to the higher than average competition for this substrate. The acetate planktonic communities also showed the lowest proportion of dissimilatory sulphate reduction compared to all other samples.

The acetate attached communities showed the inverse prevalence of tested metabolic features (Figure 8-11). These communities showed some of the lowest proportions of citrate oxidation and FeFe hydrogenase genes but showed a far higher prevalence of NiFe group 3 hydrogenases, dissimilatory sulphate reduction, formate metabolism and genes for the urea cycle. The lactate samples showed similar degrees of dissimilatory sulphate reduction, formate oxidation and genes for the urea cycle to that of the acetate attached community. However, the lactate communities showed a higher prevalence of NiFe group 4 hydrogenases, lactate oxidation, citrate oxidation and FeFe hydrogenases compared to the acetate attached communities (Figure 8-11).

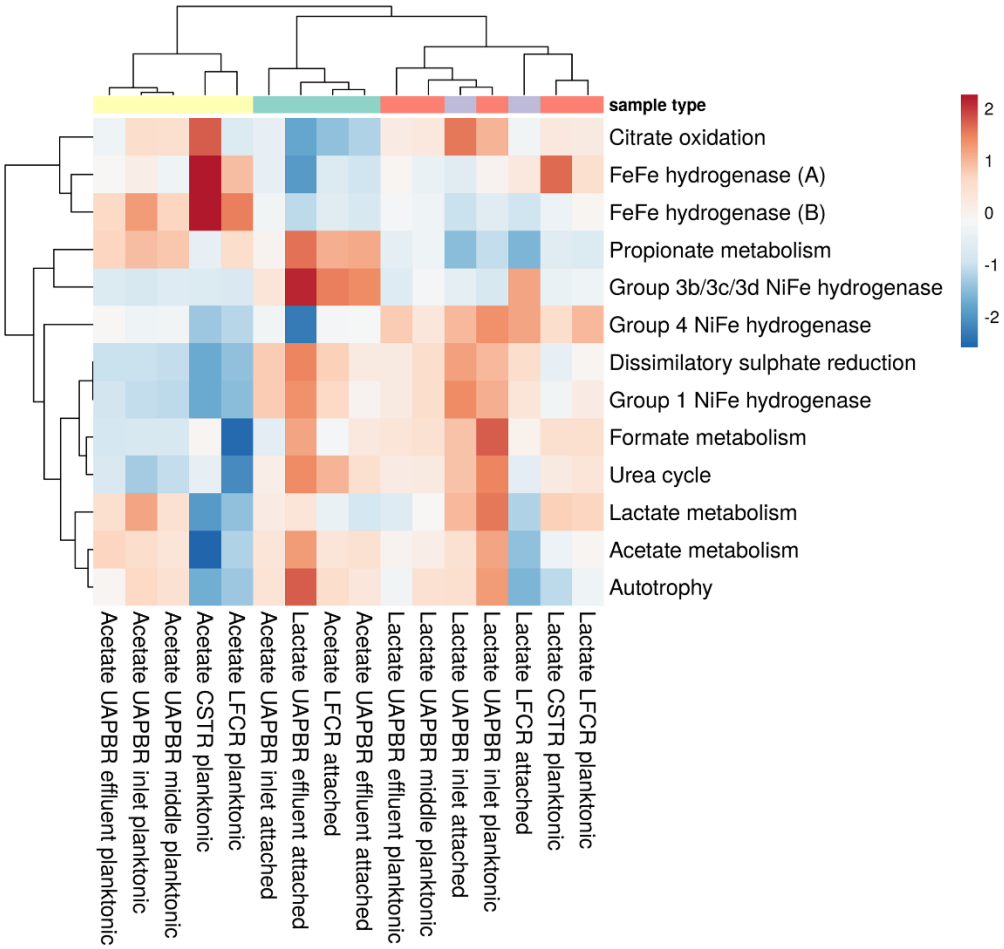


Figure 8-11 The distribution of various metabolic features among the BSR reactor microbial communities. The proportion of a microbial community possessing a various metabolic feature was used to perform hierarchical clustering (using correlation), on the reactor communities and each metabolic feature. Unit variance centering was performed on each row of the heatmap. The degree of variance from the mean of each row is shown in the legend. The reactor community samples are categorised into sample type as (■) acetate attached, (■) acetate planktonic, (■) lactate attached and (■) lactate planktonic. The lactate UAPBR effluent attached was classified as "acetate attached" as this community was never exposed to lactate due to all lactate being consumed in the inlet zone of this reactor. Planktonic communities in this zone remain classified as "lactate planktonic" as this community originates from the inlet zone and is transported to the effluent zone by plug flow. The metabolic features "Acetate oxidation" and the "urea cycle" were omitted as the proportions of these genes were largely uniform throughout all reactor communities. Group 1 hydrogenases were omitted as these genes almost perfectly co-occurred with dissimilatory sulphate reduction.

## 8.7 CSTR metagenomes

The acetate CSTR was dominated by a number of high abundance Synergistales and Sphaerochaete genomes which possessed genes for the urea cycle and citrate uptake and oxidation (Figure 8-12). These genomes also contained FeFe hydrogenases and some NiFe group 4 hydrogenases (hydrogen evolving; Vignais and Colbeau, 2004). The (i) minimal acetate oxidation, the (ii) complete oxidation of citrate and the (iii) degree of acetate generation from yeast extract oxidation observed in the acetate CSTR (Chapter 5) allows a substantial degree of amino acid and citrate fermentation to be attributed to these Synergistales and Sphaerochaete microorganisms. This fermentation together with the presence of group 4 hydrogenases indicates the generation of hydrogen. This Synergistales_64_17 was also the most abundant microorganism in the lactate CSTR and may, therefore, play the same role in this reactor.

Several lower abundance microorganisms, including a *Desulfovibrio* and a *Desulfomicrobium* genome, possessed genes for carbon fixation. These genomes also contained genes for NiFe group 1 hydrogenases which have been characterised to oxidise hydrogen and are therefore capable of providing an electron donor for the proposed autotrophy.

Alternatively, all SRB genomes in acetate CSTR contained genes for acetate oxidation and may well be using acetate as their electron donor, which was presumed in Chapter 5 and is supported by solution chemistry data at multiple HRT (Section 4.4.1). Desulfovibrio_desulfuricans_58_43 was the only genome containing both genes for dissimilatory sulphate reduction and citrate oxidation. The possibility that this organism was able to couple sulphate reduction and citrate oxidation cannot be excluded. However, this microorganism was shown to experience a nearly 100-fold reduction in relative abundance at a three-day HRT (0.014 $h^{-1}$) and does not subsequently recover (Section 4.4.3). This indicates that citrate oxidation was not linked to sulphate reduction at HRT shorter than four-days. The attributing of particular electron donors to sulphate reduction is expanded in Section 8.11 (BSR mixotrophic metabolic model).

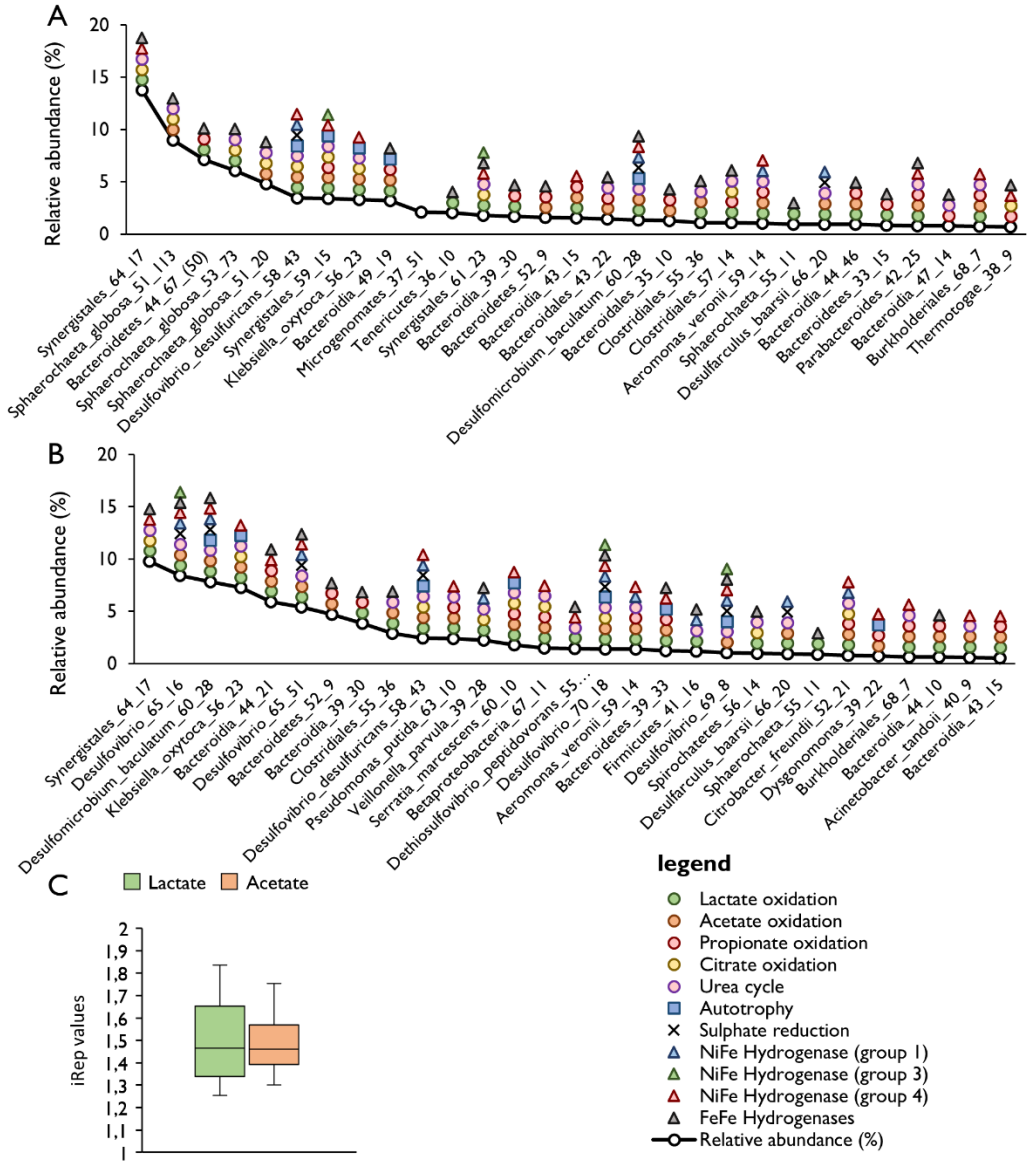


Figure 8-12 Rank abundance and metabolic potential of the most dominant genomes in the (A) acetate and (B) lactate supplemented CSTRs at a four-day HRT (0.01 $h^{-1}$). The genes and gene pathways used to infer metabolic potential are shown in Appendix A.5.1. Community stability (C) is represented as iRep values of all recovered genomes within the acetate ($n$=34) and lactate ($n$=30) CSTRs. iRep values are displayed as box and whisker plots – the box represents the interquartile range (IQR; from the 25$^{th}$ percentile, to the median and to the 75$^{th}$ percentile). The maximum and minimum of each plot were calculated as the 75$^{th}$ percentile plus 1.5 multiplied by the IQR and 25$^{th}$ percentile minus 1.5 multiplied by the IQR, respectively.

Six dominant SRB were found within the lactate CSTR, the same *Desulfovibrio* and *Desulfomicrobium* that were seen in the acetate CSTR as well as two other *Desulfovibrio* and a *Desulfarculus* genome. The second-most predominant non-SRB with the ability to oxidise lactate was a *Klebsiella oytoca*. Although presumed to be one of the SRB's major competitor for lactate, this microorganism also contained the genes necessary for acetate, citrate and amino acid oxidation. This genome was tentatively matched to an Enterobacter OTU (OTU 16) from the 16S rRNA gene amplicon sequencing, however, this could not be confirmed as no 16S rRNA gene was binned with the genome. OTU 16 showed similar abundance patterns across the 17 samples and is the only OTU classified to the shared family of Enterobacteriaceae. This OTU becomes one of the most dominant OTUs in both the lactate CSTR and LFCR at HRT from a two-day HRT.

## 8.8 UAPBR metagenomes

### 8.8.1 Acetate UAPBR

The observed relative abundance of the genomes of the acetate UAPBRs were clustered based on their differential relative abundance across the three planktonic microbial communities and the inlet and effluent attached communities (Figure 8-13). Hierarchical clustering revealed a differential dominance of most microorganisms for one or multiple of these communities, with a striking separation of many SRB genomes on this basis.

Five of these clusters have been annotated in Figure 8-13. SRB were present in each of these, except the cluster I that formed from microorganisms which increased in abundance from the inlet to the effluent planktonic community. Many of these organisms, the most abundant of which was Paracoccus_69_26, were found to be capable of sulphide oxidation via the *sox* gene pathway (Figure 8-5). It is possible that small quantities of oxygen may have entered the headspace above the effluent port and mediated minor quantities of sulphide oxidation.

Cluster II in Figure 8-13 grouped microorganisms which were prevalent in the three planktonic microbial communities and included some organisms which also prevalent in an attached community. These included the dominant SRB Desulfovibrio_desulfuricans_58_43, and Desulfomicrobium_baculatum_60_28. In addition, Bacteroidetes_41_9_47_32 was also observed in these communities in high abundance. This genome was also detected in the middle-planktonic and effluent planktonic and attached community of the lactate UAPBR. This genome contained genes for acetate oxidation and the rTCA but did not contain genes for citrate oxidation, nor the urea cycle, indicating that this microorganism was a direct competitor with SRB for acetate and/or

bicarbonate and hydrogen. Paracoccus_versutus_68_139 was found in the planktonic communities of the inlet and middle zones before showing a pronounced reduction in abundance in the effluent planktonic community. This microorganism contained genes for citrate oxidation, the urea cycle and hydrogen evolving group NiFe hydrogenases. It is thought that this microorganism may have been the dominant fermenter within this system and likely the greatest contributor towards the hydrogen that was potentially produced in this reactor.

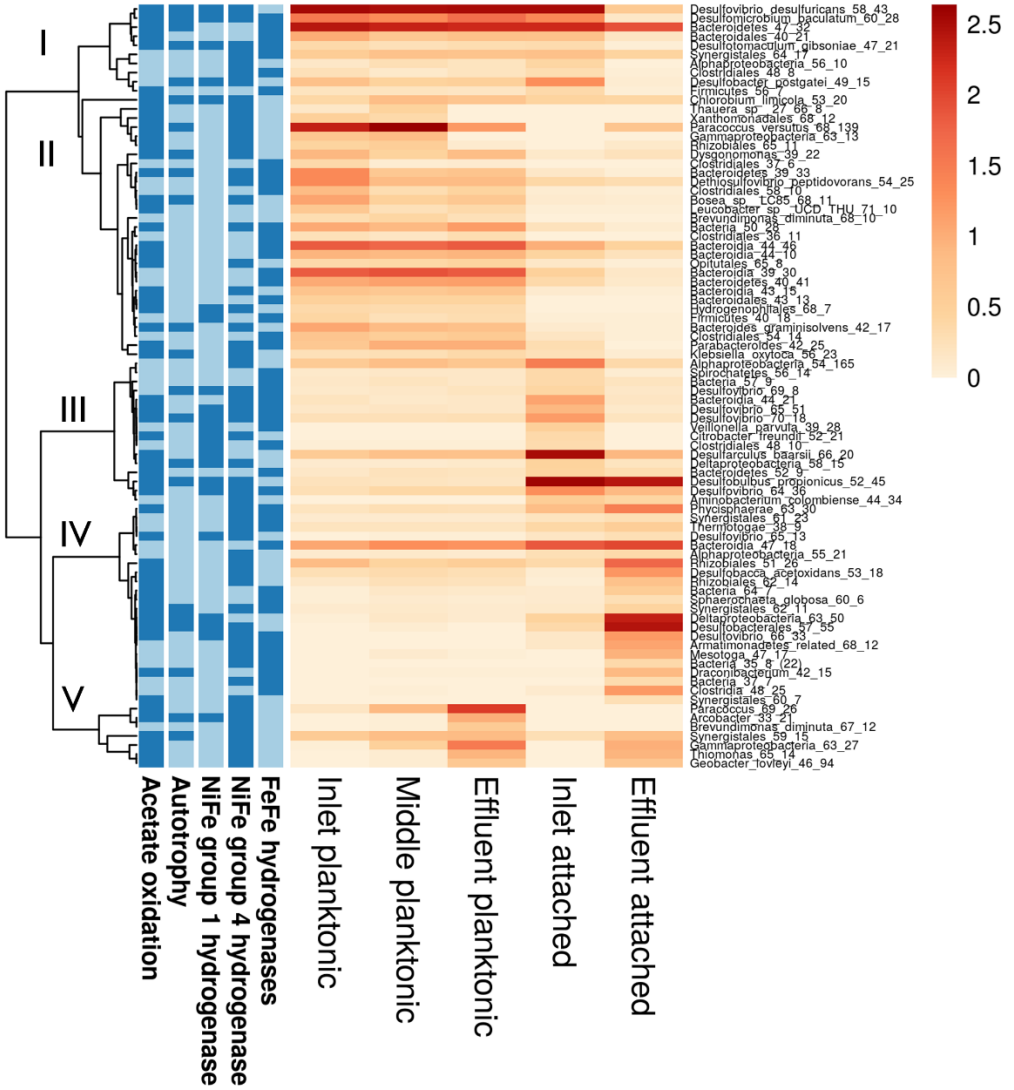


Figure 8-13 The distribution of recovered genomes throughout the microbial communities of the acetate supplemented up-flow anaerobic packed bed reactor (UAPBR) shown as ln(x +1) transformed relative abundances. Hierarchical clustering was performed using correlation distance and average linkage. The presence (■) and absence (■) of metabolic features within each genome are shown.

Four SRB, namely Desulfobacterales_57_55, Deltaproteobacteria_63_50, Desulfobacca_acetoxidans_53_18 and Desulfovibrio_66_33 were found nearly exclusively in the attached

community of the effluent zone (cluster IV). It can, therefore, be concluded that these SRB are sulphate scavengers. The two lower-abundance SRBs, namely Desulfobacca_acetoxidans_53_18 and Desulfovibrio_66_33, contained genes for acetate oxidation but not for carbon fixation. Whereas the higher abundant SRBs contained genes for both acetate oxidation and carbon fixation and it is, therefore, likely that these microorganisms employ mixotrophic metabolism of both acetate oxidation and carbon fixation. Further evidence to describe this form of metabolism is described in Section 8.11. All of these SRB contain genes for NiFe group 1 hydrogenases and are thus able to consume hydrogen produced within this reactor.

Twelve genomes, three of which were SRB, were found to be similar in abundance in both the inlet and effluent attached communities (Figure 8-13). The localisation of these SRB, in particular, is an interesting occurrence as these microorganisms appear to be adept at rapid sulphate reduction within the inlet zone as well as sulphate scavenging in the effluent region of the reactor.

Another cluster (cluster III) was constituted by microorganisms which showed the highest abundance in the inlet attached community, the most prevalent of which was the SRB Desulfarculus_baarsii_66_20. Coincidentally, this SRB was also found to be present in only the inlet attached community of the lactate UAPBR. Of the seven most abundant SRB identified in this reactor, this was the only SRB to not contain a pathway for carbon fixation. Genes linked to acetate oxidation, and four of five the genes encoding the enzymes of the urea cycle were identified within this genome, indicating its likely carbon sources.

### 8.8.2 Lactate UAPBR

Hierarchical clustering of the relative abundances of all of the genomes recovered from the five communities of the lactate UAPBR (Figure 8-14) resolved into three clusters, namely genomes which appear primarily in the planktonic communities (II), those which occur in the effluent attached communities (I) and those which occur predominantly in the inlet attached community (III).

A small number of microorganisms, the majority of which were SRB, dominated each of these five communities. As seen in the acetate UAPBR, Desulfovibrio_desulfuricans_58_43 and Desulfomicrobium_baculatum_60_28 dominated the inlet, middle and effluent planktonic communities as well as the inlet attached community of this reactor system. Deltaproteobacteria_63_50 was found above 50% relative abundance in the effluent attached community of this reactor. Based on the localisation of this SRB to the effluent zone, as well as its metabolic potential, this SRB is potentially aligned implicated attributed with acetate oxidation and potentially carbon fixation.

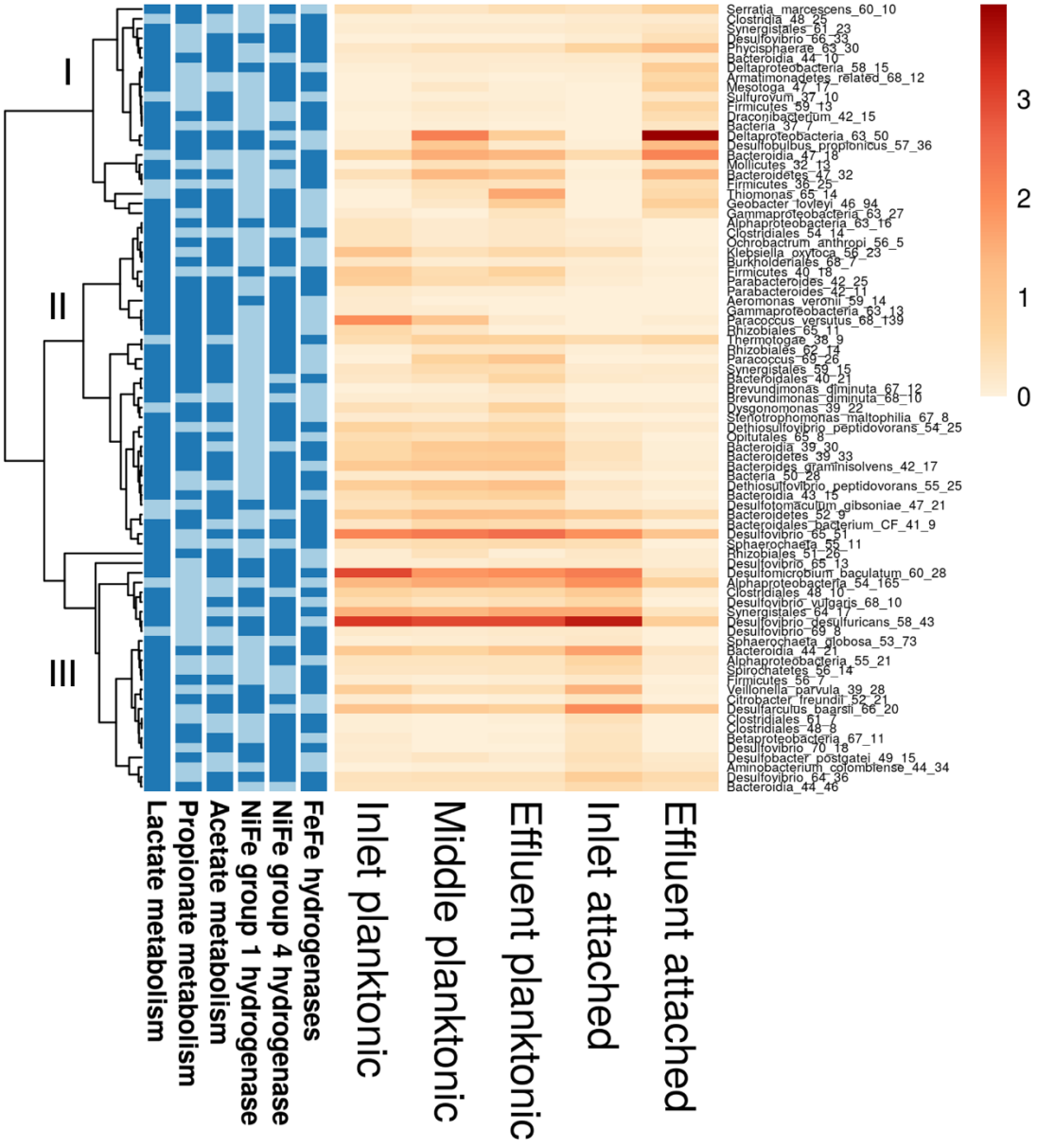


Figure 8-14 The distribution of recovered genomes throughout the microbial communities of the lactate supplemented up-flow anaerobic packed bed reactor (UAPBR) shown as ln(x +1) transformed relative abundances. Hierarchical clustering was performed using correlation distance and average linkage. The presence (■) and absence (■) of metabolic features within each genome are shown.

Bacteroidia_47_18 found in the effluent attached community had the genetic potential to oxidise acetate. As concluded for the Bacteroidetes genome identified in the lactate UAPBR effluent, it is believed that Bacteroidia_47_18 too was competing with SRB for acetate. Although, within the context of reactor performance, the activity of this microorganism would lead to further removal of COD from the effluent stream. Four dominant organisms were seen in the inlet zone, attached

and the three planktonic communities: Paracoccus_versutus_68_139, Alphaproteobacteria_54_165, Bacteroidia_44_21 and Synergistales_64_17, each of which contained genes for group 4 NiFe hydrogenases. *Paracoccus versutus*, thought to be the main competitor with planktonic SRB for lactate in this reactor, decreases in abundance between the inlet planktonic community and middle and effluent planktonic communities, which is consistent with the consumption of lactate exclusively in the inlet zone.

## 8.9 LFCRs

Genome-resolved metagenomics revealed that the LFCRs were less dominated by SRB in comparison to the UAPBRs' microbial communities (Figure 8-15). The biofilm communities of the acetate and lactate LFCRs held considerably more SRB diversity than was seen in the corresponding planktonic communities. Only two predominant SRB were observed within the acetate LFCR planktonic community at a four-day HRT. These were the frequently occurring *Desulfovibrio_desulfuricans_58_43*, which was linked to the *Desulfovibrio* OTU (6) which washed out of the CSTR and LFCR planktonic communities at reduced HRT, and the Clostridia *Desulfotomaculum gibsoniae* which was also present in the corresponding biofilm community. Both of these genomes contained genes for sulphate reduction, acetate oxidation, autotrophy and hydrogen consumption. The biofilm community within this reactor was dominated by a Desulfobacterales which was present above 25% relative abundance. This genome, as was seen in five of the seven predominant SRB in this community, contained genes for autotrophy and hydrogen consumption. The representation of autotrophic genes in this community was one of the highest observed from the sixteen bioreactor samples, occurring in 45% of the microorganisms within this sample. This compared to the lactate biofilm community were autotrophic gene pathways were represented in just 19% of the bacterial community.

The lactate LFCR planktonic community was dominated by the two frequently occurring Desulfovibrio_desulfuricans_58_43 and Desulfomicrobium_baculatum_60_28, as seen in the lactate CSTR. Two further *Desulfovibrio* genome bins were identified in this sample, both containing lactate dehydrogenase genes. The major competitor of the SRB, for lactate, is likely a *Klebsiella oxytoca*. This is the same *Klebsiella* identified in the planktonic community of the lactate CSTR at a four-day HRT. The Synergistales_64_17 present in this planktonic community is also likely to compete with SRB for available lactate. However, as previously stated, its abundance and frequency in both acetate and lactate systems, together with its genomic potential for citrate oxidation and the urea cycle, suggest this microorganism is more likely involved in the fermentation of citrate and/or amino acids.

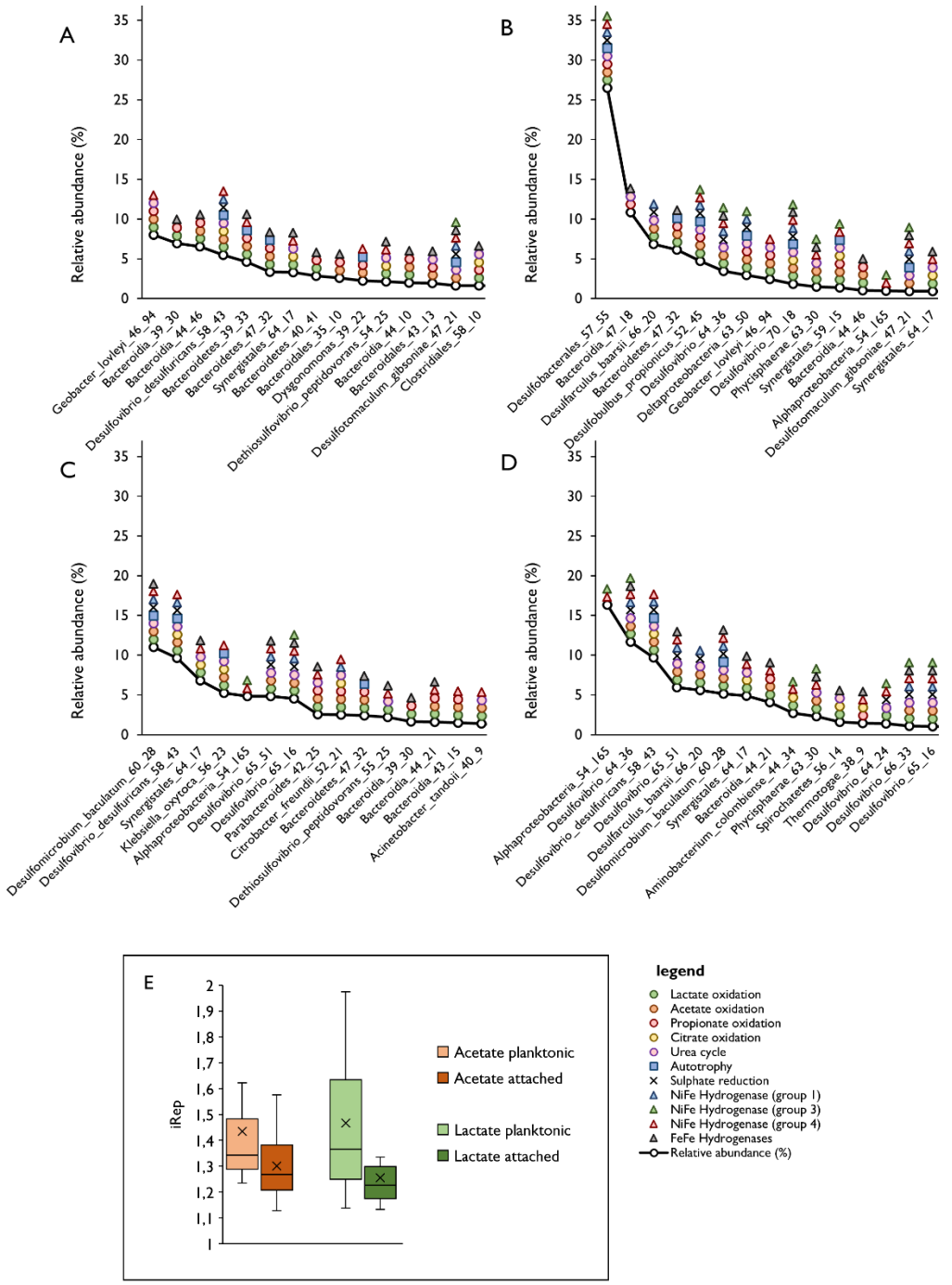


Figure 8-15 Rank abundance and metabolic potential of the most dominant genomes in the (A) acetate planktonic, (B) acetate attached, (C) lactate planktonic and (D) lactate attached LFCR microbial communities at a four-day HRT (0.01 $h^{-1}$). The genes and gene pathways used to infer metabolic potential are described in Appendix A.5.1. Community stability (E) is represented as iRep values of all recovered genomes within the acetate planktonic (*n*=20), acetate attached (*n*=9), lactate planktonic (19) and lactate attached (*n*=13) LFCRs. iRep values are displayed as box and whisker plots – the box represents the interquartile range (IQR; from the 25$^{th}$ percentile, to the median and to the 75$^{th}$ percentile). The maximum and minimum of each plot were calculated as the 75$^{th}$ percentile plus 1.5*IQR and 25$^{th}$ percentile minus 1.5*IQR, respectively.

Within the biofilm community of the lactate LFCR, six *Desulfovibrio*, the *Desulfomicrobium* and a *Desulfarculus* genome were recovered. These SRB are able to metabolise lactate and most were also able to metabolise acetate. However, very few microorganisms (12%) in this biofilm community possessed the genes required for propionate oxidation. The proportion of the lactate planktonic community able to metabolise propionate was nearly three-fold greater than in this corresponding biofilm community. No SRB present in the lactate-supplemented LFCR was able to metabolise propionate – representing a valuable substrate that was not linked to sulphate reduction.

## 8.10 Versatility of recovered SRB

The SRB genomes recovered from the BSR reactor communities were found to be metabolically versatile. Aside from the already mentioned VFA and hydrogen metabolisms and autotrophic pathways, all of the recovered SRB contained genes for gluconeogenesis, glycolysis and several glycosyl transferases indicating the capacity of these microorganisms to metabolise sugars (Table 8-5). A select few of these SRB also contained genes for the beta-oxidation of long-chain fatty acids. These genes co-occurred with genes encoding Quinone reductase complexes involved in the re-oxidation of NADH. The link between Quinone reductase complex and beta-oxidation of fatty acids was made by Spero et al. (2015), but these authors, after surveying over 900 bacteria genomes, were unable identify SRB containing these complexes.

Table 8-5 Genome summary of the SRB genomes identified in this study. Genes were predicted using prodigal and compared to KEGG, Uniref100 and Uniprot gene databases. The number of identified genes relating to each genome feature is shown.

| | Gluconeogenesis | Glycosyl Transferase | Glycolysis | TCA Cycle | Beta oxidation Fatty acids | Amylolytic Degradation | Cell surface Fibronectin | Cell surface teichoic acid | Quinone reductase complex | Flagella related proteins | Pili Pilins | Oxidative stress | Arsenate reductase | Cas proteins | Peptidoglycan biosynthesis | Lipopolysaccharide biosynthesis |
|---|---|---|---|---|---|---|---|---|---|---|---|---|---|---|---|---|
| Desulfovibrio_desulfuricans_58_43 | 17 | 33 | 17 | 14 | 0 | 2 | 0 | 1 | 5 | 34 | 0 | 6 | 0 | 0 | 5 | 0 |
| Desulfobacterales_57_55 | 15 | 48 | 18 | 25 | 23 | 4 | 2 | 1 | 12 | 46 | 1 | 12 | 0 | 0 | 5 | 9 |
| Desulfobacca_acetoxidans_53_18 | 18 | 27 | 13 | 12 | 0 | 1 | 1 | 2 | 1 | 0 | 3 | 5 | 0 | 4 | 1 | 16 |
| Deltaproteobacteria_63_50 | 20 | 35 | 16 | 21 | 21 | 2 | 1 | 0 | 4 | 33 | 2 | 9 | 1 | 0 | 7 | 10 |
| Desulfarculus_baarsii_66_20 | 18 | 55 | 15 | 12 | 19 | 0 | 1 | 0 | 12 | 38 | 1 | 4 | 0 | 0 | 1 | 11 |
| Desulfovibrio_66_33 | 28 | 46 | 23 | 18 | 1 | 0 | 0 | 0 | 5 | 48 | 1 | 8 | 0 | 0 | 8 | 3 |
| Desulfovibrio_64_36 | 21 | 33 | 20 | 16 | 1 | 1 | 0 | 1 | 4 | 46 | 1 | 7 | 0 | 0 | 7 | 1 |
| Desulfobulbus_propionicus_52_45 | 18 | 16 | 15 | 18 | 2 | 0 | 1 | 0 | 4 | 33 | 3 | 4 | 0 | 0 | 1 | 7 |
| Desulfovibrio_69_8 | 25 | 45 | 23 | 12 | 0 | 0 | 0 | 0 | 5 | 46 | 1 | 5 | 1 | 0 | 4 | 6 |
| Desulfobacter_postgatei_49_15 | 15 | 23 | 15 | 21 | 6 | 3 | 0 | 0 | 3 | 47 | 2 | 4 | 0 | 0 | 14 | 14 |
| Desulfovibrio_65_12 | 31 | 43 | 29 | 19 | 1 | 1 | 4 | 1 | 5 | 60 | 1 | 11 | 1 | 0 | 7 | 4 |
| Desulfovibrio_69_9 | 21 | 47 | 18 | 7 | 0 | 0 | 0 | 0 | 2 | 39 | 1 | 7 | 1 | 0 | 3 | 5 |
| Desulfovibrio_70_18 | 16 | 54 | 16 | 9 | 1 | 0 | 0 | 0 | 5 | 52 | 0 | 5 | 0 | 0 | 4 | 7 |
| Desulfovibrio_64_24 | 28 | 49 | 21 | 11 | 2 | 0 | 0 | 2 | 4 | 42 | 2 | 8 | 1 | 0 | 8 | 7 |
| Desulfovibrio_65_13 | 28 | 50 | 27 | 13 | 2 | 0 | 0 | 1 | 5 | 56 | 2 | 9 | 0 | 0 | 11 | 3 |
| Desulfovibrio_65_16 | 17 | 48 | 17 | 7 | 1 | 0 | 0 | 0 | 3 | 38 | 0 | 8 | 1 | 0 | 3 | 5 |
| Deltaproteobacteria_58_15 | 16 | 40 | 17 | 15 | 20 | 1 | 1 | 0 | 14 | 47 | 3 | 3 | 0 | 4 | 4 | 9 |
| Desulfobulbus_propionicus_57_36 | 19 | 29 | 18 | 19 | 2 | 2 | 1 | 0 | 2 | 39 | 7 | 6 | 0 | 0 | 1 | 9 |
| Desulfomicrobium_baculatum_60_28 | 15 | 50 | 13 | 11 | 0 | 1 | 0 | 1 | 6 | 36 | 5 | 9 | 0 | 0 | 1 | 6 |
| Desulfovibrio_65_51 | 21 | 55 | 21 | 11 | 1 | 0 | 0 | 1 | 6 | 48 | 4 | 7 | 0 | 0 | 8 | 5 |
| Desulfovibrio_vulgaris_68_10 | 20 | 43 | 17 | 14 | 0 | 0 | 0 | 0 | 9 | 45 | 1 | 9 | 0 | 0 | 5 | 6 |
| Desulfotomaculum_gibsoniae_47_21 | 10 | 9 | 12 | 9 | 16 | 0 | 3 | 0 | 1 | 38 | 0 | 4 | 0 | 0 | 1 | 1 |

The versatility of SRB has been long recognised and is evident in the already published genome sequences of a number of SRB (Copeland et al., 2009; Göker et al., 2011; Pagani et al., 2011; Wirth et al., 2011). This SRB versatility is illustrated in Figure 8-16, describing the genomes features of Desulfobulbus_propionicus_57_36. This SRB contained genes for cytochrome bd oxidase, a cytochrome involved in reducing oxidative stress. This gene and others involved with dealing with oxidative stress were found in every SRB genome suggesting these microorganisms may be more oxygen tolerant than previously thought. Four *Desulfovibrio* genomes and a genome classified only to Deltaproteobacteria also contained genes for arsenate reductase, involved in arsenate detoxification.

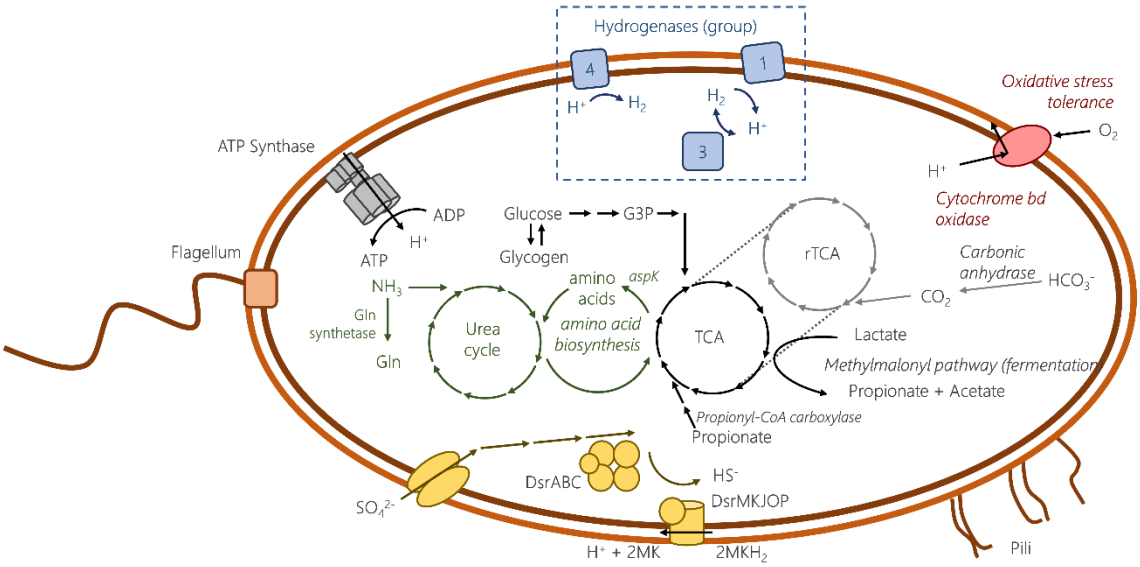


Figure 8-16 Schematic genome summary of the dissimilatory sulphate reducing bacterium BSR_Ace_UAPBR_inlet_at_2_Desulfobulbus_propionicus_52_45. The group to which the NiFe hydrogenase belong are shown in the schematic (blue). Pathways and reactions relating to nitrogen metabolism are shown in green, sulphur metabolism in yellow and oxygen metabolism in red.

## 8.11 BSR mixotrophic metabolic model

The incorporation of citrate and yeast extract in the reactor medium is thought to have led to the selection of fermentative microorganisms in both the acetate and lactate supplemented reactor systems. This is based on the wide distribution of hydrogen-evolving hydrogenase genes found in genomes also containing genes for citrate uptake and oxidation as well as genes associated with the urea cycle. BSR_Ace_UAPBR_inlet_at_2_Synergistales_64_17 was the most common of these fermentative microorganisms, appearing in above 1% relative abundance in 11 of the 17 sequenced samples. The hydrogen produced during this fermentation would offer a valuable source of reducing power for microorganisms with viable electron acceptors. The uptake of this hydrogen by SRB also containing autotrophic genes pathways may also explain the considerable deficit of bicarbonate in the acetate-supplemented systems described in Chapters 4-6. However, in these chapters, it was shown that acetate oxidation had also occurred. This led to the proposed metabolic model (Figure 8-17) whereby mixotrophic sulphate reduction occurs through the oxidation of acetate and hydrogen together and potentially with the fixation of $CO_2/HCO_3^-$ into biomass. This model suggests that reactions governed by Equations 8-1, 2-5 and 2-6, summarised below, are catalysed collectively by the SRB community within these systems. It is unclear whether

individual SRB are performing all three reactions simultaneously or if the SRB's carbon and energy requirements are met using only one or two of these reactions.

| | | | |
|---|---|---|---|
| $4\ H_2 + 2\ HCO_3^- + H^+$ | $\rightarrow$ Acetate$^-$ + $4\ H_20$ | $\Delta G°$' -104.4 (kJ/reaction) | Equation 8-1 |
| $4\ H_2 + SO_4^{2-} + H^+$ | $\rightarrow 4\ H_20 + HS^-$ | $\Delta G°$' -152.0 (kJ/reaction) | Equation 2-6 |
| Acetate + $SO_4^2$ | $\rightarrow 2\ HCO_3^- + HS^-$ | $\Delta G°$' -47.6 (kJ/reaction) | Equation 2-7 |

SRB benefiting from interspecies hydrogen transfer have been reported (Cord-Ruwisch et al., 1988; Ozuolmez et al., 2015) and coupled carbon fixation has been demonstrated in members of the genus *Desulfovibrio* (Sorokin, 1966; Badziong et al., 1979). Further evidence to substantiate this proposed metabolic model is outlined below. Evidence of autotrophy in a largely heterotrophic microbial community was described by Handley et al. (2013). These authors amended an aquifer with acetate and performed a genome-resolved metagenomic analysis of the resulting microbial community. They concluded that acetate was oxidised, linked to either sulphate or nitrate reduction. Evidence for acetate oxidation was found in the presence of genes for the TCA and modified TCA cycle. It was concluded that the produced carbon dioxide was in turn fixed by an Epsilonbacteria containing genes for the rTCA cycle. The electron donor and acceptor for this microorganism were proposed as sulphide and nitrate respectively.

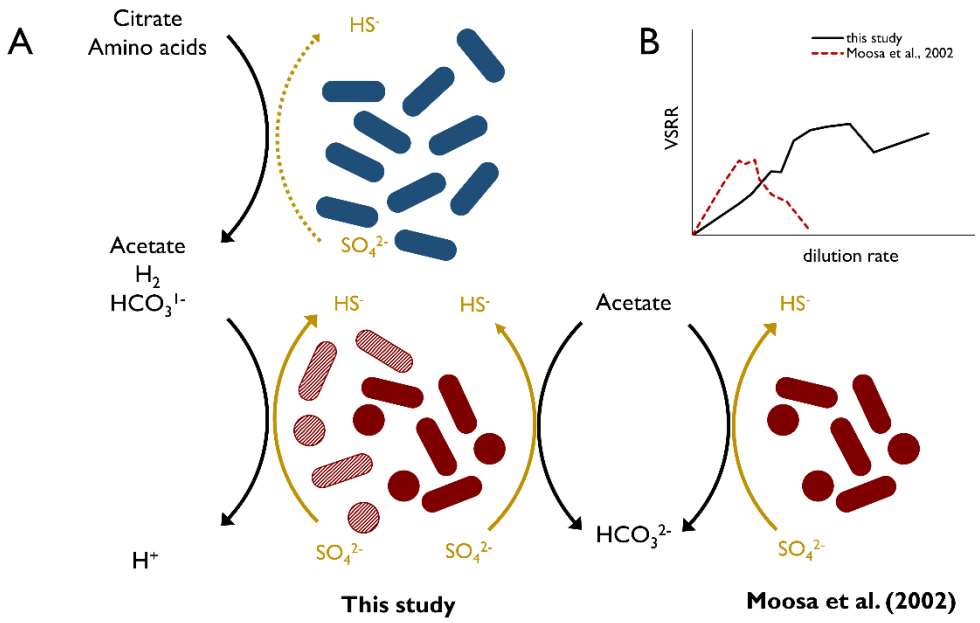


Figure 8-17 The proposed (A) metabolic model of the microbial communities found in the acetate supplemented BSR reactors systems of this study and that of Moosa et al. (2002). Acetate was provided as the sole source of reduced carbon in the study conducted by Moosa et al (2002). However, in this study, fermentative microorganisms (blue) consume citrate and amino acids in the reactor medium, generating acetate, bicarbonate and $H_2$. A portion of acetate is consumed heterotrophically (solid-red) to bicarbonate while several other microorganisms (lined) possibly function autotrophically and mixotrophically – fixing the generated bicarbonate and consuming $H_2$ as the electron donor. Genes for the reverse TCA and the Wood Ljungdahl pathway were present in several sulphate-reducing microorganisms. It is proposed that the SRB community function mixotrophically, oxidising acetate and consuming the hydrogen and bicarbonate produced from fermentation. The availability of $H_2$ in the BSR reactors of this study is thought to explain (B) the sustained volumetric sulphate reduction rates (VSRR) achieved at higher dilution rates, compared to that of Moosa et al. (2002).

The low bicarbonate concentrations observed in the acetate-supplemented BSR reactors is a possible indication of autotrophic growth. This was substantiated by the presence of carbon fixation pathways in a number of genomes, many of which were SRB. For autotrophy to have taken place on the scale observed, from the deficit of bicarbonate in these reactor systems, a substantial source of reducing power would be required. These autotrophic pathways co-occurred in these genomes with hydrogenase genes implicated in hydrogen consumption. It was concluded that a number of other dominant microorganisms were producing hydrogen based on the presence of NiFe group 4 and FeFe hydrogenase genes, together with genes for the urea cycle and citrate uptake and oxidation. This is corroborated by the lack of viable electron acceptors provided in the reactor medium. This lack of alternative electron acceptors, such as nitrate, sulphur and metals, is thought to have selected for fermentative microorganisms capable of removing electrons in the form of organic carbon and hydrogen.

Genome resolved metagenomics revealed that many of the identified SRB would be capable of the proposed form of mixotrophic sulphate reduction. Many SRB contained genes required for acetate oxidation together with NiFe group 1 hydrogenases, and autotrophic pathways. However, the SRB within the BSR reactors were also capable of catalysing amino acid and citrate oxidation. The possibility that sulphate reduction may have been linked to citrate or amino acid oxidation must first be discussed (below) and substantiated using reactor performance data.

Genes for citrate uptake and oxidation were found in one SRB genome, Desulfovibrio_desulfuricans_58_43, which was dominant in a number of planktonic reactor samples at a four-day HRT. This SRB was matched to the OTU *Desulfovibrio* (6) on the basis of taxonomic classification and abundance patterns across 16 reactor samples, although no 16S rRNA gene was binned with this genome. This OTU was shown to experience a substantial reduction in abundance at subsequently shortened HRT (Chapters 4 and 5). This SRB may have been performing citrate oxidation linked sulphate reduction but this would only be possible at a four-day HRT and cannot be linked to the performance of the reactors at shorter HRT. Many SRB contained genes for the urea cycle, indicating that these microorganisms may have been consuming amino acids as a source of carbon. However, solution chemistry data collected before and after an abrupt modification to the media composition, prior to the start of the residence time study, suggests little direct dependence of SRB on yeast extract. The yeast extract concentration in the reactor medium was reduced in the six reactors from 1.0 to 0.4 g/L (Section 4.4.2). The sulphate conversion did not experience a significant perturbation immediately after this point but decreased gradually from 55 to 45% sulphate conversion over the following100 days (Section 4.4.2). Should amino acids have been the primary source of carbon for SRB in these systems the reactors would likely have shown a considerable reduction in sulphate reducing performance after reducing this substrate by 60%. This suggests that SRB benefitted from the higher yeast extract concentration but were not entirely dependent.

The inclusion of yeast extract and citrate in the reactor medium, even if not used directly by SRB, has strong implications for sulphate reducing performance. Moosa et al. (2002) operated an identical CSTR with a similar SRB inoculum. In the study performed by Moosa et al. (2002), acetate was provided as the sole source of organic carbon. No citrate nor yeast extract was included in the medium and was instead supplemented with a trace metal solution. In that instance, the generation of hydrogen was likely to be minimal due to the absence of readily fermentable substrates. During the study performed by Moosa et al. (2002), the residual acetate concentration increased steadily as sulphate conversion decreased with the reduction of the operated HRT. Sulphate reduction linked to acetate oxidation was confirmed in the study conducted by Moosa et al. (2002) and without hydrogen as an electron donor, autotrophy would not have been possible

in this system. The maximum VSRR achieved by the reactor system was below 7.3 mg/L.h at a 3.8-day HRT. At shorter HRT, the VSRR decreased abruptly leading to total system failure at a two-day HRT. In contrast, the acetate-supplemented CSTR described in this thesis achieved a maximum VSRR of 10.9 mg/L.h at a 1.5-day HRT and did not experience system failure – demonstrating a 23% sulphate conversion at a one-day HRT. It is expected that the mixotrophic sulphate reduction is the reason for the differing performance between this study and that of Moosa et al. (2002).

## 8.12 Conclusion

Genome-resolved metagenomics was successfully employed to characterise the microbial communities of the six BSR reactors operated in this study. A total of 163 genome bins were recovered and, owing to the low complexity of individual samples, these bins showed little contamination and a high degree of completeness. The majority of the recovered genomes were classified as Proteobacteria (59), Firmicutes (29) or Bacteroidetes (28). Of the SRB recovered, one was classified as a Clostridia and the remaining as Deltaproteobacteria.

Relatively few of the 163 recovered genomes were found across more than a handful of bioreactor samples. Similarities between bioreactor communities became more evident when comparing these communities based on the proportion of metabolic potential represented within each community. Hierarchical clustering of the proportions of various metabolic features across samples yielded three clear clusters which comprised all acetate-attached, acetate-planktonic and lactate communities. The separation of these communities indicates that the electron donors and biofilm and planktonic environments are the key deterministic factors which shape these microbial communities. The reasons for the success of individual genomes over similar genomes is not always clear and may be explained by a combination of stochastic and deterministic factors including differing growth kinetics between microorganisms participating in similar forms of metabolism.

The indices of replication, iRep values, determined for each of the microbial community samples revealed that all members of the biofilm community (>1% relative abundance) are reproducing at a lower, but comparable rate to that of the planktonic communities in the same reactor zone. All microorganisms within the biofilms had an iRep value greater than one, indicating no dormant organisms were present in the biofilms. This affirms the contribution of the biofilms to sulphate reducing performance in BSR reactor systems, even when the operated HRT is long enough for planktonic cell concentrations to remain high. The biofilms communities of these systems are, therefore, more dynamic than initially thought. This was evident in the changes in the composition of these communities between a four- and one-day HRT (Chapters 3 to 5).

One of the most striking features of the metagenomes recovered from the BSR reactors was the widespread distribution of genes encoding various hydrogenases. It is concluded that fermentative microorganisms metabolising lactate, citrate and amino acids use these hydrogenases to remove electrons from the cell. The lack of alternate viable electron acceptors present in the reactor medium is thought to be the major driver of this phenomenon. The enrichment of hydrogen consuming hydrogenases is likely an adaptation of the community to in-turn metabolise the produced hydrogen. Each SRB genome recovered was found with multiple forms of hydrogenases, all containing the hydrogen consuming NiFe group 1 hydrogenase. Many of these SRB, as well as a handful of other Proteobacteria and Bacteroidetes genomes, also contained genes for autotrophy. The rTCA was the most common form of autotrophic pathway followed by the Wood-Ljungdahl pathway.

The widespread presence of hydrogen evolving hydrogenase genes in fermentative microorganisms, and the presence of hydrogen consuming and autotrophic pathways within SRB led to the proposed BSR mixotrophic model. It is proposed that SRB, predominantly within the acetate-supplemented systems, consume acetate provided in the reactor medium together with hydrogen and bicarbonate produced during fermentation, simultaneously. This form of metabolism has been previously described in pure and co-cultures of SRB. However, this mixotrophic SRB metabolism has yet to be demonstrated in BSR reactor systems. The comparison of the performance of the acetate CSTR of this study and that of Moosa et al. (2002) reveals that this mixotrophic acetate oxidation offers an enormous improvement in reactor performance over solely acetate oxidation linked sulphate reduction. It is concluded that the inclusion of low concentrations of fermentable material, in the absence of viable electron acceptors besides sulphate, would enable the generation of hydrogen in semi-passive BSR reactor systems. This hydrogen would directly benefit the growth of SRB in these reactors leading to enhanced performance and system robustness.

# Chapter 9 Conclusions and Recommendations

This thesis sought to improve the understanding of the microbial communities associated with BSR reactor systems. This arose from (i) a lack of robust, implementable, semi-passive BSR systems for the sustainable remediation of ARD and (ii) our limited understanding of BSR microbial communities' structure and function and their ultimate impact on reactor performance.

The reactor configurations and operating conditions, informed by literature, investigated in this study were selected to allow successful operation as semi-passive systems whilst generating a range of differing physiochemical environments which could be studied in relation to the inhabiting microbial ecology. The LFCRs were well-mixed systems fitted with carbon microfibre support structures to encourage biofilm formation. The UAPBRs investigated in this study were governed by plug flow, leading to the generation of continuum of changing environments as substrates were consumed and products generated throughout the reactors. Polyurethane foam was incorporated as an inert packing in these plug-flow reactors to stimulate biofilm formation. The third reactor configuration, the well-mixed CSTR, supported the growth of primarily suspended biomass with no additional biomass retention. This provided a useful system to which the LFCRs and UAPBRs could be compared, both in terms of their microbial ecology and system performance. The operation of these systems in duplicate and supplemented with acetate and lactate, separately, allowed the impacts of electron donor on the performance and ecology of each system to be simultaneously assessed.

The performance and microbial community dynamics of these systems were monitored during an extended HRT study. The microbial ecology was assessed using a combination of genome-resolved and 16S rRNA gene sequencing. To the best of our knowledge, this is the first-ever use of genome-resolved metagenomics in the study of BSR reactor systems. The 16S rRNA gene sequencing was used to characterise the composition of the microbial communities throughout these reactor systems and monitor changes in these communities as the applied HRT was reduced. The extensive use of 16S rRNA gene sequencing meant that the ideal growth conditions of both SRB and competing, co-existing and syntrophic microorganisms could be determined. Genome-resolved metagenomics was used in parallel, overcoming a major limitation of 16S rRNA gene studies: the lack of functional and metabolic information. Genome-resolved metagenomics allowed unprecedented insight into the metabolism and roles these microorganisms played within these reactor systems. The major findings arising from these studies are discussed below and are summarised in Figure 9-1.

# 9.1 Conclusions

### 9.1.1 Effective performance of several semi-passive reactor systems

The reactor systems presented in this thesis, specifically the acetate-supplemented LFCR and both UAPBRs, demonstrated competitive sulphate reducing performance compared to studies described in the literature. The success of these reactors is especially significant as these reactors contain no moving parts and can, therefore, be implemented as semi-passive systems with low energy requirements.

The lactate-supplemented UAPBR demonstrated the greatest sulphate reducing performance of the six bioreactors, exhibiting a sulphate conversion of 96% at a one-day HRT and 1 g $SO_4^{2-}$/ ℓ feed concentration. This corresponded to a VSRR of 40.1 mg/ℓ.h over the length of the reactor. The success of this reactor was largely attributed to the out-competition of fermentative microorganisms for lactate by SRB in the inlet zone, and the effective utilisation of acetate and propionate by a largely distinct group of SRB in the middle and effluent zones.

Acetate is an attractive electron donor for BSR because of its low cost and availability but offers low associated SRB growth rates. The performance of the acetate-supplemented LFCR and UAPBR is therefore promising for the viability of acetate as an electron donor for BSR systems. The UAPBR supplemented with acetate demonstrated notable performance, achieving a VSRR of 23.2 mg/ℓ.h and sulphate conversion of 56%, at a one-day HRT. This reactor operated optimally at 2.3-day HRT, achieving a sulphate conversion of close to 80% and a VSRR of 14.2 mg/ℓ.h. The acetate-supplemented LFCR, following a period of poor performance was able to achieve a VSRR of 17.1 mg/ℓ.h and a sulphate conversion of 41% at a one-day HRT, and was able to achieve a sulphate conversion of 58% at a two-day HRT.

The aspects to which the success of these reactors have been attributed are described throughout the sections below.

### 9.1.2 Hydrogen metabolism and its implication for reactor performance

Genome-resolved metagenomics revealed that all SRB within the BSR reactors were capable of hydrogen consumption through the use of Group 1 NiFe hydrogenases. This finding was not unexpected as the ability of SRB to consume hydrogen has been well documented (Fauque et al., 1988; Peters et al., 2015; Timmers et al., 2018) However, the presence of hydrogen evolving hydrogenases in the majority of microorganisms not capable of dissimilatory sulphate reduction was not anticipated. It is concluded that the applied operating conditions selected for microorganisms capable of using hydrogenases as a means of removing electrons from the cell due to the absence of alternative electron acceptors and inhibition of methanogenic microorganisms

during culture establishment. The generation of hydrogen within these systems, by amino acid, citrate and lactate fermenting microorganisms, and the subsequent utilisation of this hydrogen by SRB is believed to have facilitated the enhanced growth rates of SRB. This was evident in the nearly two-fold increase in the doubling time of SRB in the acetate-supplemented CSTR, compared to the similarly operated CSTR documented by Moosa et al. (2002). A remarkable aspect of this finding is that hydrogen can be generated in a passive system through supplementation with small amounts of fermentable material – if influent conditions are favourable and/or controlled to select for the growth of particular hydrogen-evolving microorganisms. This phenomenon undoubtedly takes place in passive BSR systems supplemented with complex electron donors such as cellulose and manure but is seldom appropriately observed or discussed.

The enhanced growth rate of acetate-oxidising SRB, in the presence of hydrogen, offers a further advantage. A major difficulty when using organic electron donors for BSR is preventing the discharge of high COD-containing effluents (Widdel, 1988). Several electron donors used for BSR are incompletely oxidised resulting in the generation of acetate -the major component of this COD. The increased growth rates of acetate-consuming SRB in the presence of hydrogen represents a strategy to reduce the acetate concentration in the effluent of BSR reactors. BSR reactor systems may benefit through operation at lower electron donor concentrations and supplemented with hydrogen, or fermentable material as discussed above. This could be optimised to potentially lead to similar reaction rates but leading to reduced acetate concentrations in the effluent of these systems.

### 9.1.3 Lactate and acetate oxidation are spatially separated

Lactate was supplied to the bioreactors of this study at 1200 mg/L. The incomplete oxidation of this lactate by SRB (Equation 2-10) corresponds with the reduction of 6.8 mM of the 10.2 mM sulphate in the medium, assuming no lactate fermentation (Equation 2-12). The successful use of this electron donor, therefore, required the initial out-competition of fermentative microorganisms by SRB for lactate, and subsequent growth of SRB capable of oxidising the produced acetate and propionate arising from lactate oxidation. The oxidation of electron donors other than lactate was minimal in the lactate-supplemented CSTR. However, the oxidation of acetate and propionate was anticipated in the lactate-supplemented LFCR and was hypothesised (Section 2.10.1) to be facilitated through the incorporation of carbon support structures for biofilm formation thereby allowing slower-growing acetate-oxidising SRB to avoid washout and become dominant in the reactor. This hypothesis was disproven as little acetate nor propionate oxidation was observed in this reactor. Acetate and propionate oxidation were observed in the lactate-supplemented UAPBR, but the oxidation of these electron donors occurred almost exclusively in the middle and effluent zones where no lactate was available. The SRB which were

specific to these zones were *Desulfatiglans* (91), *Desulfobulbus* (27), *Desulfobacca* (46) and *Desulfosarcina* (53), none of which were present in the lactate-supplemented LFCR. The poor performance of the lactate-supplemented LFCR is partially attributed to the failure to cultivate these SRB in this well-mixed system.

The inability of acetate-oxidising SRB to become dominant in these biofilm communities in the presence of lactate is attributed to the remarkably active and competitive environment posed by these biofilm communities. This accounts for the inability of the lactate-supplemented LFCR to cultivate acetate-oxidising SRB as the reactor presents as a well-mixed system with lactate available throughout.

This work demonstrates that lactate, a relatively expensive electron donor, can be used at far lower concentrations than routinely reported in literature. This requires that reactors be operated to ensure sulphate reduction coupled to the oxidation of propionate and acetate can occur. Based on our observations, we find that this can be stimulated through zoning of BSR reactor systems to spatially separate lactate, propionate and acetate oxidation. This also requires the formation of biofilms within the reactors, as described below.

### 9.1.4 The biofilms of BSR systems are active and dynamic

The biofilm communities within the BSR systems were highly active and dynamic in response to changing physicochemical conditions. Indices of replication calculated for microorganisms within BSR reactor communities revealed that the average iRep score of the biofilm communities, at a four-day HRT, were marginally lower than the planktonic community within each respective zone. This indicates that microorganisms within these biofilms were both metabolically active and undergoing active growth. This was substantiated by the considerable changes in the composition of the biofilm communities of the acetate-supplemented LFCR between a four- and one-day HRT. This explains why slower-growing acetate-oxidising bacteria were unable to become dominant in the biofilm communities of the lactate supplemented LFCR - these organisms were likely outcompeted for space in the presence of lactate due to greater growth rates associated with lactate-oxidising microorganisms in these biofilms.

### 9.1.5 Biofilms provide system robustness

The susceptibility of planktonic SRB to the reduction in the applied HRT and the evidence of the microbial activity of biofilms suggests that performance and system robustness could be enhanced by further increasing the surface area to volume within BSR reactors, thereby increasing the biofilm-SRB biomass in the reactor. This would decrease the reliance on the planktonic SRB for performance and minimise the growth of many of the identified lactate-fermenting planktonic

microorganisms, such as *Veillonella* (11) and *Enterobacter* (16) in this study. In addition, all SRB which were identified in planktonic communities were also found within biofilms, but not vice versa, indicating SRB diversity would not be negatively affected were the role of the planktonic communities be reduced.

### 9.1.6 SRB favour specific conditions

*Desulfovibrio* (6), *Desulfomicrobium* (1) and *Desulfobacter* (18) were common to most BSR reactors and reactor environments. The remainder of the identified SRB were present in only a handful of reactor communities. The specific localisation of these SRB provided strong insight into these microorganisms preferred growth conditions. The major factors identified were the available electron donors, planktonic and biofilm conditions and the concentration of sulphate in the environment. Examples of these included the implication of *Desulfobulbus* (27) in propionate oxidation in the lactate-supplemented UAPBR and the scavenging of low concentrations of sulphate by *Desulfatitalea* (177) and *Desulfatiglans* (91) in the biofilm communities within the effluent zones of the UAPBRs.

The preferential growth of SRBs for differing environmental conditions is highly pertinent to the inoculation and operation of BSR systems. The current approach to inoculation of BSR systems often recognises the need for microbial diversity but overlooks the need for particular SRB to fulfil particular roles within these systems. With this and further studies, it can become possible to design BSR inoculums and monitor BSR systems to ensure all required roles within these systems are met.

## 9.2 Recommendations for future studies

Several recommendations for further study are made in this section based on the conclusions outlined above. A schematic summarising some of the major implications for the operation and design of BSR reactor systems, based on the above conclusions, is shown in Figure 9-1.

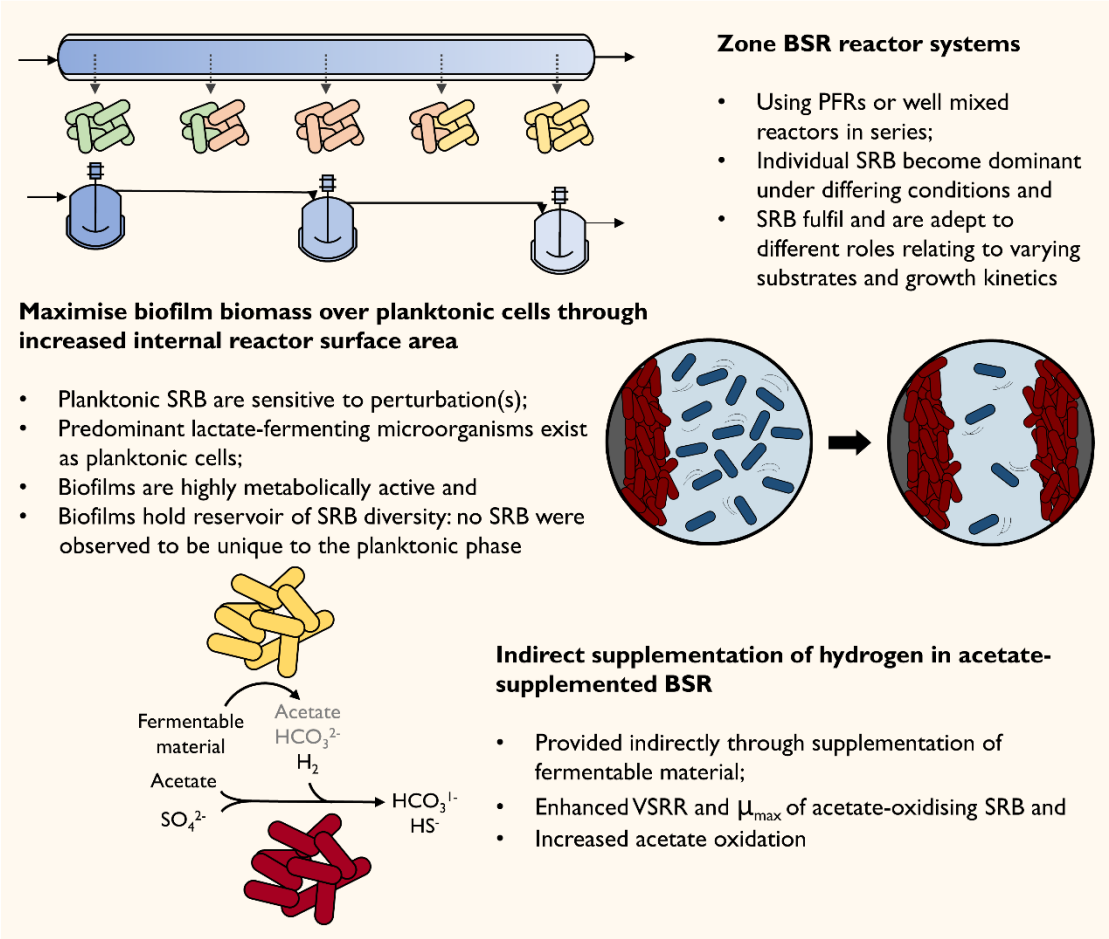


Figure 9-1 Schematic summary of suggested operation and design parameters of semi-passive BSR reactor systems arising from the conclusions of this work. These operational conditions include the zoning of BSR reactor configurations to produce a range of ecological niches to which various SRB are able to become dominant, enhance the degree of biomass retention within the system to increase process robustness and supplement the process with a fermentable material for the passive generation of hydrogen which has been shown here to enhance the growth rates of acetate-oxidising SRB.

### 9.2.1 Operation of semi-passive BSR systems supplemented with acetate and hydrogen

The unanticipated evidence of hydrogen generation in these reactors was concluded to have facilitated the higher reactions rates in reactors where acetate oxidation by SRB was taking place. The additional supplementation of hydrogen in acetate-supplemented BSR systems should be further investigated, including the kinetics of mixed BSR cultures grown on acetate and hydrogen and the generation of hydrogen from low-cost sources. This hydrogen could be supplied indirectly through the additional of fermentable material, as conjectured in this study.

### 9.2.2 Evidence of microbial interactions in metagenomes

The generation of 163 high-quality genome bins, associated with these BSR reactors has provided a database of not only SRB genomes but genomes of microorganisms associated with BSR systems. The spatial separation of many acetate-oxidising SRB from lactate oxidising microorganisms suggests either out-competition for space or antagonistic effects such as the production of antimicrobial compounds. Further investigation into these 163 genomes should aim to understand additional interactions between these microorganisms through investigations into secondary metabolite gene clusters within these genomes. Hypotheses which may arise from such an investigation should be tested through transcriptomic and/or metabolomic analyses.

### 9.2.3 BSR Inoculum development

Gene-amplicon sequencing of the six BSR reactor microbial communities revealed that individual SRB are often successful in specific environments. These environments have been characterised in this study based on electron donors present, the concentration of available sulphate and biofilm and planktonic conditions. Future studies, in pure culture or further metagenomics, should look to further characterise the ideal, and non-ideal, growth conditions and growth kinetics of these SRB and associated microorganisms. From this work, together with the cultivation or enrichment of these microorganisms, it will become viable to assemble desired inoculums for specific reactor configurations and required operating conditions. This would aim to increase sulphate conversions, reduce start-up periods and minimise downtime following system perturbations.

### 9.2.4 Modification of the lactate-supplemented LFCR

The lactate-supplemented LFCR underperformed compared to the lactate-supplemented CSTR and acetate-supplemented LFCR. It is recommended that the performance of the lactate-supplemented LFCR be investigated with the following changes made to the operation of the reactor:

The surface area to volume ratio within the reactor should be increased to allow additional biofilm formation and limit the contribution of the planktonic phase to lactate oxidation and sulphate reduction. Secondly, the removal of acetate from this system is thought to require zoning due to the competition between acetate-oxidisers and faster-growing lactate oxidisers. Therefore, two LFCRs should be connected in series allowing lactate oxidation to occur within a primary reactor and acetate oxidation and sulphate scavenging to take place in a secondary reactor.

## 9.3 Final remarks

This work integrates detailed reactor performance data with gene-amplicon and genome resolved metagenomic analyses. The field of BSR would benefit greatly from further genome-resolved metagenomic and ecological studies into these systems to inform process design and operation. The provision of the genomes of the SRB and many other microorganisms from these systems is anticipated to serve as a useful tool for genetic analyses into the microorganisms associated with BSR. The outcomes of this work have several implications for the operation and design of future and current BSR systems. A number of these outcomes relate specifically to the robustness and performance of semi-passive reactor systems supplemented with low-cost electron donors. The major results of this work, therefore, are aimed to inform the development of low-cost BSR systems for the remediation of diffuse sources of ARD. Within South Africa, the development of these systems is urgently required.

# References


Abram, J.W. and Nedwell, D. B. (1978). 'Inhibition of methanogenesis by sulphate-reducing bacteria competing for transferred hydrogen', Archives of Microbiology, 117(1), pp. 89–92.

Acinas, S.G., Marcelino, L.A., Klepac-Ceraj, V. and Polz, M. F. (2004). 'Divergence and redundancy of 16S rRNA sequences in genomes with multiple rrn operons', Journal of Bacteriology, 186(9), pp. 2629–2635.

Akcil, A. and Koldas, S. (2006). 'Acid Mine Drainage (AMD): causes, treatment and case studies', Journal of Cleaner Production, 14(12–13), pp. 1139–1145.

Alneberg, J., Bjarnason, B.S., Bruijn, I.D., Schirmer, M., Quick, J., Ijaz, U.Z., Lahti, L., Loman, N.J., Andersson, A.F. and Quince, C. (2014). 'Binning metagenomic contigs by coverage and composition', Nature methods, 11(11), pp. 1144–1151.

Amann, R.I., Binder, B.J., Olson, R.J., Chisholm, S.W., Devereux, R. and Stahl, D.A. (1990). 'Combination of 16S rRNA-targeted oligonucleotide probes with flow cytometry for analyzing mixed microbial populations', Applied and Environmental Microbiology, 56(6), pp. 1919–1925.

Amann, R.I., Ludwig, W. and Schleifer, K.H. (1995). 'Phylogenetic identification and in situ detection of individual microbial cells without cultivation', Microbiological Reviews, 59(1), pp. 143–169.

American Public Health Association (APHA) (1975). Standard methods for the examination of water and wastewater. 14th edn. APHA.

Anantharaman, K., Brown, C.T., Hug, L.A., Sharon, I., Castelle, C.J., Probst, A.J., Thomas, B.C., Singh, A., Wilkins, M. J., Karaoz, U., Brodie, E.L., Williams, K.H., Hubbard, S.S. and Banfield, J.F. (2016). 'Thousands of microbial genomes shed light on interconnected biogeochemical processes in an aquifer system', Nature Communications, 7, pp. 1–11.

Anantharaman, K., Hausmann, B., Jungbluth, S.P., Kantor, R.S., Lavy, A., Warren, L.A., Rappé, M. S., Pester, M., Loy, A., Thomas, B.C. and Banfield, J.F. (2018). 'Expanded diversity of microbial groups that shape the dissimilatory sulfur cycle', The ISME Journal, 12(7), pp. 1715–1728.

Arnold, M., Gericke, M. and Muhlbauer, R. (2016). 'Technologies for sulphate removal with valorisation options', in Proceedings of the IMWA symposium: Mining Meets Water – Conflicts and Solutions, pp. 1343–1346.

Ashe, N.L., McLean, I., and Nodwell, M. (2008). 'Review of operations of the biosulphide process plant at the copper Queen mine, Bisbee, Arizona.' In Proceedings of the 6th international symposium on hydrometallurgy, Society for Mining, Metallurgy and Exploration, Inc., Phoenix, Arizona, pp. 98-107.

Aube, B.C. and Payant, S. (1997). 'The Geco process: a new high density sludge treatment for acid mine drainage', in Fourth International Conference on Acid Rock Drainage, pp. 165–80.

Bachmann, A., Beard, V.L. and McCarty, P.L. (1985). 'Performance characteristics of the anaerobic baffled reactor', Water Research, 19(1), pp. 99–106.

Badziong, W., Ditter, B. and Thauer, R.K. (1979). 'Acetate and carbon dioxide assimilation by *Desulfovibrio vulgaris* (Marburg), growing on hydrogen and sulfate as sole energy source', Archives of Microbiology, 123(3), pp. 301–305.

Baena, S., Fardeau, M., Ollivier, B., Labat, M., Thomas, P., Garcia, J. and Patel, B. (1999). '*Aminomonas paucivorans* gen. nov., sp. nov., a mesophilic, anaerobic, amino-acid-utilizing bacterium', International Journal of Systematic Bacteriology, 49, pp. 975–982.

Baker, B.J. and Banfield, J.F. (2003). 'Microbial communities in acid mine drainage.', FEMS Microbiology Ecology, 44(2), pp. 139–52.

Baldrian, P. (2013). 'The Variability of the 16S rRNA gene in bacterial genomes and its consequences for bacterial community analyses', PloS one, 8(2), pp. 1–10.

Balintova, M., Demcak, S. and Holub, M. (2015). 'Sulphate removal from mine water– precipitation and bacterial sulphate reduction', in Proceedings of the International Conference on Engineering Sciences and Technologies, Tatranská Štrba, High Tatras Mountains, Slovak Republic, May 2015, pp. 239–244.

Barber, W.P. and Stuckey, D.C. (2000). 'Effect of sulfate reduction on chemical oxygen demand removal in an anaerobic baffled reactor', Water Environment Research, 72(5), pp. 593–601.

Barlett, M., Zhuang, K., Mahadevan, R. and Lovley, D. (2012). 'Integrative analysis of *Geobacter* spp. and sulfate-reducing bacteria during uranium bioremediation', Biogeosciences, 9(3), pp. 1033–1040.

Barton, L. and Torres, F. (1995). Sulfate-Reducing Bacteria. Springer Science+Business Media, LLC.

Baskaran, V.K. (2005). Kinetics of anaerobic sulphate reduction in immobilised cell bioreactors. *PhD thesis, University of Saskatchewan*.

Baskaran, V. and Nemati, M. (2006). 'Anaerobic reduction of sulfate in immobilized cell bioreactors, using a microbial culture originated from an oil reservoir', Biochemical Engineering Journal, 31(2), pp. 148–159.

El Bayoumy, M.A., Bewtra, J.K., Ali, H. I. and Biswas, N. (1999). 'Removal of heavy metals and COD by SRB in UAFF reactor', Journal of Environmental Engineering, 125, pp. 532–539.

Bayrakdar, A., Sahinkaya, E., Gungor, M., Uyanik, S. and Atasoy, A.D. (2009). 'Performance of sulfidogenic anaerobic baffled reactor (ABR) treating acidic and zinc-containing wastewater', Bioresource Technology, 100, pp. 4354–4360.

de Beer, M., Maree, J. P., Wilsenach, J., Motaung, S., Bologo, L. and Radebe, V. (2010). 'Acid mine water reclamation using the abc process', Mine Water and Innovative Thinking, pp. 115–118.

Beller, H., Chain, P., Letain, T., Chakicherla, A., Larimer, F., Richardson, P., Coleman, M., Wood, A. and Kelly, D. (2006). 'The genome sequence of the obligately chemolithoautotrophic, facultatively anaerobic bacterium *Thiobacillus denitrificans*', Journal of Bacteriology, 188(4), pp. 1473–1488.

Bendall, M., Stevens, S., Chan, L., Malfatti, S., Schwientek, P., Tremblay, J., Schackwitz, W., Martin, J., Pati, A., Bushnell, B., Froula, J., Kang, D., Tringe, S., Bertilsson, S., Moran, M., Shade, A., Newton, R., … Malmstrom, R. (2016). 'Genome-wide selective sweeps and gene-specific sweeps in natural bacterial populations', The ISME Journal, 10(7), pp. 1589–1601.

Bergmeyer, H., Holz, G., Klotzsch, H. and Lang, G. (1963). 'Phosphotransacetylase from *Clostridium kluyveri*. Culture of the bacterium, isolation, crystalisation and properties of the enzyme', Biochem Z, 338, pp. 114–121.

Berney, M., Greening, C., Conrad, R., Jacobs, W. and Cook, G. (2014). 'An obligately aerobic soil bacterium activates fermentative hydrogen production to survive reductive stress during hypoxia', Proceedings of the National Academy of Sciences of the USA, 111, pp. 11479–11484.

Bertolino, S.M., Rodrigues, I.C.B., Guerra-Sá, R., Aquino, S.F. and Leão, V.A. (2012). 'Implications of volatile fatty acid profile on the metabolic pathway during continuous sulfate reduction', Journal of Environmental Management, 103, pp. 15–23.

Blancato, V., Repizo, G., Sua, C. and Magni, C. (2008). 'Transcriptional regulation of the citrate gene cluster of enterococcus faecalis involves the GNTR family transcriptional activator CitO', Journal of Bacteriology, 190(22), pp. 7419–7430.

Boonstra, J., van Lier, R., Janssen, G., Dijkman, H. and Buisman, C. (1999). 'Biological treatment of acid mine drainage', in International biohydrometallurgy symposium IBS', pp. 559–567.

Boshoff, G., Duncan, J. and Rose, P.D. (2004). 'Tannery effluent as a carbon source for biological sulphate reduction', Water Research, 38(11), pp. 2651–2658.

Brand, T., Roest, K. and Brdjanovic, D. (2014). 'Temperature effect on acetate and propionate consumption by sulfate-reducing bacteria in saline wastewater', Applied Microbiology and Biotechnology, 98, pp. 4245–4255.

Brandis-Heep, A., Gebhardt, N.A., Thauer, R.K., Widdel, F. and Pfennig, N. (1983). 'Anaerobic acetate oxidation to $CO_2$ by *Desulfobacter postgatei*', Archives of Microbiology, 136(3), pp. 222–229.

Branton, D., Deamer, D., Marziali, A., Bayley, H., Benner, S., Butler, T., Ventra, M., Garaj, S., Hibbs, A. and Huang, X. (2010). 'The potential and challenges of nanopore sequencing', Nanoscience And Technology, pp. 261–268.

Breitbart, M., Hewson, I., Felts, B., Mahaffy, J., Nulton, J., Salamon, P. and Rohwer, F. (2003). 'Metagenomic analyses of an uncultured viral community from human feces metagenomic analyses of an uncultured viral community from human feces', Journal of Bacteriology, 185(20), pp. 6220–6223.

Brown, C., Olm, M., Thomas, B. and Banfield, J.F. (2016). 'Measurement of bacterial replication rates in microbial communities', Nature Biotechnology, 34(12), pp. 1256–1263.

Brysch, K., Schneider, I.C., Fuchs, G. and Widdel, F. (1987). 'Lithoautotrophic growth of sulfate-reducing bacteria, and description of *Desulfobacterium autotrophicum* gen. nov., sp. nov.', Archives of Microbiology, 148, pp. 264–274.

Burmølle, M., Ren, D., Bjarnsholt, T. and Sørensen, S.J. (2014). 'Interactions in multi-species biofilms: do they actually matter?', Trends in Microbiology, pp. 84–91.

Burns, A.S., Pugh, C.W., Segid, Y.T., Behum, P.T., Lefticariu, L. and Bender, K.S. (2012). 'Performance and microbial community dynamics of a sulfate-reducing bioreactor treating coal generated acid mine drainage', Biodegradation, 23(3), pp. 415–429.

Callahan, B.J., McMurdie, P.J., Rosen, M.J., Han, A.W., Johnson, A.J. and Holmes, S.P. (2016). 'DADA2: high-resolution sample inference from Illumina amplicon data', Nature methods, 13(7), p. 581.

Caporaso, J., Kuczynski, J., Stombaugh, J., Bittinger, K., Bushman, F.D., Costello, E.K., Fierer, N., Pena, A.G., Goodrich, J.K. and Gordon, J.I. (2010). 'QIIME allows analysis of high throughput community sequencing data', Nature Methods, 7(5), pp. 335–336.

Caporaso, J.G., Lauber, C.L., Walters, W.A., Berg-Lyons, D., Huntley, J., Fierer, N., Owens, S.M., Betley, J., Fraser, L., Bauer, M., Caporaso, J.G., Lauber, C.L., Walters, W.A., Berg-Lyons, D., Huntley, J., Fierer, N., Owens, S.M., … Fras, M. (2012). 'Ultra-high-throughput microbial community analysis on the Illumina HiSeq and MiSeq platforms', The ISME Journal, 6(8), pp. 1621–1624.

Celis, L., Gallegos-Garcia, M., Vidriales, G. and Razo-Flores, E. (2013). 'Rapid start-up of a sulfidogenic biofilm reactor: Overcoming low acetate consumption', Journal of Chemical Technology and Biotechnology, 88(9), pp. 1672–1679.

Chen, C., Mueller, R. and Griebe, T. (1994). 'Kinetic analysis of microbial sulfate reduction by *desulfovibrio desulfuricans* in an anaerobic upflow porous media biofilm reactor', Biotechnology and Bioengineering, 43(4), pp. 267–274.

Chen, Y.R. and Hashimoto, A.G. (1980). 'Substrate utilization kinetic model for biological treatment process', Biotechnology and Bioengineering, 22(10), pp. 2081–2095.

Chiume, R., Minnaar, S.H., Ngoma, I.E., Bryan, C.G. and Harrison, S.T.L. (2012). 'Microbial colonisation in heaps for mineral bioleaching and the influence of irrigation rate', Minerals Engineering, 39, pp. 156–164.

Chuichulcherm, S., Nagpal, L., Peeva, A. and Livingston (2001). 'Treatment of metal-containing wastewaters with a novel extractive membrane reactor using sulfate-reducing bacteria', Journal of Chemical Technology & Biotechnology, 76, pp. 61–68.

Cline, J.D. (1969). 'metric determination of hydrogen sulfide in natural waters', Limnology and Oceanography, 14(3), pp. 454–458.

Cogho, V.E. and van Niekerk, A.M. (2009). 'Optimum coal mine water reclamation project', in International Mine Water Conference, pp. 130–140.

Compeau, P.E., Pevzner, P.A. and Tesler, G. (2011). 'How to apply de Bruijn graphs to genome assembly', Nature Biotechnology, 29(11), p. 987.

Copeland, A., Spring, S., Göker, M., Schneider, S., Lapidus, A., del Rio, T., Tice, H., Cheng, J., Lucas, S., Chen, F., Nolan, M., Bruce, D., Goodwin, L., Pitluck, S., Ivanova, N., Mavromatis, K., Ovchinnikova, G., … Lucas, S. (2009). 'Complete genome sequence of *Desulfomicrobium baculatum* type strain (X T)', Standards in Genomic Sciences, 1(1), pp. 29–37.

Cord-Ruwisch, R., Seitz, H. and Conrad, R. (1988). 'The capacity of hydrogenotrophic anaerobic bacteria to compete for traces of hydrogen depends on the redox potential of the terminal electron acceptor', Archives of Microbiology, 149(4), pp. 350–357.

Cotton, C.A., Edlich-Muth, C. and Bar-Even, A. (2018). 'Reinforcing carbon fixation: $CO_2$ reduction replacing and supporting carboxylation', Current Opinion in Biotechnology, 49, pp. 49–56.

Coulton, R., Bullen, C., Dolan, J., Hallett, C., Wright, J. and Marsden, C. (2003). 'Wheal Jane mine water active treatment plant - design, construction and operation', Land Contamination & Reclamation, 11(2), pp. 245–252.

Dar, S., Kleerebezem, R., Stams, A., Kuenen, J. and Muyzer, G. (2008). 'Competition and coexistence of sulfate-reducing bacteria, acetogens and methanogens in a lab-scale anaerobic

bioreactor as affected by changing substrate to sulfate ratio', Applied Microbiology and Biotechnology, 78(6), pp. 1045–1055.

Dar, S., Yao, L., Van Dongen, U., Kuenen, J. and Muyzer, G. (2007). 'Analysis of diversity and activity of sulfate-reducing bacterial communities in sulfidogenic bioreactors using 16S rRNA and dsrB genes as molecular markers', Applied and Environmental Microbiology, 73(2), pp. 594–604.

Das, B.K., Mandal, S.M. and Bhattacharya, J. (2012). 'Understanding of the biochemical events in a chemo-bioreactor during continuous acid mine drainage treatment', Environmental Earth Sciences, 66(2), pp. 607–614.

Davidova, I.A. and Stams, A.J.M. (1996). 'Sulfate reduction with methanol by a thermophilic consortium obtained from a methanogenic reactor', Applied Microbiology and Biotechnology, 46, pp. 297–302.

Denef, V.J., Mueller, R.S., and Banfield, J.F. (2010). 'AMD biofilms: using model communities to study microbial evolution and ecological complexity in nature', The ISME Journal, 4, pp. 599–610.

Desai, C., Pathak, H. and Madamwar, D. (2010). 'Advances in molecular and "-omics" technologies to gauge microbial communities and bioremediation at xenobiotic/anthropogen contaminated sites', Bioresource Technology, 101(6), pp. 1558–1569.

Dev, S., Roy, S. and Bhattacharya, J. (2016). 'Understanding the performance of sulfate reducing bacteria based packed bed reactor by growth kinetics study and microbial profiling', Journal of Environmental Management, 177, pp. 101–110.

Ding, Y., Liang, Z., Guo, Z., Li, Z., Hou, X. and Jin, C. (2019). 'The performance and microbial community identification in mesophilic and atmospheric anaerobic membrane bioreactor for municipal wastewater treatment associated with different hydraulic retention times', Water (Switzerland), 11(1), pp. 1–16.

Dini-Andreote, F., Stegen, J.C., Van Elsas, J.D. and Salles, J.F. (2015). 'Disentangling mechanisms that mediate the balance between stochastic and deterministic processes in microbial succession', Proceedings of the National Academy of Sciences of the United States of America, 112(11), pp. E1326–E1332.

Dries, J., De Smul, A., Goethals, L., Grootaerd, H. and Verstraete, W. (1998). 'High rate biological treatment of sulfate-rich wastewater in an acetate-fed EGSB reactor', Biodegradation, 9(2), pp. 103–111.

Duruibe, J.O., Ogwuegbu, M.O.C. and Egwurugwu, J.N. (2007). 'Heavy metal pollution and human biotoxic effects', International Journal of physical sciences, 2(5), pp. 112–118.

Dvorak, D., Hedin, R., Edenborn, H. and McIntire, P. (1992). 'Treatment of metal-contaminated water using bacterial sulfate reduction: Results from pilot-scale reactors', Biotechnology and Bioengineering, 40(5), pp. 609–616.

Edgar, R.C. (2004). 'MUSCLE: multiple sequence alignment with high accuracy and high throughput.', Nucleic acids research, 32(5), pp. 1792–7.

Edgar, R.C. (2010). 'Search and clustering orders of magnitude faster than BLAST', Bioinformatics, 26(19), pp. 2460–2461.

Elliott, P., Ragusa, S. and Catcheside, D. (1998). 'Growth of sulfate-reducing bacteria under acidic conditions in an upflow anaerobic bioreactor as a treatment system for acid mine drainage', Water Research, 32(12), pp. 3724–3730.

Esposito, G., Lens, P., Pirozzi, F. (2006). 'User-friendly mathematical model for the design of sulfate reducing H2/CO2 fed bioreactor', Journal of Environmental Engineering, 135, pp. 167–175.

Fauque, G., Moura, H.D., Peck, J.J.G., Huynh, B.H., Dervartanian, D.V., Teixeira, M., Przybyla, A. E., Lespinat, P.A., Moura, I. and Legall, J. (1988). 'The three classes of hydrogenases from sulfate-reducing bacteria of the genus *Desulfovibrio*', FEMS Microbiology Reviews, 54, pp. 299–344.

Faust, K. and Raes, J. (2012). 'Microbial interactions: from networks to models', Nature Reviews Microbiology, 10, pp. 538–550.

Feris, L. and Kotze, L.J. (2014). 'The regulation of acid mine drainage in South Africa: law and governance perspectives', Potchefstroom Electronic Law Journal, 17(5), pp. 2104–2163.

Flemming, C. and Wingender, J. (2010). 'The biofilm matrix', Nature Reviews Microbiology, 8, pp. 623–633.

Flusberg, B.A., Webster, D.R., Lee, J.H., Travers, K.J., Olivares, E.C., Clark, T.A., Korlach, J. and Stephen, W. (2010). 'Direct detection of DNA methylation during single-molecule, real time sequencing', Nature methods, 7(6), p. 461.

Foti, M., Sorokin, D., Lomans, B., Mussman, M., Zacharova, E., Pimenov, N., Kuenen, J. and Muyzer, G. (2007). 'Diversity, activity, and abundance of sulfate-reducing bacteria in saline and hypersaline soda lakes', Applied and Environmental Microbiology, 73(7), pp. 2093–100.

Galiana-Aleixandre, M.V., Mendoza-Roca, J.A., & Bes-Pia, A. (2011). 'Reducing sulphates concentration in the tannery effluent by applying pollution prevention techniques and nanofiltration', Journal of Cleaner Production, 19(1), pp. 91–98.

Garcin, E., Vernede, X., Hatchikian, E.C., Volbeda, A., Frey, M. and Fontecilla-Camps, J.C. (1999). 'The crystal structure of a reduced [NiFeSe] hydrogenase provides an image of the activated catalytic center', Structure, (7), pp. 557–566.

Gazea, B., Adam, K. and Kontopoulos, A. (1996). 'A review of passive systems for the treatment of acid mine drainage', Minerals Engineering, 9(1), pp. 23–42.

Göker, M., Teshima, H., Lapidus, A., Nolan, M., Lucas, S., Hammon, N., Deshpande, S., Cheng, J. F., Tapia, R., Han, C., Goodwin, L., Pitluck, S., Huntemann, M., Liolios, K., Ivanova, N., Pagani, I., Mavromatis, K., … Klenk, H. P. (2011). 'Complete genome sequence of the acetate-degrading sulfate reducer *Desulfobacca acetoxidans* type strain (ASRB2 T)', Standards in Genomic Sciences, 4(3), pp. 393–401.

Gopal, H. (2005). Selection of carbon sources for the treatment of acid mine drainage by biological sulphate reduction in South Africa. *PhD dissertation*, *University of Cape Town*.

Govender, E., Bryan, C.G. and Harrison, S.T.L. (2013). 'Quantification of growth and colonisation of low grade sulphidic ores by acidophilic chemoautotrophs using a novel experimental system', Minerals Engineering, 48, pp. 108–115.

Grandgirard, J., Poinsot, D., Krespi, L., Nénon, J.P. and Cortesero, A.M. (2002). 'Costs of secondary parasitism in the facultative hyperparasitoid Pachycrepoideus dubius: Does host size matter?', Entomologia Experimentalis et Applicata, 103(3), pp. 239–248.

Greenberg, A.E. and Eaton, A.D. (eds) (1999). Standard methods for the examination of water and wastewater. APHA American Public Health Association.

Greening, C., Biswas, A., Carere, C., Jackson, C., Taylor, M., Stott, M., Cook, G. and Morales, S. (2016). 'Genomic and metagenomic surveys of hydrogenase distribution indicate $H_2$ is a widely utilised energy source for microbial growth and survival', The ISME Journal, 10(3), pp. 761–777.

Grein, F., Pereira, I.A.C. and Dahl, C. (2010). 'Biochemical characterization of individual components of the *Allochromatium vinosum* DsrMKJOP transmembrane complex aids understanding of complex function in vivo', Journal of Bacteriology, 192(24), pp. 6369–6377.

Grobicki, A. and Stuckey, D.C. (1989). 'The role of formate in the anaerobic baffled reactor', Water Research, 23(12), pp. 1599–1602.

Gunsalus, R., Romesser, J. and Wolfe, R. (1978). 'Preparation of coenzyme M analogues and their activity in the methyl coenzyme M reductase system of Methanobacterium thermoautotrophicum', Biochemistry, 17(12), pp. 2374–2377.

Gunther, P. and Mey, W. (2006). 'Selection of mine water treatment technologies for the Emalahleni (Witbank) water reclamation project', Water Institute of South Africa Conference, pp. 1–14.

Haagensen, J.A.J., Hansen, S.K., Christensen, B.B., Pamp, S.J. and Molin, S. (2015). 'Development of spatial distribution patterns by biofilm cells', Applied and Environmental Microbiology, 81(18), pp. 6120–6128.

Haas, C. and Polprasert, C. (1993). 'Biological sulfide prestripping for metal and COD removal', Water Environment Research, 65, pp. 645– 649.

Handley, K.M., Verberkmoes, N.C., Steefel, C.I., Williams, K.H., Sharon, I., Miller, C.S., Frischkorn, K.R., Chourey, K., Thomas, B.C., Shah, M.B., Long, P.., Hettich, R.L. and Banfield, J.F. (2013). 'Biostimulation induces syntrophic interactions that impact C, S and N cycling in a sediment microbial community', The ISME Journal, 7(4), pp. 800–816.

Hao, O.J. (2000). 'Metal effects on sulfur cycle bacteria and metal removal by sulfate reducing bacteria, in Environmental Technologies to Treat Sulfur Pollution: Principles and Engineering', in Lens, P.N.L. and HulshoffPol, P. (eds) Environmental Technologies to Treat Sulfur Pollution: Principles and Engineering. IWA Publishing, London (UK), pp. 393–414.

Hao, T, Xiang, P., Mackey, H., Chi, K., Lu, H., Chui, H., van Loosdrecht, M. and Chen, G. (2014). 'A review of biological sulfate conversions in wastewater treatment', Water Research, 65, pp. 1–21.

Harada, H., Uemura, S. and Momonoi, K. (1994). 'Interaction between sulfate reducing bacteria and methane producing bacteria in uasb reactors fed with low strength wastes containing different levels of sulfate', Water Research, 28, pp. 355–367.

Harrison, S.T.L., Van Hille, R.P., Mokone, T., Motleleng, L., Smart, M., Legrand, C. and Marais, T. (2014). Addressing the challenges facing biological sulphate reduction as a strategy for amd treatment: analysis of the reactor stage: raw materials products and process kinetics.

Hays, S.G., Patrick, W.G., Ziesack, M., Oxman, N. and Silver, P.A. (2015). 'Better together: Engineering and application of microbial symbioses', Current Opinion in Biotechnology, 36, pp. 40–49.

Hessler, T., Harrison, S.T.L. and Huddy, R.J. (2018). 'The preferential localisation of SRB in an acetate supplemented up-flow anaerobic packed bed reactor', in 11th ICARD | IMWA | MWD Conference – "Risk to Opportunity", pp. 1069–1074.

Hessler, T., Marais, T., Huddy, R.J., van Hille, R. and Harrison, S.T.L. (2017). 'Comparative analysis of the sulfate-reducing performance and microbial colonisation of three continuous reactor configurations with varying degrees of biomass retention', Solid State Phenomena, 262, pp. 638–642.

Hibbing, M.E., Fuqua, C., Parsek, M.R. and Peterson, S.B. (2010). 'Bacterial competition: surviving and thriving in the microbial jungle', National Review of Microbiology, 8(1), pp. 15–25.

van Hille, R.P., van Wyk, N., Motleleng, L. and Mooruth, N. (2011). 'Lessons in passive treatment : Towards efficient operation of a sulphate reduction – sulphide oxidation system', in International Mine Water Conference, pp. 491–496.

van Hille, R., Marais, T. and Harrison, S.T.L. (2015). 'Biomass Retention and Recycling to Enhance Sulfate Reduction Kinetics', In: Agreeing on solutions for more sustainable mine water management – Proceedings of the 10th ICARD & IMWA Annual Conference. – electronic document (paper 250); Santiago, Chile (GECAMIN), pp. 1–14.

Van Hille, R., Mooruth, N., Marais, T., Naidoo, N., Moss, G., Harrison, S. and Muhlbauer, R. (2016). 'Development of a pilot-scale semi-passive system for the bioremediation of ARD', in Proceedings IMWA 2016, Freiberg/Germany, pp. 957–964.

Hilpert, W. and Dimroth, P. (1991). 'On the mechanism of sodium ion translocation by methylmalonyl-CoA decarboxylase form *Veillonella alcalescens*', European Journal of Biochemistry, 195, pp. 79–86.

Hoffert, J.R. (1947). 'Acid Mine Drainage', Industrial & Engineering Chemistry, 39(5), pp. 642–646.

Holtzhausen, L. (2005). 'Research Seeks Answers for Century-Old Problem', The Water Wheel, pp. 16–21.

Houchins, J.P. and Burris, R.H. (1981). 'Occurrence and localization of two distinct hydrogenases in the heterocystous cyanobacterium *Anabaena* sp. strain 7120', Journal of Bacteriology, 146, pp. 209–214.

Huang, J., Wen, Y., Ding, N., Xu, Y. and Zhou, Q. (2012). 'Effect of sulfate on anaerobic reduction of nitrobenzene with acetate or propionate as an electron donor', Water Research, 46(14), pp. 4361–4370.

Hug, L.A., Baker, B.J., Anantharaman, K., Brown, C.T., Probst, A.J., Castelle, C.J., Butterfield, C.N., Hernsdorf, A.W., Amano, Y., Ise, K., Suzuki, Y., Dudek, N., Relman, D.A., Finstad, K.M., Amundson, R., Thomas, B.C. and Banfield, J.F. (2016). 'A new view of the tree of life', Nature Microbiology, 1(5), pp. 1–6.

Hug, L.A. and Co, R. (2018). 'It Takes a Village: Microbial Communities Thrive through Interactions and Metabolic Handoffs', mSystems, 3(2), pp. e00152-17.

Hutcheson, K. (1970). 'A test for comparing diversities based on the shannon formula', Journal of Theoretical Biology, 29(1), pp. 151–154.

Hutton, B., Kahan, I., Naidu, T. and Gunther, P. (2009). 'Operating and maintenance experience at the Emalahleni Water Reclamation Plant', in International Mine Water Conference, pp. 415–430.

Hyatt, D., Chen, G.-L., Locascio, P.F., Land, M.L., Larimer, F.W. and Hauser, L.J. (2010). 'Prodigal: prokaryotic gene recognition and translation initiation site identification.', BMC bioinformatics, 11, p. 119.

Icgen, B. and Harrison, S. (2006). 'Exposure to sulfide causes populations shifts in sulfate-reducing consortia', Research in Microbiology, 157(8), pp. 784–791.

Icgen, B., Moosa, S. and Harrison, S.T.L. (2007). 'A study of the relative dominance of selected anaerobic sulfate-reducing bacteria in a continuous bioreactor by fluorescence in situ hybridization', Microbial Ecology, 53(1), pp. 43–52.

Ingvorsen, K., Zehnder, A. and Jørgensen, B. (1984). 'Kinetics of sulphate and acetat uptake by *Desulfobacter postgatei*', Applied and Environmental Microbiology, 47(2), pp. 403–408.

Itoh, T., Suzuki, K.I., Sanches, P.C. and Nakase, T. (1999). '*Caldivirga maquilingensis* gen. nov., sp. nov. a new genus of rod-shaped crenarchaeote isolated from a hot spring in the Philippines', International Journal of Systematic Bacteriology, 49(3), pp. 1157–1163.

Jansen, K., Thauer, R.K., Widdel, F. and Fuchs, G. (1984). 'Carbon assimilation pathways in sulfate reducing bacteria. Formate, carbon dioxide, carbon monoxide, and acetate assimilation by *Desulfovibrio baarsii*', Archives of Microbiology, 138(3), pp. 257–262.

Janssen, A.J.H. and Buisman, C.J.N. (1998). 'Thiopaq Process for biological removal of sulphide', European Patent Office Office.

Johnson (2000). 'Biological removal of sulfurous compounds from inorganic wastewaters', in Lens, P. and Hulshoff, P.L. (eds) Environmental Technologies to Treat Sulfur Pollution: Principles and Engineering. International Association on Water Quality, pp. 175–206.

Johnson, D.B. and Hallberg, K.B. (2002). 'Pitfalls of passive mine water treatment', Reviews in Environmental Science and Biotechnology, 1(4), pp. 335–343.

Johnson, D.B. and Hallberg, K.B. (2005). 'Acid mine drainage remediation options: A review', Science of the Total Environment, 338, pp. 3–14.

Jormakka, M., Byrne, B. and Iwata, S. (2003). 'Formate dehydrogenase - A versatile enzyme in changing environments', Current Opinion in Structural Biology, 13(4), pp. 418–423.

Jumas-Bilak, E., Roudière, L. and Marchandin, H. (2009). 'Despcription of "Synergistetes" phyl. nov. and emended description of the phylum "*Deferribacteres*" and of the family Syntrophomonadaceae, phylum "Firmicutes"', International Journal of Systematic and Evolutionary Microbiology, 59(5), pp. 1028–1035.

Kaksonen, A. (2004). The Performance , kinetics and microbiology of sulfidogenic fluidized-bed reactors treating acidic metal- and sulfate-containing wastewater. *PhD dissertation, Tampere University of Technology*.

Kaksonen, A.H., Plumb, J.J., Franzmann, P.D. and Puhakka, J.A. (2004). 'Simple organic electron donors support diverse sulfate-reducing communities in fluidized-bed reactors treating acidic metal- and sulfate-containing wastewater', FEMS Microbiology Ecology, 47(3), pp. 279–289.

Kaksonen, A.H. and Puhakka, J.A. (2007). 'Sulfate reduction based bioprocesses for the treatment of acid mine drainage and the recovery of metals', Engineering in Life Sciences, 7(6), pp. 541–564.

Kanehisa, M. and Goto, S. (2000). 'KEGG: kyoto encyclopedia of genes and genomes', Nucleic Acids Research, 28(1), pp. 27–30.

Kang, D., Froula, J., Egan, R. and Wang, Z. (2015). 'MetaBAT, an efficient tool for accurately reconstructing single genomes from complex microbial communities', PeerJ, 3, pp. 1–15.

Kantor, R. (2016). Genome-resolved meta-omics analyses of microbial interactions in mining-impacted systems. *PhD dissertation, University of California Berkeley.*

Kantor, R.S., Huddy, R.J., Iyer, R., Thomas, B.C., Brown, C.T., Anantharaman, K., Tringe, S., Hettich, R.L., Harrison, S.T.L. and Banfield, J.F. (2017). 'Genome-resolved meta-omics ties microbial dynamics to process performance in biotechnology for thiocyanate degradation', Environmental Science and Technology, 51(5), pp. 2944–2953.

Kantor, R.S., van Zyl, A.W., van Hille, R.P., Thomas, B.C., Harrison, S.T.L. and Banfield, J.F. (2015). 'Bioreactor microbial ecosystems for thiocyanate and cyanide degradation unravelled with genome-resolved metagenomics.', Environmental microbiology, 17(12), pp. 4929–41.

Kantor, R.S., van Zyl, A. W., van Hille, R.P., Thomas, B.C., Harrison, S.T.L. and Banfield, J. F. (2015). 'Bioreactor microbial ecosystems for thiocyanate and cyanide degradation unravelled with genome-resolved metagenomics', Environmental Microbiology, 17(12), pp. 4929–4941.

Kim, J., Lee, S., Shin, H., Kim, S. and Cho, B. (2012). 'Elucidation of bacterial genome complexity using next-generation sequencing', Biotechnology and Bioprocess Engineering, 17(5), pp. 887–899.

Kim, J., Lim, J. and Lee, C. (2013). 'Quantitative real-time PCR approaches for microbial community studies in wastewater treatment systems : Applications and considerations', Biotechnology Advances, 31(8), pp. 1358–1373.

Klein, M., Friedrich, M., Roger, A.J., Hugenholtz, P., Fishbain, S., Abicht, H., Blackall, L.L., Stahl, D. A. and Wagner, M. (2001). 'Multiple lateral transfers of dissimilatory sulfite reductase genes between major lineages of sulfate-reducing prokaryotes', Journal of Bacteriology, 183(20), pp. 6028–6035.

Kleinmann, R.L.P. (1998). 'Treatment of mine drainage by anoxic limestone drains', in Acidic Mining Lakes. Springer Berlin Heidelberg, pp. 303–320.

Kolmert, A. and Johnson, D.B. (2001). 'Remediation of acidic waste waters using immobilised, acidophilic sulfate-reducing bacteria', Journal of Chemical Technology and Biotechnology, 76(8), pp. 836–843.

Kolter, R. (2010). 'Biofilms in lab and nature: a molecular geneticist's voyage to microbial ecology', International Microbiology, 13, pp. 1–7.

Konhauser, K., Fyfe, W.S., Ferris, F.G. and Beveridge, T.J. (1993). 'Metal sorption and mineral precipitation by bacteria in two Amazonian river systems: Rio Solimlles and Rio Negro.', Brazilian Journal of Geology, 21, pp. 1103–1106.

Kuo, W.C. and Shu, T.Y. (2004). 'Biological pre-treatment of wastewater containing sulfate using anaerobic immobilized cells', Journal of Hazardous Materials, 113(1–3), pp. 147–155.

Kvalseth, T.O. (1983). 'Note on the $R_2$ measure of goodness of fit for nonlinear models', Bulletin of the Psychonomic Society, 21(1), pp. 79–80.

Laanbroek, H.J., Veldkamp, H., Postgate, J.R., Lynch, J.M. and Le Roux, N. (1982). 'Microbial interactions in sediment communities', Biological Sciences, 297(1088), pp. 533–550.

Langille, M.G.I., Zaneveld, J., Caporaso, J.G., McDonald, D., Knights, D., Reyes, J.A., Clemente, J.C., Burkepile, D.E., Vega Thurber, R.L., Knight, R., Beiko, R.G. and Huttenhower, C. (2013). 'Predictive functional profiling of microbial communities using 16S rRNA marker gene sequences', Nature Biotechnology, 31(9), pp. 814–821.

Langmead, B. and Salzberg, S.L. (2012). 'Fast gapped-read alignment with Bowtie 2', Nature Methods, 9(4), pp. 357–359.

Lasdon, L.S., Waren, A.D., Jain, A. and Ratner, M. (1976). Design and testing of a generalized reduced gradient code for nonlinear programming. Scientific report.

Lee, K., Periasamy, S., Mukherjee, M., Xie, C., Kjelleberg, S. and Rice, S.A. (2014). 'Biofilm development and enhanced stress resistance of a model, mixed-species community biofilm', The ISME Journal, p. 894.

Lefticariu, L., Walters, E.R., Pugh, C.W. and Bender, K.S. (2015). 'Sulfate reducing bioreactor dependence on organic substrates for remediation of coal-generated acid mine drainage: Field experiments', Applied Geochemistry, 63, pp. 70–82.

Lei, S., Xu, X., Cheng, Z., Xiong, J., Ma, R., Zhang, L., Yang, X., Zhu, Y., Zhang, B. and Tian, B. (2019). 'Analysis of the community composition and bacterial diversity of the rhizosphere microbiome across different plant taxa', MicrobiologyOpen, 8(6), pp. 1–10.

Lens, P.N.L., Gastesi, R. and Lettinga, G. (2003). 'Use of sulfate reducing cell suspension bioreactors for the treatment of SO2 rich flue gases', Biodegradation, 14(3), pp. 229–240.

Lens, P., Vallero, M., Esposito, G. and Zandvoort, M. (2002). 'Perspectives of sulfate reducing bioreactors in environmental biotechnology', Reviews in Environmental Science and Biotechnology, 1(4), pp. 311–325.

Lettinga, A.F.M. van Velsen, S.W. Hobma, W.J. de Zeeuw, A.K. (1980). 'Use of the upflow sludge blanket (USB) reactor concept for biological wastewater treatment, espe cially anaerobic treatment', Biotechnolology and Bioengineering., 22, pp. 699– 734.

Letunic, I. and Bork, P. (2006). 'Interactive tree of life (iTOL): an online tool for phylogenetic tree display and annotation', Bioinformatics, 23, pp. 127–128.

Levenspiel, O. (1999). Chemical Reaction Engineering, Chemical Engineering Science. John Wiley & Sons. Industrial & engineering chemistry research 38, no. 11: 4140-4143.

Li, D., Liu, C., Luo, R., Sadakane, K. and Lam, T. (2015). 'Sequence analysis MEGAHIT : an ultra-fast single-node solution for large and complex metagenomics assembly via succinct de Bruijn graph', Bioinformatics, 31(10), pp. 1674–1676.

Li, J., Yu, L., Yu, D., Wang, D., Zhang, P. and Ji, Z. (2014). 'Performance and granulation in an upflow anaerobic sludge blanket (UASB) reactor treating saline sulfate wastewater', Biodegradation, 25(1), pp. 127–136.

Li, W., Fu, L., Niu, B., Wu, S. and Wooley, J. (2012). 'Ultrafast clustering algorithms for metagenomic sequence analysis', Briefings in Bioinformatics, 13(6), pp. 656–668.

Liamleam, W. and Annachhatre, A.P. (2007). 'Electron donors for biological sulfate reduction', Biotechnology Advances, 25(5), pp. 452–463.

Lin, K. and Lee, K. (2001). 'Verification of anaerobic biofilm model for phenol degradation with sulfate reduction', Journal of Environmental Engineering, 127 (2), pp. 119–125.

Liu, M., Lü, Z., Chen, Z., Yu, S. and Gao, C. (2011). 'Comparison of reverse osmosis and nanofiltration membranes in the treatment of biologically treated textile effluent for water reuse', Desalination, 281, pp. 372–378.

Londry, K.L. and Des Marais, D. (2003). 'Stable carbon isotope fractionation by sulfate-reducing bacteria', Applied and Environmental Microbiology, 69(5), pp. 2942–2949.

Loubinoux, J., Bronowicki, J., Pereira, I., Mougenel, J. and Faou, A. (2002). 'Sulfate-reducing bacteria in human feces and their association with inflammatory bowel diseases', FEMS microbiology ecology, 40(2), pp. 107–12.

Louca, S., Doebeli, M. and Parfrey, L. W. (2018). 'Correcting for 16S rRNA gene copy numbers in microbiome surveys remains an unsolved problem', Microbiome, 6(41), pp. 1–12.

Lovley, D.R., Dwyer, D.F. and Klug, M.J. (1982). 'Kinetic analysis of competition between sulfate reducers and methanogens for hydrogen in sediments', Applied and Environmental Microbiology, 43(6), pp. 1373–1379.

Luo, C., Tsementzi, D., Kyrpides, N., Read, T. and Konstantinidis, K.T. (2012). 'Direct comparisons of Illumina vs. Roche 454 sequencing technologies on the same microbial community DNA sample', PLoS ONE, 7(2), p. e30087.

Ma, K., Schicho, R., Kelly, R. and Adams, M.W. (1993). 'Hydrogenase of the hyperthermophile *Pyrococcus furiosus* is an elemental sulfur reductase or sulfhydrogenase: evidence for a sulfur-reducing hydrogenase ancestor', Proceedings of the National Academy of Sciences of the USA, 90, pp. 5341–5344.

Magoč, T. and Salzberg, S.L. (2011). 'FLASH: Fast length adjustment of short reads to improve genome assemblies', Bioinformatics, 27(21), pp. 2957–2963.

Makaula, D. (2019). Developing quantitative approaches to determine microbial colonisation and activity in mineral bioloeaching and characterisation of acid rock drainage. *PhD dissertation, University of Cape Town.*

Marais, T. (under review). A novel semi-passive process for sulphate removal and elemental sulphur recovery centred on a hybrid linear flow channel reactor. *PhD dissertation, University of Cape Town.*

Marais, T., Huddy, R., Van Hille, R. and Harrison, S.T.L. (2017). 'Effect of operational parameters on the performance of an integrated semi-passive bioprocess', in Mine Water and Circular Economy.

Marais, T.S., Huddy, R.J., Harrison, S.T.L. and Hille, R.P. Van (2020). 'Demonstration of simultaneous biological sulphate reduction and partial sulphide oxidation in a hybrid linear flow channel reactor', Journal of Water Process Engineering, 34, pp. 101143.

Maree, J.P. and Strydom, W.F. (1985). 'Biological sulphate removal in an upflow packed bed reactor, 1985', Water Research, 19, pp. 1101–1106.

Matsumoto, S., Shimada, H. and Sasaoka, T. (2016). 'The key factor of acid mine drainage (AMD) in the history of the contribution of mining industry to the prosperity of the United States and South Africa: A Review', Natural Resources, 7, pp. 445–460.

Matz, C. and Kjelleberg, S. (2005). 'Off the hook—how bacteria survive protozoan grazing', Trends in Microbiology, 13, pp. 302–307.

McCarthy, T.S. (2011). 'The impact of acid mine drainage in South Africa', South African Journal of Science, 107(5/6), pp. 1–7.

Methé, B.A., Nelson, K.E., Eisen, J.A., Paulsen, I.T., Nelson, W., Heidelberg, J.F., Wu, D., Wu, M., Ward, N., Beanan, M.J., Dodson, R.J., Madupu, R., Brinkac, L.M., Deboy, R.T., Durkin, A.S., Gwinn,

M., Kolonay, J.F., … Brinkac, L. M. (2003). 'Genome of *Geobacter sulfurreducens* : Metal Reduction in Subsurface Environments', Science, 302(5652), pp. 1967–1969.

Metsalu, T. and Vilo, J. (2015). 'ClustVis: A web tool for visualizing clustering of multivariate data using Principal Component Analysis and heatmap', Nucleic Acids Research, 43(W1), pp. W566–W570.

Meyer, B. and Kuever, J. (2007). 'Molecular analysis of the diversity of sulfate-reducing and sulfur-oxidizing prokaryotes in the environment, using aprA as functional marker gene.', Applied and Environmental Microbiology, 73(23), pp. 7664–79.

Mirjafari, P. and Baldwin, S.A. (2016). 'Decline in performance of biochemical reactors for sulphate removal from mine-influenced water is accompanied by changes in organic matter characteristics and microbial population composition', Water (Switzerland), 8(4), pp. 124–142.

Möller, D., Schauder, R., Fuchs, G. and Thauer, R.K. (1987). 'Acetate oxidation to CO2 via a citric acid cycle involving an ATP-citrate lyase: a mechanism for the synthesis of ATP via substrate level phosphorylation in *Desulfobacter postgatei* growing on acetate and sulfate', Archives of Microbiology, 148(3), pp. 202–207.

Molwantwa, J.B. and Rose, P.D. (2013). 'Development of a Linear Flow Channel Reactor for sulphur removal in acid mine wastewater treatment operations', Water SA, 39(5), pp. 649–654.

Moosa, S. (2000). A kinetic study on anaerobic sulphate reduction - Effect of sulphate and temperature. *MSc dissertation, University of Cape Town.*

Moosa, S., Nemati, M. and Harrison, S.T.L. (2002). 'A kinetic study on anaerobic reduction of sulphate, Part I: Effect of sulphate concentration', Chemical Engineering Science, 57(14), pp. 2773–2780.

Moosa, S., Nemati, M. and Harrison, S.T.L. (2005). 'A kinetic study on anaerobic reduction of sulphate, part II: Incorporation of temperature effects in the kinetic model', Chemical Engineering Science, 60(13), pp. 3517–3524.

Moosa, S., Nemati, M. and Harrison, S.T.L. (2002). 'A kinetic study on anaerobic reduction of sulphate, Part I: Effect of sulphate concentration', Chemical Engineering Science, 57(14), pp. 2773–2780.

Morais-Silva, F.O., Santos, C.I., Rodrigues, R., Pereira, I. and Rodrigues-Pousada, C. (2013). 'Roles of HynAB and Ech, the only two hydrogenases found in the model sulfate reducer *Desulfovibrio gigas*', Journal of Bacteriology, 195(20), pp. 4753–4760.

Mulunda, F.B.N. (2013). Exploring the linkages between land management institutions, land degradation and acid mine drainage: The Case of the West Rand Goldfield. *PhD dissertation, University of Cape Town.*

Muyzer, G. and Stams, A.J.M. (2008). 'The ecology and biotechnology of sulphate-reducing bacteria', Nature Reviews - Microbiology, 6(6), pp. 441–454.

Nadell, C., Drescher, K. and Foster, K. (2016). 'Spatial structure, cooperation and competition inbiofilms', Nature Reviews - Microbiology, 14, pp. 589–600.

Nasir, S., Ibrahim, E., & Arief, A.T. (2016). 'Design and experimental testing of small-scale acid mine drainage treatment plant', Journal of Materials and Environmental Science, 8, pp. 2912–2918.

Neale, J.W., Gericke, M. and Mühlbauer, R. (2018). 'On-site pilot-scale demonstration of a low-cost biological process for the treatment of high-sulphate mine waters', in IMWA proceedings -

Mine Water – Risk to Opportunity (Vol I). Pretoria, South Africa (Tshwane University of Technology), pp. 164–171.

Neidhardt, F.C., Ingraham, J.L., & Schaechter, M. (1990). Physiology of the bacterial cell: a molecular approach. 20th edn. Edited by M. S. A. Sunderland.

Ng, S.K. and Hamilton, I.R. (1971). 'Lactate metabolism by *Veillonella parvula*.', Journal of Bacteriology, 105(3), pp. 999–1005.

Nicolet, Y., Piras, C., Legrand, P., Hatchikian, C.E. and Fontecilla, C. (1999). '*Desulfovibrio desulfuricans* iron hydrogenase: the structure shows unusual coordination to an active site Fe binuclear center', Structure, 7, pp. 13–23.

Nielsen, G., Hatam, I., Abuan, K.A., Janin, A., Coudert, L., Blais, J.F. and Baldwin, S.A. (2018). 'Semi-passive in-situ pilot scale bioreactor successfully removed sulphate and metals from mine impacted water under subarctic climatic conditions', Water Research, 140, pp. 268–279.

Nocker, A., Burr, M. and Camper, A.K. (2007). 'Genotypic microbial community profiling: a critical technical review', Microbial ecology, 54(2), pp. 276–289.

Novhe, N.O., Yibas, B., Coetzee, H., Atanasova, M., Netshitungulwana, R., Modiba, M. and Mashalane, T. (2016). 'Long-Term remediation of acid mine drainage from abandoned coal mine using intergrated (anaerobic and aerobic ) passive treatment system , in South Africa : a Pilot Study', Mining Meets Water -Conflicts and Solutions, (1), pp. 668–675.

Nurk, S., Meleshko, D., Korobeynikov, A. and Pevzner, P.A. (2017). 'metaSPAdes: a new versatile metagenomic assembler', Genome Research, 27(5), pp. 824–834.

O'Flaherty, V., Mahony, T., O'Kennedy, R. and Colleran, E. (1998). 'Effect of pH on growth kinetics and sulphide toxicity thresholds of a range of methanogenic, syntrophic and sulphate-reducing bacteria', Process Biochemistry, 33(5), pp. 555–569.

O'Toole, G.A. and Wong, G.C. (2016). 'Sensational biofilms: surface sensing in bacteria', Current Opinion in Microbiology, 30, pp. 139–146.

Oliveira, T.F., Franklin, E., Afonso, J.P., Khan, A.R., Oldham, N.J., Pereira, I.A.C. and Archer, M. (2011). 'Structural insights into dissimilatory sulfite reductases: Structure of desulforubidin from *Desulfomicrobium norvegicum*', Frontiers in Microbiology, 2(APR), pp. 1–12.

Olm, M.R., Brown, C.T., Brooks, B. and Banfield, J.F. (2017). 'dRep : a tool for fast and accurate genomic comparisons that enables improved genome recovery from metagenomes through de-replication', The ISME Journal, 11(12), pp. 2864–2868.

Omil, F., Lens, P., Visser, A., Hulshoff Pol, L.W. and Lettinga, G. (1998). 'Long-term competition between sulfate reducing and methanogenic bacteria in UASB reactors treating volatile fatty acids', Biotechnology and Bioengineering, 57(6), pp. 676–685.

Omil, F., Oude Elferink, S., Lens, P., Hulshoff, L.W. and Lettinga, G. (1997). 'Effect of the inoculation with *Desulforhabdus amnigenus* and pH or $O_2$ shocks on the competition between sulphate reducing and methanogenic bacteria in an acetate fed UASB reactor', Bioresource Technology, 60(2), pp. 113–122.

Oude Elferink, S., Akkermans-van Vliet, W., Bogte, J. and Stams, A. (1999). '*Desulfobacca acetoxidans* gen. nov., sp. nov., a novel acetate-degrading sulfate reducer isolated from sulfidogenic granular sludge', International Journal of Systematic Bacteriology, 49(2), pp. 345–350.

Oyekola, O.O. (2008). An investigation into the relationship between process kinetics and microbial community dynamics in a lactate-fed sulphidogenic CSTR as a function of residence time and sulphate loading. *PhD dissertation, University of Cape Town.*

Oyekola, O.O., Harrison, S.T.L. and van Hille, R.P. (2012). 'Effect of culture conditions on the competambienitive interaction between lactate oxidizers and fermenters in a biological sulfate reduction system', Bioresource Technology, 104, pp. 616–621.

Oyekola, O.O., van Hille, R.P. and Harrison, S.T.L. (2009a). 'Competition between lactate oxidisers and fermenters under biosulphidogenic conditions: implications in the biological treatment of AMD', Advanced Materials Research, 71–73, pp. 689–692.

Oyekola, O.O., van Hille, R.P. and Harrison, S.T.L. (2009b). 'Study of anaerobic lactate metabolism under biosulfidogenic conditions.', Water Research, 43(14), pp. 3345–54.

Oyekola, O.O., van Hille, R.P. and Harrison, S.T.L. (2010). 'Kinetic analysis of biological sulphate reduction using lactate as carbon source and electron donor: Effect of sulphate concentration', Chemical Engineering Science, 65(16), pp. 4771–4781.

Ozuolmez, D., Na, H., Lever, M. . and Kjeldsen, K.U. (2015). 'Methanogenic archaea and sulfate reducing bacteria co-cultured on acetate : teamwork or coexistence ?', Frontiers in Microbiology, 6, p. 492.

Pagani, I., Lapidus, A., Nolan, M., Lucas, S., Hammon, N., Desh-Pande, S., Cheng, J.F., Chertkov, O., Davenport, K., Tapia, R., Han, C., Goodwin, L., Pitluck, S., Liolios, K., Mavromatis, K., Ivanova, N., Mikhailova, N., … Klenk, H.P. (2011). 'Complete genome sequence of *Desulfobulbus propionicus* type strain (1pr3 T)', Standards in Genomic Sciences, 4(1), pp. 100–110.

Pareek, S., Azuma, J., Shimizu, Y. and Matsui, S. (2001). 'Hydrolysis of newspaper polysaccharides under sulfate reducing and methane producing conditions', Biodegradation, 11, pp. 229–237.

Parks, D.H., Imelfort, M., Skennerton, C.T., Hugenholtz, P. and Tyson, G.W. (2015). 'CheckM: assessing the quality of microbial genomes recovered from isolates, single cells, and metagenomes', Genome Research, 25, pp. 1043–1055.

Peng, Y., Leung, H.C., Yiu, S.M. and Chin, F.Y. (2012). 'IDBA-UD: a de novo assembler for single-cell and metagenomic sequencing data with highly uneven depth', Bioinformatics, 28(11), pp. 1420–1428.

Pereira, I., Haveman, S. and Voordouw, G. (2007). 'Biochemical, genetic and genomic characterization of anaerobic electron transport pathways in sulphate-reducing delta-proteobacteria', in L.L. Barton, & W.A.A.H. (ed.) Sulphate-reducing bacteria: Environmental and engineered systems. Cambridge: Cambridge University Press, pp. 215–240.

Peters, J.W., Schut, G.J., Boyd, E.S., Mulder, D.W., Shepard, E.M., Broderick, J.B., King, P.W. and Adams, M.W.W. (2015). '[FeFe]- and [NiFe]-hydrogenase diversity, mechanism, and maturation', Biochimica et Biophysica Acta - Molecular Cell Research, 1853(6), pp. 1350–1369.

Pirt, S.J. (1965). 'The maintenance energy of bacteria in growing cultures.', Proceedings of the Royal Society of London. Series B. Biological Sciences., 163, pp. 329–336.

Plumlee, G.S., Smith, K.S., Montour, M.R., Ficklin, W.H. and Mosier, E. (1999). 'Geologic controls on the composition of natural waters and mine waters draining diverse mineral-deposit types', The environmental geochemistry of mineral deposits. Part B: case studies and research topics, 6(373–432).

Price, M.N., Dehal, P.S. and Arkin, A.P. (2009). 'Fasttree: Computing large minimum evolution trees with profiles instead of a distance matrix', Molecular Biology and Evolution, 26(7), pp. 1641–1650.

Probst, A.J., Castelle, C.J., Singh, A., Brown, C.T., Anantharaman, K., Sharon, I., Hug, L.A., Burstein, D., Emerson, J.B., Thomas, B.C. and Banfield, J.F. (2017). 'Genomic resolution of a cold subsurface aquifer community provides metabolic insights for novel microbes adapted to high $CO_2$ concentrations', Environmental Microbiology, 19(2), pp. 459–474.

Pruden, A., Messner, N., Pereyra, L., Hanson, R.E., Hiibel, S.R. and Reardon, K.F. (2007). 'The effect of inoculum on the performance of sulfate-reducing columns treating heavy metal contaminated water', Water Research, 41(4), pp. 904–914.

Rabus, R., Hansen, T.A. and Widdel, F. (2006). 'Dissimilatory sulfate-and sulfur-reducing prokaryotes.', Springer New York, pp. 659–678.

Rabus, R., Venceslau, S.S., Wöhlbrand, L., Voordouw, G., Wall, J.D. and Pereira, I.A.C. (2015). 'A post-genomic view of the ecophysiology, catabolism and biotechnological relevance of sulphate-reducing prokaryotes', in Advances in Microbial Physiology. Academic Press, pp. 55–321.

Raes, J., O Korbel, J., Lercher, M., von Mering, C. and Bork, P. (2007). 'Prediction of effective genome size in metagenomic samples', Genome Biology, 8(1), pp. 1–11.

Ragsdale, S.W. (2008). 'Enzymology of the Woods-Ljundahl pathway of acetogenesis', Annals of the New York Academy of Sciences, 1125, pp. 129–136.

Rahman, S.F., Kantor, R.S., Huddy, R., Thomas, B.C., van Zyl, A.W., Harrison, S. T. L. and Banfield, J. F. (2017). 'Genome-resolved metagenomics of a bioremediation system for degradation of thiocyanate in mine water containing suspended solid tailings', MicrobiologyOpen, 6(3), pp. 1–9.

Rendueles, O. and Ghigo, J.M. (2015). 'Mechanisms of competition in biofilm communities', Microbiology Spectrum, 3(3).

Rogosa, M. (1963). 'The Genus *Veillonella*', Journal of Bacteriology, 87(1), pp. 162–170.

Rose, P. (2013). 'Review: Long-term sustainability in the management of acid mine drainage wastewaters – development of the Rhodes BioSURE Process', Water SA, 39(5), p. 582.

Roume, H., Heintz-Buschart, A., Muller, E., May, P., Satagopam, V., Laczny, C.C., Narayanasamy, S., Lebrun, L.A., Hoopmann, M.R., Schupp, J.M., Gillece, J.D., Hicks, H.D., Engelthaler, D.M., Sauter, T., Moritz, R.L. and Wilmes, P. (2015). 'Comparative integrated omics: identification of key functionalities in microbial community-wide metabolic networks', npj Biofilms and Microbiomes, 57(6), pp. 10–13.

Ruckert, C. (2016). 'Sulfate reduction in microorganisms — recent advances and biotechnological applications', Current Opinion in Microbiology, 33, pp. 140–146.

Sáez- Navarrete, C., Zamorano, A., Ferrada, C. and Rodríguez, L. (2009). 'Sulphate reduction and biomass growth rates for *Desulfobacterium autotrophicum* in yeast extract - Supplemented media at 38°C', Desalination, 248(1–3), pp. 377–383.

Santos, A.A., Venceslau, S.S., Grein, F., Leavitt, W.D., Dahl, C., Johnston, D.T. and Pereira, I.A.C. (2015). 'A protein trisulfide couples dissimilatory sulfate reduction to energy conservation', Science, 350(6267), pp. 1541–1545.

Sarti, A. and Zaiat, M. (2011). 'Anaerobic treatment of sulphate-rich wastewater in an anaerobic sequential batch reactor (AnSBR) using butanol as the carbon source', Journal of Environmental Management, 92(6), pp. 1537–1541.

Sato, Y., Hamai, T., Hori, T., Habe, H., Kobayashi, M. and Sakata, T. (2018). 'Year-Round Performance of a Passive Sulfate-Reducing Bioreactor that Uses Rice Bran as an Organic Carbon Source to Treat Acid Mine Drainage', Mine Water and the Environment, 37(3), pp. 586–594.

Schauder, R., Eikmanns, B., Thauer, R.K., Widdel, F. and Fuchs, G. (1986). 'Acetate oxidation to CO2 in anaerobic bacteria via a novel pathway not involving reactions of the citric acid cycle', Archives of Microbiology, 145(2), pp. 162–172.

Schauder, R., Widdel, F. and Fuchs, G. (1987). 'Carbon assimilation pathways in sulfate reducing bacteria. 2. Enzymes of a reductive citric acid cycle in the autotrophic *Desulfobacter hydrogenophilus'*, Archives of Microbiology, 148, pp. 218–225.

Scheiman, J., Luber, J.M., Chavkin, T.A., MacDonald, T., Tung, A., Pham, L.D., Wibowo, M.C., Wurth, R.C., Punthambaker, S., Tierney, B.T., Yang, Z., Hattab, M.W., Avila-Pacheco, J., Clish, C. B., Lessard, S., Church, G.M. and Kostic, A.D. (2019). 'Meta-omics analysis of elite athletes identifies a performance-enhancing microbe that functions via lactate metabolism', Nature Medicine, 25(7), pp. 1104–1109.

Schloss, P.D.; Westcott, S.L.; Ryabin, T.; Hall, J.R.; Hartmann, M.; Hollister, E.B. and Lesniewski, R.A.; Oakley, B.B.; Parks, D.H.; Robinson, C. J. (2009). 'Introducing mothur: opensource, platform-independent, community-supported software for describing and comparing microbial communities.', Applied and Environmental Microbiology, 75(23), pp. 7537–7541.

Scholz, M.B., Lo, C. and Chain, P.S. (2012). 'Next generation sequencing and bioinformatic bottlenecks: the current state of metagenomic data analysis', Current Opinion in Biotechnology, 23(1), pp. 9–15.

Schrenk, M.O., Edwards, K.J., Goodman, R.M., Hamers, R.J. and Banfield, J. F. (1998). 'Distribution of *Thiobacillus ferrooxidans* and *Leptospirillum ferrooxidans*: Implications for Generation of Acid Mine Drainage', Science, 279(5356), pp. 1519–1522.

Schröder, I., Rech, S., Krafft, T. and Macy, J.M. (1997). 'Purification and characterization of the selenate reductase from *Thauera selenatis*', Journal of Biological Chemistry, 272(38), pp. 23765–23768.

Seeliger, S., Janssen, P.H. and Schink, B. (2002). 'Energetics and kinetics of lactate fermentation to acetate and propionate via methylmalonyl-CoA or acrylyl-CoA', FEMS Microbiology Letters, 211(1), pp. 65–70.

Selmer, T., Willanzheimer, A. and Hetzel, M. (2002). 'Propionate CoA-transferase from *Clostridium propionicum*. Cloning of gene and identification of glutamate 324 at the active site', European Journal of Biochemistry, 269, pp. 372–380.

Shade, A., Peter, H., Allison, S.D., Baho, D., Berga, M., Bürgmann, H., Huber, D.H., Langenheder, S., Lennon, J.T. and Martiny, J.B. (2012). 'Fundamentals of microbial community resistance and resilience', Frontiers in Microbiology, 3, p. 417.

Sharon, I., Morowitz, M.J., Thomas, B.C., Costello, E.K., Relman, D.A. and Banfield, J.F. (2013). 'Time series community genomics analysis reveals rapid shifts in bacterial species, strains, and phage during infant gut colonization.', Genome Research, 23(1), pp. 111–20.

Shen, Y. and Buick, R. (2004). 'The antiquity of microbial sulfate reduction', Earth-Science Reviews, pp. 243–272.

Shi, J., Lin, H., Yuan, X. and Zhao, Y. (2011). 'Isolation and characterization of a novel sulfuroxidizing chemolithoautotroph *Halothiobacillus* from Pb polluted paddy soil', African Journal of Biotechnology, 10(20), pp. 4121–4126.

Shin, J., Lee, Sooin, Go, M., Lee, Sang, Kim, S., Lee, C. and Cho, B. (2016). 'Analysis of the mouse gut microbiome using full-length 16S rRNA amplicon sequencing', Scientific Reports, 6(1), p. 29681.

Shu, D., He, Y., Yue, H., Zhu, L. and Wang, Q. (2015). 'Metagenomic insights into the effects of volatile fatty acids on microbial community structures and functional genes in organotrophic anammox process', Bioresource Technology, 196, pp. 621–633.

Sieber, C.M., Probst, A.J., Sharrar, A., Thomas, B.C., Hess, M., Tringe, S.G. and Banfield, J.F. (2018). 'Recovery of genomes from metagenomes via a dereplication, aggregation and scoring strategy', Nature Microbiology, 3, pp. 836–843.

Simate, G.S. and Ndlovu, S. (2014). 'Acid mine drainage: Challenges and opportunities', Journal of Environmental Chemical Engineering, 2(3), pp. 1785–1803.

Simon, C. and Daniel, R. (2011). 'Metagenomic analyses: past and future trends.', Applied and Environmental Microbiology, 77(4), pp. 1153–61.

Skousen, J.G., Sexstone, A. and Ziemkiewicz, P.F. (2000). 'Acid mine drainage control and treatment', Reclamation of Drastically Disturbed Lands, 41, pp. 131–168.

Sorokin, Y.I. (1966). 'Role of carbon dioxide and acetate in biosynthesis by sulphate-reducing bacteria', Nature, 210(5035), pp. 551–552.

Speece, R.E. (1983). 'Anaerobic biotechnology for industrial Wastewater treatment', Environmental Science and Technology, 17, pp. 416–427.

Spero, M.A., Aylward, F.O., Currie, C.R. and Donohue, T.J. (2015). 'Phylogenomic analysis and predicted physiological role of the proton-translocating NADH: Quinone oxidoreductase (complex I) across bacteria', mBio, 6(2), pp. 1–14.

Stams, A.J.M., Huisman, J., Garcia Encina, P.A. and Muyzer, G. (2009). 'Citric acid wastewater as electron donor for biological sulfate reduction', Applied Microbiology and Biotechnology, 83(5), pp. 957–963.

Starke, R., Keller, A., Jehmlich, N., Vogt, C., Richnow, H.H., Kleinsteuber, S., von Bergen, M. and Seifert, J. (2016). 'Pulsed $^{13}C_2$-acetate protein-sip unveils Epsilonproteobacteria as dominant acetate utilizers in a sulfate-reducing microbial community mineralizing benzene', Microbial Ecology, 71(4), pp. 901–911.

Steed, V.S., Suidan, M.T., Gupta, M., Miyahara, T., Acheson, C.M. and Sayles, G.D. (2000). 'Development of a sulfate-reducing biological process to remove heavy metals from acid mine drainage', Water Environment Research, 72(5), pp. 530–535.

Stegen, J.C., Lin, X., Konopka, A.E. and Fredrickson, J.K. (2012). 'Stochastic and deterministic assembly processes in subsurface microbial communities', The ISME Journal, 6(9), pp. 1653–1664.

Stieb, M., and Schink, B. (1989). 'Anaerobic degradation of isobutyrate by methanogenic enrichment cultures and by a *Desulfococcus multivorans* strain', Archives of Microbiology, 151, pp. 126–132.

Stubner, S. (2004). 'Quantification of gram-negative sulphate-reducing bacteria in rice field soil by 16S rRNA gene-targeted real-time PCR', Journal of Microbiological Methods, 57(2), pp. 219–230.

Sul, W.J., Park, J., Quensen, J.F., Rodrigues, J.L.M., Seliger, L., Tsoi, T.V., Zylstra, G.J. and Tiedje, J.M. (2009). 'DNA-stable isotope probing integrated with metagenomics for retrieval of biphenyl dioxygenase genes from polychlorinated biphenyl-contaminated river sediment', Applied and Environmental Microbiology, 75(17), pp. 5501–5506.

Surkov, A., Dubinina, G., Lysenko, A., Glöckner, F. and Kuever, J. (2001). '*Dethiosulfovibrio russensis* sp. nov., *Dethiosulfovibrio marinus* sp. nov. and *Dethiosulfovibrio acidaminovorans* sp. nov., novel anaerobic, thiosulfate- and sulfur-reducing bacteria isolated from "Thiodenron" sulfur mats in different saline environments', International Journal of Systematic and Evolutionary Microbiology, 51(2), pp. 327–337.

Thauer, R.K., Jungermann, K. and Decker, K. (1977). 'Energy conservation in chemotrophic anaerobic bacteria.', Bacteriological Reviews, 41(1), pp. 100–180.

Thauer, R.K., Stackebrandt, E. and Hamilton, W.A. (2007). Sulphate-Reducing Bacteria: Environmental and engineered systems. Cambridge University Press.

Thomas, T., Gilbert, J. and Meyer, F. (2012). 'Metagenomics - a guide from sampling to data analysis', Microbial Informatics and Experimentation, 2(1), p. 3.

Timmers, P.H.A., Vavourakis, C.D., Kleerebezem, R., Damsté, J.S., Muyzer, G., Stams, A.J., Sorokin, D. and Plugge, C.M. (2018). 'Metabolism and occurrence of methanogenic and sulfate-reducing syntrophic acetate oxidizing communities in haloalkaline environments', Frontiers in Microbiology, 9, pp. 1–18.

Tomlinson, D.L., Wilson, J.G. and Harris, C.R. and Jeffrey, D.W. (1980). 'Problems in the assessment of heavy-metal levels in estuaries and the formation of a pollution index', Helgoländer meeresuntersuchungen, 33(1), p. 566.

Trumm, D. (2010). 'Selection of active and passive treatment systems for AMD - Flow charts for New Zealand conditions', New Zealand Journal of Geology and Geophysics, 53(2–3), pp. 195–210.

Turnbaugh, P.J., Ley, R.E., Hamady, M., Fraser-Liggett, C.M., Knight, R. and Gordon, J.I. (2007). 'The human microbiome project', Nature, 449, p. 804.

Tyson, G.W., Chapman, J., Hugenholtz, P., Allen, E.E., Ram, R.J., Richardson, P.M., Solovyev, V.V., Rubin, E.M., Rokhsar, D.S. and Banfield, J.F. (2004). 'Community structure and metabolism through reconstruction of microbial genomes from the environment', Nature, 428(6978), pp. 37–43.

US EPA (1999). Health effects from exposure to high levels of sulfate in drinking water study.

Vanwonterghem, I., Jensen, P.D., Dennis, P.G., Hugenholtz, P., Rabaey, K. and Tyson, G.W. (2014). 'Deterministic processes guide long-term synchronised population dynamics in replicate anaerobic digesters', The ISME Journal, 8(10), pp. 2015–2028.

Vanwonterghem, I., Jensen, P.D., Rabaey, K. and Tyson, G.W. (2016). 'Genome-centric resolution of microbial diversity , metabolism and interactions in anaerobic digestion', Environmental Microbiology, 18(9), pp. 3144–3158.

Vasquez, Y., Escobar, M.C., Neculita, C.M., Arbeli, Z. and Roldan, F. (2016). 'Biochemical passive reactors for treatment of acid mine drainage: Effect of hydraulic retention time on changes in

efficiency, composition of reactive mixture, and microbial activity', Chemosphere, 153, pp. 244–253.

Vasquez, Y., Escobar, M.C., Saenz, J.S., Quiceno-Vallejo, M.F., Neculita, C.M., Arbeli, Z. and Roldan, F. (2018). 'Effect of hydraulic retention time on microbial community in biochemical passive reactors during treatment of acid mine drainage', Bioresource Technology, 247(4), pp. 624–632.

Vavilin, V.A., Vasiliev, V.B., Rytov, S.V. and Ponomarev, A.V. (1994). 'Self-oscillating coexistence of methanogens and sulfate-reducers under hydrogen sulfide inhibition and the pH-regulating effect', Bioresource Technology, 49, pp. 105–119.

Vignais, P. and Colbeau, A. (2004). 'Molecular biology of microbial hydrogenases', Current Issues in Molecular Biology, 6, pp. 159–188.

Vollmers, J., Wiegand, S. and Kaster, A.K. (2017). 'Comparing and evaluating metagenome assembly tools from a microbiologist's perspective-Not only size matters!', PloS one, 12(1), pp. 1–31.

Voolapalli, R.K. and Stuckey, D.C. (2001). 'Hydrogen production in anaerobic reactors during shock loads - Influence of formate production and H2 kinetics', Water Research, 35(7), pp. 1831–1841.

Vossoughi, M., Shakeri, M. and Alemzadeh, I. (2003). 'Performance of anaerobic baffled reactor treating synthetic wastewater influenced by decreasing COD/SO4 ratios', Chemical Engineering and Processing: Process Intensification, 42(10), pp. 811–816.

Wagner, M., Roger, A.J., Flax, J.L., Brusseau, G.A. and Stahl, D.A. (1998). 'Phylogeny of dissimilatory sulfite reductases supports an early origin of sulfate respiration', Journal of Bacteriology, 180(11), pp. 2975–2982.

Wall, J.D., Arkin, A.P., Balci, N.C. and Rapp-Giles, B. (2008). 'Genetics and genomics of sulfate respiration in *Desulfovibrio*', in Friedrich, C.D. & C.G. (ed.) Microbial sulfur metabolism. Heidelberg: Springer-Verlag, pp. 1–12.

Watzlaf GR, Schroeder KT, Kairies C (2000). 'Long-term performance of alkalinity-producing passive systems for the treatment of mine drainage.' In Proceedings of the 2000 National Meeting of the American Society for Surface Mining and Reclamation, (262274), pp. 262–274.

Weedon, F.R., Hartzell, A. and Setterstrom, C. (1940). 'Toxicity of ammonia, chlorine, hydrogen cyanide, hydrogen sulphide, and sulphur dioxide gases', Contributions. Boyce Thompson Institute for Plant Research, 11(5), pp. 365–385.

White, C. and Gadd, G.M. (1996). 'Mixed sulphate-reducing bacterial cultures for bioprecipitation of toxic metals: Factorial and response-surface analysis of the effects of dilution rate, sulphate and substrate concentration', Microbiology, 142(8), pp. 2197–2205.

Widdel, F. (1988). 'Microbiology and ecology of sulphate-reducing bacteria', Biology of Anaerobic Microorganisms, John Wiley and Sons, pp. 469–585.

Widdel, F. and Pfennig, N. (1982). 'Studies on dissimilatory sulfate-reducing bacteria that decompose fatty acids II. Incomplete oxidation of propionate by *Desulfobulbus propionicus* gen. nov., sp. nov', Archives of Microbiology, 131(4), pp. 360–365.

Wirth, R., Chertkov, O., Held, B., Lapidus, A., Nolan, M., Lucas, S., Hammon, N., Deshpande, S., Cheng, J.F., Tapia, R., Han, C., Goodwin, L., Pitluck, S., Liolios, K., Ioanna, P., Ivanova, N.,

Mavromatis, K., … Klenk, H.P. (2011). 'Complete genome sequence of *Desulfurococcus mucosus* type strain (O7/1 T)', Standards in Genomic Sciences, 4(2), pp. 173–182.

Wu,Y., Simmons, B.A. and Singer, S.W. (2016). 'MaxBin 2.0: an automated binning algorithm to recover genomes from multiple metagenomic datasets', Bioinformatics, 32(4), pp. 605–607.

Xu, R., Yang, Z.H., Zheng, Y., Liu, J.B., Xiong, W.P., Zhang, Y.R., Lu, Y., Xue, W.J. and Fan, C.Z. (2018). 'Organic loading rate and hydraulic retention time shape distinct ecological networks of anaerobic digestion related microbiome', Bioresource Technology, 262, pp. 184–193.

Younger, P.L., Jayaweera, A., Elliot, A., Wood, R., Amos, P., Daugherty, A.J., Martin, A., Bowden, L., Aplin, A.C. and Barrie, J.D. (2003). 'Passive treatment of acidic mine waters in subsurface-flow systems: exploring RAPS and permeable reactive barriers', Land Contamination and Reclamation, 11(2), pp. 127–135.

Yu, X., Niks, D., Mulchandani, A. and Hille, R. (2017). 'Efficient reduction of $CO_2$ by the molybdenum-containing formate dehydrogenase from *Cupriavidus necator* (*Ralstonia eutropha*)', Journal of Biological Chemistry, 292(41), pp. 16872–16879.

Yuan, C., Lei, J., Cole, J. and Sun, Y. (2015). 'Reconstructing 16S rRNA genes in metagenomic data', Bioinformatics, 31(12), pp. i35–i43.

Zagury, G.J., Kulnieks, V.I. and Neculita, C.M. (2006). 'Characterization and reactivity assessment of organic substrates for sulphate-reducing bacteria in acid mine drainage treatment.', Chemosphere, 64(6), pp. 944–54.

Zagury, G.J. and Neculita, C. (2007). 'Passive Treatment of Acid Mine Drainage in Bioreactors : Short Review , Applications , and Research Needs', in In Proceedings of the 60th Canadian geotechnical conference and 8th joint CGS/IAH-CNC specialty groundwater conference, Ottawa, Canada, pp. 1439–1446.

Zaluski, M., Foote, M., Manchester, K., Canty, M., Willis, M., Consort, J. and Al, E. (1999). 'Design and construction of bioreactors with sulphate-reducing bacteria for acid mine drainage control, in Phytoremediation and Innovative Strategies for Specialized Remedial Apllications', in The Fifth International in Situ and On-site Bioremediation Symposium, San Diego, California (USA) Applications, pp. 205–210.

Zhang, X., Niu, J., Liang, Y., Liu, X. and Yin, H. (2016). 'Metagenome-scale analysis yields insights into the structure and function of microbial communities in a copper bioleaching heap', BMC Genetics, 17(1), p. 21.

Zheng, Y., Xiao, Y., Yang, Z., Wu, S., Xu, H., Liang, F. and Zhao, F. (2014). 'The bacterial communities of bioelectrochemical systems associated with the sulfate removal under different pHs', Process Biochemistry, 49(8), pp. 1345–1351.

Zhou, J., Zhou, X., Li, Y. and Xing, J. (2015). 'Bacterial communities in haloalkaliphilic sulfate-reducing bioreactors under different electron donors revealed by 16S rRNA MiSeq sequencing', Journal of Hazardous Materials, 295, pp. 176–184.

Zoetemeyer, R.J., van Den Heuve, J.C. and Cohen, A. (1982). 'pH influence on acidogenic dissimilation of glucose in an anaerobic digestor', Water Research, 16, pp. 303–311.

Zverlov, V., Klein, M., Lücker, S., Friedrich, M., Kellermann, J., Stahl, D.A., Loy, A., Wagner, M., Lu, S., Friedrich, M., Kellermann, J., Stahl, D., Loy, A. and Wagner, M. (2005). 'Lateral gene transfer of dissimilatory (bi)sulfite reductase revisited.', Journal of Bacteriology, 187(6), pp. 2203–8.

# Appendices

## A.1 Materials and Methodology

### A.1.1 Miscellaneous reagents

**Sodium 2-bromoethanesulfonate solution (BESA)**

Analytical grade sodium 2-bromoethanesulphonate was dissolved in appropriate reactor medium to 10 mM (CSTR, LFCR) and 20 mM (UAPBR).

**Phosphate-buffered saline (PBS)**

A 1x PBS solution was prepared containing 2.7 mM potassium chloride, 137 mM sodium chloride, and 1.76 mM potassium phosphate, at pH 7.4

### A.1.2 Sulphate assay

**Conditioning reagent**

Conditioning reagent was prepared by dissolving 75 g of sodium chloride in 30 mℓ hydrochloric acid (32%), 50 mℓ glycerol,100 mℓ absolute ethanol and 300 mℓ deionised water.

**Sulphate standard solution and standard curve**

A sulphate standard curve was generated concurrently with every sulphate assay. A standard stock solution of 10 g/ℓ sulphate was prepared by dissolving 14.78 g of analytical grade $Na_2SO_4$ in deionised water. This was diluted to a final concentration of 1 g/ℓ using deionised water and used to generate a standard curve of final sulphate concentrations of 10 to 50 mg/ℓ (Figure A1-1). Each standard curve was prepared in duplicate.

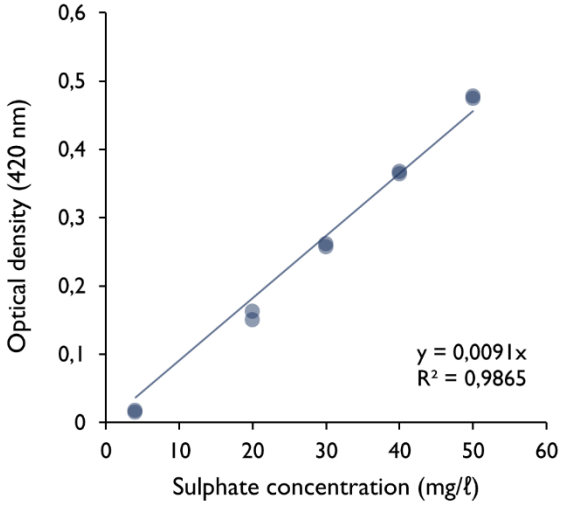


Figure A1-1 Sulphate standard curve generated using the methodology described in Section 3.5.1. The gradient of the standard curve and the $R^2$ goodness of fit are shown on the plot.

### A.1.3 Sulphide assay

**N,N-dimethyl-p-phenylenediamine solution (DMPD)**

A 19 mM DMPD solution was prepared by dissolving 2 g of DMPD in 500 mℓ of 6 M hydrochloric acid.

**Ferric Chloride solution**

A 22 mM ferric chloride solution was prepared by dissolving 8 g of ferric chloride in 500 mℓ of 6 M hydrochloric acid .

**Zinc acetate solution**

A 6.8 mM zinc acetate solution was prepared by dissolving 2.5 g of zinc acetate in 500 mℓ of 6 M hydrochloric acid.

### A.1.4 Volatile fatty acid analysis

Volatile fatty acids (VFAs) were determined using HPLC against a standard curve of each respective VFA as shown in Figure A1-2. These standard curves were generated using analytical grade reagents which diluted using deionised water to six concentrations between 100 and 600 mg/ℓ. The differing elution times of each of these VFAs allowed these VFAs to be combined into a single sample before analysis.

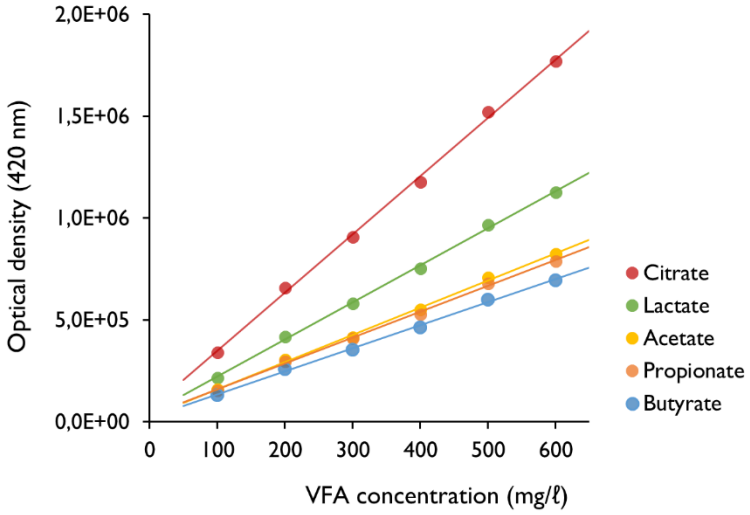


Figure A1-2 Standard curves of the assayed volatile fatty acids (VFAs) with concentrations between 100 and 600 mg/ℓ of each respective VFA.

## A.2 Hydrodynamics of the LFCR

Prior studies have demonstrated the LFCR to achieve complete mixing well within a single hydraulic residence time (Marais et al., 2020; Marais, 2020). The hydrodynamics of the LFCR were evaluated in this study using a step-up saline tracer study. The 2.4 ℓ LFCR was filled with deionised water and a conductivity probe was placed at the effluent port. Deionised water was initially supplied continuously to the reactor, via a peristaltic pump, at a six-hour HRT. After three minutes, the incoming deionised water was changed for a 1M NaCl tracer solution (t = 00:00:00,

Figure A2-1) and the six-hour HRT maintained. The residence time distribution (RTD), or F-curve, generated during the step-up tracer study showed a strong resemblance to that of an ideal CSTR (Figure A2-1).

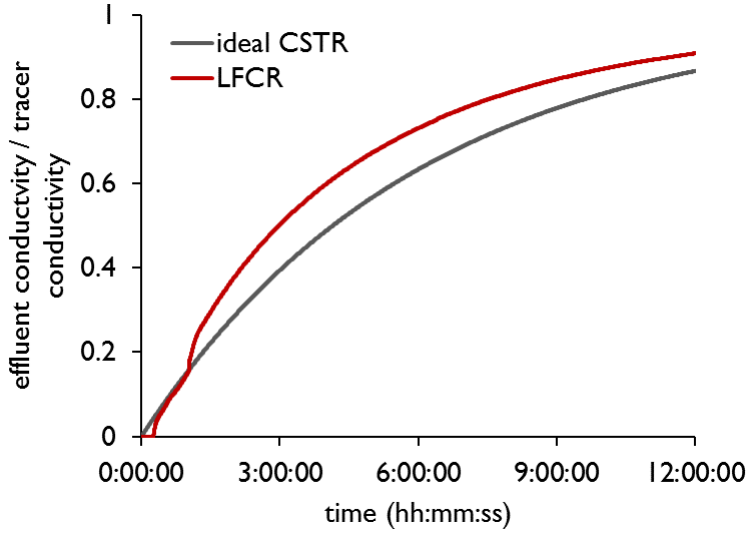


Figure A2-1 Residence time distribution (RTD) of the LFCR and a theoretical CSTR each operated at a six-hour HRT. This RTD curve was generated during a step up saline tracer experiment whereby a conductivity probe was placed at the effluent of the reactor, the reactor was filled with deionised water and a 1 M NaCl solution was pumped continuously into the reactor via the inlet port at a dilution rate of 0.167 $h^{-1}$.

The F-curve of the ideal CSTR was generated using the mixing equation shown below (Equation A2-1). This equation describes the concentration of a solute ($C_1$) in a step up tracer experiment, given the concentration of the solute in the incoming stream ($C_i$), the applied hydraulic retention time ($\tau$) and the time following the start of the continuous input of the tracer ($t$).

$$C_1 = C_i \cdot \mathrm{e}^{-\frac{t}{\tau}}$$

Equation A2-1

The general shape of the RTD curve of the LFCR and its strong resemblance to that of the ideal CSTR allowed the conclusion that the LFCR is a relatively well-mixed system. Deviations from the F-curve of the CSTR in the first three hours of the experiment suggest some elements of non-ideal flow occur within the reactor. For this reason, it was decided that the LFCR should be compartmentalised into two discrete zones (Section 3.3.2) which are both sampled simultaneously.

## A.3 Cell detachment protocol

A cell detachment protocol was adapted from Chiume et al. (2012) and Govender et al. (2013) to enable the quantification of microbial cells attached to and associated with the incorporated solid support structures within the LFCRs and UAPBRs. The detachment protocol, described in Section 3.6.2, was validated for use as described below.

Twelve pieces of polyurethane foam were removed from each of the UAPBRs and twelve groupings of carbon microfibres were removed from each of the LFCRs prior to the establishment

of steady-state at a four-day HRT. These twelve units of support structures were divided into three groups of four pieces and placed into one of three 50 mℓ sterilin tubes containing 30 mℓ of reactor medium without a supplemented electron donor. These solid support structures were taken through the cell detachment protocol as described in Section 3.6.2. Following each of the seven Tween ® 20 wash steps of this procedure, the supernatant from two of the three repeats were sampled and the quantity of cells detached from the four units of solid support structures were quantified by direct cell counting (Section 3.6.1). Where too few cells to be counted were present, the number of cells recovered was recorded to be zero. After seven wash steps had been performed, a piece of solid support structure was assessed for SEM analysis (Section 3.6.3; Figure A3-2 and Figure A3-4). The third repeat of four solid support structures were similarly taken through the cell detachment protocol but no cell quantification was performed. Instead, a representative piece of solid support structure was removed after the associated cells had been removed and after the first, second, fifth and seventh wash step had been performed. These were assessed by SEM analysis (Section 3.6.3; Figure A3-2 and Figure A3-4).

The number of cells removed from the four units of polyurethane foam and carbon microfibres are shown in Figure A3-1 and Figure A3-3, respectively. These indicate that the majority of the cells detached from the polyurethane foam and the carbon microfibres were recovered in the first two to three Tween wash steps. No cells were recovered from the colonised carbon microfibres nor from the polyurethane foam removed from the acetate-supplemented reactors after four washes. Relatively small quantities of cells could be recovered from the polyurethane foam removed from the lactate-supplemented UAPBR between the fourth and seventh wash step. SEM analysis (Figure A3-2 and Figure A3-4) confirmed that the large majority of attached cells were removed during the initial wash steps and very few cells remained attached to the support structures after seven wash steps. It was therefore concluded that seven Tween wash steps were sufficient to recover the large majority of cells from these solid support structures.

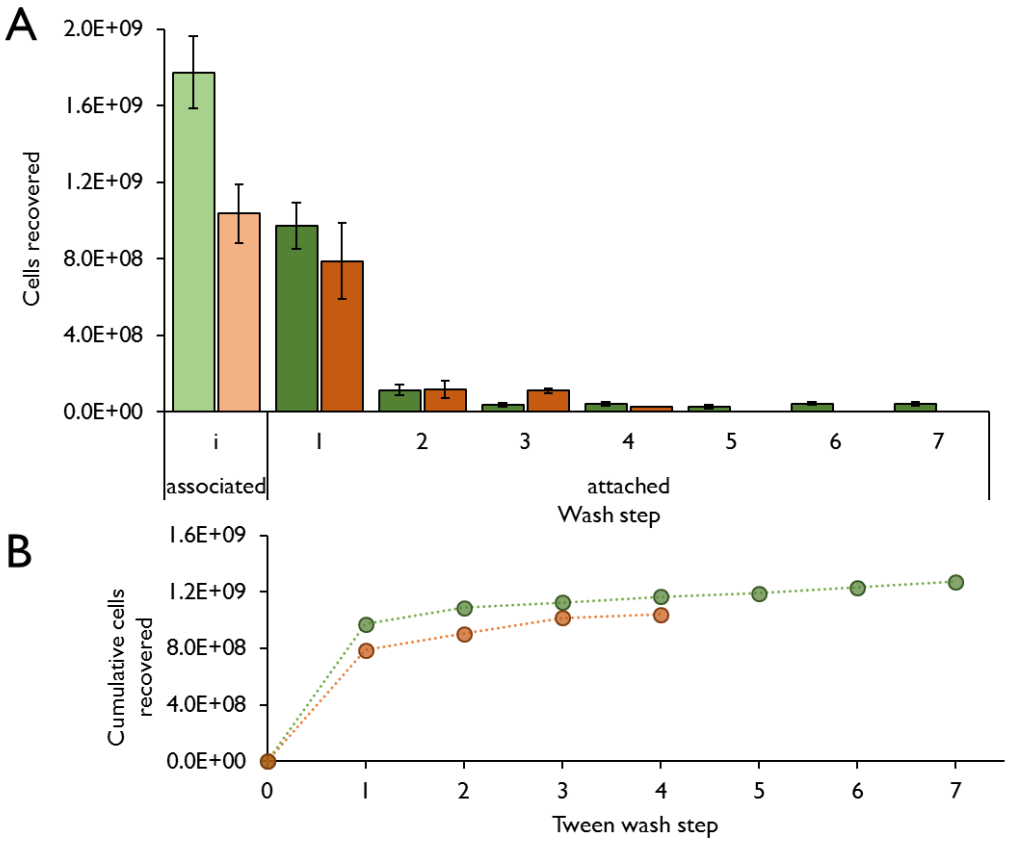


Figure A3-1 The quantity of cells recovered from individual groupings of carbon microfibres removed from the lactate (green) and acetate (orange) supplemented LFCRs, following each step of the cell recovery protocol (Section 3.6.2). Mild agitation was used to dislodge matrix-associated cells from the carbon microfibres. Matrix attached cells were detached by sequential washes containing 0.4% (v/v) Tween® 20 of the carbon microfibres with vigorous agitation for two minutes. The number of cells recovered from (A) individual wash steps and (B) cumulatively recovered between each wash step is shown. A total of seven wash steps using Tween® 20 were confirmed to remove the large majority of cells from the surface of the carbon microfibres (Figure A3-2). Error bars represent one standard deviation from the mean of two repeats each counted in duplicate.

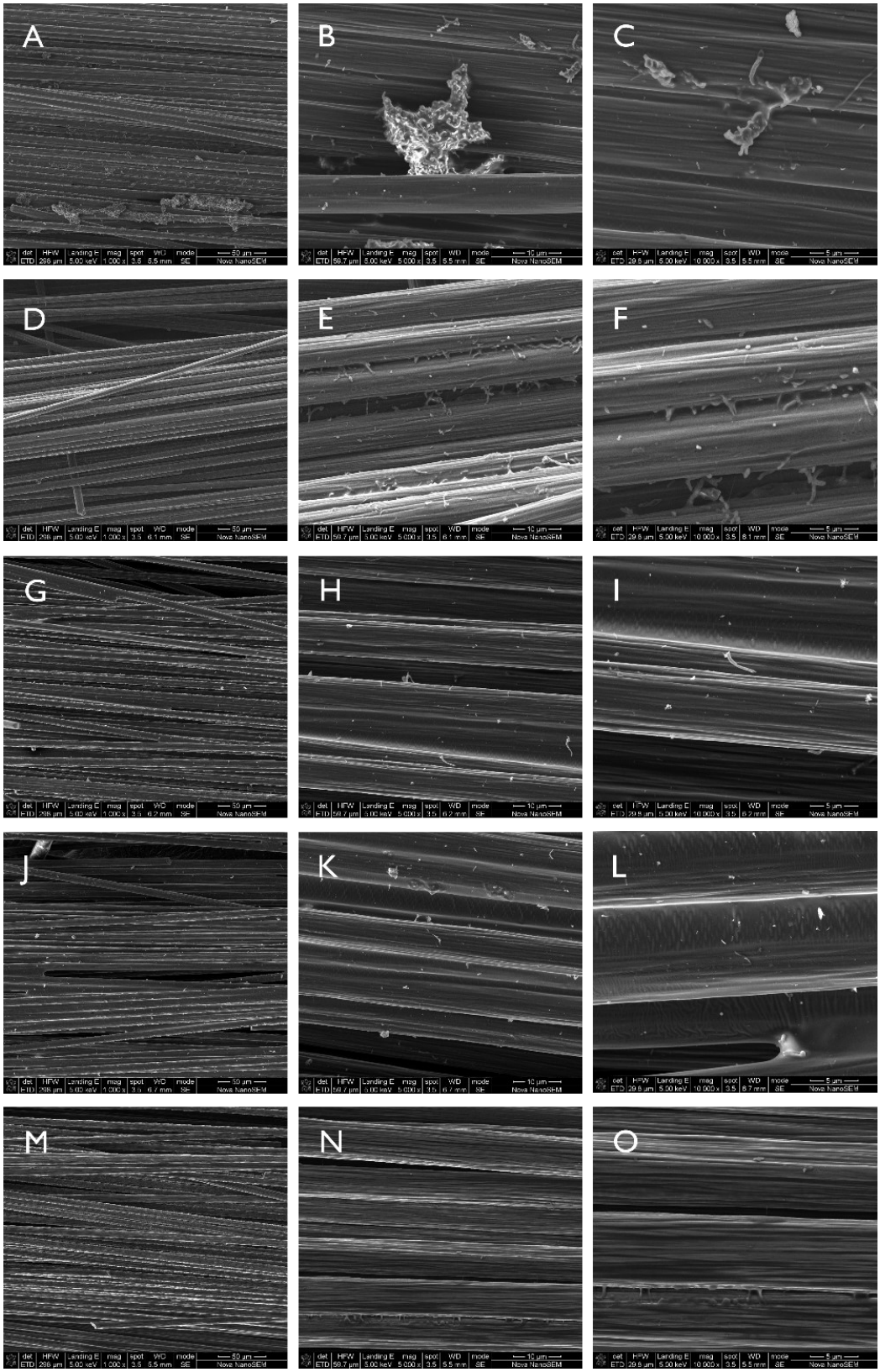


Figure A3-2 SEM micrographs of the carbon microfibres, removed from the acetate-supplemented LFCR, during consequitive steps during a cell detchemnet protocol (Section 3.6.2). Carbon microfibres were viewed immediately following the removal of associated cells (A-C), the first wash step (D-F), the second wash step (G-I), the fith wash step (J- L) and the seventh (M-O) wash step. Scale bars are shown in each micrograph.

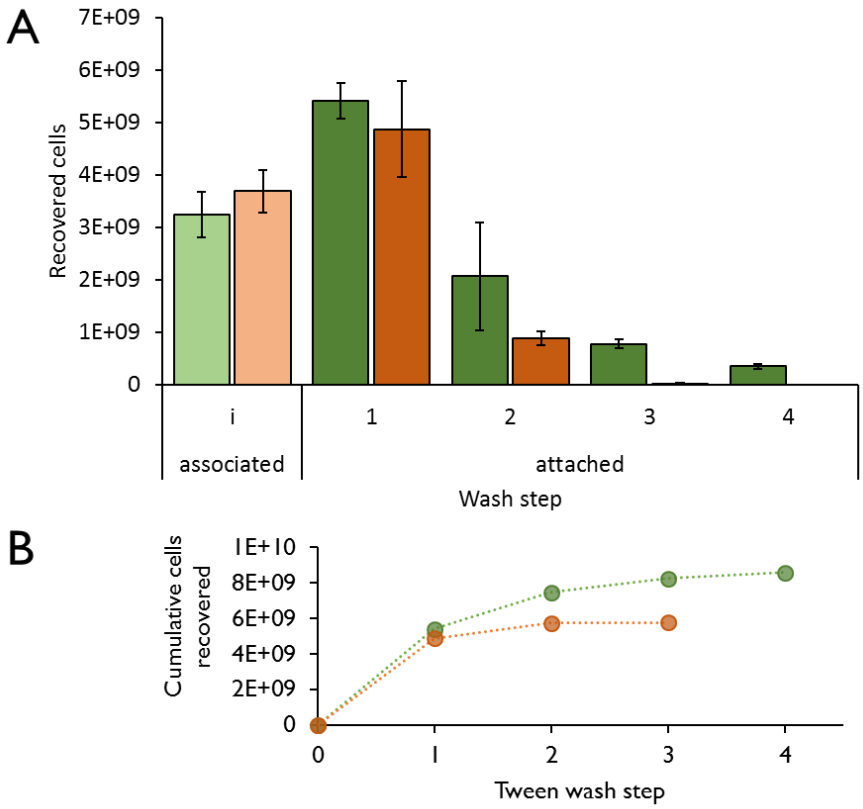


Figure A3-3 The quantity of cells recovered from individual units of polyurethane foam removed from the lactate (green) and acetate (orange) supplemented UAPBRs, following each step of the cell recovery protocol (Section 3.6.2). Mild agitation was used to dislodge matrix-associated cells from the polyurethane foam packing. Matrix attached cells were detached by sequential washes containing 0.4% (v/v) Tween® 20 of the polyurethane foam packing with vigorous agitation for two minutes. The number of cells recovered from (A) individual wash steps and (B) cumulatively recovered between each wash step is shown. A total of seven wash steps using Tween® 20 were confirmed to remove the large majority of cells from the surface of the polyurethane foam (Figure A3-4). Error bars represent one standard deviation from the mean of two repeats each counted in duplicate.

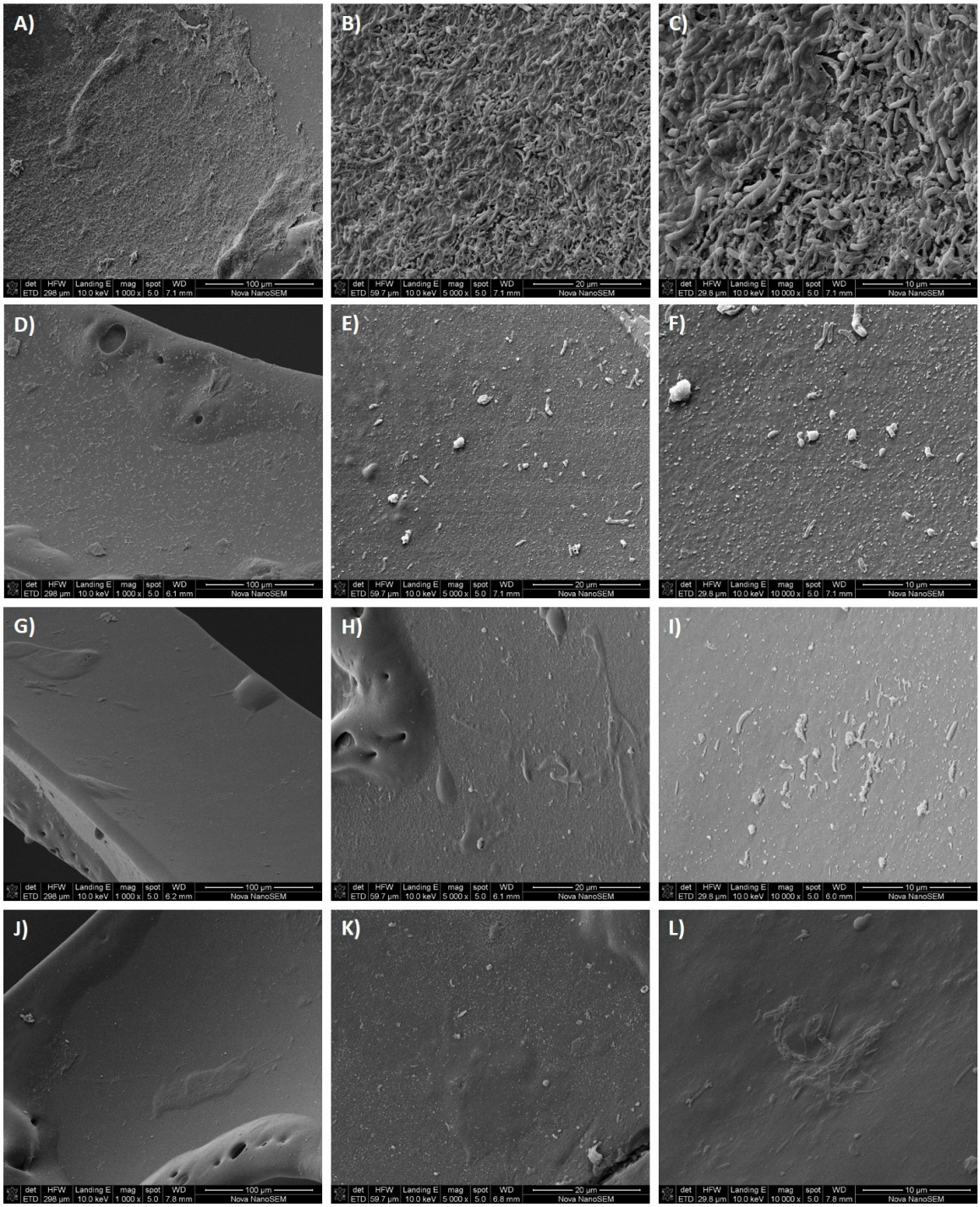


Figure A3-4 SEM micrographs of the carbon microfibres, removed from the acetate-supplemented UAPBR, during consequitive steps during a cell detchemnet protocol (Section 3.6.2). Polyurethane foam pieces were viewed immediately following the removal of associated cells (A-C), the first wash step (D-F), the second wash step (G-I), the fith wash step (J- L) and the seventh (M-O) wash step. Scale bars are shown in each micrograph.

# A.4 16S rRNA gene amplicon sequencing

## A.4.1 alpha diversity and sequencing statistics

Table A4-1 The alpha diversity and sequencing statistics associated with the 16s rRNA gene amplicons sequencing of the microbial communities associated with the acetate-supplemented BSR reactors.

| | HRT (days) | Phase | OTUs | Chao1 | Shannon | Inverse Simpson | Goods Coverage |
|---|---|---|---|---|---|---|---|
| | 5 | Planktonic | 141 | 155.3 | 4.57 | 0.9251 | 0.9983 |
| | 4 | Planktonic | 167 | 202.5 | 4.36 | 0.9074 | 0.9980 |
| | 4 | Planktonic | 119 | 150.1 | 3.96 | 0.8803 | 0.9970 |
| | 3 | Planktonic | 217 | 259.5 | 4.35 | 0.9119 | 0.9979 |
| | 2.6 | Planktonic | 253 | 321.1 | 5.08 | 0.9424 | 0.9974 |
| CSTR | 2.3 | Planktonic | 252 | 305.0 | 4.60 | 0.9144 | 0.9979 |
| | 2 | Planktonic | 280 | 386.6 | 4.77 | 0.9192 | 0.9976 |
| | 1.5 | Planktonic | 231 | 267.4 | 3.51 | 0.7639 | 0.9987 |
| | 1.3 | Planktonic | 246 | 315.8 | 3.54 | 0.7714 | 0.9984 |
| | 1 | Planktonic | 219 | 262.1 | 3.96 | 0.8558 | 0.9982 |
| | 1 | Planktonic | 219 | 278.1 | 4.00 | 0.8591 | 0.9982 |
| | 4 | Planktonic | 162 | 197.2 | 4.37 | 0.8914 | 0.9972 |
| | 4 | Planktonic | 158 | 174.7 | 4.45 | 0.8983 | 0.9979 |
| | 4 | Associated | 202 | 224.0 | 4.54 | 0.8897 | 0.9985 |
| | 4 | Associated | 190 | 263.9 | 4.33 | 0.8606 | 0.9974 |
| | 4 | Attached | 182 | 211.1 | 3.74 | 0.7756 | 0.9982 |
| | 4 | Attached | 206 | 231.1 | 3.88 | 0.7777 | 0.9983 |
| | 3 | Planktonic | 254 | 309.8 | 4.04 | 0.8516 | 0.9977 |
| | 3 | Planktonic | 277 | 349.0 | 3.92 | 0.8429 | 0.9981 |
| | 1.5 | Planktonic | 274 | 319.0 | 4.79 | 0.9318 | 0.9976 |
| LFCR | 1.5 | Planktonic | 249 | 299.1 | 4.54 | 0.9092 | 0.9976 |
| | 1 | Planktonic | 237 | 296.2 | 4.89 | 0.9271 | 0.9979 |
| | 1 | Planktonic | 262 | 359.8 | 4.87 | 0.9268 | 0.9975 |
| | 1 | Planktonic | 196 | 263.0 | 4.12 | 0.8629 | 0.9970 |
| | 1 | Associated | 302 | 347.6 | 4.44 | 0.8747 | 0.9981 |
| | 1 | Associated | 296 | 328.2 | 5.00 | 0.9300 | 0.9981 |
| | 1 | Associated | 301 | 330.3 | 5.02 | 0.9210 | 0.9987 |
| | 1 | Attached | 307 | 349.0 | 4.72 | 0.8881 | 0.9986 |
| | 1 | Attached | 306 | 359.0 | 4.54 | 0.8796 | 0.9983 |
| | 1 | Attached | 312 | 364.8 | 4.82 | 0.8947 | 0.9977 |
| | 4 | Planktonic | 179 | 214.1 | 4.59 | 0.9217 | 0.9979 |
| | 4 | Planktonic | 192 | 221.1 | 4.40 | 0.8938 | 0.9969 |
| | 4 | Planktonic | 174 | 213.0 | 4.48 | 0.9088 | 0.9973 |
| | 4 | Associated | 179 | 204.2 | 4.68 | 0.9258 | 0.9979 |
| | 4 | Associated | 185 | 204.0 | 4.82 | 0.9395 | 0.9975 |
| | 4 | Attached | 188 | 212.2 | 4.10 | 0.8859 | 0.9983 |
| | 4 | Attached | 166 | 226.1 | 3.57 | 0.8254 | 0.9970 |
| | 3 | Planktonic | 314 | 381.0 | 4.47 | 0.8388 | 0.9981 |
| | 3 | Planktonic | 313 | 366.8 | 4.71 | 0.8786 | 0.9975 |
| | 3 | Planktonic | 202 | 234.8 | 3.17 | 0.6844 | 0.9961 |
| | 2 | Planktonic | 331 | 383.8 | 4.86 | 0.9237 | 0.9974 |
| | 2 | Planktonic | 348 | 410.1 | 5.57 | 0.9574 | 0.9977 |
| | 2 | Planktonic | 286 | 355.0 | 5.05 | 0.9381 | 0.9974 |
| | 1 | Planktonic | 283 | 407.5 | 4.91 | 0.9254 | 0.9965 |
| | 1 | Planktonic | 320 | 384.2 | 4.97 | 0.9280 | 0.9969 |
| UAPBR | 1 | Planktonic | 260 | 304.6 | 4.45 | 0.9074 | 0.9975 |
| | 1 | Planktonic | 276 | 353.0 | 4.85 | 0.9265 | 0.9961 |
| | 1 | Associated | 313 | 344.4 | 3.92 | 0.7361 | 0.9983 |
| | 1 | Associated | 320 | 363.9 | 4.28 | 0.7903 | 0.9972 |
| | 1 | Associated | 291 | 323.8 | 4.07 | 0.7850 | 0.9980 |
| | 1 | Associated | 293 | 351.0 | 3.99 | 0.7848 | 0.9972 |
| | 1 | Associated | 280 | 375.3 | 4.05 | 0.8523 | 0.9970 |
| | 1 | Associated | 290 | 338.8 | 4.26 | 0.8815 | 0.9975 |
| | 1 | Associated | 262 | 323.7 | 4.18 | 0.8752 | 0.9971 |
| | 1 | Attached | 293 | 328.6 | 3.57 | 0.7293 | 0.9984 |
| | 1 | Attached | 280 | 357.0 | 4.04 | 0.8425 | 0.9977 |
| | 1 | Attached | 282 | 355.3 | 3.43 | 0.7086 | 0.9972 |
| | 1 | Attached | 271 | 299.8 | 3.76 | 0.7818 | 0.9981 |
| | 1 | Attached | 244 | 297.1 | 3.65 | 0.7790 | 0.9971 |
| | 1 | Attached | 314 | 373.9 | 3.87 | 0.7887 | 0.9983 |
| | 1 | Attached | 310 | 370.3 | 3.66 | 0.7457 | 0.9977 |

Table A4-2 The alpha diversity and sequencing statistics associated with the 16s rRNA gene amplicon sequencing of the microbial communities associated with the lactate-supplemented BSR reactors.

| | HRT (days) | Phase | OTUs | Chao1 | Shannon | Inverse Simpson | Goods Coverage |
|---|---|---|---|---|---|---|---|
| | 5 | Planktonic | 101 | 134.8 | 3.17 | 0.7893 | 0.9982 |
| | 4 | Planktonic | 117 | 137.0 | 3.74 | 0.8738 | 0.9991 |
| | 4 | Planktonic | 106 | 129.1 | 3.71 | 0.8752 | 0.9990 |
| | 3 | Planktonic | 126 | 157.7 | 2.82 | 0.7234 | 0.9959 |
| | 2.6 | Planktonic | 203 | 240.9 | 3.58 | 0.8281 | 0.9986 |
| CSTR | 2.3 | Planktonic | 194 | 237.4 | 4.22 | 0.9122 | 0.9984 |
| | 2 | Planktonic | 183 | 245.6 | 3.83 | 0.8720 | 0.9984 |
| | 1.5 | Planktonic | 173 | 230.4 | 3.75 | 0.8789 | 0.9985 |
| | 1.3 | Planktonic | 169 | 195.5 | 3.46 | 0.8104 | 0.9988 |
| | 1 | Planktonic | 205 | 238.8 | 4.36 | 0.9138 | 0.9982 |
| | 1 | Planktonic | 206 | 257.0 | 4.36 | 0.9122 | 0.9984 |
| | 4 | Planktonic | 120 | 147.3 | 4.24 | 0.9178 | 0.9983 |
| | 4 | Planktonic | 134 | 168.4 | 4.44 | 0.9225 | 0.9980 |
| | 4 | Associated | 153 | 170.3 | 4.29 | 0.8973 | 0.9983 |
| | 4 | Associated | 136 | 198.0 | 4.10 | 0.9014 | 0.9977 |
| | 4 | Attached | 176 | 212.3 | 4.97 | 0.9432 | 0.9978 |
| | 4 | Attached | 171 | 182.5 | 4.70 | 0.9299 | 0.9986 |
| | 3 | Planktonic | 211 | 303.1 | 3.54 | 0.8001 | 0.9975 |
| | 3 | Planktonic | 193 | 216.6 | 3.39 | 0.7621 | 0.9988 |
| | 1.5 | Planktonic | 163 | 233.8 | 3.16 | 0.8025 | 0.9976 |
| LFCR | 1.5 | Planktonic | 169 | 201.8 | 3.92 | 0.8952 | 0.9984 |
| | 1 | Planktonic | 170 | 208.1 | 4.00 | 0.9015 | 0.9978 |
| | 1 | Planktonic | 174 | 229.0 | 3.11 | 0.7940 | 0.9982 |
| | 1 | Planktonic | 116 | 166.6 | 2.70 | 0.7618 | 0.9972 |
| | 1 | Associated | 180 | 216.4 | 4.21 | 0.9121 | 0.9983 |
| | 1 | Associated | 205 | 256.3 | 4.20 | 0.9089 | 0.9978 |
| | 1 | Associated | 172 | 219.0 | 4.36 | 0.9207 | 0.9979 |
| | 1 | Attached | 206 | 250.2 | 4.49 | 0.9276 | 0.9983 |
| | 1 | Attached | 180 | 221.1 | 4.35 | 0.9148 | 0.9985 |
| | 1 | Attached | 216 | 271.1 | 4.40 | 0.9182 | 0.9980 |
| | 4 | Planktonic | 135 | 151.3 | 3.99 | 0.8807 | 0.9983 |
| | 4 | Planktonic | 176 | 213.3 | 4.35 | 0.8948 | 0.9976 |
| | 4 | Planktonic | 161 | 192.7 | 4.36 | 0.9070 | 0.9977 |
| | 4 | Associated | 168 | 227.4 | 4.01 | 0.8796 | 0.9972 |
| | 4 | Attached | 157 | 200.0 | 3.63 | 0.7925 | 0.9972 |
| | 4 | Associated | 129 | 141.7 | 3.47 | 0.8200 | 0.9992 |
| | 4 | Attached | 123 | 144.4 | 3.18 | 0.7744 | 0.9984 |
| | 3 | Planktonic | 317 | 394.1 | 5.02 | 0.9322 | 0.9967 |
| | 3 | Planktonic | 227 | 280.3 | 4.02 | 0.8848 | 0.9981 |
| | 3 | Planktonic | 354 | 437.0 | 4.97 | 0.9370 | 0.9978 |
| | 2 | Planktonic | 278 | 357.4 | 4.18 | 0.8462 | 0.9981 |
| | 2 | Planktonic | 236 | 272.4 | 3.95 | 0.8714 | 0.9984 |
| | 2 | Planktonic | 287 | 362.1 | 4.70 | 0.9233 | 0.9977 |
| | 1 | Planktonic | 301 | 374.1 | 4.33 | 0.8833 | 0.9976 |
| | 1 | Planktonic | 306 | 371.9 | 4.40 | 0.8894 | 0.9979 |
| UAPBR | 1 | Planktonic | 207 | 259.5 | 4.03 | 0.8967 | 0.9979 |
| | 1 | Planktonic | 287 | 394.1 | 4.16 | 0.8835 | 0.9975 |
| | 1 | Associated | 240 | 346.4 | 4.56 | 0.9003 | 0.9976 |
| | 1 | Associated | 233 | 312.6 | 3.95 | 0.8550 | 0.9980 |
| | 1 | Associated | 272 | 355.3 | 4.05 | 0.8586 | 0.9974 |
| | 1 | Associated | 319 | 361.2 | 5.02 | 0.9374 | 0.9976 |
| | 1 | Associated | 303 | 344.6 | 5.01 | 0.9376 | 0.9979 |
| | 1 | Attached | 248 | 280.8 | 4.46 | 0.8937 | 0.9981 |
| | 1 | Attached | 228 | 263.8 | 3.44 | 0.8042 | 0.9979 |
| | 1 | Attached | 271 | 336.1 | 4.22 | 0.8744 | 0.9978 |
| | 1 | Attached | 329 | 400.2 | 4.96 | 0.9274 | 0.9983 |
| | 1 | Attached | 299 | 391.9 | 4.93 | 0.9254 | 0.9975 |
| | 1 | Associated | 257 | 324.0 | 4.03 | 0.8351 | 0.9976 |
| | 1 | Associated | 230 | 285.3 | 4.00 | 0.8332 | 0.9985 |
| | 1 | Attached | 240 | 280.6 | 3.93 | 0.8392 | 0.9982 |
| | 1 | Attached | 217 | 268.1 | 3.68 | 0.8119 | 0.9981 |

# A.5 Genome-resolved metagenomics

## A.5.1 Investigated metabolic pathways

Table A5-1 Metabolic pathways and associated genes used to ascribe a genome with the genetic capcity to perform various metabolic reactions.

**Wood-Ljungdahl pathway**
fdhA_formate_dehydrogenase
carbon-monoxide_dehydrogenase
fhs_formyl-tetrahydrofolate synthase
methenyltetrahydrofolate_cyclohydrolase
methylenetetrahydrofolate_dehydrogenase
acsB_ acetyl-CoA synthase
methyltetrahydrofolate:corrinoid/iron-sulfur_protein
methylenetetrahydrofolate_reductase

**Reverse TCA**
kora_2-oxoglutarate oxidoreductase
citryl-CoA lyase_ccl and citryl-CoA synthase_ccsa
pyruvate_synthase
pep_carboxylase
frdA_Fumarate reductase
aconitate_hydratase

isocitrate_dehydrogenase
malate_dehydrogenase
Phosphoenolpyruvate_synthase
succinyl-coa_synthase

**CBB pathway**
phosphoglycerate_kinase
rubisco
fructose-bisphosphate_aldolase
fructose-bisphosphatase
phosphoribulokinase
ribose-5-phosphate_isomerase
Glyceraldehyde 3-phosphate_dehydrogenase
transaldolase
sedoheptulose-bisphosphatase
ribulose-phosphate_3-epimerase

**Acetate metabolism**
acetate_kinase
acetyl-coa_synthetase
phosphate_acetyltransferase
Phosphoenolpyruvate_carboxylase
Phosphoenolpyruvate_synthase
pyruvate_ferredoxin_oxidoreductase
methyltetrahydrofolate:corrinoid/iron-sulfur_protein
carbon-monoxide_dehydrogenase
fold_methylenetetrahydrofolate dehydrogenase
fhs_formyl-tetrahydrofolate synthase
methylenetetrahydrofolate_reductase
methenyltetrahydrofolate_cyclohydrolase
methylenetetrahydrofolate_dehydrogenase
pyruvate_carboxylase
citrate_synthase

**Glycolysis**
Hexokinase
Glucose6phosphate isomerase
Phosphofructokinase
Fructosebisphosphate aldolase
Triosephosphate isomerase
Glyceraldehyde3phosphate dehydrogenase
Phosphoglycerate kinase
Phosphoglycerate mutase
Phosphopyruvate hydratase
Pyruvate kinase

**Lactate and propionate metabolism**
cytochrome_c553_(lactate_degradatoin)
lactate_permease_(carbon:lactate)
l-lactate_dehydrogeanse_(nad_&_cytochrome)_(carbon:lactate)
2-oxoglutarate/2-oxoacid_..._(carbon:lactate)
pyruvate_synthase/oxidoreductase_(carbon:lactate)
formate_c-acetyltransferase_(carbon:lactate)

pyruvate_dehydrogenase_(carbon:lactate)
acetyl-coa_synthetase_(carbon:lactate)
phosphate_acetyltransferase_(carbon:lactate)
acylphosphatase_(carbon:lactate)
acetate_kinase_(carbon:lactate)
dihydrolipoamide_dehydrogenase_(carbon:lactate)
pyruvate_carboxylase_(carbon:lactate)
fumarate_hydratase_(carbon:lactate)
malate_dehydrogenase_(carbon:lactate)
methylmalonyl-coa_mutase_(carbon:lacate:propionate)
methylmalonyl-coa/ethylmalonyl-coa_epimerase_(carbon:lactate:propionate)
methylmalonyl-coa_carboxyltransferase_(carbon:lactate"propionate)
malonate-semialdehyde_dehydrogenase_(carbon:lactate:propionate)
phosphate_acetyltransferase_(carbon:lactate:propionate)
acetate_or_propionate_kinase_(carbon:lactate:propionate)
propionate_coa_transferase_(carbon:lactate:propionate)
butyryl-coa_dehydrogenase_(carbon:lactate:propionate)
formate_c-acetyltransferase_(carbon:lactate:propionate)
pyruvate_ferredoxin_oxidoreductase_(carbon:lactate:propionate)
methylcitrate_synthase_(carbon:propionate)
methylmalonyl-coa_carboxytransferase_(carbon:propionate)
propionyl_coa_carboxylase_(carbon:propionate)

**Citrate metabolism**
citrate_transporter_(carbon:citrate)
citrate_lyase_(carbon:citrate)

**Urea cycle**
Argininosuccinate_lyase
Argininosuccinate_synthase
Carbamoyl_phosphate_synthase
Ornithine_carbamoyltransferase_
Ureohydrolase_Arginase

**Sulphur metabolism**
sulphate_adenylyltransferase_sat_(so4_reduction:)
sulfite_reductase_cysJ_(so4_reduction:ass)
cysH_paps_reductase_(so4_reduction:ass)
adenylyl-sulfate_kinase_(so4_reduction:ass)
dsrAB_dissimilatory sulfite_redutase(so4_reduction:dis)
aps_reducatse_aprab_(so4_reduction:dis)
soxAX_cysteine_s-thiosulfotransferase_(sulphideoxidation)
soxXY_sulphur_oxidation_protein_(sulphide_oxidation)
soxB_sulfosulfanyl_cysteine_sulfohydrolase_(sulphide_oxidation)
soxcd_sulfane_dehydrogenase_(sulphide_oxidation)

**TCA cycle**
Citrate synthase
Aconitase
Isocitrate dehydrogenase
ketoglutarate dehydrogenase
Succinyl coenzyme A synthetase
Succinate dehydrogenase
Fumarase
Malate dehydrogenase

## A.5.2 Genome bin statistics

Table A5-2 Genome statistics of the total 163 recovered microbial genome bins. These genome bins are described by their GC percentage, the average coverage from the dereplicated genome bin, the number of contigs in the genome bin, the number of features/genes, the estimated genome completeness and contamination, the size of the genome, the median contig length in each bin (N50).

| Genome bin | GC (%) | coverage | contigs | features | completeness (%) | contamination (%) | genome size (Mbp) | N50 (bp) |
|---|---|---|---|---|---|---|---|---|
| BSR_Ace_LFCR_na_at_2_+ulfobacterales_57_55 | 57 | 55 | 72 | 5265 | 98 | 3 | 5.8 | 1.7E+05 |
| BSR_Ace_UAPBR_inlet_at_2_Synergistales_64_17 | 64 | 17 | 156 | 2483 | 100 | 0 | 2.6 | 3.7E+04 |
| BSR_Lac_UAPBR_inlet_at_Bacteroidia_47_18 | 47 | 18 | 31 | 1604 | 95 | 1 | 1.8 | 1.5E+05 |
| BSR_Ace_C_na_Sphaerochaeta_globosa_51_113 | 51 | 113 | 335 | 3337 | 90 | 1 | 3.4 | 2.3E+04 |
| BSR_Ace_LFCR_na_p_Geobacter_lovleyi_46_94 | 46 | 94 | 69 | 3300 | 99 | 0 | 3.4 | 1.2E+05 |
| BSR_Ace_C_na_2_Bacteroidetes_44_67_(50) | 44 | 67 | 90 | 2215 | 95 | 2 | 2.5 | 5.8E+04 |
| BSR_Lac_LFCR_na_p_Bacteroidia_39_30 | 39 | 30 | 37 | 2195 | 97 | 0 | 2.5 | 4.1E+05 |
| BSR_Ace_UAPBR_effluent_at_Desulfarculus_baarsii_66_20 | 66 | 20 | 66 | 3341 | 99 | 0 | 3.6 | 1.4E+05 |
| BSR_Ace_UAPBR_middle_p_1_Bacteroidia_44_46 | 44 | 46 | 86 | 3205 | 100 | 1 | 3.7 | 9.9E+04 |
| BSR_Ace_UAPBR_inlet_at_2_BJP_IG2103_Bacteroidetes_41_9_47_32 | 47 | 32 | 161 | 3533 | 98 | 2 | 4.4 | 6.4E+04 |
| BSR_Ace_C_na_Sphaerochaeta_globosa_53_73 | 53 | 73 | 389 | 3657 | 98 | 2 | 3.6 | 2.2E+04 |
| BSR_Ace_C_na_Desulfovibrio_desulfuricans_58_43 | 58 | 43 | 43 | 2859 | 100 | 0 | 3.5 | 1.7E+05 |
| BSR_Ace_LFCR_na_p_Sphaerochaeta_globosa_51_20 | 51 | 20 | 55 | 2929 | 98 | 0 | 3.1 | 1.0E+05 |
| BSR_Ace_UAPBR_inlet_at_2_Desulfobulbus_propionicus_52_45 | 52 | 45 | 36 | 2519 | 100 | 0 | 2.8 | 1.6E+05 |
| BSR_Ace_UAPBR_inlet_p_GWF2_Bacteroidetes_43_11_curated_39_33 | 39 | 33 | 98 | 3143 | 98 | 2 | 4.1 | 6.3E+04 |
| BSR_Ace_UAPBR_inlet_at_1_Desulfovibrio_64_36 | 64 | 36 | 37 | 3090 | 100 | 0 | 3.4 | 1.5E+05 |
| BSR_Ace_UAPBR_effluent_at_Synergistales_59_15 | 59 | 15 | 161 | 3972 | 100 | 0 | 4.2 | 5.5E+04 |
| BSR_Ace_C_na_Klebsiella_oxytoca_56_23 | 56 | 23 | 93 | 5737 | 100 | 0 | 6.0 | 1.3E+05 |
| BSR_Ace_C_na_2_Bacteroidia_49_19 | 49 | 19 | 46 | 2988 | 97 | 2 | 3.8 | 1.7E+05 |
| BSR_Ace_UAPBR_effluent_at_2_Deltaproteobacteria_63_50 | 63 | 50 | 95 | 4046 | 99 | 3 | 4.4 | 7.8E+04 |
| BSR_Ace_UAPBR_effluent_p_Bacteroidetes_40_41 | 40 | 41 | 28 | 2366 | 97 | 1 | 2.8 | 2.2E+05 |
| BSR_Ace_C_na_2_Bacteroidales_35_10 | 35 | 10 | 183 | 2567 | 99 | 1 | 3.0 | 2.8E+04 |
| BSR_Ace_LFCR_na_p_Dysgonomonas_39_22 | 39 | 22 | 27 | 3408 | 99 | 0 | 4.1 | 3.2E+05 |
| BSR_Ace_UAPBR_inlet_p_1_Dethiosulfovibrio_peptidovorans_54_25 | 54 | 25 | 50 | 2592 | 100 | 0 | 2.7 | 1.3E+05 |
| BSR_Ace_C_na_2_Microgenomates_37_51 | 37 | 51 | 24 | 965 | 64 | 0 | 0.9 | 2.4E+05 |
| BSR_Ace_LFCR_na_p_RIFOXYB2_FULL_Tenericutes_36_25_curated_36_10 | 36 | 10 | 120 | 1606 | 99 | 1 | 1.6 | 2.0E+04 |
| BSR_Lac_C_na_Bacteroidia_44_10 | 44 | 10 | 253 | 3064 | 93 | 1 | 3.4 | 3.0E+04 |
| BSR_Ace_LFCR_na_p_1_Bacteroidales_43_13 | 43 | 13 | 49 | 2671 | 100 | 1 | 3.2 | 1.1E+05 |
| BSR_Lac_C_na_Desulfovibrio_70_18 | 70 | 18 | 74 | 3273 | 100 | 0 | 3.6 | 2.0E+05 |
| BSR_Ace_C_na_Synergistales_61_23 | 61 | 23 | 36 | 3215 | 100 | 2 | 3.4 | 2.2E+05 |
| BSR_Ace_LFCR_na_p_Desulfotomaculum_gibsoniae_47_21 | 47 | 21 | 33 | 3029 | 97 | 1 | 3.1 | 1.5E+05 |
| BSR_Ace_LFCR_na_p_1_Clostridiales_58_10 | 58 | 10 | 86 | 3043 | 98 | 0 | 3.1 | 6.5E+04 |
| BSR_Lac_UAPBR_effluent_at_1_GWC2_Bacteroidetes_46_850_curated_52_9 | 52 | 9 | 120 | 1776 | 97 | 1 | 2.0 | 2.4E+04 |
| BSR_Ace_C_na_Bacteroidia_43_15 | 43 | 15 | 97 | 3695 | 99 | 1 | 4.5 | 1.1E+05 |
| BSR_Ace_UAPBR_effluent_at_Phycisphaerae_63_30 | 63 | 30 | 66 | 4332 | 100 | 1 | 5.3 | 1.3E+05 |
| BSR_Ace_UAPBR_middle_p_Bacteria_50_28 | 50 | 28 | 52 | 2215 | 95 | 1 | 2.8 | 1.1E+05 |
| BSR_Ace_C_na_Bacteroidales_43_22 | 43 | 22 | 35 | 2824 | 100 | 1 | 3.4 | 1.6E+05 |
| BSR_Lac_UAPBR_effluent_p_2_Desulfomicrobium_baculatum_60_28 | 60 | 28 | 38 | 3782 | 99 | 0 | 4.1 | 3.6E+05 |
| BSR_Ace_UAPBR_effluent_p_Clostridiales_54_14 | 54 | 14 | 35 | 3038 | 99 | 0 | 3.2 | 1.7E+05 |
| BSR_Ace_LFCR_na_p_Sphaerochaeta_globosa_45_14 | 45 | 14 | 64 | 2994 | 98 | 1 | 3.3 | 8.6E+04 |
| BSR_Ace_UAPBR_inlet_p_Bacteroidales_40_21 | 40 | 21 | 67 | 3329 | 100 | 1 | 4.0 | 9.9E+04 |
| BSR_Lac_C_na_Clostridiales_55_36 | 55 | 36 | 53 | 3098 | 99 | 0 | 3.6 | 1.5E+05 |
| BSR_Ace_C_na_Clostridiales_57_14 | 57 | 14 | 63 | 3532 | 98 | 1 | 3.7 | 1.7E+05 |
| BSR_Lac_C_na_Aeromonas_veronii_59_14 | 59 | 14 | 35 | 4213 | 100 | 0 | 4.5 | 2.5E+05 |
| BSR_Lac_LFCR_na_p_Clostridiales_36_11 | 36 | 11 | 85 | 2442 | 97 | 0 | 2.5 | 5.0E+04 |

| | | | | | | | | |
|---|---|---|---|---|---|---|---|---|
| BSR_Lac_LFCR_na_at_1_Alphaproteobacteria_54_165 | 54 | 165 | 43 | 2098 | 90 | 0 | 2.1 | 1.6E+05 |
| BSR_Lac_UAPBR_middle_p_Sphaerochaeta_55_11 | 55 | 11 | 78 | 1948 | 98 | 0 | 2.1 | 4.6E+04 |
| BSR_Ace_C_na_Bacteroidetes_33_15 | 33 | 15 | 56 | 2079 | 97 | 1 | 2.4 | 1.3E+05 |
| BSR_Ace_UAPBR_effluent_at_Bacteria_64_7 | 64 | 7 | 669 | 4147 | 89 | 4 | 4.9 | 9.2E+03 |
| BSR_Ace_UAPBR_middle_p_Parabacteroides_42_25 | 42 | 25 | 71 | 3556 | 99 | 0 | 4.2 | 1.1E+05 |
| BSR_Ace_C_na_Bacteroidia_47_14 | 47 | 14 | 182 | 2191 | 92 | 4 | 2.4 | 2.2E+04 |
| BSR_Ace_C_na_Burkholderiales_68_7 | 68 | 7 | 588 | 4356 | 88 | 0 | 4.3 | 8.9E+03 |
| BSR_Lac_UAPBR_middle_p_1_Thermotogae_38_9 | 38 | 9 | 229 | 2310 | 93 | 1 | 2.3 | 1.3E+04 |
| BSR_Ace_LFCR_na_p_Parabacteroides_42_11 | 42 | 11 | 412 | 3591 | 98 | 3 | 4.0 | 2.0E+04 |
| BSR_Ace_LFCR_na_p_Oscillibacter_valericigenes_56_9 | 56 | 9 | 161 | 2816 | 99 | 0 | 2.8 | 2.8E+04 |
| BSR_Ace_UAPBR_effluent_at_Gammaproteobacteria_63_27 | 63 | 27 | 157 | 2921 | 100 | 0 | 3.1 | 4.5E+04 |
| BSR_Ace_UAPBR_effluent_p_Chlorobium_limicola_53_20 | 53 | 20 | 55 | 2443 | 98 | 0 | 2.6 | 1.1E+05 |
| BSR_Ace_UAPBR_effluent_p_2_Thiomonas_65_14 | 65 | 14 | 129 | 2942 | 99 | 1 | 3.0 | 4.1E+04 |
| BSR_Ace_LFCR_na_at_Clostridiales_56_12 | 56 | 12 | 21 | 1929 | 95 | 0 | 1.9 | 1.8E+05 |
| BSR_Lac_LFCR_na_at_2_Bacteroidia_44_21 | 44 | 21 | 90 | 3694 | 100 | 2 | 4.6 | 7.9E+04 |
| BSR_Lac_C_na_Spirochatetes_56_14 | 56 | 14 | 26 | 2811 | 99 | 0 | 3.0 | 1.6E+05 |
| BSR_Ace_UAPBR_inlet_at_Bacteria_57_9 | 57 | 9 | 165 | 2368 | 96 | 0 | 2.5 | 2.1E+04 |
| BSR_Ace_LFCR_na_p_Clostridiales_45_11 | 45 | 11 | 50 | 1754 | 95 | 0 | 1.8 | 6.5E+04 |
| BSR_Lac_UAPBR_effluent_p_2_Desulfovibrio_65_51 | 65 | 51 | 74 | 3562 | 100 | 0 | 3.9 | 1.3E+05 |
| BSR_Lac_UAPBR_effluent_at_Firmicutes_36_25 | 36 | 25 | 4 | 1139 | 99 | 0 | 1.2 | 6.0E+05 |
| BSR_Lac_LFCR_na_at_Clostridiales_48_8 | 48 | 8 | 228 | 2376 | 91 | 1 | 2.3 | 1.4E+04 |
| BSR_Ace_UAPBR_inlet_at_Firmicutes_56_7 | 56 | 7 | 466 | 3096 | 81 | 1 | 3.1 | 7.7E+03 |
| BSR_Ace_UAPBR_effluent_at_Armatimonadetes_related_68_12 | 68 | 12 | 542 | 5961 | 94 | 4 | 8.6 | 2.3E+04 |
| BSR_Lac_UAPBR_inlet_p_1_Bacteroides_graminisolvens_42_17 | 42 | 17 | 27 | 3002 | 99 | 1 | 3.6 | 1.8E+05 |
| BSR_Ace_UAPBR_inlet_at_Desulfovibrio_69_8 | 69 | 8 | 345 | 3274 | 95 | 1 | 3.1 | 1.2E+04 |
| BSR_Ace_C_na_Bacteroidia_45_6 | 45 | 6 | 1345 | 3799 | 85 | 10 | 3.3 | 2.8E+03 |
| BSR_Lac_LFCR_na_at_1_Aminobacterium_colombiense_44_34 | 44 | 34 | 27 | 2024 | 100 | 0 | 2.1 | 1.3E+05 |
| BSR_Ace_C_na_1_Firmicutes_37_11 | 37 | 11 | 91 | 992 | 97 | 3 | 0.9 | 1.6E+04 |
| BSR_Ace_LFCR_na_at_Aminobacterium_colombiense_45_9 | 45 | 9 | 89 | 1972 | 100 | 0 | 1.9 | 4.2E+04 |
| BSR_Ace_UAPBR_effluent_at_Desulfovibrio_66_33 | 66 | 33 | 185 | 3530 | 92 | 2 | 3.7 | 3.2E+04 |
| BSR_Lac_C_na_Dethiosulfovibrio_peptidovorans_55_25 | 55 | 25 | 17 | 2522 | 100 | 1 | 2.6 | 2.8E+05 |
| BSR_Ace_LFCR_na_p_Spirochatetes_56_7 | 56 | 7 | 320 | 2447 | 86 | 1 | 2.3 | 8.4E+03 |
| BSR_Ace_UAPBR_inlet_p_Desulfobacter_postgatei_49_15 | 49 | 15 | 114 | 3241 | 98 | 0 | 3.6 | 5.6E+04 |
| BSR_Lac_UAPBR_inlet_p_1_Firmicutes_40_18 | 40 | 18 | 47 | 3313 | 97 | 0 | 3.4 | 1.5E+05 |
| BSR_Ace_UAPBR_inlet_p_Clostridiales_37_6 | 37 | 6 | 1127 | 3864 | 80 | 6 | 3.4 | 3.9E+03 |
| BSR_inoc_BJP_IG2069_Synergistales_47_25_46_13 | 46 | 13 | 241 | 2210 | 96 | 0 | 2.1 | 1.3E+04 |
| BSR_Ace_LFCR_na_p_Bacteria_61_6 | 61 | 6 | 713 | 2433 | 85 | 7 | 2.2 | 3.9E+03 |
| BSR_Ace_UAPBR_effluent_at_Synergistales_60_7 | 60 | 7 | 308 | 2004 | 75 | 3 | 1.9 | 7.3E+03 |
| BSR_Ace_LFCR_na_p_Dethiosulfovibrio_peptidovorans_54_6 | 54 | 6 | 650 | 2469 | 86 | 0 | 2.1 | 4.1E+03 |
| BSR_Lac_LFCR_na_at_Desulfovibrio_65_13 | 65 | 13 | 841 | 4034 | 91 | 8 | 3.6 | 6.4E+03 |
| BSR_Ace_LFCR_na_at_Bacteria_35_8_(22) | 35 | 8 | 256 | 1826 | 83 | 0 | 1.8 | 8.0E+03 |
| BSR_Ace_UAPBR_effluent_at_Synergistales_62_11 | 62 | 11 | 317 | 2805 | 86 | 2 | 2.7 | 2.2E+04 |
| BSR_inoc_Mesotoga_50_21 | 50 | 22 | 210 | 2891 | 99 | 6 | 3.0 | 3.0E+04 |
| BSR_Ace_UAPBR_effluent_at_Sphaerochaeta_globosa_60_6 | 60 | 6 | 798 | 3096 | 87 | 6 | 2.6 | 4.3E+03 |
| BSR_Lac_UAPBR_effluent_at_Deltaproteobacteria_58_15 | 58 | 15 | 64 | 4157 | 99 | 1 | 4.6 | 1.2E+05 |
| BSR_inoc_2_Alphaproteobacteria_63_16 | 63 | 16 | 25 | 4502 | 98 | 1 | 4.9 | 4.4E+05 |
| BSR_Ace_C_na_Firmicutes_38_9 | 38 | 9 | 76 | 1066 | 91 | 2 | 1.1 | 2.0E+04 |
| BSR_Lac_UAPBR_effluent_at_Bacteria_37_7 | 36 | 7 | 571 | 2579 | 95 | 3 | 2.4 | 7.8E+03 |
| BSR_Ace_UAPBR_middle_p_Paracoccus_versutus_68_139 | 68 | 139 | 103 | 5132 | 99 | 1 | 5.1 | 1.2E+05 |
| BSR_Ace_C_na_Firmicutes_32_7 | 32 | 7 | 279 | 1602 | 77 | 10 | 1.4 | 5.2E+03 |
| BSR_Lac_LFCR_na_at_Clostridiales_36_8 | 36 | 8 | 211 | 2061 | 92 | 0 | 1.9 | 1.2E+04 |
| BSR_Ace_UAPBR_middle_p_Alphaproteobacteria_56_10 | 56 | 10 | 113 | 1796 | 90 | 1 | 1.7 | 2.5E+04 |
| BSR_Ace_LFCR_na_at_Synergistales_46_5 | 46 | 5 | 893 | 2240 | 88 | 3 | 1.7 | 2.1E+03 |
| BSR_Lac_C_na_Oscillibacter_valericigenes_58_8 | 58 | 8 | 216 | 2715 | 94 | 1 | 2.7 | 1.9E+04 |
| BSR_Lac_LFCR_na_at_Aminobacterium_colombiense_42_11 | 42 | 11 | 97 | 2350 | 93 | 0 | 2.3 | 3.8E+04 |
| BSR_Ace_UAPBR_effluent_at_Firmicutes_35_5 | 35 | 5 | 599 | 1760 | 82 | 11 | 1.3 | 2.4E+03 |
| BSR_Ace_UAPBR_effluent_at_1_Desulfobacca_acetoxidans_53_18 | 53 | 18 | 79 | 2918 | 98 | 1 | 3.2 | 6.3E+04 |
| BSR_Lac_UAPBR_inlet_at_Alphaproteobacteria_55_21 | 55 | 21 | 75 | 2117 | 89 | 1 | 2.1 | 5.8E+04 |
| BSR_inoc_Sphaerochaeta_globosa_51_10 | 52 | 10 | 679 | 3440 | 82 | 6 | 3.1 | 8.0E+03 |
| BSR_Lac_UAPBR_effluent_at_Serratia_marcescens_60_10 | 60 | 10 | 170 | 4894 | 99 | 0 | 5.1 | 4.9E+04 |

| | | | | | | | | |
|---|---|---|---|---|---|---|---|---|
| BSR_Lac_C_na_Firmicutes_41_16 | 41 | 16 | 75 | 3349 | 97 | 0 | 3.5 | 9.5E+04 |
| BSR_Lac_UAPBR_effluent_at_Firmicutes_59_13 | 59 | 13 | 156 | 3209 | 95 | 3 | 3.4 | 4.2E+04 |
| BSR_Lac_UAPBR_inlet_p_Opitutales_65_8 | 65 | 8 | 453 | 3351 | 91 | 1 | 4.2 | 1.3E+04 |
| BSR_Lac_LFCR_na_at_Desulfovibrio_64_24 | 64 | 24 | 660 | 3492 | 76 | 3 | 3.2 | 7.9E+03 |
| BSR_inoc_Firmicutes_35_7 | 35 | 7 | 609 | 2108 | 85 | 7 | 1.6 | 3.4E+03 |
| BSR_Lac_UAPBR_inlet_at_2_Clostridiales_48_10 | 48 | 10 | 309 | 2848 | 96 | 0 | 2.9 | 1.2E+04 |
| BSR_Lac_LFCR_na_p_2_Acinetobacter_tandoii_40_9 | 40 | 9 | 169 | 3381 | 96 | 0 | 3.3 | 3.2E+04 |
| BSR_Ace_UAPBR_effluent_at_Rhizobiales_62_14 | 62 | 14 | 67 | 3753 | 89 | 1 | 3.9 | 9.2E+04 |
| BSR_inoc_Spirochatetes_46_10 | 46 | 10 | 58 | 1761 | 95 | 0 | 1.8 | 5.3E+04 |
| BSR_inoc_2_Bacteroidia_46_15 | 46 | 15 | 78 | 2136 | 95 | 1 | 2.3 | 5.6E+04 |
| BSR_Ace_UAPBR_effluent_p_2_Arcobacter_33_21 | 33 | 21 | 26 | 2237 | 100 | 0 | 2.3 | 1.2E+05 |
| BSR_inoc_2_BJP_IG2069_Synergistales_47_25_47_14 | 47 | 14 | 78 | 1990 | 100 | 0 | 2.0 | 5.5E+04 |
| BSR_Ace_UAPBR_effluent_at_1_Rhizobiales_51_26 | 51 | 26 | 56 | 3993 | 100 | 0 | 4.3 | 2.7E+05 |
| BSR_inoc_Wolinella_succinogenes_49_6 | 49 | 6 | 518 | 2331 | 94 | 5 | 1.9 | 4.9E+03 |
| BSR_Lac_LFCR_na_p_Citrobacter_freundii_52_21 | 52 | 21 | 93 | 5103 | 100 | 1 | 5.2 | 1.6E+05 |
| BSR_Lac_UAPBR_middle_p_Bacteroidales_bacterium_CF_41_9 | 41 | 9 | 440 | 3330 | 96 | 2 | 3.4 | 1.4E+04 |
| BSR_Lac_LFCR_na_at_Desulfovibrio_65_16 | 65 | 16 | 48 | 3194 | 99 | 0 | 3.4 | 2.4E+05 |
| BSR_inoc_Bacteroidetes_46_9 | 46 | 9 | 282 | 3451 | 92 | 1 | 4.0 | 1.9E+04 |
| BSR_Lac_LFCR_na_p_Stenotrophomonas_maltophilia_67_8 | 67 | 8 | 431 | 4574 | 99 | 0 | 4.6 | 1.8E+04 |
| BSR_inoc_Firmicutes_43_6 | 43 | 6 | 210 | 1344 | 84 | 7 | 1.2 | 6.6E+03 |
| BSR_Ace_UAPBR_middle_p_Thauera_sp__27_66_8 | 66 | 8 | 366 | 3839 | 96 | 1 | 4.0 | 1.5E+04 |
| BSR_Lac_C_na_Betaproteobacteria_67_11 | 67 | 11 | 293 | 5934 | 99 | 1 | 6.3 | 4.1E+04 |
| BSR_Ace_UAPBR_effluent_at_2_Draconibacterium_42_15 | 42 | 15 | 263 | 2739 | 99 | 2 | 3.0 | 1.6E+04 |
| BSR_inoc_Sphaerochaeta_globosa_50_11 | 50 | 11 | 486 | 2849 | 77 | 13 | 2.7 | 6.2E+03 |
| BSR_Lac_LFCR_na_p_Arcobacter_butzleri_27_17 | 27 | 17 | 34 | 2353 | 100 | 0 | 2.3 | 1.5E+05 |
| BSR_Lac_UAPBR_inlet_at_Clostridiales_61_7 | 61 | 7 | 465 | 3080 | 83 | 0 | 3.2 | 7.9E+03 |
| BSR_Lac_UAPBR_effluent_at_Sulfurovum_37_10 | 37 | 10 | 90 | 1741 | 98 | 2 | 1.6 | 2.9E+04 |
| BSR_Lac_UAPBR_inlet_p_Ochrobactrum_anthropi_56_5 | 56 | 5 | 2173 | 5681 | 84 | 12 | 4.5 | 2.3E+03 |
| BSR_inoc_Bordetella_65_7 | 65 | 7 | 525 | 4230 | 89 | 1 | 4.1 | 9.4E+03 |
| BSR_inoc_Desulfovibrio_65_12 | 65 | 12 | 483 | 4525 | 92 | 11 | 4.6 | 1.5E+04 |
| BSR_inoc_2_Dethiosulfovibrio_peptidovorans_54_30 | 54 | 30 | 100 | 2725 | 100 | 1 | 2.8 | 5.3E+04 |
| BSR_Lac_C_na_Desulfovibrio_69_9 | 69 | 9 | 318 | 2990 | 89 | 1 | 2.8 | 1.2E+04 |
| BSR_Lac_UAPBR_inlet_p_1_Veillonella_parvula_39_28 | 39 | 28 | 18 | 1874 | 100 | 0 | 2.0 | 4.3E+05 |
| BSR_Ace_UAPBR_effluent_at_1_Clostridia_48_25 | 48 | 25 | 28 | 2032 | 89 | 0 | 2.1 | 1.4E+05 |
| BSR_inoc_Pseudomonas_aeruginosa_67_10 | 67 | 10 | 212 | 5839 | 99 | 1 | 6.1 | 5.0E+04 |
| BSR_Lac_UAPBR_inlet_p_Rhizobiales_65_11 | 65 | 11 | 140 | 3996 | 100 | 1 | 4.1 | 7.2E+04 |
| BSR_Lac_UAPBR_effluent_at_Desulfobulbus_propionicus_57_36 | 57 | 36 | 99 | 3354 | 100 | 0 | 3.8 | 7.1E+04 |
| BSR_inoc_Bacteroidia_40_18 | 40 | 18 | 86 | 2094 | 94 | 2 | 2.5 | 4.3E+04 |
| BSR_Ace_UAPBR_effluent_p_Brevundimonas_diminuta_67_12 | 67 | 13 | 181 | 3445 | 99 | 3 | 3.4 | 3.2E+04 |
| BSR_Lac_C_na_1_Pseudomonas_putida_63_10 | 63 | 10 | 508 | 5624 | 98 | 2 | 5.8 | 2.7E+04 |
| BSR_Ace_UAPBR_inlet_p_Leucobacter_sp__UCD_THU_71_10 | 71 | 10 | 98 | 3824 | 100 | 1 | 4.1 | 7.3E+04 |
| BSR_Ace_UAPBR_middle_p_Paracoccus_69_26 | 69 | 26 | 22 | 2973 | 99 | 0 | 3.1 | 1.8E+05 |
| BSR_inoc_Tenericutes_37_12 | 37 | 12 | 61 | 1378 | 96 | 3 | 1.5 | 5.8E+04 |
| BSR_Ace_UAPBR_inlet_p_2_Bosea_sp__LC85_68_11 | 68 | 11 | 82 | 4471 | 99 | 1 | 4.6 | 9.6E+04 |
| BSR_Ace_UAPBR_middle_p_Brevundimonas_diminuta_68_10 | 68 | 10 | 219 | 3018 | 92 | 0 | 2.9 | 1.8E+04 |
| BSR_Ace_UAPBR_middle_p_Gammaproteobacteria_63_13 | 63 | 13 | 52 | 4897 | 100 | 2 | 5.4 | 2.1E+05 |
| BSR_Lac_UAPBR_effluent_at_Mollicutes_32_13 | 32 | 13 | 35 | 1704 | 99 | 0 | 1.8 | 9.6E+04 |
| BSR_Lac_UAPBR_inlet_at_Desulfovibrio_vulgaris_68_10 | 68 | 10 | 146 | 3242 | 99 | 1 | 3.8 | 4.1E+04 |
| BSR_inoc_Mesotoga_48_20 | 48 | 20 | 200 | 2646 | 92 | 1 | 2.8 | 2.6E+04 |
| BSR_inoc_2_Mollicutes_45_98 | 45 | 98 | 37 | 1574 | 97 | 0 | 1.7 | 1.5E+05 |
| BSR_Lac_UAPBR_effluent_at_Mesotoga_47_17 | 47 | 17 | 117 | 2922 | 100 | 0 | 3.1 | 6.8E+04 |
| BSR_inoc_Euryarchaeota_62_7 | 62 | 7 | 295 | 2209 | 93 | 13 | 2.0 | 8.9E+03 |
| BSR_Ace_UAPBR_effluent_p_Hydrogenophilales_68_7 | 68 | 7 | 520 | 3075 | 93 | 3 | 2.7 | 7.1E+03 |
| BSR_inoc_Thiotrichales_48_37 | 48 | 37 | 70 | 2654 | 100 | 0 | 2.8 | 1.0E+05 |
| BSR_Ace_UAPBR_inlet_p_Xanthomonadales_68_12 | 68 | 12 | 53 | 2642 | 92 | 7 | 3.0 | 1.2E+05 |
| BSR_inoc_Arcobacter_butzleri_29_10 | 29 | 10 | 161 | 1363 | 83 | 1 | 1.2 | 9.4E+03 |
| BSR_inoc_Tistrella_mobilis_68_15 | 68 | 15 | 51 | 5342 | 100 | 0 | 6.0 | 2.5E+05 |
| BSR_inoc_Cloacimonetes_37_5 | 37 | 5 | 556 | 1514 | 76 | 4 | 1.3 | 2.7E+03 |